THE BEHAVIOUR OF PROFILED STEEL SHEET/CONCRETE COMPOSITE SLABS

Imad E.H. Shobaki

School of Environment & Life Sciences

Division of Civil & Environmental Engineering

University of Salford, Salford, UK

Submitted in Partial Fulfilment for the Degree of

Doctor of Philosophy, October 2000

THE BEHAVIOUR OF PROFILED STEEL SHEET/CONCRETE COMPOSITE SLABS

Imad E.H SHOBAKI

Ph.D. Thesis 2000

Contents

Contents i

List of illustrations vii

List of tables xi

Acknowledgements xii

Abstract xiii

Notation xiv

Abbreviations xviii

Chapter One: Introduction

1.1 Introduction 1

1.2 Composite slabs with profiled steel sheets 3

1.3 Profiled steel sheeting 4

1.4 Shapes and position of embossments 4

1.5 Definition of shear-bond strength 5

1.6 Composite structures using profiled steel sheeting 6

1.7 Advantages of composite structures 7

1.8 The use of composite structures 7

1.9 Composite behaviour 8

1.10 Scope of the problem investigated in this thesis 8

1.11 Outline of the thesis 10

Chapter Two: Shear-Bond in Composite Construction

2.1 Introduction 17

2.2 Bond in conventional reinforced concrete 17

2.2.1 Bond for coated reinforcing bars and sheeting. 18

2.2.2 Bond stress-slip relationship 19

2.2.3 Anchorage length 20

2.3 Composite beams 21
2.3.1 General 21
2.3.2 Composite beams with solid concrete slabs 21
2.3.3 Composite beams with composite concrete slabs 22

2.4 Profiled composite slabs 23
2.4.1 General 23
2.4.2 Design criteria and failure modes 24
2.4.3 Ductility 26
2.4.4 Propped and unpropped construction 27
2.4.4.1 Temporary supports (propped) 27
2.4.4.2 Deflection during construction (unpropped) 28

2.5 Design methods 29
2.5.1 The 'm-k' method 29
2.5.2 The partial shear connection method 31
2.5.2.1 General 31
2.5.2.2. Determination of the bending resistance 32
2.5.2.3 Determination of the horizontal shear strength τu.Rd 34
2.5.2.4 Extension of partial connection method 35

2.6 Mechanical interlock and friction 36

2.7 Numerical modelling 37

Chapter Three: Small Scale Tests on Composite Slabs to investigate Longitudinal Shear/Slip Behaviour

Summary 45

3.1 Introduction 46

3.2 Conventional reinforced concrete 47

3.3 Composite slabs 48

3.4 Push-off and Pull-out tests 49
3.4.1 General 49
3.4.2 Preparation of the specimens 50
3.4.3 Test set-up 51
3.4.4 Test results and comments 51

3.5 Frictional coefficient 53

3.6 Discussion 54

3.7 Conclusions 54

Chapter Four: Full-Scale Tests

4.1 Introduction **77**

4.2 Composite slabs **77**

4.3 Materials **78**
4.3.1 Profiled steel sheeting 78
4.3.2 Concrete 78
4.3.3 Mesh reinforcement 78
4.3.4 Additional reinforcement 79

4. 4 Casting **79**

4.5 Test set-up **80**

4.6 Arrangement **80**
4.6.1 Slip gauges 80
4.6.2 Deflection gauges 81

4.7 Test loading procedure **81**

4.8 History of load-deflection behaviour **82**

4.9 Load-end slip behaviour **82**

4.10 Failure characteristics **82**

4.11 Slab behaviour during load application **83**
4.11.1 Results summary 83

4.12 Regression line **85**

4.13 Evaluation of design loads **85**

4.14 Discussion of results **86**
4. 14.1 Slabs behaviour and failure mode 86

4. 15 Design loads using the m-k method **86**

4.16 Evaluation of test results according to partial shear connection method in EC4 ..... **88**
4.16.1 Determination of design load 89

4.17 Conclusions **94**

Chapter Five: Finite Element Analysis

5.1 Introduction 122

5.2 The finite element method (FEM): 123

5.3 Advantages of the finite element method 123

5.4 ANSYS 125

5.4.1 The required data file to run ANSYS software[54] 126

5.4.1.1 Model construction: 126

5.4.1.2 Load application and solution: 126

5.4.1.3 Results review: 127

5.4.2 Element characteristics 127

5.4.2.1 Lists of element types two-dimensional and three-dimensional elements: 127

5.4.3 Structural analysis 128

5.4.3.1 Static analysis 129

5.4.3.2 Modal analysis 129

5.4.3.3 Harmonic analysis 129

5.4.3.4 Transient dynamic analysis 130

5.4.2.5 Spectrum analysis 130

5.4.3.6 Buckling analysis 130

5.5 Non-linear structural analysis 130

5.5.1 Geometric non-linearities 131

5.5.2 Material non-linearities 132

5.5.2.1 Plasticity 132

5.5.2.2 Contact non-linearities 132

5.5.2.3 Friction 133

5.5.3 Changing status (including contact) 134

5.5.4 Incremental loading and equilibrium iterations 135

5.6 Modelling composite slabs 135

Chapter Six: Finite Element Modelling of Tests

6.1 Introduction 141

6.2 Finite element model 142

6.2.1 Concrete 144

6.2.2 Steel sheeting 144

6.2.3 Non-linear stress strain materials 145

6.3 Mechanical interlock 147

6.3.1 Contact non-linearities 147

6.3.2 Contact stiffness 147

6.3.3 Choosing the contact stiffness 148
6.3.4 Combination element 149
6.3.4.1 Element geometry and input data 149
6.3.4.2 Characteristics of the element 150
6.3.4.3 Determination of F1 and F2 for structural applications 150
6.3.5 Point-to-point 3-D contact element 151
6.3.5.1 Element geometry and input data 151
6.3.6 Point-to-surface 3-D contact element 152
6.3.6.1 Element geometry 152

6.4 Example use of modelling procedure 153

6.5 Comparison of numerical analysis with test results 153

6.6 Discussion and conclusions 154

Chapter Seven: Finite Element Modelling of Embossment Performance

7.1 Introduction 183

7.2 Elements used in modelling 183
(a) Finite strain shell element: 184
(b) 3-D structural solid element 184
(c) 3-D point-to-surface contact element 184

7.3 Material properties 185
(a) Steel plate element: 185
(b) Concrete: 185

7.4 Modelling of steel plate only 186
7.4.1 General 186
7.4.2 Effect of the aspect ratio-single embossment 187
7.4.3 Behaviour of several embossments under horizontal load 188

7.5 Modelling concrete with steel sheet and embossments 189
7.5.1 General 189
7.5.2 Effect of the aspect ratio of the embossments 189
7.5.3 Behaviour of several embossments under horizontal load 190
7.5.4 Effect of uniform load distribution 191

7.6 Conclusions and future work 192

Chapter Eight: Review, Conclusions and Future Work

8.1 Introduction **213**

8.2 Summary of research and main conclusions **213**
8.2.1 Introduction 213
8.2.2 Shear-bond in composite construction 214
8.2.3 Push-off and pull-out tests 214
8.2.4 Full-scale tests 216
8.2.5 Modelling of composite slabs 218
8.2.6 Finite element modelling of embossments 219

8.3 Recommendations (for future work) **220**

References 222

Appendix A: Self weight of concrete slab and spreader beams 228

Appendix B: Determination of design load using the partial shear connection method 229

Appendix C: Determination of design loads using the m-k method 239

Appendix D: Example of input data 243

List of Illustrations

Figure 1.1 Early composite slab supported by steel beam 12
Figure 1.2 Composite slabs supported by composite beams 12
Figure 1.3 Dovetailed (re-entrant) deck profiles 13
Figure 1.4 Trapezoidal deck profiles 14
Figure 1.5 Shapes of embossment in the web 15
Figure 1.6 Position of embossments 15
Figure1.7 Typical hybrid deck with re-entrant portions 15
Figure 1.8 Forms of shear connection in composite slabs 16

Figure 2.8 Shear span in composite slabs 41
Figure 2.8.a Effective shear span in partial shear connection method 42
Figure 2.9 Stress distribution for sagging bending if the neutral
axis is above the steel sheet 42
Figure 2.10 Stress distribution for sagging bending if the neutral 42
axis is in the steel sheet 42
Figure 2.11 Determination of the degree of shear connection from Mtest 43
Figure 2.12 Design partial interaction diagram 43
Figure 2.13 Design partial interaction diagram for a slab with end anchorage 43
Figure 2.14 Contribution of additional longitudinal reinforcement 44

Figure 3.1 Shear stress-slip relationship in reinforced concrete 59
Figure 3.2.a Pull-out test 59
Figure 3.2.b Typical push-off test for shear connection in composite beams 60
Figure 3.3.a Push-off test for one rib with full encasement of the rib 60
Figure 3.3.b Pull-out test for one rib with full encasement of the rib 60
Figure 3.3.c Pull-out test for one rib with part encasement of the rib 61
Figure 3.3.d Push-off test for one rib with part encasement of the rib 61
Figure 3.4.a Push-off test of two ribs with full encasement 61
of the whole sheet (600*600mm) 61
Figure 3.4.b Push-off test with part encasement of end ribs (600*600mm) 62
Figure 3.5.a Pull-out test in operation 62
Figure 3.5.b Pull-out test of the full encasement of the rib 63
Figure 3.5.c Push-off test with part encasement of the end ribs 63
Figure 3.5.d Push-off test with full encasement of the ribs 64
Figure 3.6.a Pull-out test with part encasement of the ribs 64
Figure 3.6.b Pull-out test with full encasement of the ribs 65
Figure 3.6.c Push-off test with full encasement of the ribs 65
Figure 3.6.d Push-off test with part encasement of the ribs 66
Figure 3.7 Failure mechanism of tests 66
Figure 3.8-17 Load-Slip behaviour for composite slab
(push-off and pull-out tests) 67-71
Figure 3.18-25 Comparison of push-off, and pull-out tests (Load-Slip) 72-75
Figure 3.26-27 Determination of frictional coefficient
(for the push-off and pull-out tests) 76
Figure 4.1 First series of composite slab tests 102

Figure 4.2 Second series of composite slab tests (additional reinforcement)..... 103
Figure 4.3 Third series of composite slab tests (135mm deep) 104
Figure 4.4 Illustration of possible failure modes 105
Figure 4.5 Profiled steel sheet (ComFlor70) 106
Figure 4.6 Test setup and load arrangement for composite slab tests 107
Figure 4.7 End slip gauges and transducers..... 108
Figure 4.8 Deflection transducers and dial gauges 108
Figure 4.9-17 Load-Central Deflection curve for Slab No.1 to 9.....109-113
Figure 4.18-26 Load-End Slip curve for Slab No.1 to 9.....113-117
Figure 4.27 Typical crack patterns 118
Figure 4.28-33 Comparison of load verses load-deflection or end slip
for the composite slabs 108

Figure 5.1 Three triangular element 137
Figure 5.2 Irregularly shaped plate shown
discretized into triangular finite elements..... 137
Figure 5.3 Rectangular plate discretized into rectangular elements. 137
Figure 5.4 Representing higher order elements 137
Figure 5.5 Non-linear behaviour of structures..... 138
Figure 5.6 Example of geometric non-linearity of the fishing rod 139
Figure 5.7 Non-linear stress-strain relationship..... 139
Figure 5.8 Stress –strain curve with the elastic and plastic parts 139
Figure 5.9 Changing status including contact..... 140
Figure 5.10 Non-linear analysis with a linear solver 140
Figure 5.11 Incremental loading..... 140

Figure 6.1.a Finite element modelling of the composite slab (full scale). 158
Figure 6.1.b Finite element modelling of the composite slab (small scale). 158
Figure 6.2 Force-deflection relationship of the contact and combine elements. 159
Figure 6.3 3-D Structural solid element..... 159
Figure 6.4 Finite strain shell element..... 160
Figure 6.5 The elasto-plastic stress-strain curve used
for concrete, an steel materials 160
Figure 6.6.a The penetration of two areas. 161
Figure 6.6.b Spring behaviour between the contact areas when contact occurs. 161
Figure 6.7.a Combine element (spring-slider and damper element). 161
Figure 6.7.b Combine behaviour. 162
Figure 6.7.c Force-deflection relationship 162
Figure 6.8.a 3-D Point-to-point contact element. 162
Figure 6.8.b Force-deflection relation-ship 163
Figure 6.9 3-D Node-to-surface contact element..... 163
Figure 6.10.a The finite element mesh for profiled steel sheeting in
small-scale test model..... 164
Figure 6.10.b The finite element mesh of concrete for the
small-scale test model..... 164
Figure 6.10.c The finite element model with the loads and supports indicated. 165
Figure 6.11.a The finite element mesh for profiled steel sheeting. 165

Figure 6.11.b The finite element mesh for concrete for the full scale tests using symmetry.....166
Figure 6.11.c The finite element model with the loads for the full-scale tests.....166
Figure 6.12 The composite slab dimensions, and the cross-section geometry of profiled steel sheet (Daniels[56]) 167
Figure 6.13 Comparison between experimental and FE results load-slip behaviour for push-off test No.1.....168
Figure 6.14 Comparison between experimental and FE results for load-slip behaviour for push-off test No.2.....168
Figure 6.15-23 Comparison between experimental and FE results for load-end slip curve for composite slabs No.3 to 11.....169-173
Figure 6.24–32 Comparison between experimental and FE results for load-central deflection curve for slabs No.3 to 11.....173-177
Figure 6.33.a Slip for the small-scale model.....178
Figure 6.33.b Close up of slip in the small scale-model.....178
Figure 6.33.c Longitudinal displacement (uz) in small-scale model.....179
Figure 6.33.d Deformation of the model at load 21.83 kN. 179
Figure 6.34.a Deflection (95mm) of the composite slab at load of 64.86 kN. 180
Figure 6.34.b Deflection (95mm) of the profiled steel sheet at load of 64.86 kN....180
Figure 6.34.c Section of the longitudinal displacement of at load of 64.86 kN. 181
Figure 6.34.d Longitudinal displacement of the composite slab.....181
Figure 6.34.e General deformation of composite slab.....182

Figure 7.1 Profiled steel sheet dimensions. 193
Figure 7.2 Concrete layer dimensions 193
Figure 7.3 Definition of aspect ratio (b/d) for embossment modelling 193
Figure 7.4-6 F.E. modelling for embossments.....194-195
Figure 7.7 Comparison of applied load versus deflection for various aspect- ratio . 196
Figure 7.8 Comparison of applied load versus longitudinal displacement various aspect ratio. 196
Figure 7.9-12 F.E. modelling for embossments.....197-198
Figure 7.13 Comparison of applied load versus longitudinal displacement for numbers of embossments. 199
Figure 7.14 Comparison of applied load versus deflection for numbers of embossments. 199
Figure 7.15-20 F.E. modelling for embossments.....200-204
Figure 7.21 Comparison of the applied load versus deflection for various aspect ratio. 205
Figure 7.22 Comparison of applied load-slip versus longitudinal displacement.....205
Figure 7.23-30 F.E. modelling for embossments.....206-209
Figure 7.31 Comparison of applied load versus deflection for various numbers of embossments.....210
Figure 7.32 Comparison of applied load versus longitudinal displacement for various numbers of embossments. 210
Figure 7.33-37 F.E. modelling for embossments.....211-212

Figure B.1 Determination of the degree of shear connection from M_{test} for slab No1 236
Figure B.2 Design partial interaction diagram for slab No.1 237
Figure B.3 Design partial interaction diagram for slab No.2 237
Figure B.4 Cross section of composite slab with reinforcement 238
Figure C.1 Evaluation of m & k for the first series of composite slabs 242
Figure C.2 Evaluation of m&k for second series of composite slabs 243

List of Tables

Table 3.1.a Profiled steel sheet details.....57
Table 3.1.b Details of push-off and pull-out tests.....57
Table 3.2 Details of typical shear stress values τ (N/mm2).....58

Table 4.1 Tensile Strength of Profiled Steel Sheeting.....96
Table 4.2 Profile Steel sheeting details 96
Table 4.3 Slab Details:.....97
Table 4.4 Test Results:.....98
Table 4.5 Regression line values: 99
Table 4.6 Shear strength and design load values
using m-k method & partial connection methods.....100
Table 4.6.a Calculation of shear stress according to partial interaction theory,
compared with the shear stress from the small-scale tests. 101

Table 6.1 The input data of the geometrical properties for the two
small-scale tests (using data from chapter 3).....155
Table 6.2 Input data for the three full scale composite slabs (data from chapter 4). 156
Table 6.3 Input data for the properties of concrete and profiled steel sheet
for the composite slabs for reported by Daniels1987[56].....156
Table 6.4 The complete input data for the FEM.....157

Acknowledgements

I must first express my deep gratitude to my supervisor, Mr. D.C. O'Leary, for his inspiration, encouragement, and the constant advice during this research.

Many thanks are due to the technical staff in the departmental laboratories and workshops.

My thanks to my parents, my wife, my brothers, and sisters for their continuous encouragement and support during the study. I also thank my daughter, and my son for bringing me so much happiness.

My thanks to all friends for their effort in giving the best advice from their experience in postgraduate studies.

Abstract

The work presented in this thesis is concerned with the effect of shear-bond on the behaviour of profiled steel sheet/concrete composite slabs. A review of the previous work carried out to investigate the influence of shear bond in composite construction and the factors which may affect shear bond resistance is presented and discussed. Also, the different empirical shear-bond equations proposed and design methods for composite slabs are reviewed. A description of push-off and pull-out tests follows and several examples of concrete/profiled steel sheeting units were tested and the results discussed. These small scale tests provided information on the load/slip relationship which was used in the subsequent modelling of the full-scale composite slabs. Full-scale composite slab tests are then considered together with a discussion of results. These are analysed using the regression approach of British Standards and the Eurocode 4. Comparison is made with the design values using the partial interaction method. The comparison indicates that both design methods are valid with the regression approach being slightly more conservative.

Finite element methods and their advantages are reviewed and the ANSYS software is introduced together with it's proprietary elements, material models and contact elements. This is followed by a description of three-dimensional finite element modelling of composite slabs (small and full scale). The load versus deflection, and load versus slip provide a comparison between the numerical analysis and test results. The finite element analysis of the composite slabs was successful. The failure load of each slab was modelled satisfactorily using the contact stiffness from the small-scale tests modified by a small percentage (less than 10%). A close correlation between the experimental and finite element analysis predictions for the load/slip and load/deflection behaviour was also obtained.

Three-dimensional finite element modelling of embossments with different parameters for the steel sheet and concrete was carried out and conclusions drawn. The general conclusions of the work follows together with recommendations for future research.

Notation

A_p Effective cross - sectional area of profiled steel sheet

A_s Cross-section area of steel reinforcement

b_r Breadth of the concrete rib

b Slab width

C Damping coefficient = Force* Time2/Length

D_p Overall depth of the steel sheeting

d_p The vertical distance from top of slab to the centroid of the steel profile.

d_s Vertical distance from top of slab to centreline of steel reinforcement

e Distance from centriod of steel sheet to its underside

E_c Young's modulus (kN/mm^2),

e_p Distance from plastic neutral axis of steel sheet to its underside

e_{sc} Distance to centroid of steel sheet in compression

F Force applied to the structure

F_1 Force in spring one

F_2 Force in spring two

f_b Bond stress

f_{bu} Design ultimate anchorage bond stress

f_{ck} Characteristic cube strength of concrete

f_{cu} Compressive strength of concrete

f_{dp} Design strength of steel sheet

FN Normal force

F_s Force required in spring 1 to cause sliding (input quantity FSLIDE)

F_s Force in the bar or group of bars

F_s Absolute value of the tangential force

f_{sk} Yield strength of steel reinforcement

FSLIDE Absolute value of the spring force that must be exceeded before sliding occurs.

f_{up} Ultimate strength of steel sheet

f_{yp} Yield strength of steel sheet

h Overall height of the shear-stud

h Thickness of the small composite tests

h_t Total depth of slab

k Contact stiffness

k Reduction factor

k_{Comp} Reduction factor for the "composite slab" only

K proportional constant represent the stiffness of the structure

[K] Global stiffness matrix

k,k_r Intercept of regression line

K_1 Stiffness of spring one

K_2 Stiffness of spring two

KN Contact stiffness

L Anchorage length

L_o Length of overhang

L_s Shear span length

L_{sf} Length for full shear connection

L_t Slab length

L_w Slab width

L_x Distance from support

m,m_r Slope of regression line

m_{Comp} Slope of regression line for the "composite slab" only

M_{pa} Plastic moment capacity of steel sheeting

M_{pr} Reduced plastic moment capacity of steel sheet

$M_{p,Rd}$ Design bending moment

M,M_{pRm} Bending moment

M_{Rc} The maximum bending moment for the "reinforced slab" only.

M_{comp} The maximum bending moment for the composite slab only

M_{Rd} design resistance moment (design bending resistance)

$M_{R.design}$ Design bending moment of profiled steel sheet

$M_{R.ult}$ Ultimate bending moment of profiled steel sheet

M_{test} Maximum bending moment from test

MU	Friction
N	Number of studs in trough
N_{as}	Force in steel reinforcement
$N_{cf,}$ Nc	Compression force in concrete
N_p,N_{st}	Force in profiled steel sheet
Q_k	Characteristic resistance of shear-connector
Q_n	Capacity of shear-connector in negative moment regions
Q_p	Capacity of shear-connector in positive moment regions.
p_s	Average load at which slip is first recorded.
p_{max}	Maximum load recorded before the slab failure.
seqv	Total stresses
sz	Stress at z direction
t	Thickness of the profiled steel
u	displacement
u_1	Displacement at node I
u_2	Displacement at node J
u_{gap}	Initial gap size
uy	Displacement at y direction (slip direction)
uz	Displacement at z direction (deflection direction)
V_1	Resistance of end anchorage
V_{1d}	Design resistance of end anchorage
V_{1k}	Characteristic resistance of end anchorage
$V_{1.Rd}$	Maximum design shear resistance
$V_{v.Rd}$	Vertical shear resistance
V_t	Experimental shear force
$V_{t"Rc"}$	Experimental shear force for the "reinforced slab"only
$V_{t"Comp"}$	Experimental shear force for the "composite slab" only
w	Total applied load
z,z_1,z_2	lever arms
β	Coefficient dependent on bar type.
x	Depth of stress block for concrete

ϕ_e Effective bar size which, for a single bar is equal to the size and for a group of bars in contact is equal to the diameter of a bar of equal total area

γ_{ap} Partial safety factor for profiled steel sheet

γ_c Partial safety factor for concrete

γ_s partial safety factor for steel reinforcement

γ_{vs} Partial safety coefficient, normally taken as 1.25

γ_m Partial safety factor.

η Degree of shear connection

η_{comp} Degree of shear connection for the composite slabs with reinforcement when the flexural capacity of the "reinforced concrete portion" has been deducted.

η_{test} Degree of shear connection from test

μ Coefficient of friction

μFN Constant friction force

τ_u Ultimate shear strength

τ_{um} Mean value of ultimate shear strength

$\tau_{u.Rd}$ Design shear strength

$\tau_{u.Rk}$ Characteristic shear strength

Abbreviations

ASDs	ANSYS Support Distributors
c.a.	Centroidal axis
DOF	Degree of freedom
FE	Finite Element
FEA	Finite Element Analysis
FEM	Finite Element Method
N-R	Newton-Raphson
p.n.a.	Plastic neutral axis
SASI	Swanson Analysis Systems, Incorporated

Chapter One

Introduction

1.1 Introduction

Composite construction is the term used for structures composed of two or more different materials. Generally in Structural Engineering, the materials may be concrete/steel, concrete/timber, timber/plastic, timber/steel, plastic/steel ... etc. Composite construction integrates the structural properties of the two materials to produce stiffer, stronger and lighter members from the efficient connection between the two materials. The shear-bond connection between the two materials is a very important factor in ensuring they act as one unit.

In construction, the most common combination of these materials is concrete and steel, producing a composite material where the bending moment caused by a static load is mainly resisted by the compressive force in the concrete and the tensile force in the steel. Probably the more common form is reinforced concrete while the subject of this work, concrete/profiled steel sheet slabs, are an efficient and popular alternative for floor slab construction.

The choice between reinforced concrete, and this other form of composite construction for a particular structure depends on many factors. When these different modes of construction are compared, the main comparison is that of total cost, including cost of materials, construction time, and whilst strength is often the predominating factor fire resistance also has a significant influence. In terms of materials reinforced concrete is the cheaper of the two, because of the relatively high price of the profiled steel sheets.

From the constructional standpoint, composite construction may often be cost effective, because it can be quickly erected especially when precast concrete units or profiled steel sheeting are used in conjunction with the steel frame to facilitate the construction of the floors. Regarding fire resistance, reinforced concrete has some

advantages, but since both types are used in the construction of multi-storey structures it would seem that the total costs are not significantly different.

The concrete/steel type of composite construction considered in this work, uses steel in the form of profiled steel sheeting. The steel sheeting is considered as an external main reinforcement for the composite member. For many reasons, the composite action may not be complete because the concrete does not completely confine the steel. This may give rise to incompatibility in the strain at the concrete/steel interface when horizontal slip has occurred at the interface in the longitudinal direction. Also, vertical movement (uplift) may occur due to lack of interlock at the interface in the vertical direction. So, a strong stiff connection at the interface is required for effective composite members.

When rolled steel sections are used, as in composite beams, shear-connecting devices are required to increase the interface stiffness in both the horizontal and vertical directions. Welded shear-stud connectors are a common form of shear-connection device. The interface can only be assumed to be fully rigid and infinitely strong if the horizontal slip that may occur at the steel/concrete interface is very small. When profiled steel sheeting is used as the steel component in a composite element, it is impractical to weld shear connectors unless they are used on the supporting beams as end anchors. The steel material may be less than 1 mm thick, so shear connection is provided either by pressed or rolled embossments (indentations) that project into the concrete. This may be enhanced by giving the profiled steel sheeting a re-entrant shape, which prevents the vertical separation of the steel from the concrete, and can result in more effective mechanical connection from the embossments.

For rolled steel sections, it is possible to produce strong ductile members that are relatively easy to design by controlling the number of shear-stud connectors used. However, for composite members formed with profiled steel sheeting, it is more difficult to ensure strong ductile behaviour and this is reflected in the design approach.

1.2 Composite slabs with profiled steel sheets

Lawson[1] defined composite slabs as slabs that comprise profiled steel decking (or sheeting) as the permanent formwork to the underside of concrete slabs spanning between the support beams.

The sheeting takes on different roles during different stages in construction. Prior to casting the concrete serves as a platform for the workmen and their equipment. During casting of concrete, the sheeting acts as formwork. After the concrete has hardened and the two components have become a composite system, the sheeting serves as reinforcement.

Composite slab systems were first developed in the late 1930s for use in tall buildings. At that time, this technique brought a considerable dead-load reduction, and was essentially seen potentially as a substitute for traditional reinforced concrete slabs. Because of their efficiency and advantages, composite slabs were soon applied to a wide range of construction projects invariably based on structural steel framing (high-rise, low-rise, and industrial buildings).

Profiled steel sheet/concrete floor systems have been used in North America since the early 1950s and since that date have been used in increasingly sophisticated ways[2]. In Europe, the first composite slabs appeared at the end of the 1950s Davies[3]. At that time, the construction was carried out using corrugated sheets supported by fabricated steel beams and covered with a thin concrete slab containing a wire mesh (Figure1.1). The connection between the sheet and the concrete was provided by pure bond, except in cases of significantly heavy load conditions, where the mesh wires were welded to the top of the sheet corrugations. In the middle of the 1960s, the first dovetailed profiled sheeting, originally designed for composite slabs, was introduced from the U.S.A to the European market. During the 1980s, the introduction of fast-track construction methods brought a new interest in steel design and consequently in composite flooring.

The initial use of composite decks was as a substitute for traditional reinforced concrete slabs. A composite floor is essentially an overlay of one-way structural elements. The primary beams, the secondary beams and the composite slab is shown in Figure 1.2.

1.3 Profiled steel sheeting

Profiled steel sheeting is manufactured from a thin strip or coil material, usually between 0.7 mm and 1.5 mm thick. It can be formed to almost any required shape to obtain a strong, stiff structural member of low weight and high efficiency.

There are two well-known forms of sheet (deck) profiles, the dovetail profile (re-entrant) and the trapezoidal profile (open ribs) with web indentations. Some profiles of each type are shown in Figures 1.3 and 1.4. The type ComFlor 70 is used for the experimental work carried out in this study. In recent times a series of hybrid profiles have been developed which incorporate the features of both trapezoidal and re-entrant forms as shown in Figure 1.7.

A thin layer of galvanising is the normal protection against corrosion of sheeting, which is sufficient for composite slabs in a dry interior atmosphere. For more severe environments, other types of protection need to be provided.

1.4 Shapes and position of embossments

Embossments may be described as sudden changes in the surface of the sheeting. They are pressed into the profiled steel surface to act as shear-connection devices. Each profiled steel sheeting product has its own geometry of embossments. Different shapes can be given to the embossments. The embossments may be pressed or rolled in the shape of vertical or inclined rectangles (trapezoidal in section), squares, chevrons, circles or staggered circles and vertical or inclined splits as shown in Figure 1.5 (Zubair[4]). The corners of the embossments and the connecting lines with the profiled steel sheeting are curved, as it is quite difficult to form sharp angles. The embossments may be pressed in the webs, flanges or the troughs (Figure 1.6). The position of the embossments may depend on the available areas to be pressed through the profiled steel sheeting. The height of embossments is limited due to the energy required for the pressing process and to avoid tearing of the sheeting. In general, the height of embossments varies between 1.5 mm to 4.0 mm.

1.5 Definition of shear-bond strength

Shear-bond can be defined as the strength of the interface between any two materials in carrying a load parallel to their longitudinal axes. It may also be defined by the value of forces transmitted from one material to the other at their interface. The relation between the horizontal load and horizontal slip can help define the shear-bond strength. The shear-bond strength has three components, chemical adhesion, friction and mechanical interlock. The chemical adhesion component arises due to chemical bond action between the cement in the concrete and the surface of the steel sheeting. The friction component depends on the normal stress and the coefficient of friction once chemical adhesion has failed. In profiled composite structures, the mechanical interlock component depends on the embossments and the re-entrant (if present) portion's geometry. The factors that may affect the capacity of the mechanical interlock component will be studied throughout this work.

Mechanical interlock provides the shear connection required for the efficient structural combination between steel profile and concrete. The idea is to prevent slip and vertical separation at the steel-concrete interface and to achieve the composite action.

Mechanical interlock is generally achieved by:

1. Embossments projecting from the sides of the profiled steel ribs into the concrete, or indentations in the web or flange of the steel profile.
2. The re-entrant shape of the steel profile, which can lock the concrete into the steel profile.

The use of end anchors is another way of transferring shear forces between the steel profile and concrete, and limiting the longitudinal slip and preventing the uplift at the interface of the steel sheet and concrete. The headed stud and the shot-fired shear connectors are the most common types of end anchor.

1.6 Composite structures using profiled steel sheeting

Composite structures using profiled steel sheeting may be classified as profiled composite slabs, profiled composite walls, profiled composite beams and profiled composite columns.

Profiled composite floor slabs have been in use since the early 1950s in the USA. But their use in the UK has become widespread. The use of such sheeting as permanent formwork is not new, but its additional function as tensile reinforcement has only been fully developed in recent years (Evans and Wright, 1988)[5].

Some form of interlocking devices provide the composite action between the profiled steel sheeting and the concrete. These devices must be capable of resisting the horizontal shear as well as preventing the vertical separation at the steel concrete interface. Some profiled steel sheets rely mainly on their shape to ensure composite action, for example re-entrant forms as shown in Figure 1.7 and 1.8. Previously, there were profiles that used transverse wires welded to the upper flanges of the profiled steel sheeting to achieve composite action. However, currently, the most common method of achieving reasonable composite action is by rolling or pressing fixed patterns of embossments into the surface of trapezoidal shaped profiled steel sheeting, which increasingly may incorporate a re-entrant feature.

The behaviour of the steel concrete interface is very complex. So, for the design of composite slabs failing in shear-bond (incomplete composite action), most codes depend on empirical formulae obtained from a regression analysis of full-scale test results. The design formula has two empirical parameters (as m and k, used in BS5950 Part: 4, 1994)[6] for each profiled steel sheeting geometry with the same type of shear-connection device. Alternatively, in Eurocode 4[7], partial shear connection theory is employed in addition to the m&k method.

To date, there are a few numerical studies modelling the embossments as shear-connecting devices, the profiled steel sheeting as tensile reinforcement and the concrete slab in compression. These numerical models together with a finite element (F.E.) procedure may be used to study and understand the behaviour of the composite slab. This work uses these procedures to model full scale, and small-scale tests which

have been carried out together with a study of embossment behaviour with and without a concrete slab.

1.7 Advantages of composite structures

The main advantages of adopting composite floors with steel deck in building may be summarised by Mathys, 1987 [8], Wright and Evans, 1987 [9], and Zubair, 1987 [4], as follows:

The steel deck supports loads during construction and protects people working below and acts as a working platform for workmen, construction equipment, and possibly a storage area for construction materials.

Steel decks are light, pre-fabricated elements that are easily transported and act as a tensile reinforcement in sagging moment region once the concrete has hardened also accommodates electrical, communication, and air distribution ducts.

The use of decks reduces slab thickness and construction loads. This can in turn result in savings in foundation, beam, and column costs. Also construction periods are reduced. When panels are fixed in place they can act as an effective in-plane bracing.

Adequate fire resistance may be insured by the use of supplementary reinforcement.

Furthermore, there are certain other factors, which should be noted:

The surface of the steel deck should be protected from damage on site or during storage. Sheets are galvanized to protect them during transport, storage and as resistance to corrosive conditions which may be experienced in buildings.

1.8 The use of composite structures

Composite slabs are often used in the following types of buildings:

- Multi-storey car parks.
- Industrial buildings.
- Office buildings.
- Commercial buildings.
- Hospitals.
- Housing.

- Renovation of existing buildings.

1.9 Composite behaviour

In 1982, the BS 5950:Part 4:1982[10] was introduced to cover the design of composite floors with steel decking. However, there was no British Standards at that time, which covered the design of composite beams with steel decks or the fire resistance of composite floor slabs. In 1992, Eurocode 4[11] Part 1.1 was issued to cover the design of composite steel and concrete structures.

As defined in Eurocode 4 Part 1.1 clause 7.1.2.2, composite behaviour is that which occurs after a floor slab comprising profiled steel sheet, plus any additional reinforcement, and hardened concrete have combined to form a single structural element. The profiled steel sheet shall be capable of transmitting horizontal shear at the interface between the sheet and the concrete, pure bond between steel sheeting and concrete is not considered effective for composite action.

Ideal composite action between the steel and concrete occurs only when:

There is no strain discontinuity at the interface; that is, there should be no relative movement or slip between the two materials in the direction parallel to the interface.

There is no separation.

If these two conditions are satisfied, it is achieved complete interaction. If one-condition is not fulfilled, partial interaction may exist. In the case where there is no connection between the two materials, it is said to have zero interaction.

1.10 Scope of the problem investigated in this thesis

Shear-bond in composite construction is the primary important factor that may affect the mode of failure and ultimate capacities of composite structures. In profiled composite slabs, the shear-bond failure is the predominant mode of failure. The current design codes for composite slabs are based on performance testing of full size slabs. The design equation for the shear-bond capacity according to BS5950: Part 4[6]: 1994 and Eurocode 4[7] is derived from data obtained by means of a performance test series which allows a plot of two parameters, m and k. Unfortunately, these factors do

not have a direct physical meaning. The development of partial shear connection theory does address the actual behaviour in producing a "design" approach to a shear bond capacity based on a shear strength τ_u. The method is described in Appendix B of Eurocode 4.

Some time ago a research project was started at University of Salford to investigate the use of profiled steel sheeting as horizontal formwork and reinforcement to a composite slabs. This pilot test showed that the bond between the steel sheeting and the concrete was a critical aspect in ensuring that the composite slab acted as a fully composite element Duffy and O'Leary[12,13].

It is clear from the above discussion that the shear-bond failure is often the critical mode of failure for composite slabs and this may also be true for any composite structure. So, the higher shear-bond resistance, the greater the capacity of the composite structure considered.

To date, a few studies have been carried out in analysing the behaviour and the function of the embossments and the re-entrant portions in the shear-bond resistance as shear-connecting devices. The aim of this research work to investigate the effect of these shear-connecting devices through experimental and finite element modelling.

To study the effect of embossments and the re-entrant portions in shear-bond resistance, the author has presented small-scale tests. Also, full-scale composite slabs were prepared and tested to investigate the behaviour of composite slabs. The full-scale tests results were analysed according to the m&k method and the partial connection method and comparisons made between the two approaches. Finite element analysis was applied to study the behaviour of composite slabs and the results compared with the experimental results. Amongst other factors, the following were considered:

- Embossments in three dimensions,
- The effect of various embossment/sheet geometries, and boundary conditions.
- Modelling of single and multiple embossments.

1.11 Outline of the thesis

The thesis contains eight chapters with chapter one and two introducing composite slabs with profiled steel sheeting.

A review of the previous work carried out to investigate the shear-bond of composite construction especially for composite slabs and the factors that may affect the shear-bond resistance are presented and discussed in chapter two. Also, the different empirical shear-bond equations proposed and design method for composite slabs are reviewed and discussed.

Chapter three contains a description of push-off and pull-out tests presented by the author. Several samples of profiled steel sheeting were tested. The results of these tests are described and discussed.

Details and results of full-scale composite slabs are given in chapter four. The description of composite slabs are detailed along with presentation and discussion of the results. Using the regression analysis of composite slabs tests results the m&k values were calculated. Also the partial-interaction method was used in predicting the capacity of the composite slab from the test results. Comparisons are made between the two design approaches.

Chapter five includes the finite element methods, advantages of the finite element method, and a review of the ANSYS, with the required data file to run by ANSYS software.

In chapter six, the 'ANSYS' software computer program and proprietary elements, materials models and contact elements are described. This is followed by a description of three-dimensional finite element modelling of composite slabs (small and full scale). The load versus deflection, and load versus slip present a comparison between the numerical analysis and the test results. The finite element analysis of the composite slabs was carried out using contact stiffness from the small-scale tests. Relatively small adjustment of this contact stiffness enabled the failure load of each composite slab to be reproduced fairly accurately, together with close correlation between the experimental and Finite Element Analysis predicted load-deflection relationships and load-slip throughout their entire load histories. The finite element models were based on actual measured material properties.

In chapter seven, three-dimensional finite element modelling of embossments is described. Different parameters for the profiled steel sheeting and concrete have been investigated. The investigation demonstrated how the behaviour of an embossed element may be studied effectively using the modelling approach.

The conclusion of this research work and the recommendations for the future research are given in chapter eight. It indicates the small-tests can give useful information in composite behaviour of the full size slab. Also that finite element modelling is a powerful aid in the development of more efficient profile shapes.

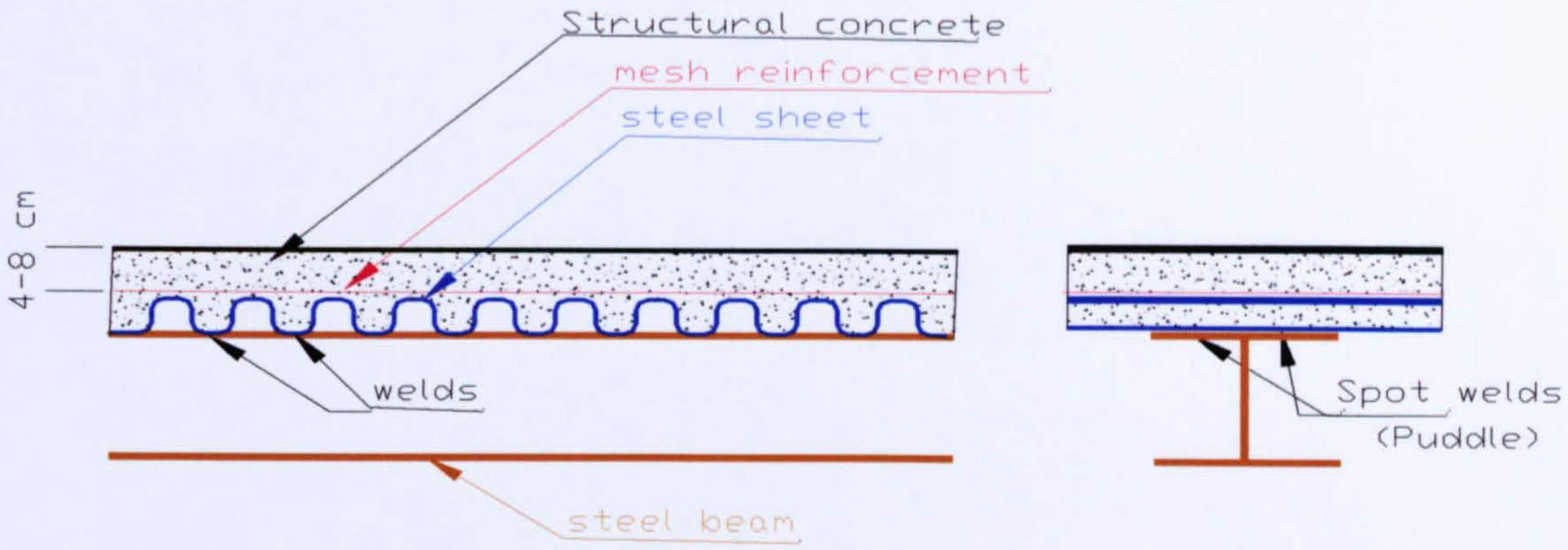

Figure 1.1 Early composite slabs supported by steel beam

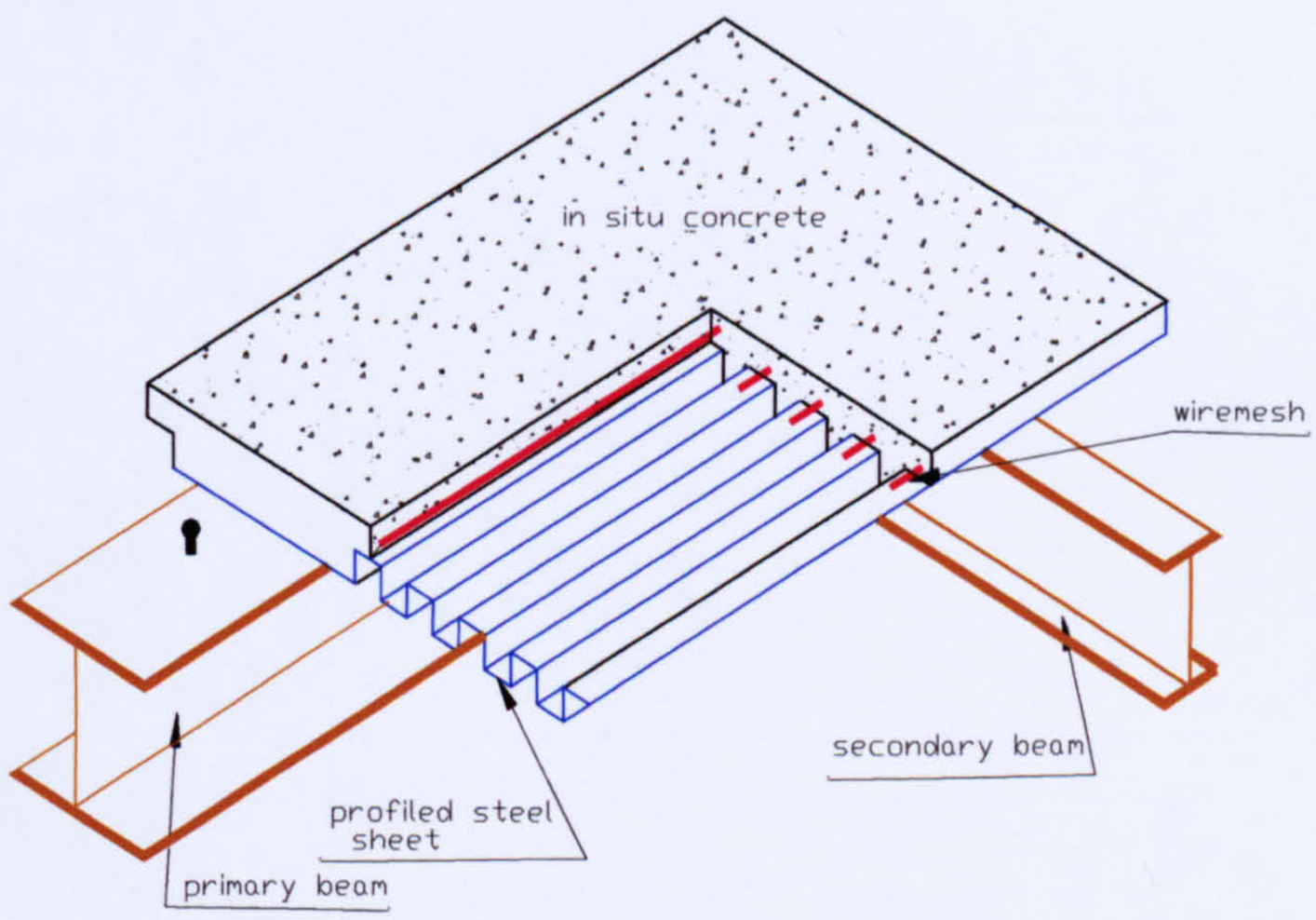

Figure 1.2 Composite slabs supported by composite beams

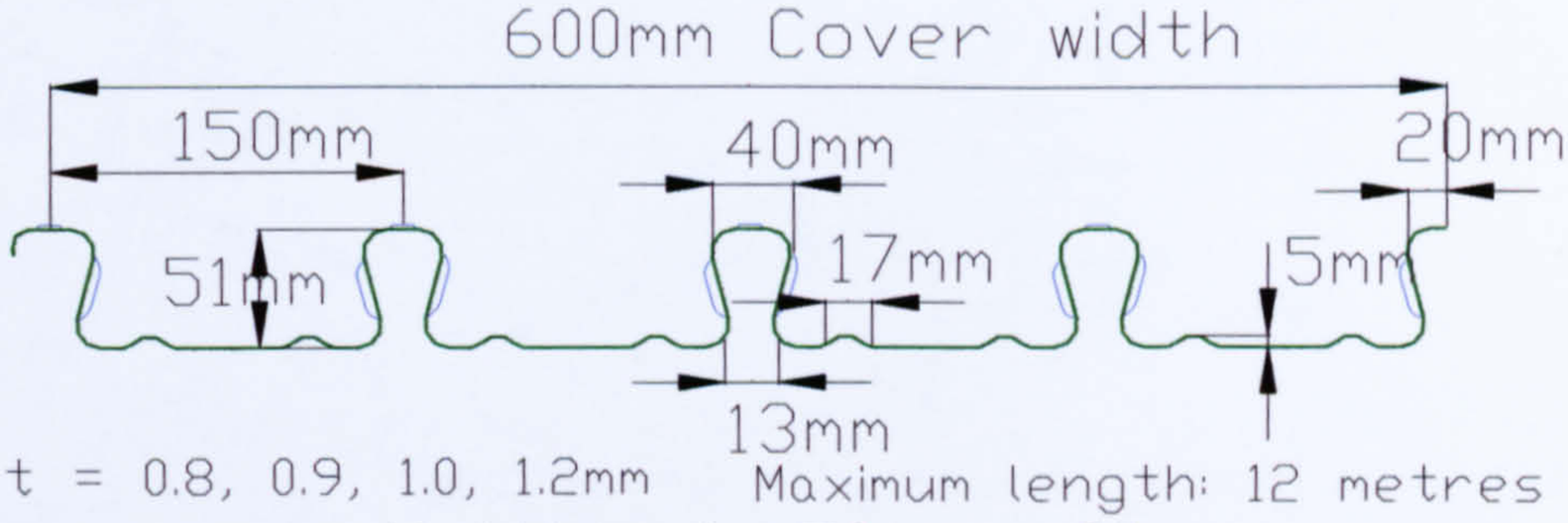

Figure 1.3 Dovetailed (re-entrant) deck profiles

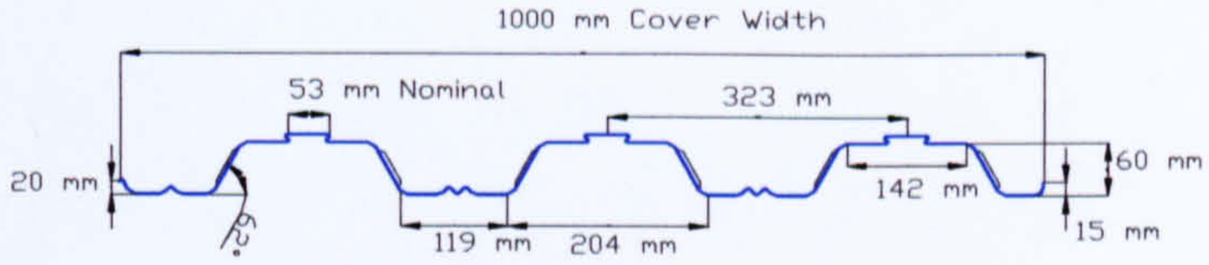

t = 0.9, 1.0, 1.1 & 1.2mm Maximum length: 12 metres

Multideck 60 profile

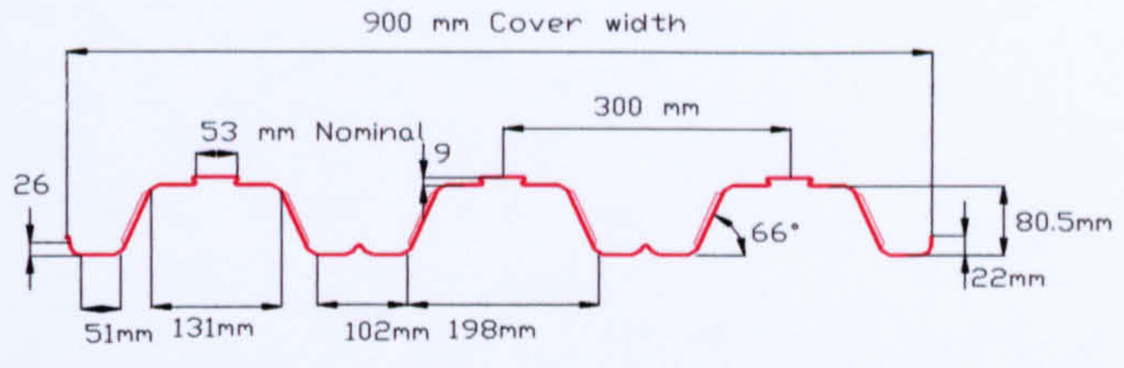

t = 1.2mm Maximum length: 12 metres

Multideck 80 profile

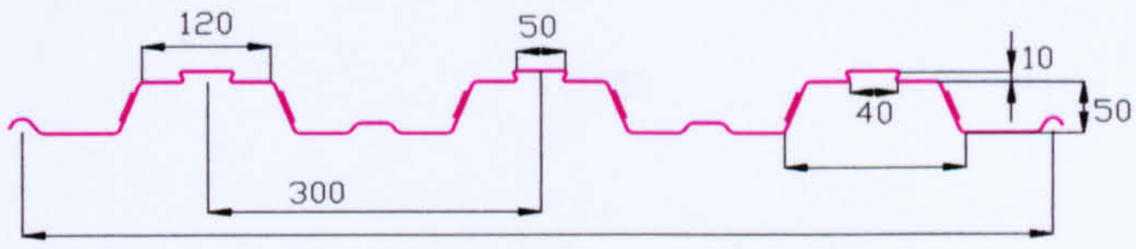

Cover width 900mm

Ribdeck AL Z35

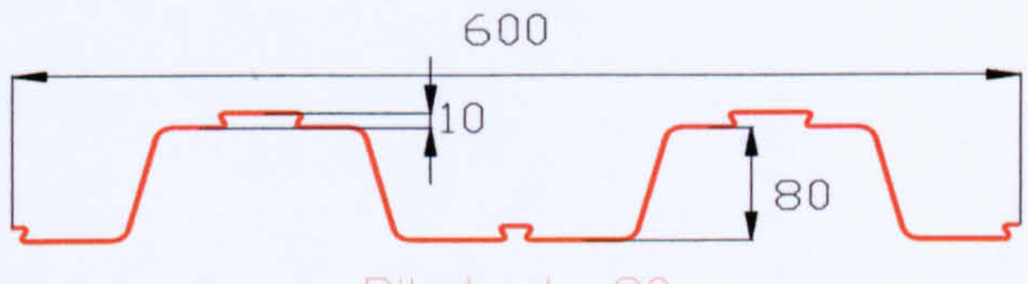

Ribdeck 80

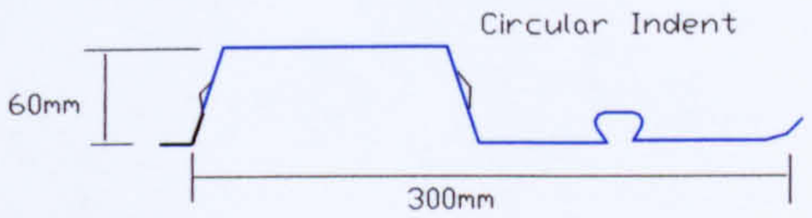

Ribdeck 60

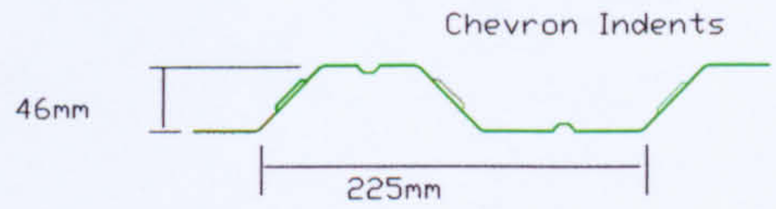

PMF.CF46

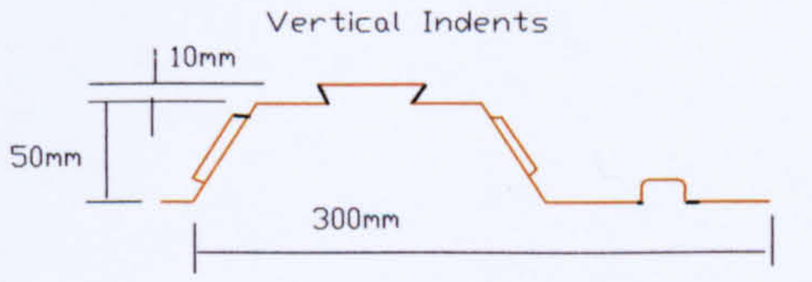

Alphalok

PMF.CF60

Figure 1.4. Trapezoidal deck profiles

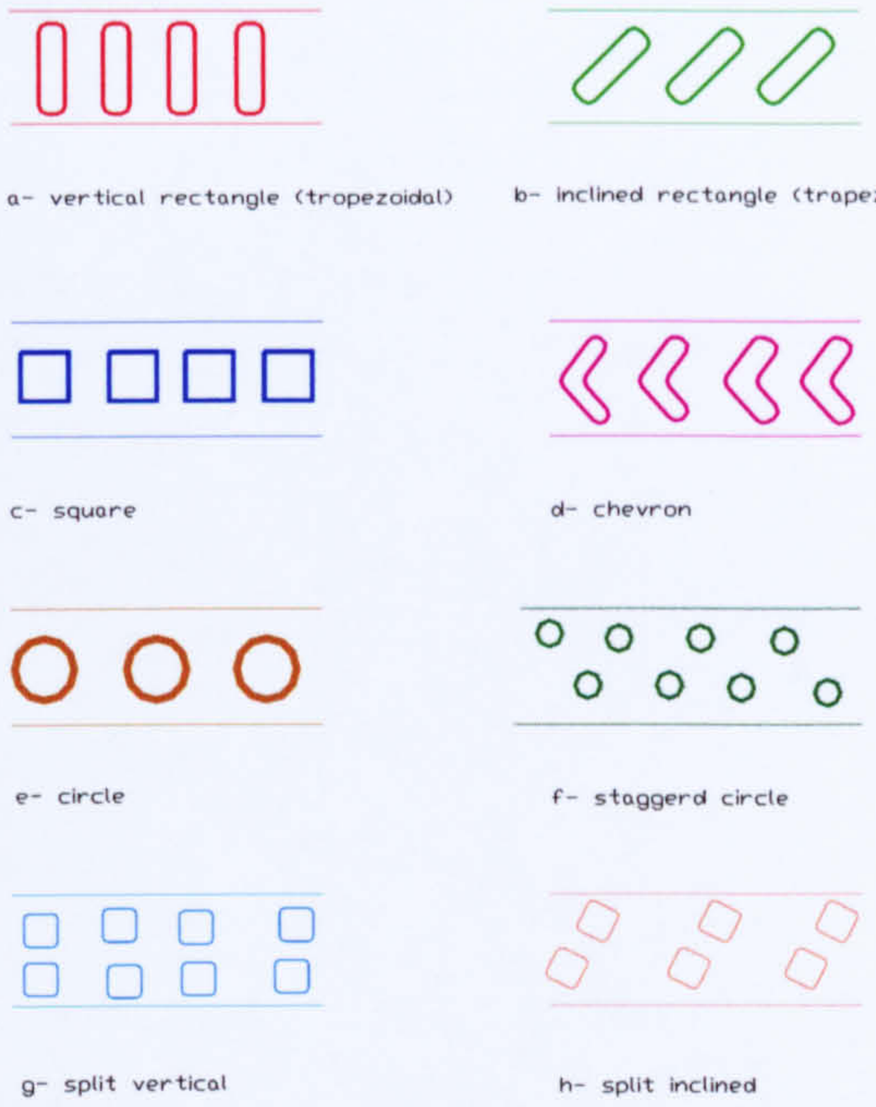

Figure 1.5 Shapes of embossment in the web

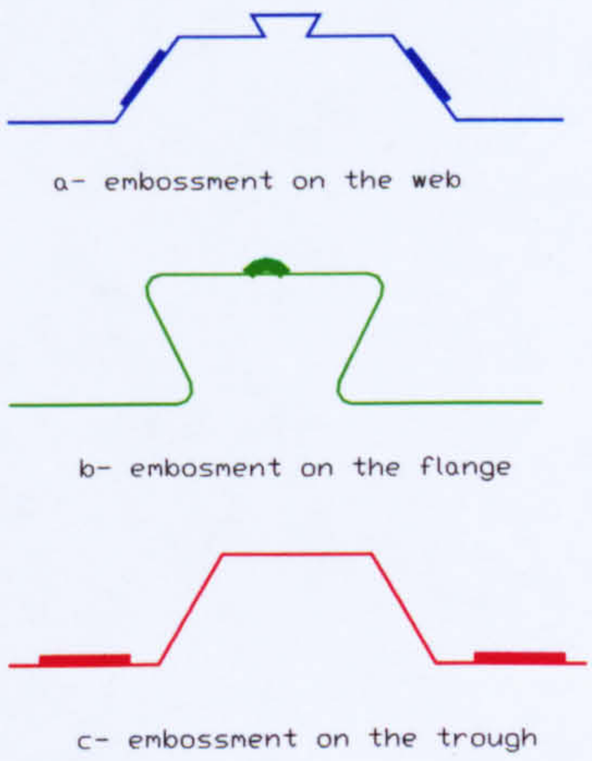

Figure 1.6 Position of embossments

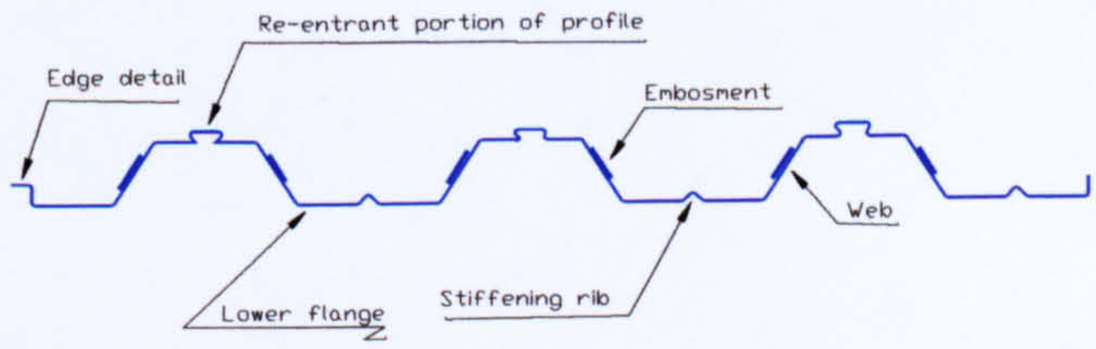

Figure1.7 Typical hybrid deck with re-entrant portions

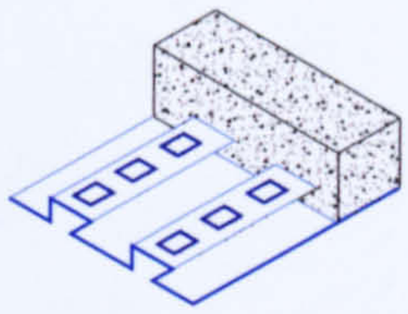

a- Embossments

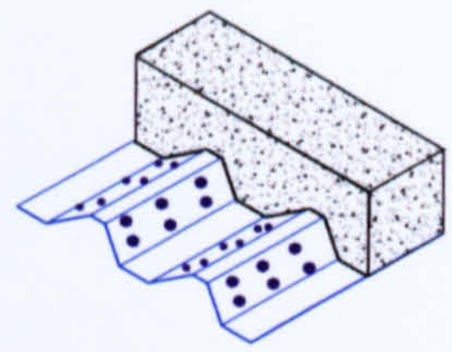

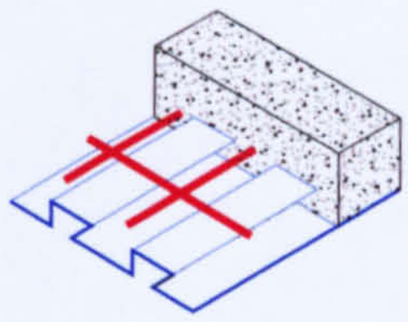

b- Welded wires

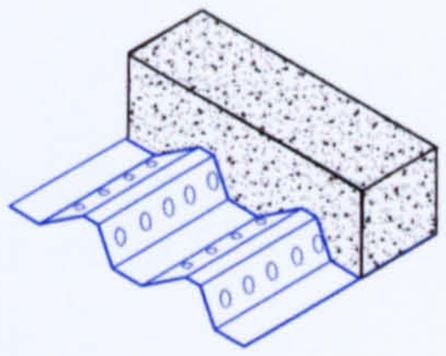

c- Holes

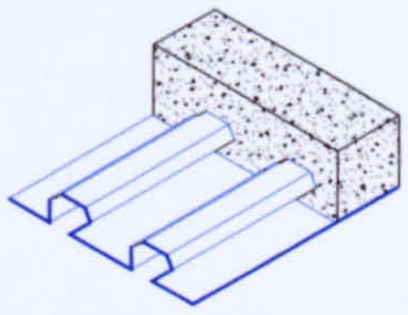

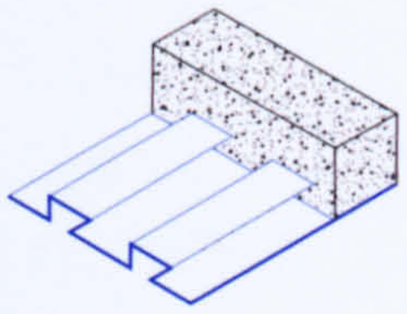

d- Re-entrant form

Figure 1.8 Forms of shear connection in composite slabs

Chapter Two

Shear-Bond in Composite Construction

2.1 Introduction

Shear-bond behaviour is a critical factor in the design of composite sections. For composite construction comprising thin gauge steel sheeting and concrete, the shear bond strength is much lower than for conventional reinforced concrete or composite hot rolled section/concrete slab construction. This is because the reinforcement in reinforced concrete members is more constrained from slip displacement by the solid cross section and full encasement of the concrete. In composite hot rolled steel section and concrete slab construction, the shear-stud connectors are also encased and provide strong mechanical interlock.

This chapter contains a general review of shear-bond strength in conventional reinforced concrete and composite construction. Also, it contains a detailed review of shear bond equations for profiled composite slabs for which there are similarities and differences with shear bond behaviour in the more well known form of composite. The two most often used design methods for composite slabs; namely the m-k method and the partial connection method, are reviewed and compared.

2.2 Bond in conventional reinforced concrete

Bond stress in conventional reinforced concrete is generally taken to mean the transferring of force from the steel bar to the surrounding concrete and vice versa. This bond results from chemical adhesion, friction and mechanical interaction between concrete and the reinforcing bars.

In general, many complex phenomena influence bond strength for reinforcing bars. Previous researchers (e.g. Naway, 1990[14], Abrishami and Mitchell, 1992[15] and

Cairns, 1994[16]) reported that many parameters may affect in the bond strength of reinforcing bars.

The rib geometry of reinforcing bars may affect the bond strength (Figure 2.1). The transfer of the force between ribbed bar and surrounding concrete is achieved principally by bearing of the ribs on the concrete. The resultant compressive force exerted by the ribs on the concrete is inclined to the bar axis. The radial component of this force creates a ring tension in the concrete cover around the bar. If the tension force generated by bond action exceeds the capacity of the ring, bond failure occurs by splitting of concrete cover. Cairns and Jones, 1995[17], reported that two failure modes may be developed as follows:

1- Splitting failure: when concrete cover is less than approximately three times bar diameter, and

2- Pull-out failure: if the concrete cover is larger or if sufficient confining reinforcement or transverse pressure opposed the splitting force.

Also, Hamad, 1995[18], tested eccentric pull-out specimens with specially machined anchored bars and full-scale beam specimens. The tested rib geometry parameters were rib face angle, rib spacing and rib height. The experimental results showed that the bond strength and bond-slip resistance varied with the rib geometry and concrete strength.

The function of embossments pressed onto the profiled steel sheeting is the same as the lugs or ribs for the reinforcing bars. But the behaviour of embossment is thought to be different[19]. Reinforcing bars are fully encased in the concrete whereas the profiled steel sheeting is in contact with the concrete on one face only. There is little opportunity for ring tension to develop and, as the sheeting is relatively flexible, the embossment may move relative to the concrete. However, the embossments may act to a limited extent as the ribs in the reinforcing bars if they are located on a relatively stiff section of the profile.

2.2.1 Bond for coated reinforcing bars and sheeting.

In recent years, epoxy-coated reinforcing bars have been used in some concrete structures exposed to corrosive conditions. The effect of the epoxy-coating layer in

bond strength has been studied by many researchers (Treece and Ersa, 1989[20], Cleary and Ramirez, 1993[21]). Most of the previous researchers reported that the friction between the concrete and the epoxy-coated bars is less than that between the concrete and un-coated bars. They reported that the reduction in the friction characteristics reduces bond between reinforcement and concrete. However, the difference in behaviour reduces with provision of heavy confining reinforcement or thick concrete cover. Yan and Mindess, 1994[22], from their experimental tests, concluded that under high rate loading, the deficiency of epoxy-coated bars; e.g. the reduction in bond strength, wider crack developed and brittleness, were reduced.

The steel deck sheeting surface is usually galvanised by zinc layer. It is, however, assumed that this will have little effect on mechanical bond. However, the zinc coating layer for galvanised profiled steel sheeting surface may increase the chemical bond[19].

2.2.2 Bond stress-slip relationship

The relationship between the horizontal load and the horizontal slip, occurring at the steel concrete interface, may be considered as a measure of bond strength. The bond stress between a reinforcing bar subjected to pull-out force was characterised, as reported by Gambarova et al, 1989[23], by four different stages (Figure 2.2) as follows:

(a) Stage 1: For small values of the bond stress, bond efficiency is ensured by chemical adhesion, and no bar slip occurs in this stage.

(b) Stage 2: For larger bond stress values, the chemical adhesion breaks, the lugs of the bar induce large bearing stresses in the concrete, transverse micro-cracks start at the tops of the lugs allowing the bar to slip, but the wedging action of the lugs remains limited (bond is assured by bearing action).

(c) Stage 3: For still larger values of bond stress, the first longitudinal cracks form as a result of the increasing wedging action of the lugs, which produces tensile hoop stresses in the surrounding concrete and a confinement action is exerted by the concrete on the bars. The bond stress is assured by bar-to-concrete interlock.

(d) Stage 4: Once the longitudinal cracks (splitting cracks) break out the whole cover and bar spacing, the bond fails abruptly if no transverse reinforcement is provided.

The characteristics of the reinforcing bar at stage 1 are the same as that for steel sheeting in profiled composite structures, where no slip occurs until chemical bond failure. Other stages for profiled composite structures may differ as no concrete cover or transverse reinforcement is provided. However, if the embossments are pressed in parts of the profile of high stiffness, the behaviour of shear-bond may be similar to that of the ribs in reinforcing bars. Typical curves of shear force-slip relationship for profiled composite section are presented in chapter three.

2.2.3 Anchorage length

BS8110: Part 1, 1985[24], assumes a constant bond stress along the anchorage length of a bar. The bond stress is obtained by dividing the force in a bar by the contact area between the concrete and reinforcement (given by the effective bar perimeter multiplied by the effective anchorage length), equation (2.1a). This must not exceed empirical limiting values, equation (2.1b). Thus according to BS8110:

$$f_b = F_s/\pi\phi_e L \qquad (2.1a)$$

$$f_{bu} = \beta\sqrt{f_{cu}} \qquad (2.1b)$$

Where:

f_b is the bond stress;

f_{bu} is the design ultimate anchorage bond stress;

f_{cu} is characteristic cube strength of concrete;

F_s is the force in the bar or group of bars;

L is the anchorage length;

ϕ_e is the effective bar size which, for a single bar is equal to the size and for a group of bars in contact is equal to the diameter of a bar of equal total area; and

β is a coefficient dependent on bar type.

2.3 Composite beams

2.3.1 General

Composite beam construction is taken here to mean the utilisation of hot rolled steel sections with a solid or profiled steel sheet/concrete composite slabs. The general type of connection between steel beams and concrete slabs is the welded shear-stud connector. The popularity of this connector is due to the fact that its strength is the same in all directions and that it is easy to attach by semi-automatic welding through the profiled steel sheeting.

The failure modes of welded stud shear-connectors may be by shearing of the steel stud or by concrete crushing. Such is the complexity of these actions that only empirical design methods have been developed to date.

Push-off tests are the main source of data on the resistance of shear-stud connectors to longitudinal shear.

2.3.2 Composite beams with solid concrete slabs

The characteristic resistance 'Q_k' of a headed stud shear connector with specific properties given by BS5950: Part 3, 1990[25], for composite beams with solid slabs (Fig. 2.3a), is given in a table. A reduction factor for the shear capacity of a stud shear connector is given as follows:

1. For positive moment:

$$Q_p = 0.8Q_k \qquad (2.2a)$$

2. For negative moment:

$$Q_n = 0.6Q_k \qquad (2.2b)$$

Where:

Q_k is characteristic resistance of shear-connector;

Q_n is capacity of shear-connector in negative moment regions;

Q_p is capacity of shear-connector in positive moment regions.

2.3.3 Composite beams with composite concrete slabs

The resistance of shear-studs in composite beams utilising composite concrete slabs (Figs. 2.3b and 2.3c), are influenced by many factors (Lloyd and Wright, 1990[26] and Johnson and Anderson, 1993)[27] as follows:

1- The geometry of the steel sheeting;

2- The direction of the ribs, perpendicular or parallel, to the span of the beam;

3- The mean breadth b and depth D of the profiled steel sheeting;

4- The diameter d and height h of the stud; and

5- The number N of the studs in one trough and their spacing.

6- The load-slip behaviour of a shear-stud connector in a trough or rib of profiled steel sheeting (Figures. 2.3b and 2.3c) is more complex than in a solid concrete slab. So, the shear capacity of the shear-stud connectors may be taken as its capacity in solid slab multiplied by a reduction factor.

7- The reduction factor for a particular shear-stud and profiled steel sheeting with specific dimensions and properties has been explained in: BS5950: Part 3, 1990[25], is as follows:

a- ribs of steel sheeting perpendicular to the beam:

1- for one stud per rib:

$$k = 0.85(b_r / D_p)\{(h / D_p - 1\} \le 1 \qquad (2.3a)$$

2 - for two studs per rib:

$$k = 0.6(b_r / D_p)\{(h / D_p - 1\} \le 0.8 \qquad (2.3b)$$

3- for three or more studs per rib:

$$k = 0.5(b_r / D_p - 1)\{(h / D_p - 1\} \le 0.6 \qquad (2.3c)$$

b- ribs of steel sheeting parallel to the beam:

1- when $b_r / D_p \le 1.5$:

$$k=1 \qquad (2.4a)$$

2- when $b_r / D_p < 1.5$:

$$k = 0.6(b_r / D_p)\{(h / D_p - 1\} \le 1 \qquad (2.4b)$$

where:

b_r is the breadth of the concrete rib;

D_p is the overall depth of the steel sheeting;

h is the overall height of the shear-stud; and

k is a reduction factor.

The height of the embossments and local bending stiffness of the steel sheeting are small compared to those of the shear-stud connectors and the steel beams in composite beams. The efficiency of the embossments as shear-connecting devices for profiled composite structures is not readily identifiable and therefore forms an important part of this work.

2.4 Profiled composite slabs

2.4.1 General

Most of composite slabs tested by earlier researchers failed under shear-bond failure. Hence the better the shear bond, the higher the load carrying capacity of these composite slabs.

Wright and Evans, 1987[9], discussed the factors that may affect the shear-bond of composite slabs as:

(1) The profile of the decking:

Profiles with large thin flange and web plates may exhibit lateral flexibility under load and distort sufficiently to break or reduce the mechanical connection of the embossments.

(2) The thickness of the steel sheet:

Although the thickness of the steel will influence flexibility of the constituent plates of a profile allowing uplifting, thinner sheets are easier to emboss and are, therefore, more likely to have a more satisfactory shear-bond capacity.

(3) The geometry of embossments:

The mechanical grip of the concrete around an embossment will be affected by the size and especially the height of the embossment.

(4) The shear span:

The length of the slab over which shear forces develop is dependent upon the load type and slab span.

(5) The quality of concrete:

The mechanical bond between concrete and steel depends upon the type, compaction and strength of the concrete.

Expanding this list to describe further the factors that may affect shear-bond leads to the following:

(1) The geometry and mechanical properties of the steel sheeting:

Moment of inertia

Depth of web

Re-entrant portions and stiffeners, and,

Yield strength of the steel

(2) Embossment geometry:

Shapes of embossments

Height of embossments

Surface area of embossments, Eccentricities of the centre of the embossment from the surface and the neutral axis of the steel sheeting (Figure 2.4), and angle of attack (defined in Figure 2.5).

(3) Geometry and mechanical properties of concrete:

Maximum and minimum depth of concrete; and

Compressive and tensile strength of concrete.

(4) The surface coating of steel deck sheeting.

This is not normally a factor where galvanized steel sheeting is used.

2.4.2 Design criteria and failure modes

The resistance of a composite slab shall be sufficient to withstand the design loads and to ensure that no ultimate limit state is reached, based on one of the following modes of failure and as shown in figure 2.6.a Considering a simply-supported composite slab, with two line loads perpendicular to the ribs, the failure can occur in three different sections, as follows:

1. Critical section I.

Flexure: bending resistance $M_{p\cdot Rd}$.

Flexural failure occurs when the plastic capacity of the slab is reached. This is possible if the resistance for the longitudinal shear transfer in the shear span is large enough to allow yielding of the entire cross section of the sheeting; i.e. full interaction is assumed at the critical cross section. Further, a certain amount of rotation capacity is required in order to reach the maximum flexural capacities.

A suspicion that a reduction of mechanical interlocking due to large strains in the sheeting exists is based on experimental evidence that the final failure of a composite slab is always caused by horizontal slip, even if the flexural resistance has been reached. This means that although the bending moment does not increase, the failure is finally caused by strains reducing the shear resistance.

This section can be critical if there is complete shear connection at the interface between the sheet and the concrete. In other words, it means the bond provides full interaction. The failure in this case is flexural.

2. Critical section II.

Longitudinal shear: longitudinal shear resistance $V_{l.Rd}$.

Failure in longitudinal shear is indicated by relative movement (end slip) between the sheeting and the concrete at the end of the test specimen at a load lower than the load which would cause flexural bending failure.

Longitudinal shear failure occurs if the shear span is not sufficiently long for the mechanical interlocking strength to develop the plastic resistance as defined above.

The resistance of shear connection determines the maximum load on the slab. The ultimate moment of resistance $M_{p.Rd}$ at section I cannot be reached. This is defined as partial shear connection and results in a longitudinal shear or shear bond failure.

3. Critical section III.

Vertical and punching shear: vertical shear resistance $V_{v.Rd}$ exceeded.

Vertical shear failure rarely occurs but may appear if a large concentrated force is applied to a composite slab. To a large extent the understanding of this failure mode is related to the shear strength of the concrete.

This section will be critical only in special cases, for example in deep slabs or short spans with loads of relatively large magnitude when a vertical shear failure occurs.

Figure 2.6.b shows the three different modes of failure, for composite slabs. $\frac{V_t}{b.d_p}$ is plotted against $\frac{A_p}{b.L_s}$.

where:

V_t = Experimental shear force

b = slab width, in mm

d_p = distance from the top of the slab to the centroid of the effective area of the steel sheeting, in mm

A_p = effective cross – section area of the decking, in mm^2

L_s = shear span length, in mm

2.4.3 Ductility

Ductility is the ability of a member to continue to deform while maintaining its load-carrying capacity. According to Eurocode 4 for composite slabs it is defined as follows:

From the load-deflection curve recorded from tests, the behaviour is classified as ductile if the failure load exceeds the load causing first recorded end slip by more than 10%. The maximum load is taken as that at a mid-span deflection of L/50. Otherwise the behaviour is classified as brittle.

Figure 2.6.c shows two main failure modes: brittle and ductile behaviour. The load applied is plotted against the midspan deflection. At the beginning of the test, the behaviour of both types of slab (brittle and ductile) is similar. The chemical, friction and mechanical interlocks are not destroyed and the composite slab acts as a homogeneous material. No significant slip occurs between the concrete and the steel sheeting. As the load increases, the stiffness of the slab decreases because of cracks in the concrete tensile area, and the horizontal shear force increases between the bearing and the point load.

When the chemical bond breaks, the first slip occurs between the steel decking and the concrete, which may induce a decrease in the load. Then only the friction and mechanical interlock supports the longitudinal shear. Any decrease in the load is directly dependent on the quality of the mechanical bond provided by the shape of steel decking.

In summary, the two modes are apparent:

- Brittle behaviour is characterised by a significant decrease in load. Moreover the load will never attain its maximum value again. This behaviour is due to the fact that the mechanical interlock is not able to ensure bond greater than the chemical bond and failure occurs by longitudinal shear.
- For ductile behaviour the load increases to a greater value than the first slip load. Thus, the mechanical interlock can provide greater bond effect than the chemical bond. The slab can then collapse either by flexure (full connection) or by longitudinal shear (partial interaction).

2.4.4 Propped and unpropped construction

Composite slabs may be designed and constructed as propped or unpropped.

In propped construction, the steel sheet is supported at intervals along its length until the concrete has reached a certain proportion, usually three-quarters, of its design strength. The whole of the dead load is then assumed to be resisted by the composite member.

When no props are used, it is assumed in elastic analysis that the steel sheet alone resists its own weight and that of the concrete slab. Other dead loads, which can be determined quite accurately from known dimensions of the structure and densities of materials, such as floor finishes and internal walls, are added later. It is assumed that these are carried by the composite member.

2.4.4.1 Temporary supports (propped)

Normally unpropped construction is preferred as it can speed erection and allow other aspects of construction to continue with less restriction. However, where safe span or construction limits would otherwise be exceeded, temporary supports should be

provided to the profiled steel sheeting until the concrete has reached an adequate strength to avoid exceeding the capacity of the profiled steel sheets under the loading of wet concrete and construction loads. Propped construction should also be used to reduce the deflection of the profiled steel sheeting, where the deflection limits would otherwise be exceeded.

Where temporary supports are used, the effects of their use and subsequent removal on the distribution of shear forces in the composite slab should be allowed for in the design of both the supporting and the supported slabs. The method of providing temporary supports should be chosen to suit the conditions on site. Normally, one of the following should be used:

a) Temporary props from beneath;

b) Temporary beams at the soffit of the sheets.

Alternative methods may be used where suitable but, in all cases, the temporary support should be capable of carrying all the loads and forces imposed on it without undue deflection.

2.4.4.2 Deflection during construction (unpropped)

Commonly, to increase the speed of construction, profiled steel sheeting is not propped during construction. The sheeting alone must then carry the weight of wet concrete, operatives and tools. The profiled steel sheeting is subjected mainly to bending and shear. Compression due to bending of the profile arises in the flanges and the web and may give rise to buckling of the thin walled steel profile. High shear occurs near the supports. In many cases the construction condition, rather than composite state, controls the design of the sheeting.

At the time of construction, deflection of the profiled sheet under loads of self-weight and wet concrete must not exceed a limiting value.

For example, in Eurocode 4, this limit is L/180 or 20 mm, where L is the span of the sheet between supports. In the case of propped profiled sheets, props are considered as rigid supports. The use (or not) of props affects the serviceability performance of the composite slab and this is reflected in manufacturer's tables.

At the ultimate limit state the shear bond resistance for the propped case has to resist the entire self weight of the slab together with the applied loads. This is considered the worst case by the codes of practice and it is therefore specified for the tests that the profiled steel sheeting is propped during casting. For a slab with full interaction and ductile behaviour, the flexural capacity is unaffected by the previous loading history.

2.5 Design methods

Several methods for the design of a composite slab exist due mainly to the fact that the failure mechanism is complex and poorly understood. A comparison of design methods and a method based on global plastic analysis was presented by Wright and Evans[28]. The backgrounds of recently established design methods are presented in Easterling[29], Patrick[30], and Bode and Sauerborn[31], and still the discussion of the design methods is on going, Patrick and Bridge[32], Bode et al[33].

2.5.1 The 'm-k' method

The 'm-k' method is still a broadly accepted method for longitudinal shear design in USA[29] and in European national codes, as well as in Eurocode 4[7].

The empirical design method, the m-k method, which is developed by Schuster, Porter, and Ekberg is based on at least two groups of three full-scale tests. Figure 2.7 shows the results of the two groups indicated by regions A and B. From each group, the characteristic value is deemed to be the one obtained by taking the minimum value of the group reduced by 10%. The design relationship is formed by the straight line, the so called "regression line", through these characteristic values for groups A and B. As shown in figure 2.7, the intersect value at the vertical axis represents the k-factor, in N/mm^2, and the slope of the regression line represents the m-factor, in N/mm^2.

The maximum design vertical shear resistance $V_{l.Rd}$ for a width of slab b, according to EC4, is calculated as follows:

$$V_{l.Rd} = V_{l.k} / \gamma_{vs} \qquad (2.5)$$

$$= b \cdot d_p [(m \cdot A_p / b \cdot L_s) + k] / \gamma_{vs} \quad (2.5)$$

Where:

m & k: experimentally determined factors.

Ap : effective cross - sectional area of the decking, in mm^2

Ls : shear span length, in mm

b : slab width, in mm

d_p : distance from the top of the slab to the centroid of the effective area of the steel sheeting, in mm.

γ_{vs} : partial safety coefficient, normally taken as 1.25

For the effective area A_p of the steel sheeting the area of embossments and indentations in the sheet should be neglected, unless it is shown by tests that a larger area is effective (clause 7.6.1.2(2) Eurocode 4 part 1.1)[7].

The m-k method does not have a definite physical representation and cannot be related directly to the shear bond. The two factors do not have a direct physical significance; they are simply empirical constants used in the determination of shear bond capacity. The method of evaluation of test data is the same; whether the failure is brittle or ductile.

For composite slabs with reinforcement the m-k procedure requires extra analysis to allow for the presence of the reinforcing bars. The capacity of the reinforced concrete slab alone is determined which is then used to determined the contribution of the composite slab to the ultimate shear obtained in the test (see section 4.16 and Appendix B).

The shear span length Ls to be taken for design, is defined as follows:

1. L/4 for a uniformly distributed load applied to the entire span length as shown below.
2. The distance between the applied load and the nearest support for two equal and symmetrically placed loads.
3. For other loading arrangements, the shear span length is determined by an approximate calculation similar to the following:

In the case of the uniformly distributed load the shear span L_s is determined by equating the area of the shear force diagram for the uniformly distributed load to that for the two points load. Referring to Figure 2.8:

A uniformly distributed load leads to the shear force diagram for case 1:

$$\text{Area 1} = 0.5\ V\ (L/2)$$

$$= VL/4$$

Whereas in the shear force diagram for two line loads, case 2:

$$\text{Area 2} = VL_s$$

Equating Area 1 to Area 2:

$$VL/4 = VL_s$$

and thus:

$$L_s = L/4$$

where

L is the effective span of composite slab;

Ls is the shear span of composite slab;

V is the point load.

2.5.2 The partial shear connection method

2.5.2.1 General

The partial connection strength method, derived primarily for composite beams[34,35], has been suggested as an appropriate method for the design of composite slabs failing in longitudinal shear. Currently, two variants of the partial connection method exist. One, which is proposed in Eurocode 4[7], was developed by J.BW Stark and H.Bode together with their collaborators, and the other was developed by Patrick 1994[36]. The importance of friction developed at the support between sheeting and concrete was first recognized by Patrick 1990[30]. Eurocode 4[7] allows the designer to use an alternative design method, the partial shear connection method, which was further developed by Bode, Sauerborn, and Minas,[33] after earlier work by Stark[37]. In this method, the shear resistance of the connection is also determined by using full-scale experiments. In order to use the partial shear connection method, the behaviour of composite slab should be ductile as defined by Eurocode 4.

Applying partial connection theory to composite slabs with ductile behaviour has the advantage that the method follows the same principles of partial connection design for

composite beams with flexible connectors. It has the further advantage, that the same mechanical model is used to evaluate slab tests, to determine the longitudinal shear strength and to carry out design calculations. In the Eurocode 4 theory, the longitudinal shear resistance $\tau_{u,}$ which is assumed to act uniformly over the entire concrete/steel sheet interface, is determined from a series of full-scale tests. This value is then used to determine design values for composite slabs using the procedures described later.

The partial connection method may be used to account for contributions from end anchorage and additional reinforcement.

During the design of composite beams, the distribution of shear forces in the interface can be manipulated by the number and spacing of shear devices. For composite slabs the shear characteristics of the connection depend on the geometry of the sheeting and the geometry and location of the indentations. They are therefore product properties. Apart from the optional shear devices at the supports, the shear force in the interface is influenced mainly by the length of the shear span, usually the distance between the loads and the supports. A typical condition is shown in Figure 2.8.a. It can be seen that the longitudinal shear τu acts over the shear span Lx leading to the development of a longitudinal force N, the resulting moment Msa (the inertial flexural capacity based on shear) is then compared to the external moment. The distribution of τ in the shear span shown in the figure is the ultimate case where after the development length at the support the distribution is considered uniform in the case of ductile behaviour. In cases where the shear span is large enough to develop the maximum normal force in the sheeting, the shear connection is full, so the bending resistance is critical (flexural failure). If, as shown in Figure 2.8.a, the shear span is smaller, the shear connection is partial, so the longitudinal shear resistance is critical (longitudinal shear failure).

2.5.2.2. Determination of the bending resistance

According to Eurocode 4[7] clause 7.6.1.2, the bending resistance of a composite slab with the neutral axis above the sheeting is calculated as follows:

$$M_{p.Rd} = N_{cf} (d_p - 0.5x) \qquad (2.6)$$

where, $N_{cf} = A_p . f_{yp}/\gamma_{ap}$

A_p is the effective area of the steel sheet in tension. The width of embossments and indentations in the steel should be neglected.

d_p is the distance from the top of the slab to the centroid of the effective area.

x is the depth of the stress block for the concrete, given by

$$x = \frac{N_{cf}}{b(0.85 f_{ck} / \gamma_c)} \qquad (2.7)$$

b is the width of the cross-section considered.

The stress distribution is given in figure 2.9.

If the neutral axis lies in the sheeting (figure 2.10), the bending resistance of a composite slab may be calculated as follows:

$M_{p.Rd} = N_{cf} . z + M_{pr}$ (2.8)

where:

$$Z = h_t - 0.5h_c - e_p + (e_p - e)\frac{N_{cf}}{A_p f_{yp} / \gamma_{ap}} \qquad (2.9)$$

M_{pr} is the reduced plastic moment capacity of the sheeting, given by:

$$M_{pr} = 1.25 M_{pa}(1 - \frac{N_{cf}}{A_p . f_{yp} / \gamma_{ap}}) \qquad (2.10)$$

$N_{cf} = h_c . b (0.85 f_{ck} / \gamma_c)$

M_{pa} is the plastic moment capacity of the effective cross-section of the sheeting.

h_t is the total depth of the slab.

e is the distance from the centroid of the effective area of the steel sheet to underside.

e_p is the distance of the plastic neutral axis of the effective area of the sheeting to its underside.

The tensile force in the sheeting $N_p = \eta . N_{cf}$ equals the concrete compression force N_c. The lever arm between the couple of these forces is z. In case of full connection, i.e., η= 100%, the bending resistance is calculated solely with the couple $N_c = |N_p| = N_{cf}$. If η= 0%, the full bending resistance of composite slab $M_{p.Rd}$ equals the plastic moment capacity M_{pa} of the sheeting. Within the range of 0 ≤ 100%, the force in the

steel sheet and concrete slab is limited by the longitudinal shear resistance in the steel-concrete interface.

Generally, the tensile force does not stress the sheeting to yield and thus the decking is able to carry an additional bending moment $M_{pr.}$

Slab tests are used to determine $\tau_{u,test}$ for the partial connection method. For each type of steel sheet, no less than six tests should are to be carried out on the specimens without additional reinforcement or end anchorage. The test specimens should be chosen so that the test information may be considered as representative for the whole range of the degree of shear connection ($\eta_{test} \leq 1.0$). The span and the slab thickness should be varied so that at least three tests have a value of η between 0.7 and 1.0.

When sufficient knowledge from former tests are available to prove that the behaviour is ductile; the test series may be reduced to three tests each having, a value of η between 0.7 and 1.0 (see Eurocode 4).

2.5.2.3 Determination of the horizontal shear strength $\tau_{u.Rd}$

To determine the design shear strength, the degree of shears connection,$\tau_{test,}$ should be calculated first. To find τ_{test}, a partial interaction diagram is produced by drawing either a straight line between M_{pa} and $M_{p.Rd}$ or more accurately as shown in figure 2.11, by calculating the true relationship between M_{pa} and M_{pRd}.

From the maximum applied loads, the bending moment M_{test} at the critical cross-section I beneath the point load due to the applied load, dead weight of the slab and spreader beams should be determined. By following the path represented by the dotted line (A -- > B -- > C in figure 2.11), a value of η_{test} is known for each test. This value is then used in the following equation to calculate the ultimate shear strength (from the test values), $\tau_{u.test}$:

$$\tau_{u.test} = \frac{\eta_{test}.N_{cf}}{b(L_s + L_o)} \qquad (2.11)$$

where;

L_o is the length of the overhang (limited to 100mm in EC4 to avoid increasing the longitudinal shear resistance from a non-contributing part of the composite slab).

L_s is the shear span.

The characteristic shear strength $\tau_{u.Rk}$ should be taken as the minimum value obtained from all tests reduced by 10%. The design shear strength $\tau_{u.Rk}$ is the characteristic shear strength $\tau_{u.Rd}$ divided by $\gamma_c = 1.25$.

With the design shear strength $\tau_{u.Rd}$ determined, the design partial connection diagram should be determined as shown in Figure 2.12.

In this diagram, the bending resistance M_{Rd} of a cross-section at a distance L_x from the nearer support is plotted against L_x The length for full shear connection L_{sf} is given by:

$$L_{sf} = \frac{N_{cf}}{b.\tau_{u.Rd}} \qquad (2.12)$$

For $L_x \leq L_{sf}$ full shear connection exists, so the bending resistance (flexural failure) is critical.

For $L_x < L_{sf}$ the shear connection is partial, so the longitudinal shear resistance is critical.

2.5.2.4 Extension of partial connection method:

The partial connection method has advantages:

- may be applied to composite slabs with end anchorages.
- may be modified to include additional reinforcing bars, which increase the load carrying capacity.
- may be used within global plastic analysis to determine the ultimate loads of continuous span composite slabs.

In the case of composite slabs with end anchorage, and as explained clearly in Annex E.4 of Eurocode[7] Part 1.1, account may be taken by adding the design strength V_{Id} of the end anchorage as follows:

$$N = b.\ L_x.\ \tau_{u.Rd} + V_{Id} \qquad (2.13)$$

This results in an increase in L_x over a distance of

$-V_{Id} / b.\ \tau_{u.Rd}$ as illustrated in Figure 2.13.

In the case of composite slabs with additional bottom reinforcement, the design partial connection diagram should be modified in accordance with Annex E.5 of Eurocode 4[7] by calculating M_{Rd} as follows (Figure 2.14):

$$M_{Rd} = N_p .z_1 + M_{pr} + N_{as} . z_2 \quad (2.14)$$

where;

$N_p = b.L_x.\tau_{u.Rd}$

$N_{as} = A_s . f_{sk} / \gamma_s$

$z_2 = ds - 0.5x$

$$z_1 = h_t - 0.5x - e_p + (e_p - e)\frac{N_p}{A_p.f_{yp}/\gamma_{ap}}$$

$$x = \frac{N_p + N_{as}}{b(0.85 \times f_{ck}/\gamma_c}$$

$$M_{pr} = 1.25M_{pa}(1 - \frac{N_p}{A_p.f_{yp}/\gamma_{ap}}) \quad (2.15)$$

A_s is the area of fully-anchored bottom reinforcement within width b.

2.6 Mechanical interlock and friction

The importance of friction was first recognized and measured by Patrick[30]. In a somewhat different construction of the test setup and using a simple procedure, friction coefficients were measured at Luleâ[38]. These two parameters, i.e. mechanical interlocking and friction, were considered as sufficient for the prediction of longitudinal shear failure when strain levels in the sheeting are relatively low[39] or when strong longitudinal slip resistance is considered[32]. The performance of the mechanical interlocking of the sheeting, in a variant of the partial connection strength method proposed in EC4, is determined by means of a full scale parametric test. The same tests are used for the statistical evaluation of the m and k values required in the design criterion for the longitudinal shear failure. In addition to the mentioned shear-bond action, an increase of the load bearing capacity of the slabs can be attained by

providing additional end anchorage which is often in the form of welded studs as used in composite beams[40].

A large variety of indentations and sheeting geometry exist on the European market offering different mechanical interlocking performance,[41]. The nominal sheeting area of such sheeting is not fully active and according to the recommendations given in EC4, the whole dimpled sheeting area should be neglected. This is however rather pessimistic for certain sheeting. It is suitable for engineering practice to estimate the effective sheeting area, as proposed in Veljkovic [42].

The mechanical interlocking performance of the sheeting can be determined considering only a small segment of the composite slab,[30,38,41]. In recently published papers[31] results of small scale tests are used in the partial connection strength method developed for possible use in the Australian Standard. Both variants of the partial connection strength method[41,7] require ductile connection performances between sheeting and concrete.

2.7 Numerical modelling

Considerable research into the nature of the shear bond resistance of composite floor decks has been carried out since the 1970s. The latest Code method[2] for deck design still relies upon performance testing of full scale specimens. Various design methods have been proposed[28,31,and 43-48] but all rely upon tests to provide data from which behaviour may be extrapolated. The tests may be full scale or small scale model specimens.

There have been attempts to model the behaviour using numerical analysis[49,50]. This is an extremely complex problem, especially if the individual embossment behaviour is to be modelled. To date, the models produced are not at a stage whereby general design, using them, may be considered.

The aim of the study has been to use experimental data together with a numerical model developed by FEM (Finite Element Method). This provides greater confidence in the numerical model and new insight into the behaviour of composite slabs failing in a ductile longitudinal shear mode.

Also by identifying the critical characteristics which influence shear bond capacities future new profile design can be more effective.

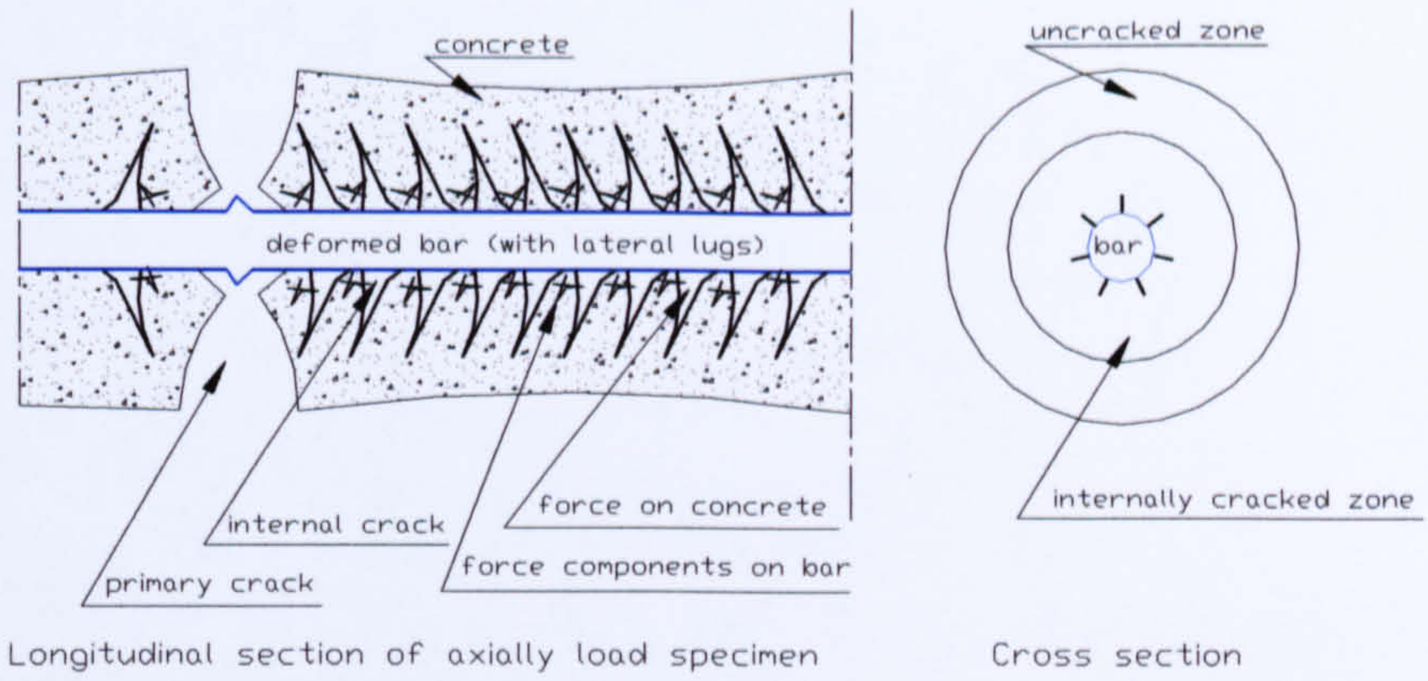

Figure 2.1 Deformation of concrete around reinforcing bars

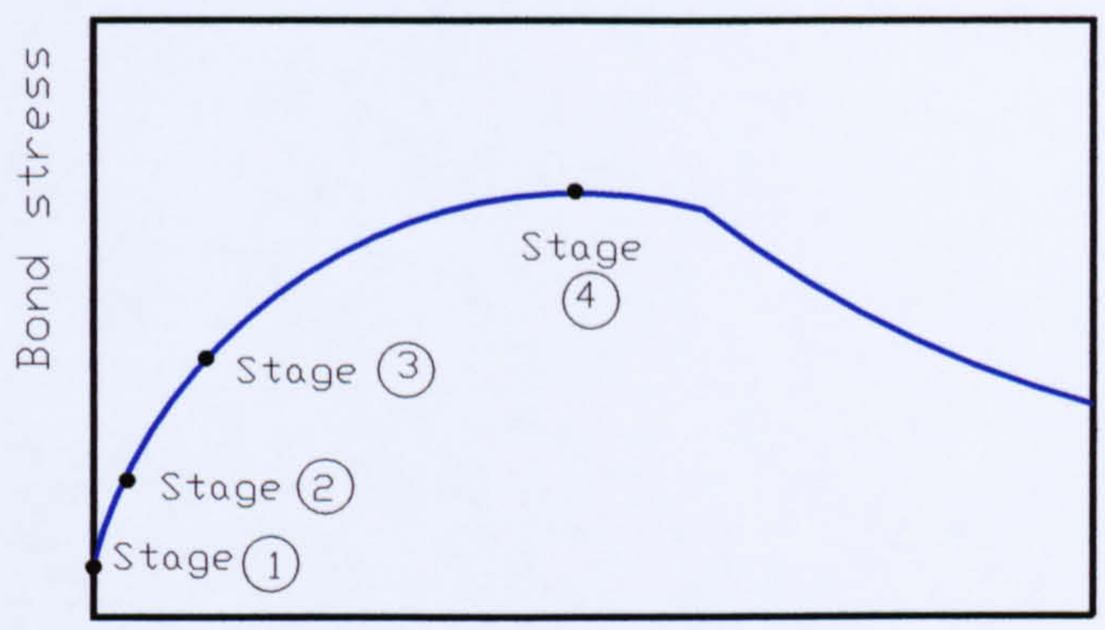

Figure 2.2 Local bond slip.

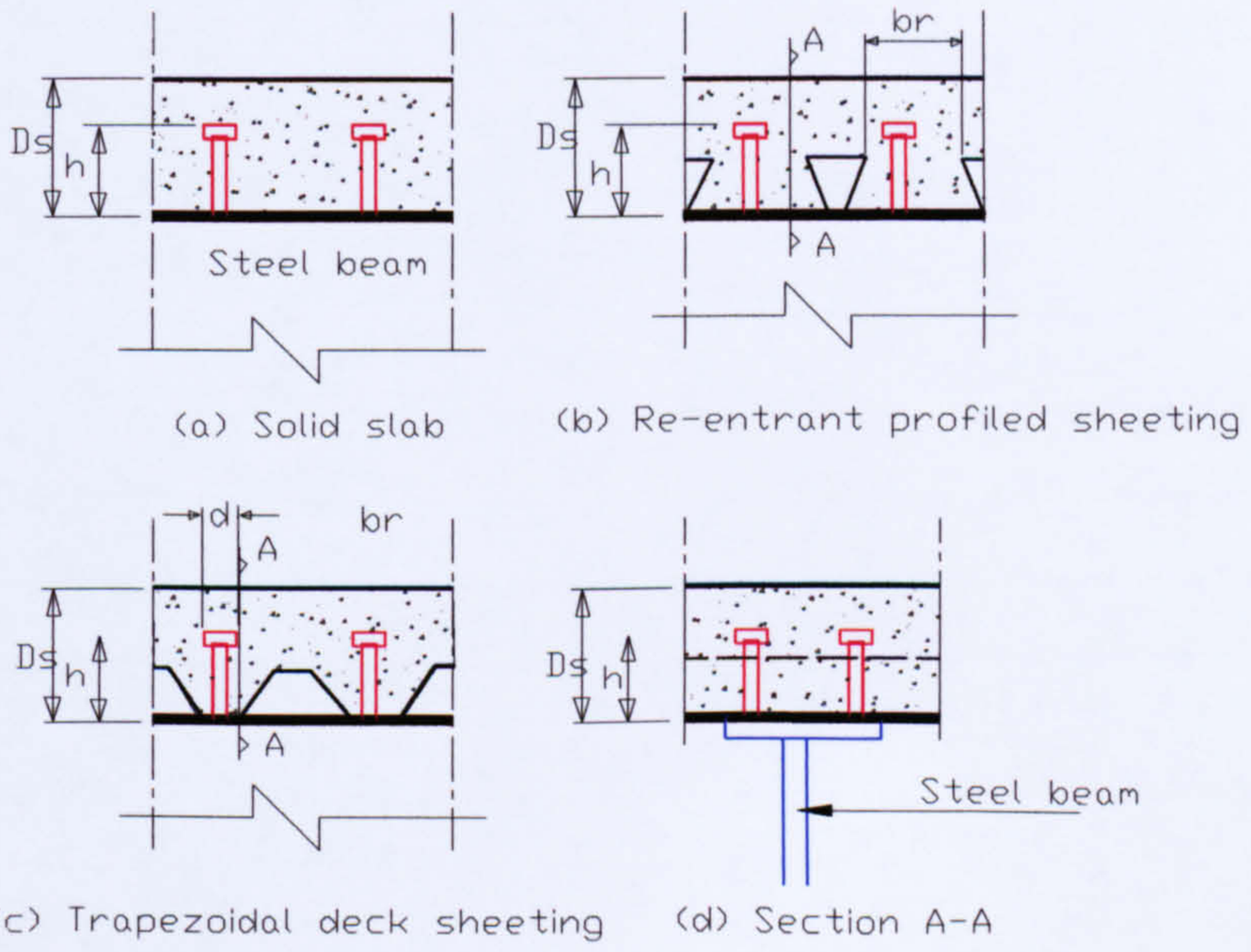

Figure 2.3 Influence of deck profile in composite beams

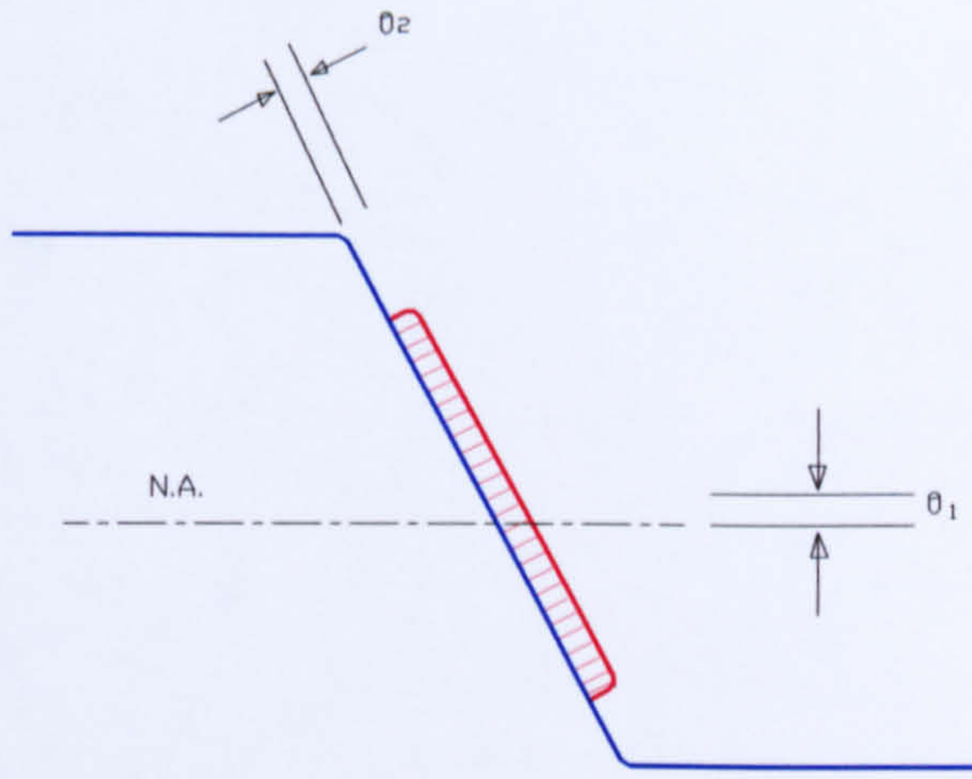

Figure 2.4 Depth of an embossment

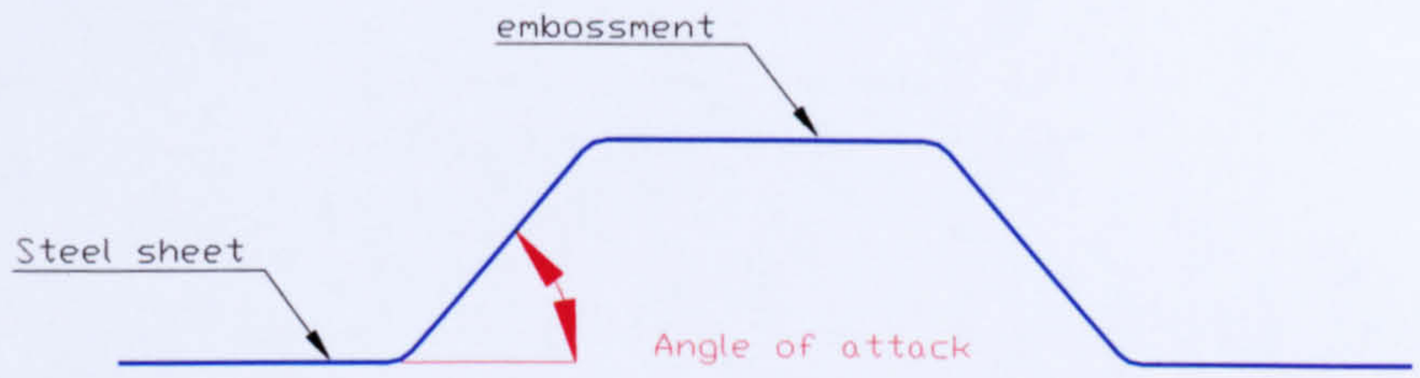

Figure 2.5 Definition angle of attack

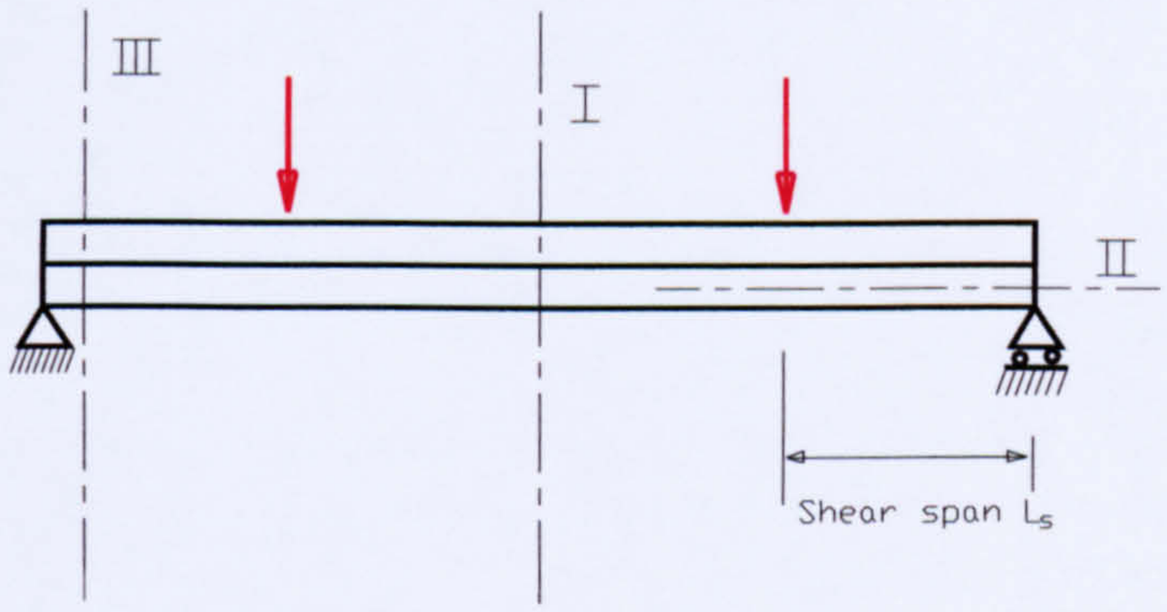

Figure 2.6.a Illustration of possible critical sections

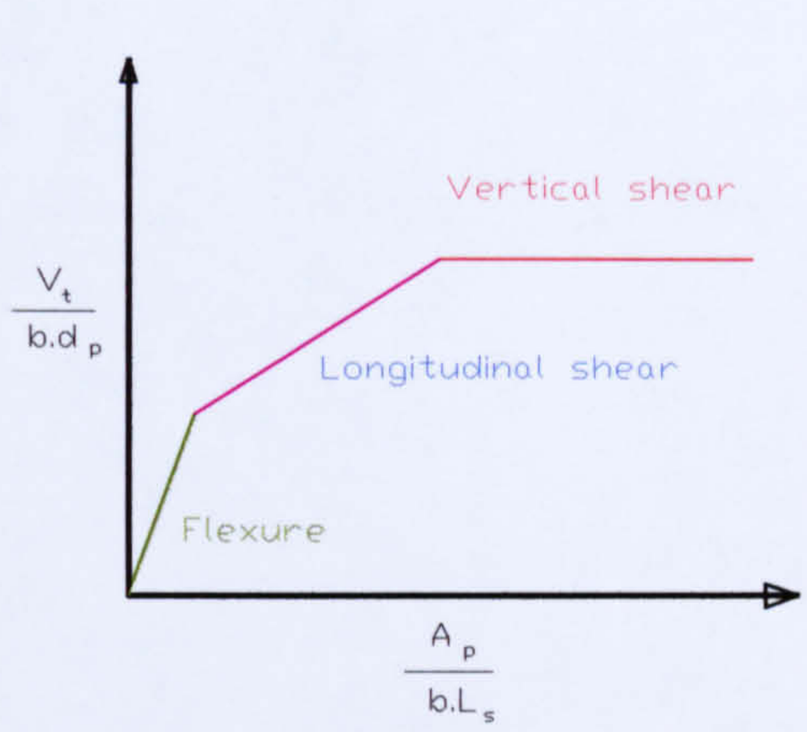

Figure 2.6.b Illustration of possible failure modes

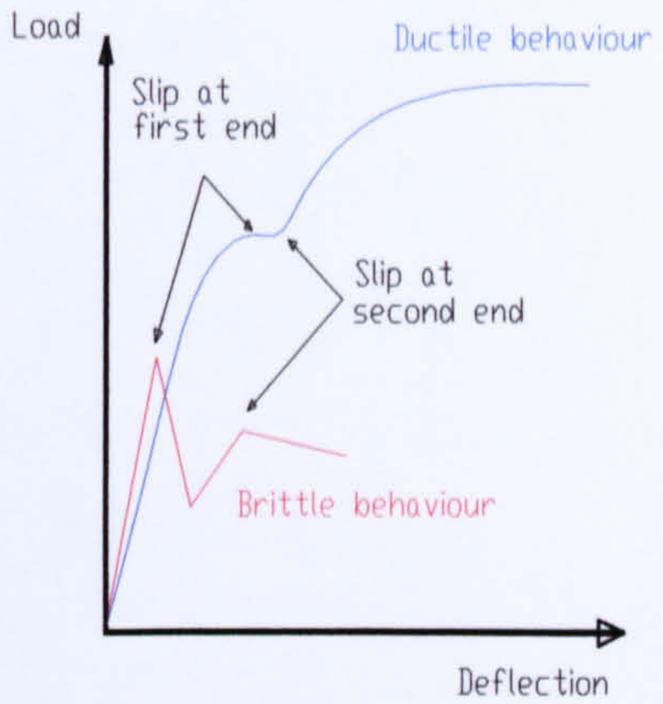

Figure 2.6.c Two typical behaviour mode of composite slabs

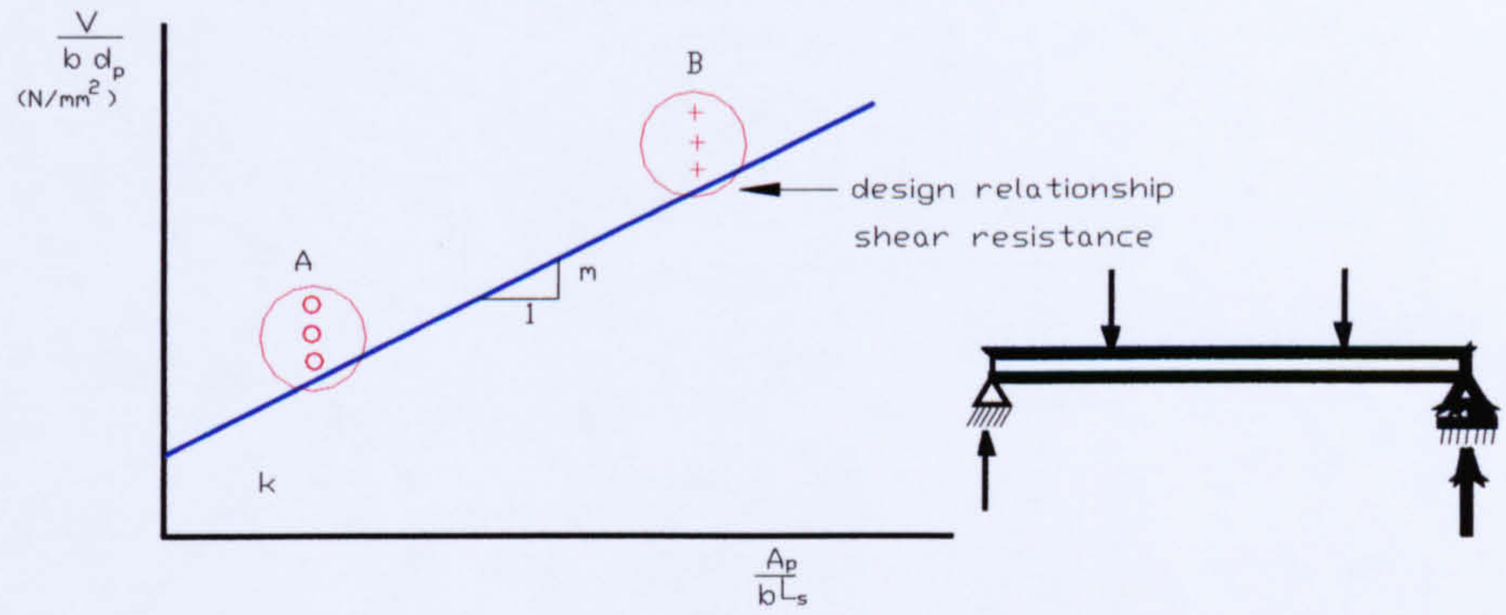

Figure 2.7 Evaluation of test results

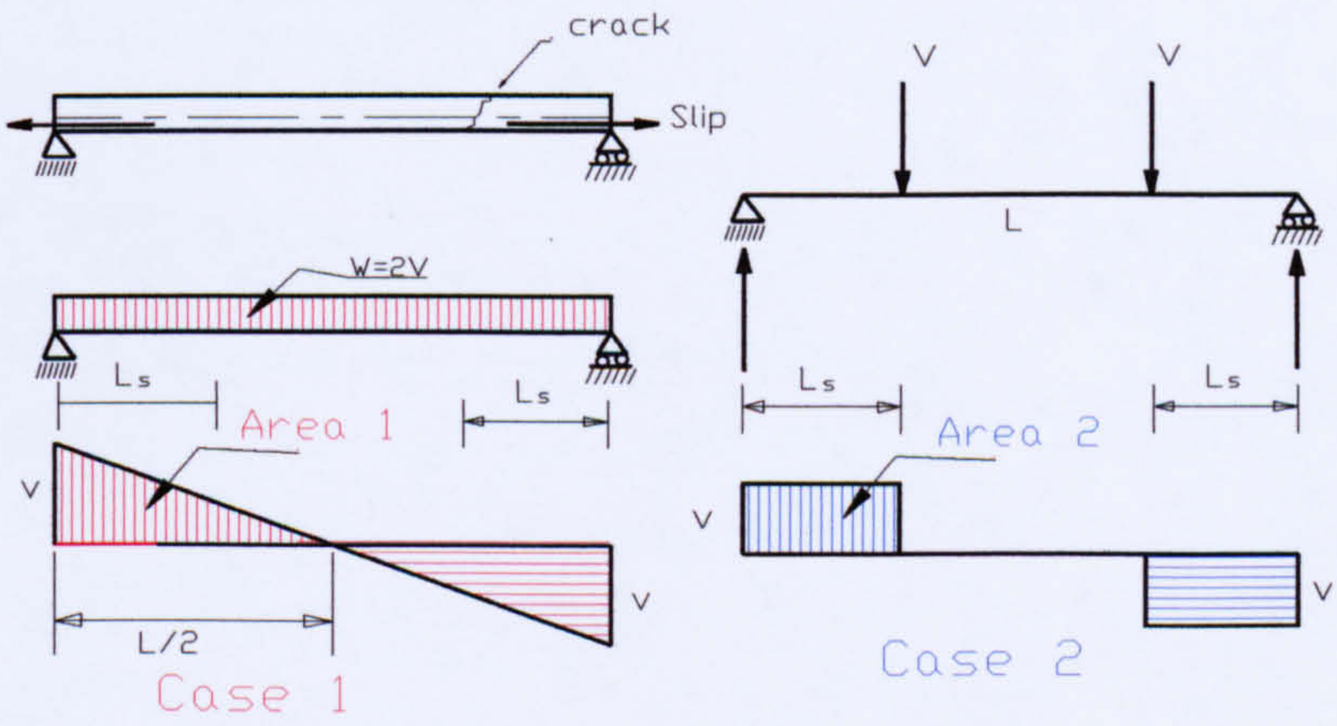

Figure 2.8 Shear span in composite slabs

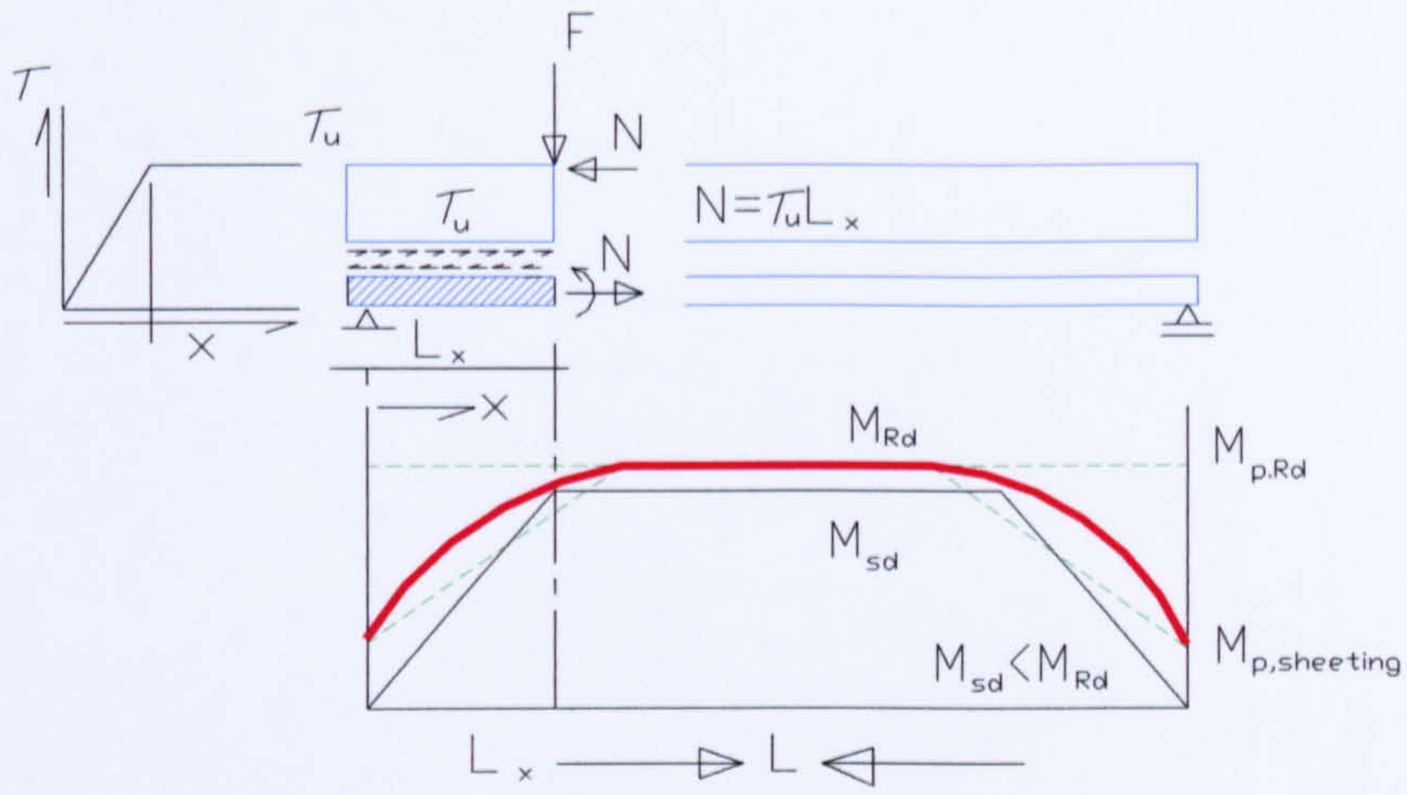

Figure 2.8.a Effective shear span in partial shear connection method

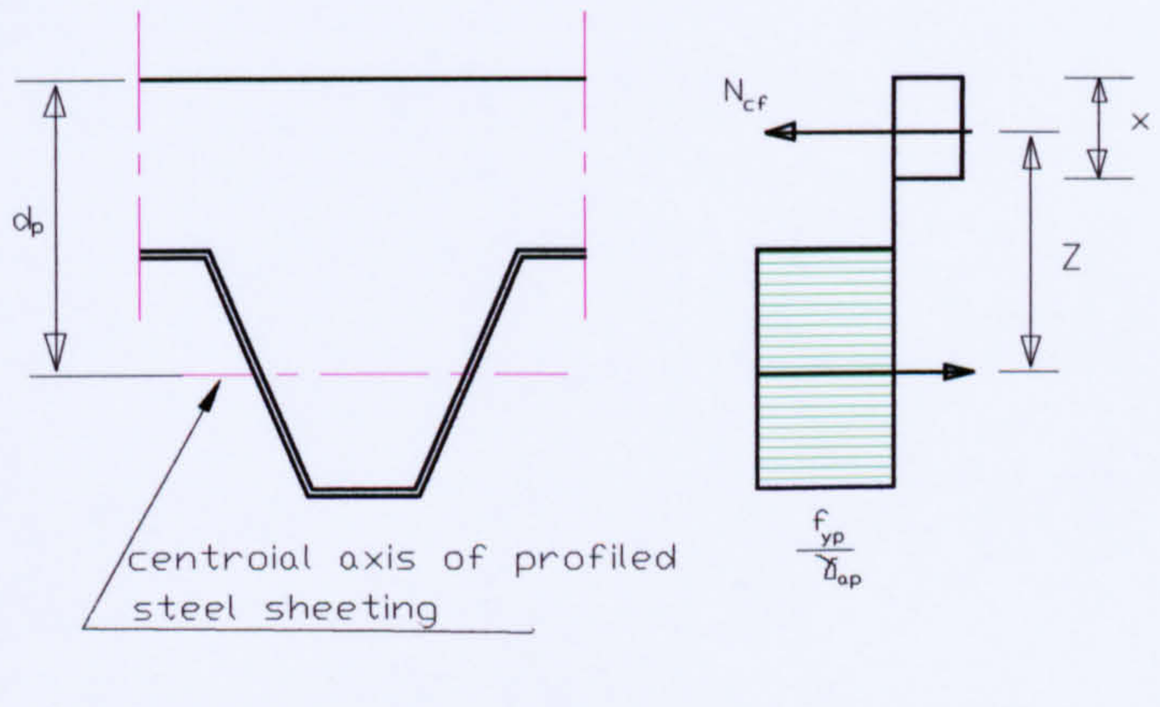

Figure 2.9 Stress distribution for sagging bending if the neutral axis is above the steel sheet

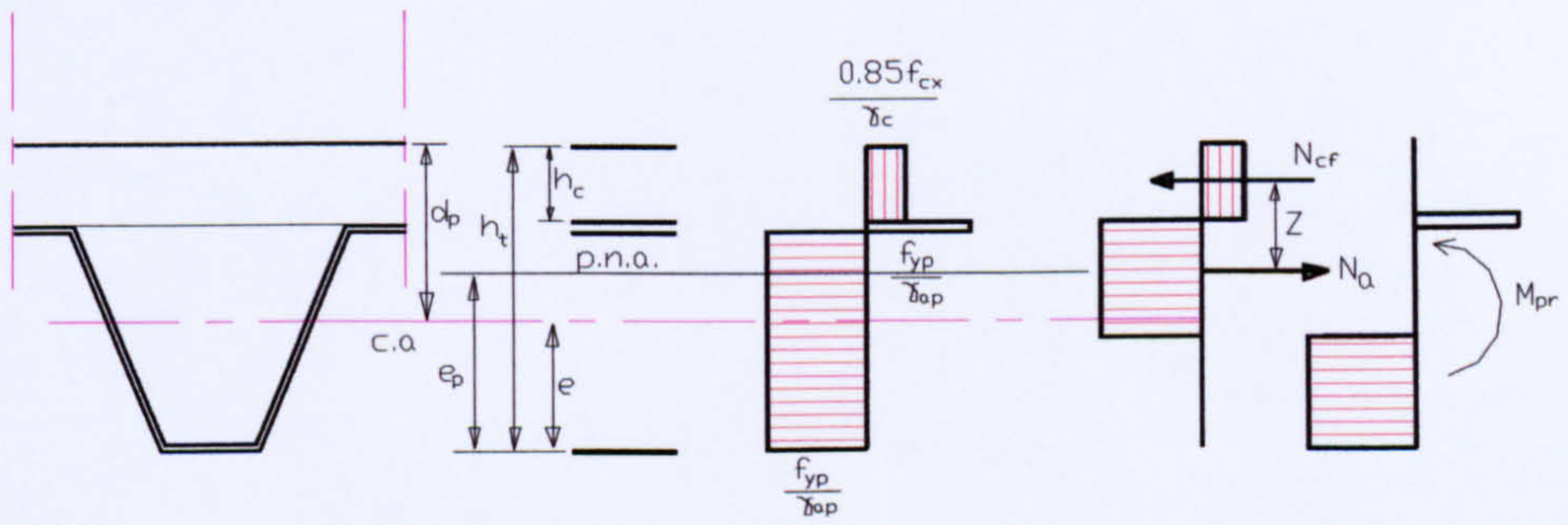

2.10 Stress distribution for sagging bending if the neutral axis is in the steel sheet

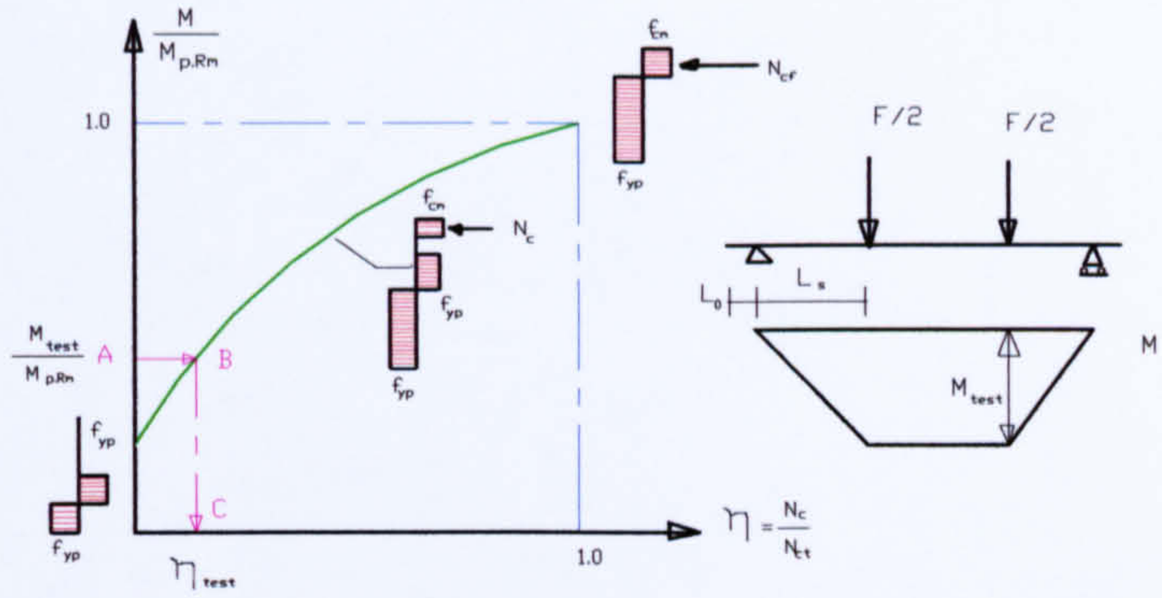

Figure 2.11 Determination of the degree of shear connection from M_{test}

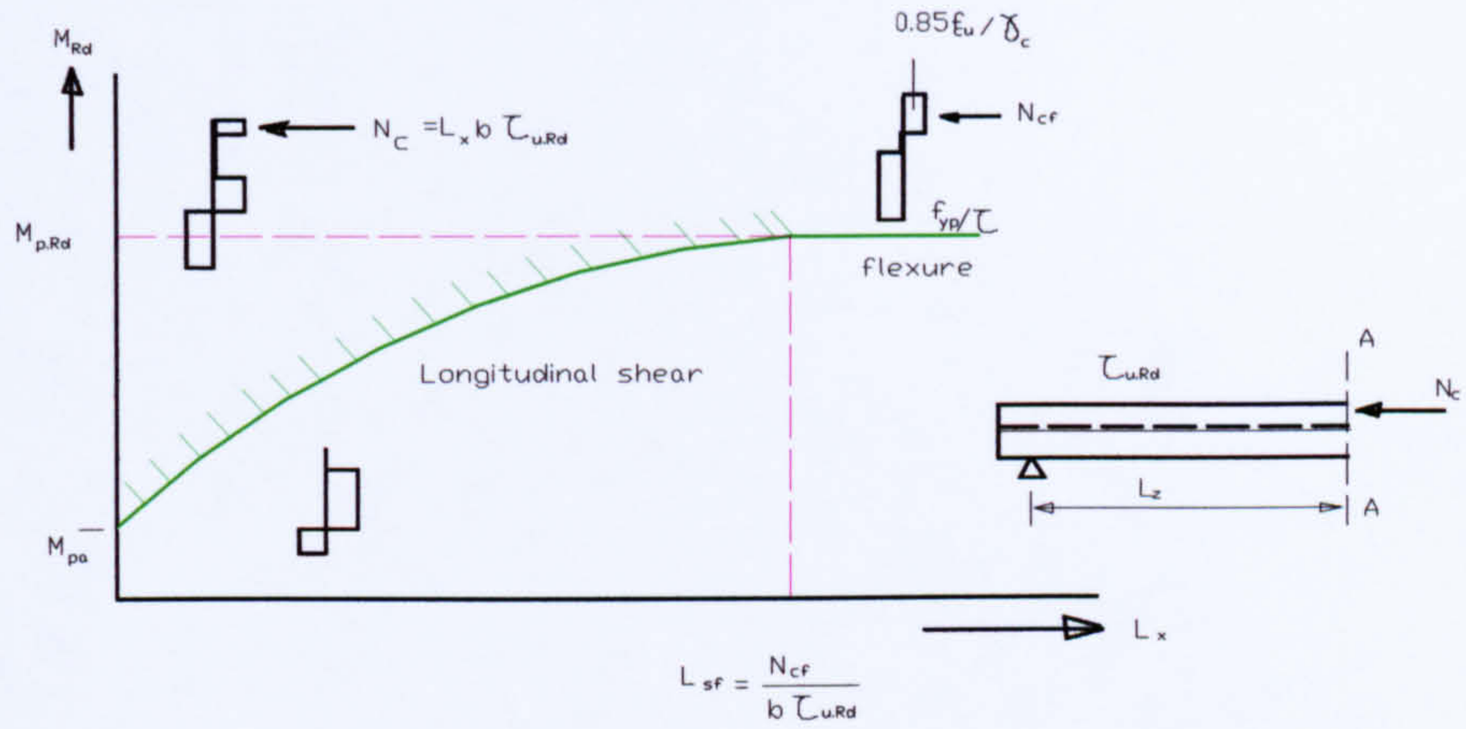

Figure 2.12 Design partial interaction diagram

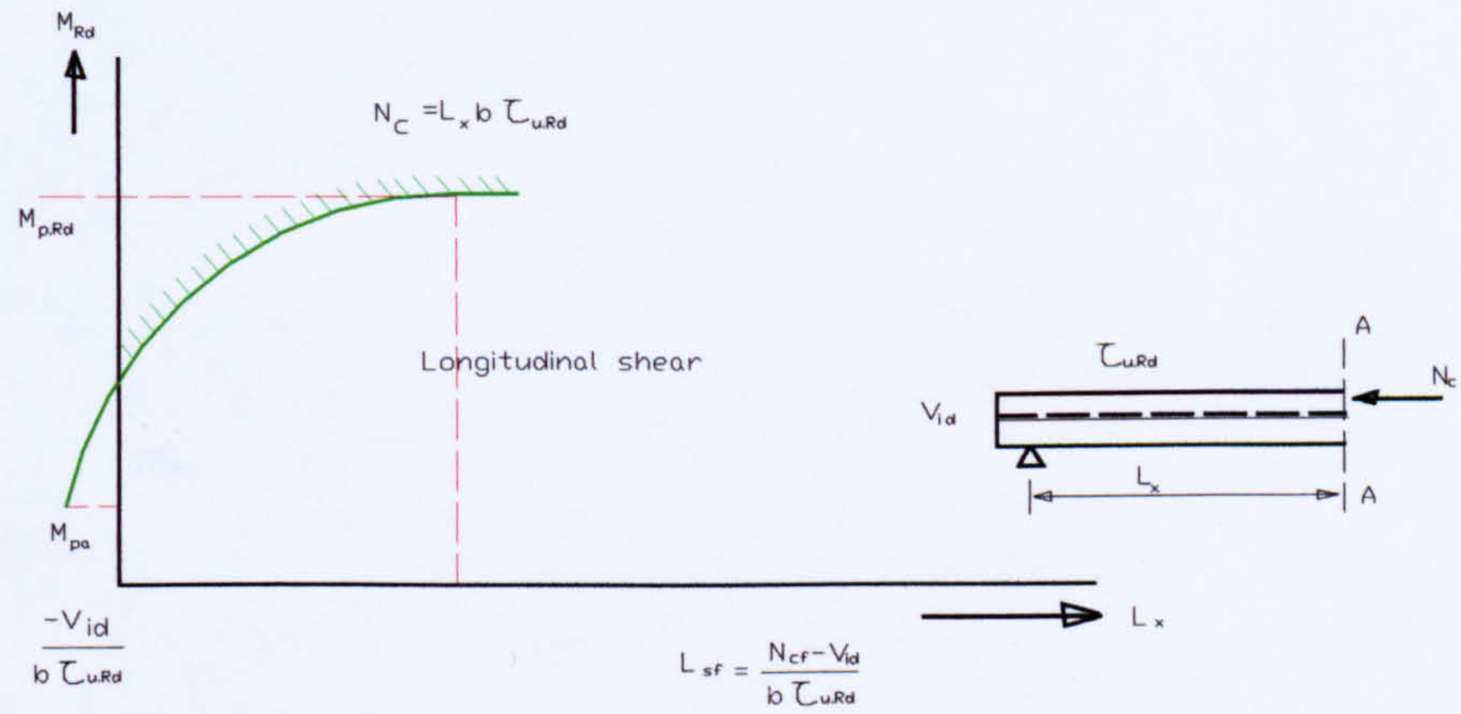

Figure 2.13 Design partial interaction diagram for a slab with end anchorage

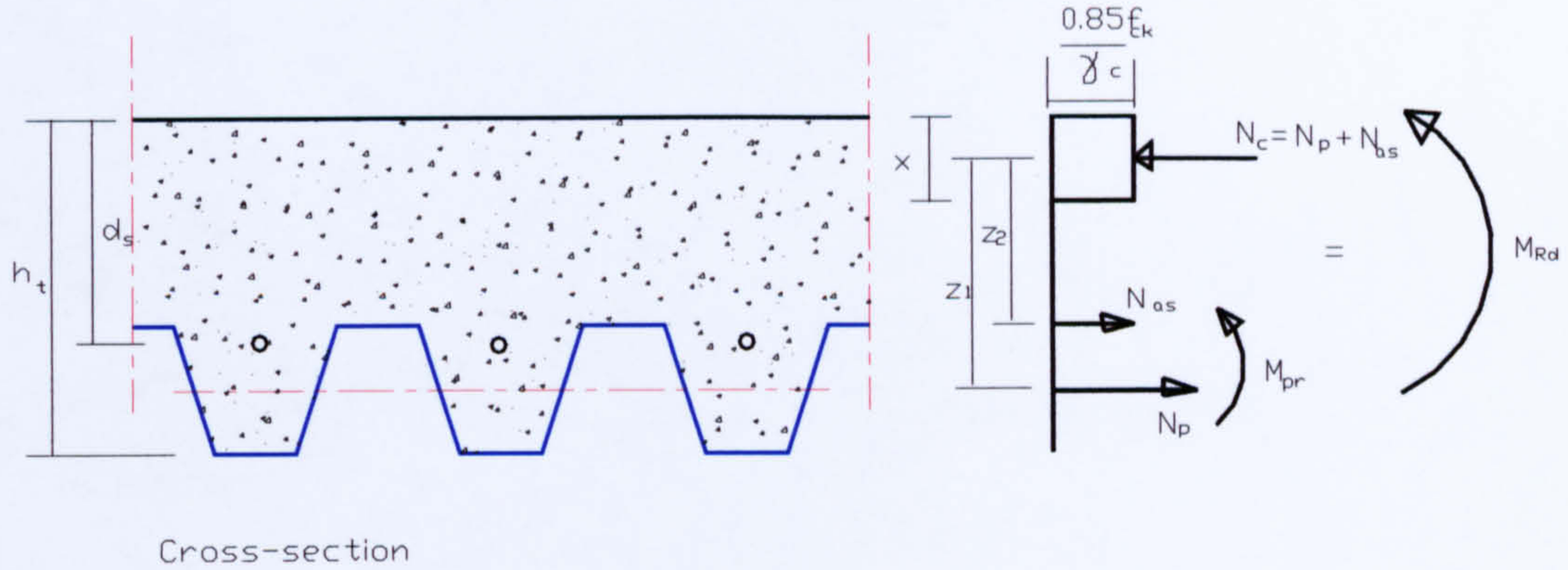

Figure 2.14 Contribution of additional longitudinal reinforcement

Chapter Three

Small Scale Tests

Tests on Composite Slabs to investigate Longitudinal Shear/Slip Behaviour

Summary

The details of control tests are reported whereby a small element of a composite slab is used to simulate the conditions during longitudinal slip failure. Called the 'push-off' or 'pull-out' test, the shear connection performance of a profile may be determined. In these tests after initiating the breakdown of the adhesive bond, a vertical force is applied in addition to the horizontal push or pull force, while continuously measuring the longitudinal slip resistance to determine the values of the horizontal shear capacity of the profile and the coefficient of friction. This information can be used directly in a partial shear connection model to predict the shear bond capacity of composite slabs. The shear transfer between sheeting and concrete depends on various parameters, the influences of these will be considered in this chapter.

The composite action between the profiled steel sheeting and the concrete in a composite slab is ensured by bond stress and mechanical interlock in the shear span and by friction, which is caused by loading and support reactions. To investigate this action, two types of small-scale tests, Push-off and Pull-out tests, were performed. Longitudinal shear-slip, and load-slip behaviour have been studied, and is discussed along with the coefficient of friction.

Based on the experimental results, and the study reported, a FEM simulation was made and described in chapter six.

3.1 Introduction

The concept of testing the shear resistance between concrete and sheeting using small specimens dates back to the seventies. Different testing equipment was used in order to obtain the shear resistance at the contact surface between concrete and sheeting. Small specimens were commonly tested for pure shear by either pulling the sheeting with the specimens placed vertically or pushing the concrete block with the specimens placed horizontally. The small-scale test has been shown to be a very economical way of developing new sheeting profiles, because it provides, of relatively low cost, very useful information about the longitudinal shear properties of the profiled sheeting. The development cost of a new sheeting profile, with optimum characteristics demanded from the producer, could be further reduced by combining the results of a small-scale test with a numerical simulation of the full scale test. Different authors have used the longitudinal shear stress (or horizontal force) - slip relationship obtained from small-scale tests. Two types of small-scale tests, push-off tests and pull-out test with friction tests, were performed in this study.

A major requirement for an efficient composite slab is the significant bond strength acting at the interface of its components. The interface must be able to resist horizontal shear and prevent vertical separation. To achieve this, profiled steel sheeting in the current market today generally utilises a fixed pattern of embossments and re-entrant portions.

The efficiency of the composite action for steel sheeting is currently thought to be reliably obtained only from test information. The methods of measuring shear-bond resistance may be by full-scale tests of concrete slabs or full-scale tests in combination with small-scale model tests.

The most widely used small scale tests are:

1. Pull-out test: similar to that used for reinforcing bars in conventional reinforced concrete, where a tensile load is applied to one end of the reinforcing bar. Pull-out tests used for composite structures will be described in this chapter.
2. Push-off test: similar to that used for composite structures as composite beams and composite slabs, where a compressive force is applied to the concrete.

In the following section, Pull-out test, and Push-off tests used for profiled composite slabs are reviewed and a pull-out, and push-off test, as modified by the author, is described and the results are presented and compared.

3.2 Conventional reinforced concrete

Since the beginning of twentieth century pull-out tests have been used to determine the bond resistance of reinforcing bars. These tests first were performed on plain reinforcing bars and later adapted for use with deformed or ribbed reinforcing bars. Load-slip curves for a number of diameters and lug patterns have been studied by many researchers (Mathey and Wastein[51], 1961, Hamad[18], 1995 and Cairns and Jones[17], 1995). A typical shear stress-slip relationship for plain and deformed reinforcing bars are shown in Fig. 3.1.

Three types of tests can determine the bond stress of the reinforcing bar as follows:

Pull-out test;

Embedment test; and

Beam test.

The Pull-out test has been widely used for comparative studies of bond behaviour. This is because it is economical to manufacture and test. But it has the disadvantage in that the concrete is in compression and steel bar is in tension; a situation that will not be encountered in practical structures at the interface between the reinforcement and the concrete.

In the Pull-out test, a bar is embedded in a cylinder or rectangular block of concrete and the force required to pull it out or make it slip excessively is measured. Figure 3.2.a shows such a test schematically (omitting details such as the bearing plate). Slip of the bar relative to concrete is measured at the bottom (loaded end) and top (free end). Failure usually occurs by longitudinal splitting of the concrete in the case of deformed bars or by pulling the bar through the concrete in the case of a very small bars or very light aggregate and by failure of the bar, if the embedment length is sufficient.

Push-off tests, sometimes called Push-out, are often used to determine concrete slab/beam connection strength. These tests consist of two concrete blocks cast on each side of the hot-rolled steel section as shown in Figure 3.3.b (BS5400: Part 5, 1979)[52]. The specimen is provided with shear connection devices as in the full-scale member. Also, Push-off tests have been performed for composite beams consisting of profiled composite slabs and hot rolled steel beam sections. Connection between the sheeting and beam is established using either conventional welded studs or other connectors. In some cases the sheeting may increase the difficulties of welding shear-connectors to the underlying beam.

Lloyd and Wright, 1990[26], carried out 42 through-deck Push-off tests. Their tests were conducted on specimens that incorporated trapezoidal profiled steel sheets and headed shear-connectors. From their experimental study, they confirmed that the resistance of through-deck welded shear-stud connectors cast in slabs with profiled steel sheeting as permanent form-work will depend on the geometry of the sheeting and stud height. Also, they concluded that the ultimate shear resistance of the connection between the composite slabs and the steel beam could be considerably less than the connection in solid slabs.

3.3 Composite slabs

The standard test for shear-bond interlock described in BS5950: Part 4: 1994[6] would require at least six test slabs to be cast for each single profile type. The span of these slabs would typically vary between 1.8 m and 4.0 m, and the breadth would be the total width of the profiled steel sheet. It is considered expensive and time-consuming to do this full standard test on every variation of embossment considered. As a result many researchers have tried to develop a small-scale test to determine the shear-connection performance of steel sheeting from which the full-scale performance can be predicted.

In order to study the relationship between shear resistance, friction and for various types and gauges of steel decking with different embossments; push-off and pull-out tests have been carried out by various investigators. These tests are carried out on

either a full width of sheeting produced commercially or on a specimen equal to the width of one rib of the profile. The main purpose of these tests is to obtain data on shear-bond characteristics of the various types of steel decks

3.4 Push-off and pull-out tests

3.4.1 General

The purpose of the small-scale tests in this study is to give insight into the mechanical inter-locking mechanism and into the behaviour of composite slabs and to use the results in a FEM model of the full scale slab behaviour. Small-scale push tests and friction tests are used to obtain interaction properties between sheeting and concrete. The focus is on the distribution of slip and longitudinal shear stresses between concrete and sheeting. It is assumed that the shear connection in a composite slab cannot function unless there is slip at the interface between concrete and the sheeting (a simple test rig was devised for this purpose).

Ten small specimen tests have been carried out, five push-off, and five pull-out. In the push-off tests the samples were pushed at one end using a hydraulic jack applying load directly to the concrete through one or two load cells. In the pull-out tests, two bars were passed through the test sample so that the hydraulic jack could apply a tensile force to the bars which reacted against the sample at the end away from the jack (as shown in Figure 3.6.a and b). The tests provided information on the load/slip behaviour of the composite, the coefficient of friction and the effectiveness of the re-entrant portion in the profiled steel sheeting.

A concrete block is cast in a width equal to one, or two rib widths of the profiled steel sheeting used from the centres of two adjacent flanges and 300 mm in length for the single rib, and 600mm in length for the double rib, as shown in Figures 3.3.a to d (for single rib with full and part- encasement of the concrete), and Figures 3.4.a and b (for double rib with full and part-encasement of the concrete). The tests were carried out using CF70 profiled steel sheeting manufactured by Precision Metal Forming Limited (PMF). Details of the profile are shown in Figure 4.5, and section 4.3.1 in chapter 4.

Static loads were to be used in these tests. The requirement in the various codes that the test slabs be subjected to a dynamic load regime cycles prior to the static test to failure appears to be directed towards the breaking of any chemical bond between the concrete and steel. It is intended that this will ensure that the static test measures the resistance of the embossments and profile shape only and is not affected by chemical bond which may not exist after the slab has been in service for some time. Wright[57] and Abdel-Syed[58], found that the failure loads of composite slabs are hardly affected by cycling. Several slabs have been tested without cycling and the failure load does not appear to differ markedly from similar slabs that have been subject to load cycles. According to the two references above, dynamic load does not affect the performance of composite slabs and therefore it was decided not to employ dynamic loading these small-scale tests.

3.4.2 Preparation of the specimens

The push-off, and pull-out test specimens were prepared according to the following procedures:

The steel sheeting is cut longitudinally into sections to include either one rib of the profile or two ribs. The sheeting is then cut transversely through its full depth, typically to a length of 350 mm.

The steel sheeting is then welded to fixed heavy I-beams from the two sides and from the back. The formwork is prepared to give a total concrete thickness of 165 mm.

A plastic tube is fixed in the middle trough at a depth of 27.5 mm from the top surface of the concrete. Concrete is prepared using the same mix as the full-scale test described in chapter 4.

The steel deck surface is well cleaned just before casting the concrete.

The specimens are compacted manually, covered and left in the formwork for the curing process.

3.4.3 Test set-up

Figures 3.5.a to d shows the test rig for the push-off and pull-out test.

For the pull-out test a steel bar is pulled through the horizontal fixed tube in the concrete block. One end of the steel bar is screwed to a nut welded to a steel bar, and the other end is screwed into a nut with a piece of steel plate acting as a washer at the back end of the concrete block. The concrete block is restrained against vertical uplifting by a roller support attached to a load cell, which is fixed to a rigid steel frame which houses a hydraulic jack. The function of the load cell was to measure the initial vertical force (5 kN, 10 kN, or 20 kN) applied to the specimen. This is achieved by bolting the jack and the load cell to a steel frame. The output reading of the load cell was then used to control the value of the vertical load. Values of 5, 10, or 20 kN were used as vertical loads and varied depending on the test.

The horizontal force was applied by a hydraulic jack at one end of the steel bars. This force was transmitted to the far end of the concrete block through the embedded tube as shown in the diagrammatic sketches, figures 3.6.a-b. The horizontal load is applied in constant increments until failure occurs. The horizontal slip at the back end, just above the applied load point, was recorded at each load increment using transducers as shown in Figure 3.5.a and Figure 3.5.d.

For the push-off test the same set-up but for the horizontal load as shown in Figures 3.6.c & d. A hydraulic jack was used to uniformly push the specimen. The horizontal slip at the back end, just above the applied load point, was recorded at each load increment using transducers as shown in Figure 3.5.a & d.

3.4.4 Test results and comments

Specimens were tested when the concrete had reached an appropriate strength. The shear stress was calculated as the horizontal load divided by the projected area in contact between sheeting and concrete. The concrete is locked in by the re-entrant portion of the sheeting, which provides resistance to vertical separation.

The mechanical interlocking forces, defined as forces produced by the presence of indentations, depend on the web stiffness and possible frictional locking produced by the shape of the re-entrant portion which causes locking of the concrete.

The maximum recorded loads are given in Table 3.1.b. The shear stresses at first slip and failure are given in Table 3.2. Comparing the shear stresses at the maximum load

of the test results (between 0.08 to 0.21 N/mm^2) and similar small test has been done by Daniels[59] (between 0.073 to 0.224 N/mm^2) shows close agreement. The overriding of concrete at the embossments Figure 3.7 is similar to that observed in the full-scale composite slab tests. The load/horizontal slip relationships for the tested profiled steel sheeting, and the shear stress with horizontal slip relationships are shown in Figures 3.8-17.

Figures 3.18-20 indicates the increase in the maximum load and shear strength which results from full interaction of the re-entrant portion of the profile in tests 1, 3, and 9, when compared to the partial contribution of the "dovetail" shape in tests 8, 6, and 10. Figures 3.21-25 shows the increase of the vertical load increases the friction and the maximum shear stress.

In Figure 3.8 for example two critical load levels can be used to define the behaviour:

1. Average load at which slip is first recorded (p_s), after the chemical bond broken down.
2. Maximum load recorded (p_{max}) before the slabs failure.

The general observations were:

- At low load, the slip was negligible (chemical bond effective).
- As slip started, the concrete block began to override the embossments at the front end of the specimen as shown in Figure 3.7.
- After failure, the concrete block was lifted away from the sheeting at the free end, and it was noticed that the concrete was restrained against vertical uplifting due to its bearing on the bottom sides of the embossments and at the re-entrant portions.
- The concrete was completely sound except at the side of the embossments and at the re-entrant portions.
- A horizontal line was marked in the concrete block at the side of the embossments due to bearing and friction.
- No changes in the load cell readings (the vertical load) were recorded until the concrete block almost left the roller support.
- No plastic deformation was observed in the profiled steel sheeting.

3.5 Frictional coefficient

Push-off, (Figure 3.6.c), and pull-out tests, (Figure 3.6.b), were used to determine the frictional coefficient between the steel sheeting (0.9mm galvanised steel CF70) and the concrete.

The procedures followed were as follows:

A hydraulic jack was used to displace the concrete block either by pushing or pulling away from the steel sheeting breaking the chemical bond.

The concrete was replaced in its original position.

A known vertical load was applied and held at the top surface of the concrete block.

A static load was applied in small increments at the end of the steel bar using hydraulic jack.

The static load was increased until the concrete block just started to move.

The horizontal static load and vertical load were removed and the concrete block was again replaced to its first position.

The vertical load was increased on the top surface of the concrete block.

The required static horizontal load to cause the concrete block to start moving was determined.

Steps 6-8 was repeated many times with increases in the vertical load applied to the top surface of the concrete block.

The relationship between the static load (horizontal force, H) caused the concrete block to move and the static vertical load on the surface of the concrete block (vertical load, V,*)* is given in Figure 3.26 for the Push-off test, and Figure 3.27 for the Pull-out test. The slope of the regression line for the results gives the coefficient of friction as 0.412 for the push-off arrangement, and 0.388 for the pull-out. It was assumed that the repetition of tests and the replacement of the concrete in its original position did not adversely affect the veracity of the tests and this appeared to be the case from the reproducibility of the values.

3.6 Discussion

In the tests, failure occurred by the concrete over-riding the embossments. Scoring of the steel and slight crushing of the concrete was observed at the base of the embossments. This was similar damage to that observed in the full scale slab tests. Little damage occurred to the re-entrant portions in the test, and in all other tests the re-entrant nib of concrete was found to be broken following failure. The load recorded in the cell remained constant until the final stages of the test when the block had lifted and moved from 5 to 25 mm.

These tests show the importance of simple friction. It is also shown that the re-entrant portion has a significant effect, according to the results in Figures 3.18 to 3.20.

It may also be surmised from the damage incurred by the concrete and embossment steel that most shear resistance would appear to be derived at the base of the embossment. Given the fact that the normal load did not vary until the very late stages of each test it may also be concluded that the over-riding of the concrete was made possible by the local deformation of the web plate.

3.7 Conclusions

Push-off, and pull-out tests are relatively quick, simple and economical, and can yield essential information about the shear connection performance of profiles with very different characteristics. Adhesion bond, mechanical interlock and friction can collectively contribute toward the total longitudinal slip resistance of a profile and can be separately identified using the test. In particular, parametric values determined from the test can be used directly in a physical model using partial shear connection theory, which accurately predicts the strengths of slabs. The test can therefore complement a test programme involving full-scale slab testing.

The results from the tests provide a very clear indication of the effectiveness of the re-entrant profile in enhancing the shear bond strength of the profile. The forms of the tests enabled a comparison to be made of the contribution of the embossed dovetail when fully encased in concrete with the half dovetail at the edge of the slab.

Figure 3.26 and 3.27 gave the frictional coefficient values 0.412 for the push-off test, and 0.388 for the pull-out test, but the push-off test gave a closer linear relationship between longitudinal and vertical load than the pull-out test.

Full encasement of the re-entrant profile with concrete instead of part-encasement increased the slip resistance of the specimen from 13 kN to 23 kN (increase in shear resistance from 0.1 to 0.2 N/mm^2) in push-off test shown in Figure 3.20. Also in the pull-out test, there was an increase in the shear resistance from 0.08 to 0.17 N/mm^2, shown in Figure 3.19.

Furthermore the double encasement of the re-entrant profile in the test No.9, compared to one full re-entrant profile and two halves of profile in test No.10, resulted in a shear load increase from 0.123 to 0.18 N/mm^2, as shown in figure 3.20.

The results in tables 3.1.b and 3.2 showed no significant difference between pull-out and push-off tests (the results were close). Table 3.2 also highlights the improvement in shear capacity resulting from the complete encasement of the dovetail rib. Tests 1 to 4 show an average $\tau_f = 0.102$ N/mm^2 for the fully encased rib while tests 5 to 8 have average τ_f value of 0.05 N/mm^2 for the partially encased rib. Tests 9 and 10 show similar behaviour for larger tests.

Comparison of the two graphs, (Figures 3.26 and 3.27) indicate that linear relationship between the vertical and horizontal loads was closer with the push-off test, which supports the conclusion that the push-off test was a more satisfactory test. The difference between the two may be explained by the control of the line of action of the longitudinal force. In the push-off test the close proximity of the jack to the sample enabled close control to be maintained. In the pull-out test the length of the tensioned bars meant that any lack of straightness as slipping pushed the concrete out of the line was exaggerated.

The push-off test was easier to carry out and is recommended with full encasement of the rib either for the full sheet or for one trapezoidal rib.

In principle, a small-scale test should create a load environment similar to that in the real structure in order to study the shear transfer mechanism. A good model should include the possibilities of bending, cracking, vertical separation and horizontal slip. However, these conditions cannot be achieved in a small-scale test. The small-scale

tests aforementioned modelled the load in two aspects (shear load represented by the 'horizontal load' and friction being induced by the 'vertical load'). This is considered the best method to obtain the actual shear stress-slip relation.

According to the shear stresses recorded in table 3.2 and plotted in graphs results the small-scale tests show an increase in capacity after first slip. This was also demonstrated in the full-scale tests, thus suggesting that small-scale tests can be used to investigate the behaviour of different trial profiles prior to embarking on an expensive full-scale tests programme. It means the small-scale test can give a good representation of the full- scale tests.

Numerical results from these tests will be used in the analysis and numerical modelling of composite slabs as presented in chapter six.

Table 3.1.a Profiled steel sheet details

Specimen No.	Total Thickness t (mm)	Depth h (mm)	Width b (mm)	Young's Modulus N/mm^2	Area of Steel A_p (mm^2/m)	Neutral Axis e_p (mm)
1- 10	0.9	70	300/600	202777	1166	30.34

Table 3.1.b Details of push-off and pull-out tests.

Test No.	Test type	Length (mm)	Width (mm)	Depth (mm)	Density of Concrete kN/m^3	Concrete cube strength N/mm^2	Maximum applied horizontal load kN	Vertical applied load kN
1	Push-off	300	300	165	23.79	44	23.15	5
2	Push-off	300	300	165	23.79	44	25.25	10
3	Pull-out	300	300	165	23.79	44	22.87	5
4	Pull-out	300	300	165	23.79	44	24.91	10
5	Pull-out	300	300	165	23.79	44	11.6	10
6	Pull-out	300	300	165	23.79	44	10.1	5
7	Push-off	300	300	165	23.79	44	14.76	10
8	Push-off	300	300	165	23.79	44	13.45	5
9	Push-off	600	600	165	23.23	34	88.95	20
10	Push-off	600	600	165	23.23	34	59.8	20

Table 3.2 Details of typical shear stress values τ (N/mm^2).

Test No.	Test type	P_f (kN)	P_{max} (kN)	τ_f (N/mm^2)	τ_{max} (N/mm^2)	A_v (%)
1	Push-off	13	23.15	0.11	0.19	72
2	Push-off	13.5	25.25	0.108	0.21	94
3	Pull-out	12.7	22.87	0.10	0.18	80
4	Pull-out	11	24.91	0.09	0.21	133
5	Pull-out	5	11.6	0.04	0.09	125
6	Pull-out	5	10.1	0.045	0.08	77
7	Push-off	8.5	14.76	0.07	0.12	71
8	Push-off	6.5	13.45	0.055	0.11	100
9	Push-off	59	88.95	0.12	0.18	50
10	Push-off	34.5	59.8	0.07	0.12	71

where

P_f = load value at the first slip

P_{max} = maximum applied load

τ_f = shear stress at the first slip

τ_{max} = shear stress at the maximum load

A_v = % increase in τ from first slip to failure

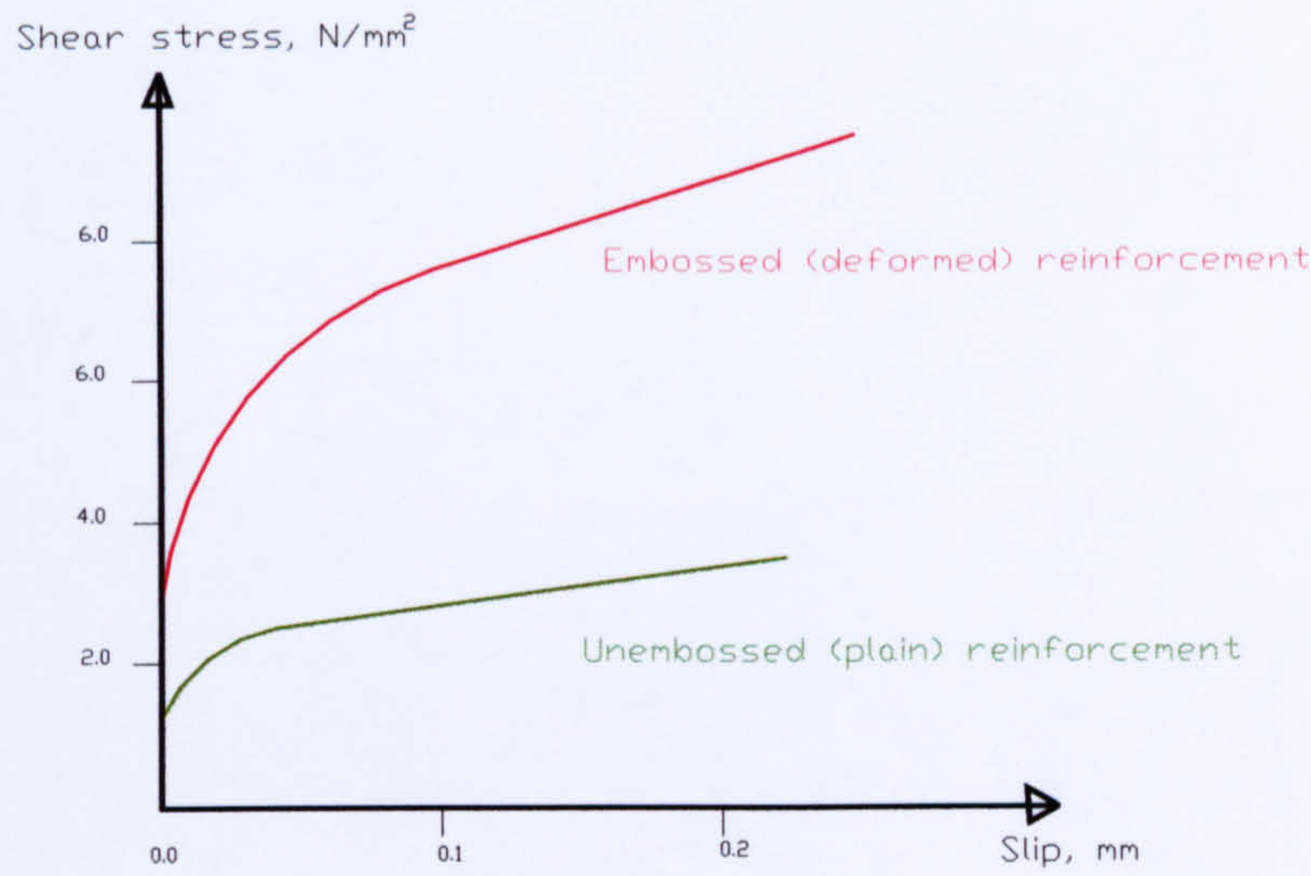

Figure 3.1 Shear stress-slip relationship in reinforced concrete

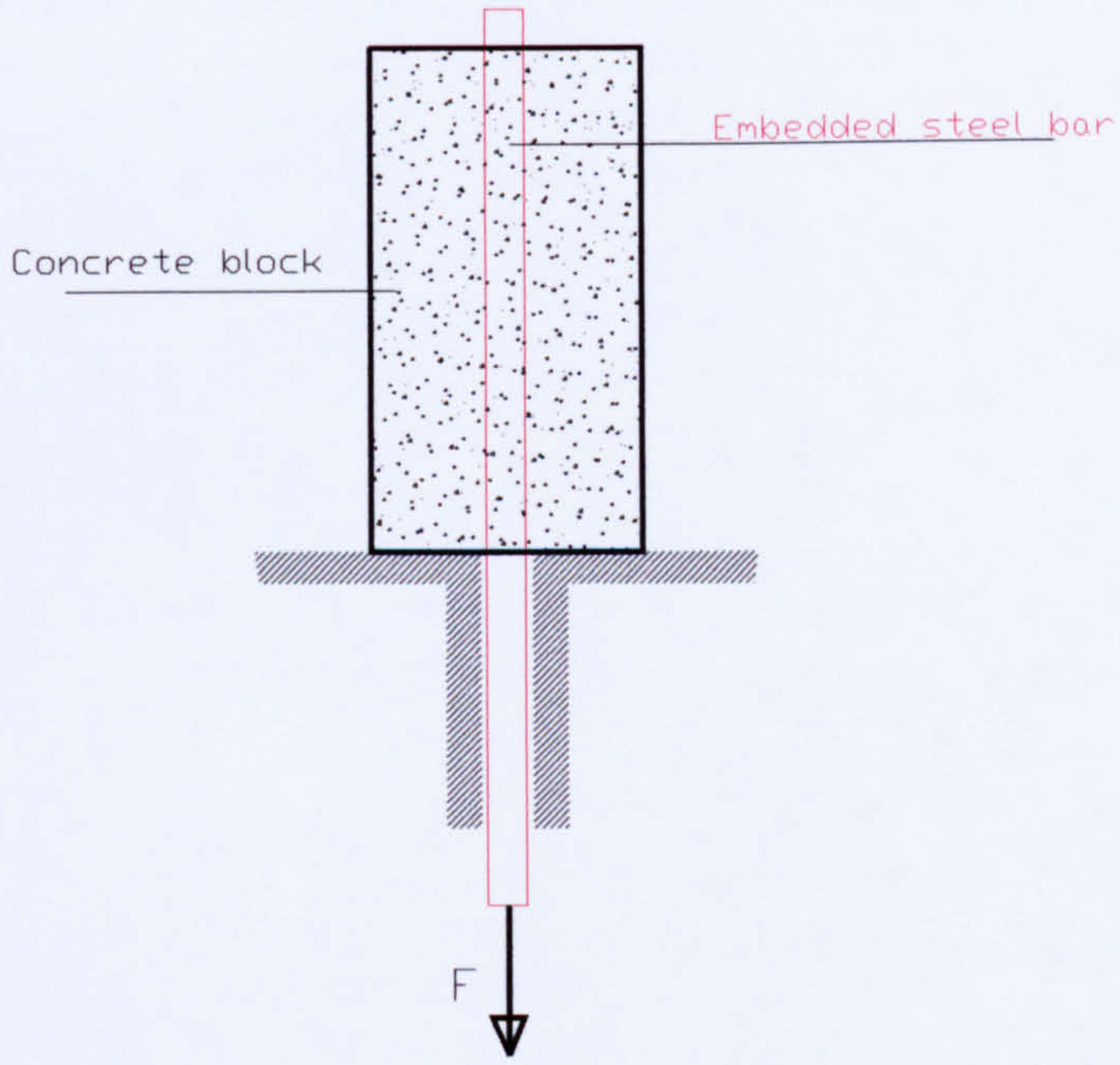

Figure 3.2.a Pull-out test

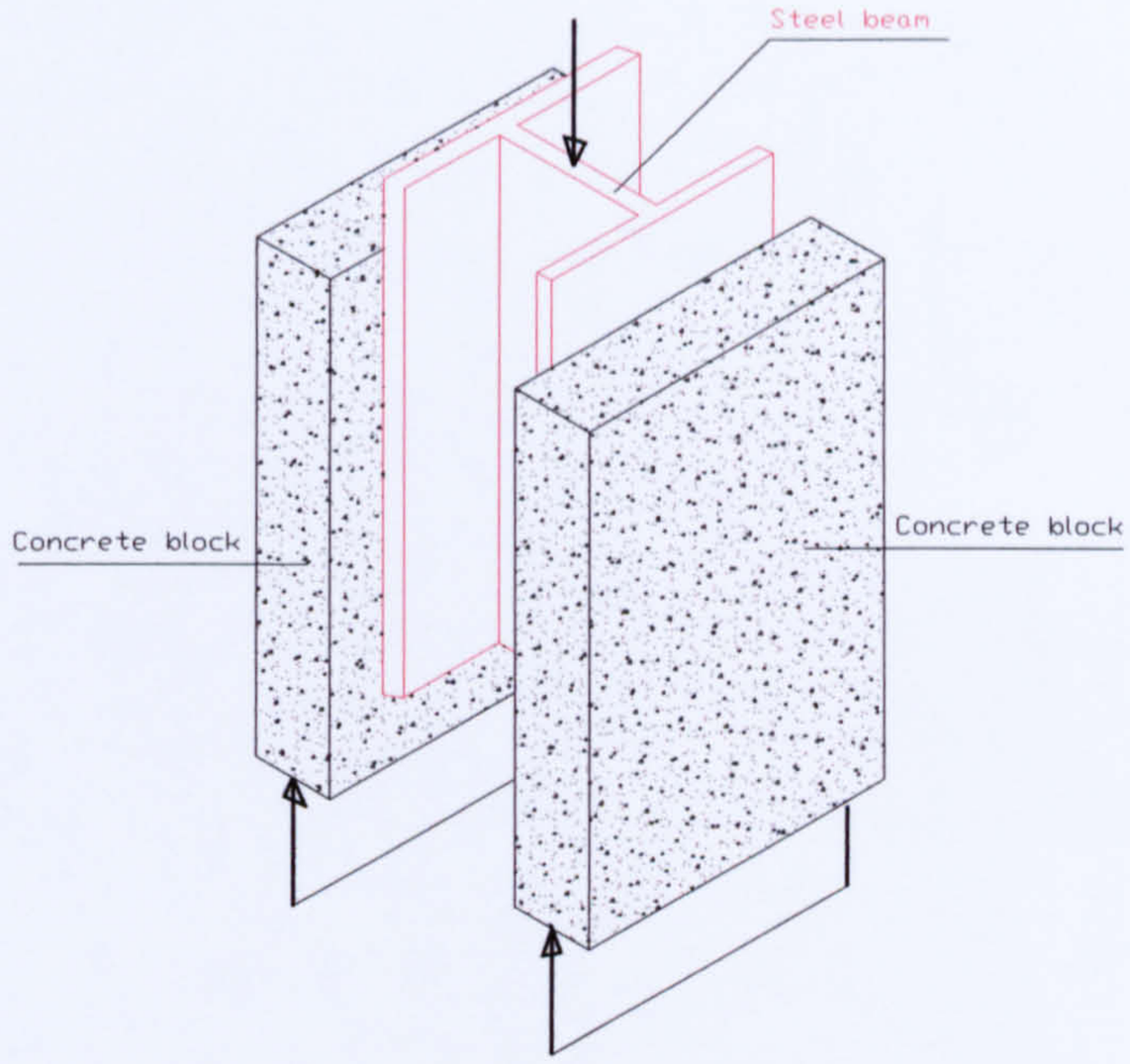

Figure 3.2.b Typical push-off test for shear connection in composite beams

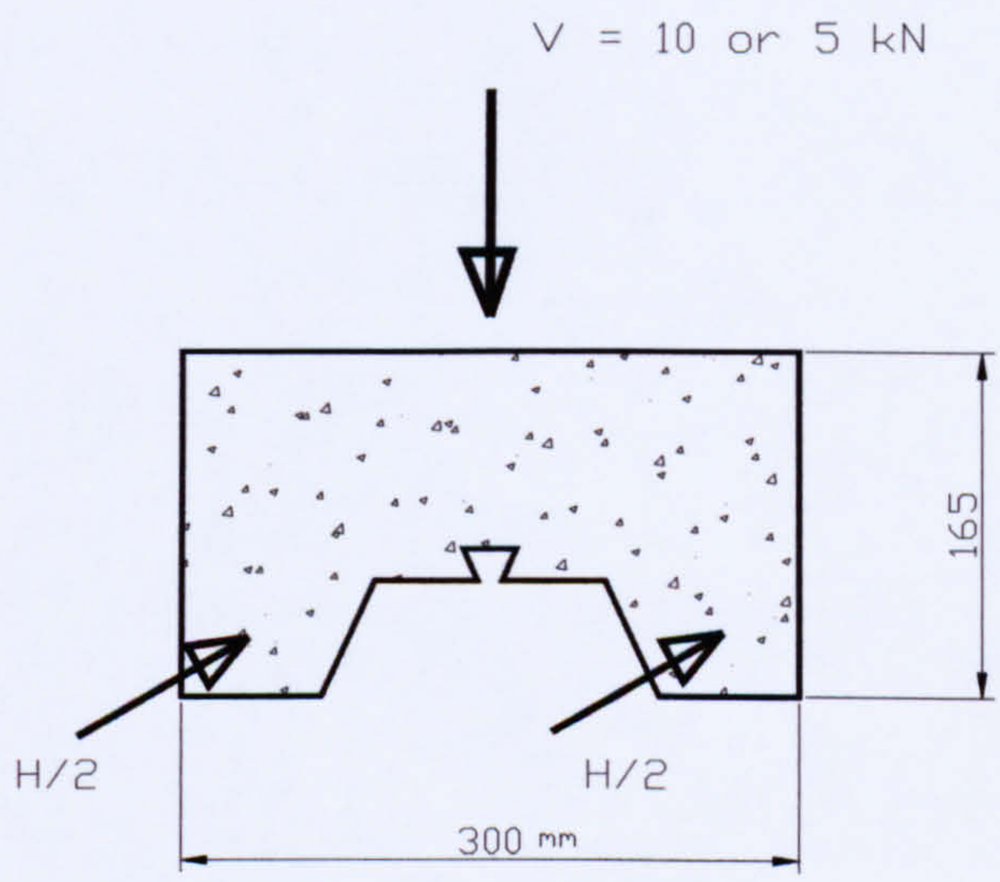

Figure 3.3.a Push-off test for one rib with full encasement of the rib

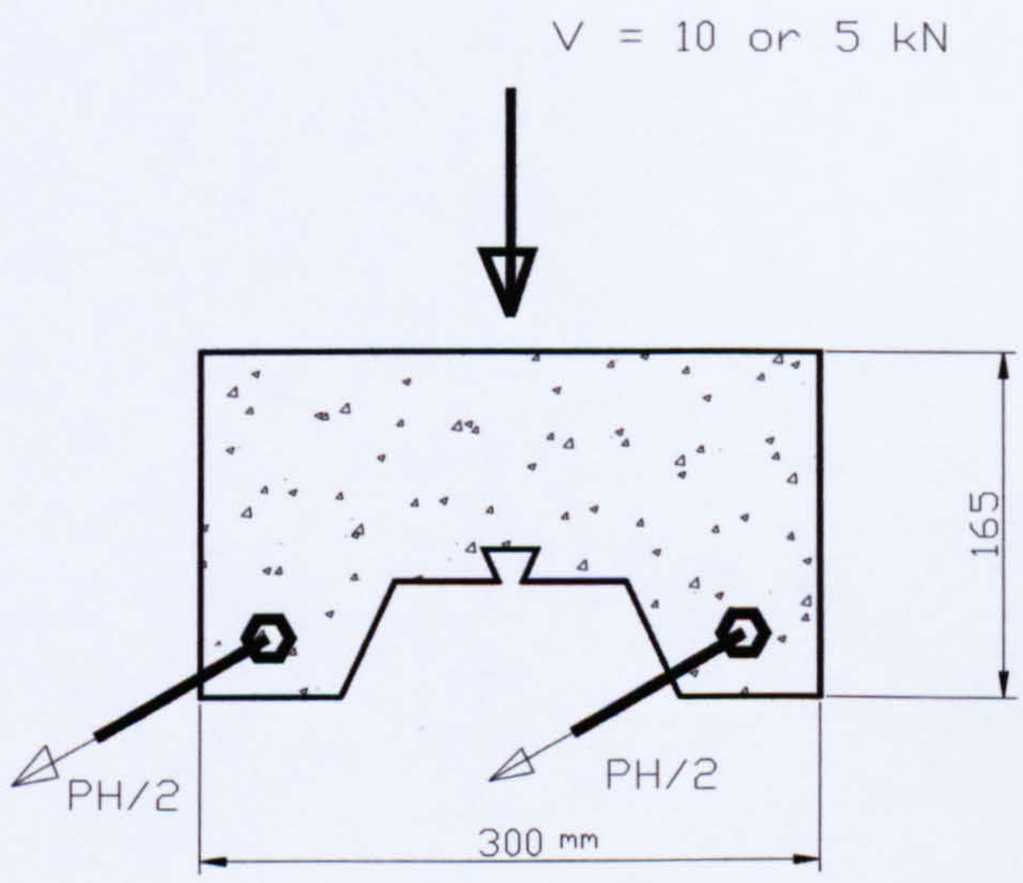

Figure 3.3.b Pull-out test for one rib with full encasement of the rib

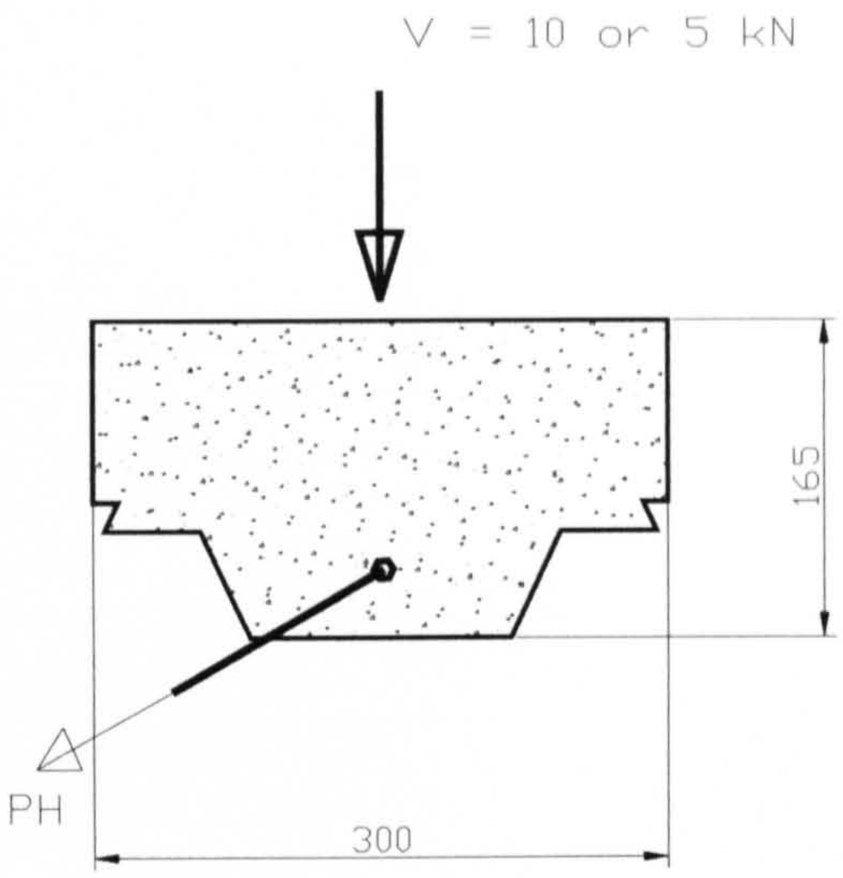

Figure 3.3.c Pull-out test for one rib with part encasement of the rib

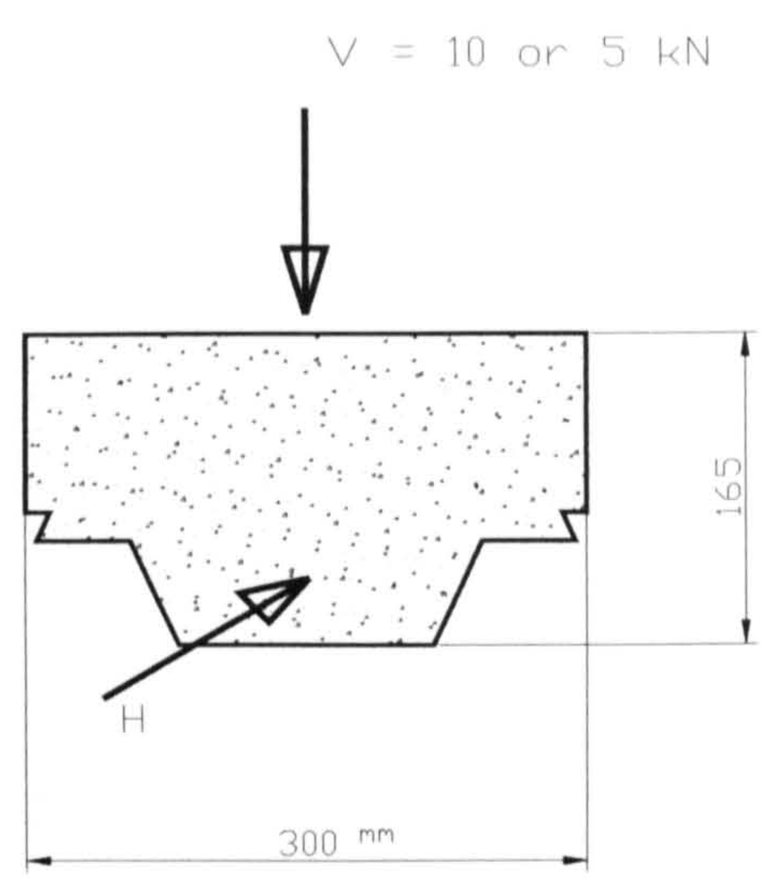

Figure 3.3.d Push-off test for one rib with part encasement of the rib

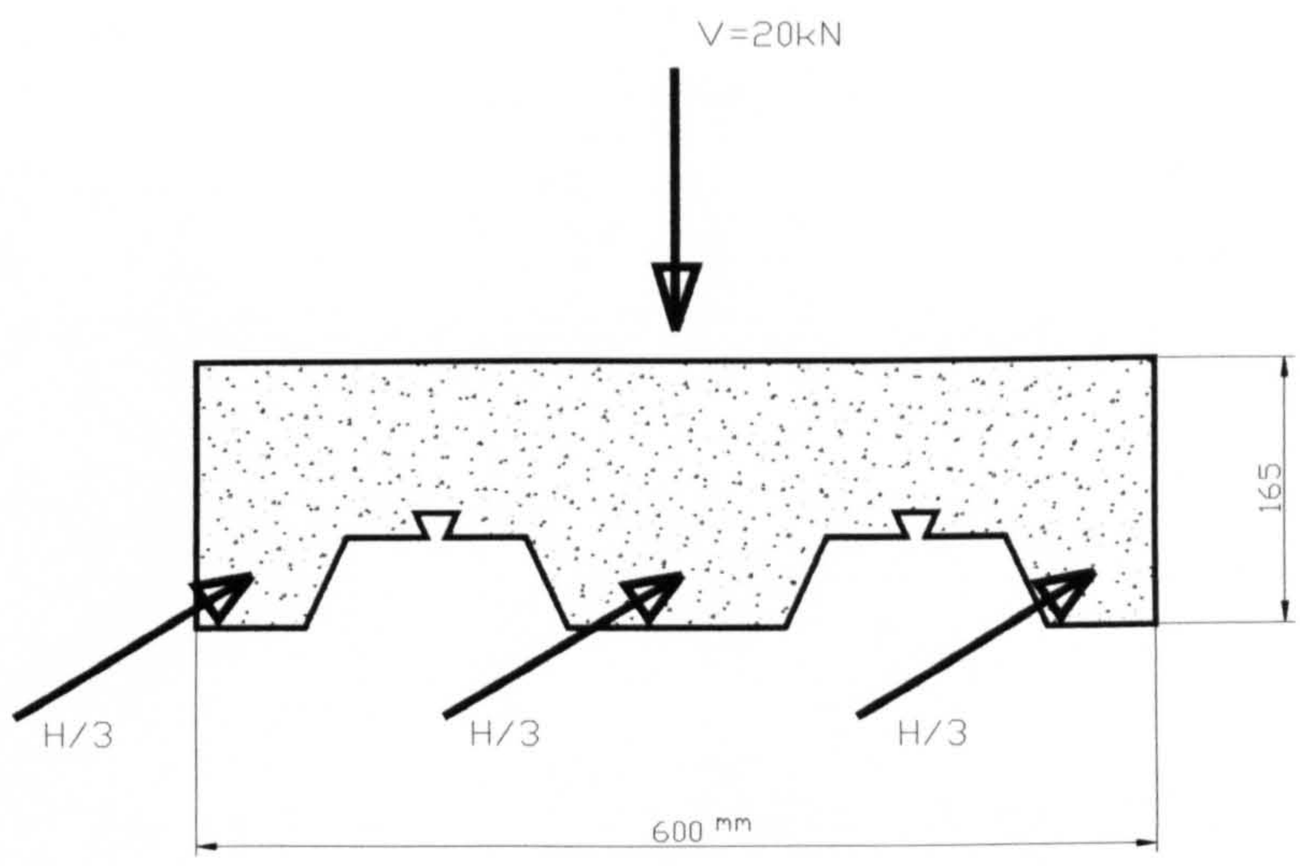

Figure 3.4.a Push-off test of two ribs with full encasement of the whole sheet (600*600mm)

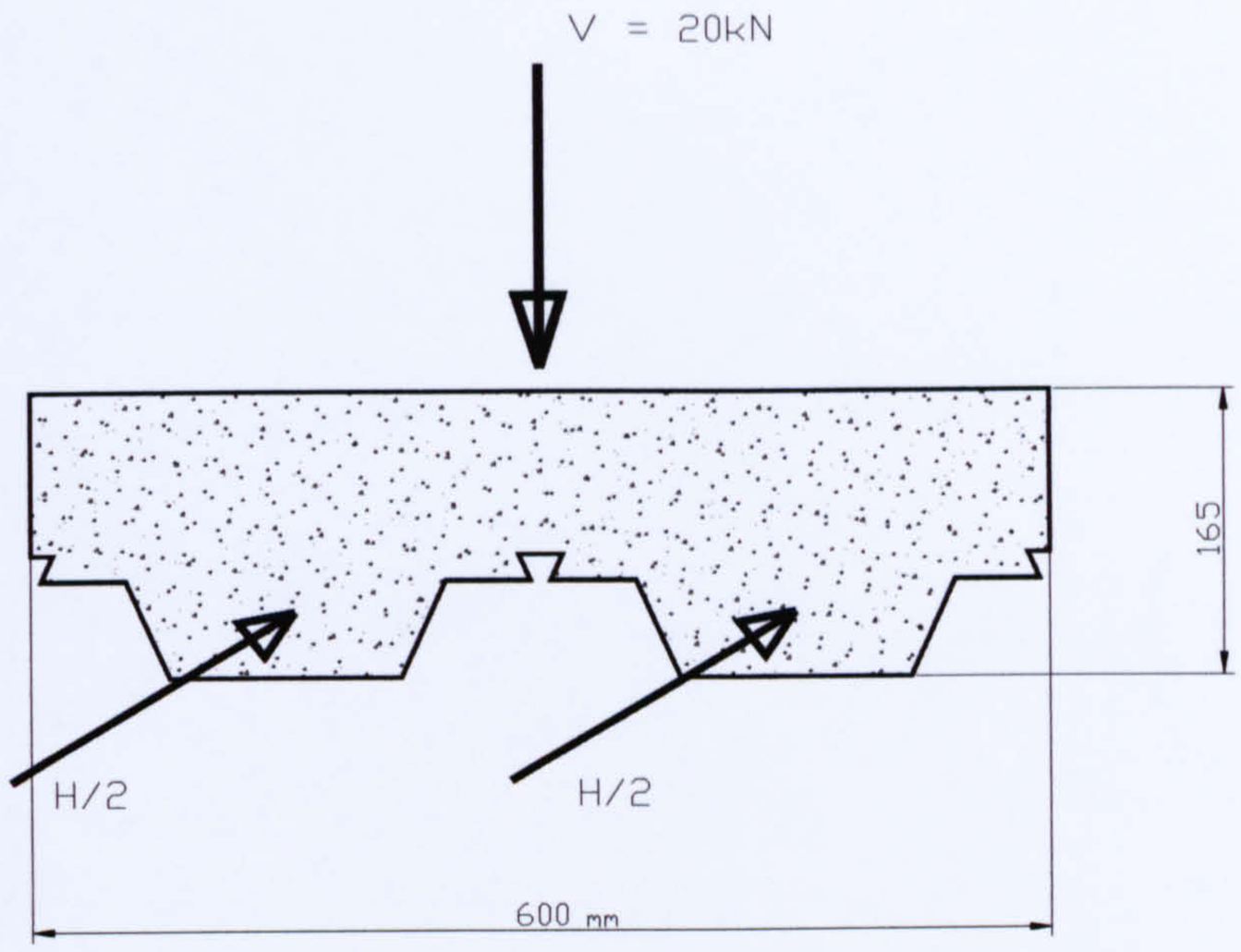

Figure 3.4.b Push-off test with part encasement of end ribs (600*600mm)

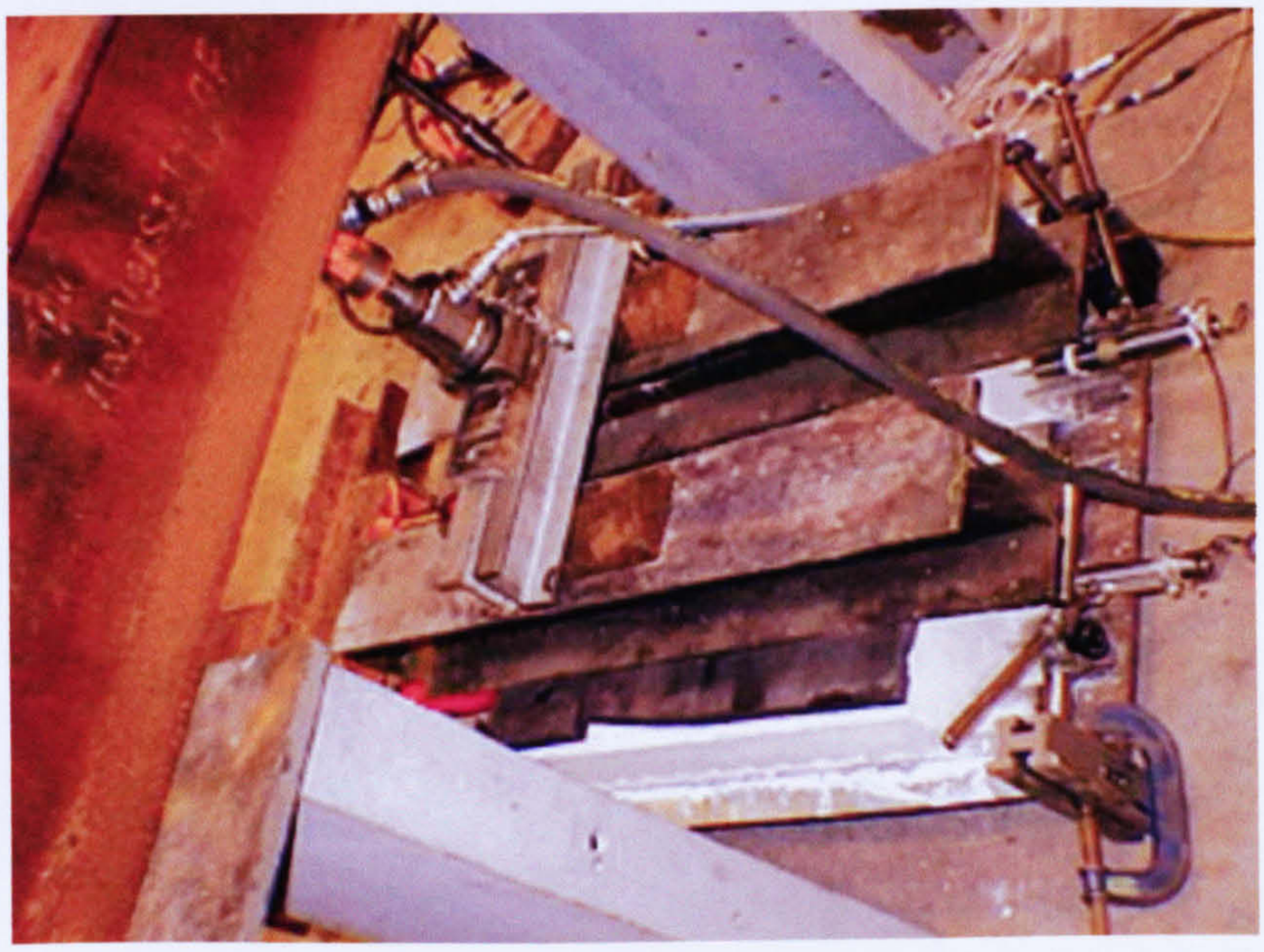

Figure 3.5.a Pull-out test in operation

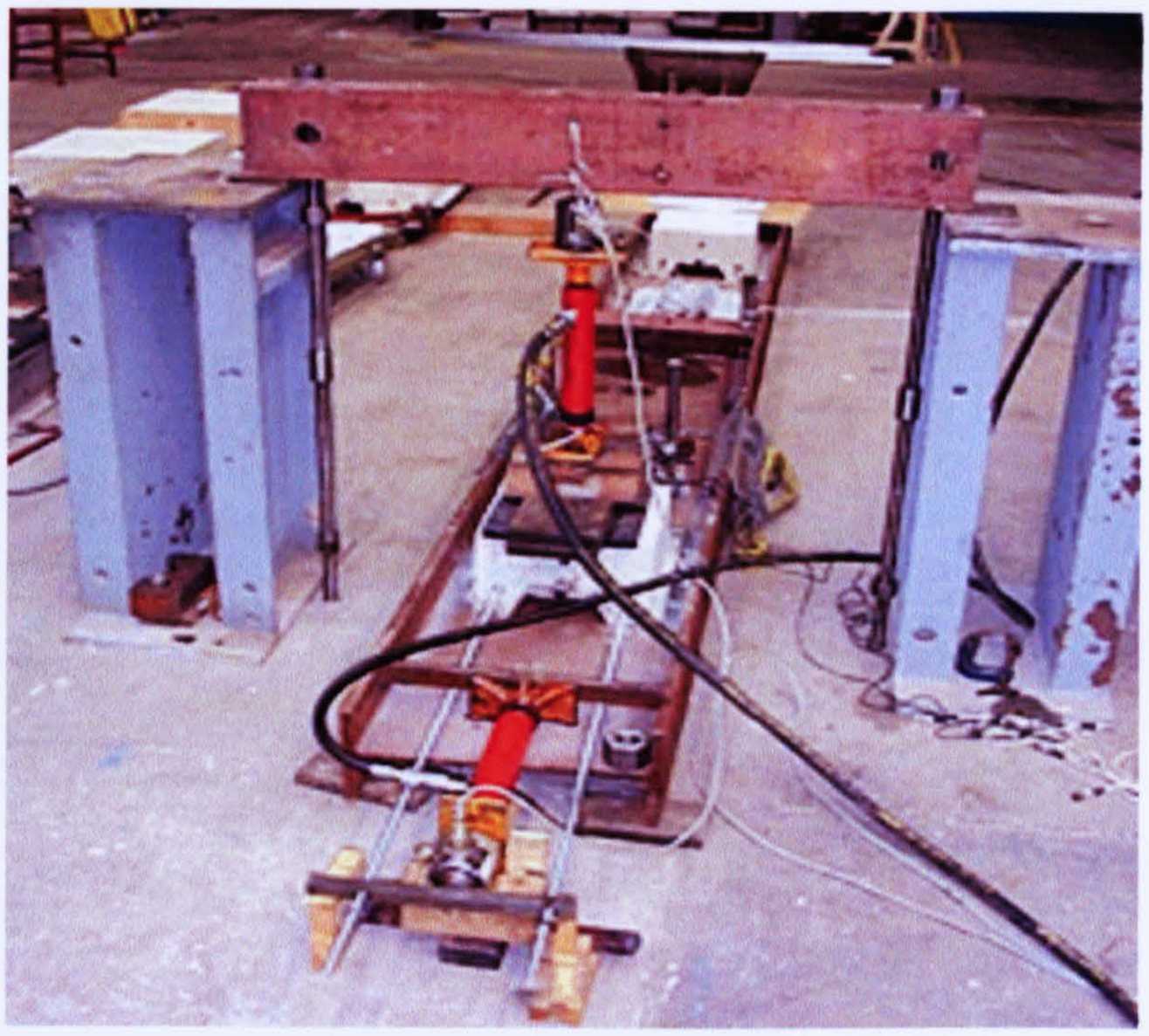

Figure 3.5.b Pull-out test of the full encasement of the rib

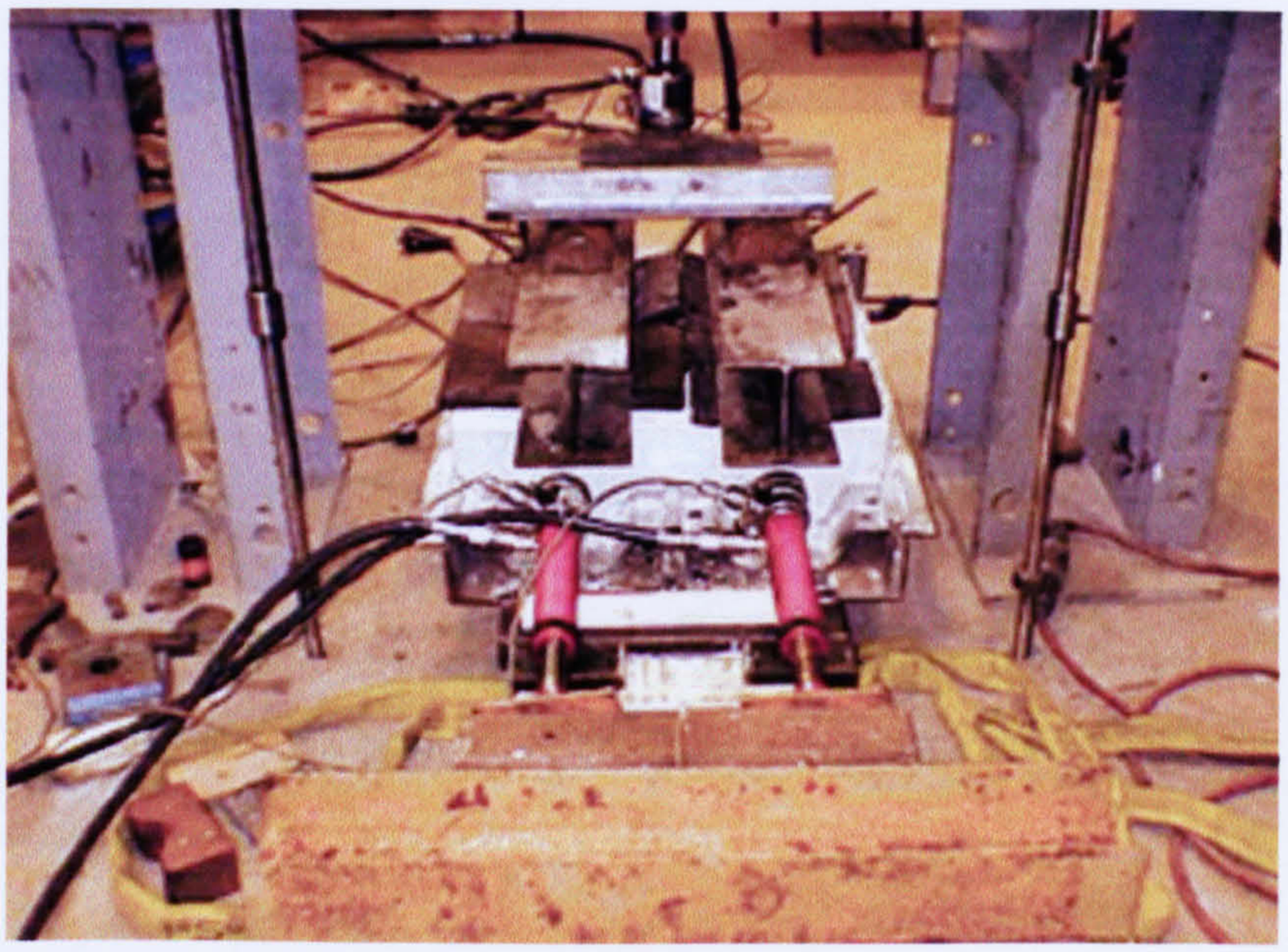

Figure 3.5.c Push-off test with part encasement of the end ribs

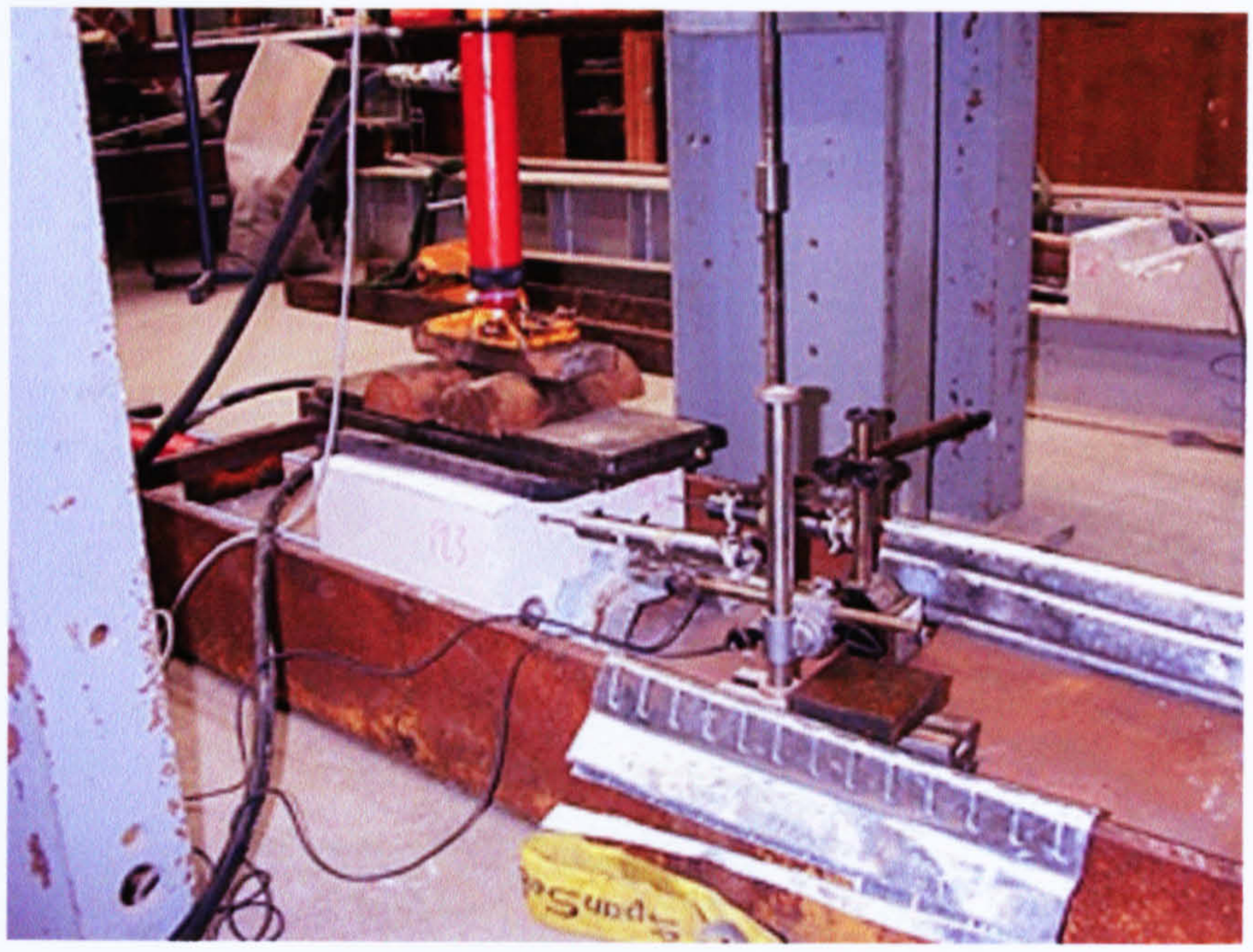

Figure 3.5.d Push-off test with full encasement of the ribs

Figure 3.6.a Pull-out test with part encasement of the ribs

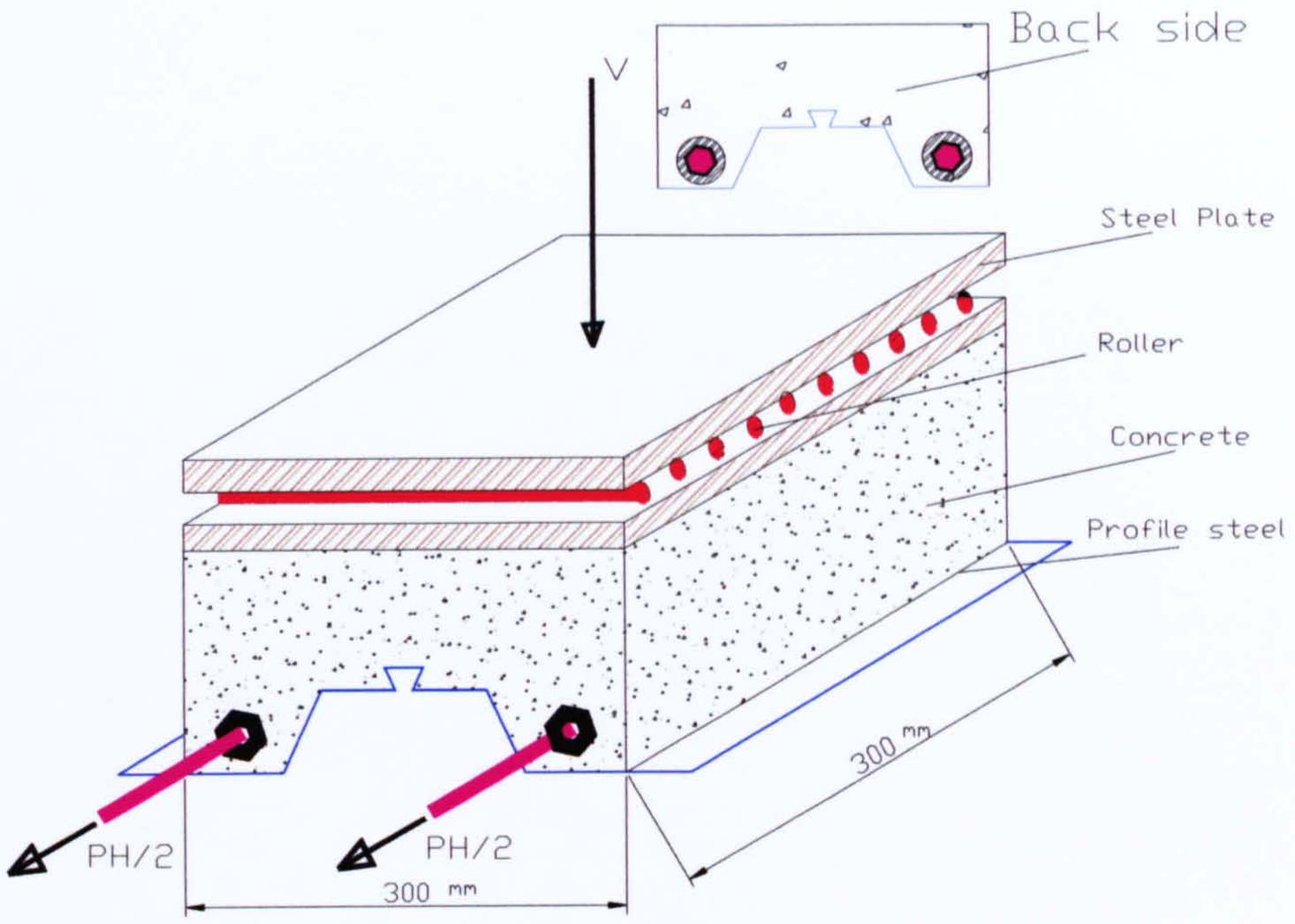

Figure 3.6.b Pull-out test with full encasement of the ribs

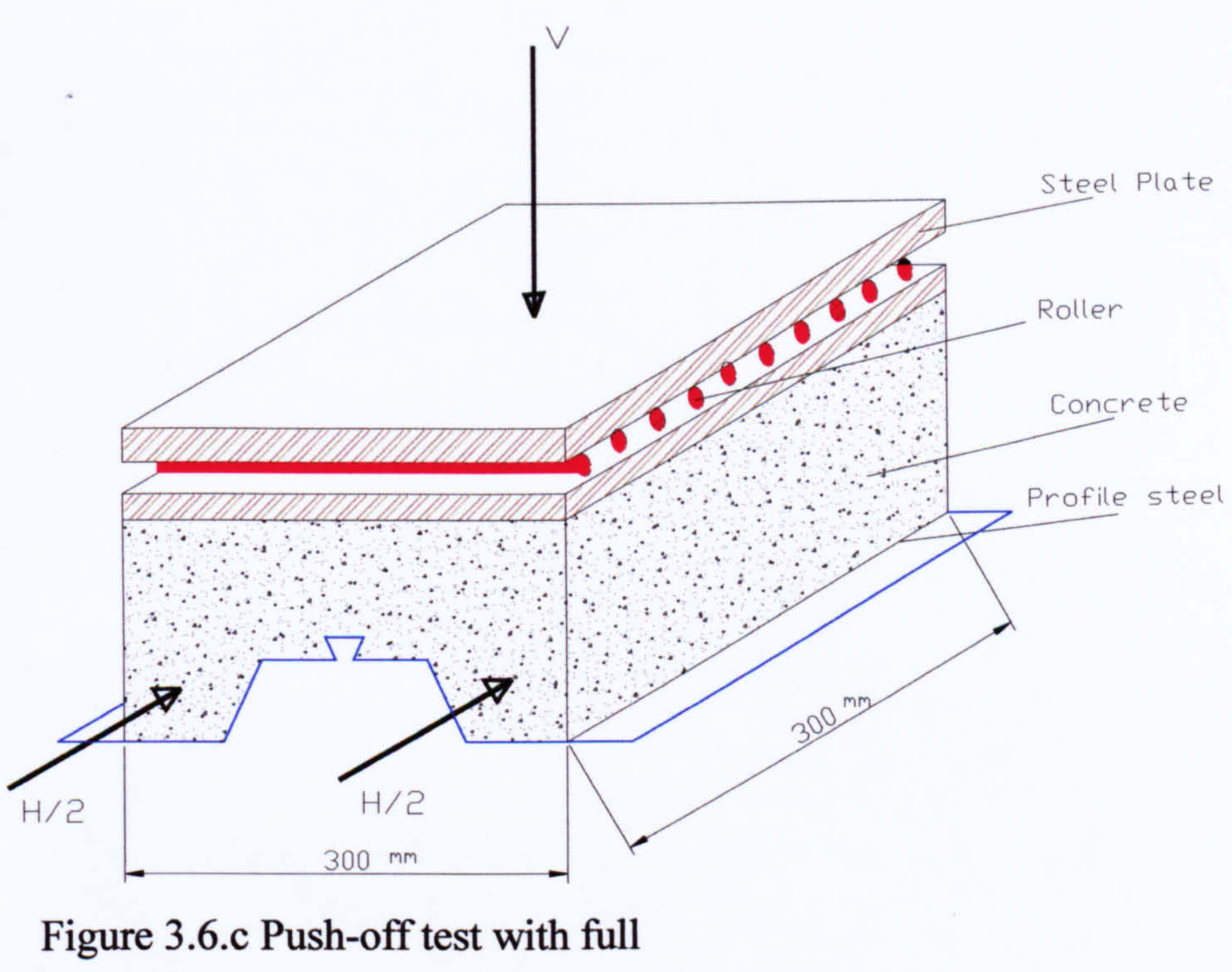

Figure 3.6.c Push-off test with full encasement of the ribs

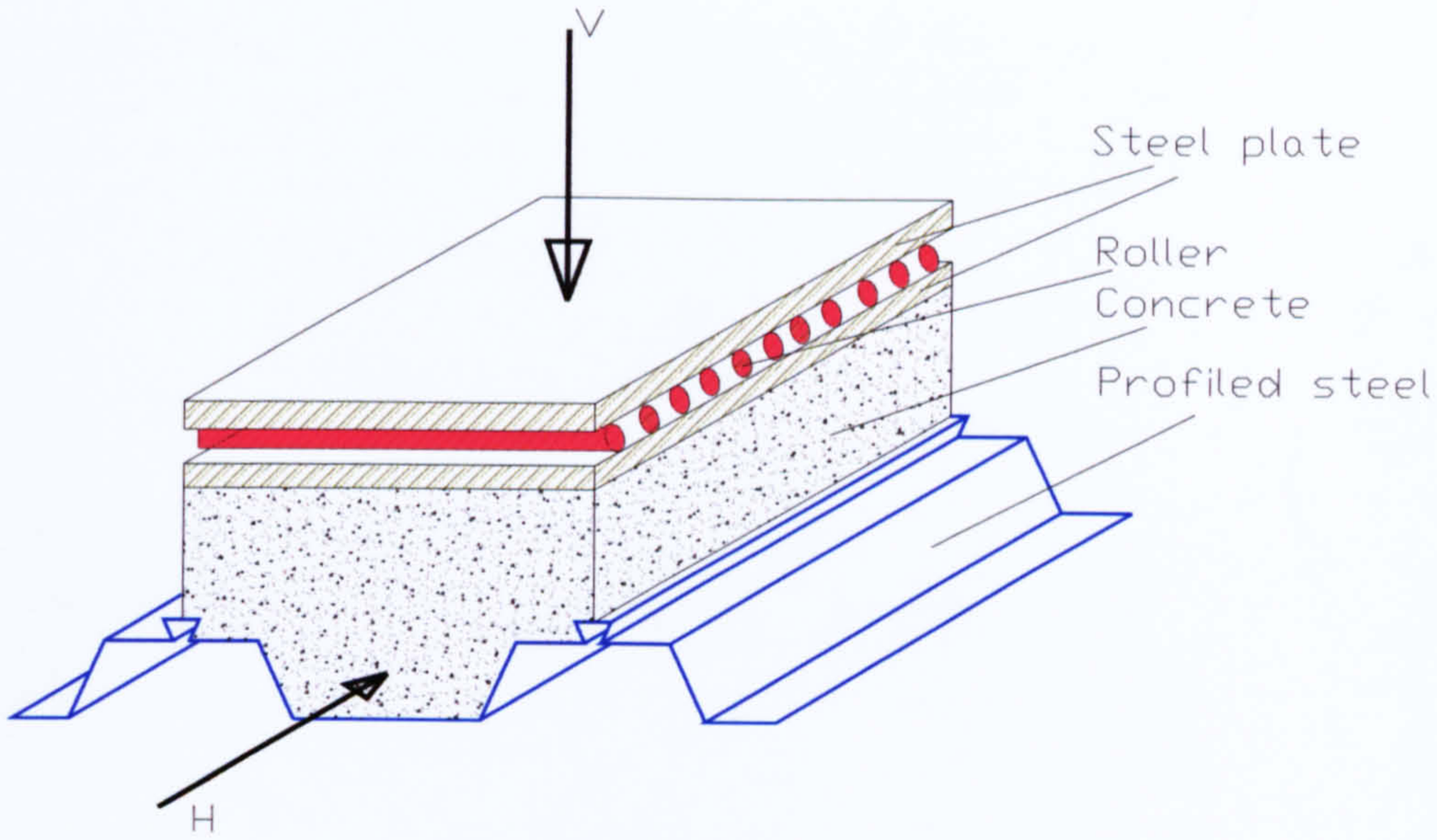

Figure 3.6.d Push-off test with part encasement of the ribs

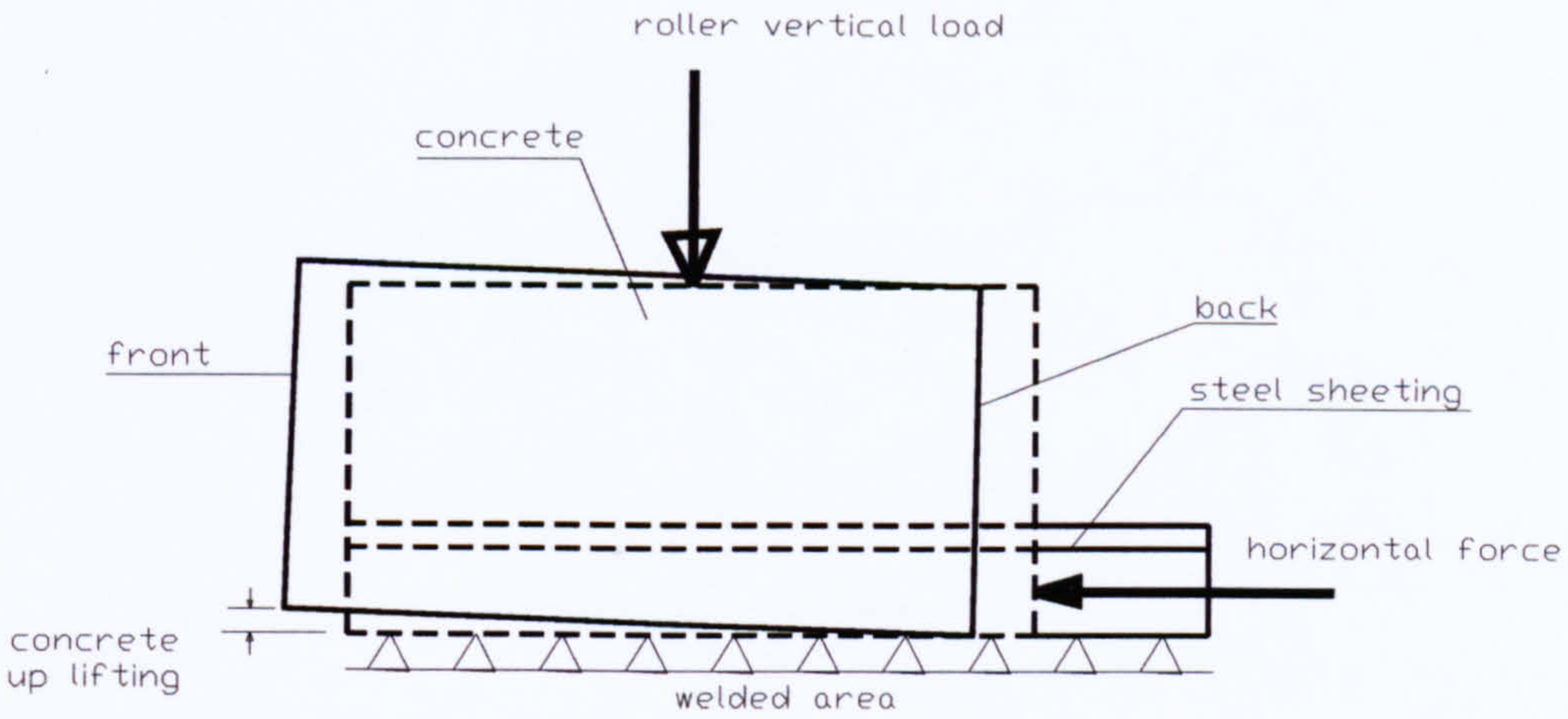

Figure 3.7 Failure mechanism of tests

Figure 3.8 Load-Slip behaviour for Composite Slab (Push-off test No. 1 with vertical load 5 kN)

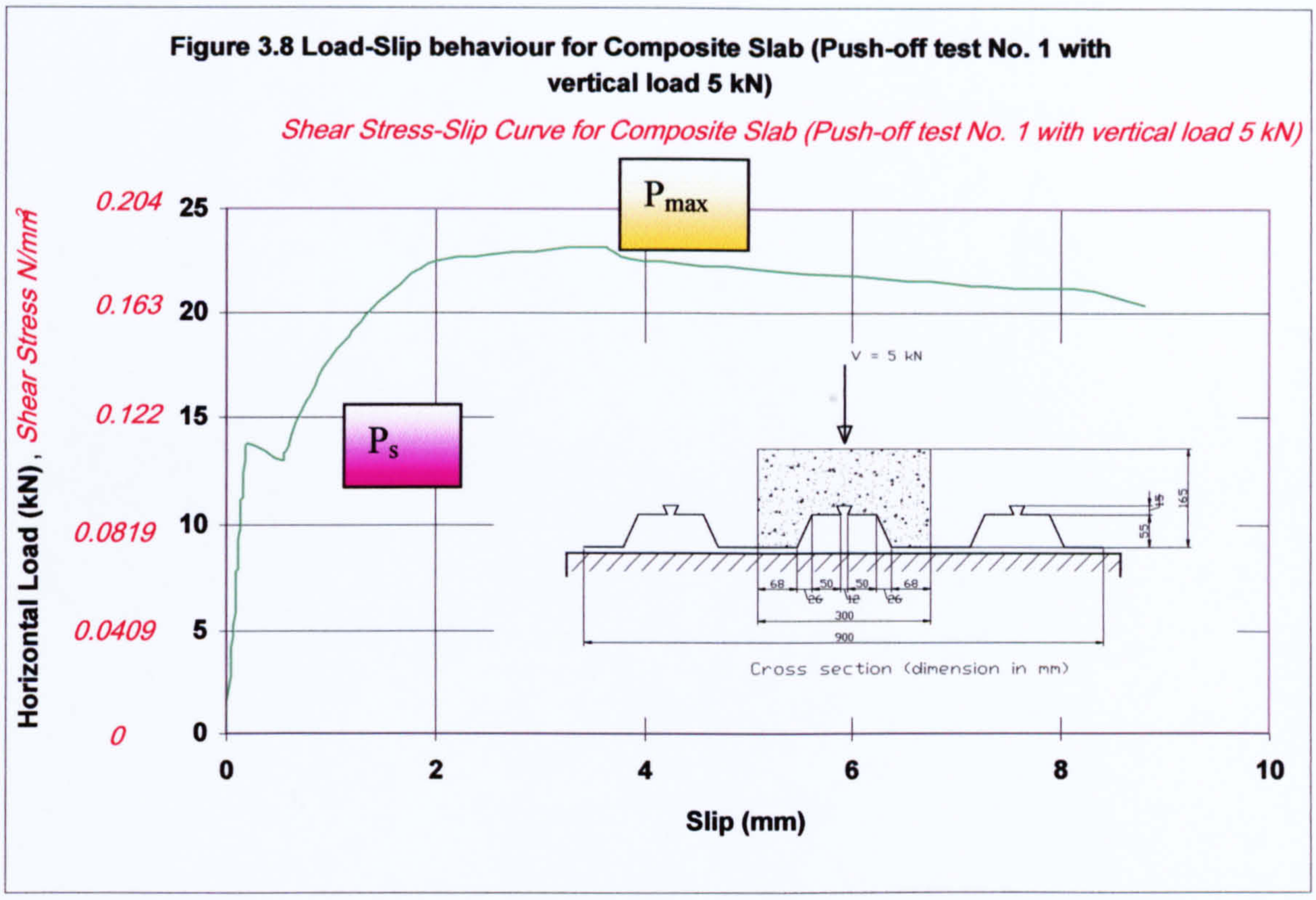

Figure 3.9 Load-Slip behaviour for Composite Slab (Push-off test No. 2 with vertical load 10 kN)

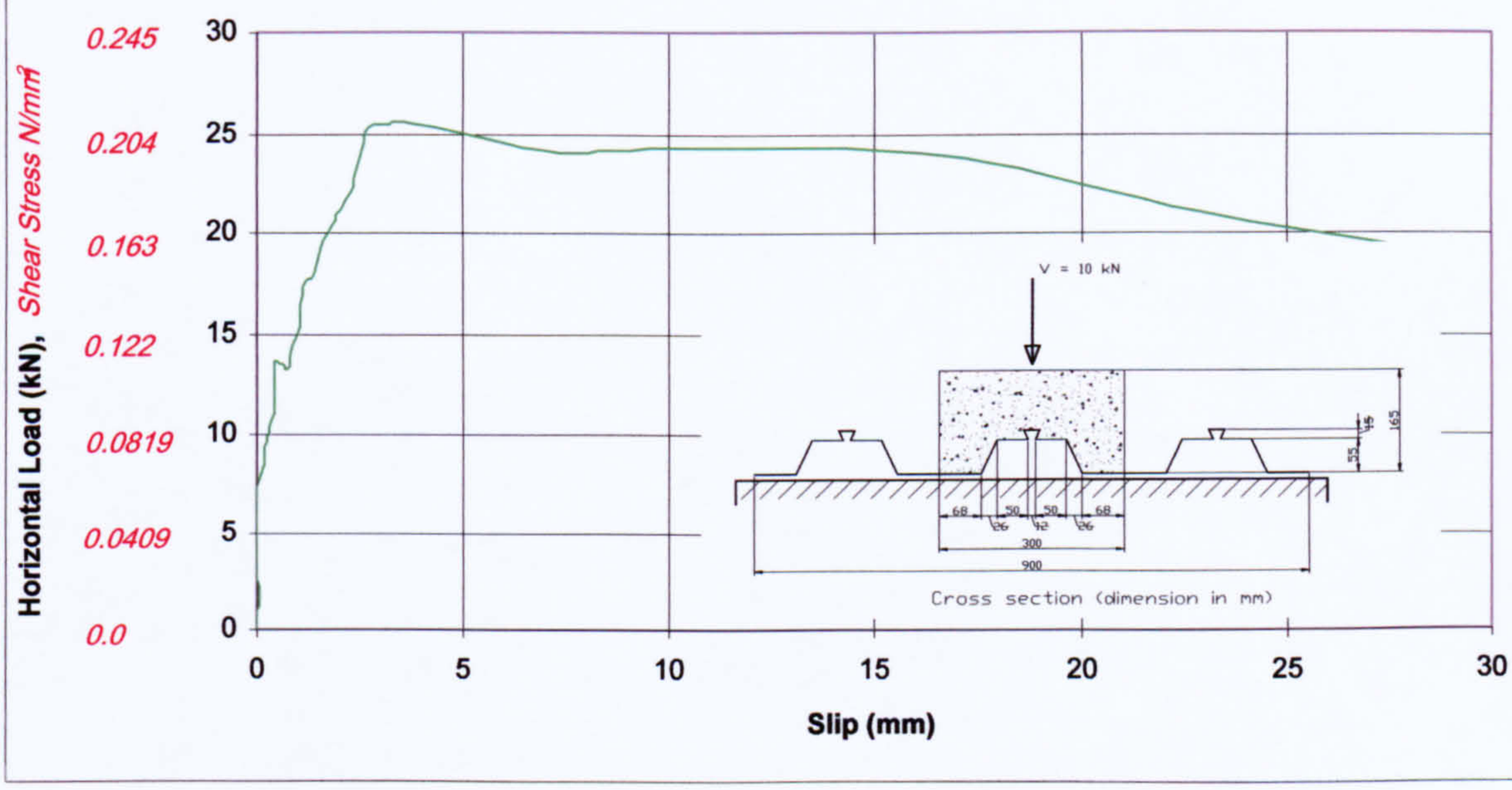

Figure 3.10 Load-Slip behaviour for Composite Slab (Pull-out test No. 3 with vertical load 5 kN)

Shear Stress-Slip curve for Composite Slab (Pull-out test No. 3 with vertical load 5kN)

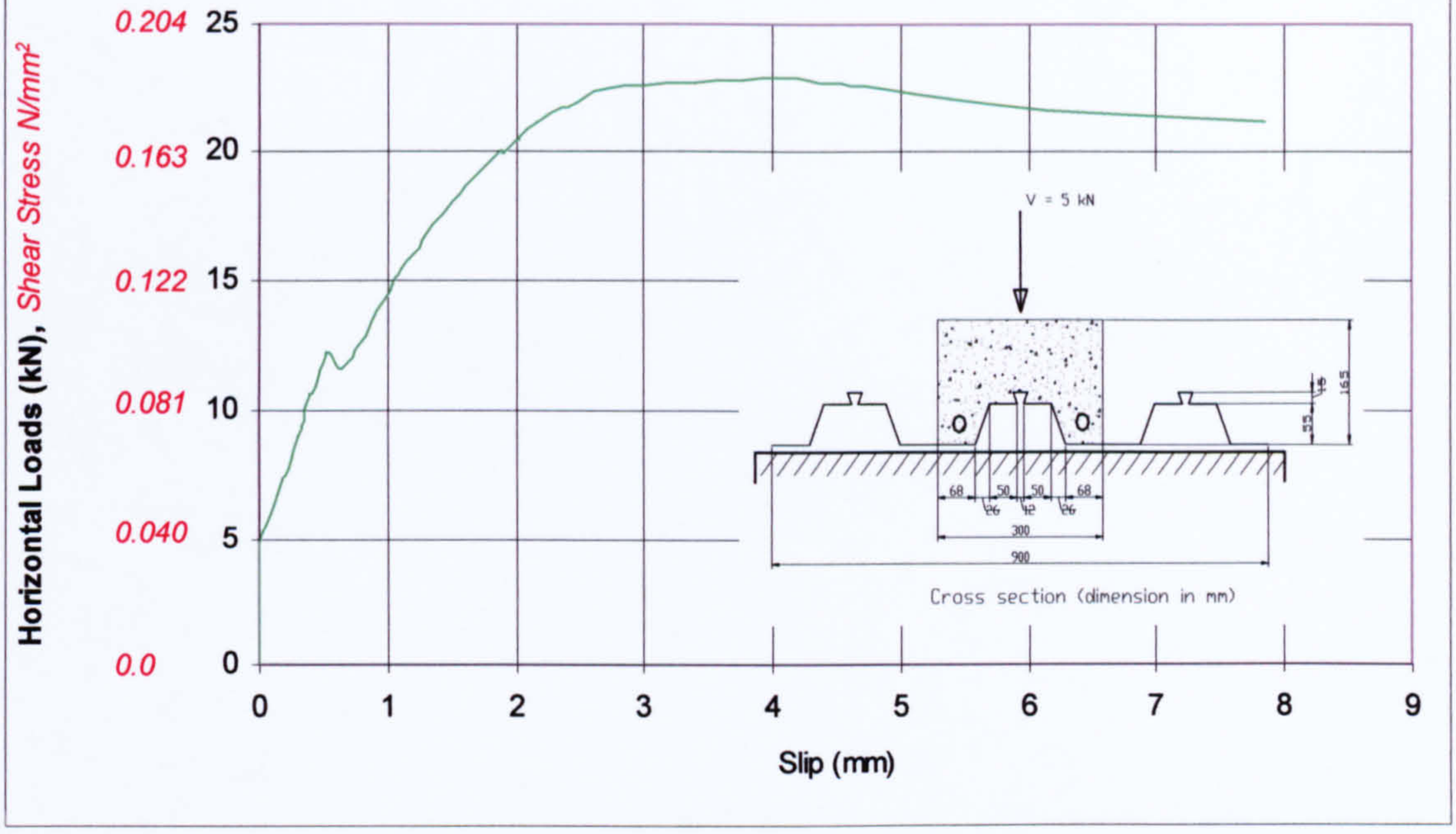

Figure 3.11 Load-Slip behaviour for Composite Slab (Pull-out test No. 4, with vertical load 10 kN)

Shear Stress-Slip curve for Composite Slab (Pull-out test No. 4 with vertical load 10 kN)

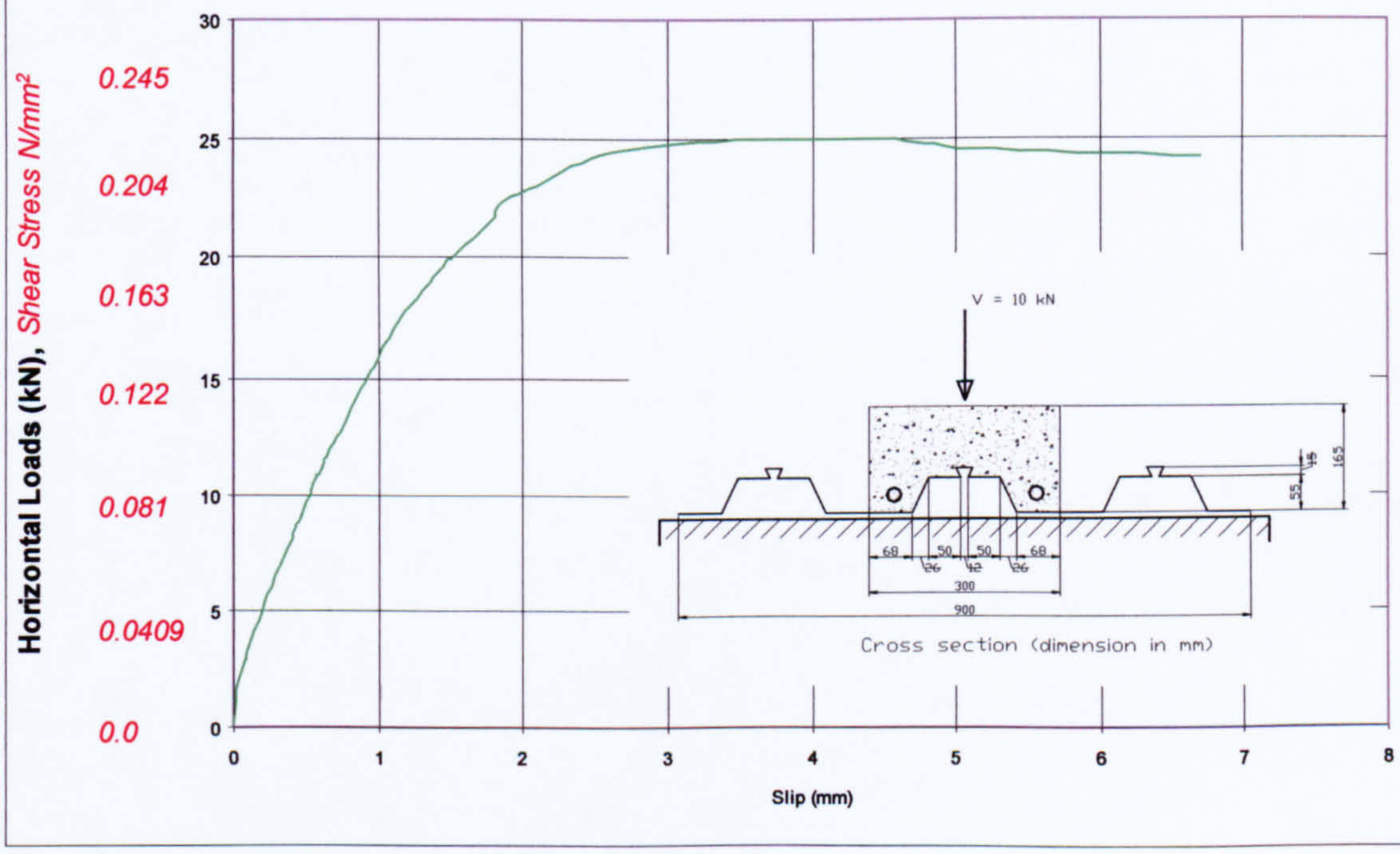

Figure 3.12 Load-Slip behaviour for Composite Slab (Pull-out test No. 5, with vertical load 10 kN)

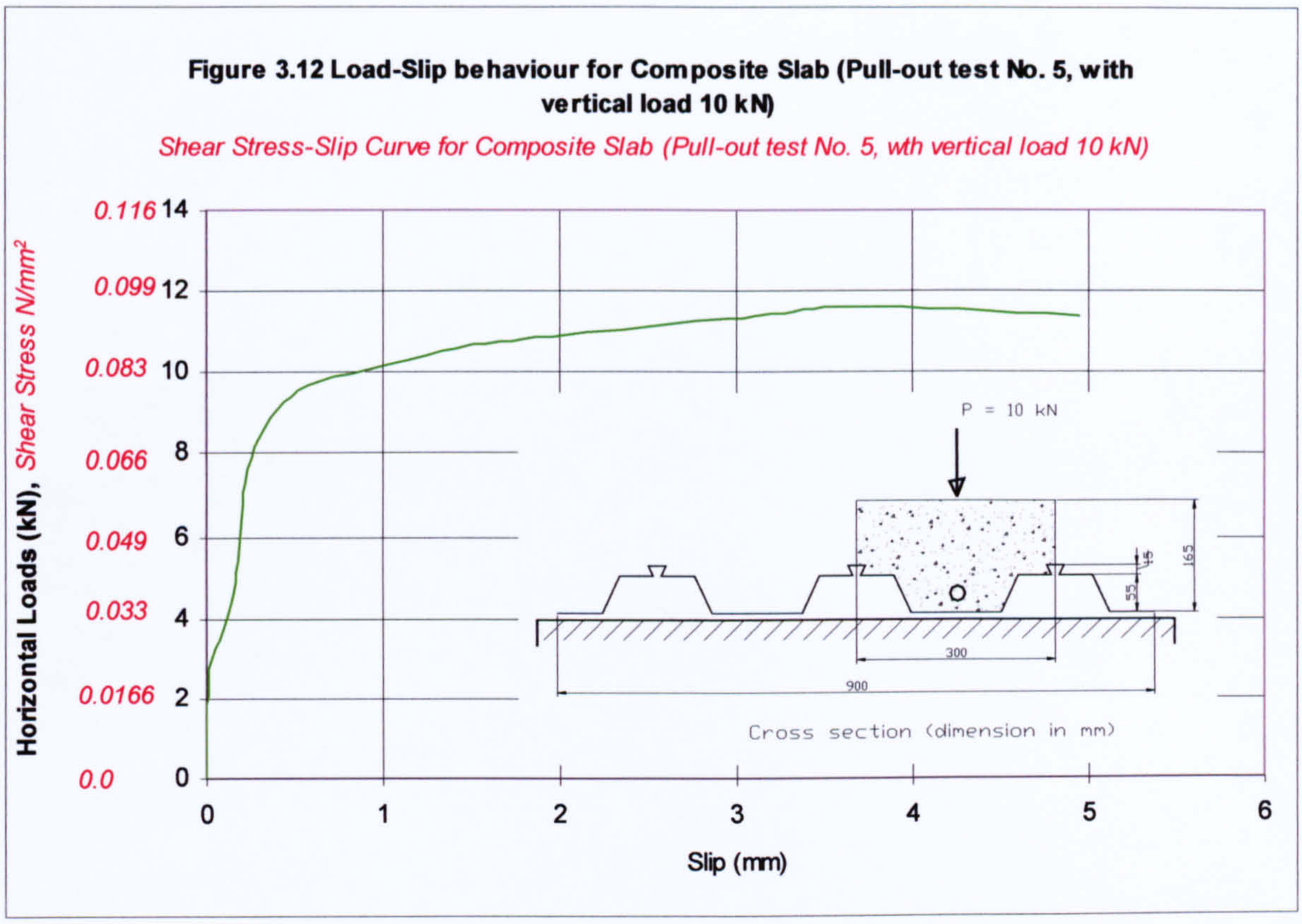

Figure 3.13 Load-Slip behaviour for Composite Slab (Pull-out test No. 6, with vertical load 5 kN)

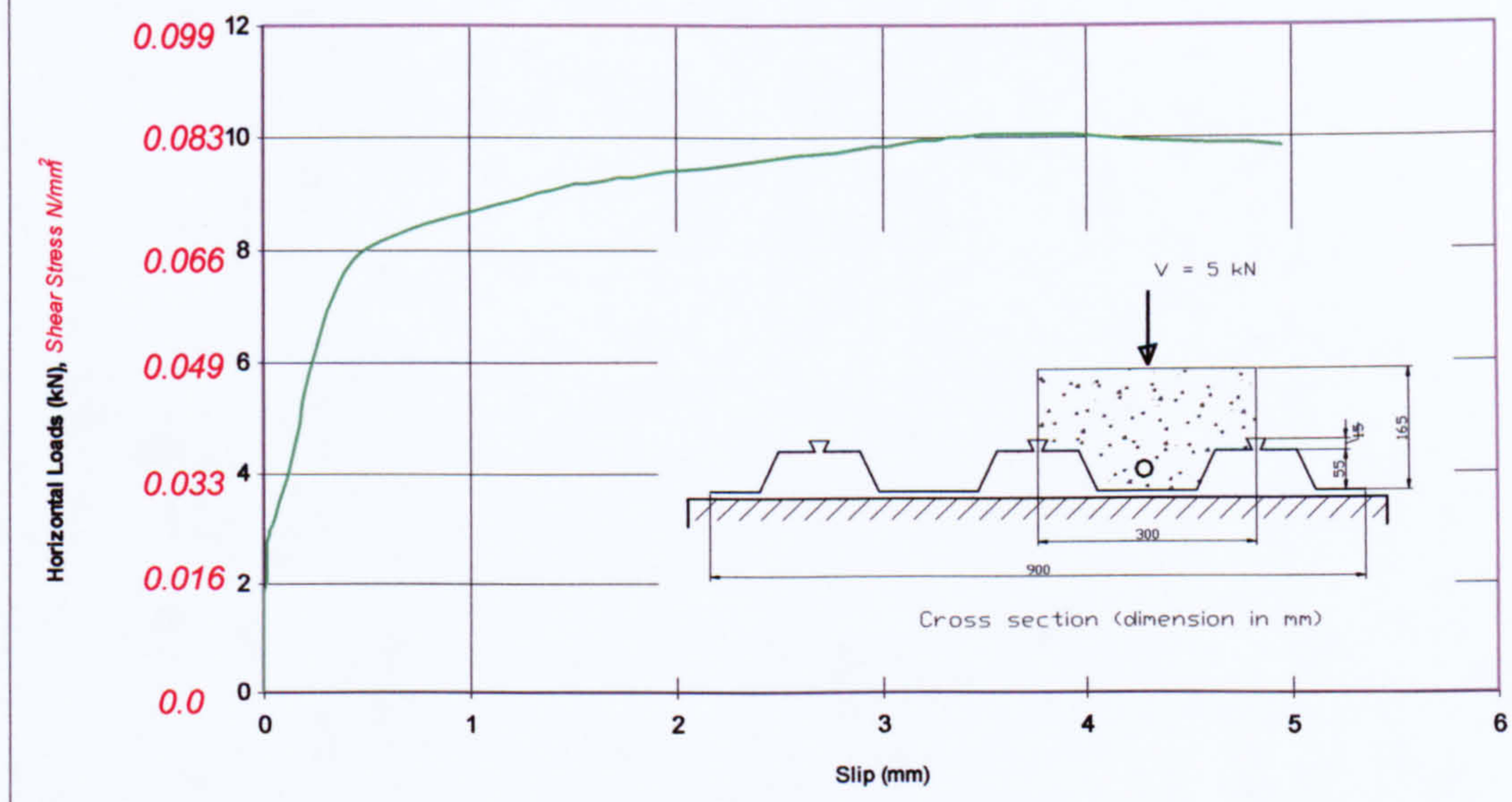

Figure 3.14 Load-Slip behaviour for Composite Slab (Push-off test No. 7, with vertical load 10 kN)

Shear Stress Curve for Composite Slab (Push-off test No. 7, with vertical load 10kN)

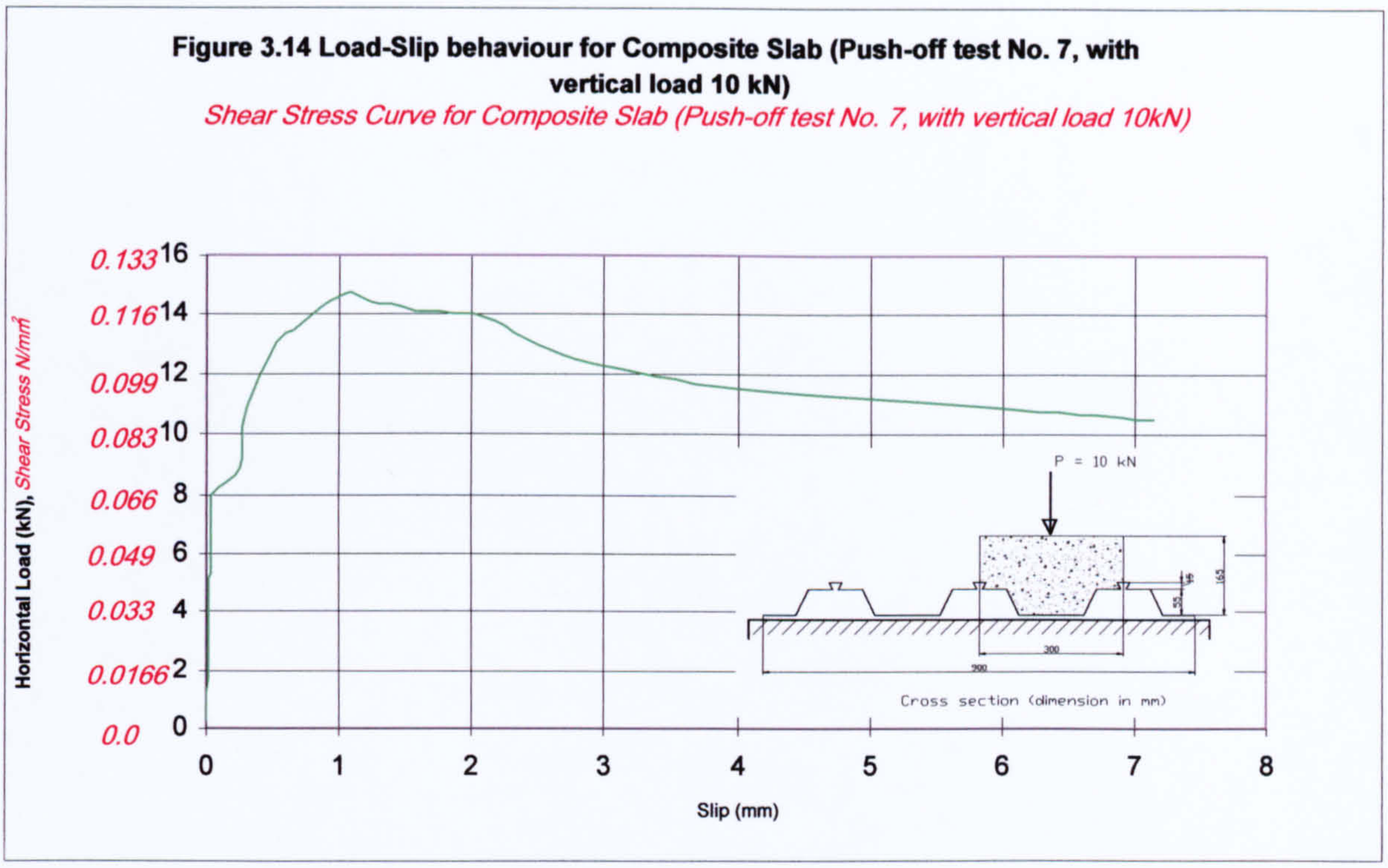

Figure 3.15 Load-Slip behaviour for Composite Slab (Push-off test No. 8, with vertical load 5kN)

Shear Stress-Slip Curve for Composite Slab (Push-off test No.8, with vertical load 5kN)

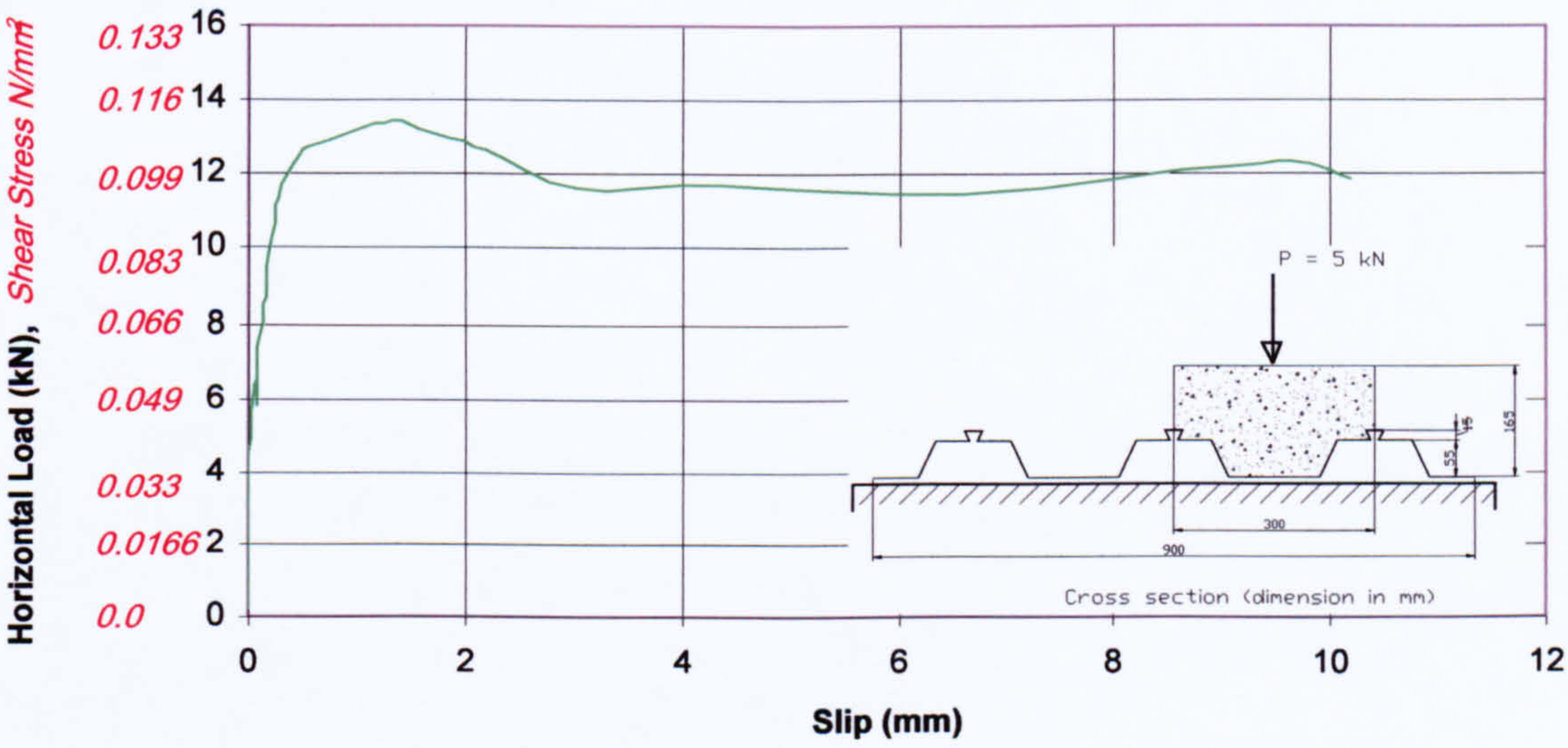

Figure 3.16 Load-Slip behaviour for Composite Slab (push-off test No. 9 with vertical load 20kN)

Shear Stress-Slip Curve for Composite Slab (Push-off test No. 9 with vertical load 20 kN)

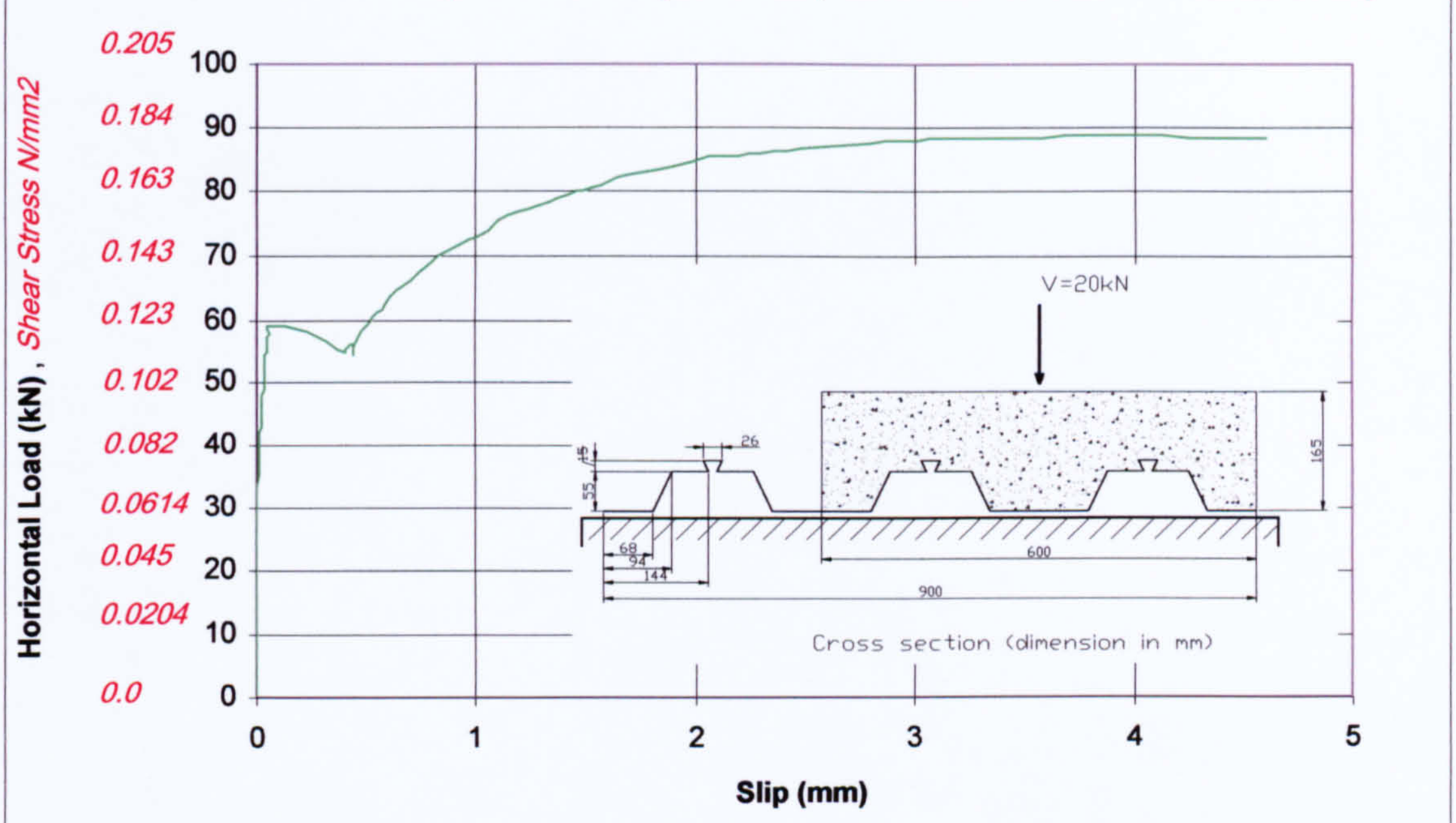

Figure 3.17 Load-Slip behaviour for Composite Slab (Push-out test No. 10 with vertical load 20kN)

Shear Stress-Slip Curve for profiled Composite Slab (Push-out test No. 10 with 20 kN)

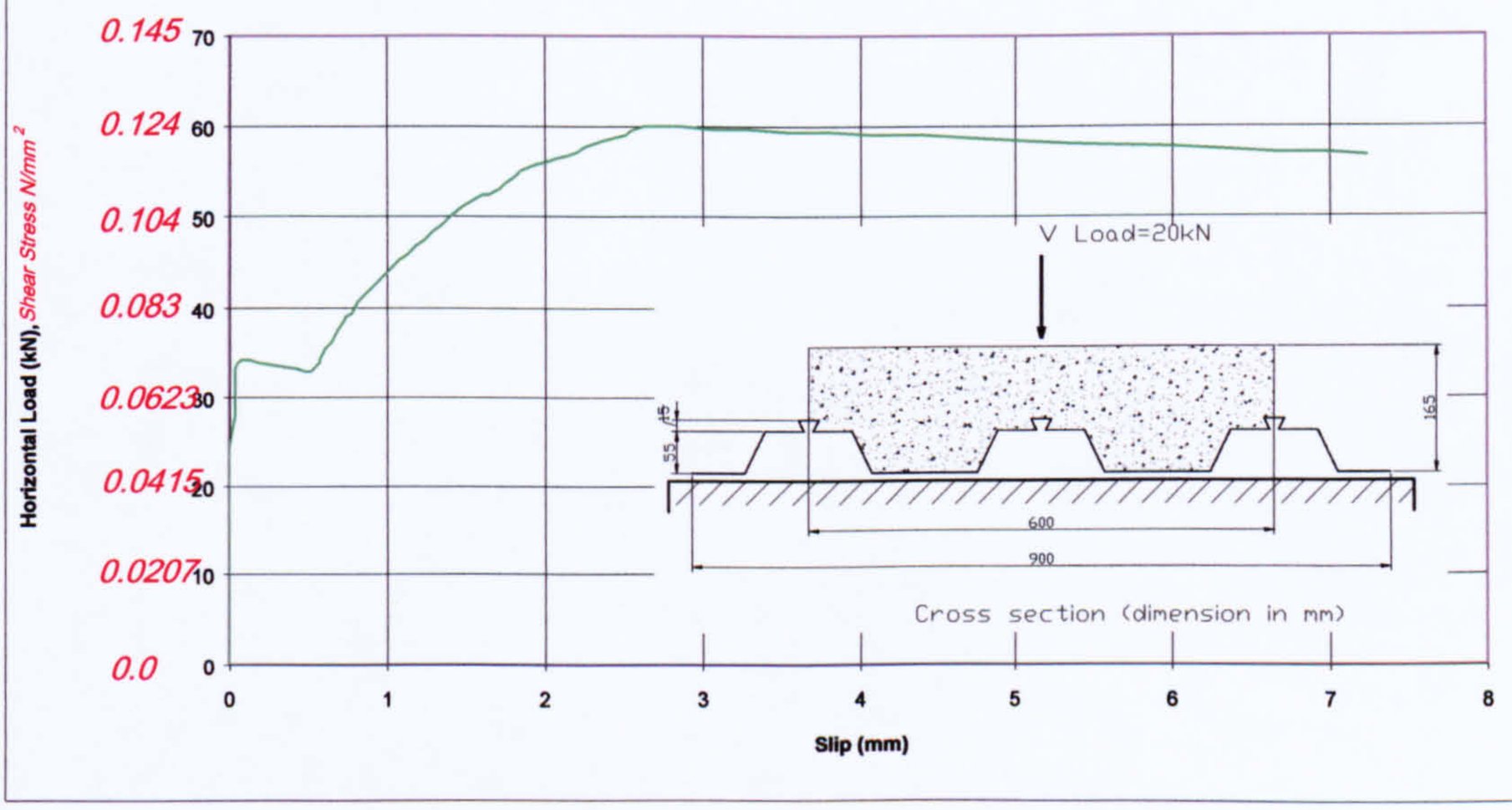

Figure 3.18 Comparison of Push-off test No 1&8 (Load-Slip)

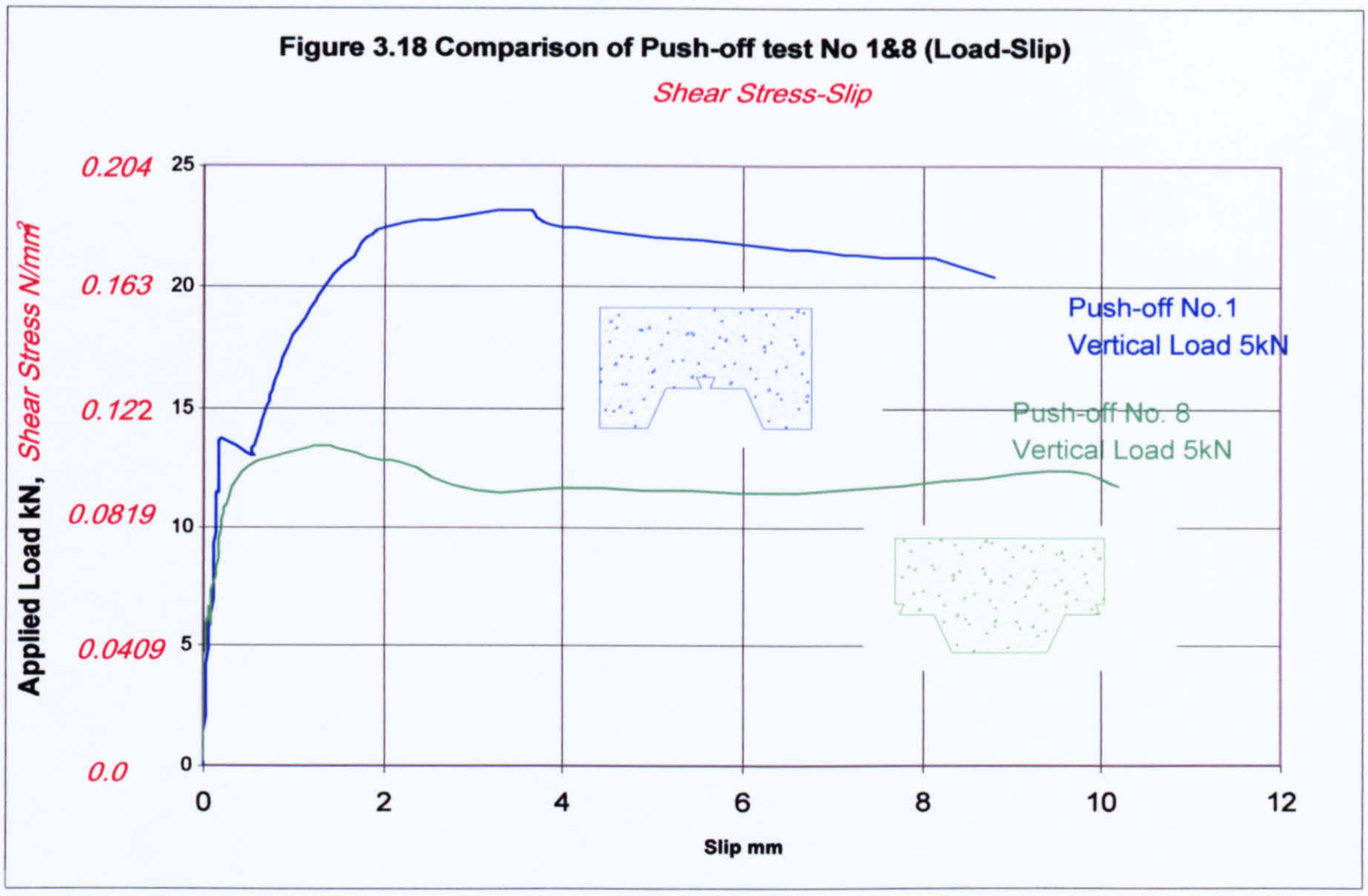

Figure 3.19 Comparison of Pull-out test No. 3&6 (Load-Slip)

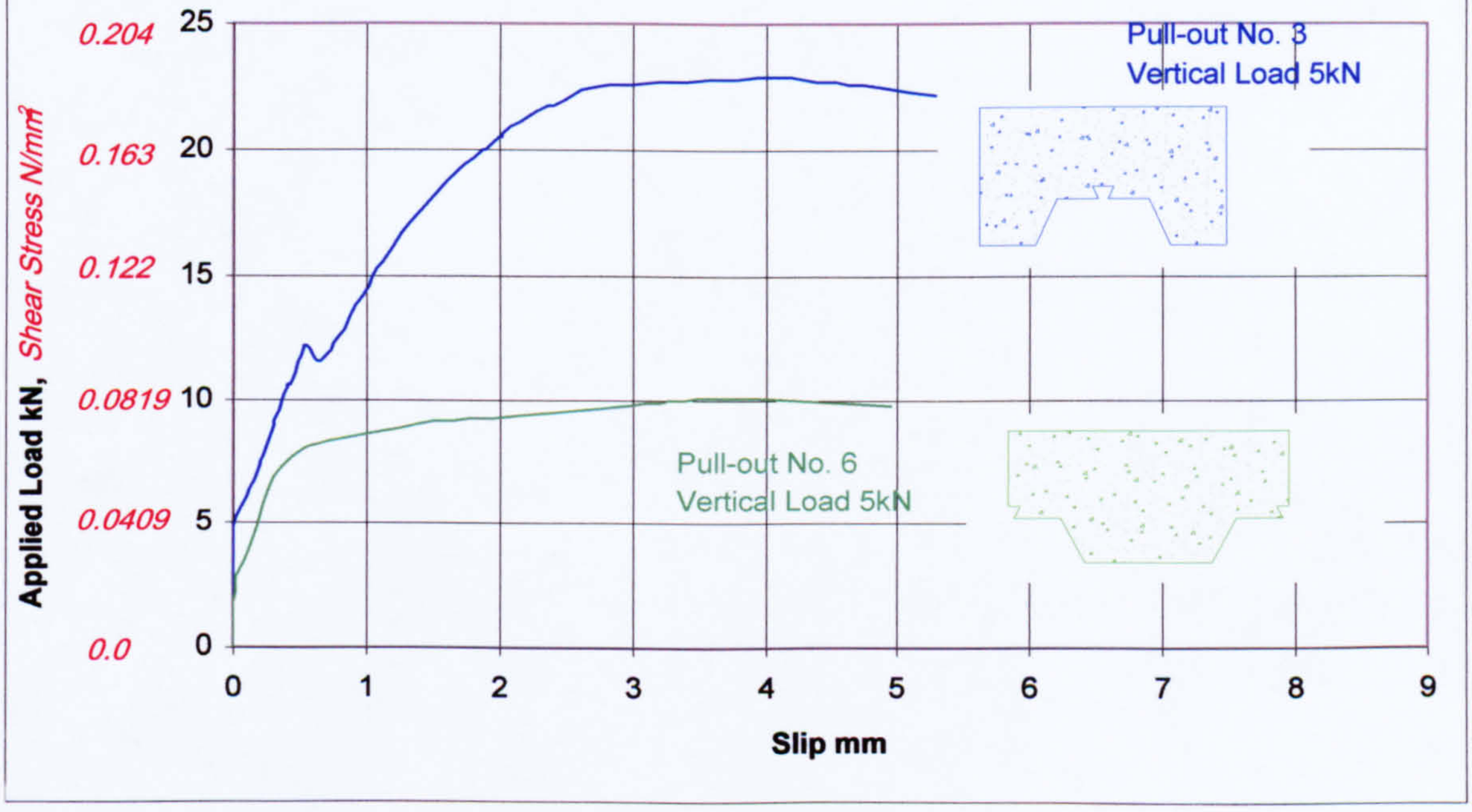

Figure 3.20 Comparison of Push-off test No. 9&10 (Load-Slip)

Shear Stress-Slip

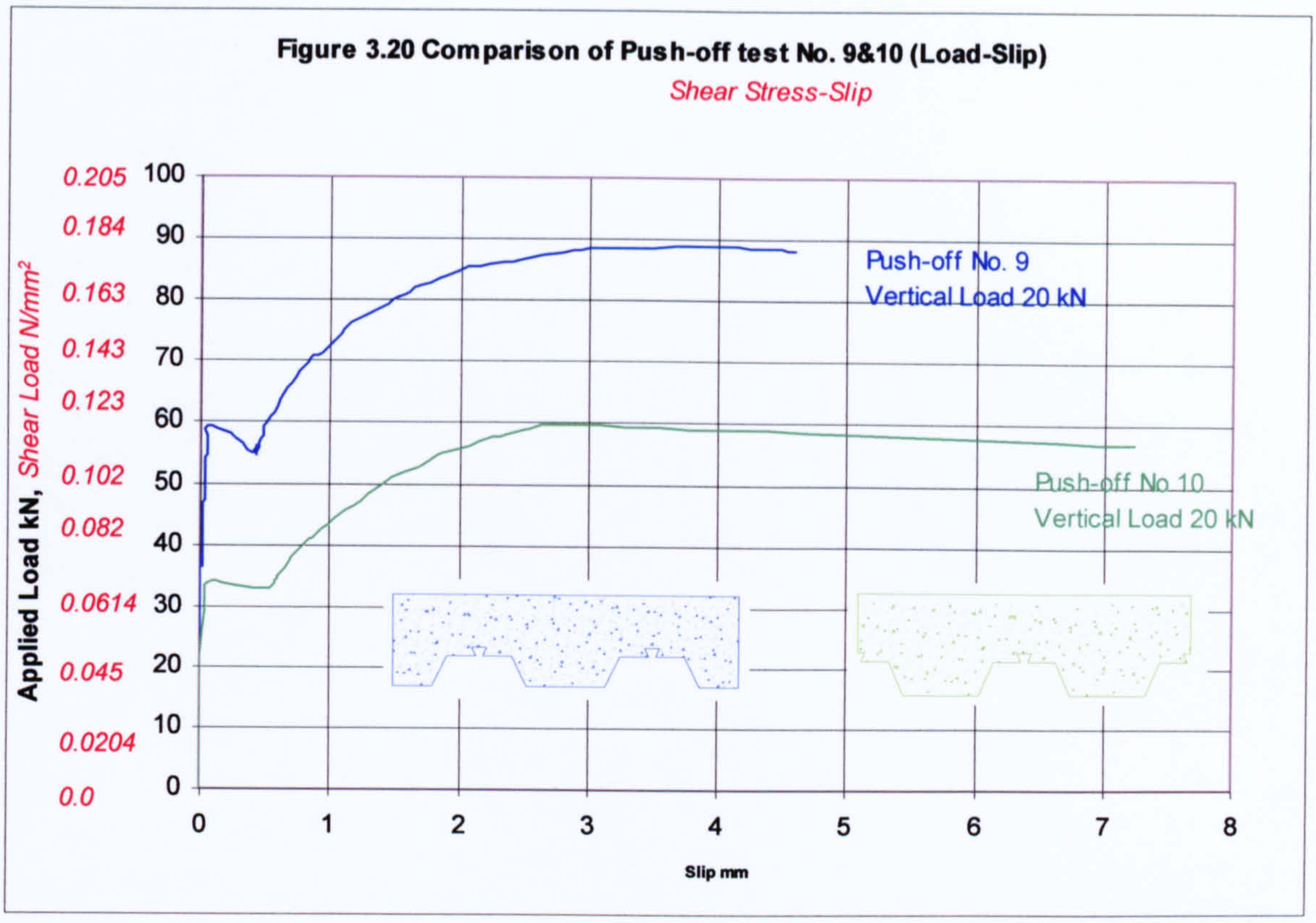

Figure 3.21 Comparison of Push-off Test No. 1&2 (Load-Slip)

Shear Stress-Slip

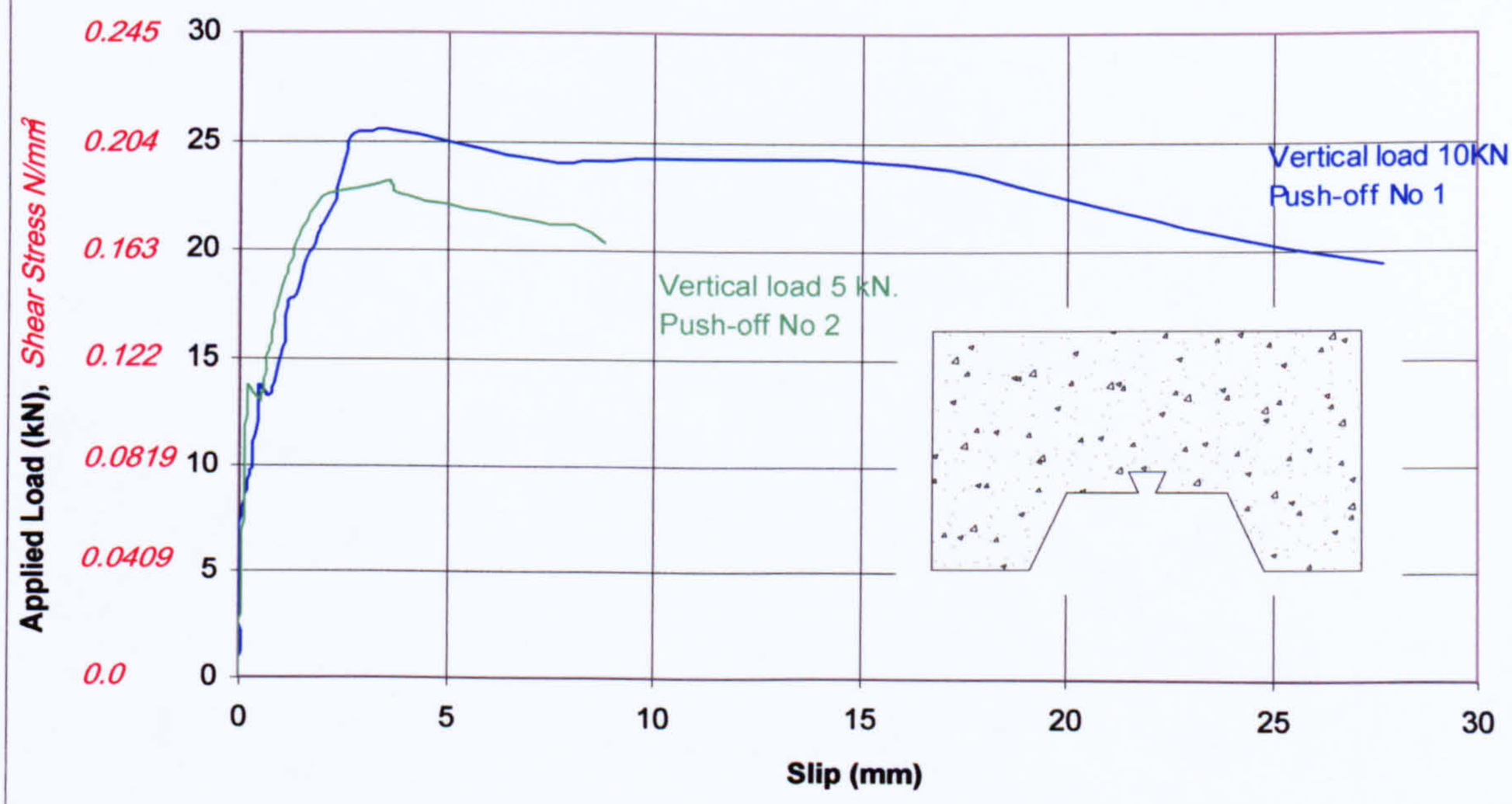

Figure 3.22 Comparison of Pull-out test No. 3&4 (Load-Slip)

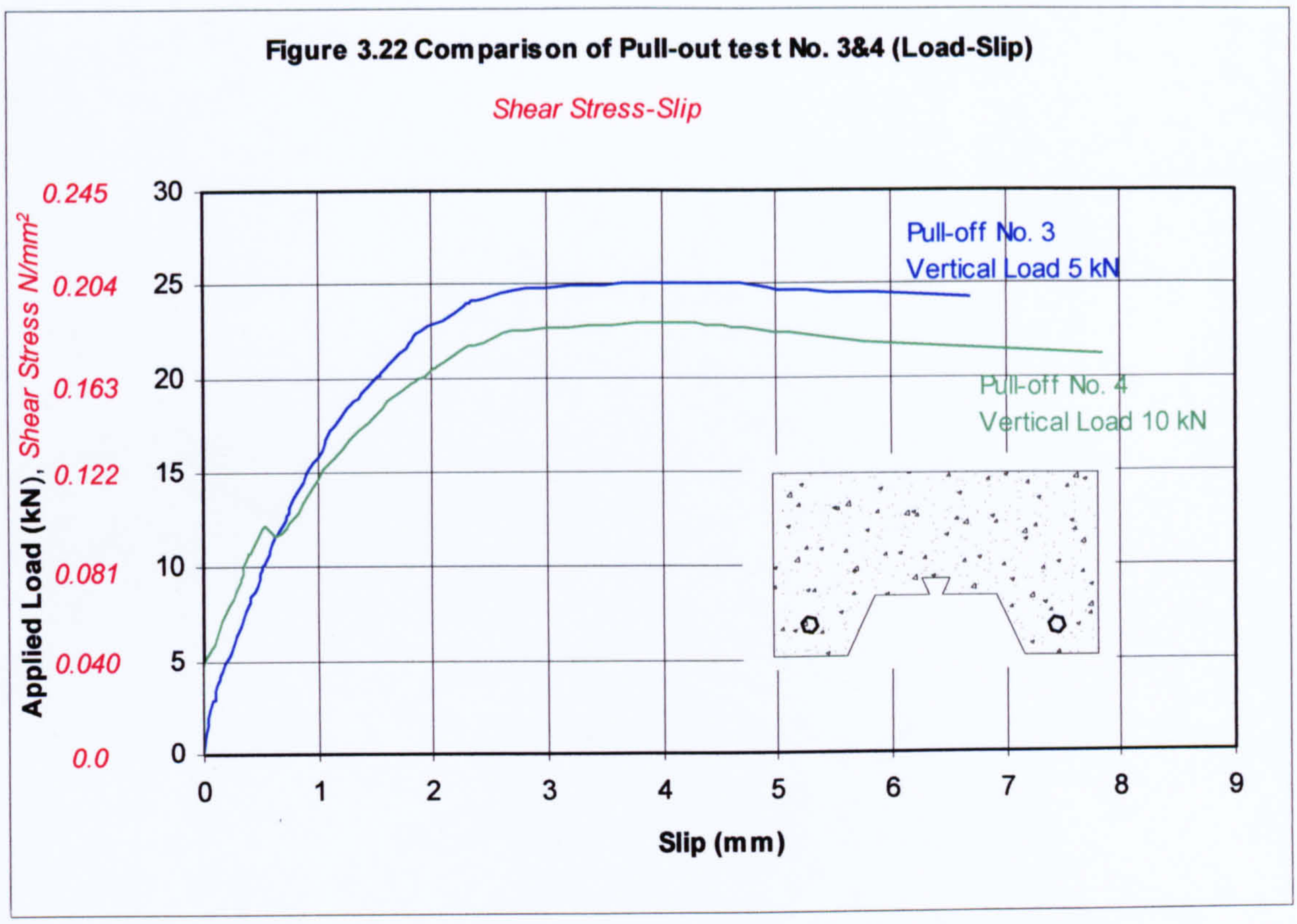

Figure 3.23 Comparison of Pull-out test No. 5&6 (Load-Slip)

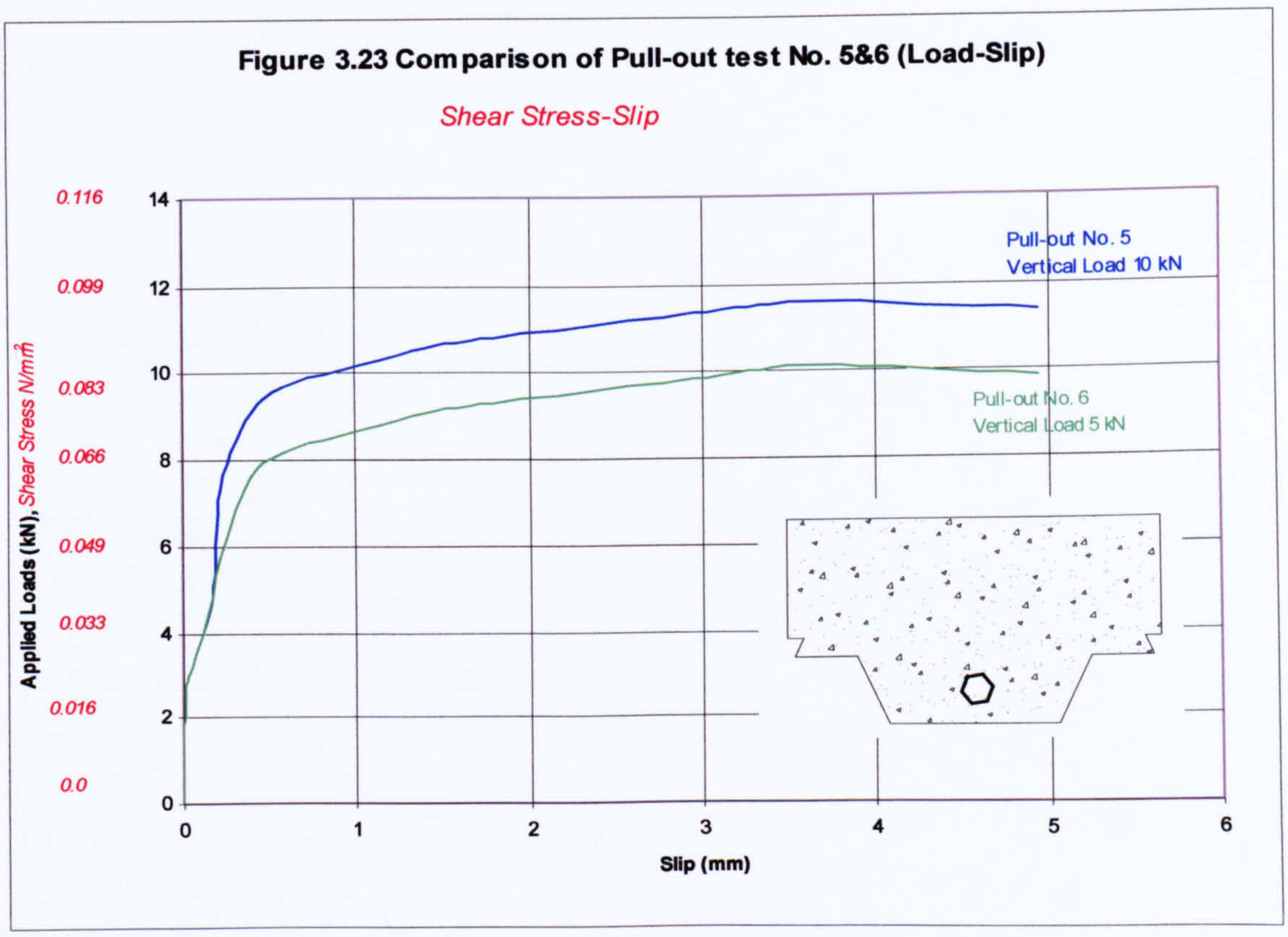

Figure 3.24 Comparison of Push-off test No. 8&7 (Load-Slip)

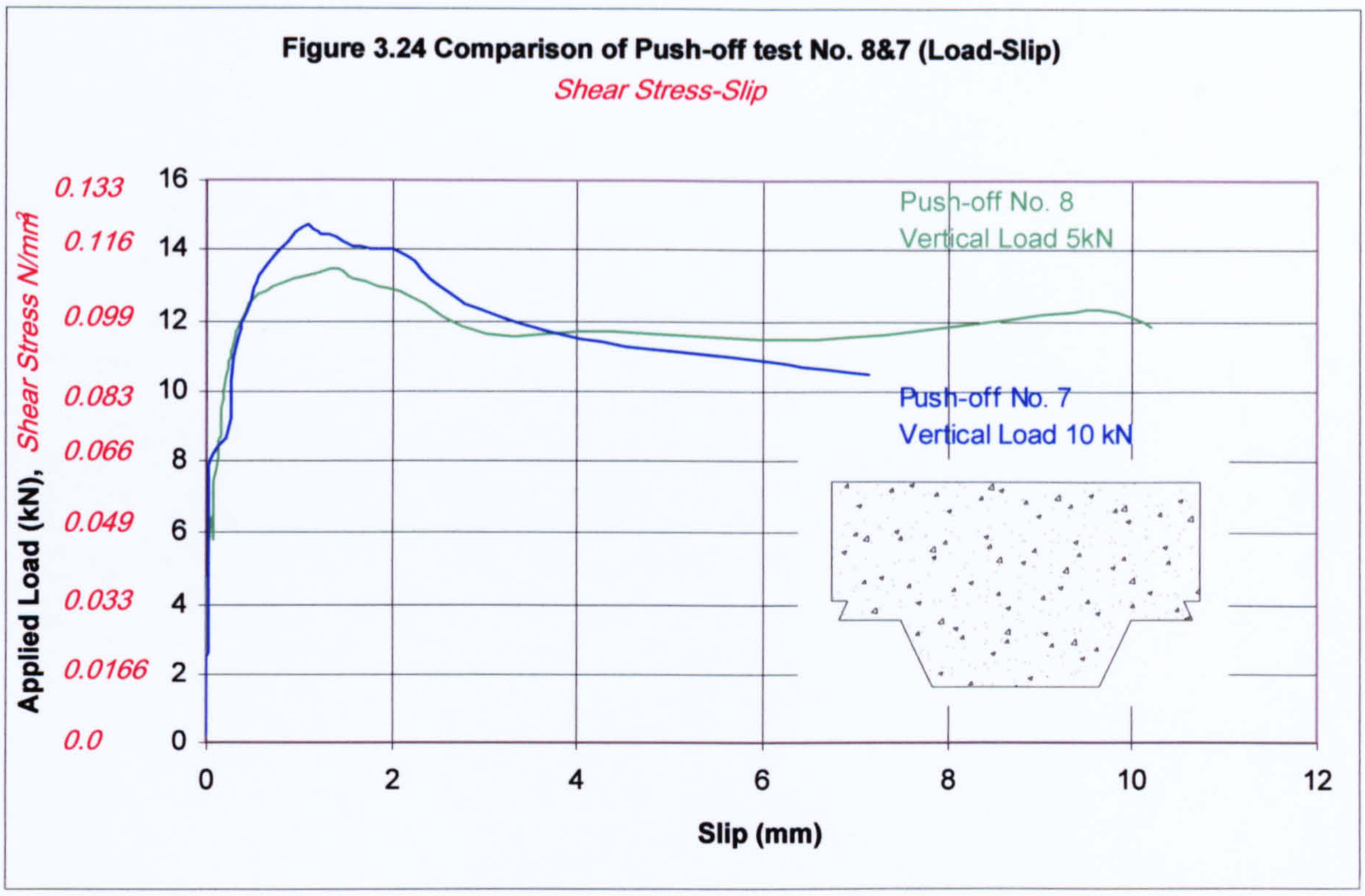

Figure 3.25 Comparison of Push-off test No 1& Pull-out No 3 (Load-Slip)

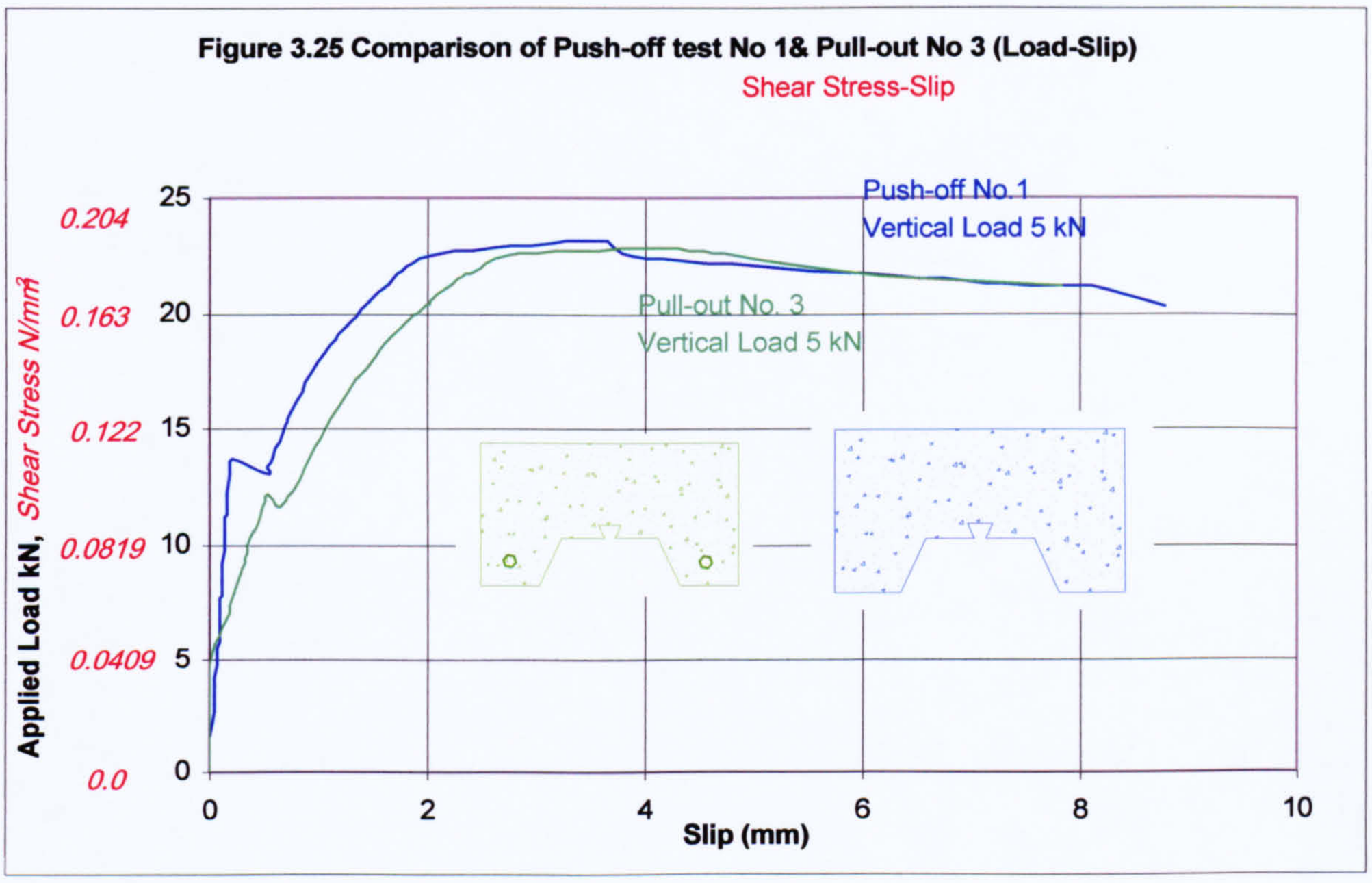

Figure 3.26 Determiniation of frictional coefficient (for the Push-off test)

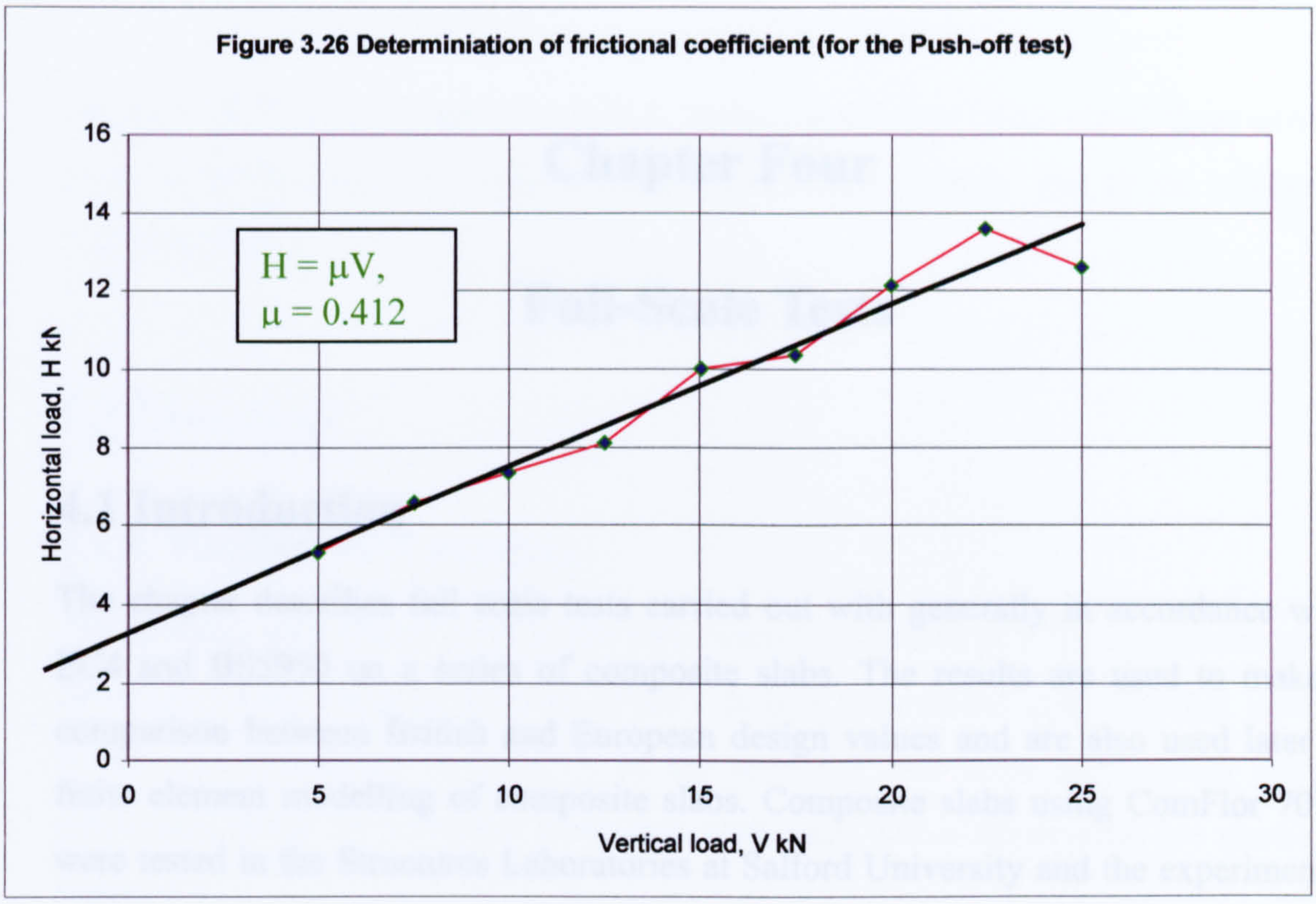

Figure 3.27 Determiniation of frictional coefficient (for the Pull-out test)

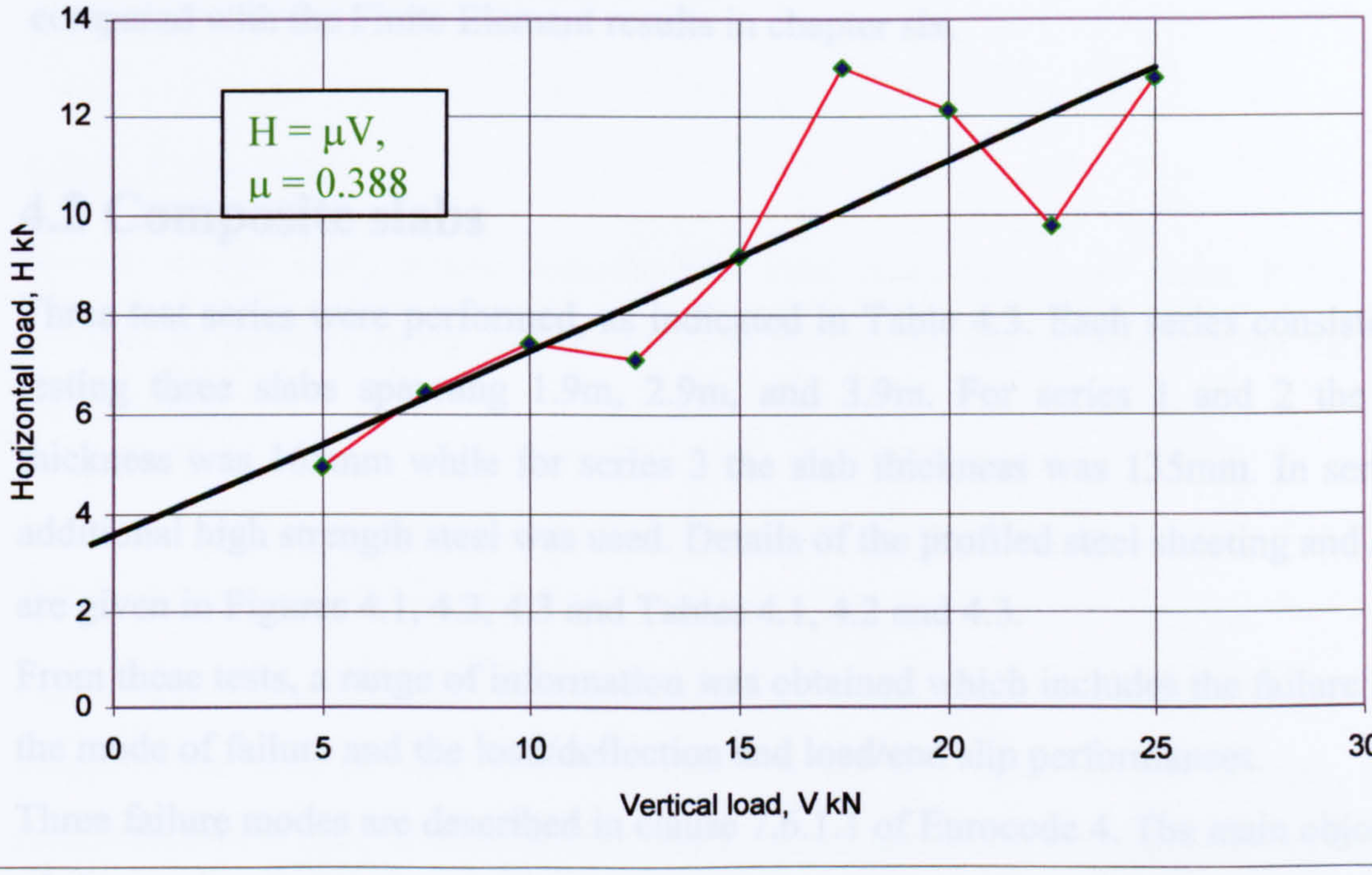

Chapter Four

Full-Scale Tests

4.1 Introduction

The chapter describes full scale tests carried out with generally in accordance with EC4 and BS5950 on a series of composite slabs. The results are used to make a comparison between British and European design values and are also used later in finite element modelling of composite slabs. Composite slabs using ComFlor 70[52] were tested in the Structures Laboratories at Salford University and the experimental evidence obtained is analysed and described in the following sections.

The data obtained in this chapter and the previous chapter (small scale tests) will be used to model the composite slab behaviour using Finite Element Analysis software (ANSYS). The results obtained from the experimental work (in this chapter) will be compared with the Finite Element results in chapter six.

4.2 Composite slabs

Three test series were performed, as indicated in Table 4.3. Each series consisted of testing three slabs spanning 1.9m, 2.9m, and 3.9m. For series 1 and 2 the slab thickness was 165mm while for series 3 the slab thickness was 135mm. In series 2 additional high strength steel was used. Details of the profiled steel sheeting and slabs are given in Figures 4.1, 4.2, 4.3 and Tables 4.1, 4.2 and 4.3.

From these tests, a range of information was obtained which includes the failure load, the mode of failure and the load/deflection and load/end slip performances.

Three failure modes are described in clause 7.6.1.1 of Eurocode 4. The main objective of the study was to determine the resistance to longitudinal shear, so ideally test results should lie in the region 2 of Figure 4.4. As the results subsequently indicate

the mode of failure of composite slabs in series 1 and 3 was longitudinal shear as were those in series 2 after the adjustment for the added capacity due to the additional reinforcement.

4.3 Materials

4.3.1 Profiled steel sheeting

The profiled steel sheets used in the tests were ComFlor70 (CF70) manufactured by Precision Metal Forming Limited (PMF). It is a trapezoidal steel flooring profile, which was introduced in 1991[53]. In the tests 0.9 mm thick steel sheets with a galvanised finish for corrosion protection were used. Other dimensions are shown in Figure 4.5.

The characteristic design strength for the sheeting was taken as 330 N/mm^2. The actual yield and ultimate stresses were found by testing five coupons, cut from the flat parts of the profiled steel sheet. The results obtained are shown in Table 4.1 and 4.2 showing the profiled steel sheeting details.

4.3.2 Concrete

Normal-weight ready mixed concrete was used in all composite slabs. It has good workability during casting. Its strength was monitored, and is shown in the table 4.3 for each test.

4.3.3 Mesh reinforcement

Mesh reinforcement (A142) was used in all the composite slabs. It was placed in the compression zone of slab, leaving a cover of 30 mm from the top of slab. Mesh reinforcement is used to resist strains due to shrinkage and temperature effects.

4.3.4 Additional reinforcement

Two12-mm diameter high strength steel deformed bars were used as an additional reinforcement in slab No.2, slab No.5, and slab No.7. A cover of 30 mm from the bottom and 30 mm from the ends was maintained. The reinforcement was of high strength with a characteristic design strength of 550 N/mm^2. The actual yield strength of the reinforcement was 823 N/mm^2.

4. 4 Casting

Two slabs were cast at a time in a timber mould. The slabs were cast propped, as required by the codes (section 2.4.4), using steel beams at 100mm centres placed below the slabs to prevent any deflection occurring before the concrete hardened. A thin layer of oil was applied to the surface of the vertical timber formwork. The surface of the profiled steel sheet was used in the as-rolled condition, no attempt being made to improve the bond by degreasing the surface.

At each casting, twelve 100 x 100 x 100mm standard cubes and two 150mm diameter,300mm deep cylinders were cast in moulds. All the samples were compacted using a poker vibrator. The day after, they were stripped and left near the slabs to be cured under the same conditions. Cubes were tested to determine the average compressive strength of concrete and its density. Half the cubes and cylinders were used at the beginning of each test, and the other half were used at the end of each test.

For slab Nos.2, 5, and 7, the additional reinforcement was added after placing the profiled steel sheet in the wooden mould. Mesh reinforcement was placed on concrete chairs with the correct cover. Four deformed steel bars 8-mm diameter used as lifting hooks were positioned in the slab to ease transportation from the mould to the testing rig. The concrete was poured and compacted by a poker vibrator. The surface was then tamped and trowelled. Three days later, the slabs were removed from the mould and left nearby for curing before testing.

4.5 Test set-up

Figure 4.6 shows the set-up used for testing the composite slabs. When slabs were ready for testing, having reached the required strength, they were lifted by a crane and positioned as shown in Figure 4.6, the middle of the slab been coincident with the centreline of the jack. All slabs were simply supported. A distance of 100mm was left between the centreline of the supports and the end of the slab (Eurocode 4 requires that the distance between the centre line of the supports and the end of the slab should not exceed 100mm). A system of spreader beams was placed on the slabs so arranged to allow two equal concentrated loads at a distance of span/4 from each support. Fibreboard packing pieces were used between the supports and the lower surface of slabs, and between the spreader beams and the upper surface of slabs.

4.6 Arrangement

The test configuration and loading procedure were according to recommendation of the Eurocode 4. All slabs were simply supported and tested with two symmetrically placed line loads. A single hydraulic jack was used to apply load, which was distributed to the slab through a spreader beam system, which resulted in two line loads being applied to the specimen. It took approximately four to eight days from the start of testing to failure of the slab. Transducers and dial gauges were used to measure deflection and end-slip. Deflection at the mid-span was registered for two points. The end-slip between the steel sheet and the concrete slab was measured at both ends of the slab. The deflections and end-slip were recorded at each loading increment.

4.6.1 Slip gauges

Slip gauges were used to measure the horizontal movement between the profiled steel sheet and concrete. They consisted of one 0.01mm dial gauge and two 0.01mm transducers at each end of slab, which were connected to a computer. They were fixed

on to steel rods in a horizontal position and glued to the lower surface of the steel sheet. Slip gauge positions are shown in Figure 4.7.

4.6.2 Deflection gauges

The instruments used to measure the mid-span deflection consisted of one dial gauge (reading to an accuracy of 0.01mm) and two transducers (0.01mm accuracy). A deflection control transducer was positioned under the slab to measure the mid-span deflection and to control load/deflection as shown in Figure 4.8.

4.7 Test loading procedure

The loading of all slabs was of two types, static loading and dynamic (cyclic) loading. Testing started with static loading applied by the hydraulic jack to the spreader beams, and transmitted to the slab as a two concentrated line loads across the slab width at a distance of span/4 from each support which is equivalent to the uniformly distributed load case (see Figure 2.8, section 2.5.1 in chapter two). The load was increased gradually in small increments (between 1-2 kN), and all the loads and displacement readings were taken at each increment. The load was then reduced to zero.

Dynamic load was applied at a maximum of approximately 0.75 the previous maximum static load. The loading was applied for 5000 cycles in approximately 3.5 to 7 hours.

The static loading was applied to the slab in deflection control. After the first cycle (static and dynamic loading), the load was increased in small increments to a value higher than that reached in the first static loading, then reduced to zero. The load-deflection and load-end slip curves were monitored using the computer when load was increased with a deflection control. A dynamic load followed the static load for 5000 cycles at a maximum of 0.75 the static load.

The specimen was finally loaded to determine the ultimate load. The load was applied from zero kN until failure occurred and reduced automatically to zero. The maximum load was recorded. Generally the failure was characterised by cracking of the concrete and folding or creasing of the steel profile, initially under the line load. The mid-span

deflection was recorded and shown in Figures 4.9-4.17. Horizontal slip at the two ends was recorded at failure, and is shown in Figures 4.18-4.26.

4.8 History of load-deflection behaviour

All slabs were tested under a number of static and dynamic (cyclic) loads applied as a two point loads across the slab width. Figures 4.9 - 4.17 represents the relationship between the applied load and the mid-span deflection. As expected, deflections of span/250 were attained in all slabs. For slabs No 1&2, deflections of span/50 were not attained before failure, although these did reach span/52.

4.9 Load-end slip behaviour

When the chemical bond between the profiled steel sheet and concrete interface in the shear span was broken, initial end slip occurs. Figures 4.18 - 4.26 were plotted using the data recorded by the end slip transducers during static loads. The gaps between the curves represent the increase in end slip caused by the dynamic load, which was applied between two static loads.

All test slabs exhibited end slip. End slip was accompanied by cracks, and increased with the increase in loading. In general, the end slip was greater in slabs with relatively long spans than shorter ones.

4.10 Failure characteristics

The test slabs failed under static loading with deflection control. From table 4.4, it can be seen that as expected composite slabs with shorter spans carried greater loads. Slabs No.1 and 2 behaved normally at span/250 deflection and reached a deflection of span/52 at failure. Cracks and end slips were observed prior to failure in all slabs.

4.11 Slab behaviour during load application

A brief account of the experimental observations for slab No.1 is given below.

Two line loads were applied to the slab of the quarter span points (725mm shear span). The load was first applied from 0 to 20 kN then reduced to 0 kN (static load run 1), followed by a dynamic load (run a) at a maximum load of 15 kN. At these two static and dynamic loads, no visual changes were observed, but there were noises suggesting either concrete cracking or bond breakdown. The load was applied again from 0 to 30 kN then reduced to 0 (static load run 2), followed by a dynamic load (run b) to a maximum of 22.5 kN. The first crack was observed. The static load was applied again from 0 to 40 kN (run3), followed by a dynamic load (run c) to a maximum load of 30 kN. There was no evidence of end slip during the dynamic loading cycles. The end slip which did occur took place during the static loading process. The same procedure was repeated until the static load with deflection control (run 8) was applied to the slab up to eventual failure. When the load reached 96.27 kN, the slab started to fail, and the cracks which developed under the two point loads, increased in size. At the same time, the end slip which had started at 52.41 kN, increased considerably. Then the load started to fall, but the central deflection and end slip continued to increase. The central deflection of span/250 had been attained, but it did not reach span/50. The maximum load reached was 96.27 kN. The maximum-recorded end slip was 6.9mm at the end of the slab.

A similar procedure, applying static and dynamic loads took place with the remaining slabs. For slabs No 6, 7 and 8 there was evidence of end slip during static loading at about the span/250 level, see Table 4.4. From the load deflection graphs, however these was little evidence of increased deflection after this initial end slip. With a poor profile the effect of initial end slip would have been far more pronounced.

4.11.1 Results summary

The overall behaviour of the composite slabs is represented by the curves of load versus mid- span deflection and load versus end-slip, as shown in Figures 4.9 to 4.26. The maximum external load and the load at which the end-slip was observed are listed

in and table 4.4 representing the load of deflections of span/50 (i.e. failure), span/250, (i.e. serviceability) load at first end slip, the amount of end slip at failure load, and the maximum applied load.

Before the end-slip had commenced, there was full interaction between the steel sheet and the concrete slab. Flexural cracks occurred at the mid span area of the slab and the width of the cracks increased with the applied load. It seemed also that the mean spacing of cracks increased with the depth of the slabs. The behaviour of the composite slabs was similar to that of an equivalent reinforced concrete slab until slip occurred at the end of the span. After the initiation of end-slip, the deflection and the end-slip continued to increase with loading, and the stiffness of the slab decreased. The maximum load was achieved when a approximately diagonal crack, had formed either under or near the concentrated load, as shown in Figure 4.27. The primary mode of failure for the slabs was shear bond. The slabs without additional reinforcement clearly failed in this mode while the slabs with additional reinforcement developed end slip at failure and subsequent calculation indicated that the "composite portion" of the slab capacity did not achieve the capacity for full interaction.

The buckling of the steel sheeting was concentrated in the webs. Also, at the final failure the concrete separated almost completely from the steel sheeting.

Figures 4.28 to 4.33 shows the comparison values of deflection, end-slip, to the load between the slabs (compared according to span, depth, and additional reinforcement).

For the majority of the slabs there was no significant evidence of bond breakdown during the dynamic tests. For slabs 7 and 8 there was some slip at a load below the serviceability load (see table 4.4) but inspection of the load/deflection graphs, Figure 4.29 and 4.30, indicates there was no significant change in the stiffness of these slabs until much higher load had been applied. For slab 5 static loads of up to 150 kN have been achieved prior to end slip developing during subsequent dynamic cycle. Again the load/deflection graph, Figure 4.29, indicates no change in stiffness.

Comparison of the applied load with mid-span deflection for the final failure of the composite slabs is shown in figure 4.28 to 4.30. It can be seen for the shortest span the same concrete depth 165mm carried loads of about 43 and 75 kN (16.5 and 43.8

kN/m^2) greater than the other slabs (in figure 4.28). Similarly in figure 4.29 and 4.30 with additional reinforcement, the shortest span carried a greater load than the longer span.

4.12 Regression line

The so-called "Regression Line" (see Appendix C), is a line representing the design relationship for longitudinal shear resistance. Table 4.5 lists all the parameters used to draw the regression line shown in figures C.1 to C.3. The force V_t is the reaction force at the support due to the maximum load including the self-weight of slab and spreader beams, or the load at a deflection of span/50, if this deflection occurs before the maximum load. In each figure mentioned above, an interpolation line for the three points representing three different spans of slabs was drawn. The factor *k* is the value in N/mm^2 at which the line intersects the Y-axis, and the factor m is the slope of the regression line in N/mm^2. A reduced value of m and k is used in design. In this study, in place of three tests in the regions A and B, one test at three spans were used to predict the m and k values. As shown in Figure, the intersect value in the vertical axis represents the k-factor, in N/mm^2, and the slope of the regression line represents the m-factor, in N/mm^2. The values of m an k obtained reduced by 10% according to Eurocode 4, though it is understood that this is a function of the number of tests carried out.

4.13 Evaluation of design loads

Table 4.6 groups the design load values found by testing and by the two methods (m-k & partial shear connection). The values of m and k are the values found from the regression lines but reduced by 10%. From the tests, the distributed failure load equals the failure load including the self weight of slab and spreader beams divided by the actual area of test slab.

Two factors are presented in the Table. The model factor is the ratio of the failure load from the test divided by the design value calculated from the test results

according to the two design techniques. The overall factor is the ratio of the failure load for the tests derived by the two design techniques code values in which all the partial factors of safety have been set to unity. This second factor indicates the closeness of the failure load and its value predicted in the design methods.

4.14 Discussion of results

The behaviour of the test slabs is discussed, and the design loads predicted by the m-*k* method and the Partial Shear Connection method are compared with the design load determined from the tests.

4. 14.1 Slabs behaviour and failure mode

In table 4.4, it can be seen that the maximum failure load exceeded the load causing first recorded end slip by more than 10% for all test slabs, therefore, according to Eurocode 4 clause 10.3.1.5 the behaviour is classified as 'ductile'.

In general, for the shorter spans and greater concrete depths, the maximum applied load is greater. Adding reinforcement to the slabs (slabs No. 2, 5, and 7) reduces the crack widths, and increases the failure load.

All slabs exhibited slip between the sheeting and the concrete before failure. This was measured at the end of the specimen. As slip increased, cracks at the lower surface of concrete also widened. At failure, a major crack formed in the slabs at approximately one-quarter to one-third of the span from the support, which was typical for a failure in longitudinal shear. As previously noted the primary mode of failure for all the slabs was shear bond.

4. 15 Design loads using the m-k method

According to the recommended procedure in Eurocode 4 for composite slabs, analysis was carried out for the test results to determine the slope *m* and intercept *k* of a linear regression line. Three tests for each variable to be investigated or three groups of two tests should be performed.

In fact, only three groups of two tests for each variable were carried out in the first test programme, and one test for each variable were carried out in the second test programme, (the first tests without reinforcement, and the second with reinforcement) as the purpose of this study was to compare the analysis of design loads for various slabs and to provide data for finite element modelling of the slabs.

The maximum design vertical shear resistance $V_{1.Rd}$ for a width of slab b, according to EC4, is calculated as follows:

$$V_{1.Rd} = V_{1.k} / \gamma_{vs}$$

$$= b \,.\, d_p \,[(m \,.\, A_p / b \,.L_s) + k] / \gamma_{vs}$$

where:

m & k: experimentally determined factors.

Ap : effective cross - sectional area of the decking, in mm^2

Ls : shear span length, in mm

b : slab width, in mm

d_p : distance from the top of the slab to the centroid of the effective area of the steel sheeting, in mm.

γ_{vs} : partial safety coefficient, normally taken as 1.25

For the effective area A_p of the steel sheeting the area of embossments and indentations in the sheet has been neglected.

As shown in Figures C.1 – C.2 (in Appendix C), a regression line was drawn and the values of m and *k* were determined. When the values of m and *k* were found for each series, the reduced values (reduced by 10%) were used in calculating the design load for each slab (Appendix C). Table 4.6 shows the values of design loads predicted by the m-*k* method.

As can be seen from Table 4.6, the design loads predicted by the m-*k* method were smaller than those found by testing, which gives a model factor greater than 1.0. The average value of 1.53 is satisfactory from a design stand point. The overall factor with all partial factors set at unity has an average value of 1.15 which indicates a satisfactory reserve of capacity between the actual failure load and predicted theoretical value.

For the composite slabs with reinforcement, see figure C.2 the design values may be obtained for all span between 1.9 m and 3.9 m using the m_r and k_r values for slabs in which at least the area of reinforcement used in the tests is utilised. Alternatively the m_r and k_r values for the un-reinforced slabs may be used to obtain the design load together with the additional load which any added reinforcement provides. The flexural capacity of the "reinforced slab" is calculated as in Table 4.6.a and the additional shear capacity that this represents is added to the "composite capacity". For these tests using this process the range of values for the model factor lay between 1.64 to 1.44 as shown in Table 4.5. These factors are slightly more conservative than the values in Table 4.6 indicating that the contribution of the reinforcement appears to enhance the composite action a conclusion similar to that indicated later in the discussion on the shear connection method values.

4.16 Evaluation of test results according to partial shear connection method in EC4

The test results have been evaluated according to the partial shear connection method, which is an alternative to the m-*k* method. The design shear strength has been obtained.

As previously mentioned, all slabs showed ductile behaviour. Therefore, the partial shear connection method is applicable. Table 4.6 groups the design loads predicted by the above mentioned method. These loads are greater than those predicted by the m-*k* method which means the model factor is lower at an average of 1.34. The average for the overall factor is 1.11 indicating also satisfactory reserve of capacity.

The partial shear connection method is briefly described in chapter two which together with the connection diagram in Figure 2.11 explains the principle of partial interaction. In order to determine the design shear strength at the interface, the connection diagram should be obtained using the following procedure.

4.16.1 Determination of design load

The partial shear connection method used for the calculation is as follows:

1- Knowing

a- thickness of profiled steel sheeting (0.9 mm thick)

b- Distance from plastic neutral axis of steel sheet to its underside (e_p =30.34 mm[given by the manufacturers])

c- The measured yield strength of sheeting, (f_{yp} = 349 N/ mm^2)

The ultimate bending moment of profiled steel, $M_{R.ult}$ can be calculated (see appendix B).

2- The design bending moment of profiled steel sheet, $M_{R.\ design}$ is obtained from the following equation:

$M_{R.\ design} = M_{pa}$

$$= M_{R.ult} \times \frac{0.87 \times f_{dp}}{f_{yp}}$$

where:

f_{dp} = the design strength of profiled steel sheeting

f_{yp} = the measured yield strength of of profiled steel sheeting

3- The ultimate resistance of the composite section $M_{p.Rm}$ using measured strengths has been calculated as follows:

a- The position of the centroidal axis of the steel sheet, e, is determined by taking the sum of each area about an arbitrary datum divided by the total area.

$$e = \frac{\sum A.Y}{\sum A}$$

b- The ultimate force in sheeting is calculated from the following equation

$N_{st} = A_p \,.\, f_{yp} = N_{cf}$ (the ultimate force in concrete)

where

A_p = Area of profile steel

f_{yp} = The measured yield strength of sheeting

c- The value of x (the depth of the stress block for the concrete) is given by:

$$x = \frac{N_{cf}}{f_{cu} \cdot \gamma \cdot b}$$

d- The lever arm Z is given as follow:

$$Z = h_t - \frac{x}{2} - e_p + (e_p - e)\frac{N_{cf}}{A_p \cdot f_{yp}}$$

where

h_t = the total depth of the slab.

e = is the distance from the centroid of the effective area of the steel sheet to its underside.

e_p = is the distance of the plastic neutral axis of the effective area of the sheeting to its underside.

e- Using one of the equations according to the Eurocode 4

$$\mathbf{M = N_c \cdot Z + M_{pr}}$$

where

Bending moment, $M_{pRm} = N_{st} \cdot Z + M_{R.ult}$

4- The maximum bending moment for the test, M_{test} is calculated using the equation:

$$M_{test} = [(\text{max. load} + \text{self weight}) / 2] \times L/4$$

5- The values of M_{pRm}, $M_{R.ult}$, and M_{tes} enable the value of the degree of interaction η_{test} to be determined.

From the maximum applied loads, the bending moment M_{test} at the critical cross-section beneath the point load due to the applied jack load, the dead weight of the slab and the spreader beams is determined. By following the path represented by the dotted

line, a value of η_{test} is known for each test (see Figure B.1 as example).

6- From the calculated M_{test} of each test, the actual degree of connection η_{test} was determined using the M-N_c diagram of each slab. The ultimate shear strength $\tau_{u.test}$ at the interface is given by:

$$\tau_{u.test} = \frac{\eta_{test}.N_{ct}}{b(L_s + L_o)}$$

where

η_{test} = degree of interaction from test results

N_{ct} = full interaction force

b = width of cross-section considered

L_s = shear span (L/4)

L_o = overhang

7- a- The characteristic shear strength $\tau_{u.Rk}$ is given by:

$$\tau_{u.Rk} = \tau_{u.test} \times 0.9$$

The characteristic shear strength $\tau_{u.Rk}$ was taken as a minimum value obtained from all tests reduced by 10%.

b- The design shear strength is the characteristic shear strength divided by the partial safety coefficient γ_v, normally taken as 1.25.

Design shear strength $\tau_{u.Rd} = \tau_{u.Rk} / \gamma_v$

c- Calculating the length for development of full shear resistance, L_{sf}

$$L_{sf} = \frac{N_{ct}}{b.\tau_{u.Rd}}$$

8- Design resistance for full interaction, $M_{p.Rd}$:

a- The value of x is given by:

$$x = \frac{N_{cf}}{f_{cu}.\gamma.b}$$

b- The value of lever arm Z is given by:

$$Z = h_t - \frac{x}{2} - e_p + (e_p - e)\frac{N_{cf}}{A_p . f_{yp}}$$

c- The design resistance for full interaction derived is as follows:

$$M_{p.Rd} = N_{cf} . Z + M_{pa}$$

9- Design resistance for L_x (assumed for $L_x < L_{sf}$, the shear is partial, so the longitudinal shear resistance is critical).

- The force in concrete in compression, N_c is calculated from

$$N_c = b . L_x . \tau_{u.Rd}$$

- The depth of concrete block x obtained from:

$$x = \frac{N_c}{\gamma . f_{cu} . b}$$

- Then the following are calculated

a- Maximum force in steel, $N_{st} = A_p \times f_{dp} \times 0.87$

b- Force in steel in compression $= (N_{st} - N_c)/2$

c- Force in steel in tension $= N_c + (N_{st} - N_c)/2$

d- Force in the upper part of flange, the neutral axis is positioned at a distance, t, in the lower part of flange, depth of flange in compression, the centroid of steel in compression, e_{sc}, and the value of lever arm Z were calculated (see appendix B)

e- The moment about the centroid of the profile steel sheet $M_{p.Rd}$ is obtained.

10- Design loads using partial interaction method:

For two point loads at L/4 from each support, the maximum bending moment M_{Rd} is found from figure B.2 in appendix B.

Then the design load using the following equation

$$M_{Rd} = \frac{WL}{8}$$

where

W is the total design load

L is the span of the composite slab

Appendix A and B show the calculation of two slabs according the partial connection method. Also shown in Appendix B is the calculation of the flexural capacity of the reinforced part of the slab for the composite slabs with additional reinforcement. Assuming complete compatibility of the "reinforced" and "composite" behaviour of these slabs enables the capacity of the reinforced slab to be deducted from the failure load leading to the contribution from the composite slab. Deduction of M_{RC} (the maximum bending moment for the steel reinforcement only) from M_{test} (the maximum bending moment for the slab test) leaves M_{comp} (the maximum bending moment of the composite slab only), which is the strength, associated with the composite slab alone when the contribution of the reinforced concrete slab has been deducted.

In all the cases, the resulting M_{comp} was less than $M_{p.RM}$ which is the flexural capacity for full interaction, and therefore η_{comp} (degree of shear connection for composite slabs with reinforcement with the flexural capacity of the reinforced concrete slabs deducted) values of less than one were found, varying between 0.91 and 0.75. Comparison of these with the tests for the same span, for instance S5 with S4, shows an increase in η for the reinforced case. This may be due to the improved crack control caused by the inclusion of the reinforcement enabling the composite interaction to perform satisfactorily up to a higher load level. There was also some variation on the value of M_{RC} due to the variation in concrete strength.

Table 4.6.a shows the values of η_{comp}, and M_{comp}.

4.17 Conclusions

Nine full-scale composite slabs were tested to failure under two concentrated line loads. Early end-slip occurred before the ultimate load had been attained in all the slabs, but ductile behaviour was observed in the slabs. The test showed differences between the slabs with and without additional reinforcement, as well, the different depth and span of the slabs. The loss of interaction between the steel sheet and the concrete occurred gradually in the slabs without any detrimental effect on the performance of the slabs.

The test results were evaluated by the m&*k* method, and by the partial shear connection method according to the Eurocode 4. The evaluation in accordance with the partial shear connection method in EC4 gives the design longitudinal shear strength.

The design values for the m-*k* method are based on the regression values reduced by 10% and the use of γ_{vs} of 1.25. Hence, the factors in table 4.6 reflect the difference between the design load, the predicted failure load and the actual failure load.

For the partial shear connection method, the analysis is based on the actual measured strengths and hence the factor of safety in table 4.6 would increase when the design strength f_{dp} = 330 N/mm^2 is used. In general, both methods are satisfactory for the prediction of design loads, with an indication, previously discussed, that the m-*k* method is generally more conservative.

The capacity of the composite slabs was calculated by both methods. The comparison of the calculated capacity with actual failure load was expressed by two ratios for both methods. These ratios represent the safety factors for the design model. The safety factors for both procedures were satisfactory with the m&k values slightly more conservative than the partial connection values.

The main conclusions from testing composite slabs with profiled steel sheeting under static and dynamic loading are:

1. Both methods of design (m&k method and Partial Shear Connection method) are satisfactory in predicting the design capacities and the primary mode of failure was shear bond.

2. Testing under static and dynamic loading gave more information on the behaviour of composite slabs after breakdown of chemical bond between steel and concrete.

3. The use of additional reinforcing bars increases the load carrying capacity and ductility. The contribution of the reinforcement is shown in table 4.6.a. Back calculation of the composite indicates that degree of shear connection η_{comp} for the composite slabs with reinforcement was less than one. The effect, however, of the reinforcement was an increase in the degree of connection when the slabs with reinforcement are compared to similar slabs without reinforcement.

4. All slabs reached a deflection of either span/50 or close to it at failure.

5. The calculated results are summarised in Table 4.6, and 4.6.a showing the shear stress according to partial connection method (values between 0.24 to 0.45 N/mm^2). These values are similar to those obtained by Veljkovic[60] (between 0.31 to 0.51), and Li An[61] (between 0.17 to 0.47).

The shear stress calculated in small-scale tests in chapter three was between 0.08 to 0.21N/mm^2. The difference between the full-scale and the small-scale values is significant and requires further study. The curvature experienced in the full-scale test may enhance the longitudinal shear resistance and this together to the manner of load application and differences between test format could give rise to these differences.

Overall the experimental study indicates that both design techniques are valid and that for the slabs with additional reinforcement there is sufficient compatibility to permit the combined action of both the composite and reinforced components of the slabs to be taken into account. The study also furnished all the necessary data for the finite element modelling which follows.

Table 4.1 Tensile Strength of Profiled Steel Sheeting

Specimen No.	Width (mm)	Thickness					Area (mm^2)	Gauge Length (mm)	Yield Load (kN)	Yield Stress (N/mm^2)	Ultimate Load (kN)	Ultimate Stress (N/mm^2)	Gauge Length After failure	% Elong-ation
		Gross (mm)	Coating (mm)			Core (mm)								
			Side 1	Side 2	Total									
1	12.45	0.9	0.02	0.019	0.039	0.861	10.71	50	3.7	354	4.717	440.42	66	32
2	12.46	0.9	0.015	0.019	0.034	0.866	10.79	50	3.836	335	4.709	436.42	67	34
3	12.46	0.9	0.025	0.0123	0.0339	0.8661	10.795	50	3.868	358	4.714	436.68	66	32
4	12.47	0.9	0.021	0.02	0.041	0.859	10.711	50	3.804	355	4.699	438.7	67	34
5	12.47	0.9	0.0183.	0.023	0.0419	0.8681	10.82	50	3.8	351	4.765	440.38	66	32
Average										349		438.52		

Table 4.2 Profiled Steel sheeting details

Slab No.	Thickness t (mm)	Depth h (mm)	Width b (mm)	Young's Modulus (N/mm^2)	Area of Steel A_p (mm^2/m)	Moment of inertia (mm^4/m)	Neutral Axis e_p (mm)
1-9	0.9	70	900	202777	1166	570000	30.34

Table 4.3 Slab Details

Slab No.	Span length L (mm)	Total Length L_t (mm)	Depth h_t (mm)	Width b (mm)	Cross-section Area of reinforcement A_s (mm^2)	Casting date	Starting date testing	Unit weight of concrete kN/m^3	Concrete Self weight Plus Spreader Beams kN	Concrete strength at failure (N/mm^2)
S 1	2900	3100	165	900	0.0	9/7/98	5/8/98	23.79	10.01	44
S 2	2900	3100	165	900	226.2	9/7/98	13/8/98	23.79	10.01	44
S 3	2900	3100	135	900	0.0	31/7/98	24/8/98	23.18	7.8	26
S 4	1900	2100	165	900	0.0	31/7/98	28/8/98	23.18	6.84	26
S 5	1900	2100	165	900	226.2	27/8/98	9/9/98	23.229	6.9	27.9
S 6	3900	4100	135	900	0.0	27/8/98	16/9/98	23.229	8.53	27
S 7	3900	4100	165	900	226.2	18/9/98	30/9/98	23.36	12.7	27
S 8	1900	2100	135	900	0.0	18/9/98	6/10/98	23.36	5.68	29
S 9	3900	4100	165	900	0.0	28/9/98	12/10/98	22.79	12.42	20

Notes,

Slabs No. 1, 4, and 9 are the first test series.

Slabs No. 2, 5, and 7 are the second test series with additional reinforcement.

Slabs No. 3, 6, and 8 are the third test series.

Table 4.4 Test Results:

Slab No.	Span (mm)	Load at deflection of span/250 (kN)	Load at first End slip (kN)	Load at deflection of span/50 (kN)	Maximum Applied Load (kN)
S 1	2900	50.2	52.41	* (95.3)	96.27
S 2	2900	82.0	90.8	* (192.7)	192.7
S 3	2900	29.1	30.6	70.6	71.3
S 4	1900	79.4	86.5	138	138.2
S 5	1900	104	**150	212	258.6
S 6	3900	19.7	19.7	55	57.3
S 7	3900	40	33.5	112.2	126.3
S 8	1900	51	36.3	98	100.18
S 9	3900	28	38.2	62.9	64.19

Notes:

1- All loads generally reached a deflection of span/50 (before maximum load was attained).

2- * = Deflection of span/50 was not reached. Values quoted are for span/52

3- Concrete self weight plus spreader beams were not added.

4- ** Dynamic loading D (see Figure 4.22) caused first end slip

Table 4.5 Regression line values:

Slab No.	V_t (N)	$V_{t"Rc"}$ (N)	$V_{t"Comp"}$ (N)	L_s (mm)	b (mm)	d_p (mm)	$\frac{A_p}{b.L_s}$	$\frac{V_t}{b.d_p}$	Design capacity using m_r,k_r w_{design} (kN/m^2) (Table 4.6)	Additional design capacity for "reinforced slab" w_r (kN/m^2)	Overall capacity $w_o=w_{design}+w_r$ (kN/m^2)	$\frac{w_{failure}}{w_o}$ ****
S 1	53140	----	----	752	900	134.66	0.00178	0.438	26.20	----	----	----
S 2	101335	32270	68700	752	900	134.66	0.00178	0.836	26.20	21.19	47.39	1.64
S 3	39200	----	----	752	900	104.66	0.00178	0.416	----	----	----	----
S 4	72420	----	----	475	900	134.66	0.00272	0.597	54.55	----	----	----
S 5	109420	48420	60970	475	900	134.66	0.00272	0.902	54.55	48.22	102.77	1.52
S 6	31765	----	----	975	900	104.66	0.001328	0.337	----	----	----	----
S 7	62450	23480	38970	975	900	134.66	0.001328	0.515	16.00	11.42	27.42	1.44
S 8	51840	----	----	475	900	104.66	0.00272	0.550	----	----	----	----
S 9	37660	----	----	975	900	134.66	0.001328	0.310	16.00	----	----	----

Notes:

V_t is the reaction force at the support due to the maximum load at deflection of span/50 if this deflection occurs before maximum load.
L_s is the shear span, which equals span/4.
d_p is the vertical distance from top of slab to the centroid of the steel profile.
b is the average width.
A_p is equal 1166 mm^2
$V_{t"Rc"}$ Experimental shear force for the "reinforced slab"only
$V_{t"Comp"}$ Experimental shear force for the "composite slab" only
**** See Table 4.6

Table 4.6 Shear strength and design load values using m-k method & partial connection methods

Slab No.	m (N/mm^2)	k (N/mm^2)	m_r (N/mm^2)	k_r (N/mm^2)	s.w (kN)	Total failure load from testing (jack load plus s.w) (kN)	Distributed failure load from testing per width of specimen (900mm) (kN/m)	Distributed failure load from testing per metre width $w_{failure}$ (kN/m^2)	Design capacity based on shear bond capacity per metre width (kN/m^2)		Model factor		Overall factor ++			
									m-k method w_{design}	Partial connection method w_{design}	m-k method $\frac{w_{failure}}{w_{design}}$	Partial connection method $\frac{w_{failure}}{w_{design}}$	m-k method Ratio	$w_{max.}$	Partial connection method Ratio	$w_{max.}$
S1	169	0.12	152	0.11	10.0	106.28	36.90	40.72	26.2	28.70	1.55	1.42	1.12	36.38	1.07	37.90
S3	169	0.12	152	0.11	7.8	79.10	27.27	30.30	20.35	26.36	1.49	1.14	1.08	28.00	1.06	28.66
S4	169	0.12	152	0.11	6.84	145.04	76.33	84.81	54.55	67.30	1.55	1.30	1.11	75.80	1.07	97.06
S6	169	0.12	152	0.11	8.53	65.83	16.88	18.75	12.44	14.11	1.51	1.33	1.08	17.28	1.06	17.66
S8	169	0.12	152	0.11	8.53	105.86	55.72	61.90	42.40	44.53	1.46	1.40	1.05	58.92	1.05	59.21
S9	169	0.12	152	0.11	12.4	76.61	19.64	21.82	16.00	17.04	1.36	1.30	1.07	20.24	1.06	20.6
S2	257	0.28	231	0.22	10.0	202.71	69.90	77.66**(52.90)**	44.36	49.51	1.75	1.57	1.39	37.90	1.21	43.50
S5	257	0.28	231	0.22	6.9	265.5	139.73	155.3**(98.65)**	89.92	97.89	1.72	1.59	1.39	70.78	1.28	77.00
S7	257	0.28	231	0.22	12.7	139.0	35.64	39.6**(26.26)**	27.7	32.66	1.42	1.21	1.05	25.12	1.09	24.00
										Average value	**1.53**	**1.34**	**1.15**		**1.11**	

s.w = self-weight plus spreader beams
Overall factor = partial safety factors taken as unity.
++ Use of unit safety factors leads to $w_{max.}$ (kN/m^2) for m and k method and partial connection method and ratios $w_{max.}/w$ (where w is the failure load predicted by the design methods with unit load factors).
(--) "Shear bond" capacity after deduction of contribution of "reinforced slab" (see Table 4.6a).

Table 4.6.a Calculation of shear stress according to partial interaction theory, compared with the shear stress from the small-scale tests.

Slab No. (full-scale)	Span (mm)	M_{test} (kN.m)	M_{Rc} (kN.m)	M_{comp} (kN.m)	$M_{p,RM}$ (kN.m)	M_{pa} (kN.m)	η_{test} (full scale)	η_{comp} (full scale)	$\tau_{u,test}$ (N/mm^2) (full-scale)	Test No. (small-scale)	τ (N/mm^2) (small-scale)
S1	2900	38.52	----	----	55.20	7.76	0.69	----	0.34	1	0.19
S3	2900	29.47	----	----	42.46	7.76	0.69	----	0.34	2	0.21
S4	1900	34.39	----	----	53.44	7.76	0.64	----	0.45	3	0.18
S6	3900	32.09	----	----	42.62	7.76	0.75	----	0.28	4	0.21
S8	1900	25.14	----	----	42.90	7.76	0.58	----	0.41	5	0.09
S9	3900	37.34	----	----	57.72	7.76	0.64	----	0.24	6	0.08
**S2	2900	73.48	23.4	50.1	55.20	7.76	1.33	0.91	0.65(0.45)	7	0.12
**S5	1900	63.05	23	40	53.74	7.76	1.17	0.75	0.83(0.53)	8	0.11
**S7	3900	67.76	22.9	44.7	53.60	7.76	1.26	0.84	0.47(0.31)	9	0.18
										10	0.12

** the composite slabs with high strength steel reinforcement.

η_{comp} degree of interaction for the composite slabs with reinforcement with the flexural capacity of the "reinforced concrete" deducted.

M_{Rc} the maximum bending moment for the "reinforced slab" only.

M_{comp} the maximum bending moment for the composite slab only

( ) represents $\tau_{u,test}$ values using η_{comp}

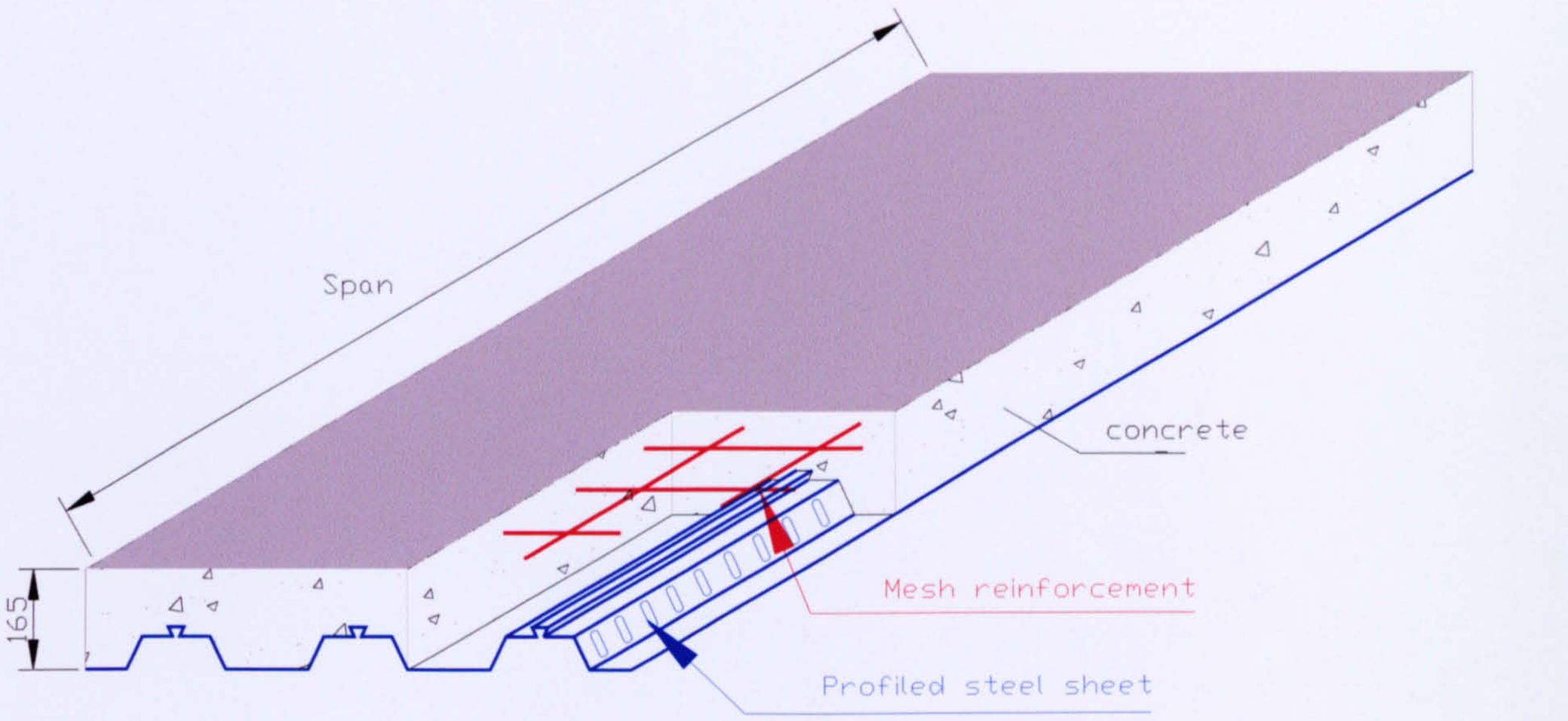

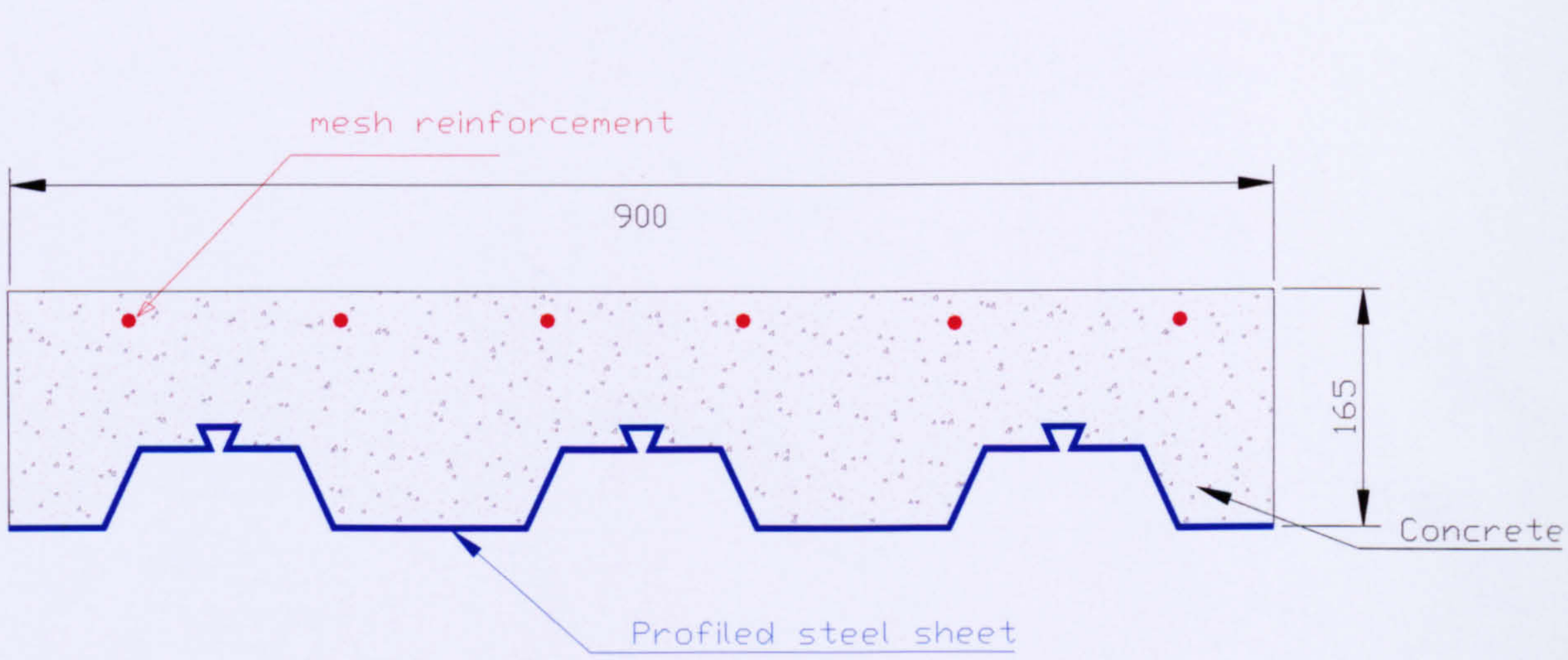

Figure 4.1 First series of composite slab tests

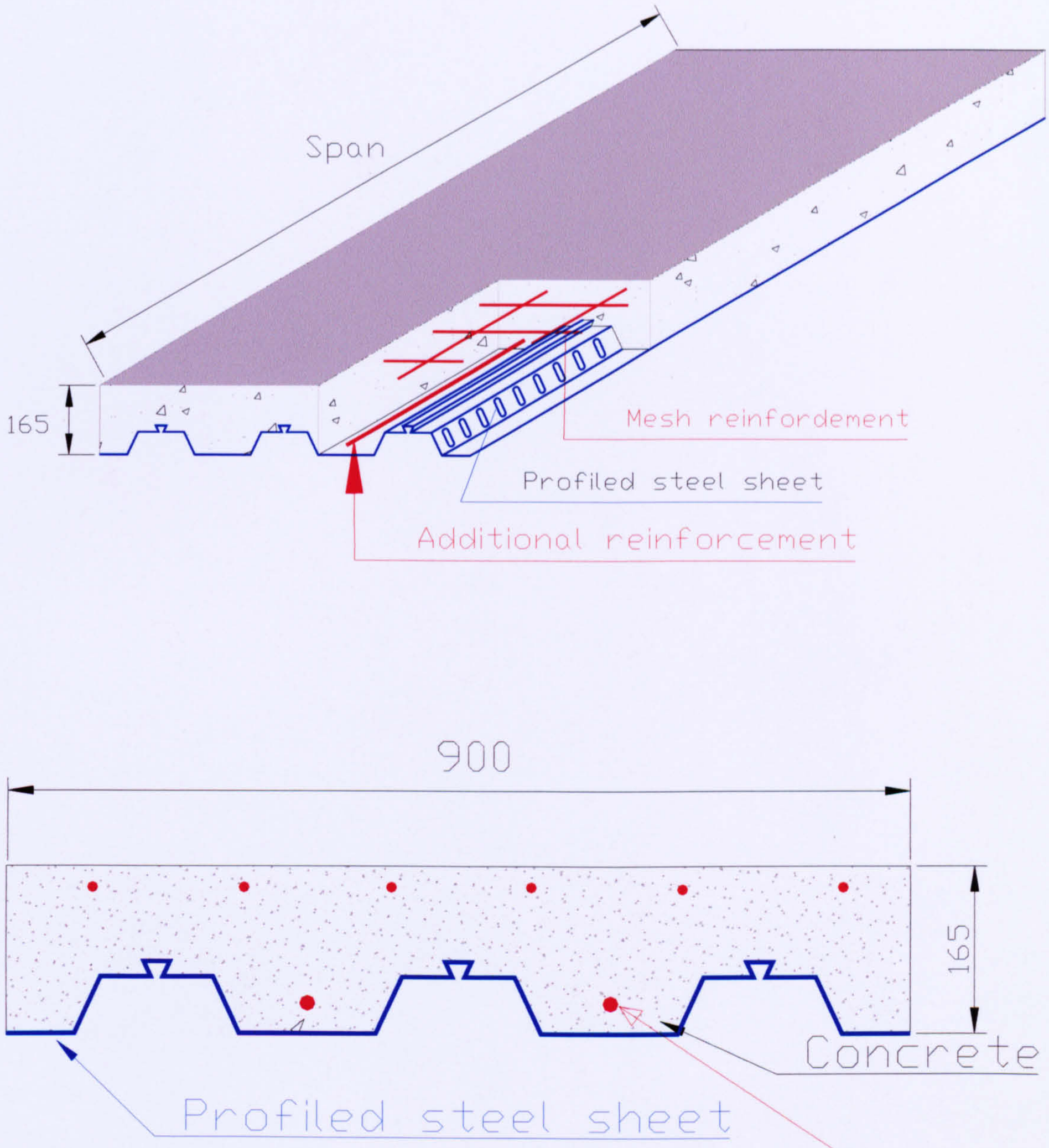

Figure 4.2 Second series of composite slab tests (additional reinforcement)

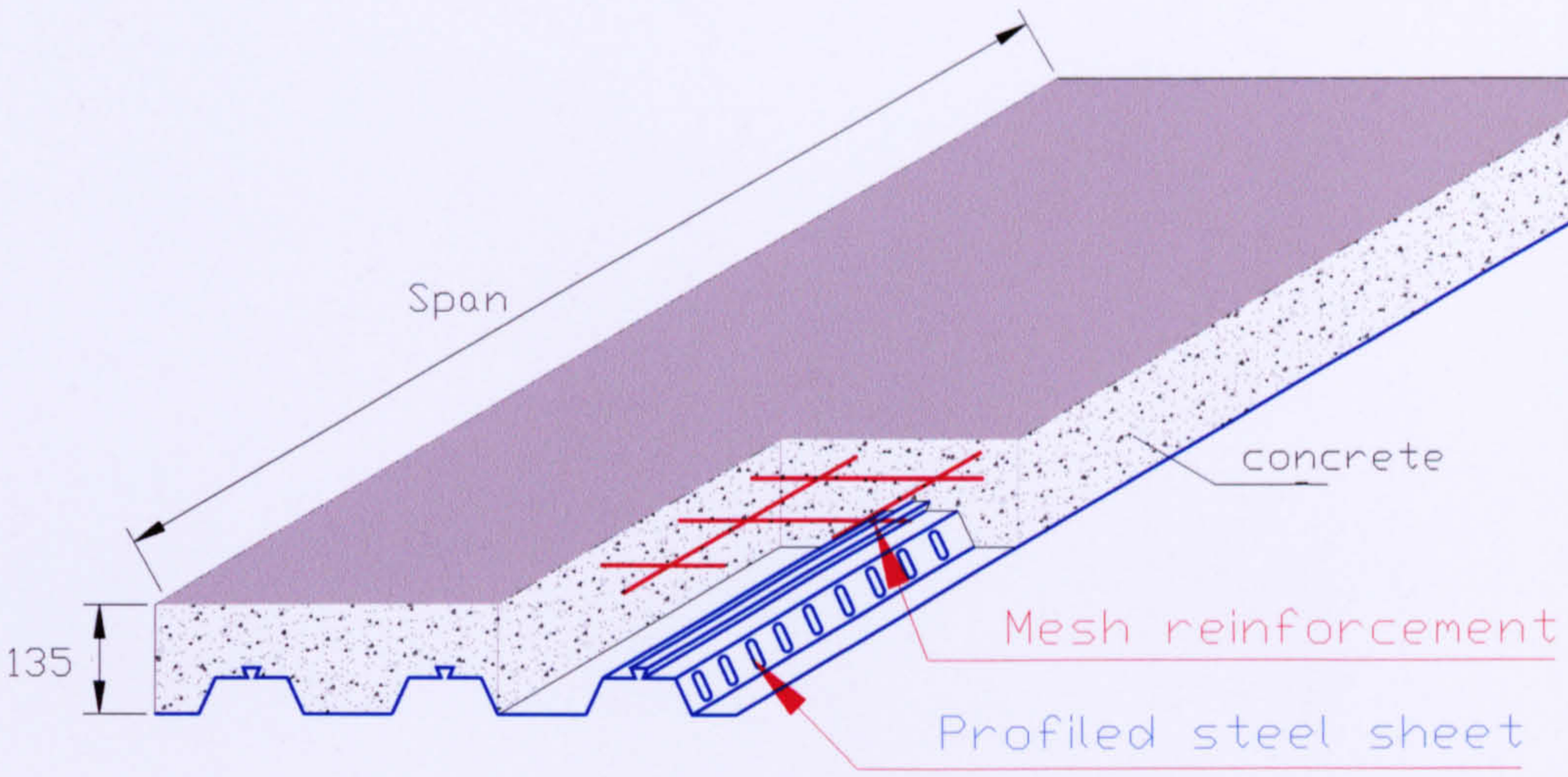

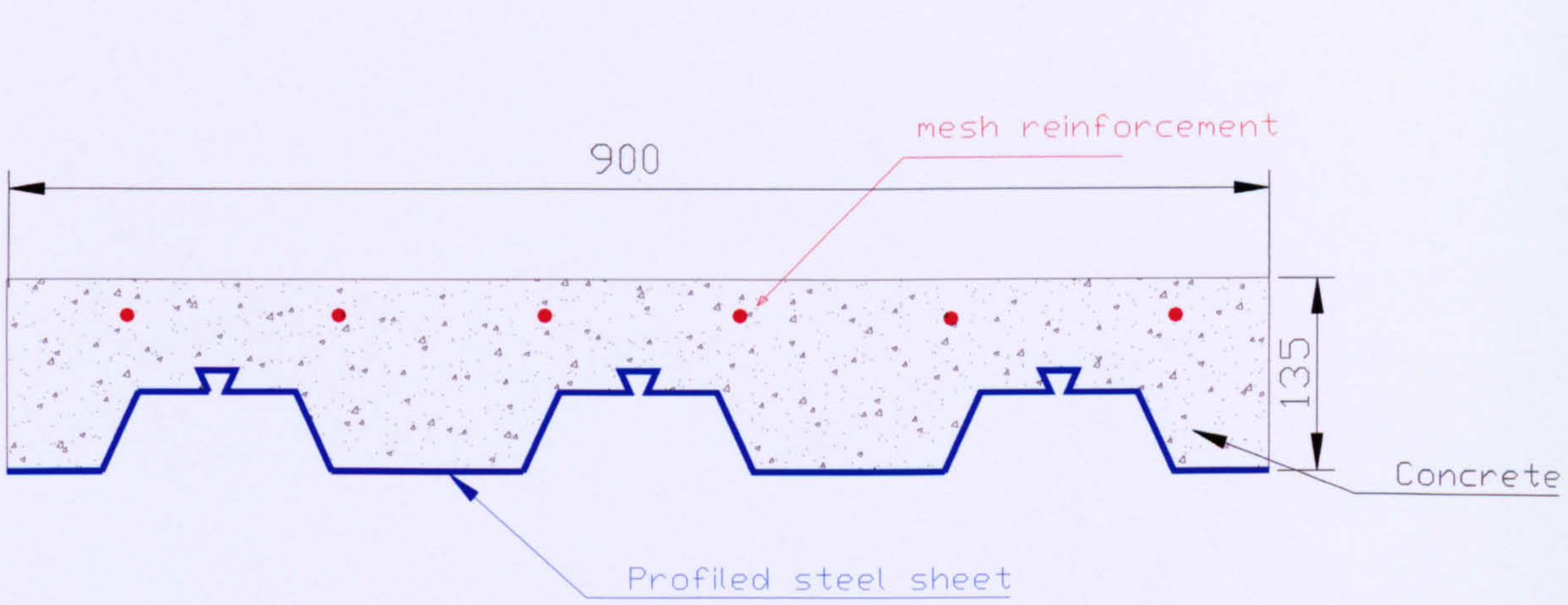

Figure 4.3 Third series of composite slab tests (135mm deep)

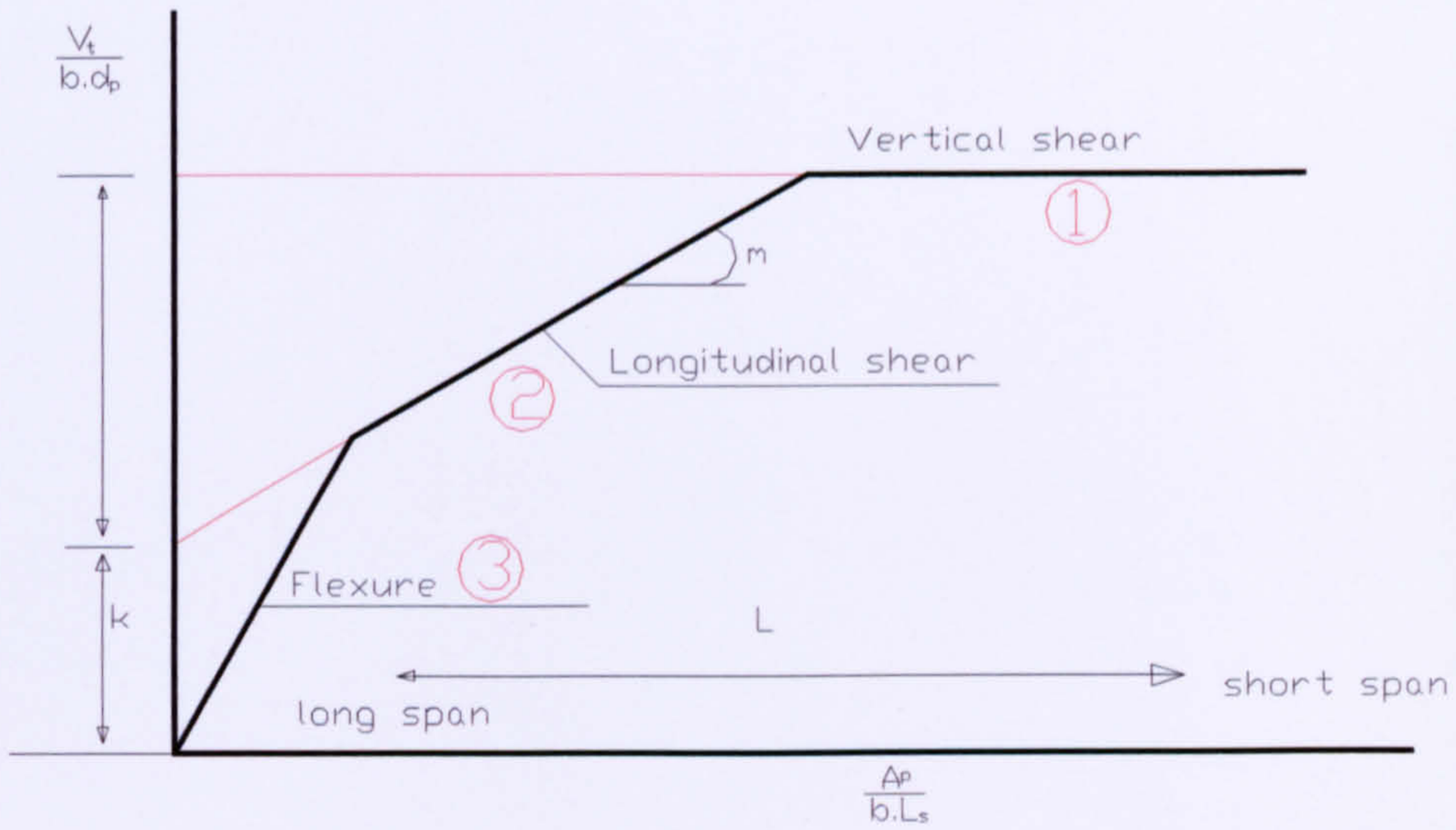

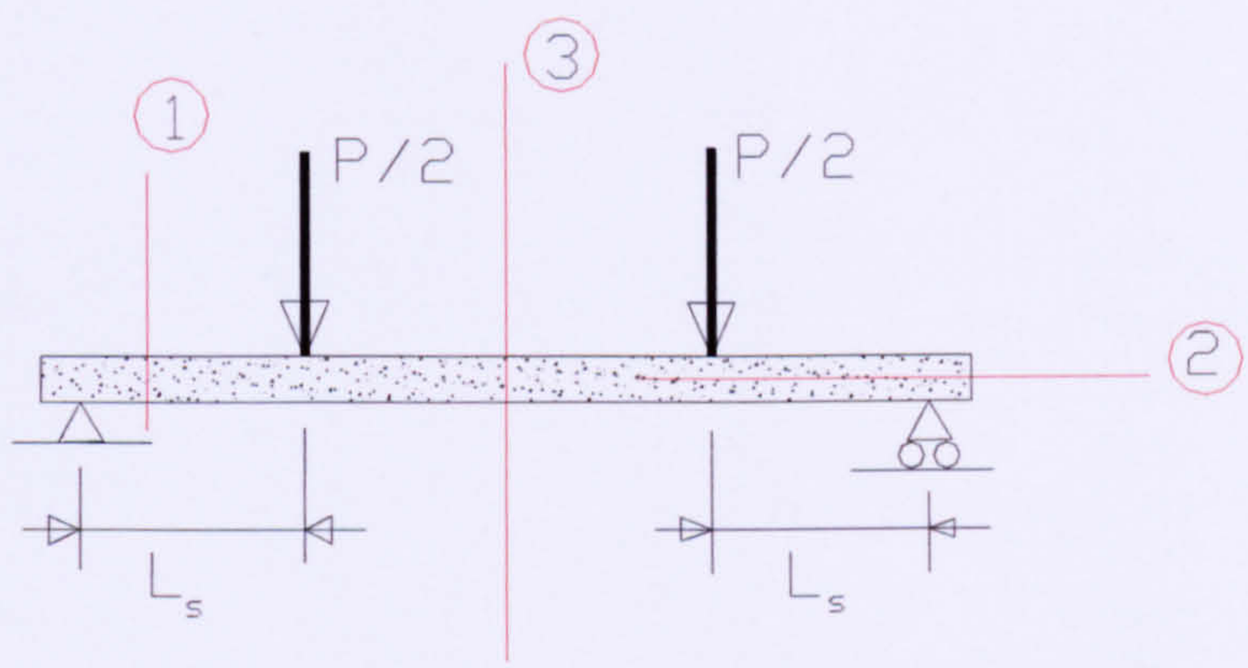

Figure 4.4 Illustration of possible failure modes

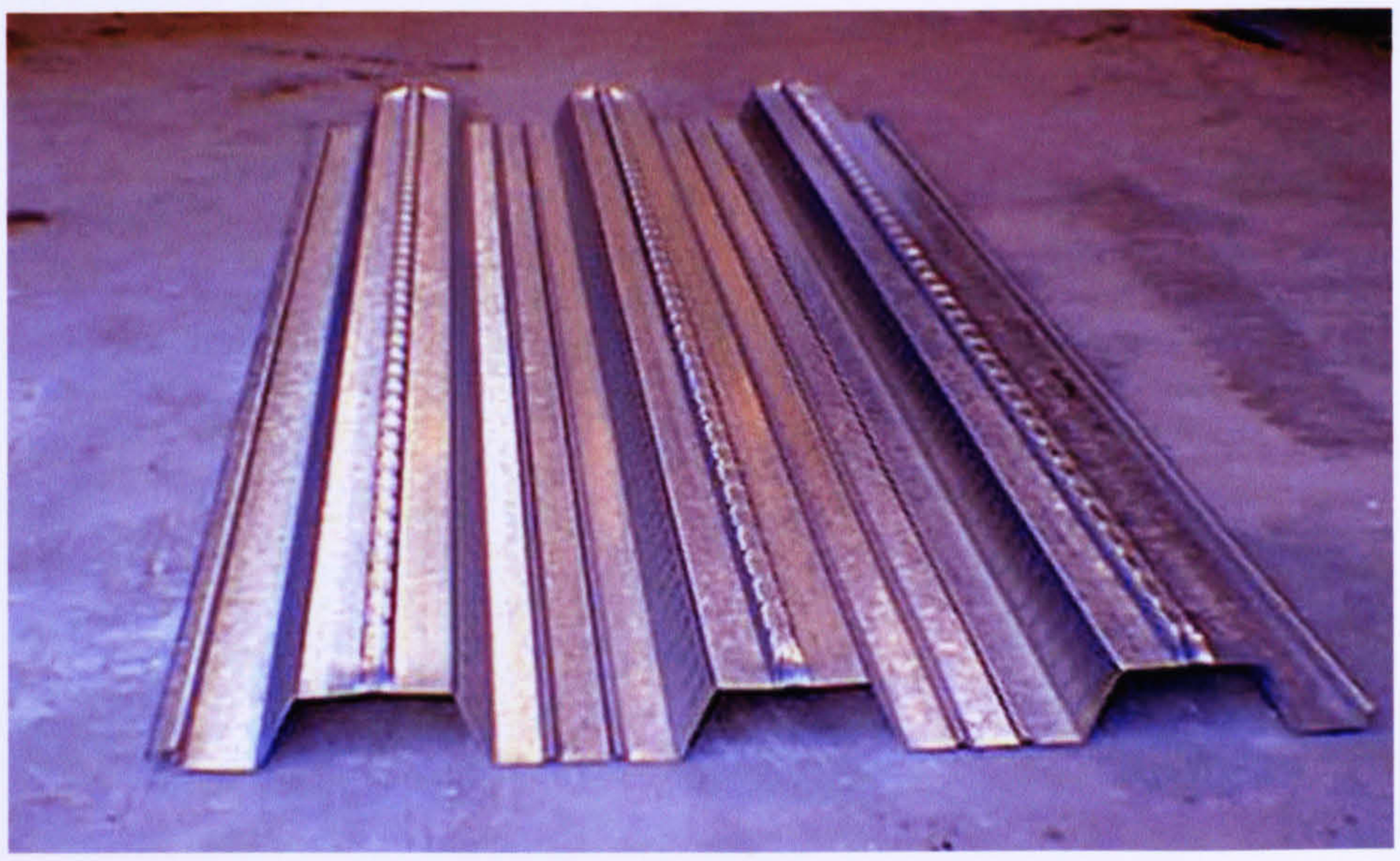

Figure 4.5 Profiled steel sheet (ComFlor70)

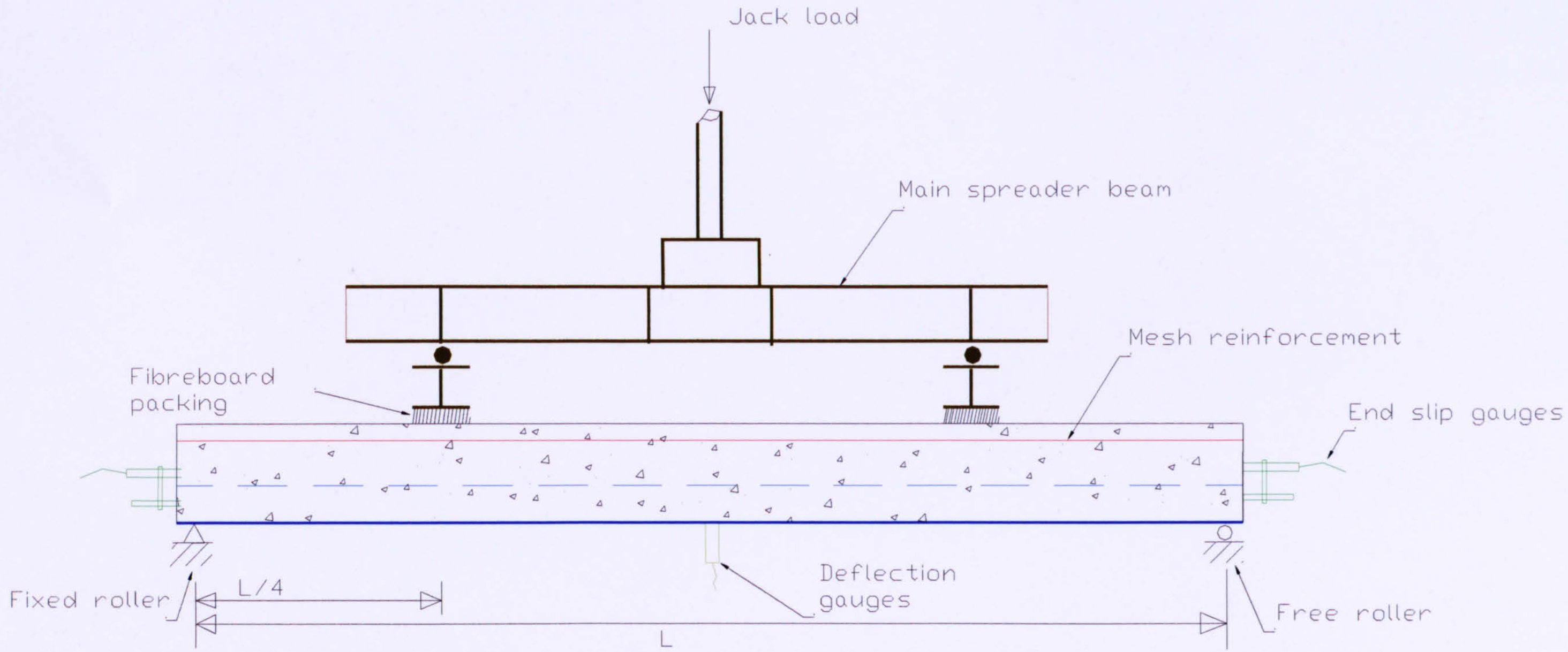

Figure 4.6 Test setup and load arrangement for composite slab tests

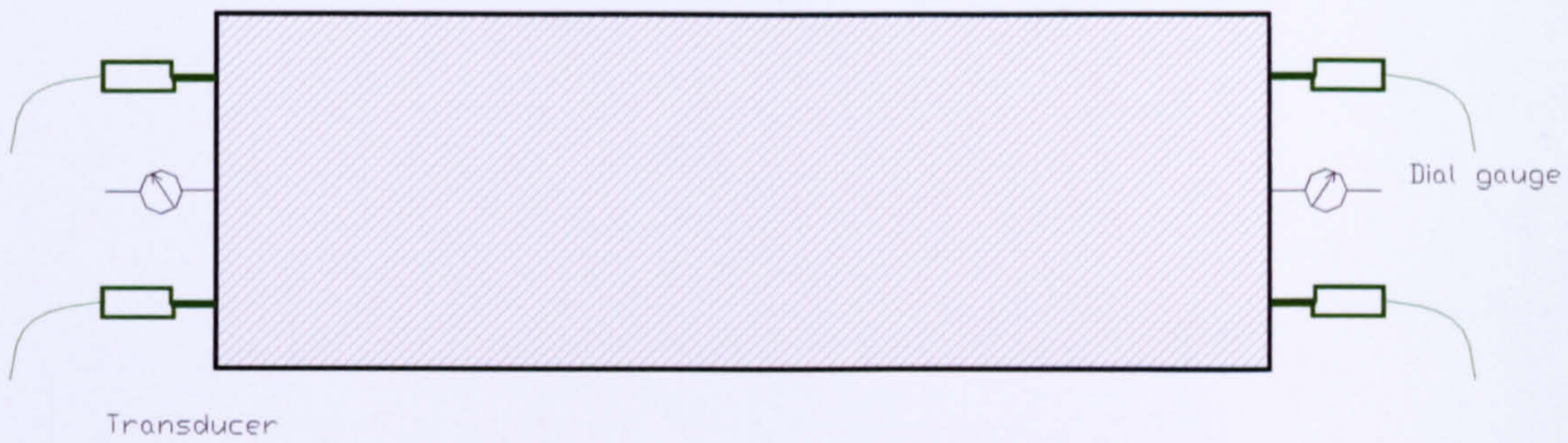

Figure 4.7 End slip gauges and transducers

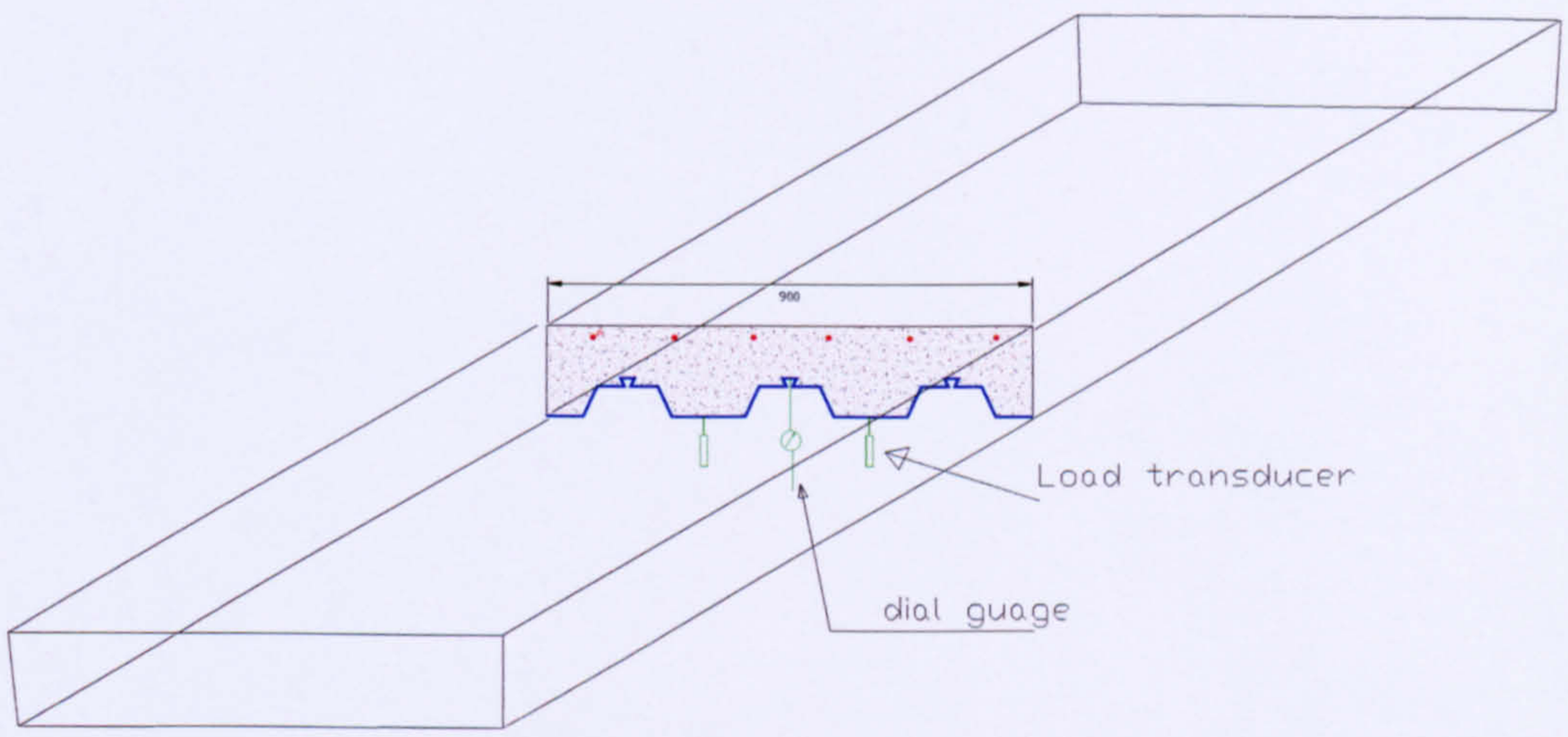

Figure 4.8 Deflection transducers and dial gauges

Figure 4.9. Load-Central Deflection curve for Slab No.1

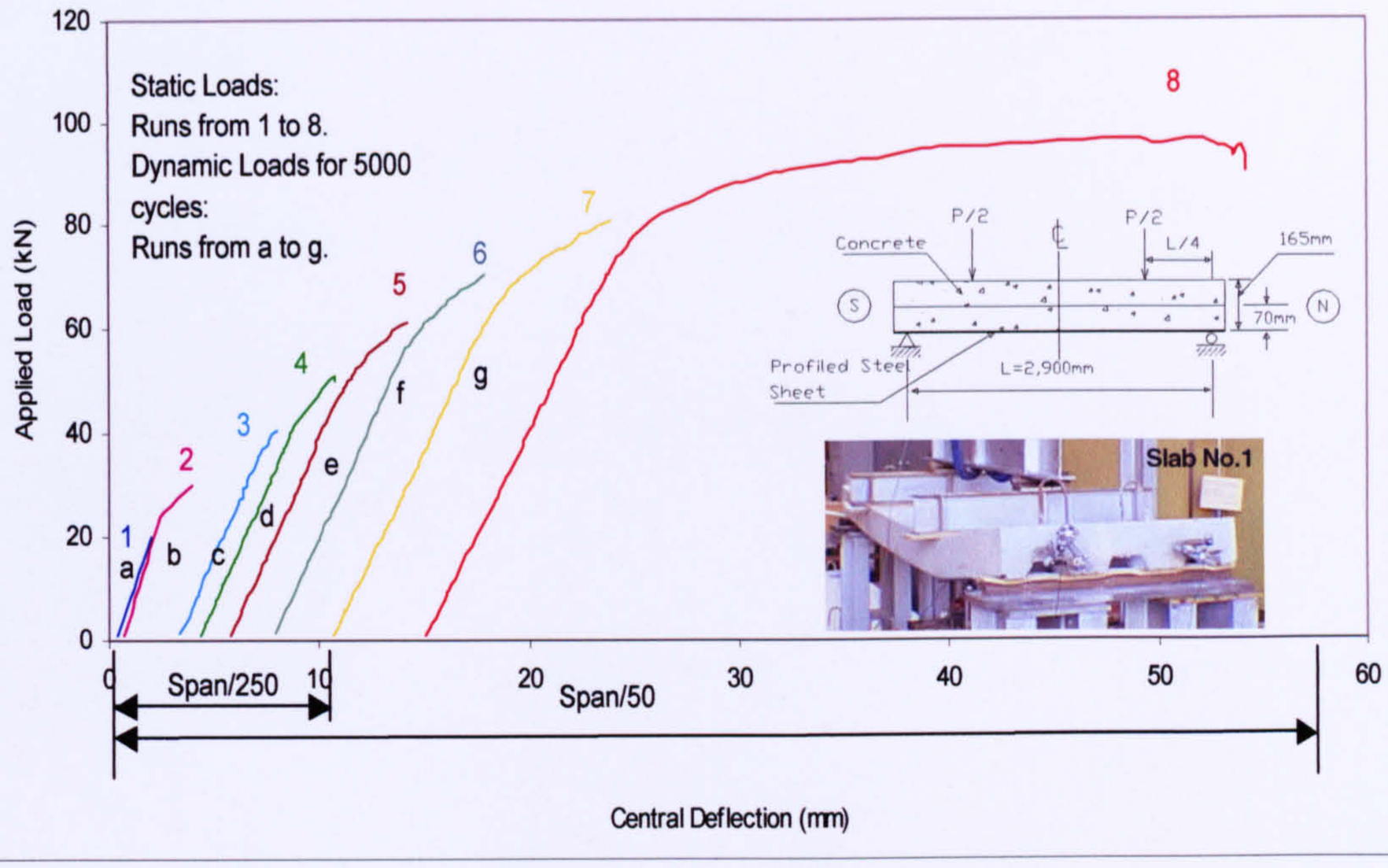

Figure 4.10. Load-Central Deflection curve for Slab No.2

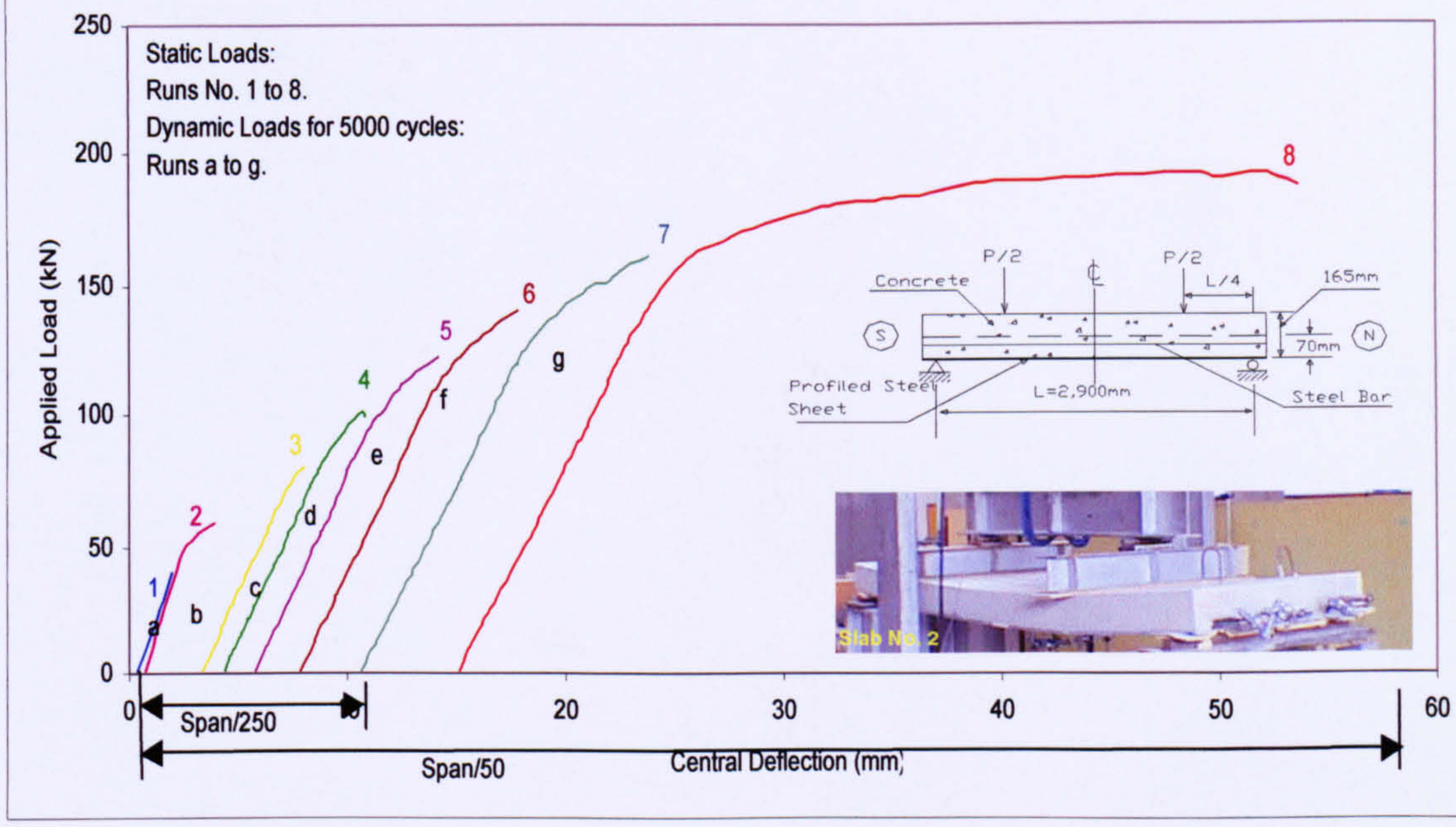

Figur4.11. Load-Central Deflection Curve for Slab No. 3

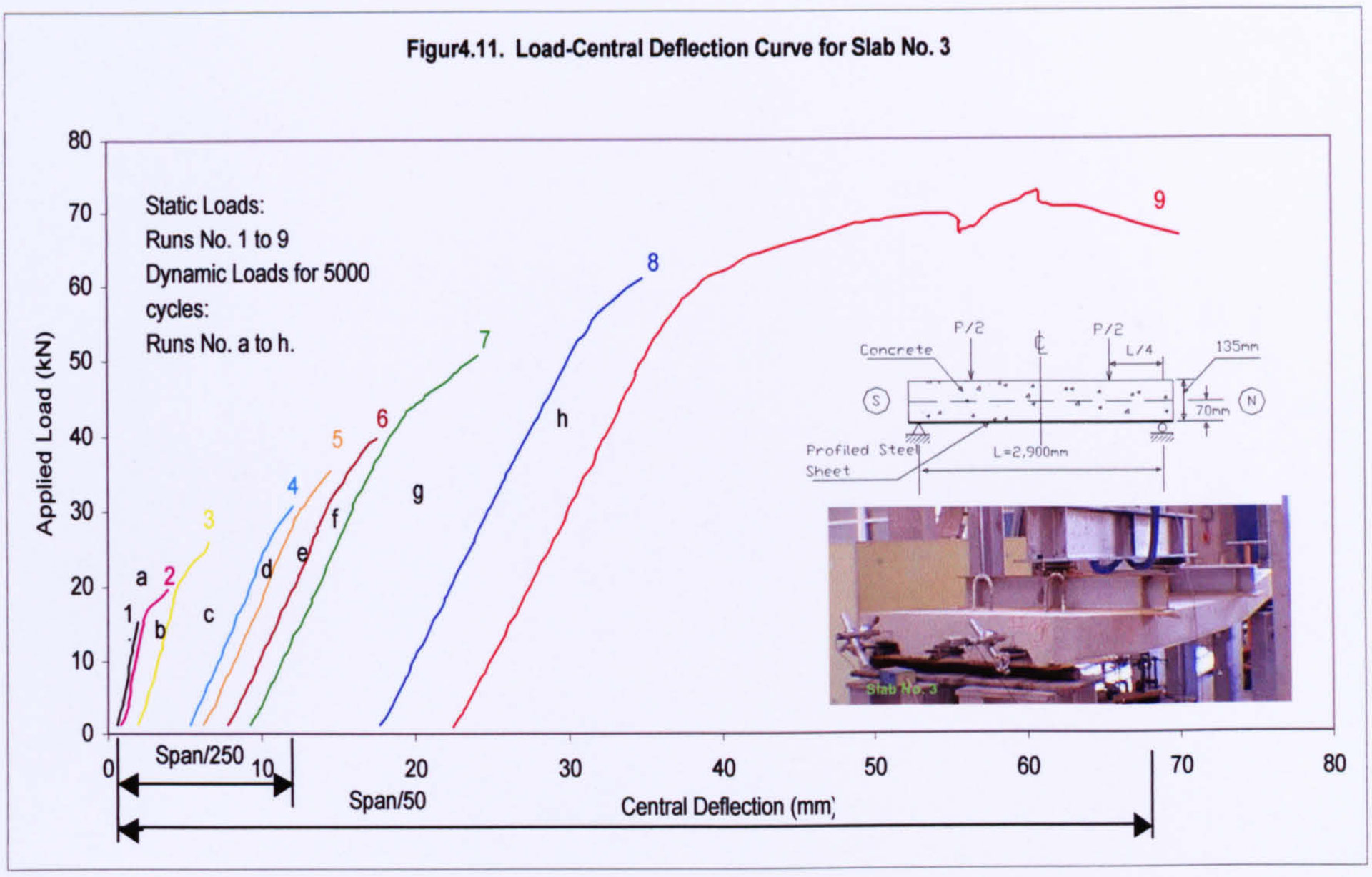

Figur 4. 12 Load-Central Deflection Curve for Slab No. 4

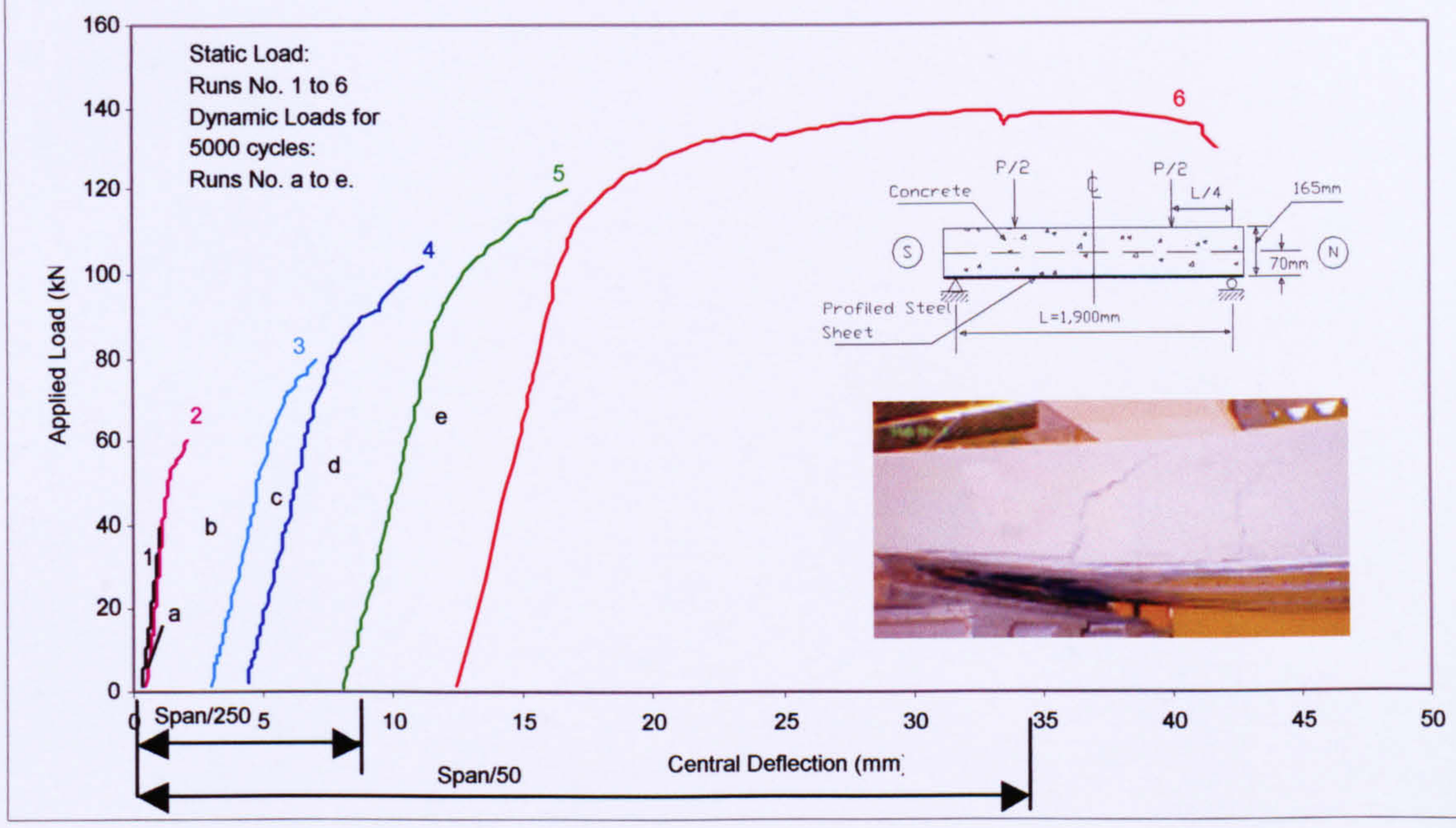

Figure 4.13 Load-Central Deflection Curve for Slab No. 5

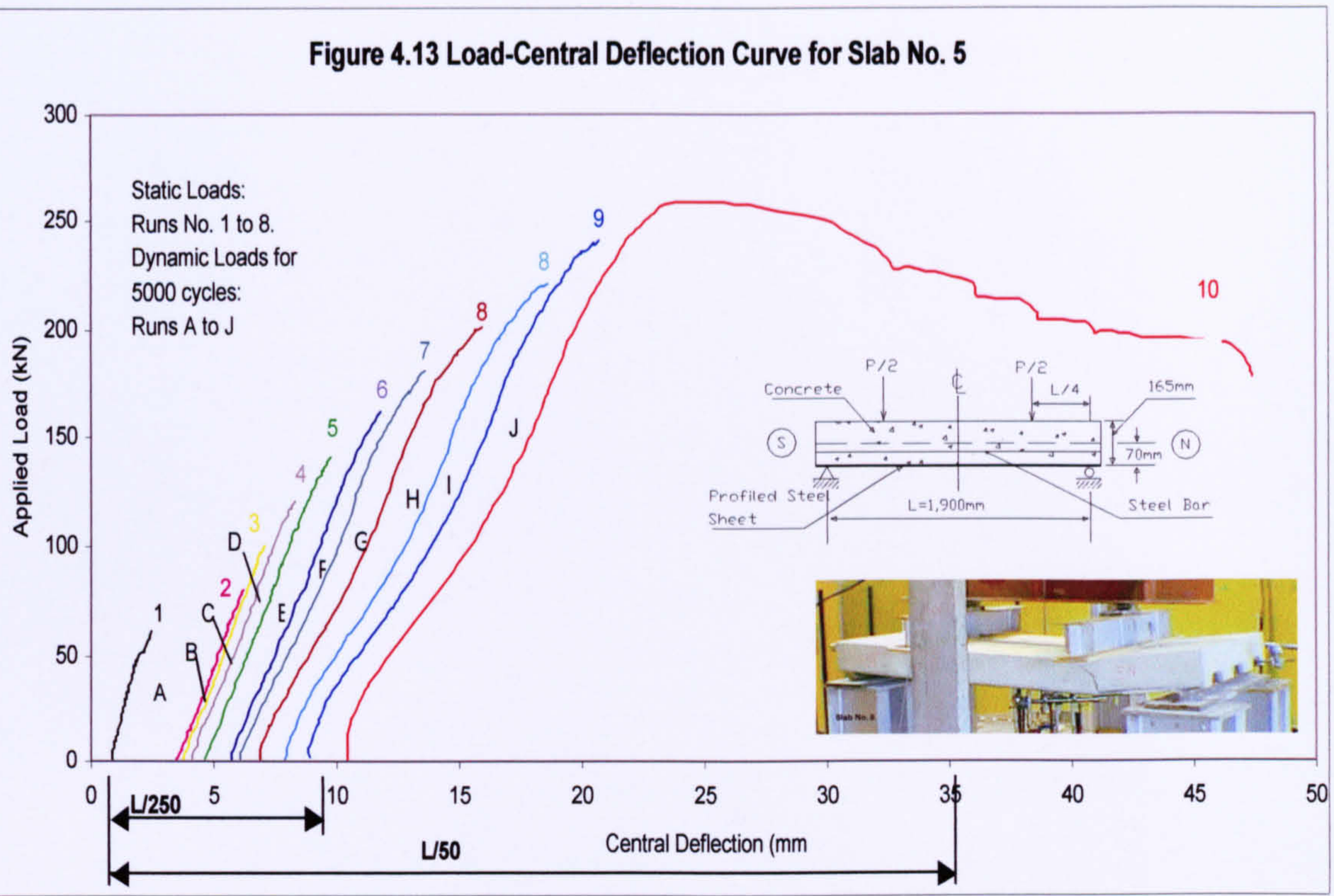

Figure 4.14 Load-Central Deflection Curve for Slab No. 6

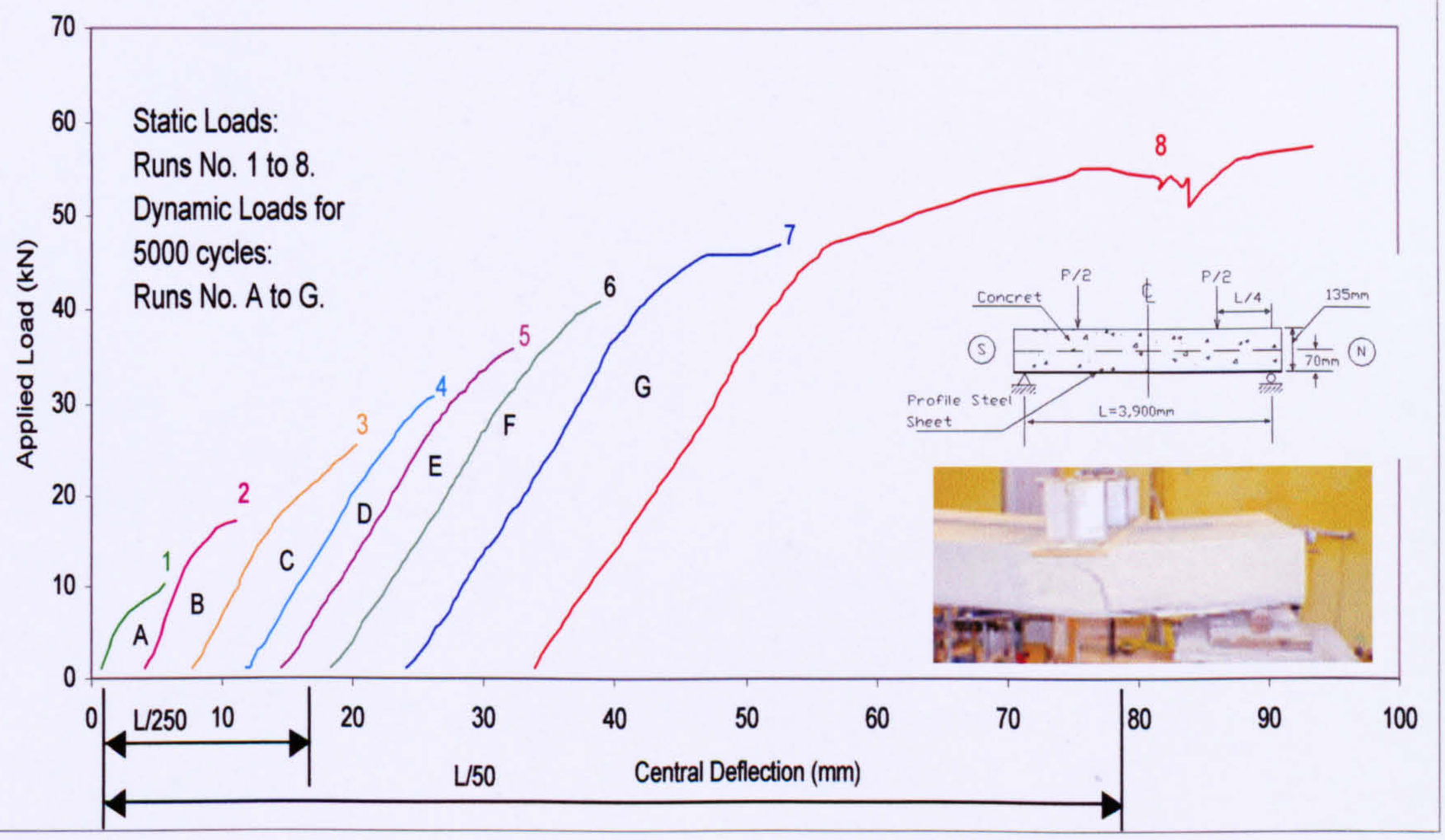

Figure 4.15 Load-Central Deflection Curve for Slab No. 7

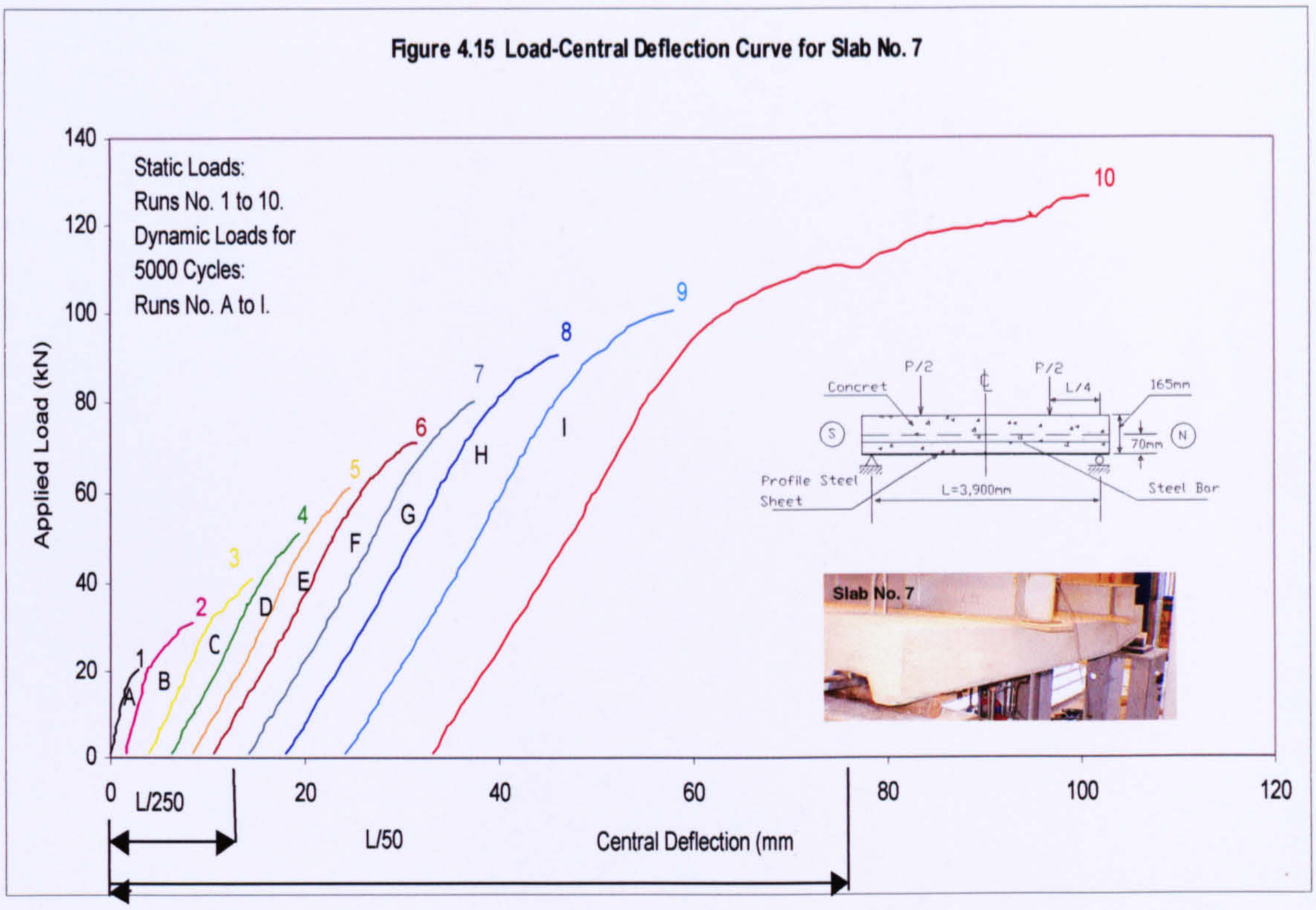

Figure 4. 16 Load-Central Deflection Curve for Slab No. 8

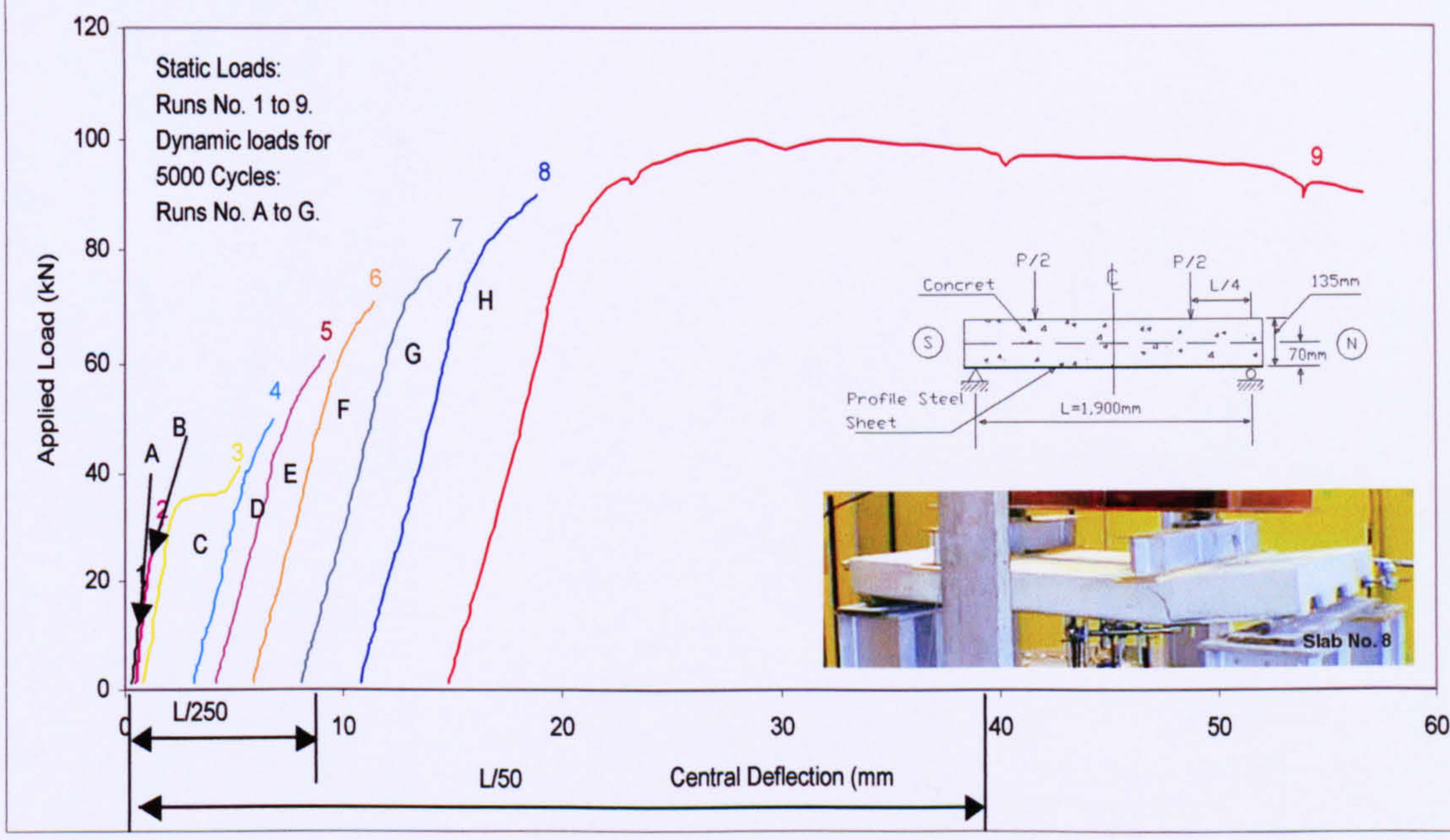

Figure 4. 17 Load-Central Deflection Curve For Slab No. 9

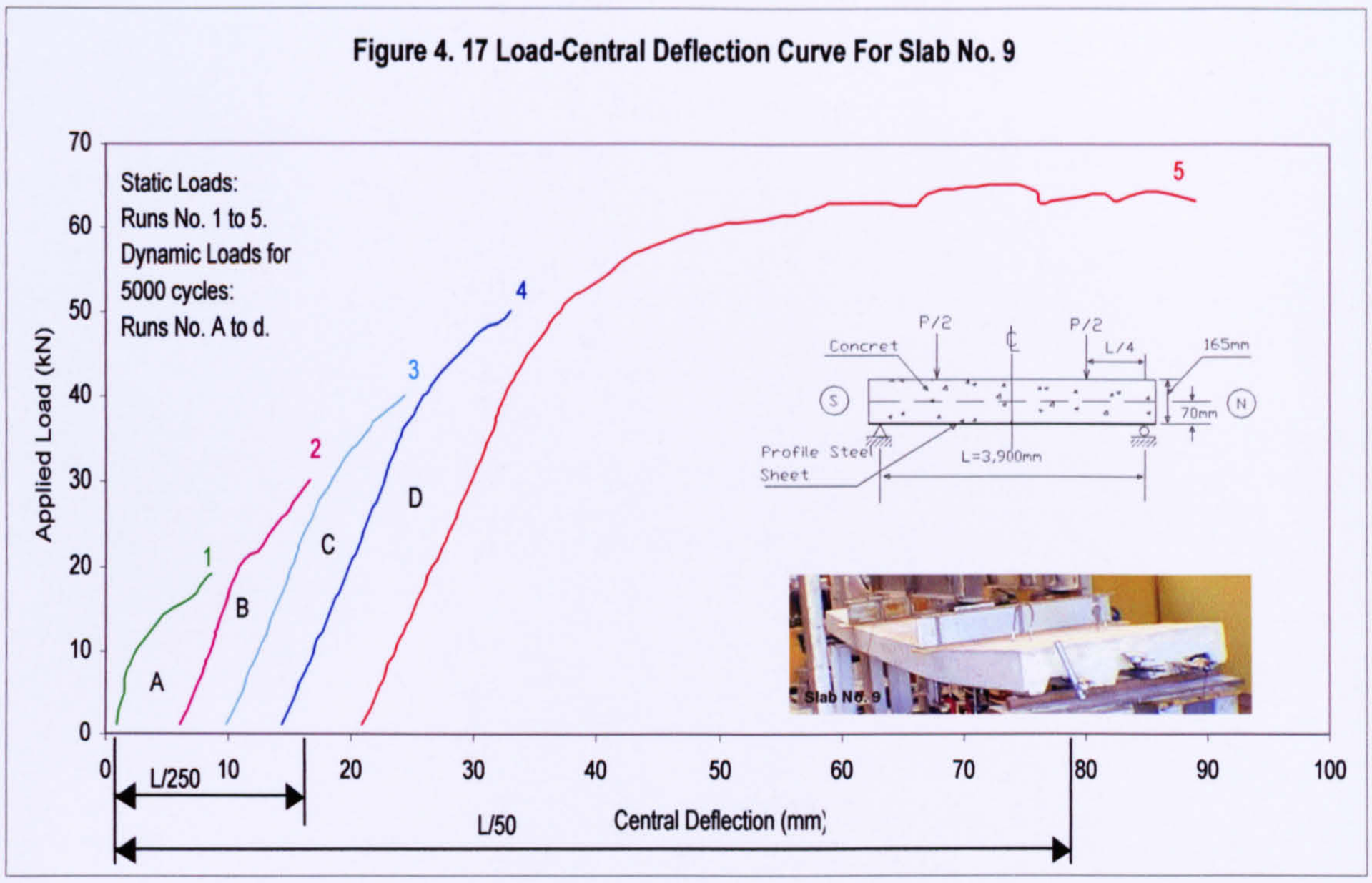

Figure 4.18 Load-End Slip curve for Slab No.1

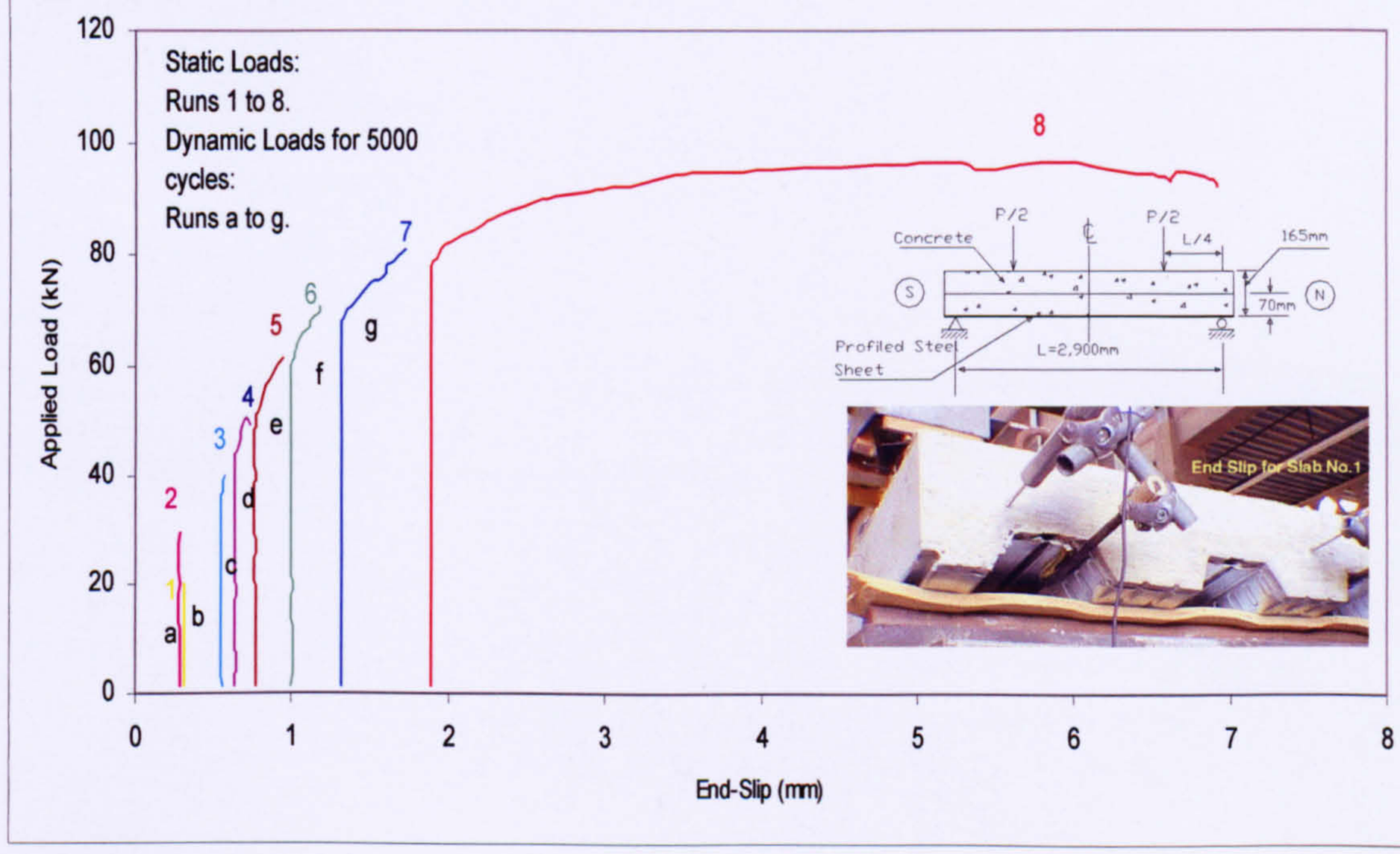

Figure 4. 19 Load-End Slip Curve Slab No.2

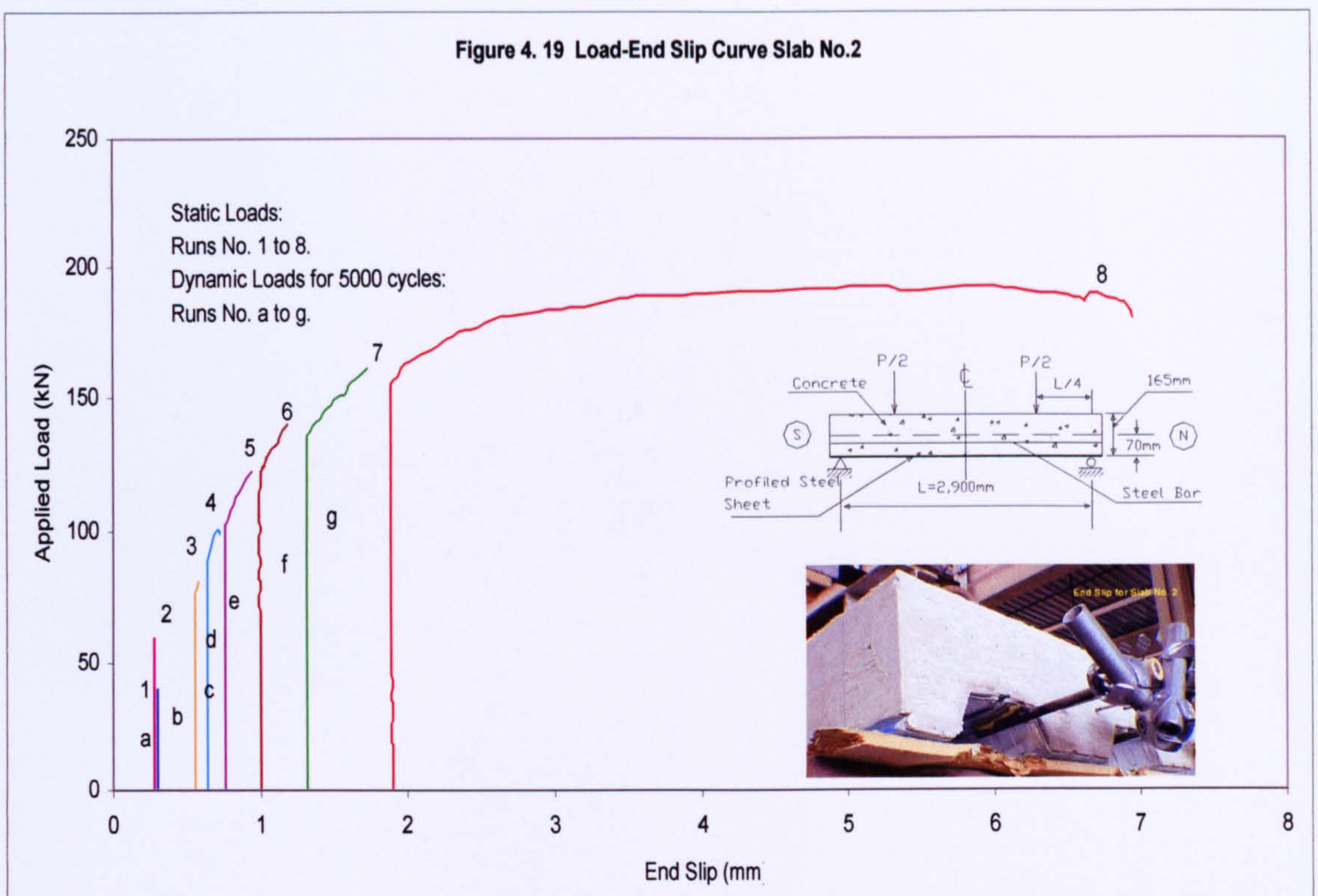

Figure 4. 20 Load-End Slip Curve Slab No. 3

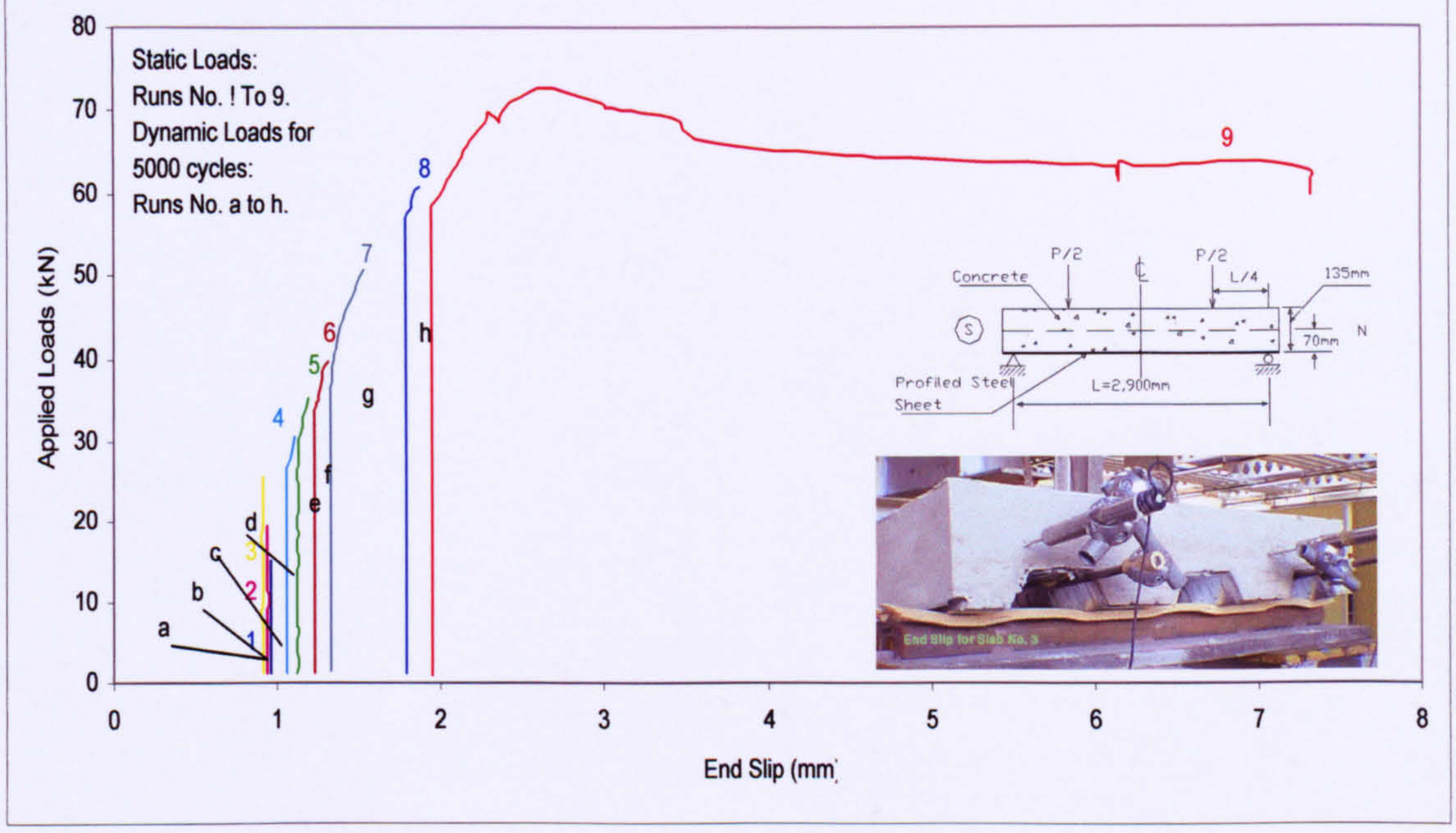

Figure 4. 21 Load-End Slip Curve For Slab No. 4

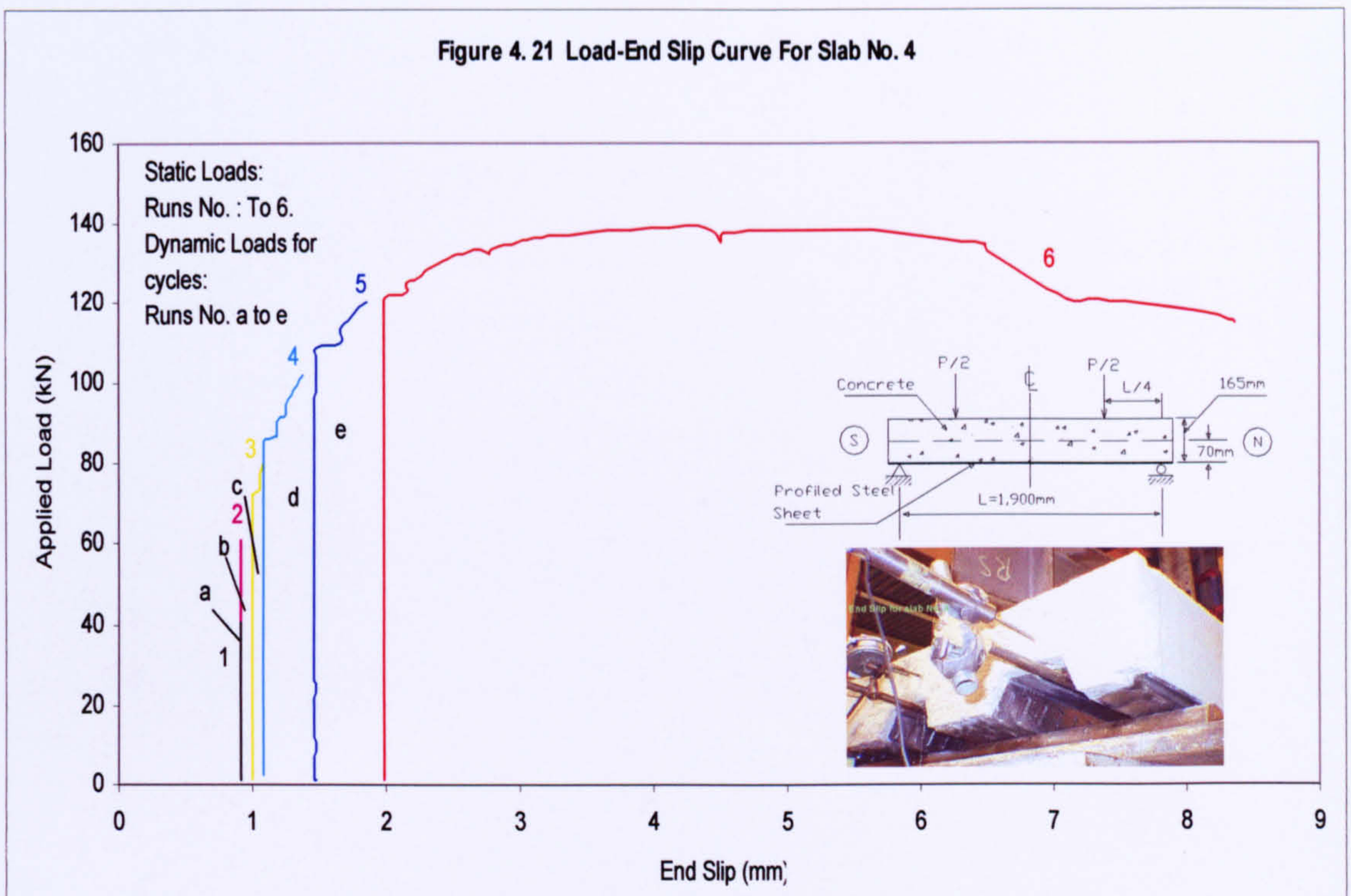

Figure 4. 22 Load-End Slip Curve Slab No. 5

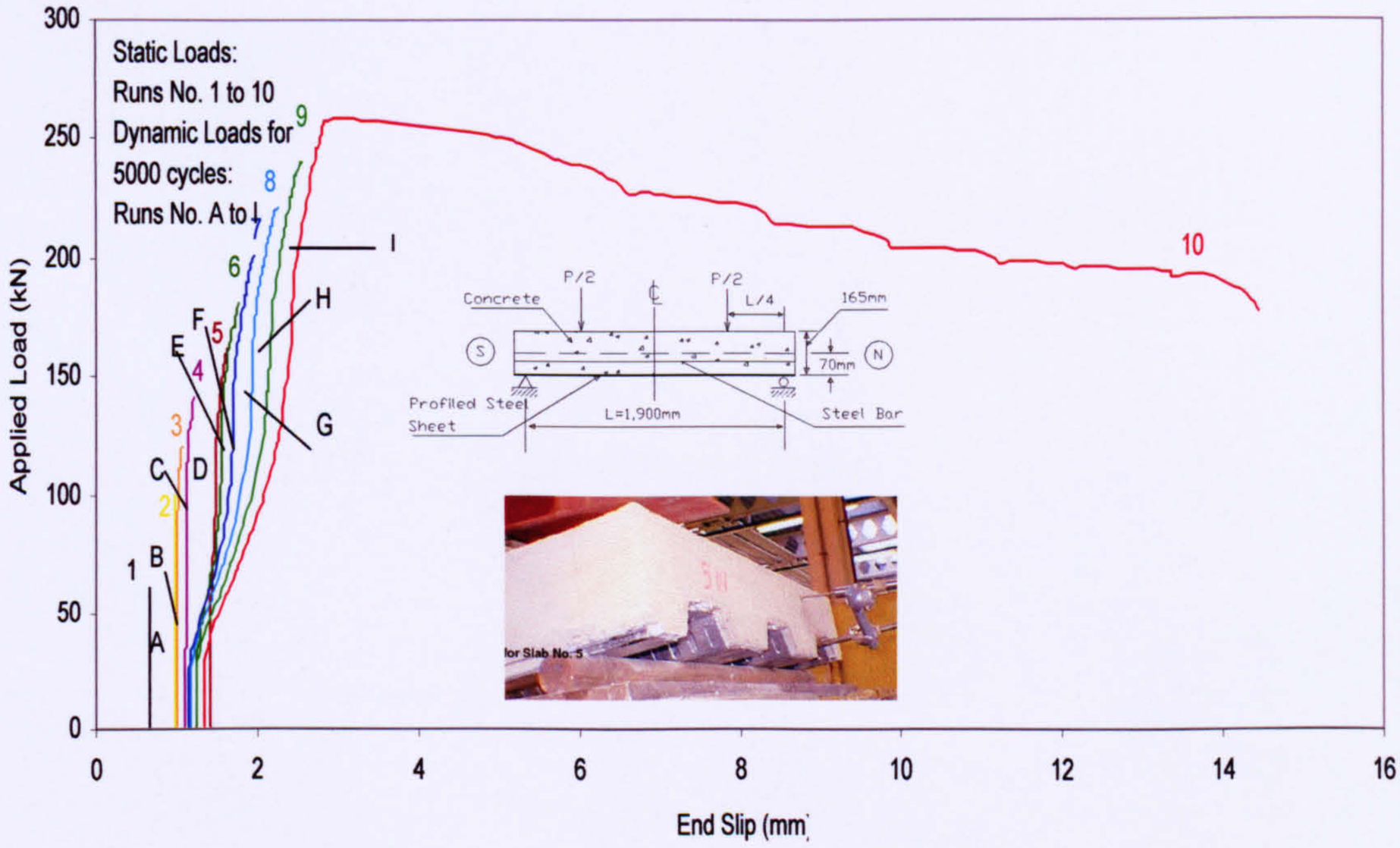

Figure 4. 23 Load-End Slip Curve Slab No. 6

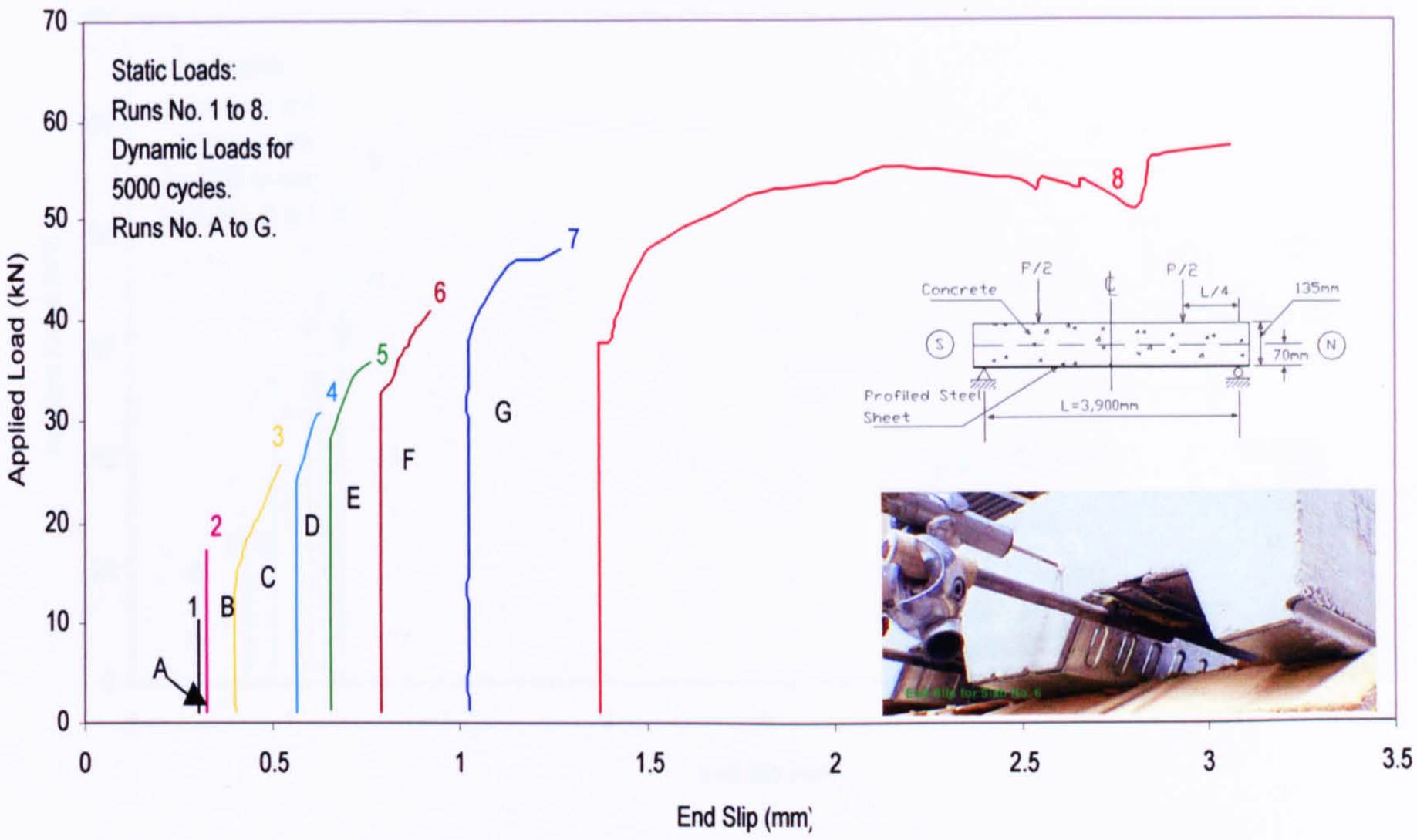

Figure 4. 24 Load-End Slip Curve for Slab No. 7

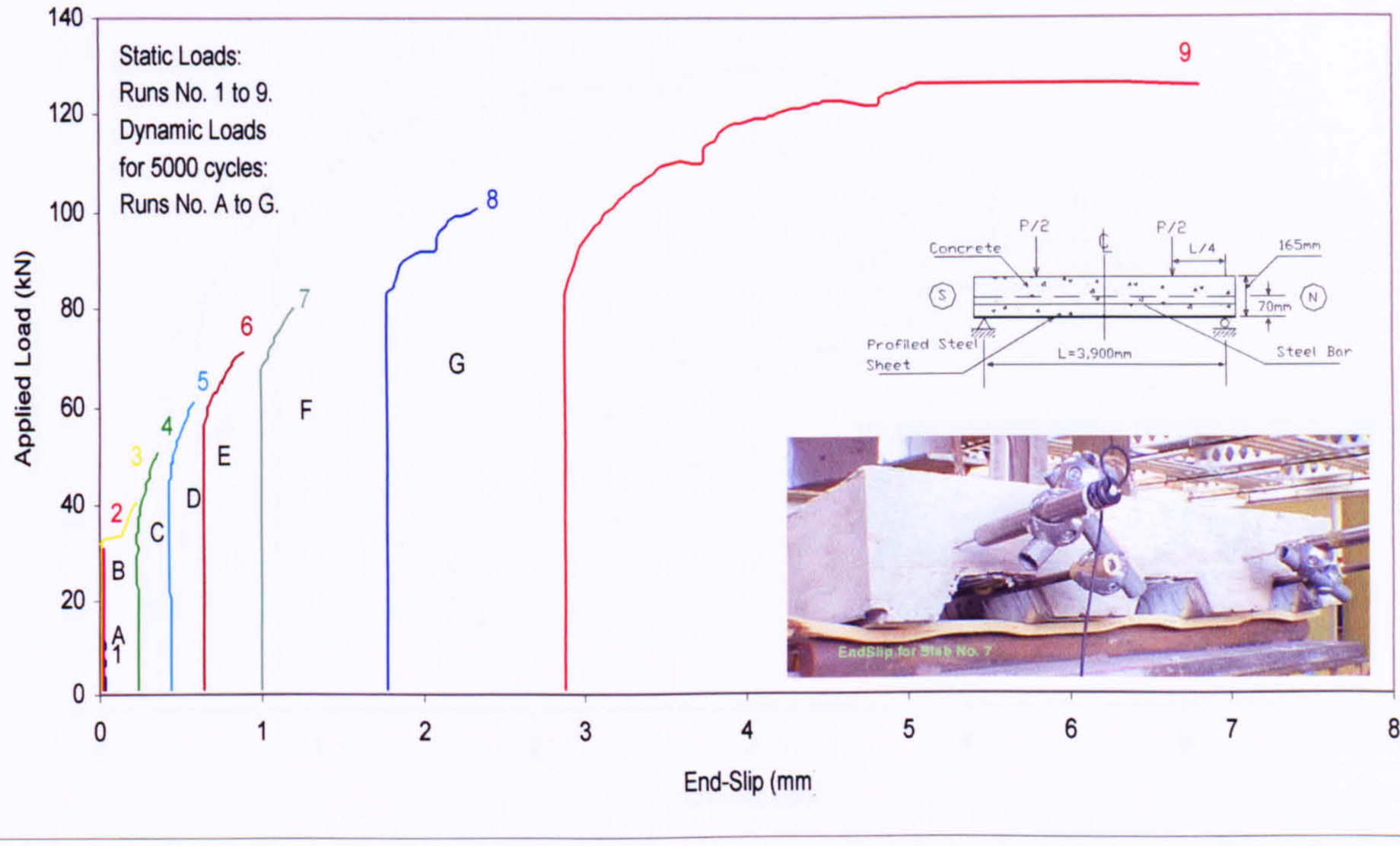

Figure 4. 25 Load-End Slip Curve for Slab No. 8

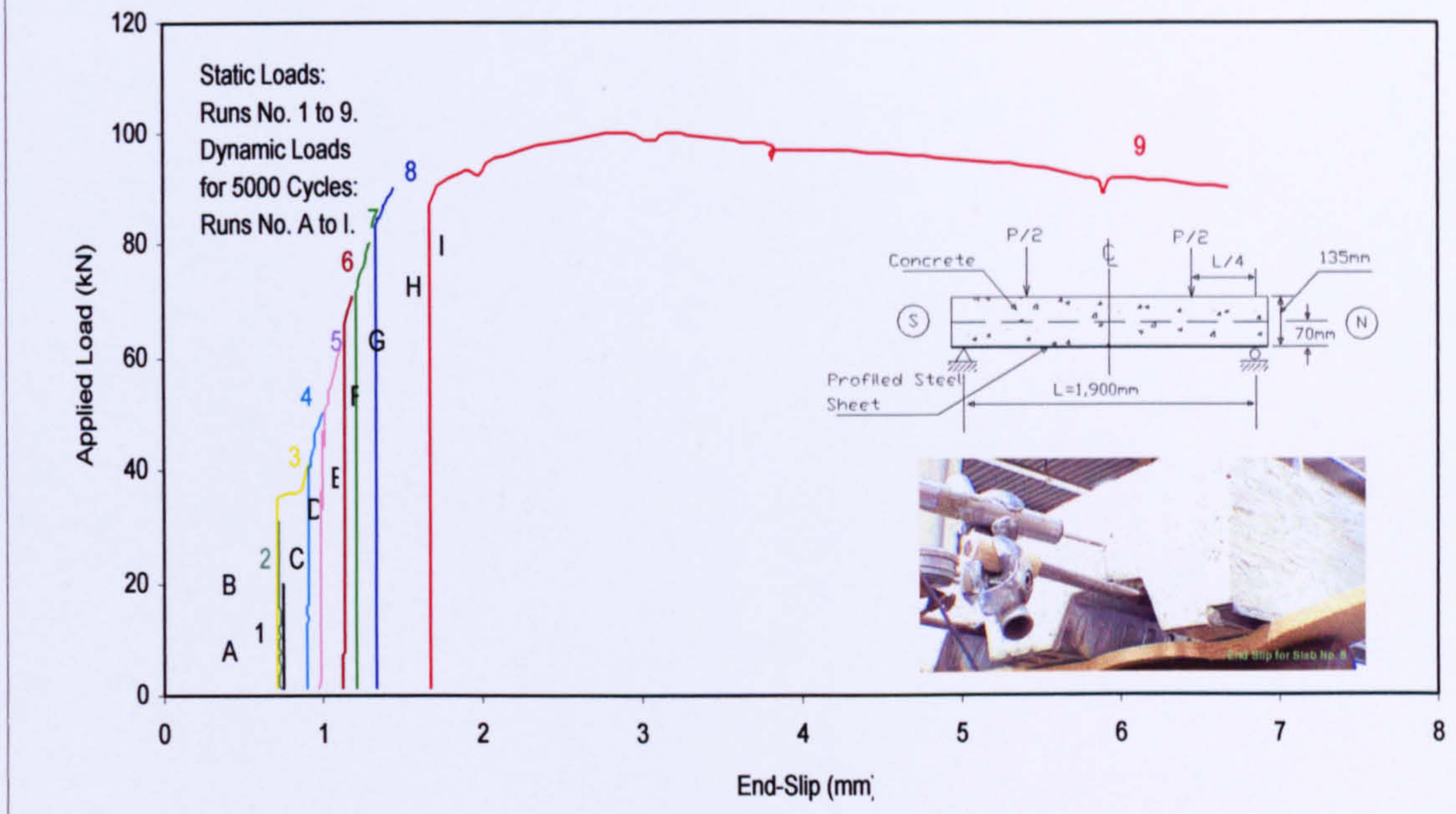

Figure 4. 26 Load-End Slip Curve for Slab No. 9

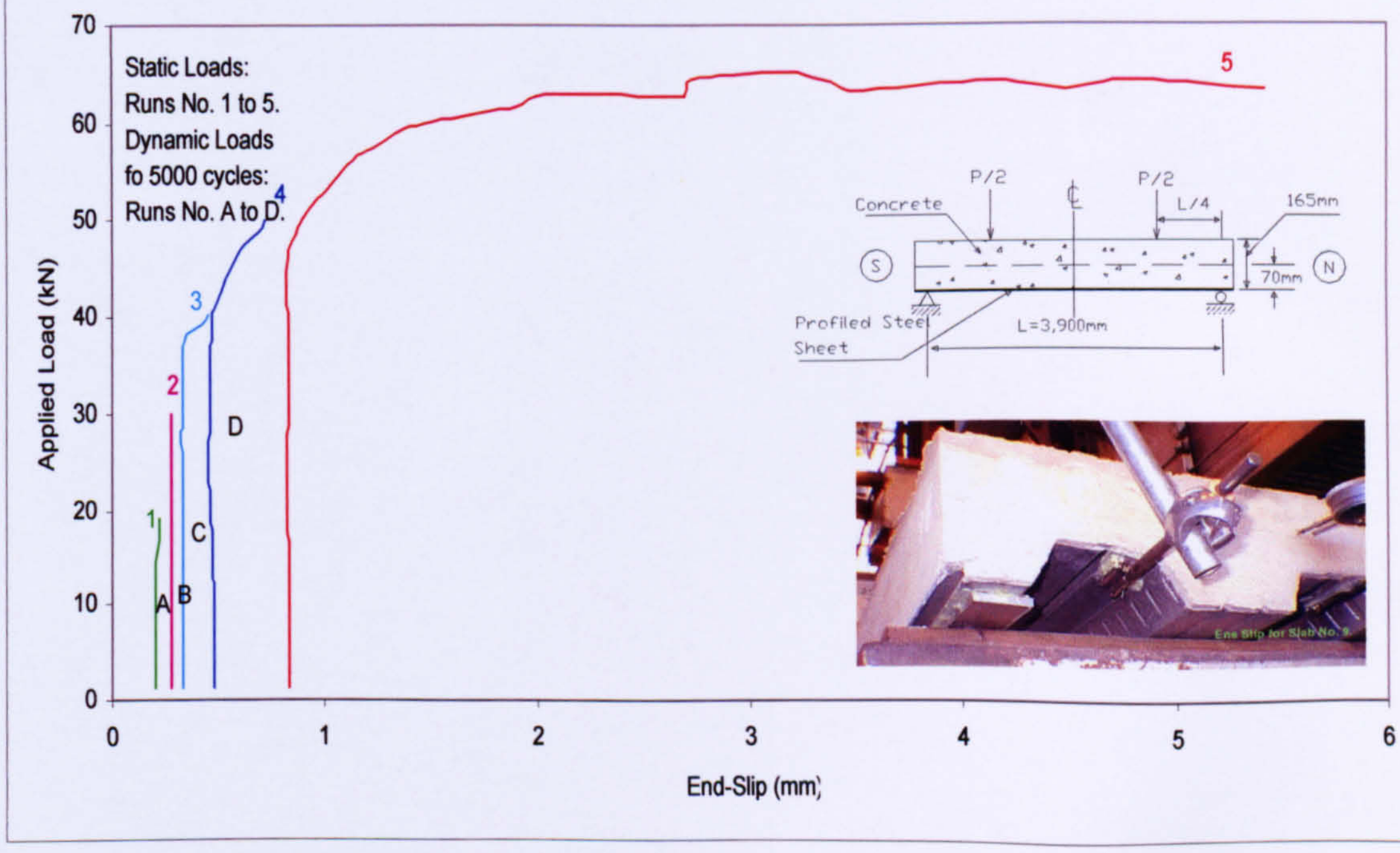

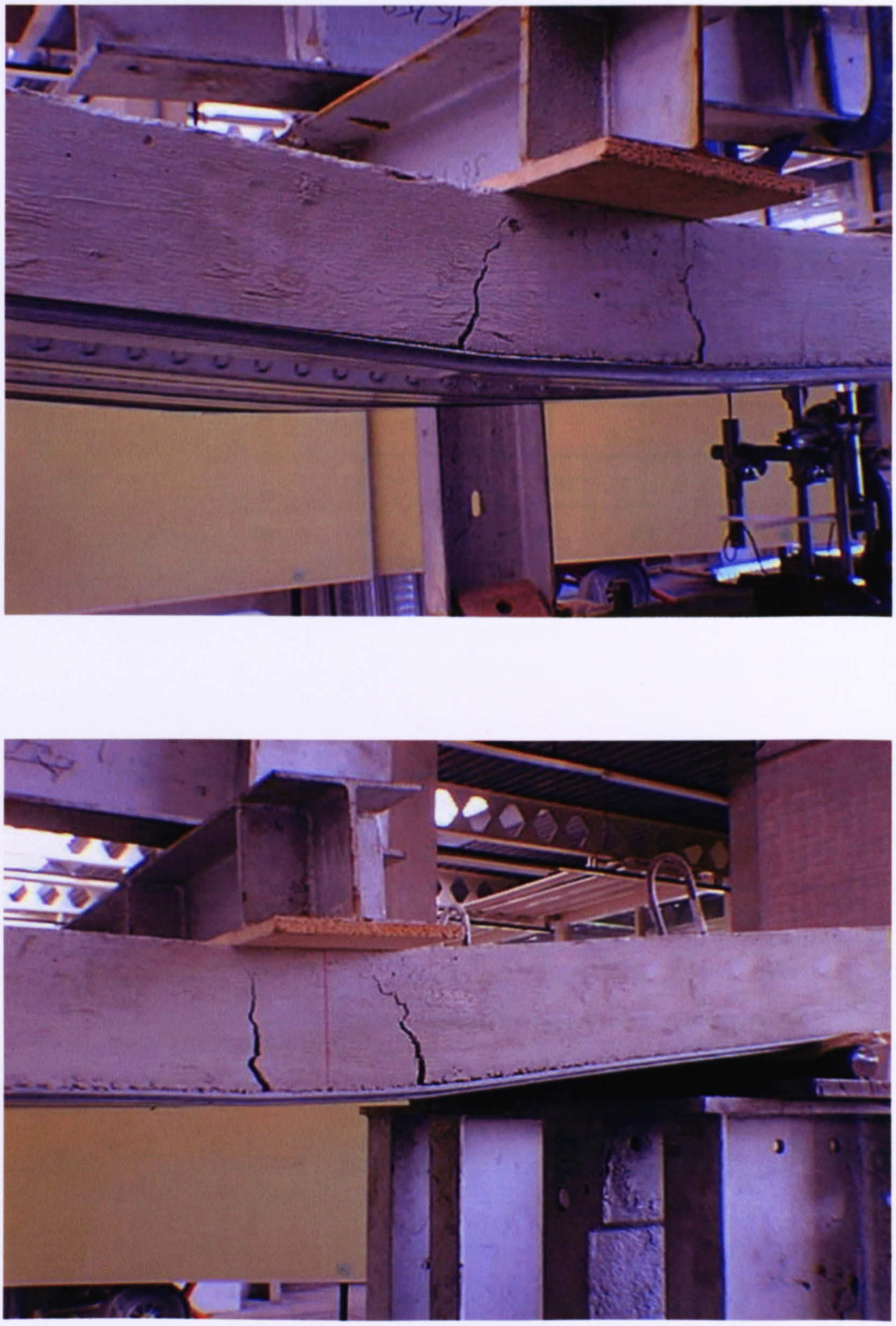

Figure 4. 27 Typical crack patterns

Figure 4. 28 Comparison of load-deflection curves for slabs. 1, 4, and 9 (165 depth)

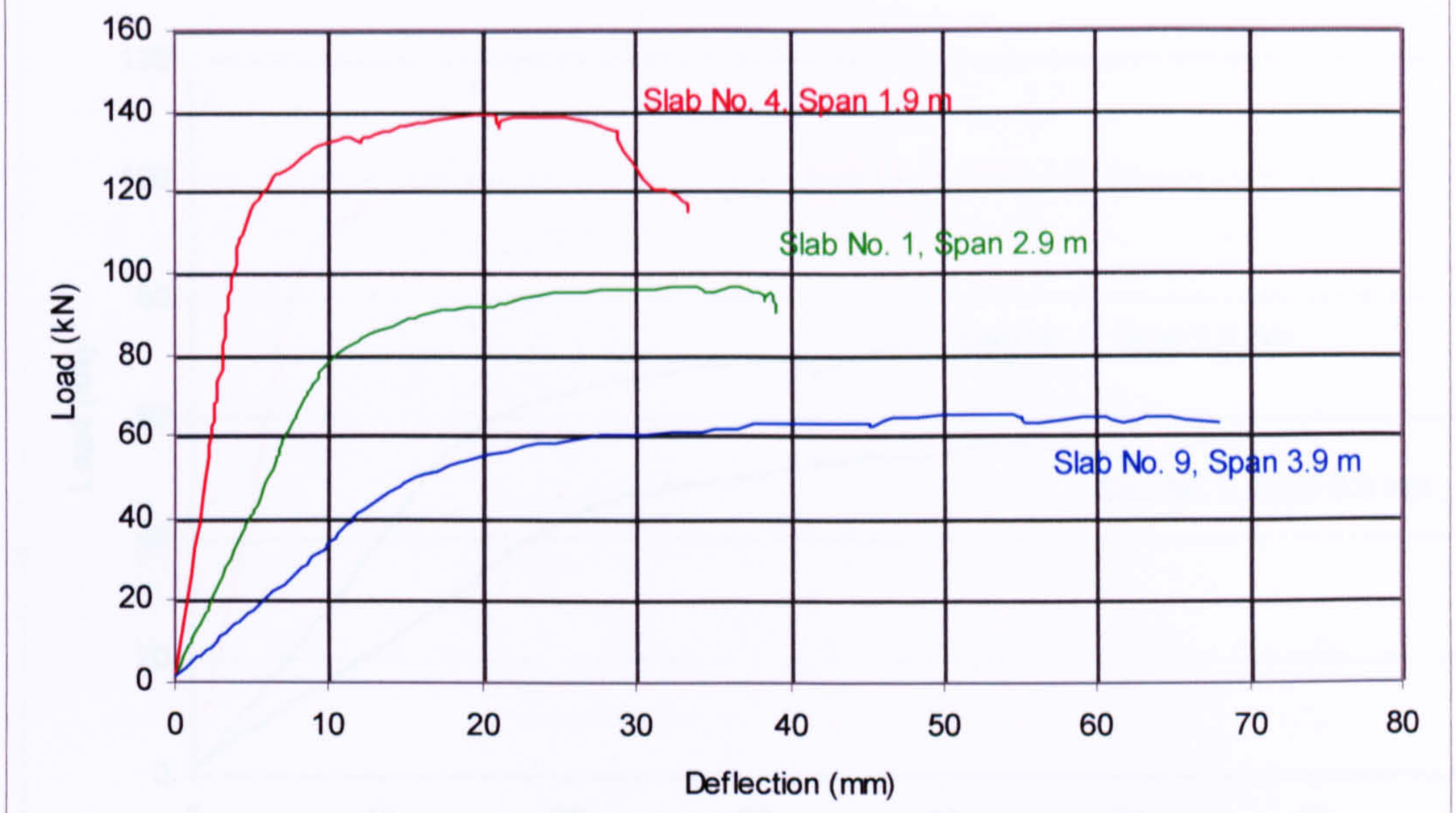

Figure 4. 29 Comparison of load-deflection curves for slabs No. 2, 5, and 7 (with reinforcement)

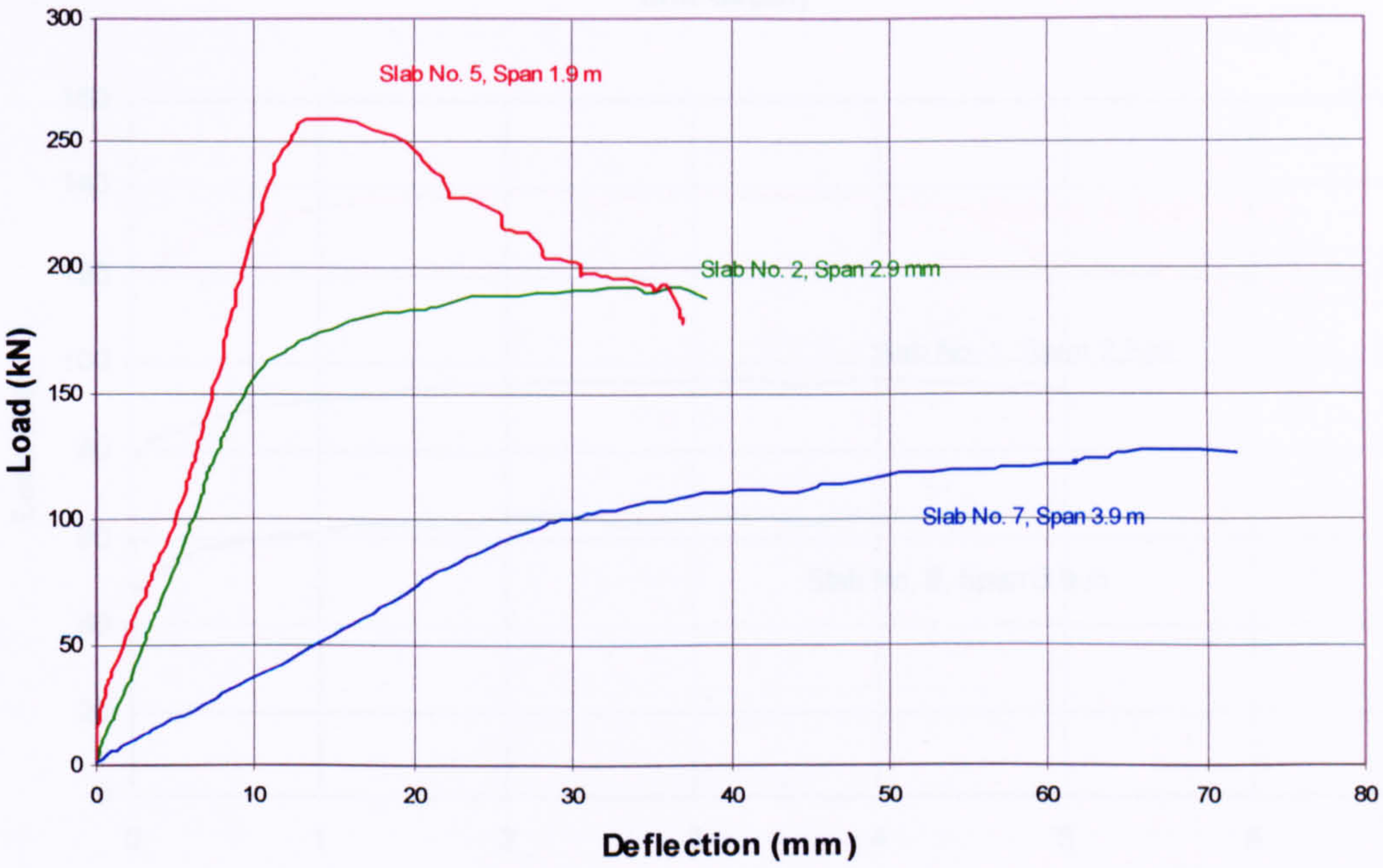

Figure 4. 30 Comparison of load-deflection curves for slabs No. 3, 6, and 8 (135 mm depth)

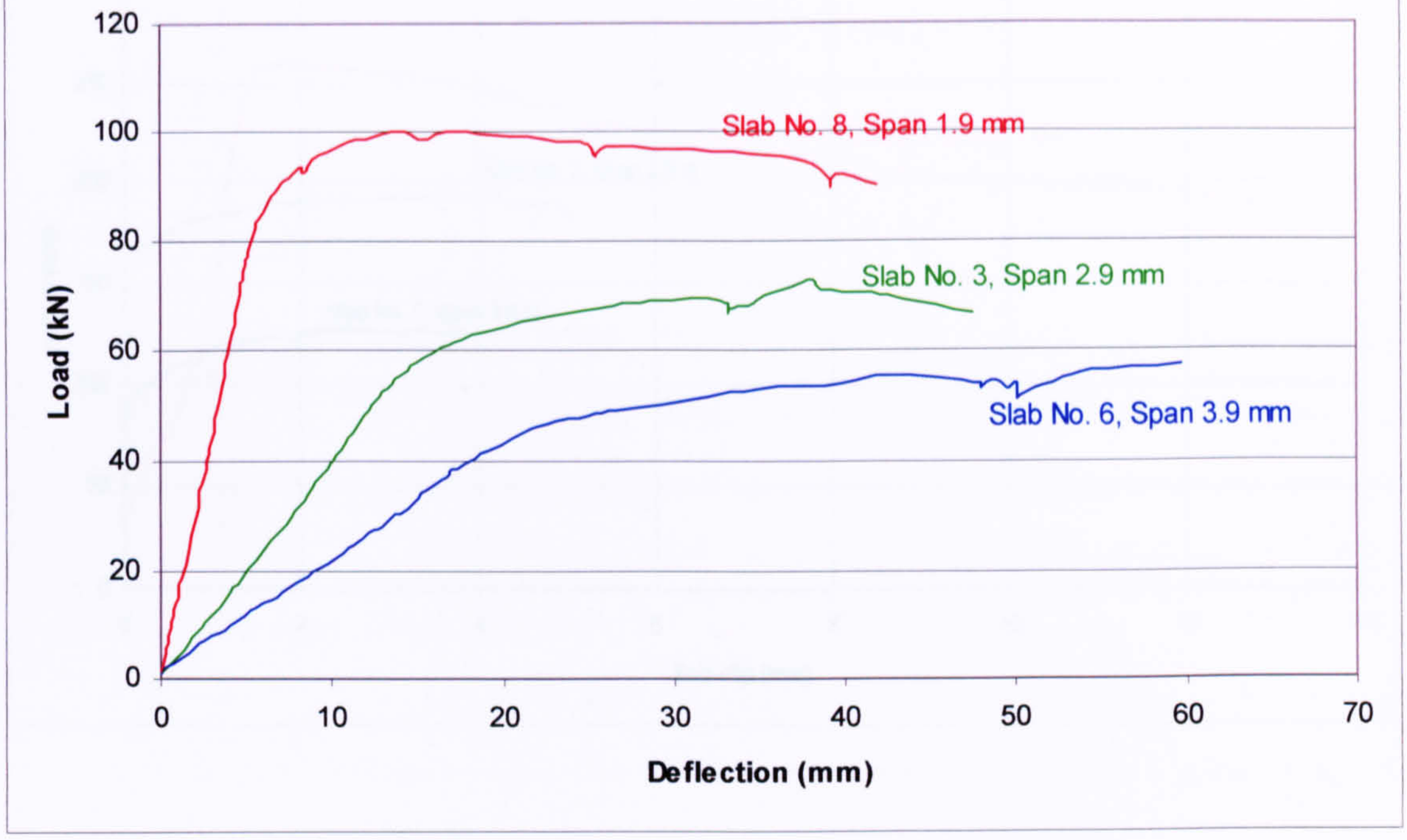

Figure 4. 31 Comparison of Load-End slip curves for slabs No. 1, 4, and 9 (165 mm depth)

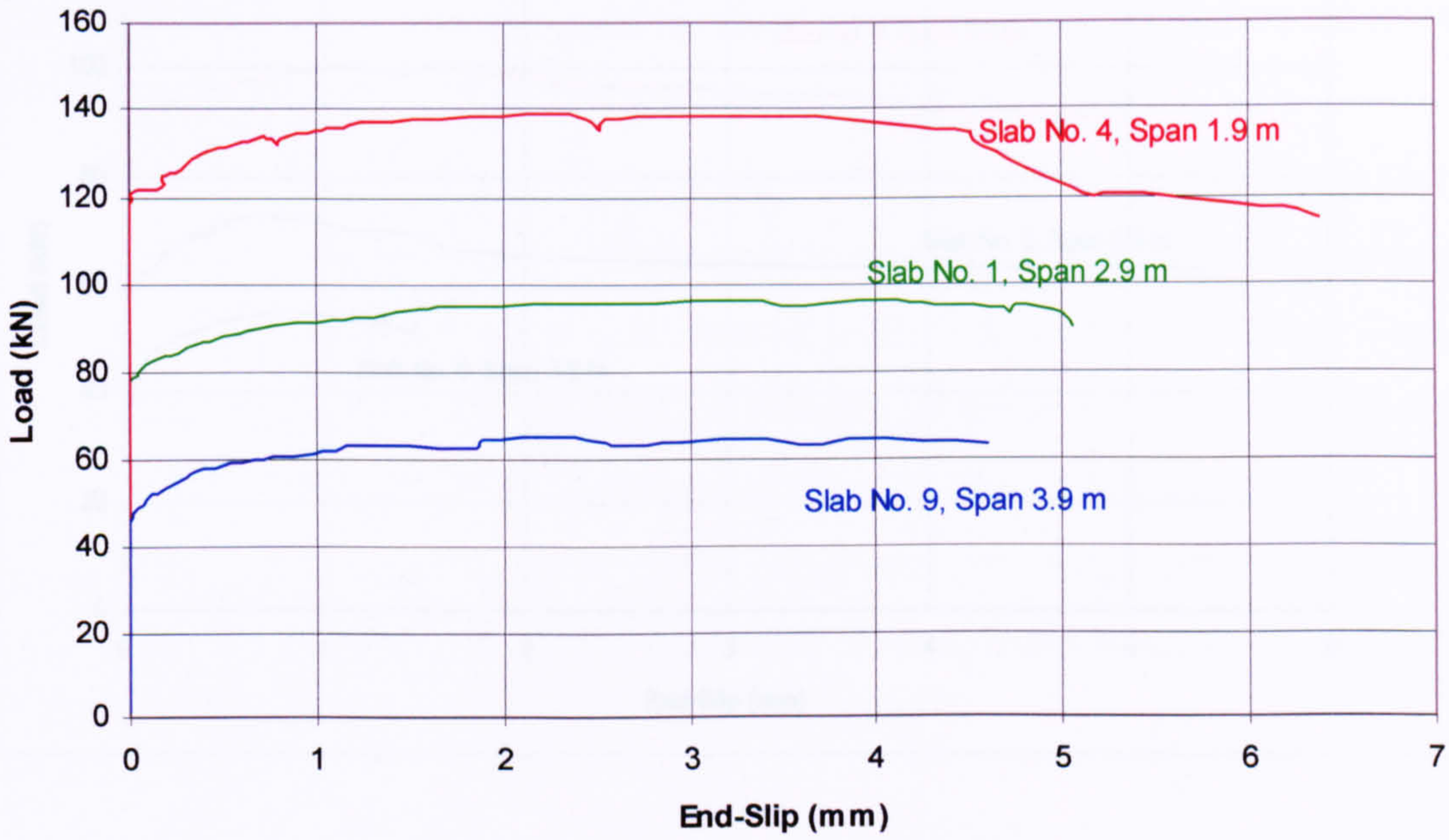

Figure 4. 32 Comparison of Load-End slip curves for slab no. 2, 5, and 7 (with reinforcement)

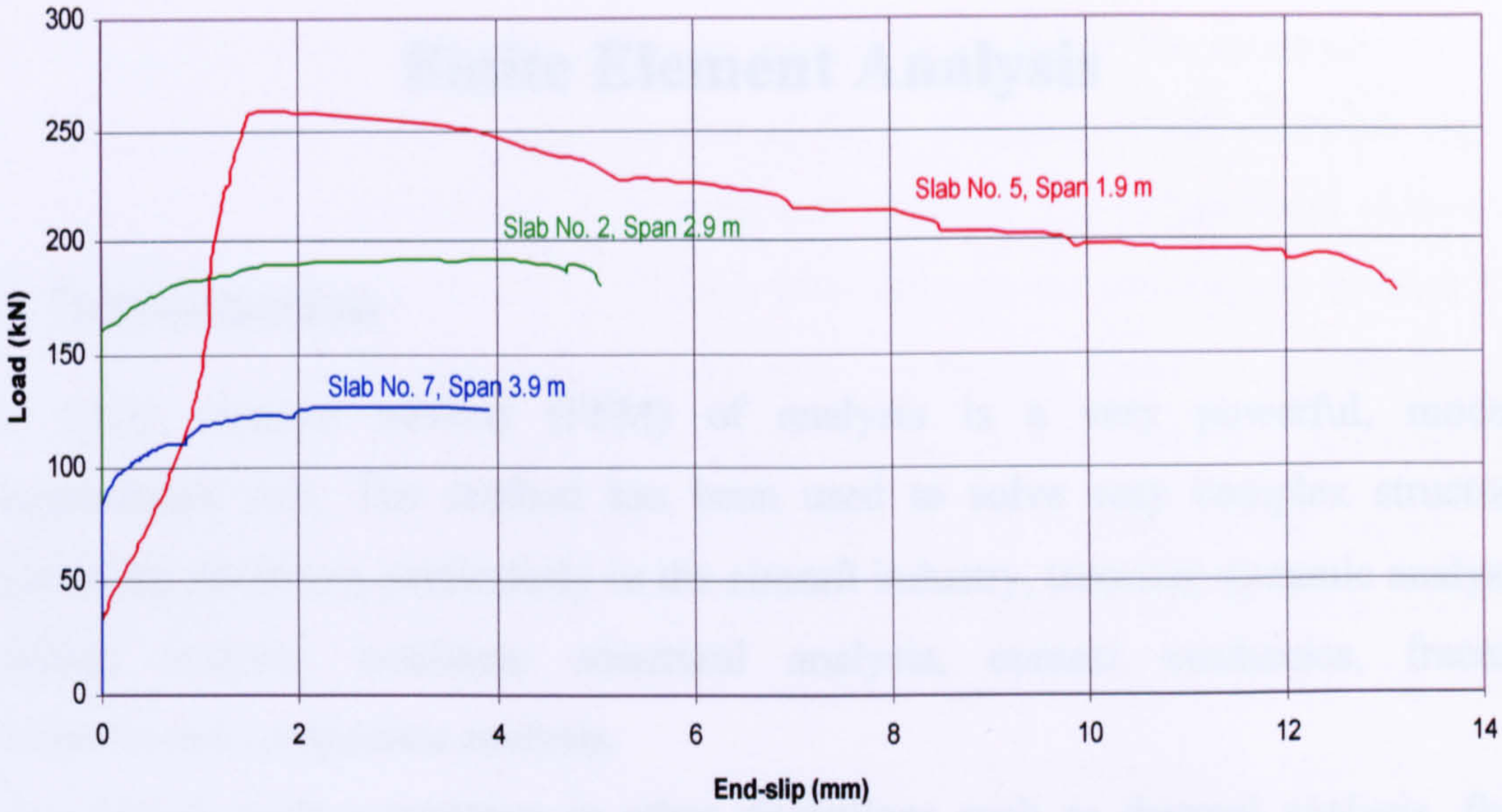

Figure 4. 33 Comparison of Load-End Slip curves for slab No. 3, 6, and 8 (135 depth)

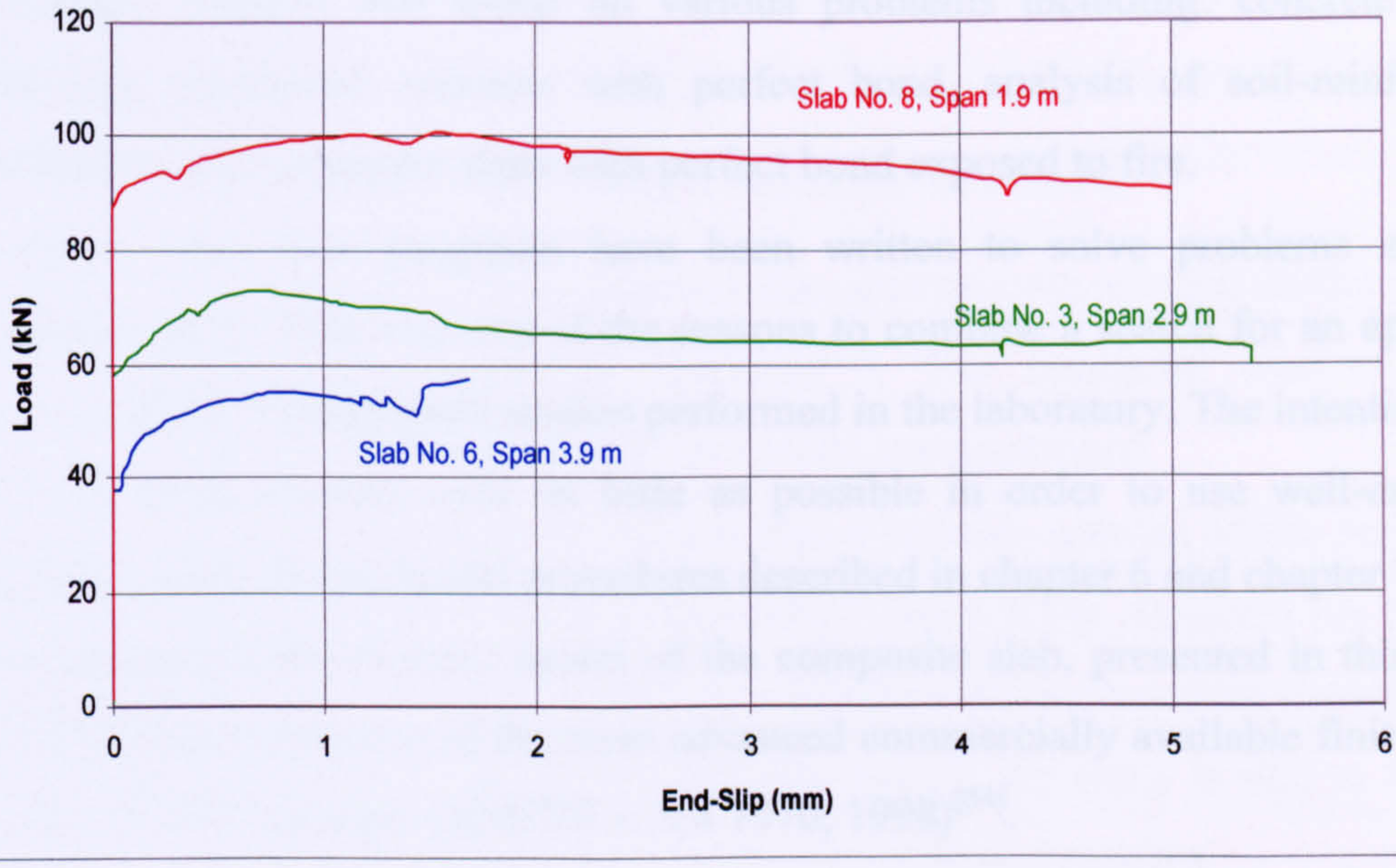

Chapter Five

Finite Element Analysis

5.1 Introduction

The finite element method (FEM) of analysis is a very powerful, modern computational tool. The method has been used to solve very complex structural engineering problems, particularly in the aircraft industry, transient dynamic analysis, buckling analysis, nonlinear structural analysis, contact mechanics, fracture mechanics and composites analysis.

It has gained wide acceptance in other disciplines such as thermal analysis, fluid mechanics and electromagnetics. The method requires the use of a digital computer because of the large number of computations involved.

Recent development of computational mechanics and material research, and fast implementation of the results in the finite element code has largely increased the possibilities for composite slab analysis using FEM. The numerical implementation of the recent research was tested on various problems including: concrete material behaviour, reinforced concrete with perfect bond, analysis of soil-reinforcement interaction, and composite slabs with perfect bond exposed to fire.

However, very few programs have been written to solve problems similar to composite slabs. This was one of the reasons to combine a search for an appropriate model with the experimental studies performed in the laboratory. The intention was to alter the finite element code as little as possible in order to use well-established material models elements and procedures described in chapter 6 and chapter 7.

The proposed finite element model of the composite slab, presented in this chapter, was developed using one of the most advanced commercially available finite element analysis (FEA) packages (ANSYS v. 5.4 1970, 1998)[54].

Chapter Five

Finite Element Analysis

5.1 Introduction

The finite element method (FEM) of analysis is a very powerful, modern computational tool. The method has been used to solve very complex structural engineering problems, particularly in the aircraft industry, transient dynamic analysis, buckling analysis, nonlinear structural analysis, contact mechanics, fracture mechanics and composites analysis.

It has gained wide acceptance in other disciplines such as thermal analysis, fluid mechanics and electromagnetics. The method requires the use of a digital computer because of the large number of computations involved.

Recent development of computational mechanics and material research, and fast implementation of the results in the finite element code has largely increased the possibilities for composite slab analysis using FEM. The numerical implementation of the recent research was tested on various problems including: concrete material behaviour, reinforced concrete with perfect bond, analysis of soil-reinforcement interaction, and composite slabs with perfect bond exposed to fire.

However, very few programs have been written to solve problems similar to composite slabs. This was one of the reasons to combine a search for an appropriate model with the experimental studies performed in the laboratory. The intention was to alter the finite element code as little as possible in order to use well-established material models elements and procedures described in chapter 6 and chapter 7.

The proposed finite element model of the composite slab, presented in this chapter, was developed using one of the most advanced commercially available finite element analysis (FEA) packages (ANSYS v. 5.4 1970, 1998)[54].

5.2 The finite element method (FEM):

The basic idea behind the finite element method is to divide the structure, body, or region being analysed into a large number of finite elements. These elements may be one, two, or three-dimensional. A popular and classical two-dimensional element is the triangle shown in Figure 5.1. When a two-dimensional structure is divided into hundreds or sometimes thousands of these non-overlapping triangles, we can see that essentially all planar geometries can be easily accommodated. Note that this particular element has three nodes (i, j, k) appropriately placed at the vertices of the triangle.

In a structural analysis application, the field variables may be displacements and/ or deflections and slopes. Therefore, in a structural finite element model, the nodal displacements and/or the nodal deflections and slopes are determined. From these, the stresses and/or bending moments within an element are easily derived. These results may then be used to obtain the shear stresses within each element if they are needed.

In summarizing, the two key ideas of the finite element method are:

1- discretization of the region being analysed into finite elements and,

2- the use of interpolating polynomials to describe the variation of a field variable within an element.

5.3 Advantages of the finite element method

The main advantages of FEM over most other approximate solution methods is that it can handle irregular geometries routinely[55]. The triangular element in two-dimensional applications is used with no special considerations.

Another significant advantage of FEM is that a variable spacing of the nodes is also routinely handled. When a body is discretized using finite elements (in FEM), the nodes are said to form a mesh. Typical two-dimensional meshes were shown in Figure 5.2 and 5.3. When the nodes are not equally spaced, the mesh is said to be graded. The finite element method lends itself to the use of graded meshes.

Another advantage of FEM, especially over analytical solution techniques (as opposed to numerical techniques) is the ease with which non-homogeneous and anisotropic materials may be handled. Materials whose properties are not specially

dependent are said to be homogeneous, whereas materials with specially dependent properties are heterogeneous.

Materials may also be classified as isotropic or anisotropic. An isotropic material is one whose properties (Young's modulus, thermal conductivity, etc.) do not exhibit a direction sensitivity. For example, even though concrete may be non-homogeneous, each direction appears to have the same (rather random) variation in thermal conductivity and, therefore, it is isotropic. Anisotropic materials, on the other hand, will have one or more properties that are direction-dependent. For example, a laminated metallic structure quite frequently will have different values of certain properties, such as Young's modulus or thermal conductivity, in different directions. Wood is another example of an anisotropic material; it is generally stiffer in the direction of the grain and hence would have a higher value of Young's modulus in this direction. Very little extra effort is required in the FEM formulation when heterogeneous and/or anisotropic materials are to be modelled, even when some parts of the structure or body are made of one material and other parts are made of different materials.

All the various types of boundary conditions that are encountered in a typical FEM application except those that require prescribed values of the field variables themselves, are automatically included in the formulation. The typical field variables are displacements in structural and stress analysis, temperatures in thermal analysis, fluid velocities and pressures in fluid flow analysis, etc. The prescribed displacements, temperatures, velocities, pressures, etc., are not automatically included in the FEM formulation and solution. They are systematically enforced just before the solution for the nodal values of the unknown field variables.

Another advantage is that higher-order elements may be implemented with relative ease. Several higher-order elements are shown in Figure 5.4. Higher-order elements require the use of higher-order interpolating polynomials. Note that additional nodes are introduced along the sides of the two-dimensional elements and between the two end nodes of the one-dimensional element. Occasionally, interior nodes are introduced as shown in Figure 5.4. The use of these nodes requires special considerations.

5.4 ANSYS

The ANSYS program was introduced by Dr. John Swanson and Swanson Analysis Systems, Incorporated (SASI)[54], in 1970. Since that time, the program, SASI, and ANSYS Support Distributors (ASDs) have grown as part of a commitment to provide the latest finite element analysis and design technology to engineers worldwide. Today, ANSYS capabilities are available on computers that range from PCs to supermainframes.

The ANSYS program is a computer program for finite element analysis and design. The program can be used to determine to find out how a given design (e.g., a machine component) works under operating conditions. The ANSYS program can also be used to calculate the proper design for given operating conditions.

The ANSYS program is a general-purpose program, it may be used for almost any type of finite element analysis in virtually any industry. The system includes facilities for linear and nonlinear stress analysis, step by step dynamic analysis, and other problems.

It has a finite element library that contains over 120 different element types. Each element type is identified by a unique number and a prefix that identifies the element category: BEAM4, PLANE77, SOLID45, CONTAC40,SHEL181...etc. It includes different material properties including linear, nonlinear, anisotropic,....etc. Different element types and load cases can be combined to represent different parts of structures. It contains an interactive post- and pre-processing graphics package, which enables plotting isometric or perspective views or models from different positions. Results may be displayed as contours, vectors, displaced shapes, or force/moment diagrams.

5.4.1 The required data file to run ANSYS software[54]

5.4.1.1 Model construction:

This is probably the most time consuming part of the analysis. In this step, the following are specified: Job-name analysis title and PREP7 is then used to define the element types (solid45, shell181, or contac40,...etc).

Element real constants are properties that are specific to a given element type, such as cross-sectional properties of a beam element. For example, the real constant for BEAM3, (a 2-D beam element) are areas, moment of inertia, shear deflection constant, initial strain, height. Not all elements require real constants.

Defining material properties for most element types depends on the application. Material properties may be linear, non-linear, and/or anisotropic.

The main objective of creating model geometry is to generate a finite model, nodes and elements, that adequately describes the model geometry.

There are two methods to create the finite element model: solid modelling and direct generation.

5.4.1.2 Load application and solution:

Defining the analysis type and analysis options: The analysis type is chosen based on the loading conditions and the response required. For example, if natural frequencies and mode shapes are to be calculated, a modal analysis would be chosen. The following analysis types are available in the ANSYS program: static, transient, harmonic...etc.

For load application, the word loads as used in the manual includes boundary conditions (constraints, supports, or boundary field specifications) as well as other externally and internally applied loads. Loads in the ANSYS program are divided into a number of categories:

Degree of freedom (DOF) Constraints, Forces, Surface Loads, Body Loads, Inertia Loads, and Coupled-field Loads. Most of these loads can be applied either on the solid model (key-points, lines and areas) or the finite element model (nodes and elements). Two important load-related terms are load step and sub-step.

To specify load step options these may be changed from load step to load step, such as number of sub-steps, time at the end of a load step, and output controls. Depending on the type of analysis being carried out, load step options may or may not be required. To initiate the Solution, the action command for calculations is SOLVE. When this command is issued, the ANSYS program takes model and loading information from the database and calculates the results. Results are written to the results files.

5.4.1.3 Results review:

Once the solution has been calculated, the ANSYS postprocessors can be used to review the results. Two postprocessors are available: POST1 and POST26.

POST1, the general post-processor is used to review results at one sub-step (time step) over the entire model.

POST26, the time history post-processor, is used to review results at specific points in the model over all time steps.

5.4.2 Element characteristics

5.4.2.1 Lists of element types

The ANSYS program has a large library of element types. The ANSYS element library consists of more than 100 different element formulations or types. An element type is identified by a name (8 characters maximum), such as BEAM3, consisting of a group label (BEAM) and a unique identifying number (3). The element descriptions are arranged in order of these identification numbers. The element is selected from the library for use in the analysis by inputting its name on the element type command ET.

Two-Dimensional and three-dimensional elements:

ANSYS models may be either two-dimensional or three-dimensional depending upon the element types used, two-dimensional models must be defined in an X-Y plane. They are easier to set up, and run faster than equivalent three-dimensional models. Two-dimensional element types may be used in three-dimensional models.

Element characteristic shape:

In general, four shapes are possible: point, line, area, or volume. A point element is typically defined by one node, e.g., a mass element. A line element is typically represented by a line or arc connecting two or three nodes. Examples are beams, spars, pipes, and axisymmetric shells. An area element has a triangular or quadrilateral shape and may be a 2-D solid element or a shell element, A volume element has a tetrahedral or brick shape and is usually a 3-D solid element.

Degrees of freedom and discipline:

The degrees of freedom of the element determine the discipline for which the element is applicable: structural, thermal, fluid, electric, magnetic, or coupled-field. The element type should be chosen such that the degrees of freedom are sufficient to characterise the model's response. Including unnecessary degrees of freedom increases the solution memory requirements and running time. Similarly, selecting element types with unnecessary features, such as using an element type with plastic capability in an elastic solution, also unnecessarily increases the analysis run time.

User Elements:A particular element type may be created and used in an analysis as a user element. User elements and other user programmable features are described in the ANSYS Advanced Analysis Techniques Guide.

5.4.3 Structural analysis

Structural analysis is probably the most common application of the finite element method. The term structure implies not only civil engineering structures such as bridges and buildings, but also mechanical components such as pistons, machine parts, tools, and the like.

Many types of structural analyses are available in the ANSYS program. The primary unknowns (nodal degrees of freedom) calculated in a structural analysis are displacements. Other quantities, such as strains, stresses, and reaction forces, are then derived from the nodal displacements.

The following types of structural analyses are available:

5.4.3.1 Static analysis

Static analysis is used to determine the displacements, stresses, strains, and forces in structures or components due to loads that do not induce significant inertia and damping effects. Steady loading and response conditions are assumed, i.e., the loads and the structure's response are assumed to vary slowly with respect to time. The kinds of loading that can be applied in a static analysis include externally applied forces and pressures, steady-state inertial forces (such as gravity or rotational velocity), imposed (non-zero) displacements, temperatures (for thermal strain).

A static analysis can be either linear or nonlinear. All types of nonlinear analysis are allowed large deformations, plasticity, creep, stress stiffening, contact elements,...etc.

Perhaps the simplest form of analysis, a static analysis calculates the effects of steady loading conditions on a structure. However, steady inertia loads, such as gravity and rotational velocity can be included. In addition, if time-varying loads can be approximated as static equivalent loads (such as the static equivalent wind and seismic loads commonly defined in many building codes), their effects can also be evaluated using a static analysis.

5.4.3.2 Modal analysis

Modal analysis is used to determine the natural frequencies and mode shapes of a structure. The natural frequencies and mode shapes are important parameters in the design of a structure for dynamic loading conditions. Different mode extraction methods are available in ANSYS.

5.4.3.3 Harmonic analysis

Harmonic response analysis is a technique used to determine the steady-state response of a linear structure to loads that vary harmonically with time. The idea is to calculate the structure's response at several frequencies and obtain a graph of some response quantity (usually displacements) versus frequency. Peak responses are then identified on the graph and stresses reviewed at those peak frequencies.

5.4.3.4 Transient dynamic analysis

Transient dynamic analysis (sometimes called time-history analysis) is a technique used to determine the dynamic response of a structure under the action of any general time-dependent loads. This type of analysis can be used to determine the time-varying displacements, strains, stresses, and forces in a structure as it responds to any combination of static, transient, and harmonic loads. The time scale of the loading is such that the inertia or damping effects are considered to be important.

5.4.2.5 Spectrum analysis

A spectrum analysis is one where the results of a modal analysis are used with a known spectrum to calculate displacements and stresses in the model. It is mainly used in place of a time-history analysis to determine the response of structures to random loading conditions such as earthquakes, wind loads, ocean wave loads, jet engine thrust, rocket motor vibrations, and so on.

5.4.3.6 Buckling analysis

Buckling analysis is a technique used to determine buckling loads - critical loads at which a structure becomes unstable - and buckled mode shapes - the characteristic shape associated with a structure's buckled response.

5.5 Non-linear structural analysis

To describe nonlinear behaviour it is necessary to review some basic principles of structural theory:

When a force (F) is applied to a structural system Figure 5.5.a, that system will displace some corresponding amount (u). The predictability of the relationship between F and u allows engineers to calculate the response of structures to give sets of loads. In many engineering applications, the relationship between F and u can be described by the linear equation known as Hooke's Law (Figure 5.5.b):

$F = Ku$

In this equation, the proportionality constant K represents the stiffness of the structural system. As long as a structure's stiffness remains constant, that structure is said to be linear, because its behaviour can be analysed using linear equations. Many engineered structural systems are designed to remain linear (or nearly so) within their normal range of service loads. Standard linear equation solvers such as are found in the ANSYS program and other finite element programs were initially developed to enable engineers to analyze complex linear structures.

However, there are significant classes of engineering applications for which the relationship between force and displacement is not constant. A plot of F versus u for such systems is not a straight line; hence, such systems are said to be nonlinear. The behaviour of such systems cannot be represented directly with a set of linear equations Figure 5.5.c.

The linear structures are usually truly non-linear to some extent, but the degree of non-linearity is often small enough for it to be neglected Figure 5.5.d.

Some structures might have linear and non-linear behaviour ranges Figure 5.5.e:

If the range of interest is just the linear range (typically the case for engineered systems subjected to service loads), there is no need for a non-linear analysis.

There are many potential causes of non-linear behaviour. They may be grouped into three main categories, which are covered in sections 5.5.1, 5.5.2, and 5.5.3.

5.5.1 Geometric non-linearities

If a structure experiences large deformations, its changing geometric configuration can cause the structure to respond non-linearly.

An example of geometric non-linearity would be the fishing rod shown in Figure 5.6. a, b, and c. Under light lateral loads, the rod tip is extremely flexible (low lateral stiffness). As lateral load increases, the rod deflects so much that the moment arm decreases appreciably, causing the rod tip to exhibit increasing stiffness at higher loads. Thus, the structure's stiffness changes as a result of displacements and geometric changes.

Four kinds of geometric non-linearities can be included in an ANSYS analysis:

Large strain, large deflection, crack, and stress stiffening.

5.5.2 Material non-linearities

Non-linear stress-strain relationships are a common cause of non-linear structural behaviour Figure 5.7.a, and b as example.

Many factors can influence a material's stress-strain properties, including load history (as in elasto-plastic response), environmental conditions and the amount of time that a load is applied (as in creep response). Elastic materials such as rubbers can also behave nonlinearly, and are modelled using special hyperelastic material properties.

5.5.2.1 Plasticity

Plasticity is a material behaviour in which the material deforms permanently under the action of some applied loads.

Most engineering materials behave linearly below some stress level, called the proportional limit. Below the proportional limit, the stress is linearly related to the strain. Additionally, most materials behave elastically below a stress level called the yield point. Below the yield point, any straining, which occurs with loading completely, disappears upon removal of the load shown in Figure 5.8.

There is usually little difference between the yield point and the proportional limit, and the program will always assume them to be the same. The portion of the stress-strain curve below the yield point is called the elastic portion, and that above is the plastic portion shown in Figure 5.8. The part of the curve beyond the yield point is called the strain hardening portion of the curve. Plasticity analyses account for material behaviour in the plastic range.

5.5.2.2 Contact non-linearities

Contact non-linearities occur when two or more components (or parts of one component) come into or out of contact with each other (or itself) during the course

of the deformation process. Contact non-linearities also occur when two components slide relative to one another.

Contact is a non-linearity because one or both of the following are unknown:

- The contacting area(s).
- The forces transmitted, both normal and tangential (frictional).

One of the purposes of the analysis is to determine these quantities.

Contact can also be a severe non-linearity since the analysis can experience an abrupt change when areas make or break contact.

Contact problems are highly non-linear and require significant computer resources to solve. It is important that the physics of the problem is understood and that time is taken to set up the model of the problem to run as efficiently as possible.

The contact stiffness is used to enforce compatibility between the contacting surfaces. The higher the value, the better this enforcement (the less the penetration). However, too high a value for contact stiffness can cause convergence difficulties.

The value must be chosen carefully in order to both minimize the penetration and at the same time minimize the number of iterations needed.

The analysis may need to run part of the way through a few times in order to arrive at a good value. Note, in this study the normal contact stiffness was being changed from one load step to another.

5.5.2.3 Friction

The tangential or sliding behaviour of two contacting bodies may be frictionless or may involve friction.

Frictionless behaviour allows the two bodies to slide relative to one another without any resistance. In the presence of friction, however, shear forces develop between the two bodies.

When the tangential forces attempting to move two bodies relative to each other are "small", the two bodies will stick together. If the forces are "large", then the two bodies will slide relative to each other. An opposing shear stress will still be

experienced by both bodies. Loading must be applied in the same manner as it occurs on the real component.

Friction is a complex phenomenon that is a function of the contacting materials, surface roughness, temperature, relative velocity of the bodies, etc.

5.5.3 Changing status (including contact)

Many common structural features exhibit nonlinear behaviour that is status-dependent Figure 5. 9. For example, a tension-only cable is either slack or taut; a roller support is either in contact or not in contact; permafrost is either frozen or thawed. The stiffness of these and other systems shifts abruptly between different values, depending on the overall status of the item. Status changes might be directly related to load (as in the case of the cable), or they might be determined by some external cause (such as disturbed thermal conditions in the permafrost). Non-linear elements and birth and death options are used to model such status changes in the ANSYS program.

Situations in which contact occurs are common to many different non-linear applications. Contact forms a distinctive and important subset to the category of changing-status non-linearities.

For a simply supported composite slab subjected to a vertical load, the non-linearity develops with the onset of slip. Beyond this point increases in load result in nonlinear behaviour due to continuing slip at the interface and crushing of the concrete. At failure of the slab, local buckling of the thin profiled steel sheet may have occurred together with significant slip and deformation of concrete

A non-linear system cannot be analyzed directly with a linear equation solver. However, it can be analyzed by using a series of linear approximations, with corrections as shown in Figure 5.10. Each linear approximation requires a separate pass, or iteration, through the program's linear equation solver.

Special techniques are required to keep track of information generated during each iteration (information such as displacements, plastic strains, etc.), as well as to calculate the corrections necessary to drive the iterative analysis to a converged solution.

The ANSYS program has been designed such that the tedious aspects of these operations are all handled automatically, once the proper features and controls have been incorporated.

The iterative process that the ANSYS program uses to solve, correct, and re-solve a non-linear analysis is called the Newton-Raphson (N-R) method. Each iteration generated in this process is known as a Newton-Raphson iteration, or an equilibrium iteration.

5.5.4 Incremental loading and equilibrium iterations

One approach to non-linear solutions is to divide the load into a series of load increments. The load increments can be applied either over several load steps or over several sub-steps within a load step. At the completion of each incremental solution, the program adjusts the stiffness matrix to reflect the non-linear changes in structural stiffness before proceeding to the next load increment, Unfortunately, a pure incremental approach inevitably accumulates error with each load increment, causing the final results to be out of equilibrium, as shown in Figure 5.11.a.

The ANSYS program overcomes this difficulty by using Newton-Raphson equilibrium iterations, which drive the solution to equilibrium convergence (within some tolerance limit) at the end of each load increment, Figure 5.11.b illustrates the use of Newton-Raphson equilibrium iterations in a single DOF non-linear analysis.

5.6 Modelling composite slabs

Realistic modelling of composite slab behaviour requires the proper choice of constitutive modelling for the following phenomena:

- Plasticity and hardening in the steel sheeting.
- Non-linear mechanical interlocking resistance of the sheeting.
- Friction between the sheeting and the concrete at the support.

FEM was used as the only possible method of structural analysis which allows such combination of material and connection parameters. The FE analysis was performed by using of ANSYS version 5.3 see chapter 6 and chapter 7.

Recent development of computational mechanics and material research, and fast implementation of the results in the finite element code has largely increased the possibilities for composite slab analysis using FEM.

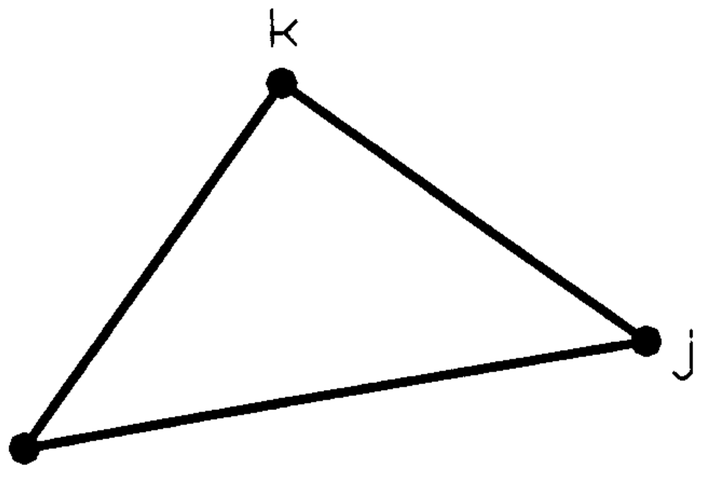

Figure 5.1 Three triangular element.

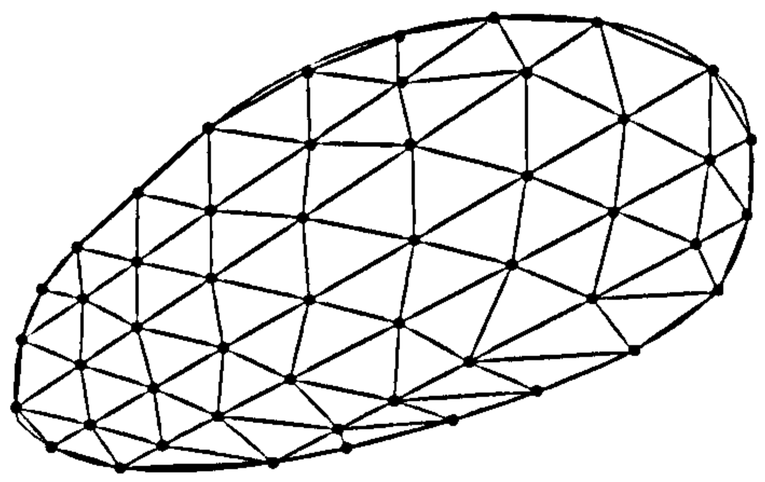

Figure 5.2 Irregularly shaped plate shown discretized into triangular finite elements.

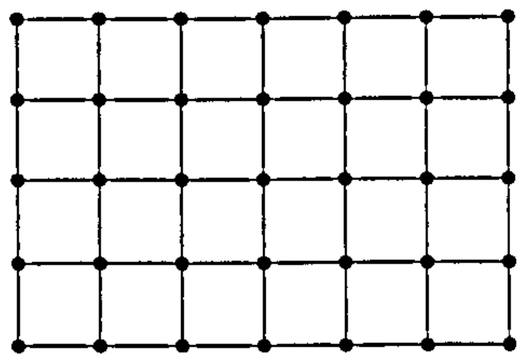

Figure 5.3 Rectangular plate discretized into rectangular elements.

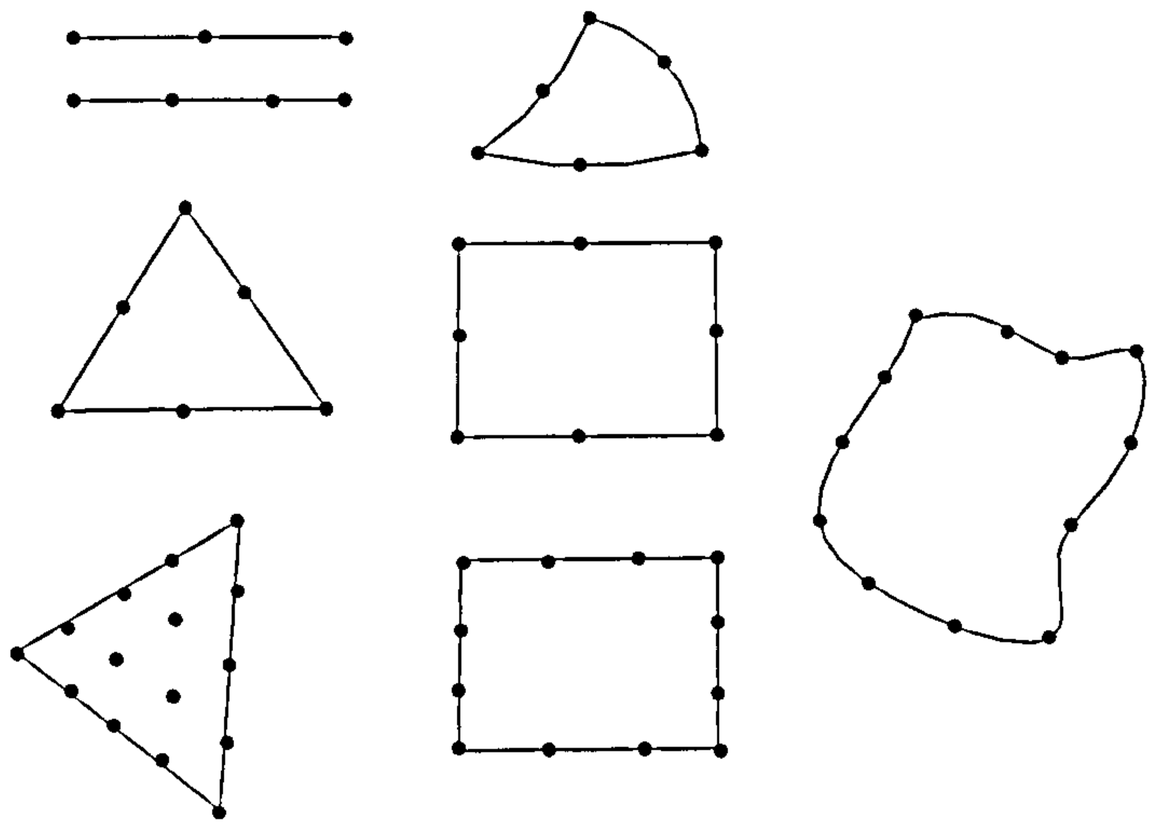

Figure 5.4 Representing higher order elements.

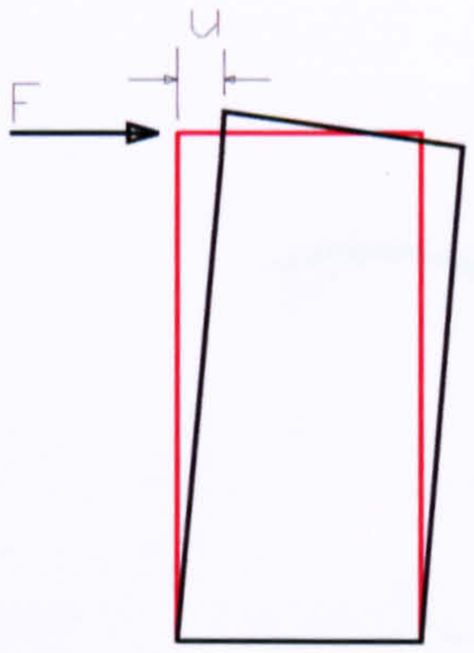

(a) $F = Ku$

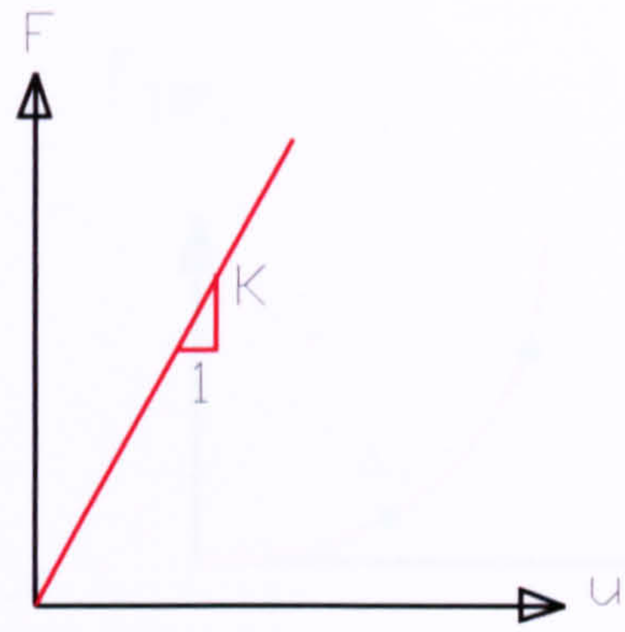

(b)

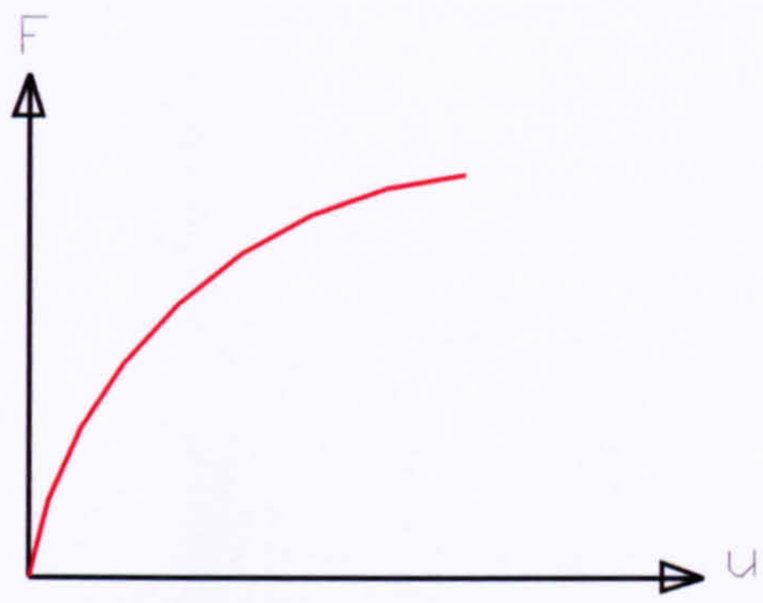

$F \neq Ku$

(c)

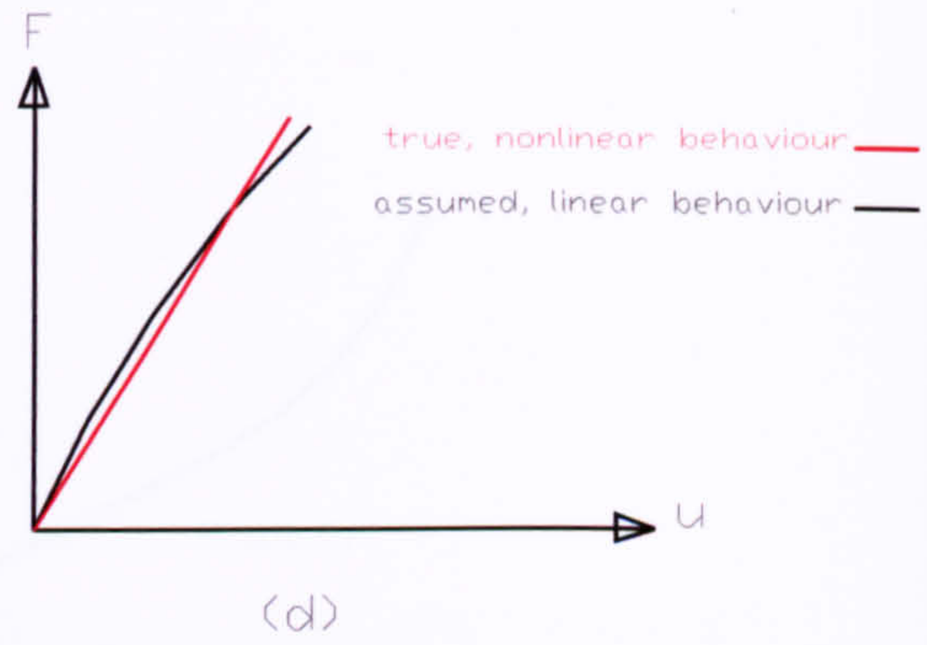

(d)

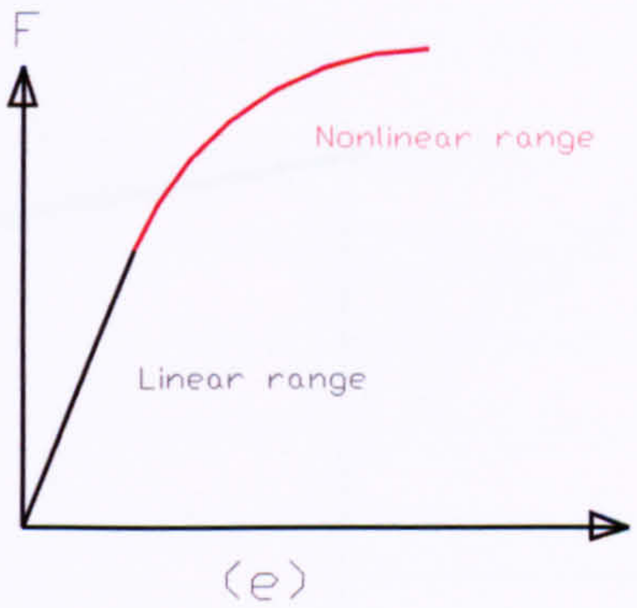

(e)

Figure 5.5 Non-linear behaviour of structures.

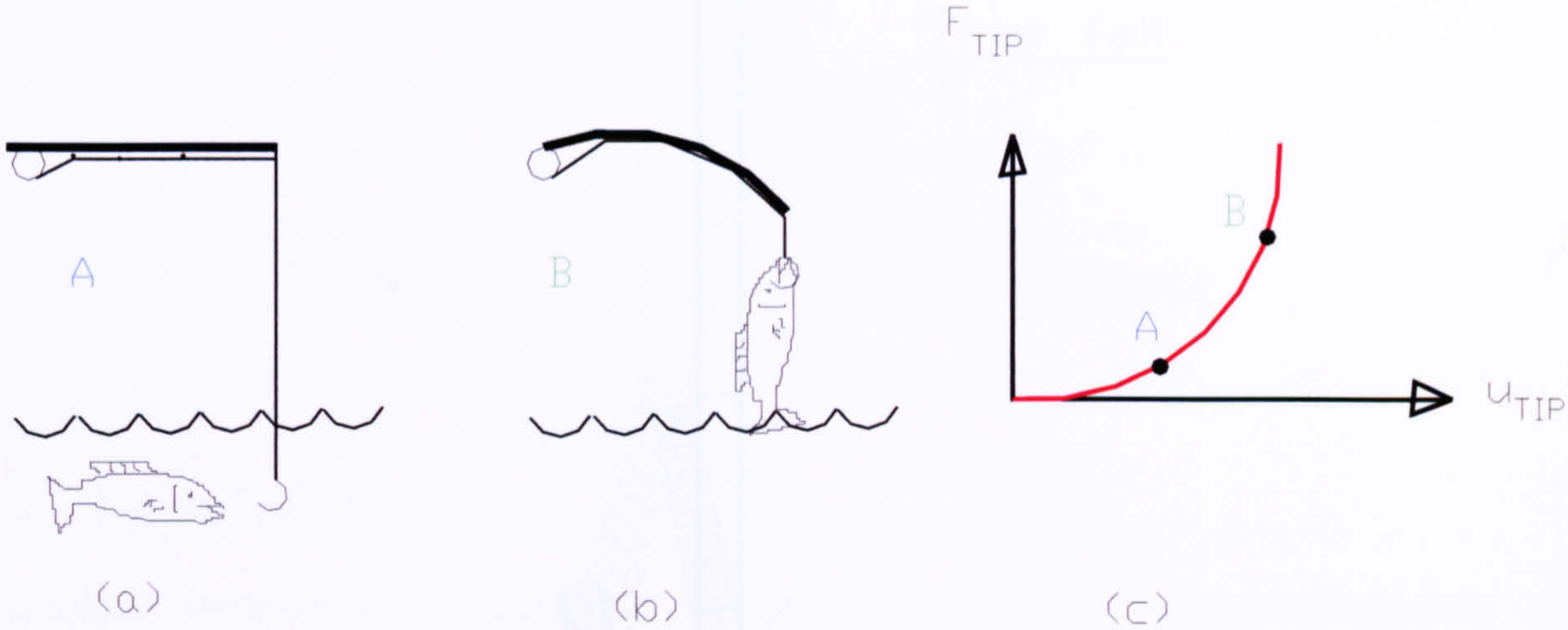

Figure 5.6 Example of geometric non-linearity of the fishing rod.

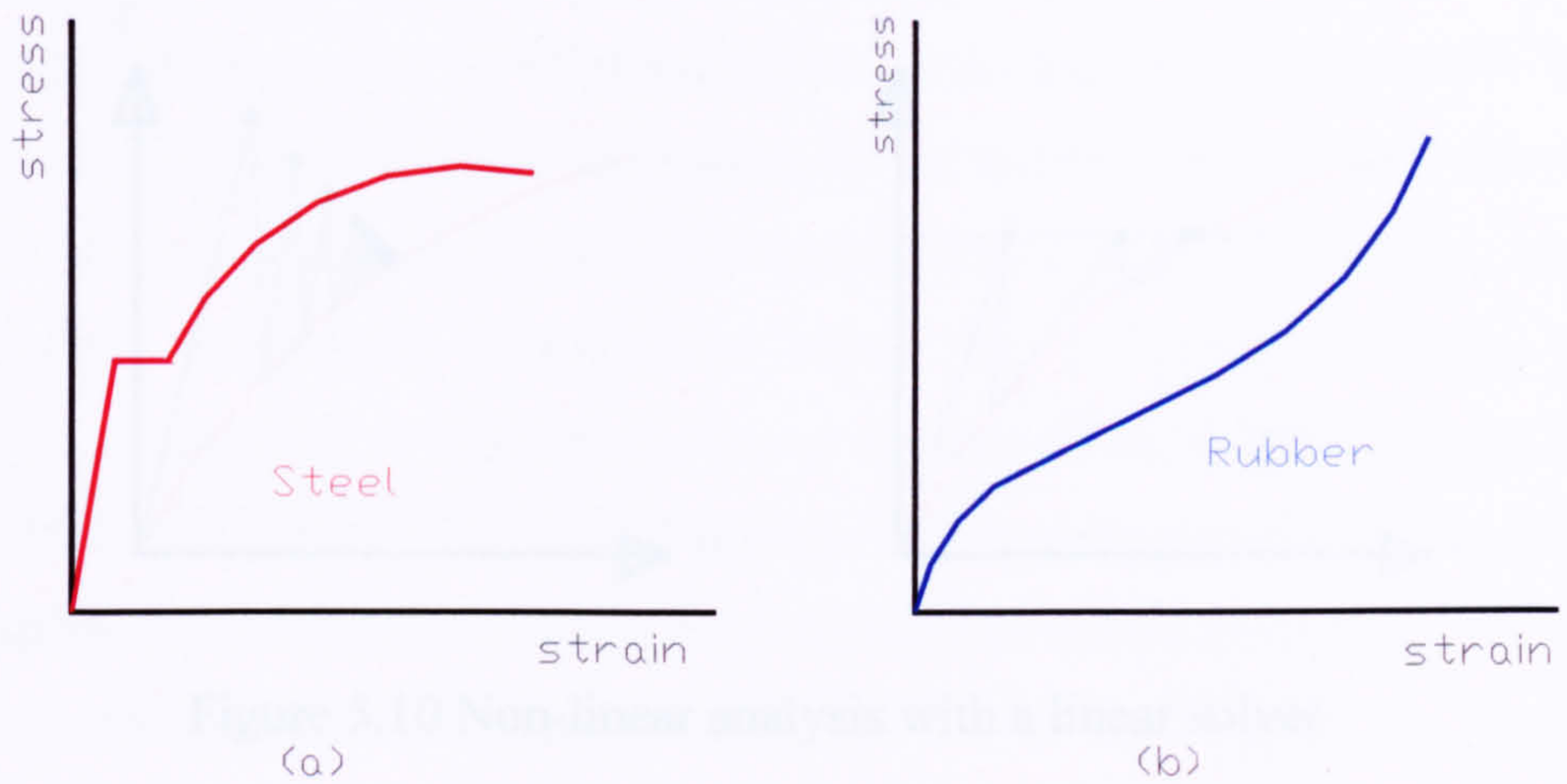

Figure 5.7 Non-linear stress-strain relationship.

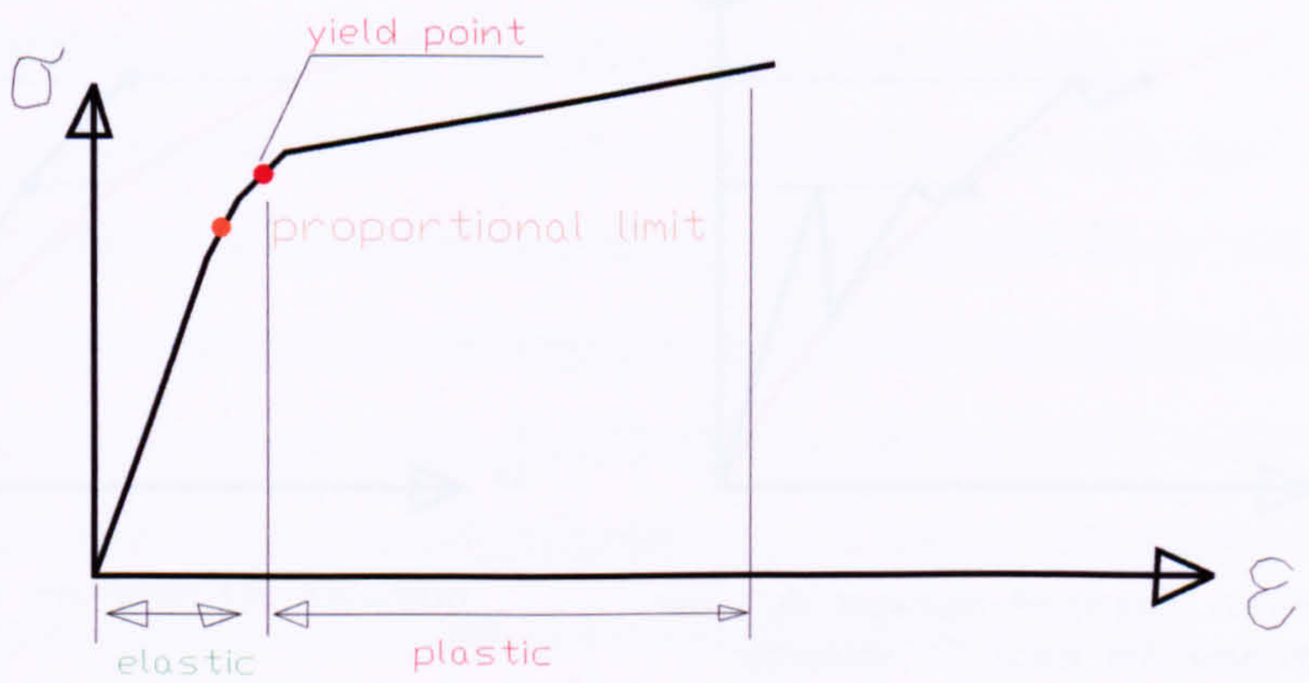

Figure 5.8 Stress –strain curve with the elastic and plastic parts.

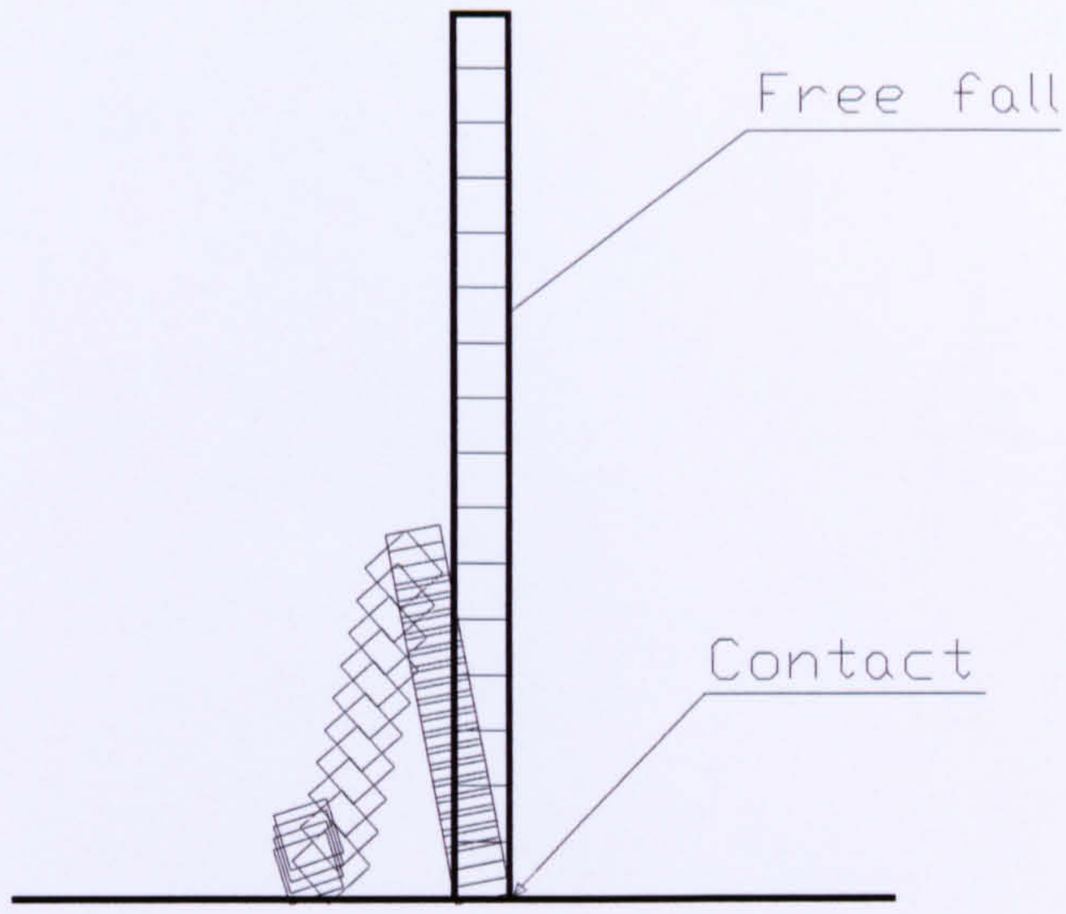

Figure 5.9 Changing status including contact.

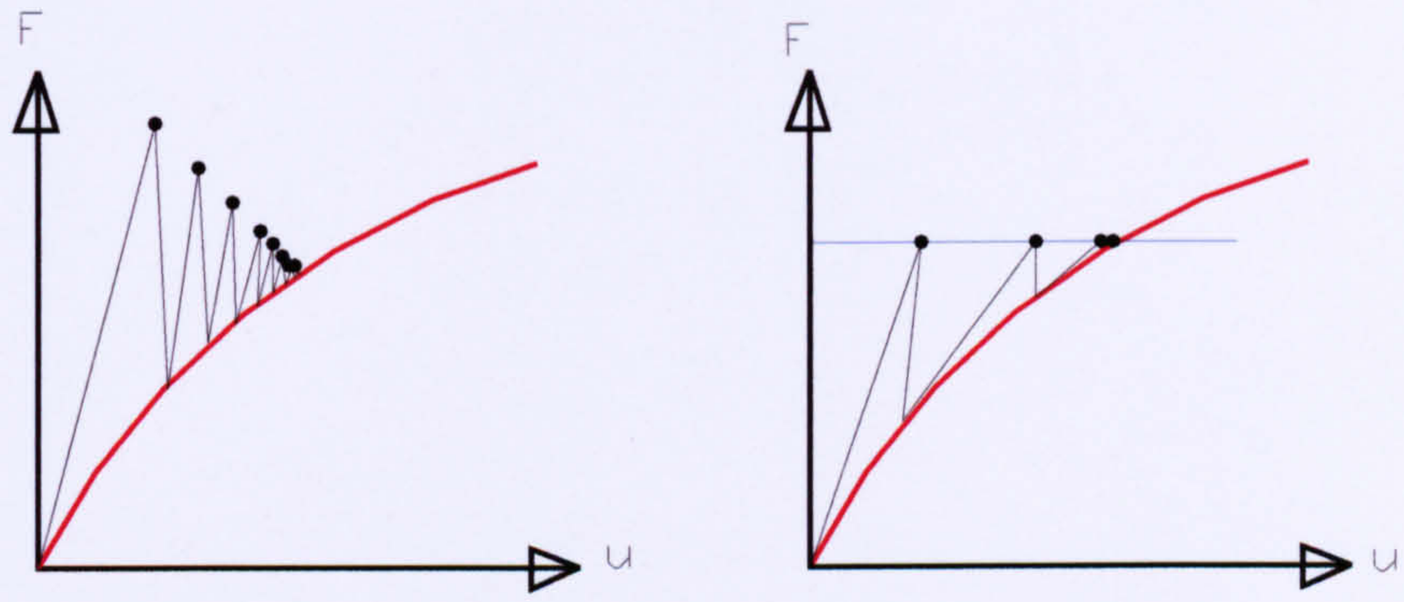

Figure 5.10 Non-linear analysis with a linear solver

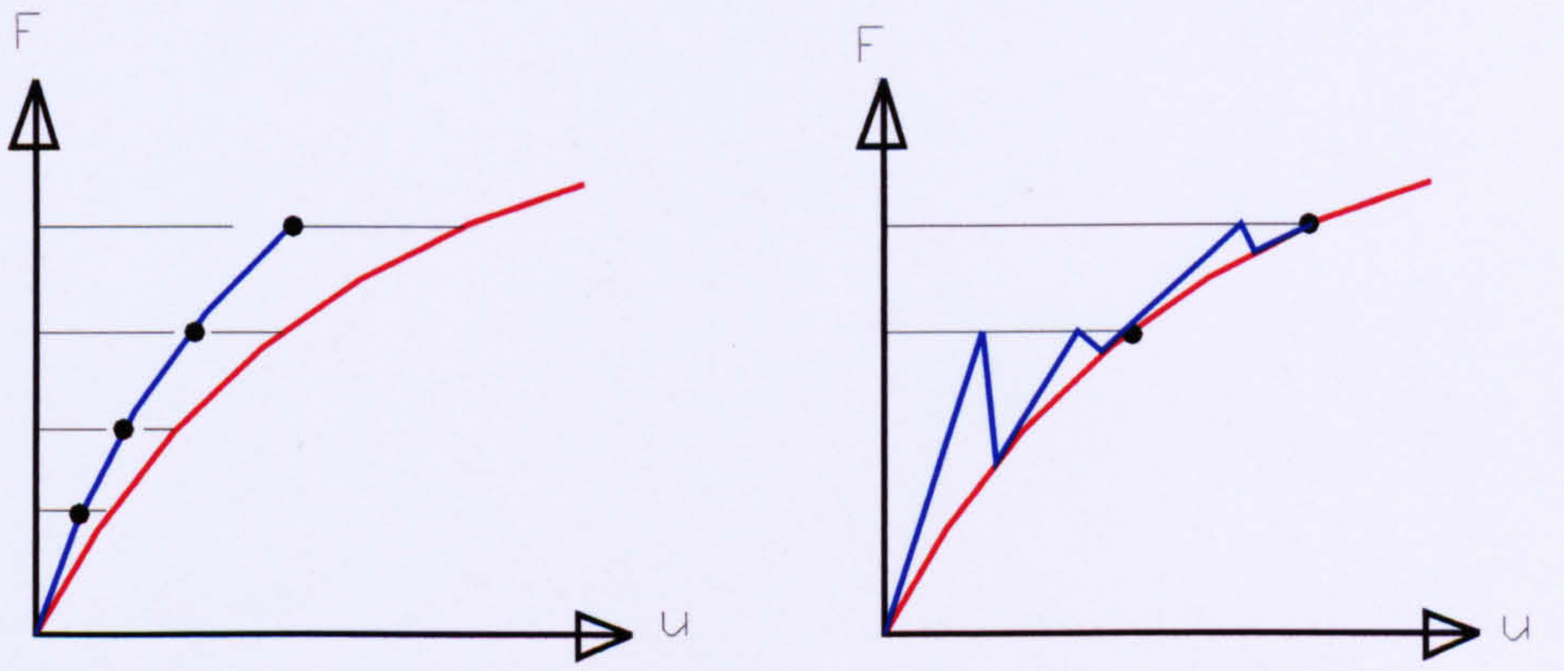

(a) Pure incremental solution

(b) Full Newton-Raphson iteractive solution (2 load increments)

Figure 5.11 Incremental loading

Chapter Six

Finite Element Modelling of Tests

6.1 Introduction

Composite steel-concrete construction allows designers to take advantage of the most favourable mechanical material properties of both steel and concrete, to produce economical structures. Currently, composite floor slabs are designed using the results of full scale tests, which is costly and time consuming.

Investigation by means of experimental tests is important and useful. The shear resistance of composite slabs can generally be determined by tests. However, the number of experiments is limited for economical reason. Meanwhile, experiments only reflect the overall behaviour of slabs. The influences of some individual variables are not easy to assess in tests and are also difficult to distinguish from each other in the test results. These disadvantages can be compensated by use of the finite element method. A flexible numerical model can be extended to carry out parametric studies and yield more information.

Recent developments, including the development of numerical techniques and knowledge of the mechanical properties of concrete and steel, have made it possible to determine the behaviour by modelling the composite slab.

Studies on composite floor slabs were started some time ago to update design approaches and to investigate modelling of composite floor slabs. These studies include the development of mathematical models for the calculation of the behaviour of the structure of various forms. In this chapter, the use of FE method is described for the prediction of behaviour of composite floor slabs. The method mainly uses the ANSYS finite element to provide the solution to such problems.

This Chapter attempts to validate use of the finite element program for modelling composite slabs by combining the development of an appropriate model with the experimental studies performed in the laboratory. The intention was to alter the finite

element code as little as possible in order to use well-established material models, elements and procedures approved for various structural problems.

The proposed finite element model of the composite slab, presented within this chapter, was developed using an advanced commercially available finite element analysis (FEA) package (ANSYS V.5.3 58,1997)[54].

A non-linear 3D analysis of a small and full-scale composite slab with partial interaction between steel sheeting and concrete has been performed and compared to experimental results with a slightly altered contact stiffness obtained from the small-scale tests, good agreement with the actual test results for longitudinal shear failure indicates proper modelling and use of correct input data.

Material and interaction properties have been determined from standard and new tests. Plasticity of the concrete, non-linear shear resistance, and friction at interface between concrete and sheeting are included in the numerical model.

6.2 Finite element model

An assembly of finite elements representing the concrete slab and profile steel sheeting, connected together by contact elements, has formed the basis for the modelling of composite slabs.

The problem of non-linear analysis of composite members can be solved in part using existing ANSYS capabilities for modelling parameters, which can affect the behaviour of such structures. The elements, which were provided as follows:

Design philosophy:

The finite element (FE) model developed used a combination of element types from the ANSYS library in order to model the composite slab. Three-dimensional Solid Elements were used to model the concrete, and Strain Shell element was used to model the profiled steel sheeting.

The composite action was completed by connecting together each of Solid and Shell Elements as follows:

For the full scale composite slabs connection was made with 3-D Point-to-Point Contact Element and Combination Element as illustrated in Figure 6.1.a. For the small-scale composite slab, 3-D Point-to-Surface Contact Element and Combination Element, as illustrated in Figure 6.1.b., were used.

To model a composite slab, it is necessary to allow adjacent steel and concrete to slip relative to each other when the bond strength or shear bond capacity has been exceeded. The relative movement of the steel sheet and concrete (when facing each other) must be controlled so that they are not able to move through each other, but are free to separate.

It is also essential to allow relative shear movements, both before and after the bond has broken, to occur in the direction that corresponds to the principal stress at interface. It was difficult to model three-dimensional behaviour of the composite slab, which can perform the above action. Thus, it was necessary to use several elements in combination to create the same effect. This combination of gap elements was matched to represent the true behaviour of the structure.

The suitability of this approach must be judged by the capability of the model to represent the measured load-deflection, measured load-slip response and the ultimate load, whilst being based on measured material properties.

The CONTAC element, which is a 3-D Point-to-Point element, is capable of supporting only compression in the direction normal to the contact surface and shear in the tangential direction.

Figure 6.2 shows the force-deflection relationship for this element in which it can be seen that the contact surfaces are free to separate in the normal direction. The stiffness (KN), of the element inhibits the movement of the two contact surfaces through each other but not prevent it. A slight overlap will occur and this is used to calculate the normal force between the contact surfaces. Coulomb friction is used to associate this normal force to the maximum sustainable shear force. If only the CONTAC element was used, the analysis would fail at an unrealistically low load. The CONTAC element is used for its abilities to prevent overlapping. However, a COMBIN element was used to increase the shear bond strength, as shown in Figure 6.2.

The COMBIN element is a one-dimensional element which has several capabilities, most of which were not used in this application. In other words, the load-deflection relationship of this element resembled the stress-bond deformation of the structure.

6.2.1 Concrete

The concrete is modelled with 3-D Structural Solid Element which is used for three-dimensional modelling of solids with or without reinforcing bars.

Eight nodes having three degrees of freedom at each node define the solid element: translations in the nodal x, y, and z directions.

The geometry, node locations, and the co-ordinate system for this element are shown in Figure 6.3.

Node and element load:

Loading is defined to be two types: node and element. Nodal loads defined at the nodes and are not directly related to the elements. These nodal loads are associated with the degrees of freedom at the node and are typically entered with the D and F commands (such as nodal displacement constraints and nodal force loads)[61]. Element loads are surface loads, body loads, and inertia loads. Element loads are always associated with a particular element (even if the input is at the nodes).

Treatment of non-linear element: These elements have non-linear geometric capability such as large strain, large deflection and stress stiffening.

6.2.2 Steel sheeting

The trapezoidal shape of sheeting is modelled with Finite Strain Shell Element. The element is suitable for analysing thin to moderately thick shell structures. It is a four nodes element with six degrees of freedom at each node: translations in the x, y, and z directions, and rotations about the x, y, and z-axes.

Element geometry:

The geometry, node locations, and the co-ordinate system for this element are shown in Figure 6.4. Four nodes define the element, I,J,K, and L. The thickness of the shell may be defined at each of its nodes. The thickness is assumed to vary smoothly over

the area of the element. As the element has a constant thickness, only one thickness needs to be input. If the thickness is not constant, all four thicknesses must be input.

Node and element load:

Pressures may be input as surface loads on the element faces as shown by the circled numbers on the Figure 6.4. Positive pressures act upon the element. Edge pressures are input as force per unit area.

Treatment of non-linear element:

The element is well suited for linear, large rotation, and/or large strain non-linear applications. Change in thickness is accounted for in non-linear analysis. The element accounts for change in thickness while calculating pressure load operators in a geometrically non-linear analysis.

6.2.3 Non-linear stress strain materials

A Multilinear Isotropic Hardening (MISO) model was used to model the stress strain curve of the concrete material. This option uses the von Mises yield criteria coupled with an isotropic work hardening assumption. In addition, this option may be preferred for large strain cycling. The uniaxial behaviour is described by a piece-wise linear stress-strain curve, starting at the origin, and with positive stress and strain values. The curve is continuous from the origin through 100 (at most) stress-strain points. The slope of the first segment of the curve must correspond to the elastic modulus of the material and no segment slope should be larger.

The curve are initialised by using Lab=MISO on the 'tb' command. The temperature for the first curve is input with the TBTEMP command, followed by tbpt commands for up to 100 stress-strain points. The constants (x,y) entered on the 'tbpt' command (two per command) are:

Constant	Meaning
x	Strain value
y	Corresponding stress value

Stress-strain-temperature curves example would be input for a multilinear isotropic hardening material as follows (see Figure 6.5):

```
tb,miso, 1, 2, 5          ! Activate a data table
tbtemp, 20.0              ! Temperature = 20.0
tbpt, defi, x1, y1        ! Strain, stress at temperature = 20
tbpt, defi, x2, y2
tbpt, defi, x3, y3
tbpt, defi, x4, y4
tbpt, defi, x5, y5
/xrange, 0, 0.02
tbplot, miso, 1
```

A Bilinear Isotropic Hardening (BISO) model was used to model the stress strain curve of the steel material. This option is similar to option MISO except that a bilinear curve is used instead of a multilinear curve. The material behaviour is described by a bilinear stress-strain curve starting at the origin and with positive stress and strain values. The initial slope of the curve is taken as the elastic modulus of the material. At the specified yield stress (c1), the curve continues along the second slope defined by the tangent modulus, c2 (having the same units as the elastic modulus). The tangent modulus cannot be less than zero nor greater than the elastic modulus.

Stress-strain-temperature curves example would be input for a Bilinear isotropic hardening material as follows (see Figure 6.5):

```
tb, biso, 1, 2            ! Activate a data table for Bilinear Isotropic
                          !Hardening option-only one set temp.
tbtemp, 20.0              ! Temperature = 20.0
tbdata, 1, c1, c2         ! Yield stress =  c1; Tangent modulus = c2
/xtange, 0, 0.01          ! x-axis of 'tbtemp' to extend from e=0 to 0.01
tbplot, biso, 1           !Display the data table
```

See appendix D for the input data of composite slab.

6.3 Mechanical interlock

6.3.1 Contact non-linearities

Contact non-linearities occur when two or more components (or parts of one component) come into or out of contact with each other (or itself) during the course of the deformation process. Contact non-linearities also occur when two components slide relative to one another.

Contact problems are highly non-linear and require significant computer resources to solve. It is important that the physics of the problem is understood and that time is taken to set up the model of the problem to run as efficiently as possible.

Contact problems present two significant difficulties. First, the regions of contact are not known until the problem has been run. Depending on the loads, material, boundary conditions, and other factors, surfaces can come into and go out of contact with each other in a largely unpredictable and abrupt manner. Second, most contact problems need to account for friction, and sliding. There are several friction laws and models to choose from, and all are non-linear. Frictional response can be chaotic, making solution convergence difficult.

ANSYS supports three contact models: node-to-node, node-to-surface, and surface-to-surface. Each type of model uses a different set of ANSYS contact elements and is appropriate for specific types of problems.

6.3.2 Contact stiffness

In order to handle a contact analysis when using the finite element method, a stiffness relationship must be represented between the two contact areas when contact occurs. Otherwise, the two areas will "pass through" each other, as shown in Figure 6.6.a.

This relationship is established through a spring, which is placed between the two contacting areas when contact occurs, see Figure 6.6.b.

Note that the spring will deflect an amount Δ such that equilibrium is satisfied, $\mathbf{F=k\Delta}$ where **k** is the spring stiffness. **k** is called the ***contact stiffness*** and has units of force/length.

This method of enforcing contact compatibility is called the penalty method. The contact stiffness is the penalty parameter.

There are other methods for establishing the relationship between the two contacting areas when contact occurs, including:

- Coupling the two surfaces.
- Applying a force to "push" the two areas back apart so that they just touch.
- Adding another Degree of freedom (DOF) to the solution set (the force needed to push the two apart).

The last method is called the Lagrange multiplier method, and a variant of this option may be used by the general contact elements. The second method is used by the reduced and mode superposition transient methods with the gap capability.

The contact stiffness is an element real constant. The amount of penetration, or incompatibility, between the two surfaces is therefore dependent on the stiffness **k**.

Ideally there should be no penetration, but this implies **k**= ∞. High values of **k** will also lead to ill-conditioning of the global stiffness matrix **[K]** as well as convergence difficulties. Practically, a high enough stiffness is required that the contact penetration is acceptably small, but not so high that convergence or ill-conditioning problems do not occur.

6.3.3 Choosing the contact stiffness

In all cases, a value for the contact stiffness, KN is input. The value of contact stiffness was estimated from the experimental results of small tests in chapter 3 section 3.4.4 and chapter 4 section 4.14.1. Table 6.4 shows the contact stiffness values which have been used for modelling (estimated from the small scale tests in chapter 3 by taking the average value of the first eight small tests, and the average of the small scale test values of Daniels[59]).

It was necessary to use several elements in combination to create the same effect of contact stiffness between concrete and profiled steel sheeting. This combination was intended to reproduce the actual behaviour. The contact between sheeting and concrete is modelled using two types of elements in combination to create the same effect (combination element and point to point contact element for full scale model or

combination element and point to surface element for the small scale). This combination with the solid and shell element was intended to reproduce the actual behaviour of a composite slab. The achievement of this must be judged on the ability of the model to reproduce the measured load-deflection response and the longitudinal slip-stress relation.

In other words, if only one type of element was used as contact between steel and concrete, the analysis would fail at an unrealistically low load. The stiffnesses taken from the small-scale tests were generally estimated from the initial stiffness up to the onset of slip. Variation of this stiffness indicated in the Table was required to achieve agreement in the behaviour between the initial linear portion of the graphs and the failure plateau. In the case where variation between +7% and –5% was required several cycles of finite element analysis were carried out.

6.3.4 Combination element

The element is a combination of a spring-slider and damper in parallel, coupled to a gap in series. A mass can be associated with one or both nodal points. The element has one degree of freedom at each node, either a nodal translation, rotation, pressure, or temperature. The mass, springs, slider, damper, and/or the gap may be removed from the element. The element can be used in any analysis.

6.3.4.1 Element geometry and input data

The combination element is shown in Figure 6.7.a. The element is defined by two nodes, two spring constants K1 and K2 (Element stiffness = Force/Length), a damping coefficient C (Force* Time2/Length), a gap size GAP (length or (Radians), and a limiting sliding force FSLIDE (Force). The FSLIDE value represents the absolute value of the spring force that must be exceeded before sliding occurs. If FSLIDE is 0.0, the sliding capability of the element is removed, that is, a rigid connection is assumed.

A "break-away" feature is available to allow the element stiffness (K1) to drop to zero once a limiting force FSLIDE has been reached. The limit is input as FSLIDE and is applicable to both tensile breaking and compressive crushing.

The force-deflection relationship for the combination element is as shown in Figure 6.7.b (for no damping). If the initial gap is zero, the element responds as a spring-damper-slider element having both tension and compression capability. If the gap is not initially zero, the element responds as follows: when the spring force (F1 + F2) is negative (compression), the gap remains closed and the element responds as a spring-damper parallel combination. As the spring force (F1) increases beyond the FSLIDE value, the element slides and the F1 component of the spring force remains constant. If FSLIDE is input with a negative sign, the stiffness drops to zero and the element moves with no resisting F1 spring force. If the spring force becomes positive (tension), the gap opens and no force is transmitted[54].

6.3.4.2 Characteristics of the element

The force-deflection relationship for the combination element under initial loading is as shown in Figure 6.7.c (for no damping).

where: F_1 = force in spring 1

F_2 = force in spring 2

K_1 = stiffness of spring 1

K_2 = stiffness of spring 2

u_{gap} = initial gap size

u_1 = displacement at node I

u_2 = displacement at node J

F_s = force required in spring 1 to cause sliding (input quantity FSLIDE)

6.3.4.3 Determination of F1 and F_2 for structural applications

For this study the gap is considered closed at the concrete/steel interface and the slider is ready to slide when the value of the stiffness equals FSLIDE.

$$F_1 = \pm F_s$$

6.3.5 Point-to-point 3-D contact element

The element represents two surfaces, which may maintain or break physical contact and may slide relative to each other. The element is capable of supporting only compression in the direction normal to the surfaces and shear (Coulomb friction) in the tangential direction. The element has three degrees of freedom at each node: translations in the nodal x, y, and z directions. The element may be initially preloaded in the normal direction, or it may be given a gap. A specified stiffness acts in the normal and tangential directions when the gap is closed and not sliding.

6.3.5.1 Element geometry and input data

The geometry, node locations, and the co-ordinate system for this element are shown in Figure 6.8.a Two nodes define the element, two stiffnesses (KN and KS), an initial gap or interference (GAP), and initial element status (START). The orientation of the interface is defined by the node locations. The interface is assumed to be perpendicular to the I-J line. The only material property used is the interface coefficient of friction μ. A zero value should be used for frictionless surfaces. The force deflection relationships for the interface element can be separated into the normal and tangential (sliding) directions as shown in Figure 6.8.b. The element condition at the first sub-step is determined from the START parameter. If the interface is closed and sticking, KN is used in the gap resistance and KS is used for sticking resistance. If the interface is closed but sliding, KN is used in the gap resistance and the constant friction force μFN is used for the sliding resistance. In the normal direction, when the normal force (FN) is negative, the interface remains in contact and responds as a linear spring. As the normal force becomes positive, contact is broken and no force is transmitted. In the tangential direction, for $FN < 0$ and the absolute value of the tangential force (FS) less than $\mu|FN|$, the interface sticks and responds as a linear spring. For $FN < 0$ and $FS = \mu|FN|$, sliding occurs. If contact is broken, $FS = 0$.

If rigid Coulomb friction is selected, KS is not used, and the elastic sticking capability is removed, This option is useful for displacement controlled problems or for certain

dynamic problems where sliding dominates. The solution output associated with the element (Force-Deflection curves are illustrated in Figure 6.8.b).

In this study, a value for the stiffness KN was required which was obtained from chapter 3 and chapter 4, with the gap initially closed and not sliding, and the average values taken for the friction from section 3.5.

6.3.6 Point-to-surface 3-D contact element

The element can be used to represent contact and sliding between two surfaces (or between a node and a surface) in three dimensions. The element has five nodes with three degrees of freedom at each node: translations in the nodal x, y, and z directions. Contact occurs when the contact node penetrates the target base. Elastic Coulomb friction and rigid Coulomb friction are allowed, where sliding is along the target base.

6.3.6.1 Element geometry

The geometry and node locations are shown in Figure 6.9. The element geometry is a pyramid with the base being a quadrilateral, vertices being nodes on one of the surfaces (called the target surface), and the opposing vertex being a node on the other surface (called the contact surface). A degenerate form of the element is allowed which takes the shape of a tetrahedron when the base is a triangle. The base on the target surface is called a target base, and the nodes defining the target base are called target nodes. The node on the contact surface that completes the pyramid is called a contact node. A geometrical display of this element shows the target base and the contact node (as a star). Nodes 1, J, K and L define the target base, and node M is the contact node.

The normal contact stiffness, KN, is used in the penalty function method to determine contact forces. KN has units of force/length, KN corresponds to a penalty stiffness that acts in the direction of the target surface normal. The value of the contact stiffness was determined from real experimental tests from chapter three and chapter four. The average values were taken from the pull-out and push-off tests for the Salford work. For the studies of Daniels[54] tests the value was taken from the data provided.

The coefficient of friction was specified from chapter three, section 3.5.

6.4 Example use of modelling procedure

Two small scale, and nine full-scale tests were performed, as indicated in table 6.1 to table 6.3, and table 6.4 shows the data that has been used. Appendix D show typical example of input data for the composite slab.

The ANSYS program is used in the analysis of several composite slabs (full and small scale), using various loads, supports, thicknesses and dimensions. The following is a description of the problems encountered and the results obtained. Figures 6.10.a to 6.11.a shows details of the finite element meshes for one small scale and for one full-scale model.

For the small-scale tests, horizontal loads were applied (with 5 kN vertical load) to push concrete relative to the profiled small-scale steel sheet (similar to the experimental procedure in chapter 3 for the first two models).

Full scale test, models No.3 to 5 similar to the experimental tests in chapter 4 were used. Two equal line loads are symmetrically placed on each model.

The models No. 6 to 11 were similar to the experimental tests at ICOM by Daniels[56]. Two equal line loads are symmetrically placed on each model or one line load is placed at midspan. The cross-sectional geometry and critical testing parameters for one model are illustrated in Figure 6.12.

For the small-scale tests the entire structure has been modelled, but for the full-scale tests are quarter of the composite slab has been modelled using symmetry.

6.5 Comparison of numerical analysis with test results

The load versus deflection, and load versus slip graphs provide a comparison between the numerical analysis and the test results. Figure 6.13 and 6.14 shows the comparison between the measured and calculated slip for two of the small-scale tests. The contact stiffness for the ANSYS model was taken from the experimental data from these tests and as could be expected the agreement is acceptable and confirms the general approach to modelling of the full-scale composite slabs.

Figures 6.15 to 6.32 shows the comparison for a selection of full-scale slabs from the Salford tests and those of Daniels at ICOM.

The comparisons are made for end slip and deflection. The input data for the modelling shows in table 6.4 includes the variation in contact stiffness required to produce the agreement obtained for end slip and deflection. The change is between –5% and +7%.

6.6 Discussion and conclusions

The non-linear analysis of composite slab structures using ANSYS has been investigated in order to examine the capability of ANSYS in dealing with composite slab structures. The procedure was to study a series of problems with different thicknesses and dimensions. The analysis of the slabs has demonstrated the validity of the modelling technique and within a reasonable range of accuracy has produced satisfactory agreement in terms of overall behaviour and failure loads. Further study should attempt to use wholly modelled small-scale model values in a full-scale composite slab representation

Table 6.1 The input data of the geometrical properties for the two small-scale tests (using data from chapter 3).

Test No.	Reference	Cross-section	h (mm)	L_t (mm)	L_w (mm)	t (mm)
1	Chapter 3 data	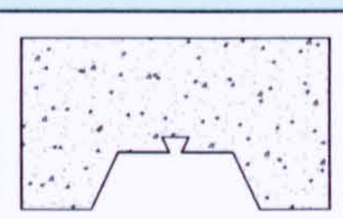	165	300	300	0.9
2	Chapter 3 data	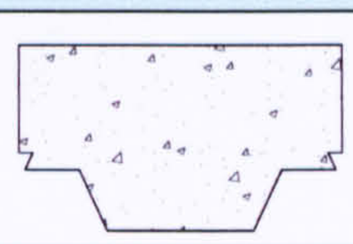	165	300	300	0.9

where:

h is the thickness of the composite tests.

L_t is the length of the slabs.

L_w is the width of the slabs.

t is the thickness of the profiled steel.

Table 6.2 Input data for the three full scale composite slabs (data from chapter 4).

Test No.	Cross-section	Reference	h (mm)	L_t (mm)	L (mm)	L_s (mm)	t (mm)
S3	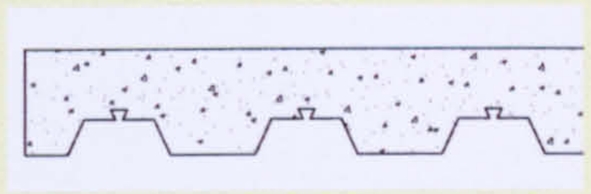	data from chapter no 4	165.00	3100	2900	725	0.9
S4			165.00	2100	3900	975	0.9
S5			135.00	4100	1900	475	0.9

Table 6.3 Input data for the properties of concrete and profiled steel sheet for the composite slabs for reported by Daniels1987[56].

Test No.	Cross-section	Reference	h (mm)	L_t (mm)	L (mm)	L_s (mm)	t (mm)
S6	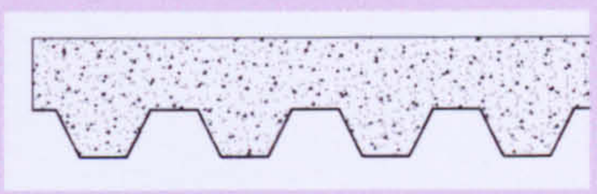	data from Daniels report 1987.	140	4150	4000	2000	1.00
S7			165	4800	4500	2250	0.75
S8			140	4150	4000	1000	1.00
S9	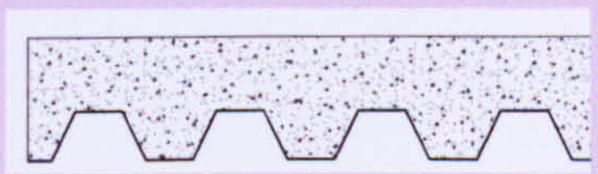		140	4150	4000	1000	1.00
S10			115	2120	1800	900	0.75
S11			165	2120	1800	900	0.75

Table 6.4 The complete input data for the FEM.

Test no.	Modulus of elasticity of concrete (N/mm^2)	Modulus of elasticity of steel (N/mm^2)	Compressive strength of concrete (N/mm^2)	Tensile strength of steel (N/mm^2)	Contact stiffness (from small-scale test) (kN/mm)	Percentage change to the contact stiffness value (%) for modelling	Poisson's ratio of concrete	Poisson's ratio of steel	Coefficient of friction
SS1	42000	202777	44	354	25.72	-----	0.2	0.3	0.4
SS2	42000	202777	44	354	13.00	-----	0.2	0.3	0.4
S3	42000	202777	44	354	18.67	+7	0.2	0.3	0.4
S4	24596	202777	20	354	18.49	+6	0.2	0.3	0.4
S5	29618	202777	29	354	17.45	-----	0.2	0.3	0.4
D6	35000	200000	40	330	21.18	-----	0.2	0.3	0.4
D7	35000	200000	40	330	14.66	- 5	0.2	0.3	0.4
D8	35000	200000	40	330	21.18	-----	0.2	0.3	0.4
D9	35000	200000	40	330	21.18	-----	0.2	0.3	0.4
D10	35000	200000	40	330	16.05	+4	0.2	0.3	0.4
D11	35000	200000	40	330	15.90	+3	0.2	0.3	0.4

SS = Small-scale tests at Salford University (SS1 is push-off test No. 1 (figure 3.8))
(SS2 is push-off test No. 8 (figure 3.15))

S = Salford University tests (S3 is slab No. 3 (figure 4.11))
(S4 is slab No. 4 (figure 4.12))
(S5 is slab No. 5 (figure 4.13))

D = Daniels tests (see reference 56 and 59)

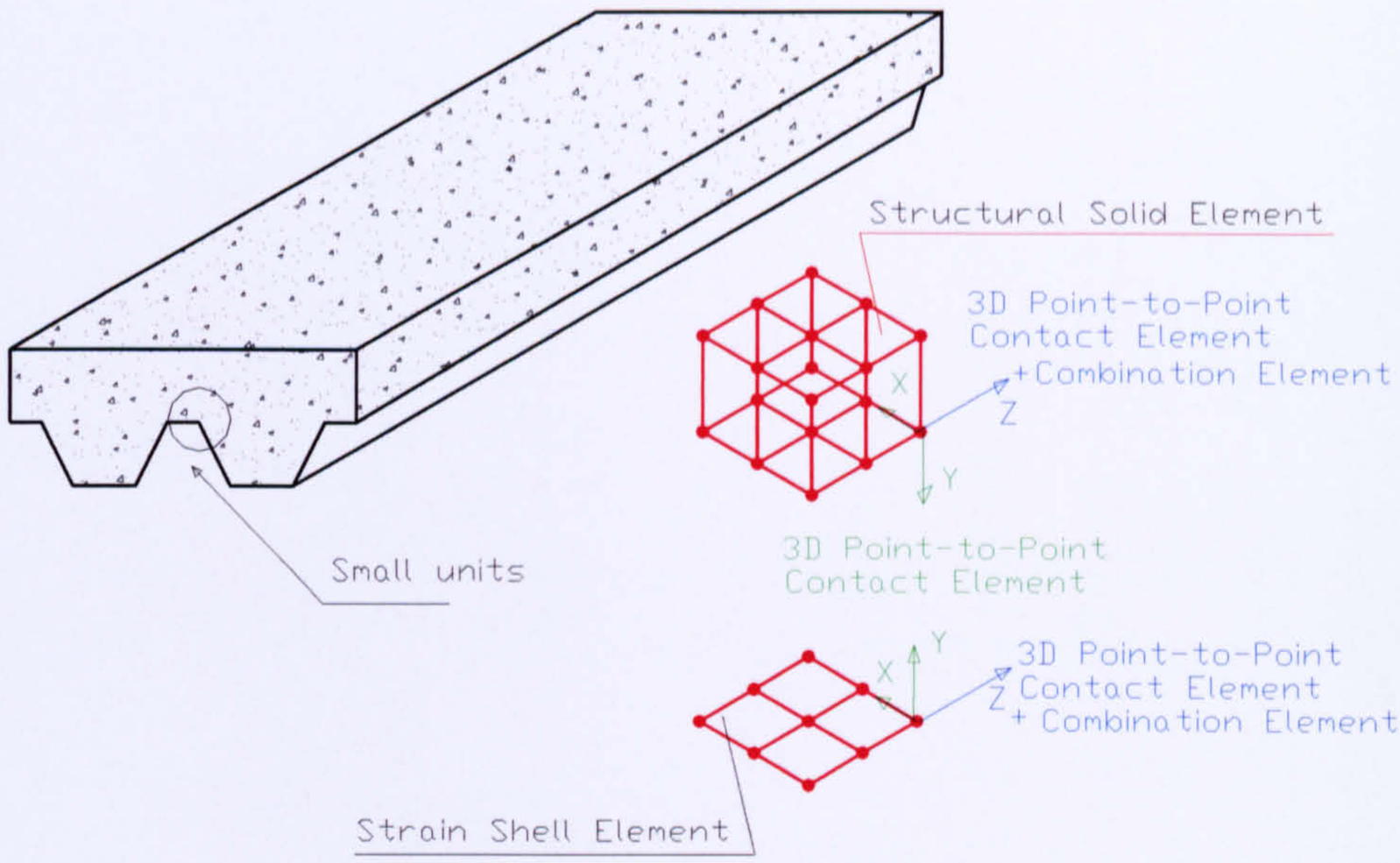

Figure 6.1.a Finite Element modelling of the Composite Slab (full scale).

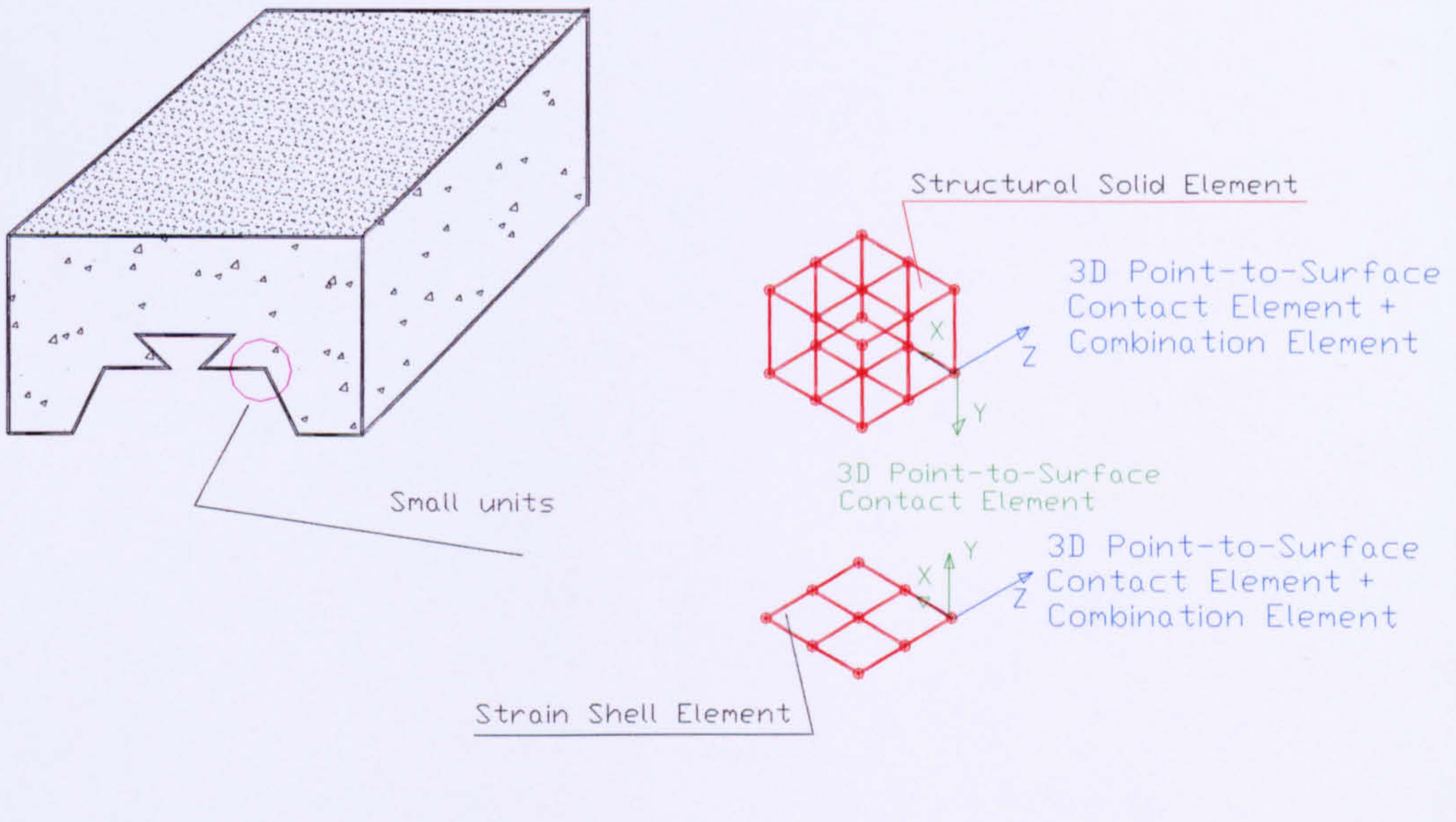

Figure 6.1.b Finite Element modelling of the Composite Slab (small scale).

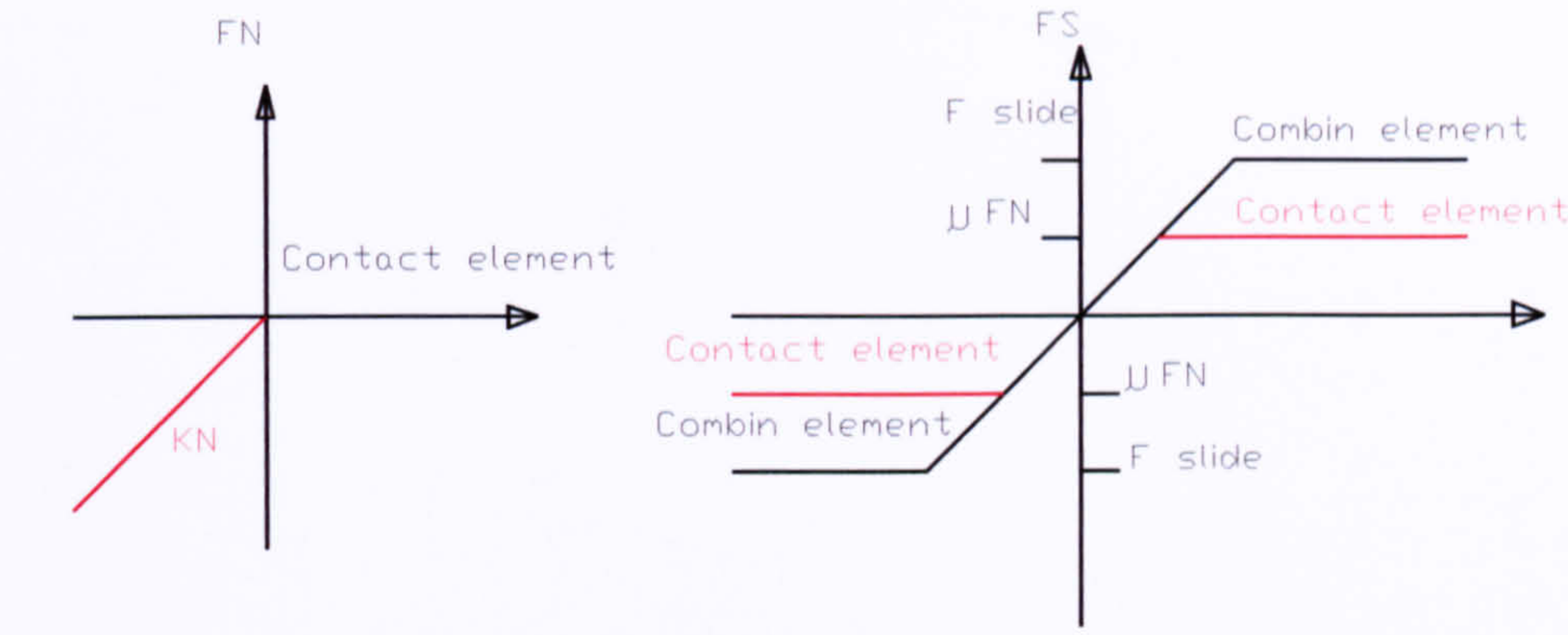

Figure 6.2 Force-Deflection relationship of the contact and combine elements.

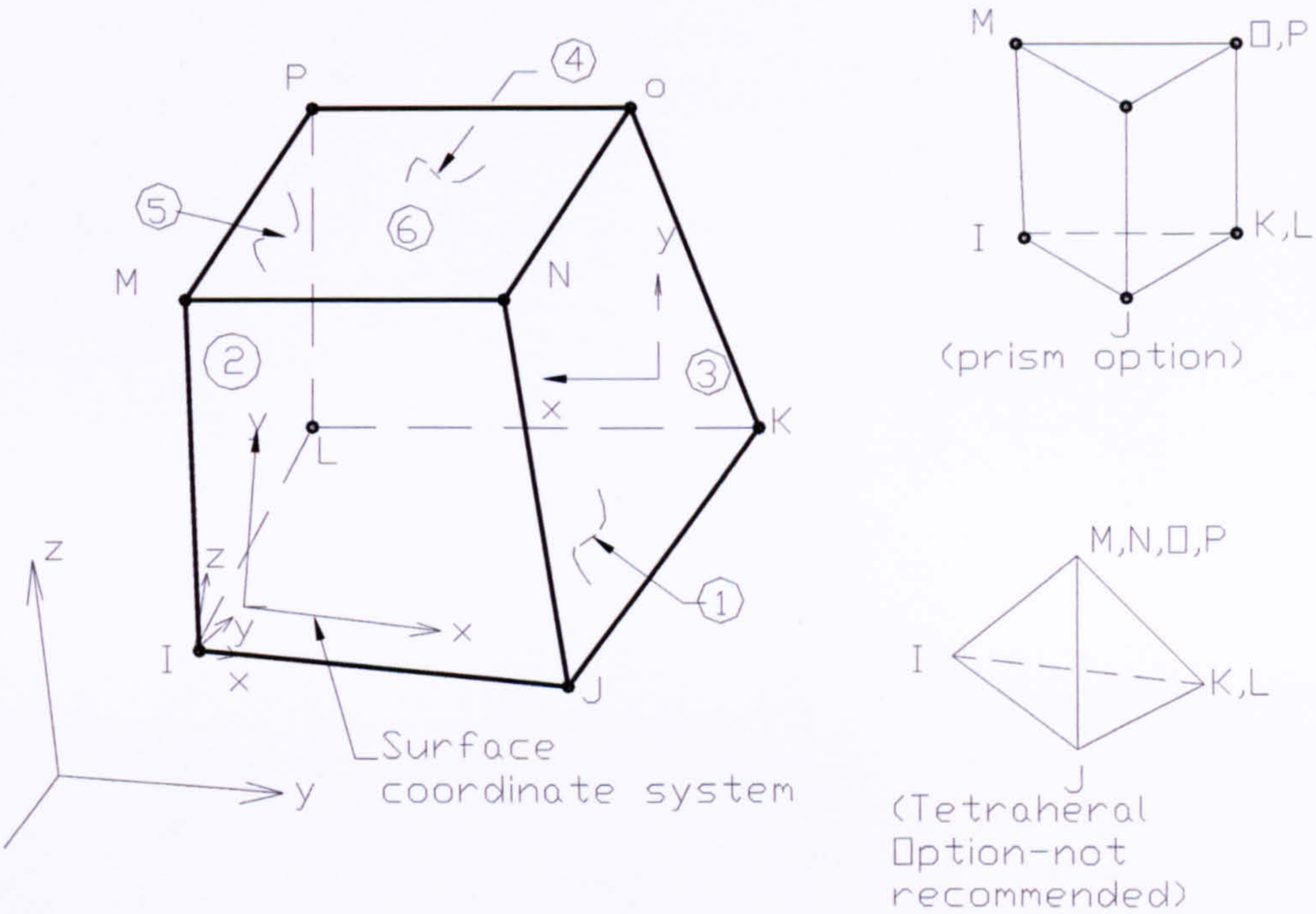

Figure 6.3 3-D Structural Solid Element

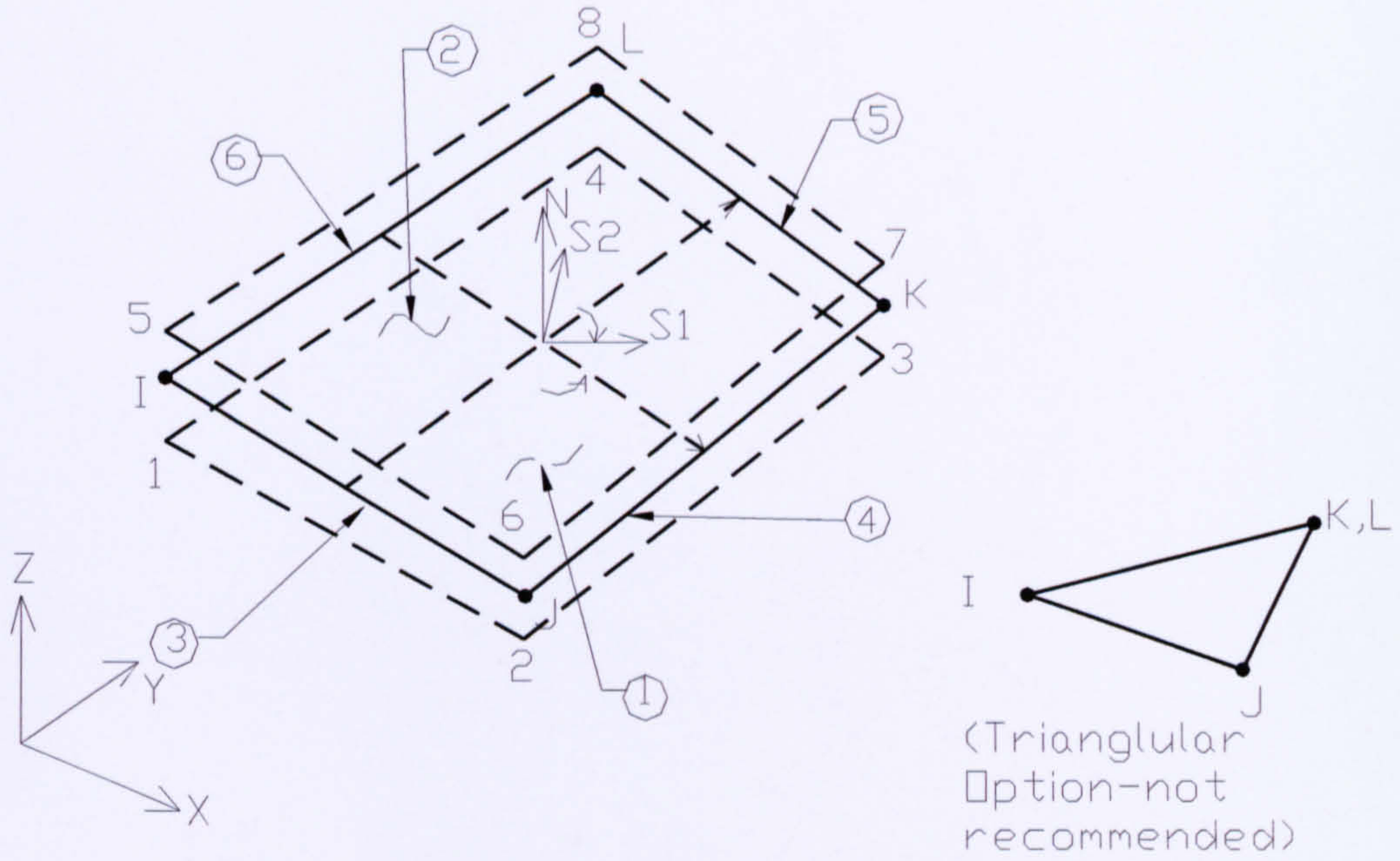

Figure 6.4 Finite Strain Shell Element

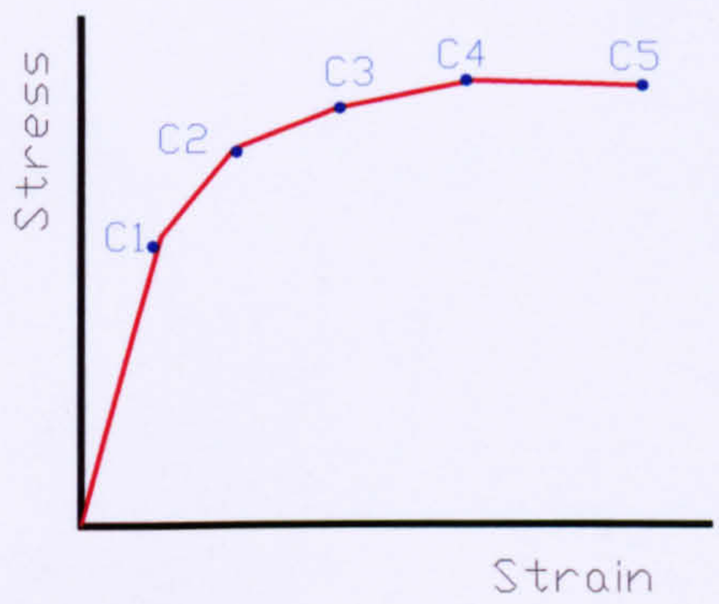

Multilinear Isotropic Hardening (MISO).
(for the concrete cases)

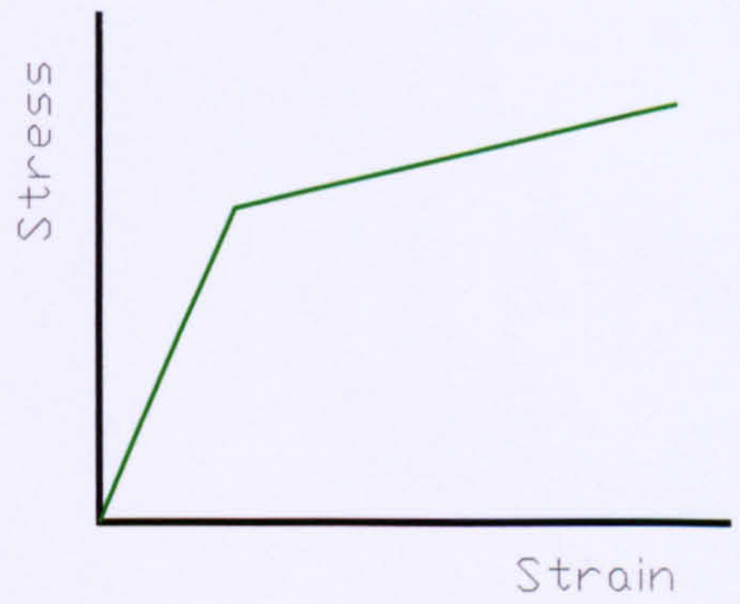

Bilinear Isotropic Hardening (BISO).
(for the profiled steel cases)

Figure 6.5 The elasto-plastic stress-strain curve used for concrete, an steel materials

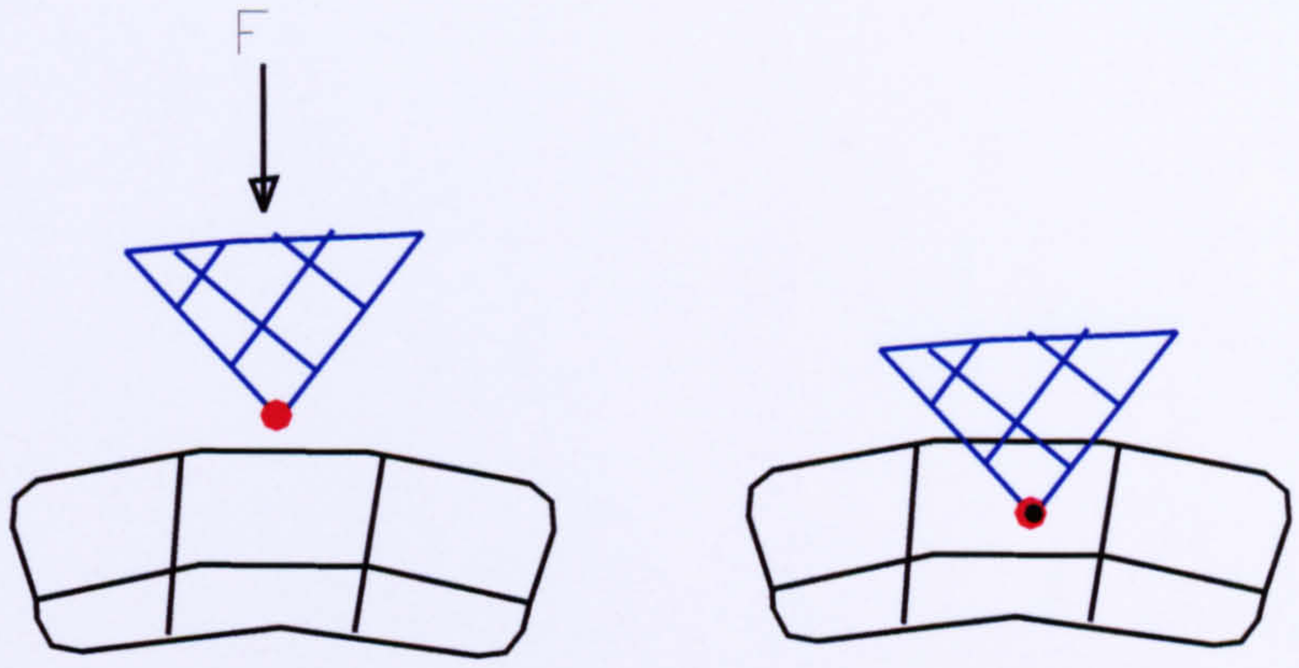

Figure 6.6.a The penetration of two areas.

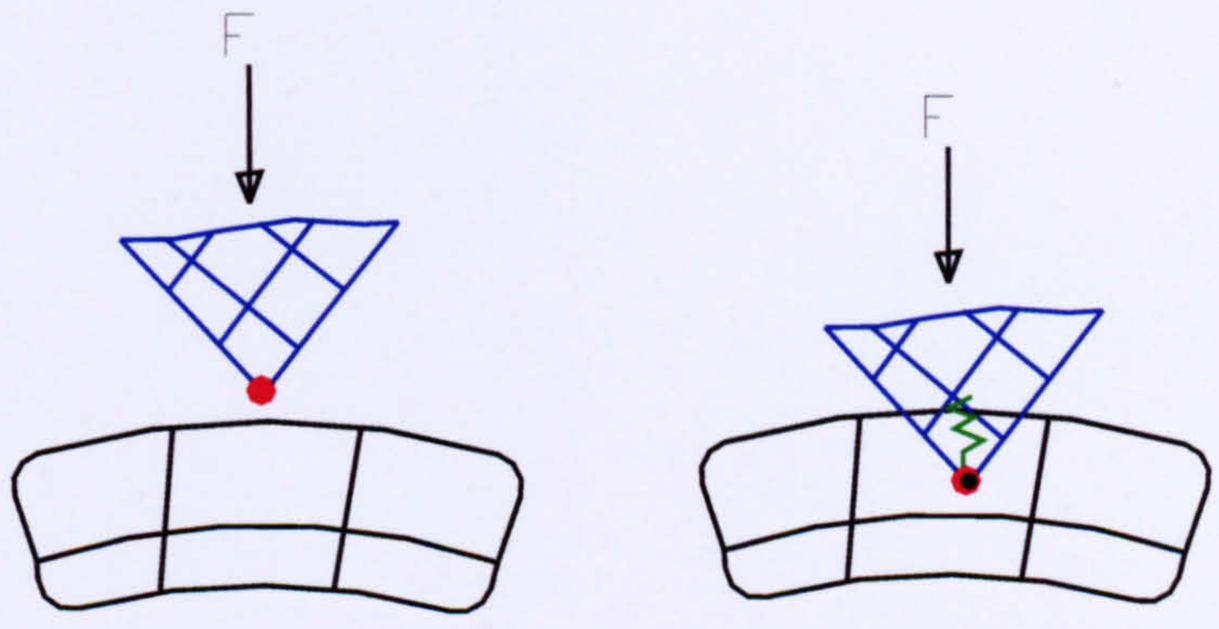

Figure 6.6.b Spring behaviour between the contact areas when contact occurs.

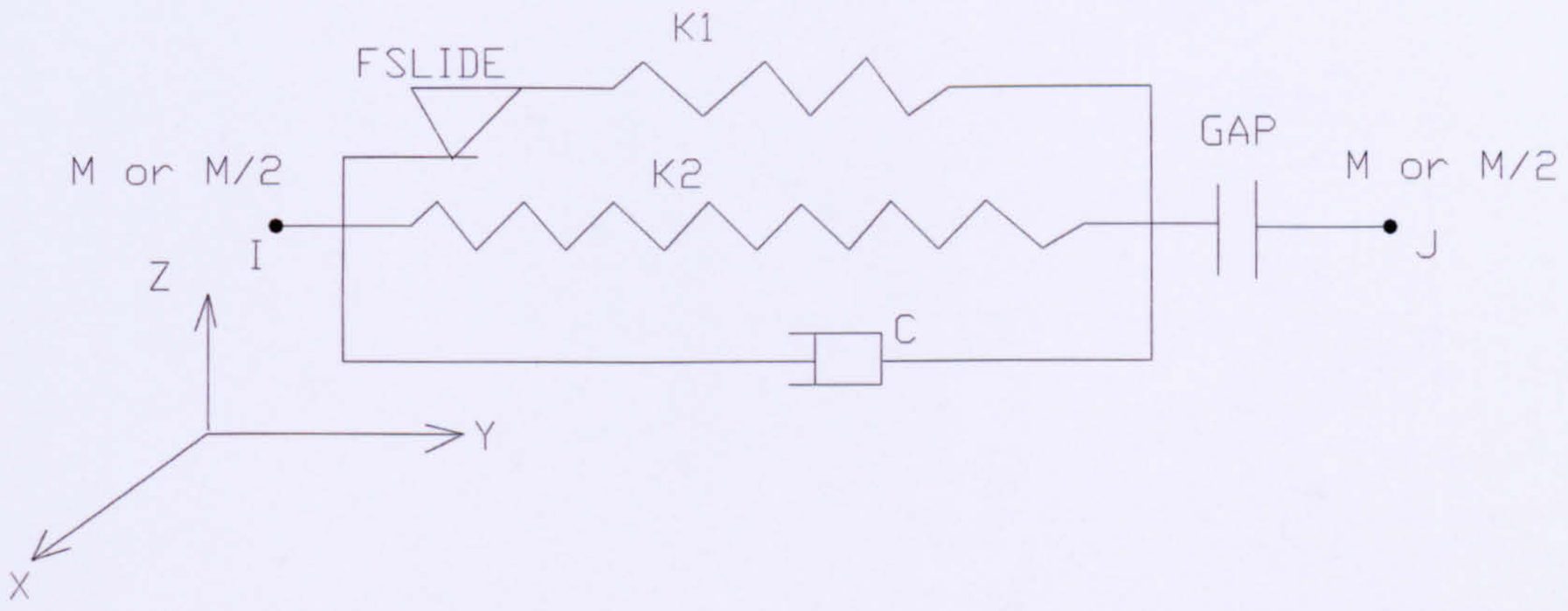

Figure 6.7.a Combine Element (spring-slider and damper element).

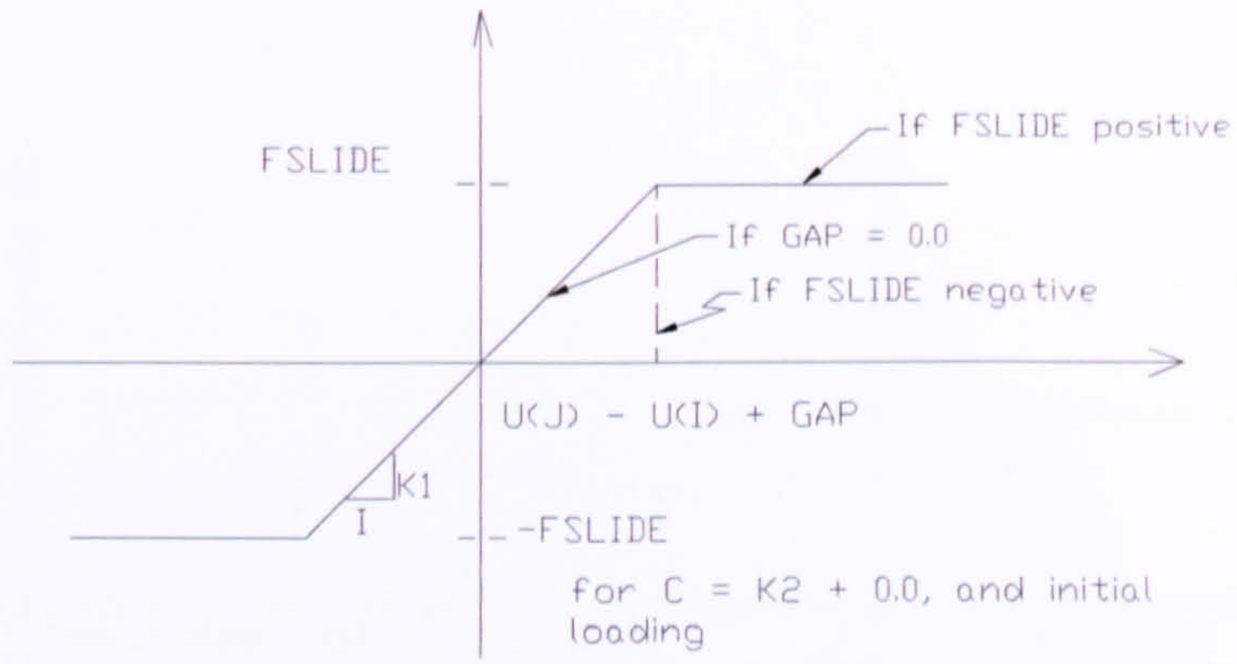

Figure 6.7.b Combine Behaviour.

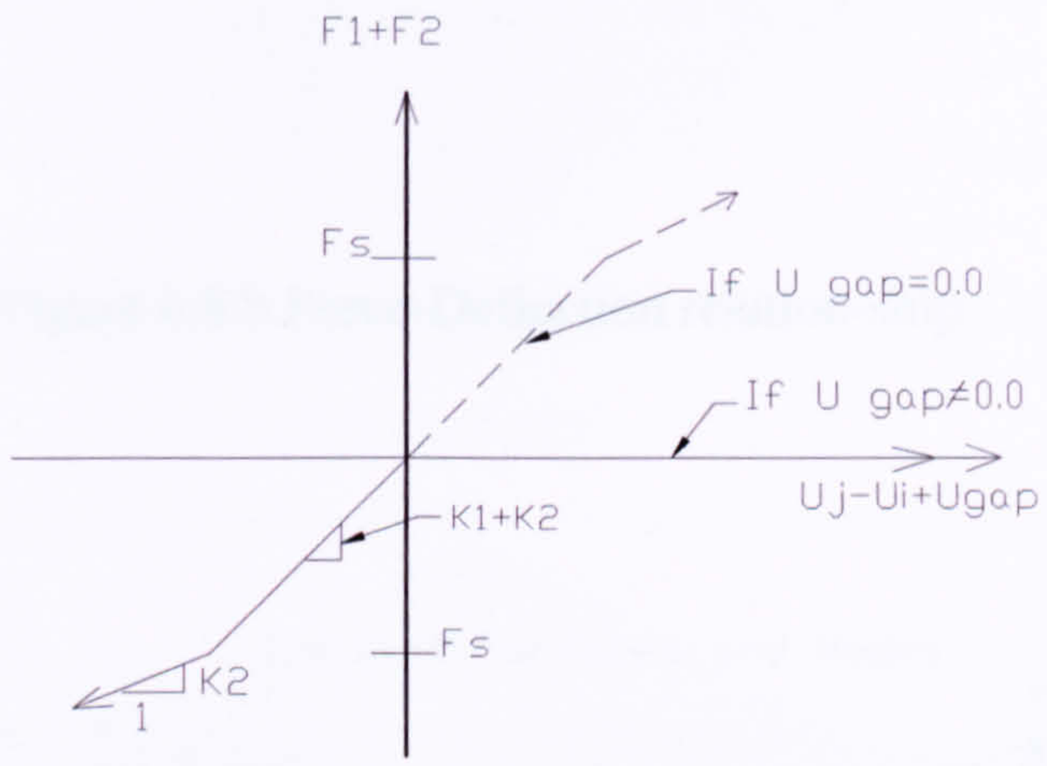

Figure 6.7.c Force-Deflection Relationship

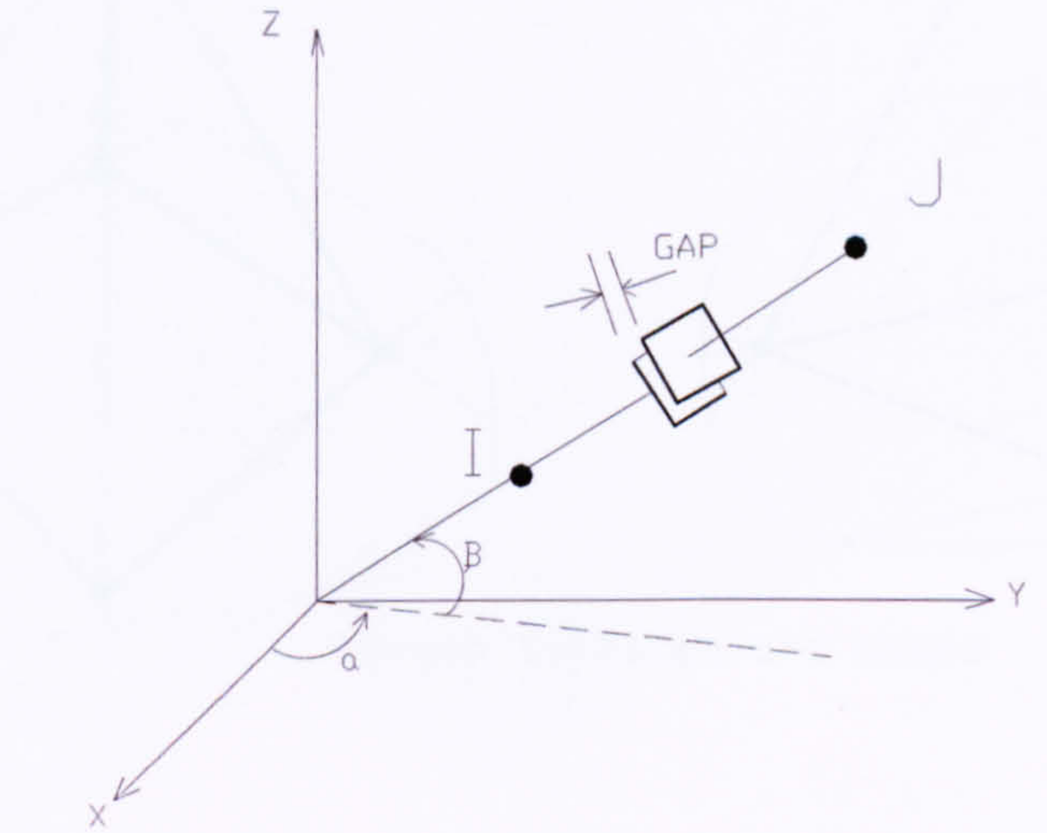

Figure 6.8.a 3-D Point-to-Point Contact Element.

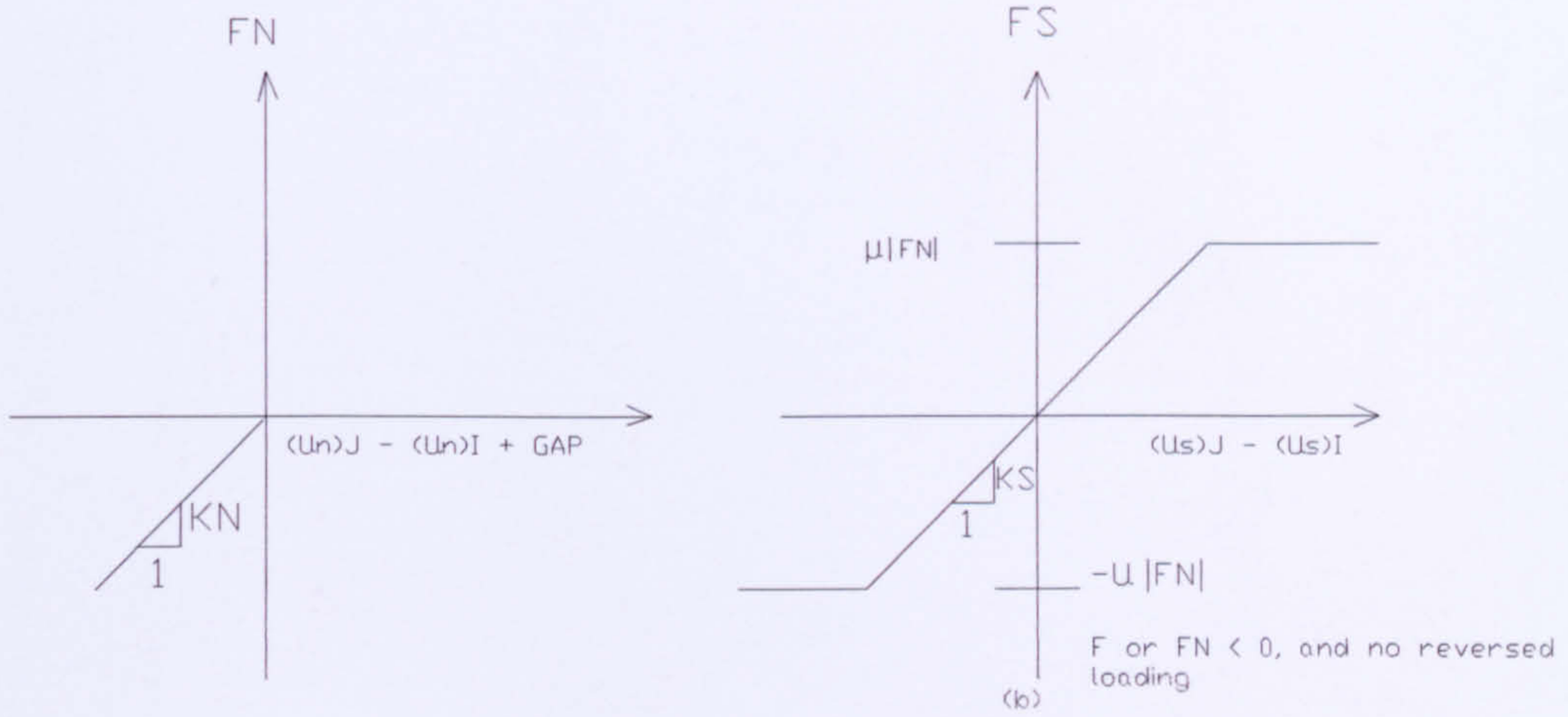

Figure 6.8.b Force-Deflection relation-ship

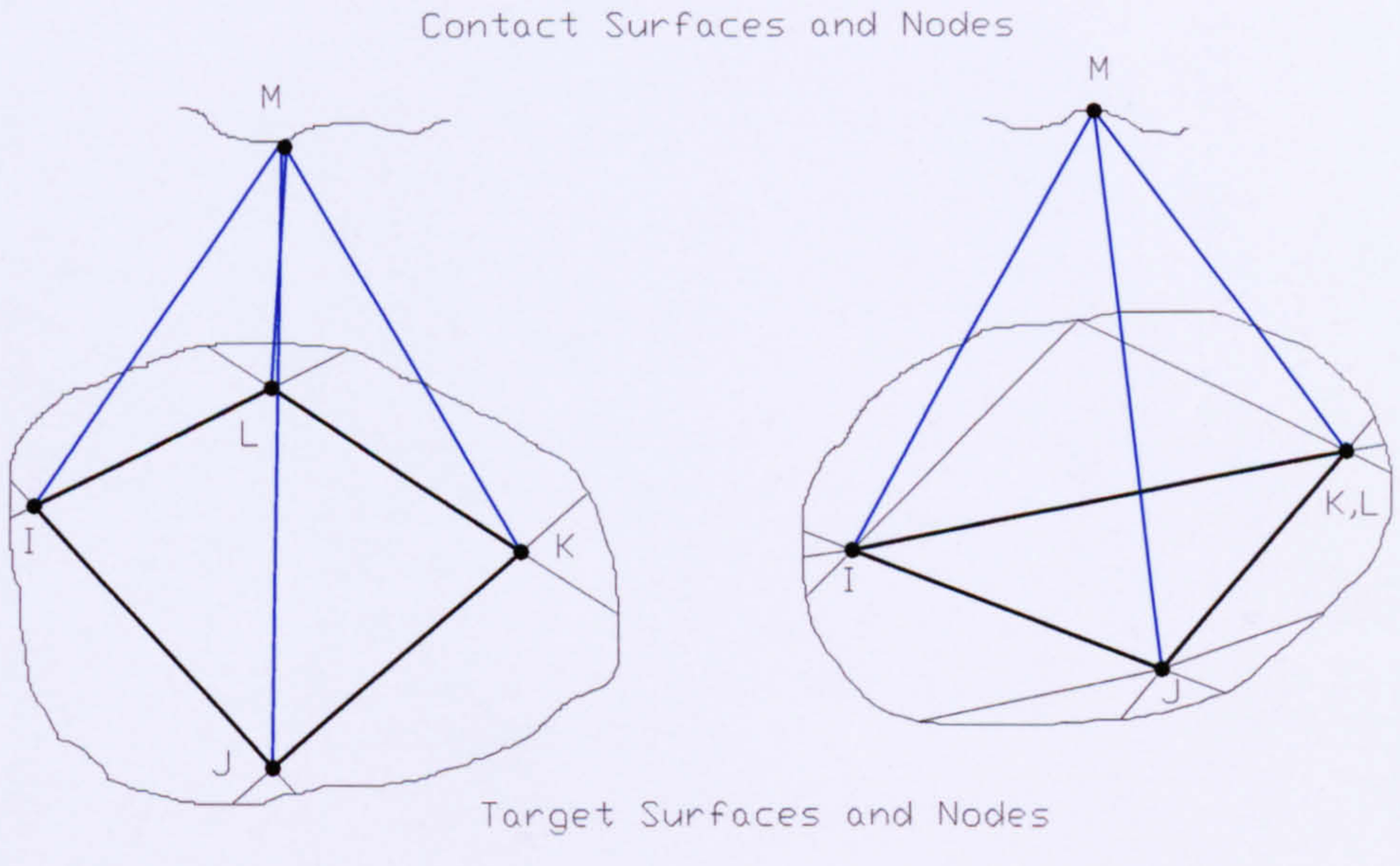

Figure 6.9 3-D Node-to-Surface Contact Element.

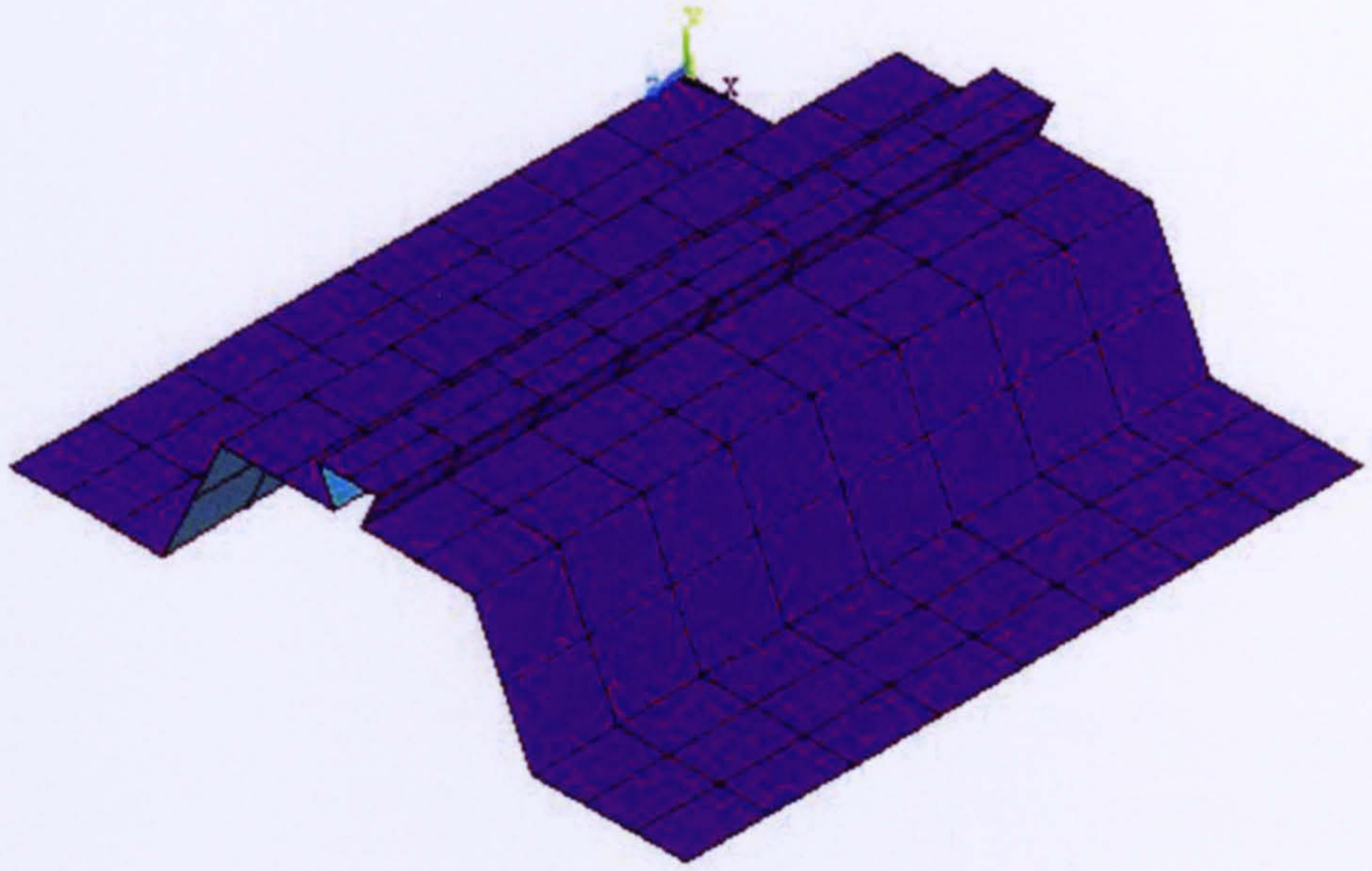

Figure 6.10.a The Finite Element mesh for profiled steel sheeting in small-scale test model

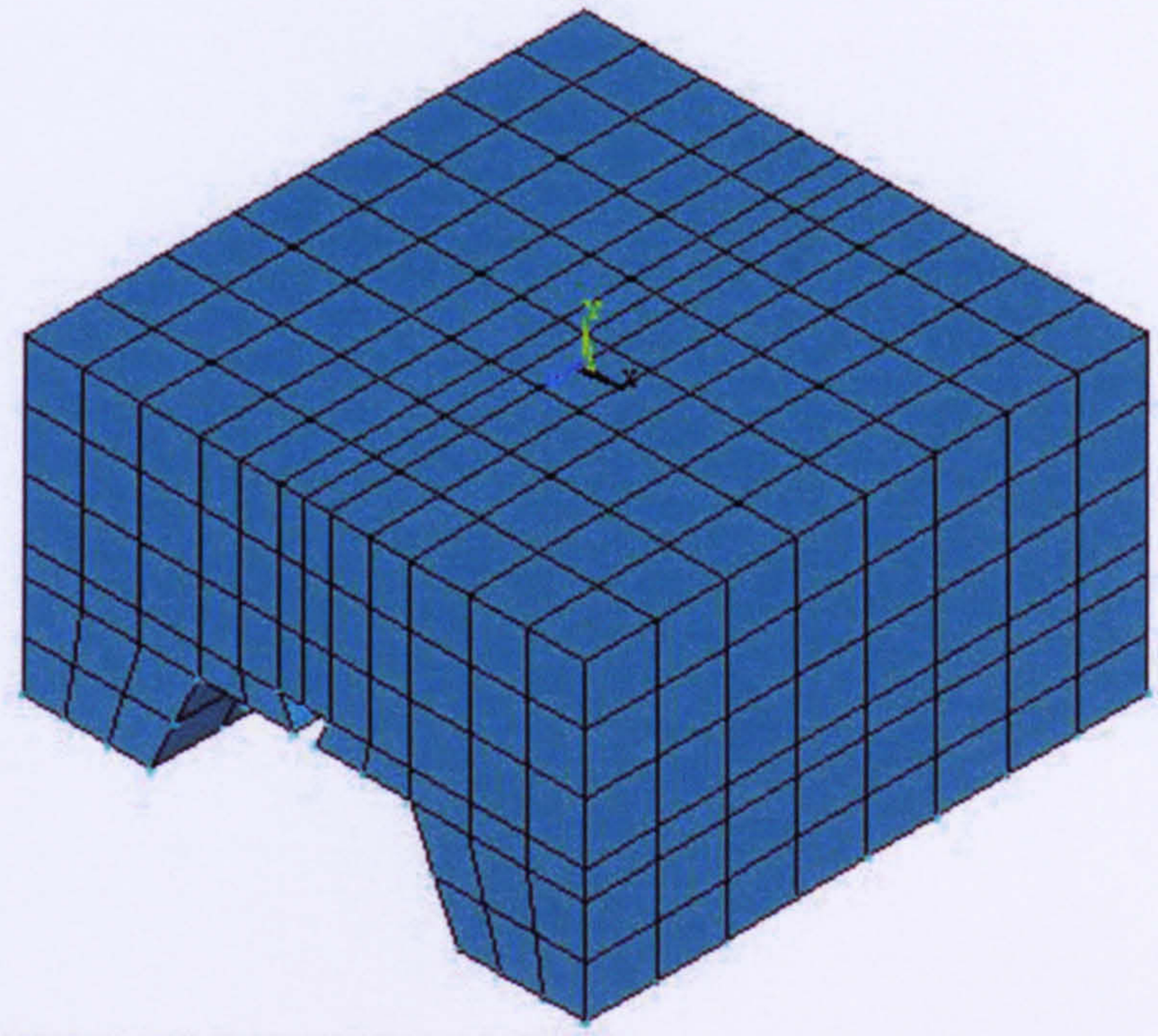

Figure 6.10.b The Finite Element mesh of concrete for the small-scale test model

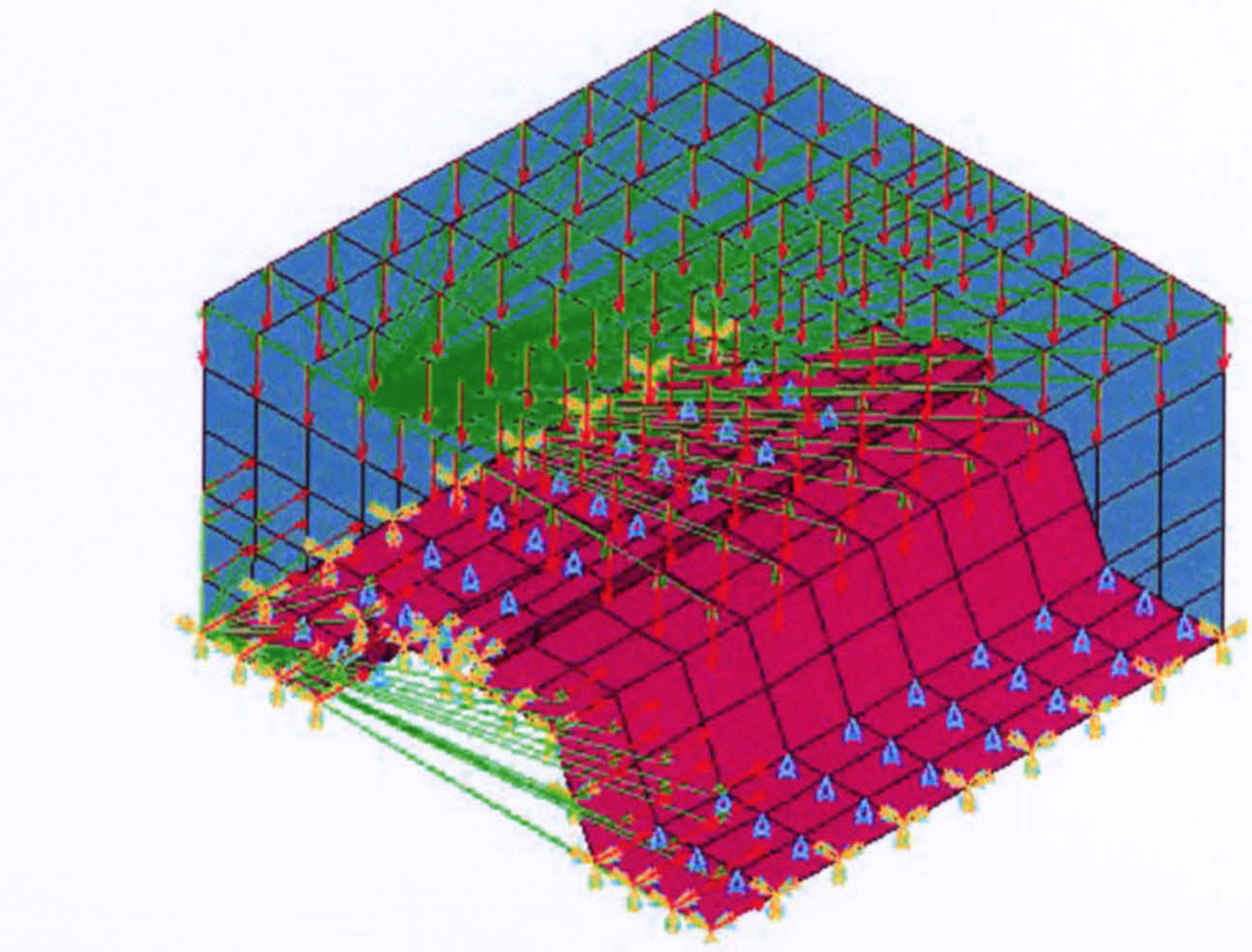

Figure 6.10.c The Finite Element model with the loads and supports indicated.

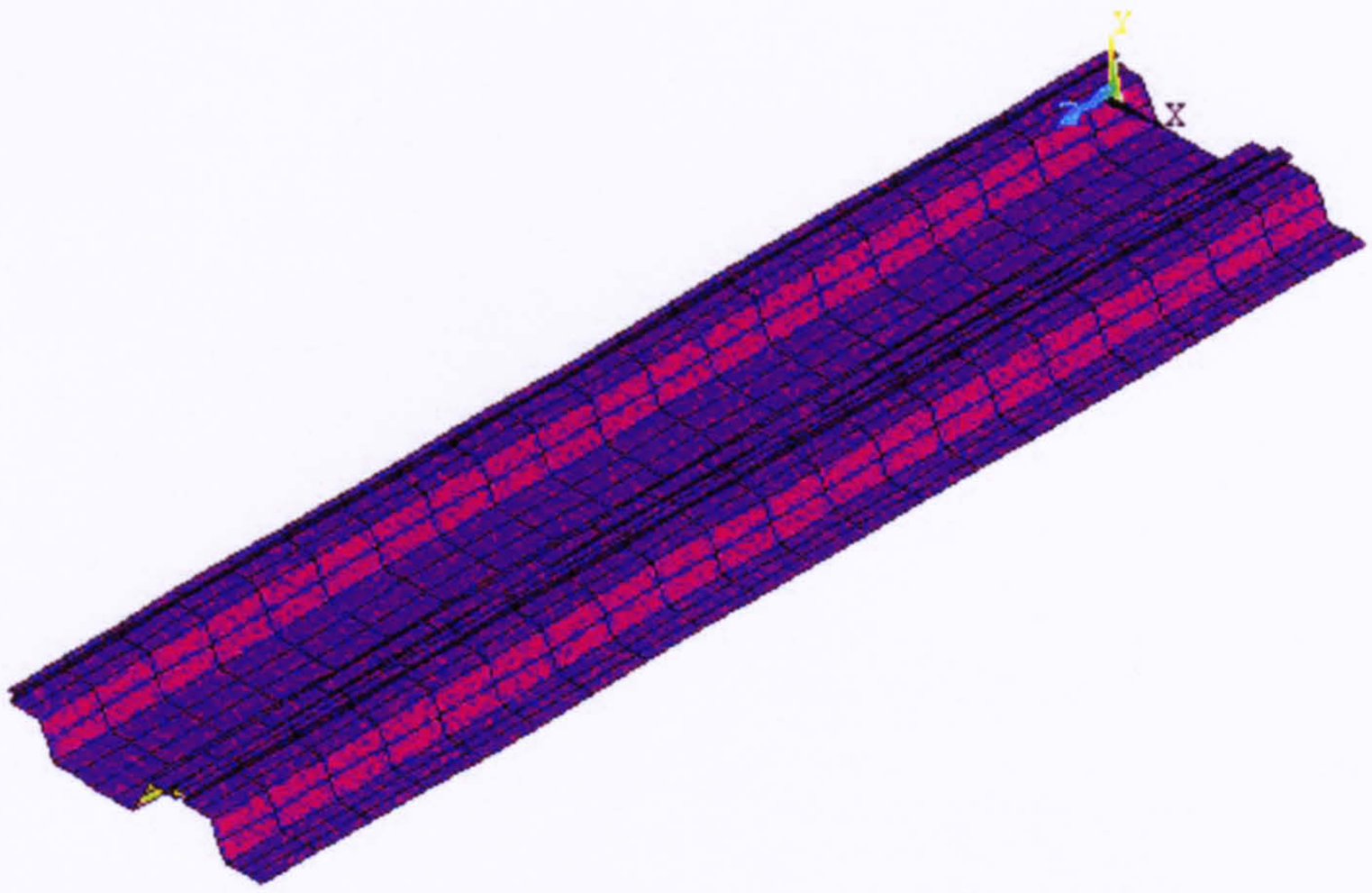

Figure 6.11.a The Finite Element mesh for profiled steel sheeting.

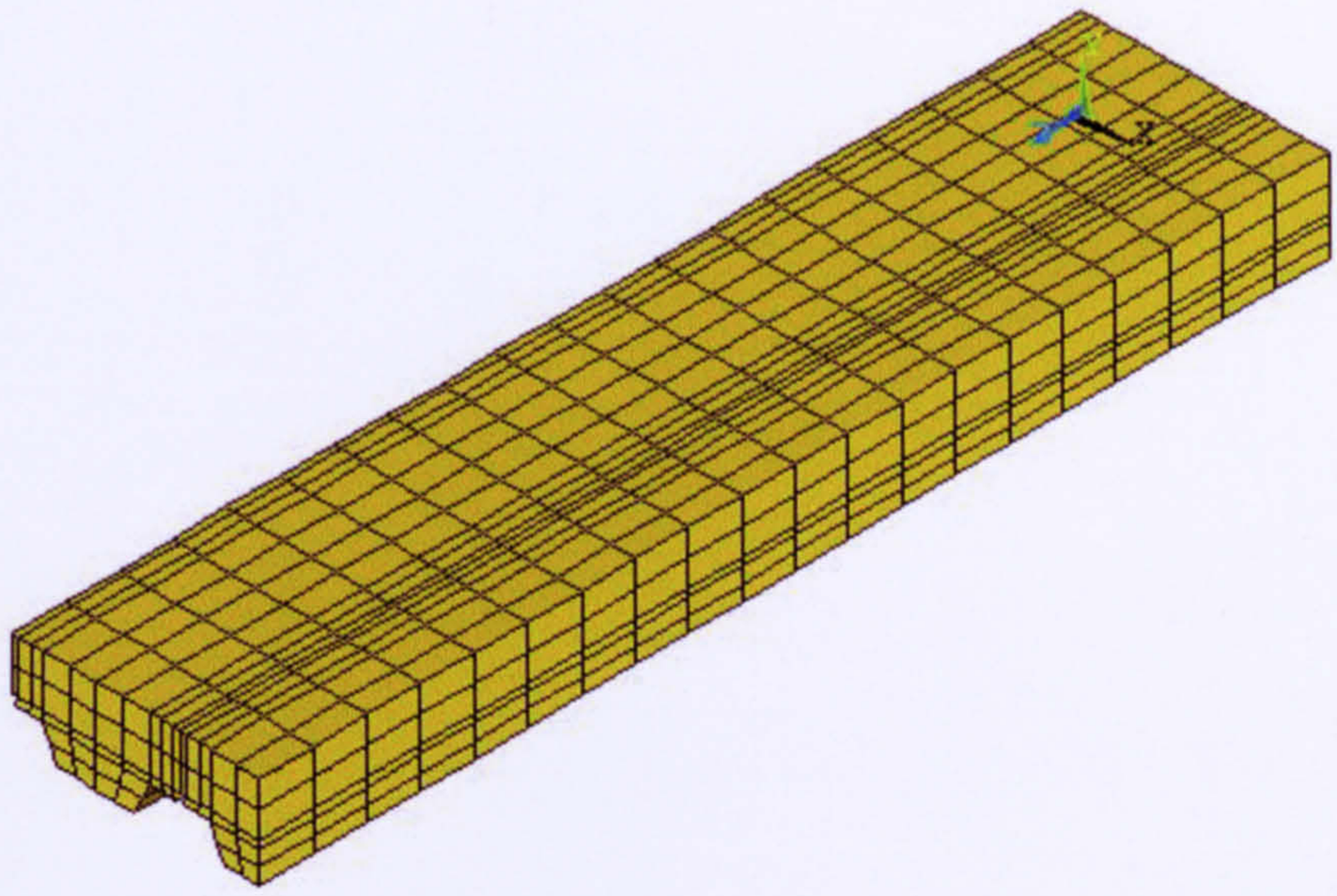

Figure 6.11.b The Finite Element mesh for concrete for the full scale tests using symmetry.

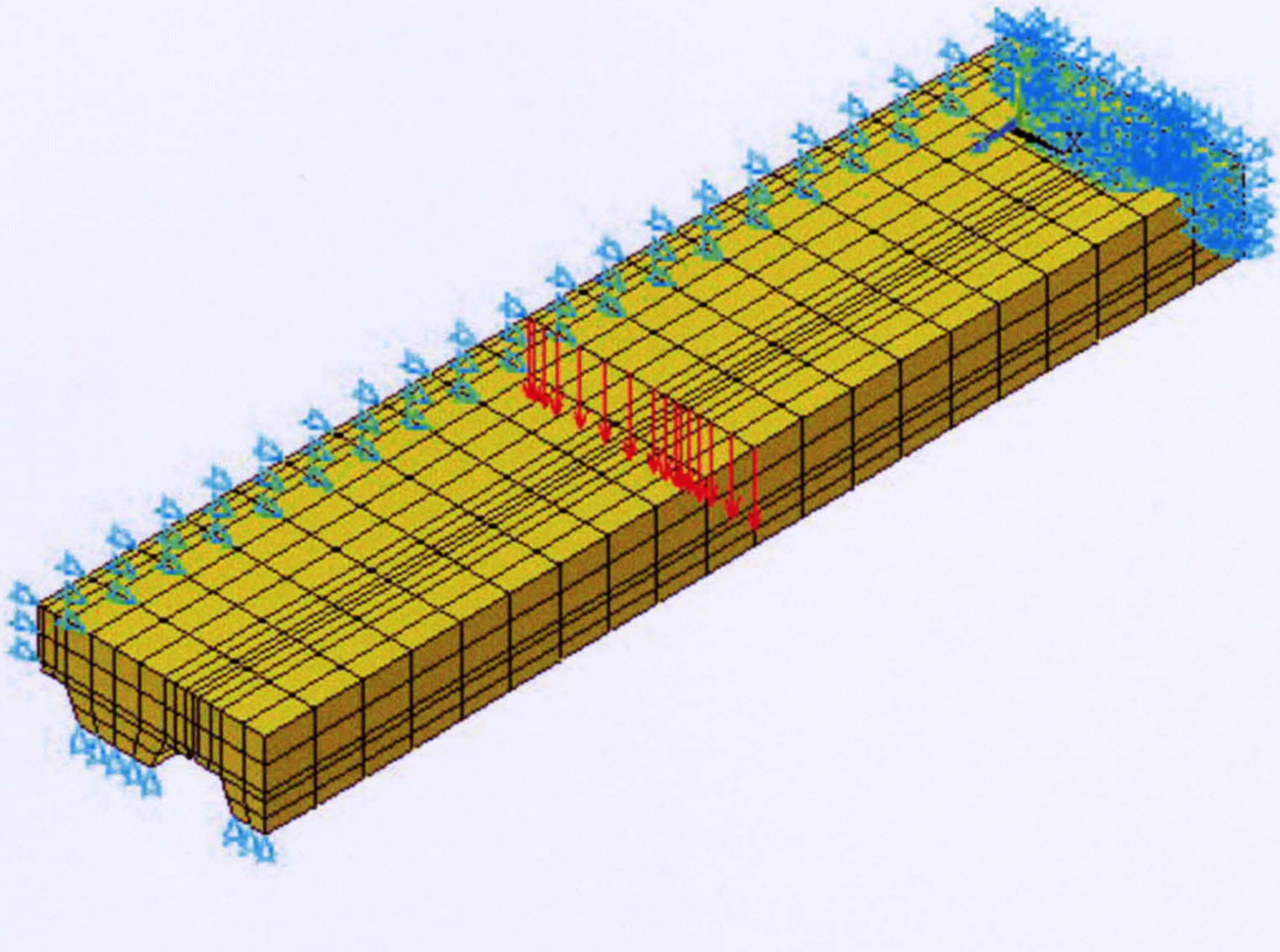

Figure 6.11.c The Finite Element model with the loads for the full scale tests.

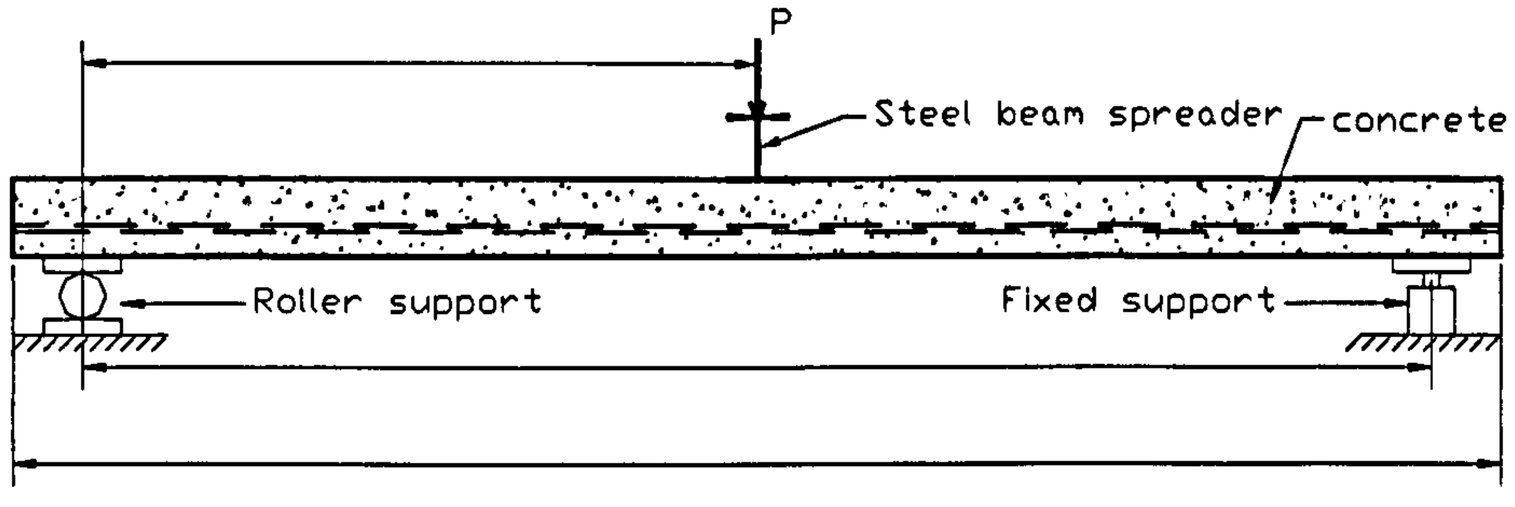

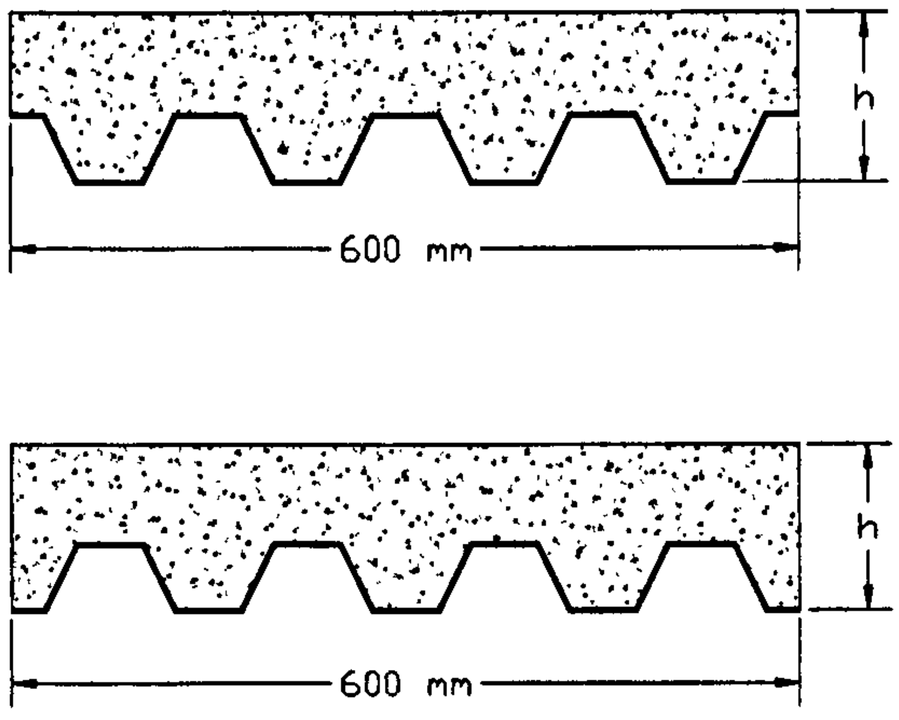

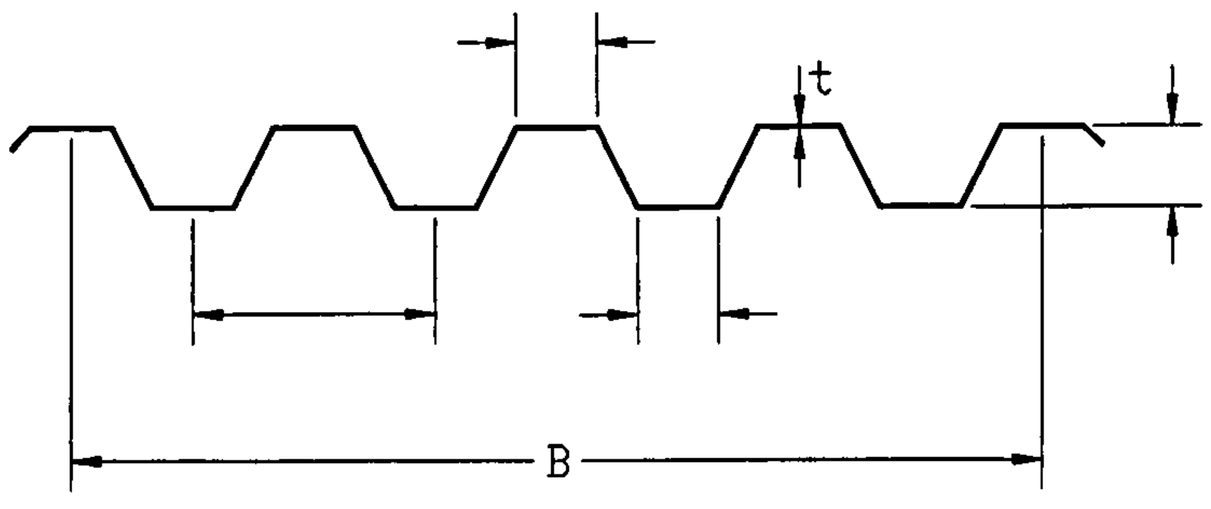

Figure 6.12 The composite slab dimensions, and the cross-section geometry of profiled steel sheet (Daniels[56]).

Figure 6.13 Comparison between experimental and FE results of Load-Slip behaviour for Composite Slab (Push-off test No. 1 with vertical load 5 kN)

and Shear Stress-Slip Curve for Composite Slab (Push-off test No. 1 with vertical load 5 kN)

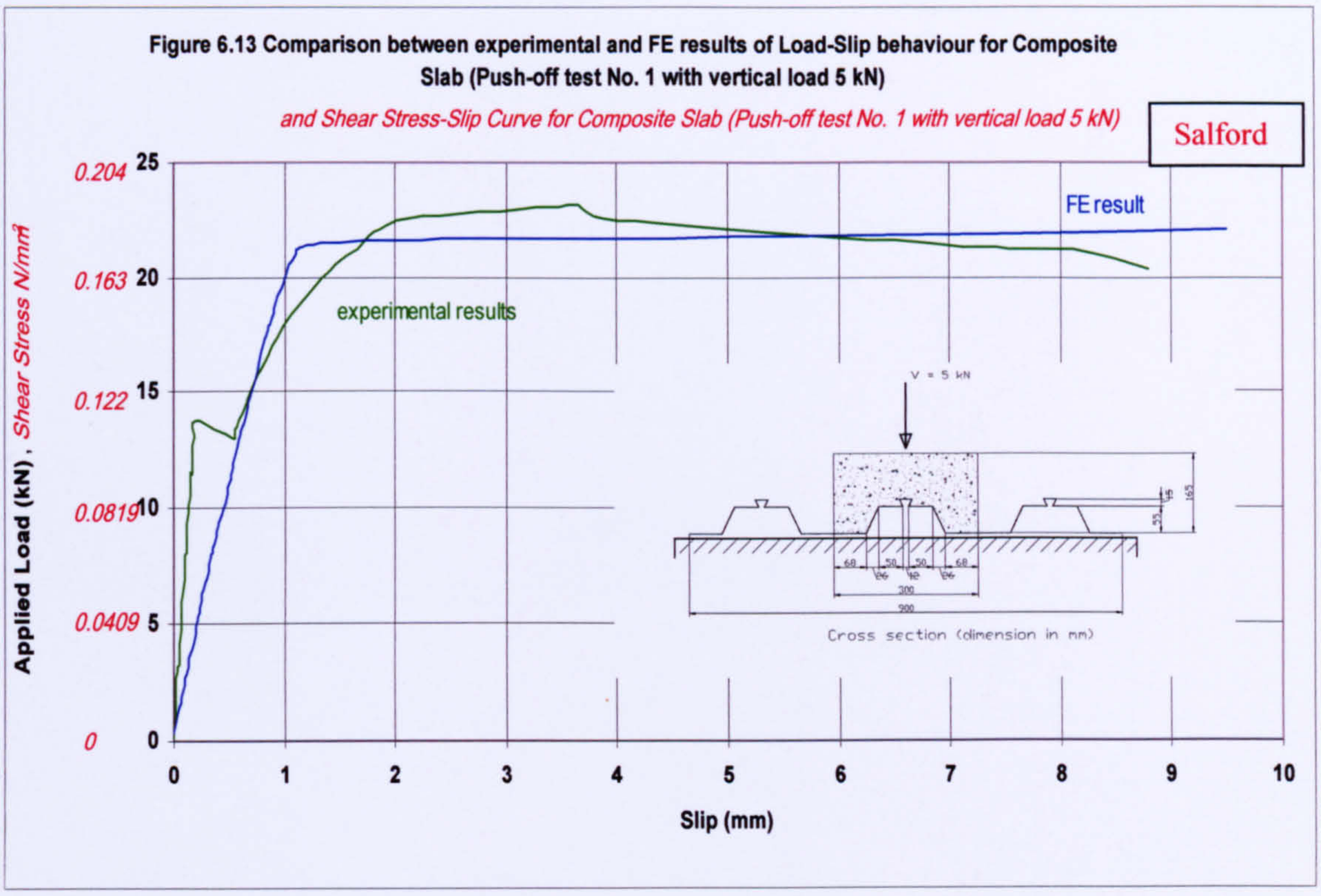

Figure 6.14 Comparison between experimental and FE results of Load-Slip behaviour for Composite Slab (Push-off test No.2, with vertical load 5kN)

and Shear Stress-Slip Curve for Composite Slab (Push-off test No.8, with vertical load 5kN)

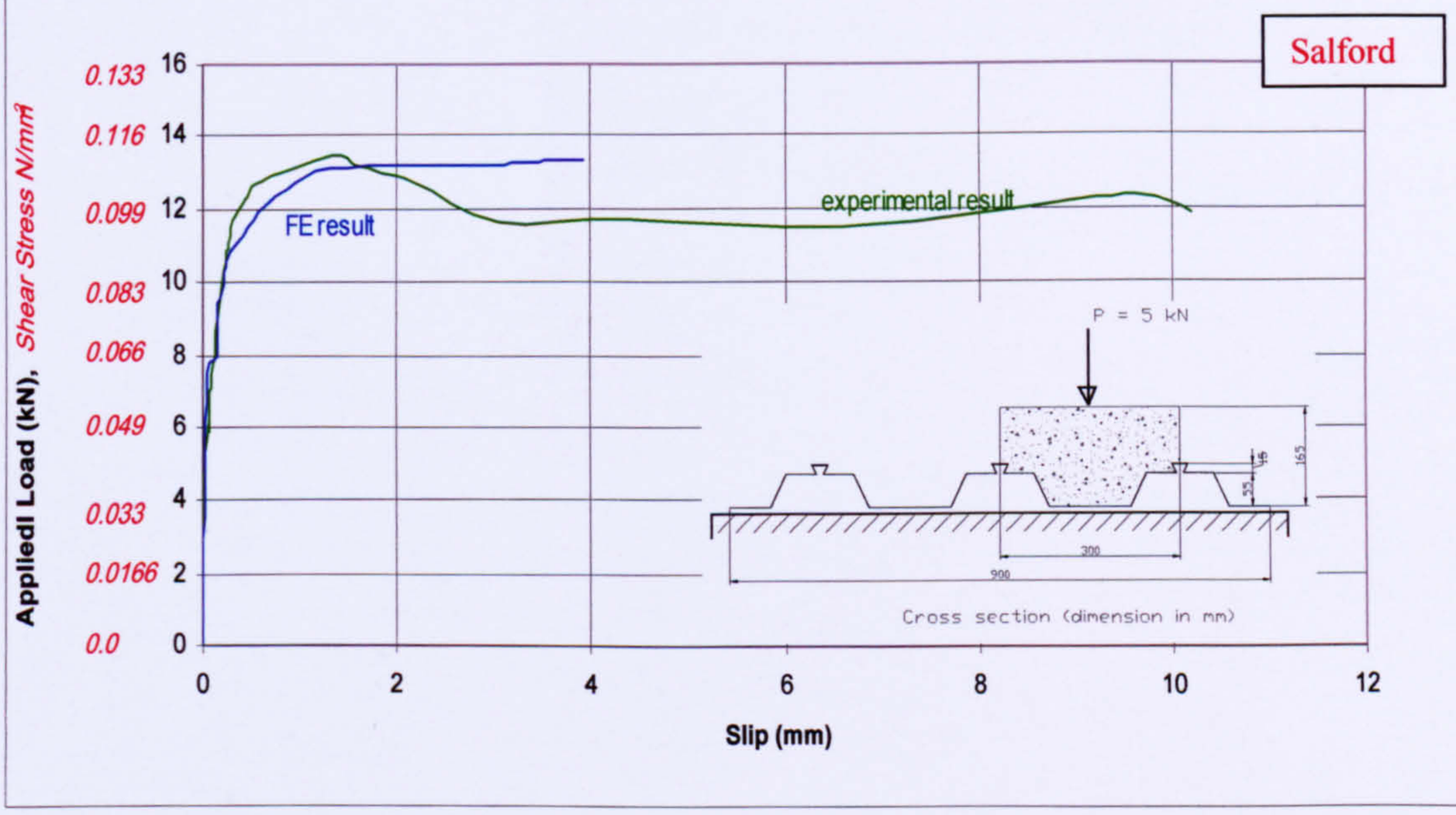

Figure 6.15 Comparison between experimental and FE results of Load-End Slip curve for composite Slab No.3

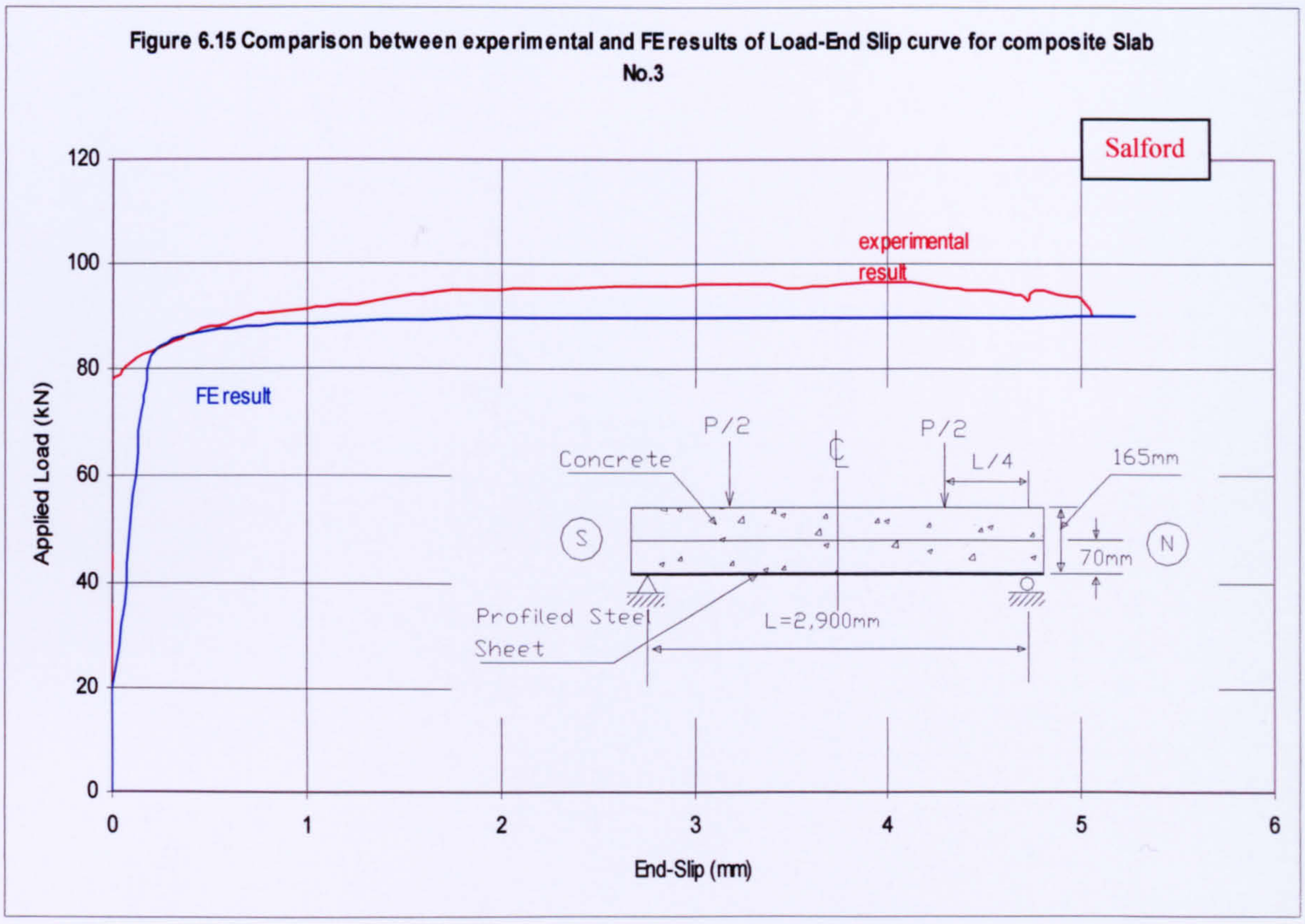

Figure 6.16 Comparison between experimental and FE results of Load-End Slip curve for composite slab No. 4

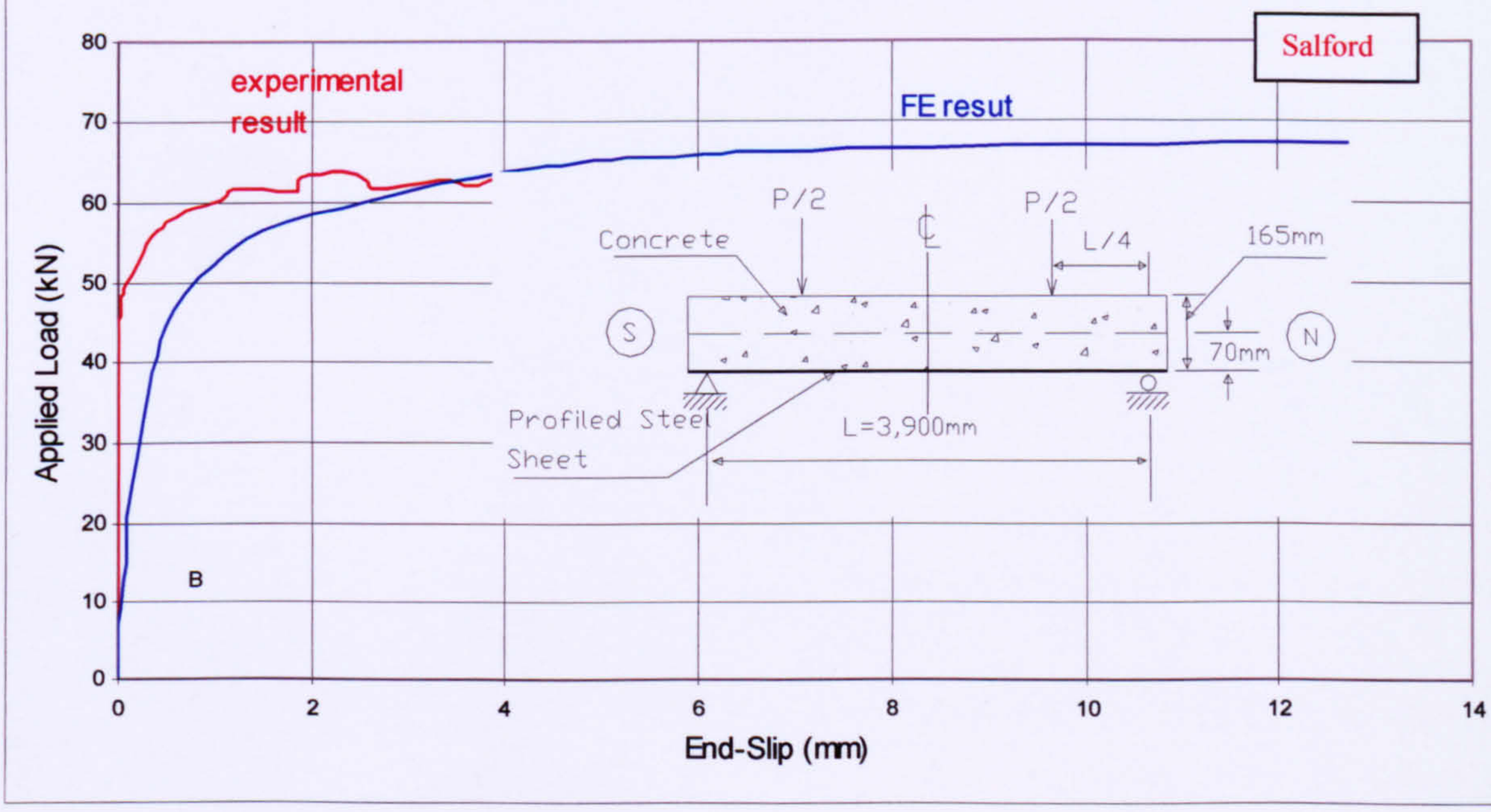

Figure 6.17 Comparison between experimental and FE results of Load-End Slip Curve for Slab No.5

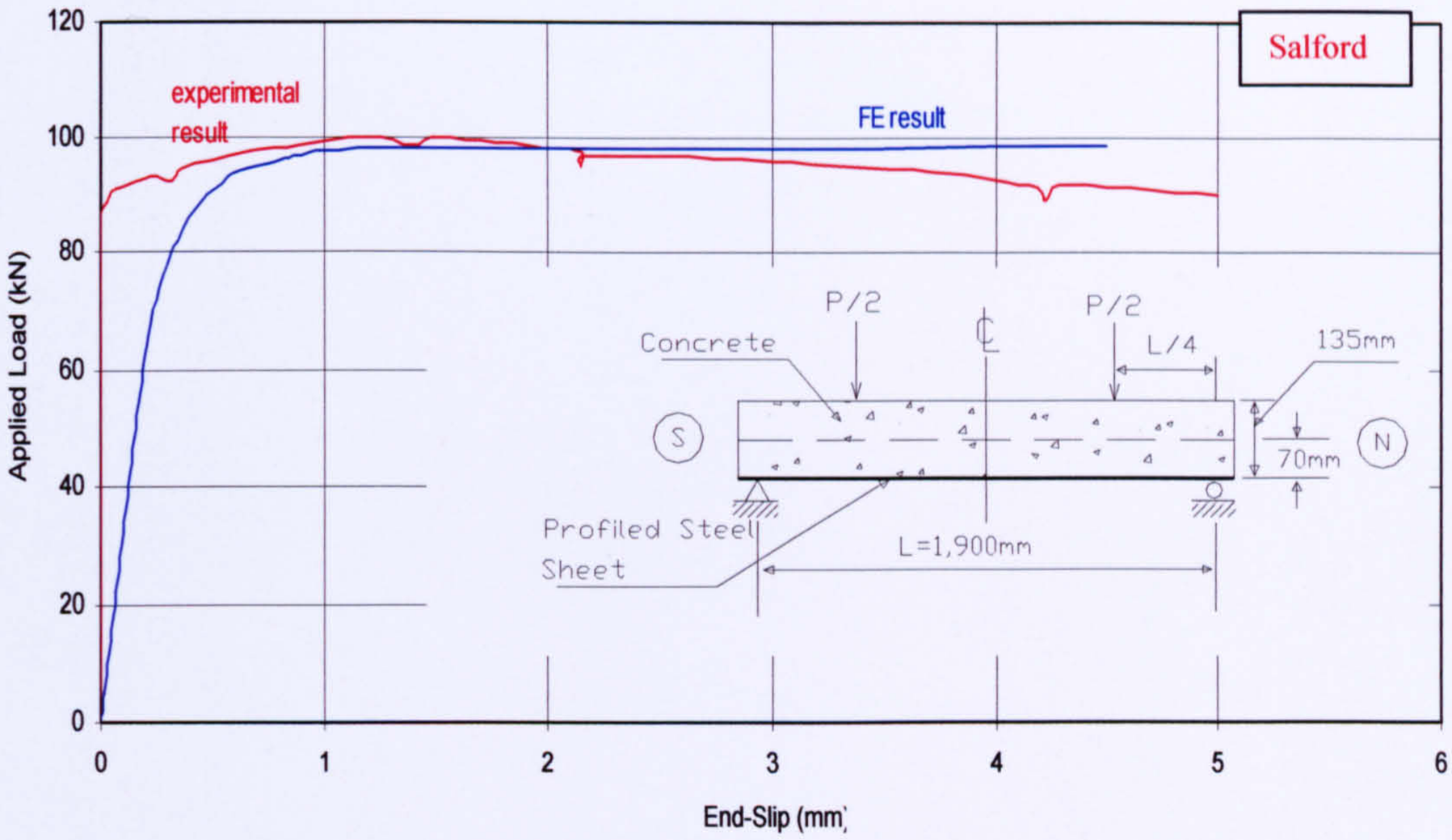

Figure 6.18 Comparison between experimental and FE results of Load-End Slip curve (Test no. 6).

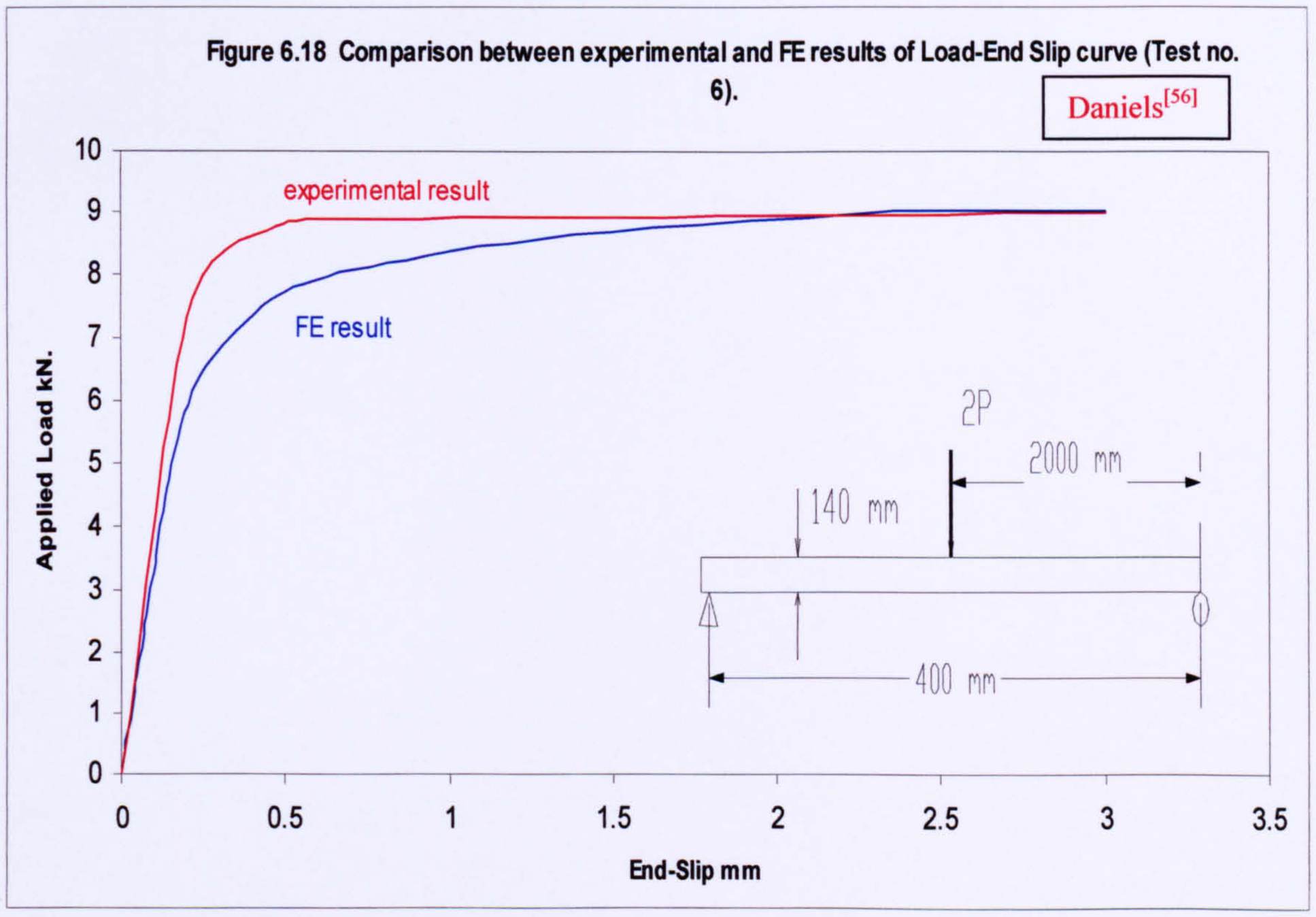

Figure 6.19 Comparison between experimental and FE results of Load-End Slip curve for Composite Slab (no. 7).

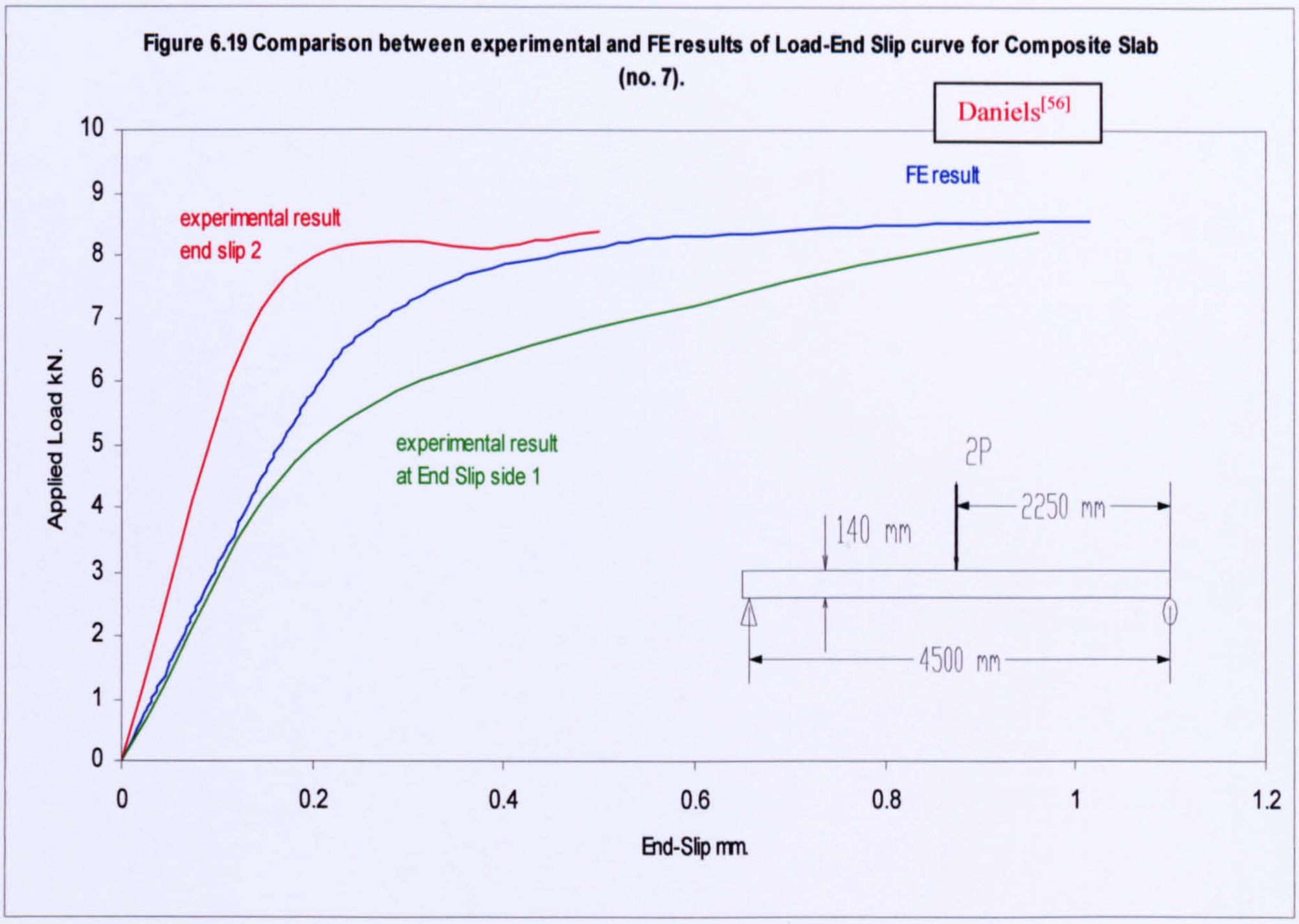

Figure 6.20 Comparison between experimental and FE resultsof Load-End Slip results of Composite Slab No 8.

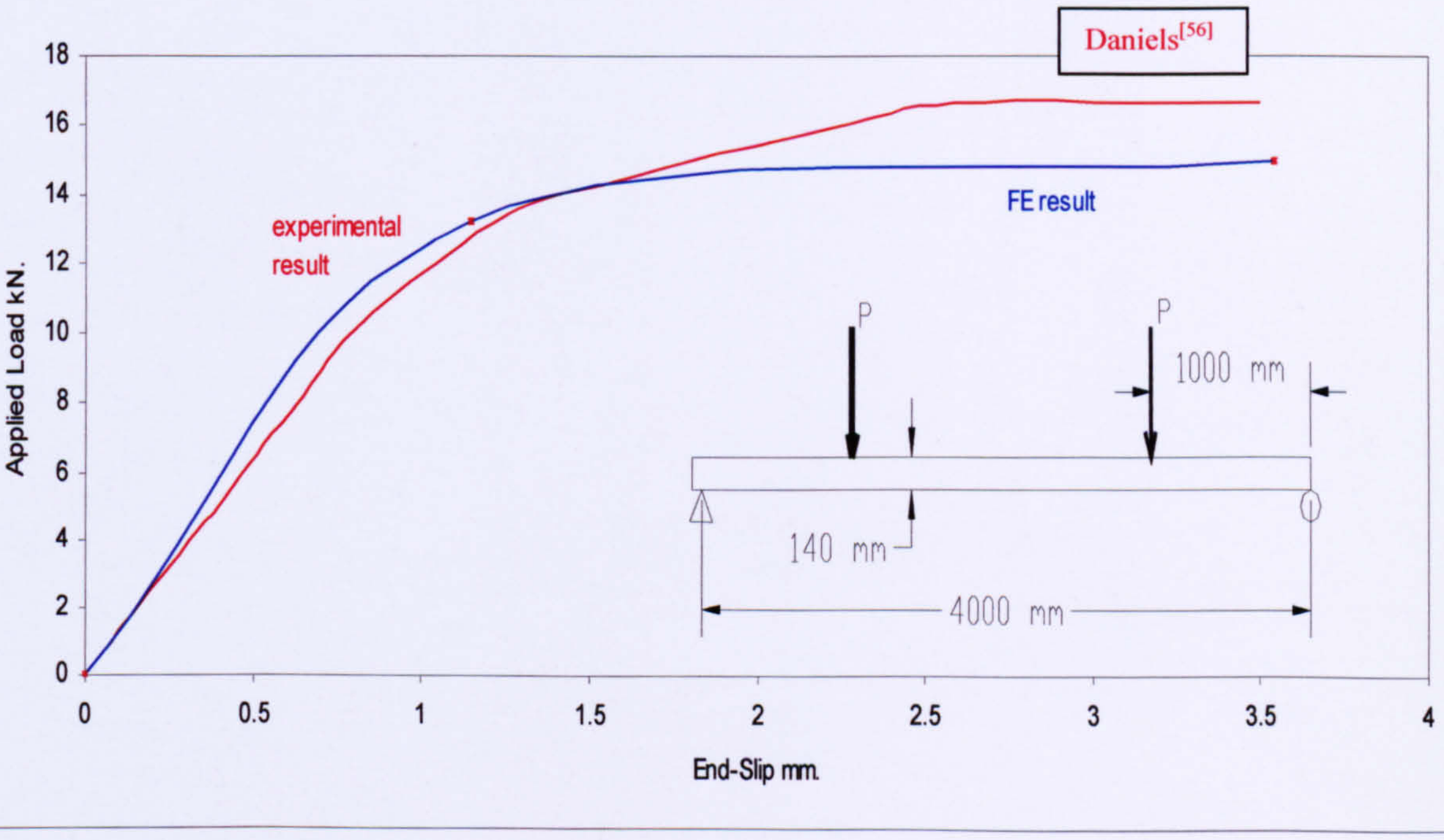

Figure 6.21 Comparison between experimental and FE results of Load-Slip curve for Composite Slab No 9.

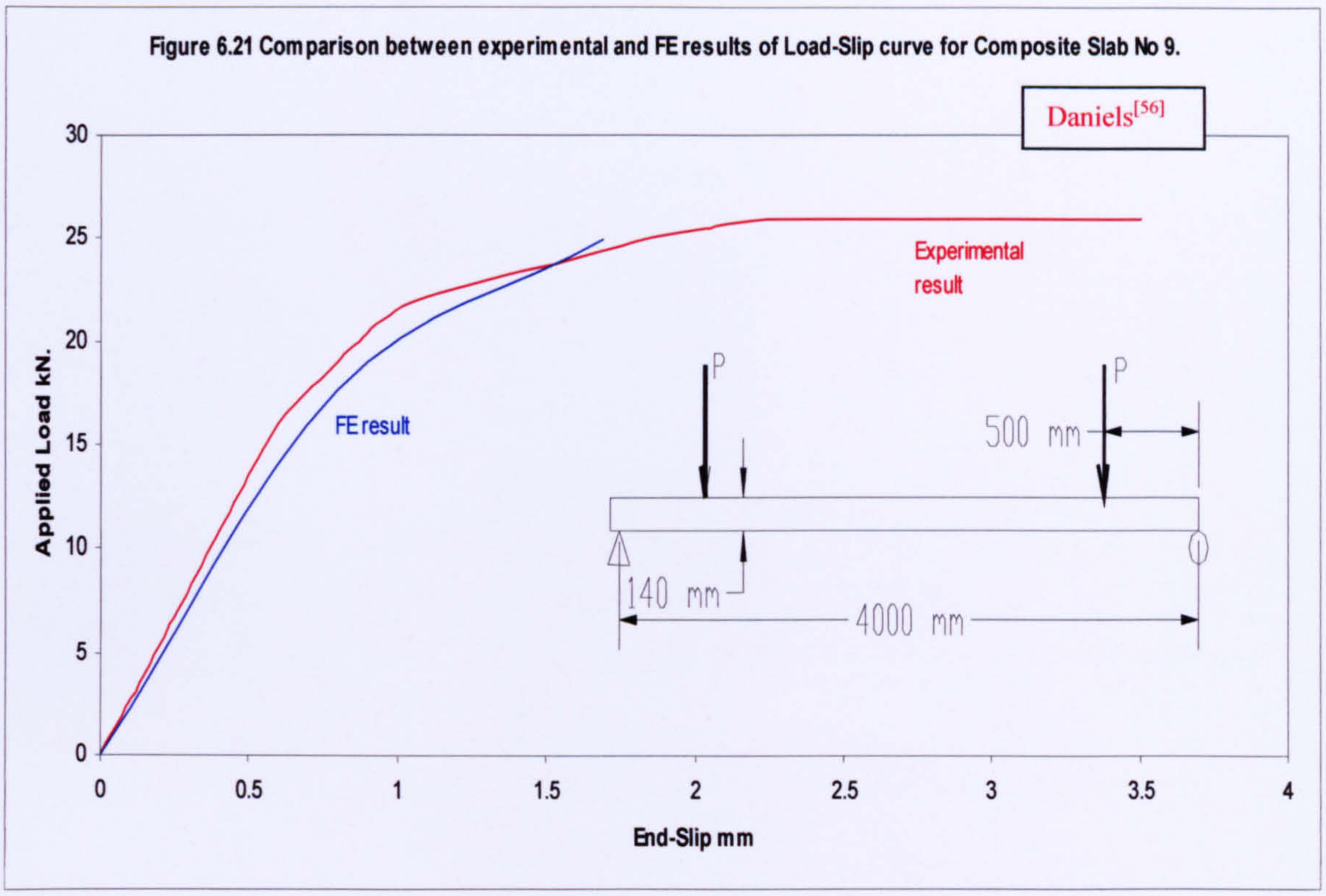

Figure 6.22 Comparison between experimental and FE results of Load-End Slip for composite slab No. 10.

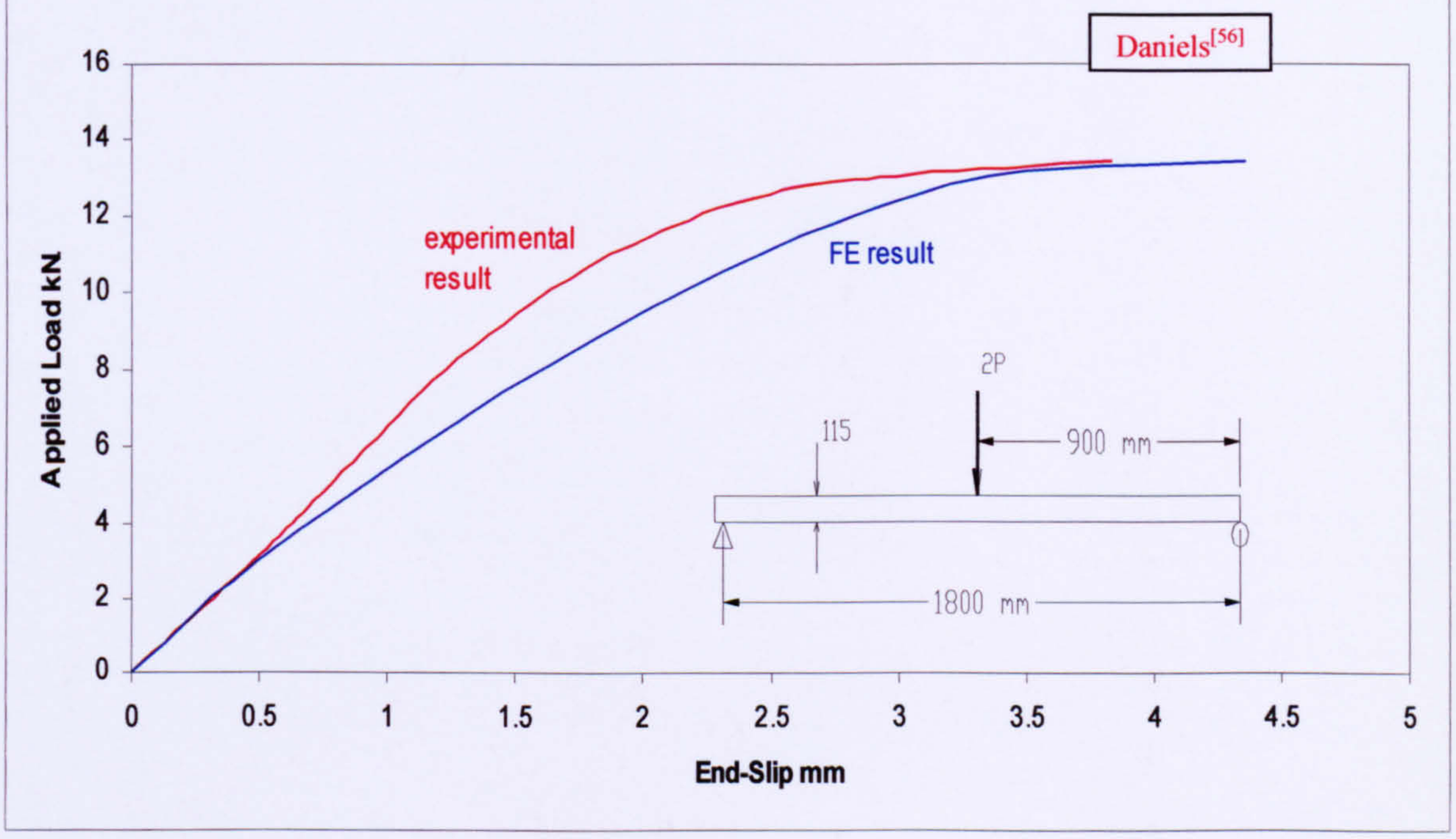

Figure 6.23 Comparison Between experimental and FE results of Load-End Slip For Composite Slab No. 11.

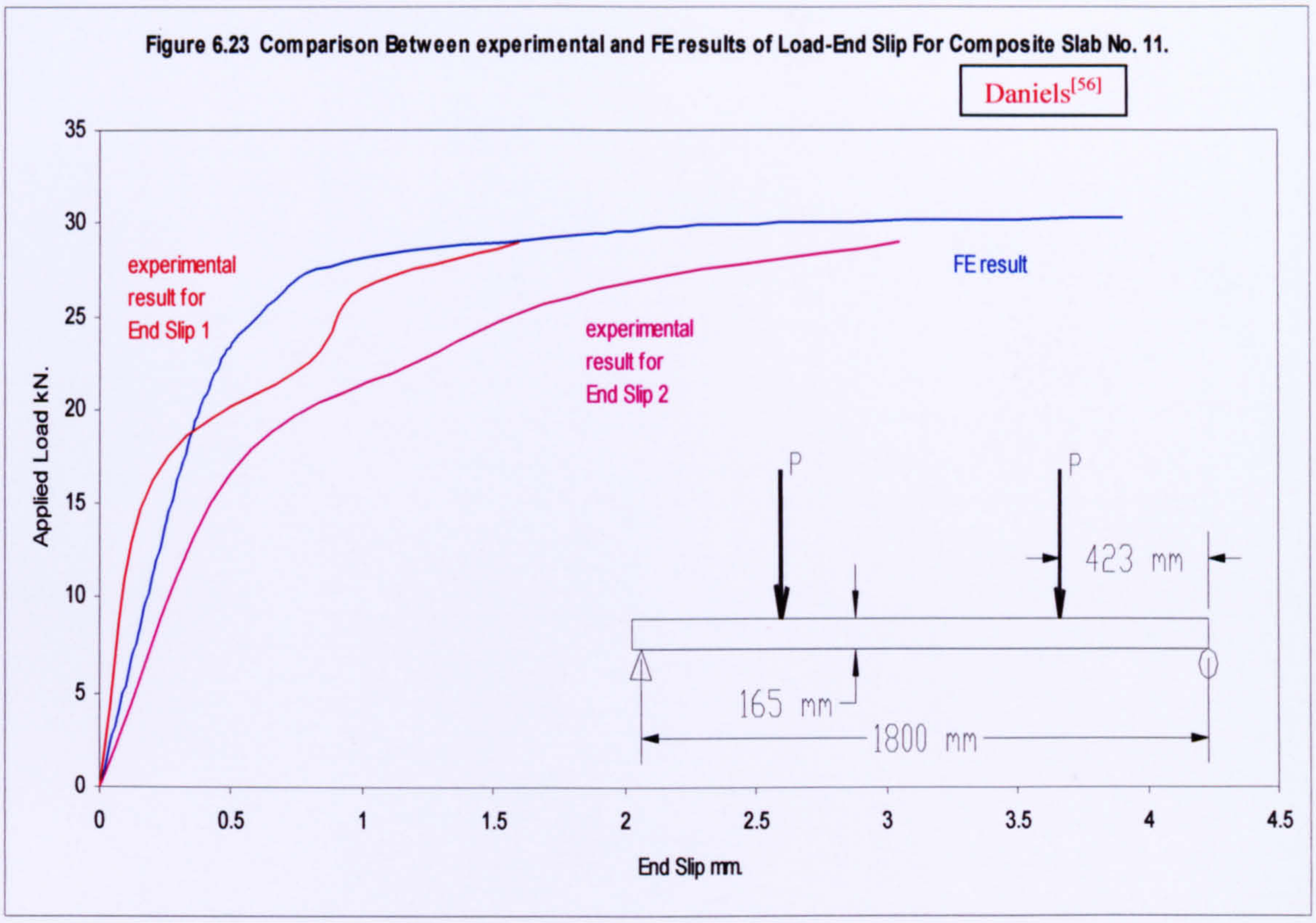

Figure 6.24 Comparison between experimental and FE results of Load-Central Deflection curve for Slab No.3

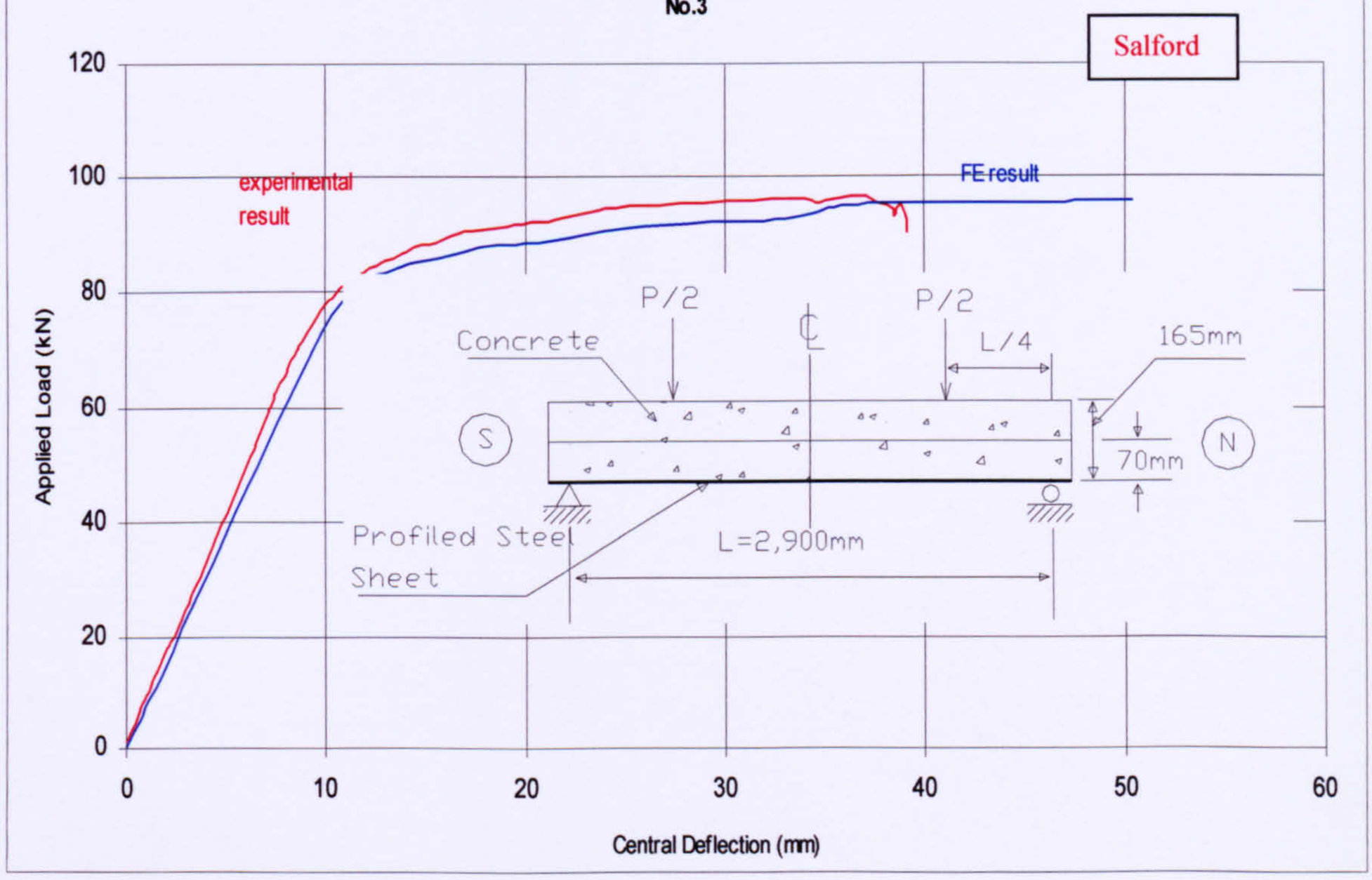

Figure 6.25 Comparison between experimental and FE results of Load-Central Deflection curve for composite slab No.4

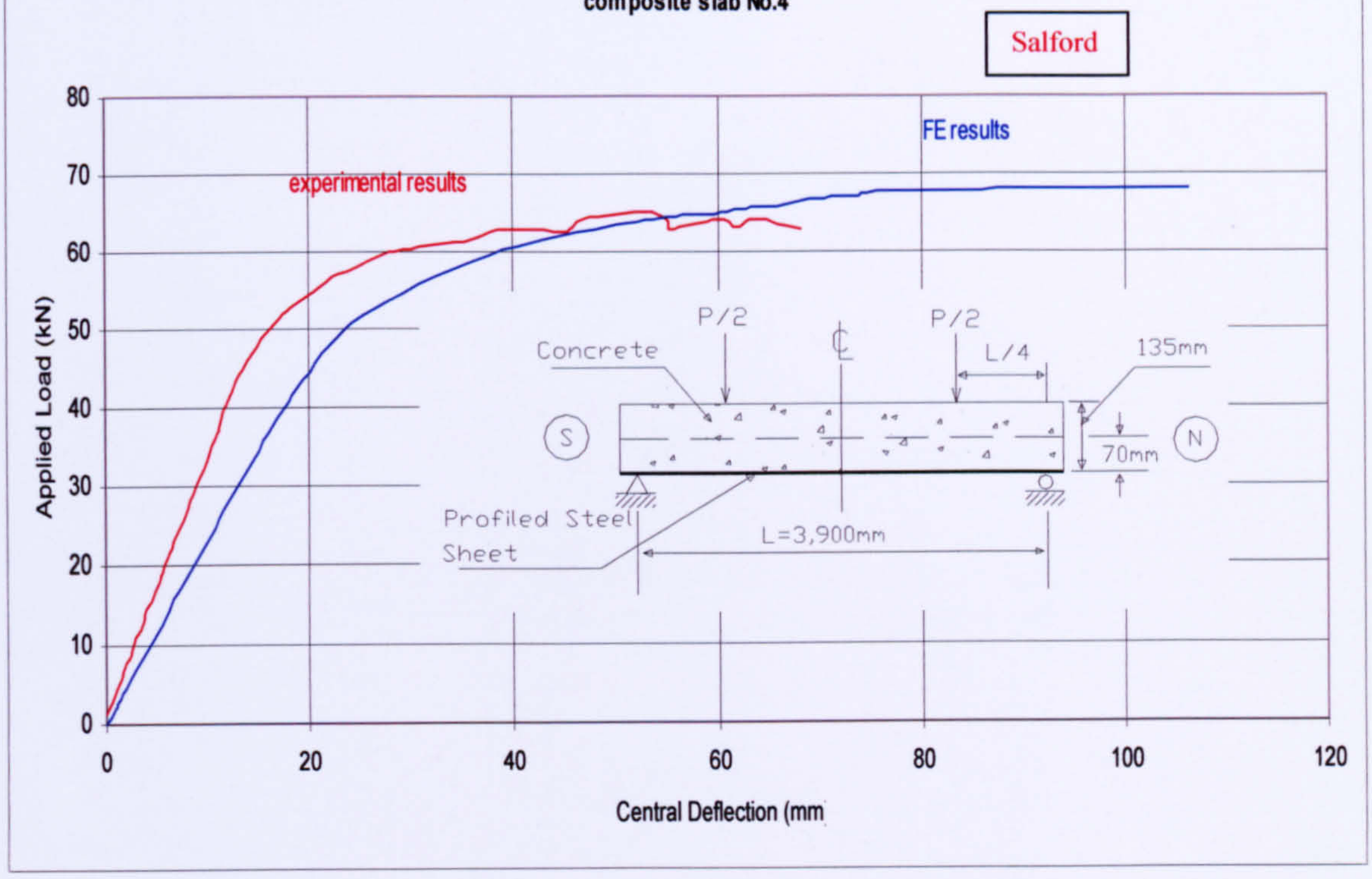

Figure 6.26 Comparison between experimental and FE results of Load-Central Deflection Curve for composite Slab No. 5

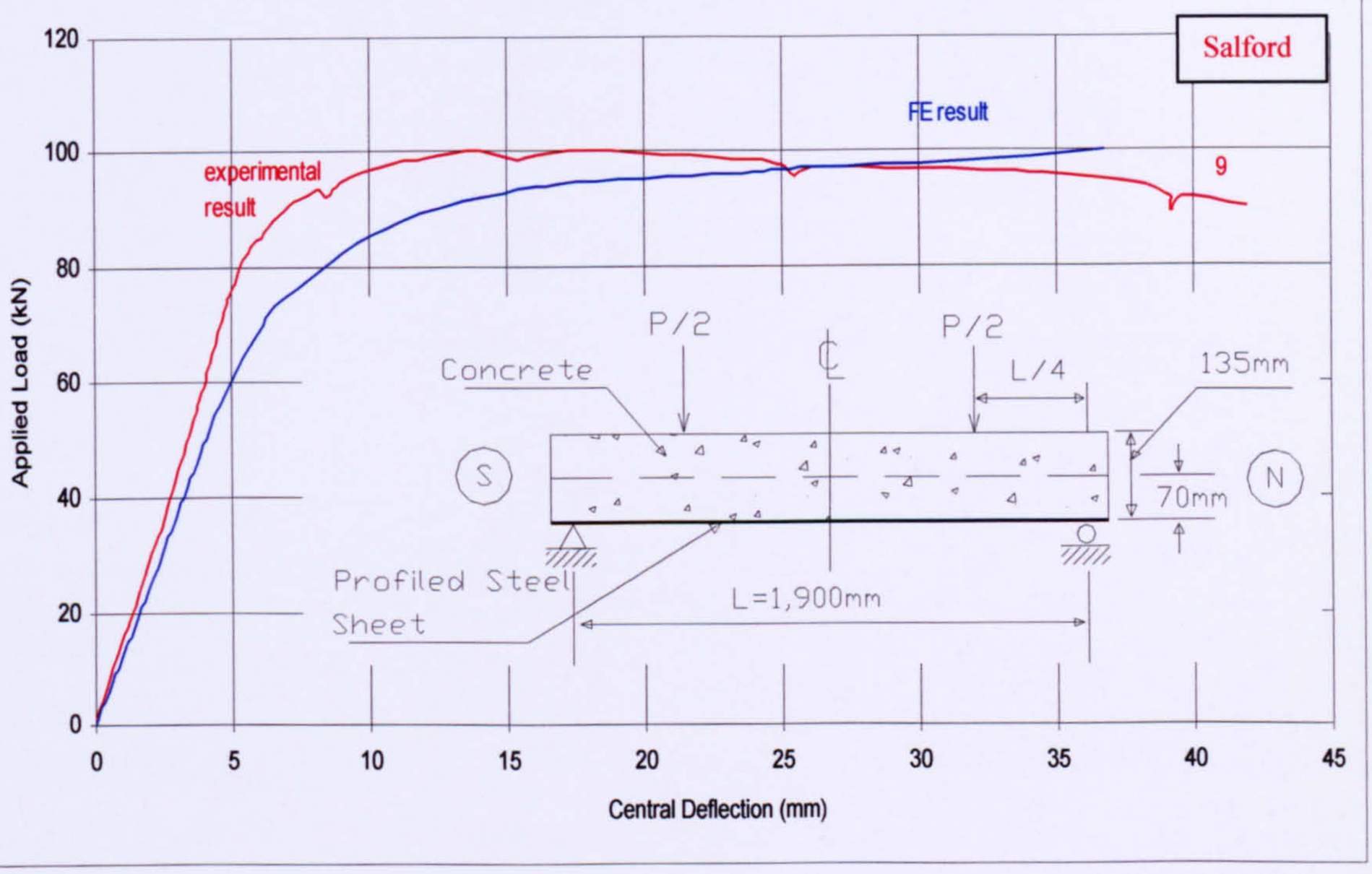

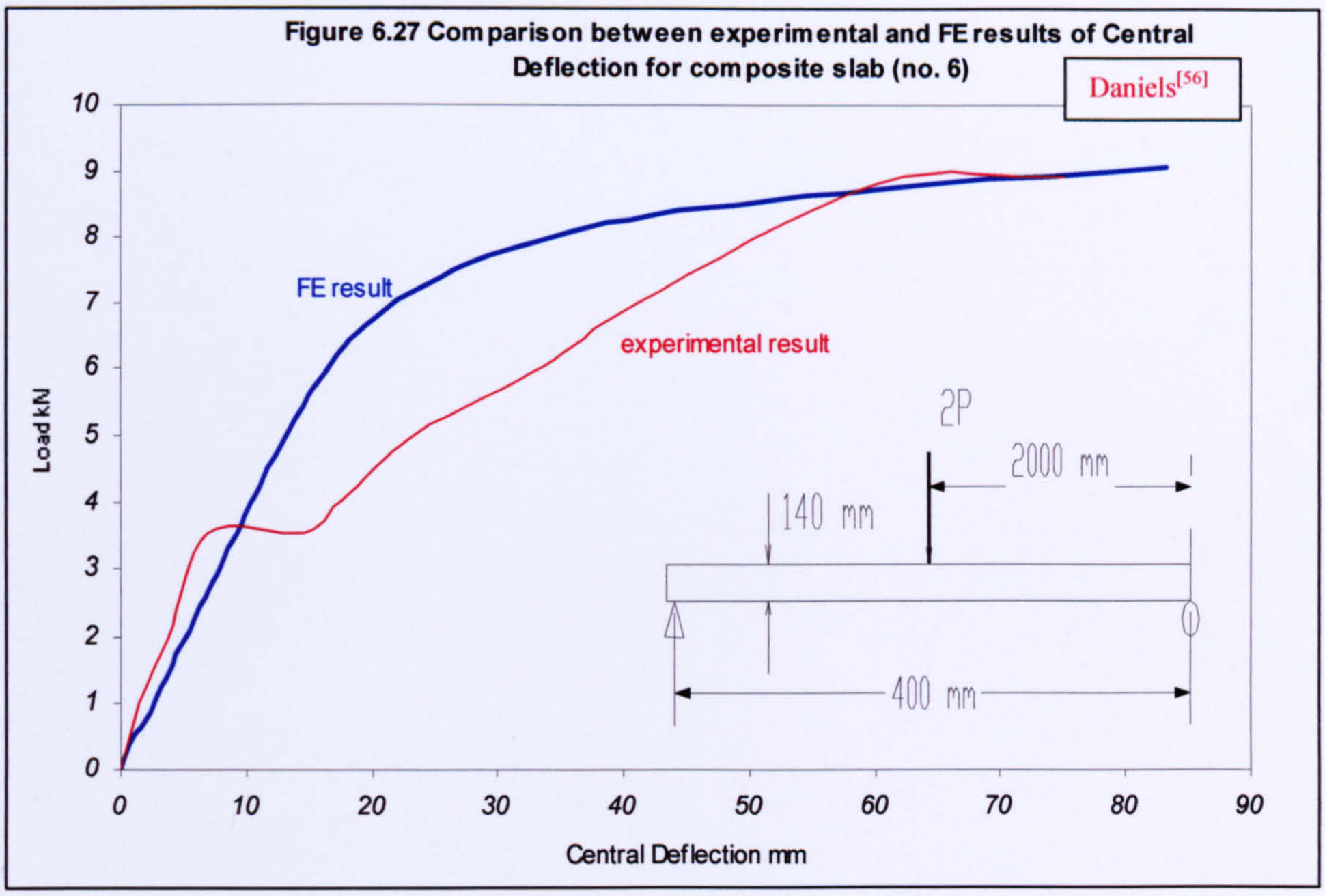

Figure 6.27 Comparison between experimental and FE results of Central Deflection for composite slab (no. 6)

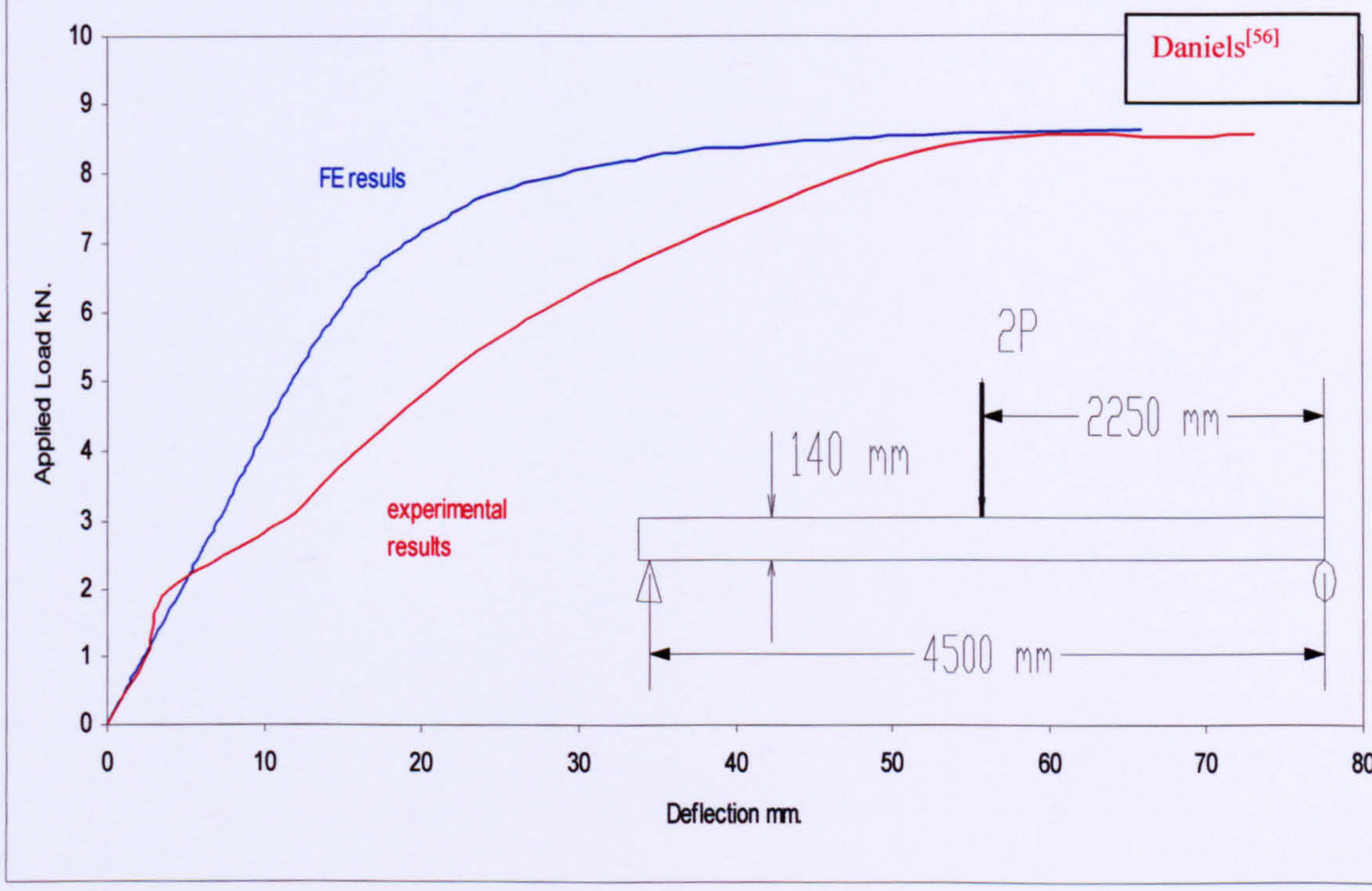

Figure 6.28 Comparison between experimental and FE results of Load-Central Deflection for Composite Slab No 7.

Figure 6.29 Comparison between experimental and FE results of Load-Central Deflection for Composite Slab No 8.

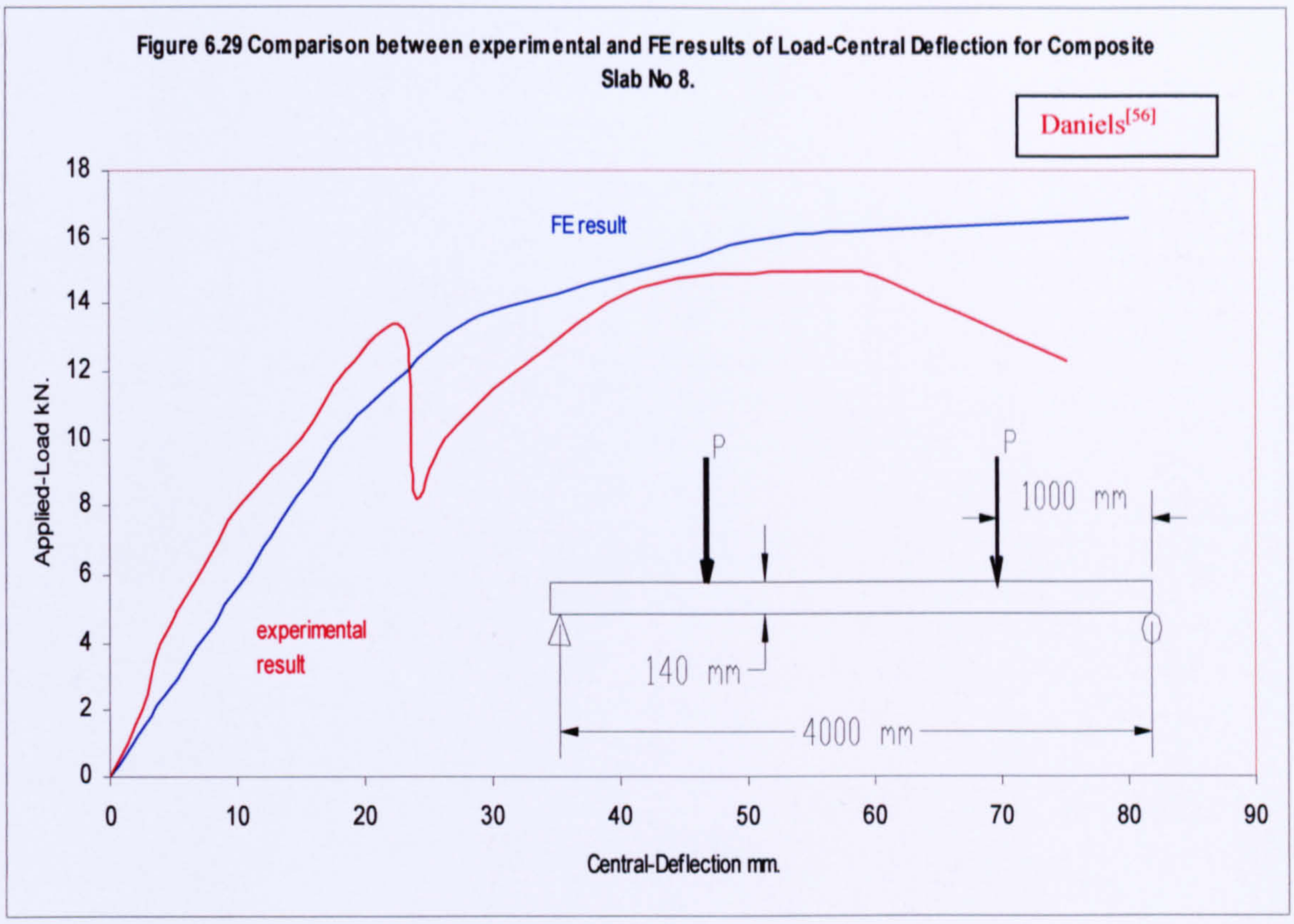

Figure 6.30 Comparison between experimental and FE results of Load-Central Deflection for Composite Slab No. 9.

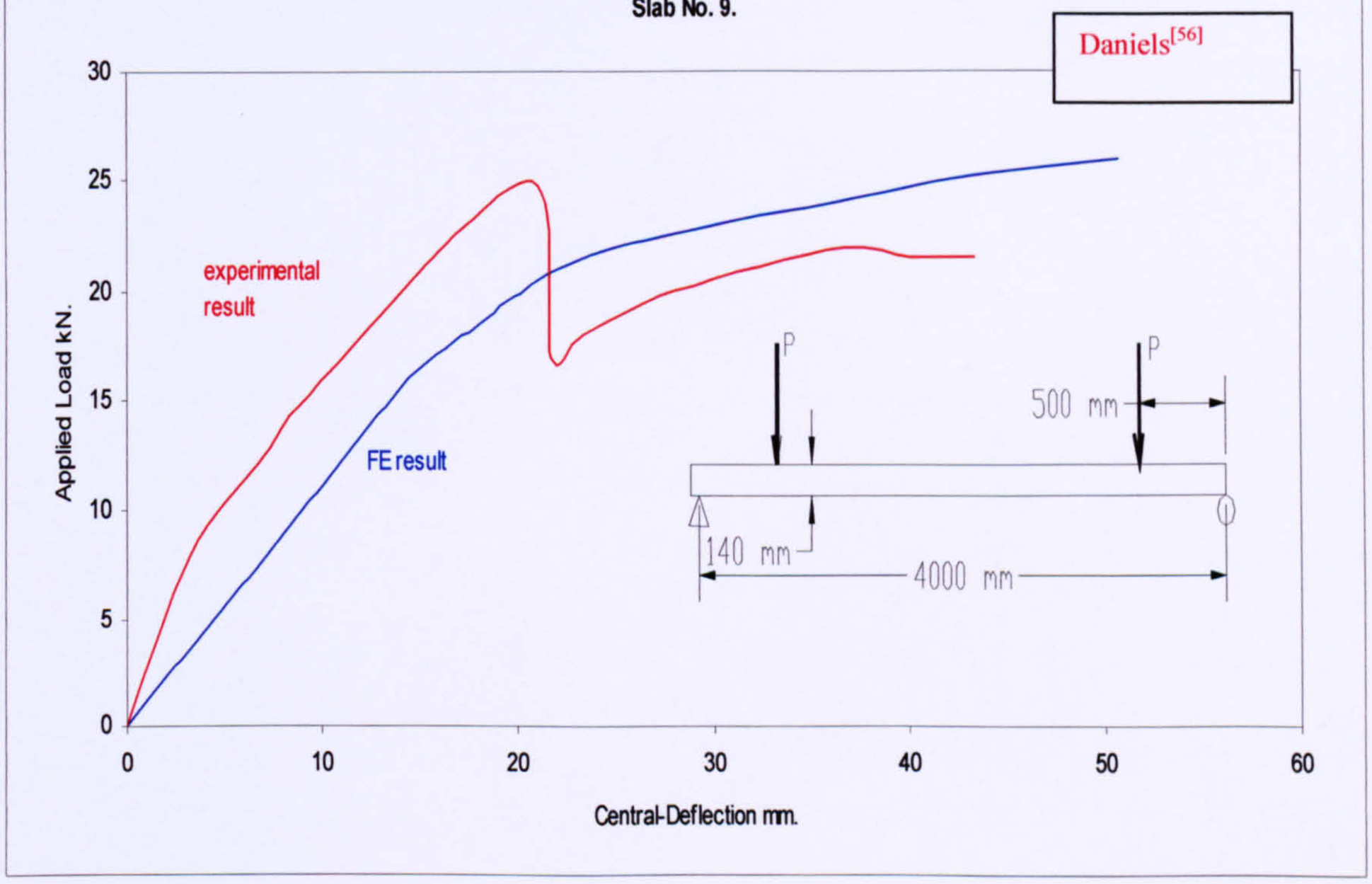

Figure 6.31 Comparison between experimental and FE results of Load-Central Deflection for Composite Slab No. 10.

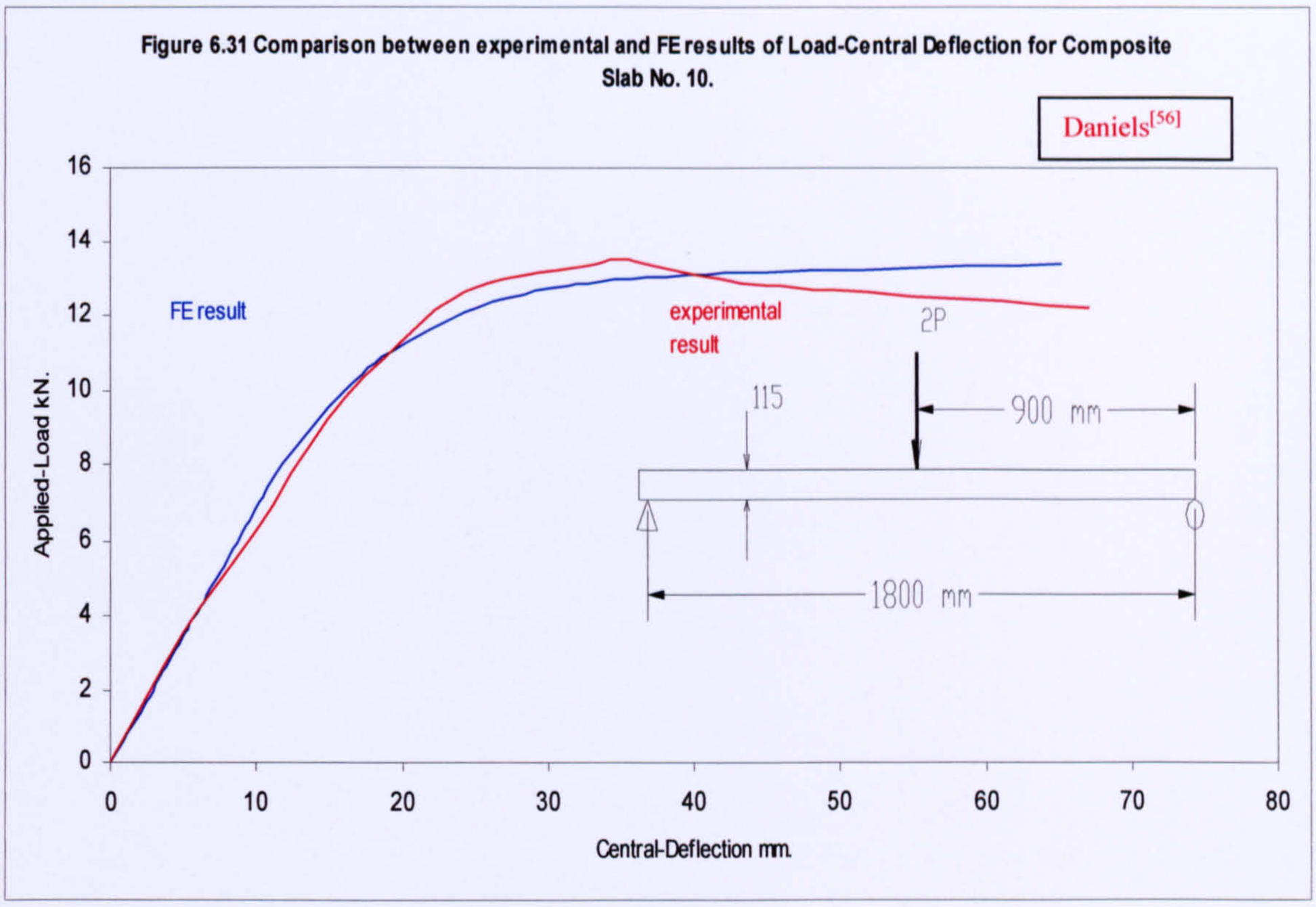

Figure 6.32 Comparison between experimental and FE results of Load-Central Deflection for Composite Slab No. 11.

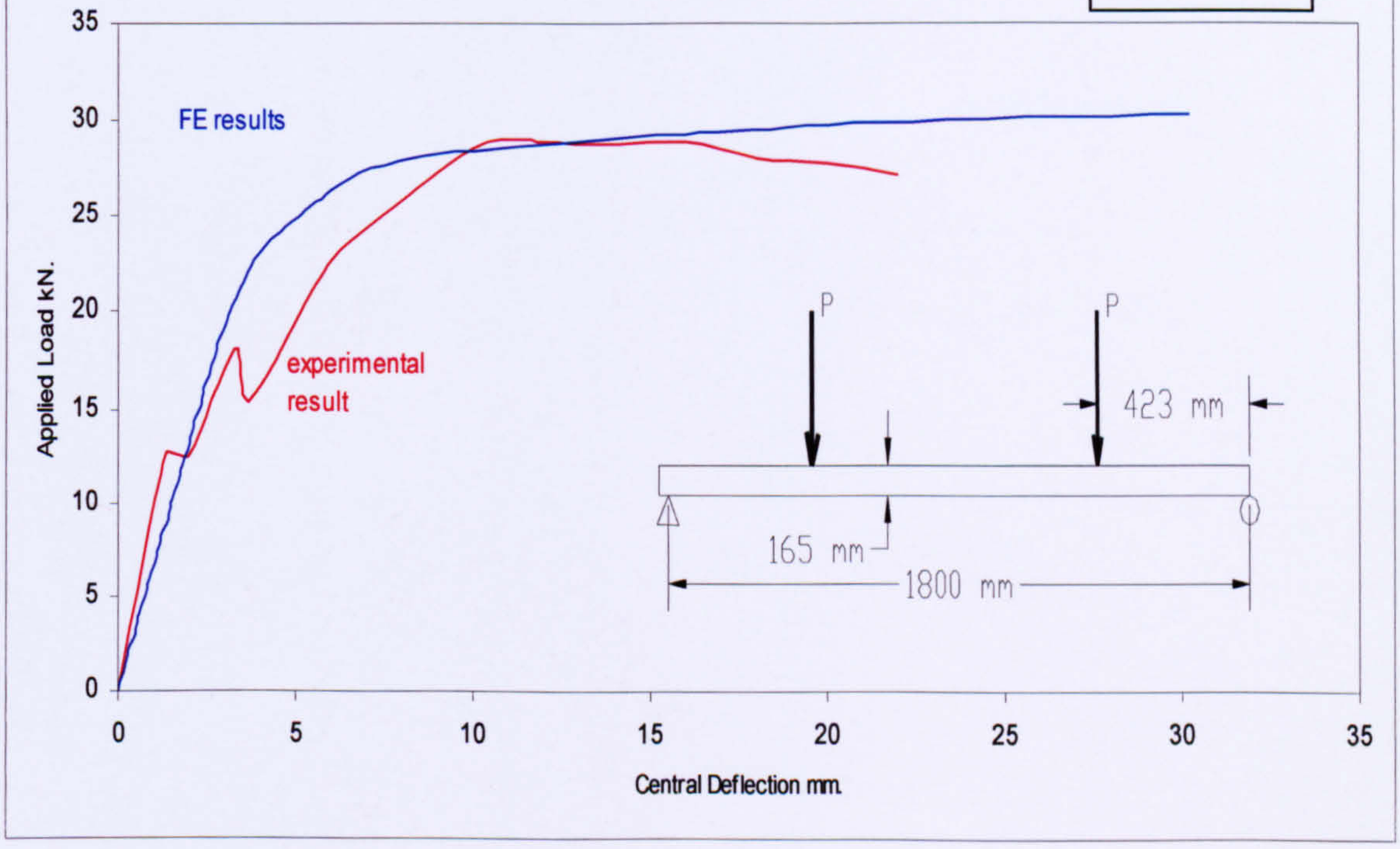

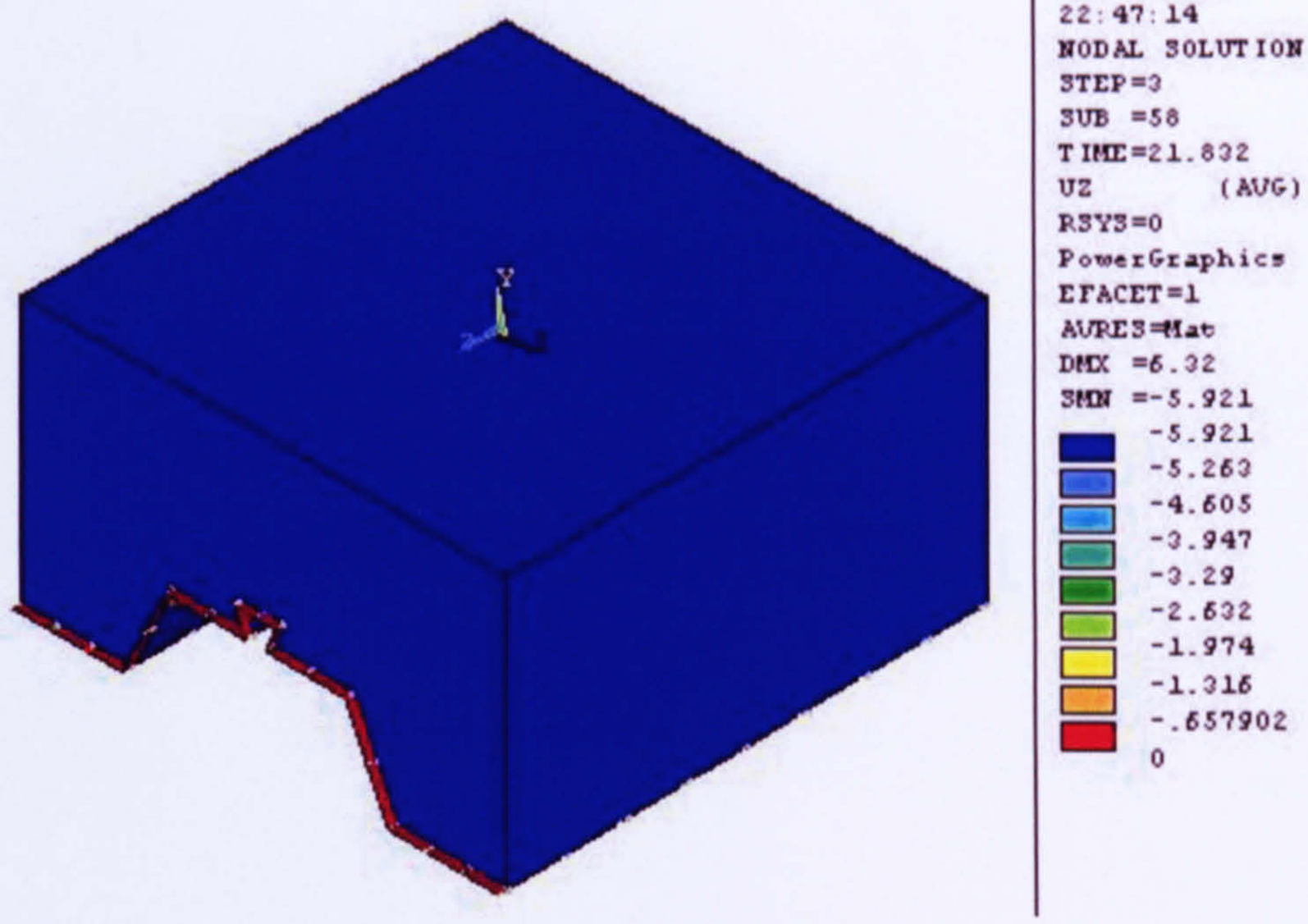

Figure 6.33.a Slip for the small-scale model.

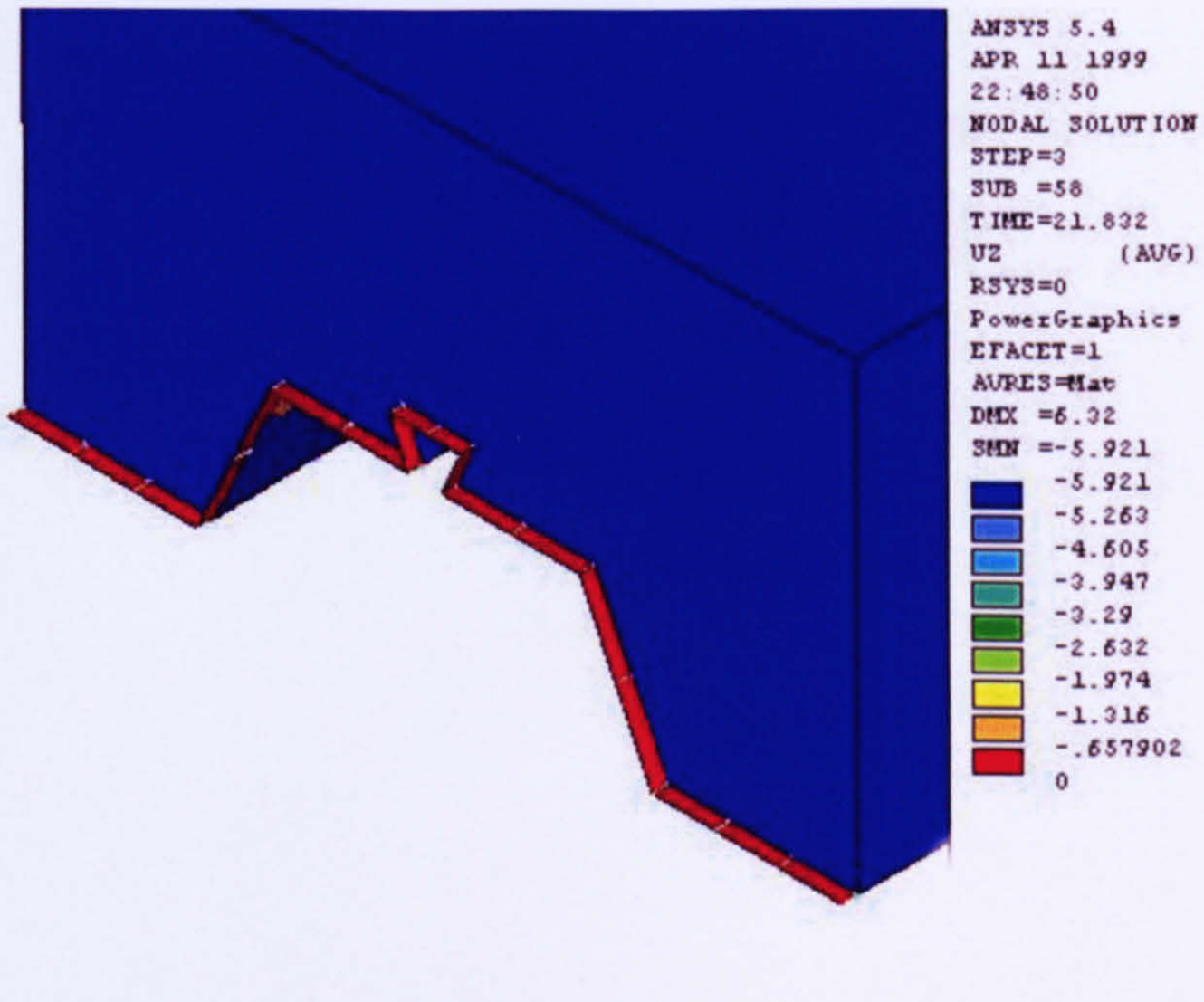

Figure 6.33.b Close up of slip in the small scale-model.

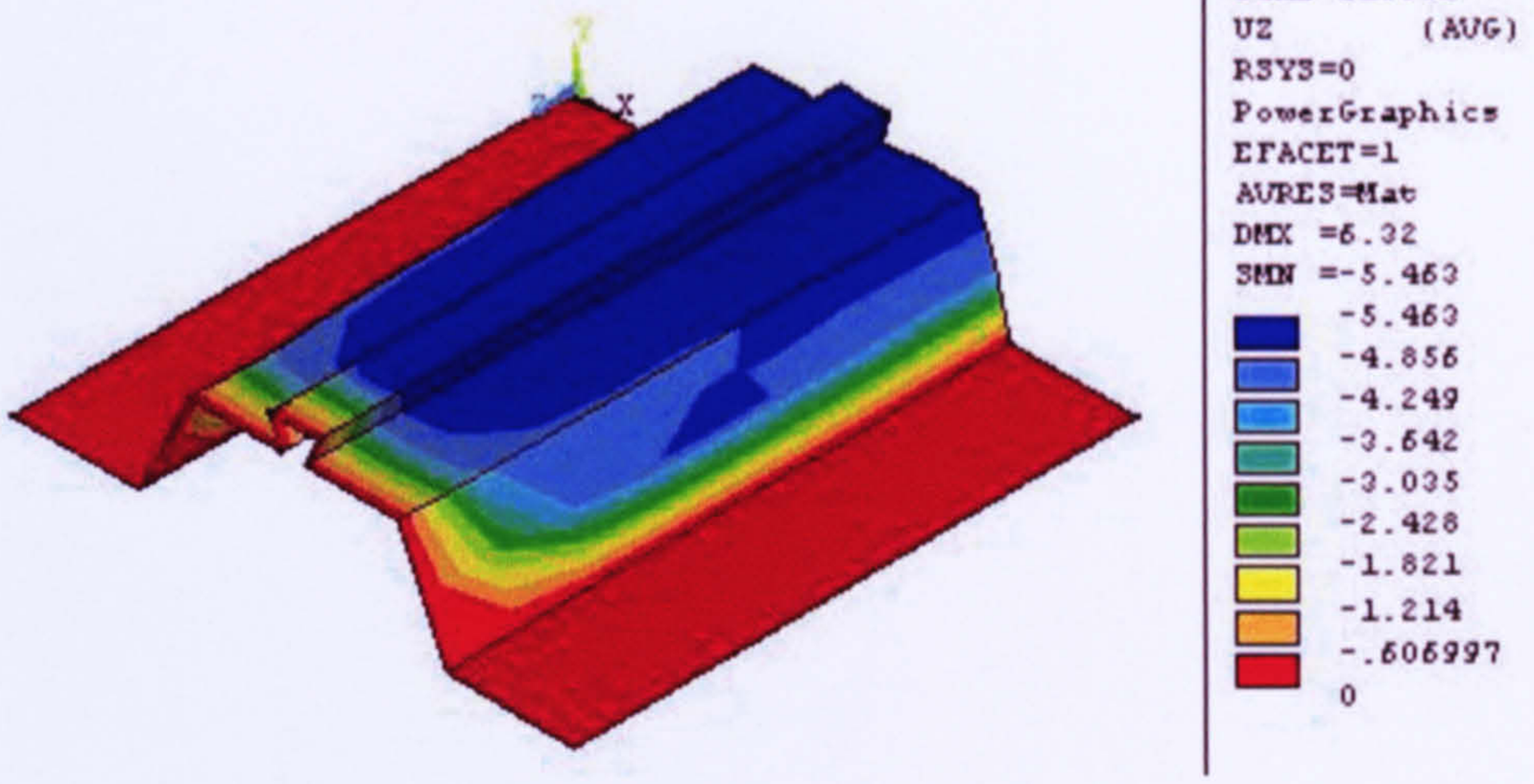

Figure 6.33.c Longitudinal displacement (uz) in small-scale model.

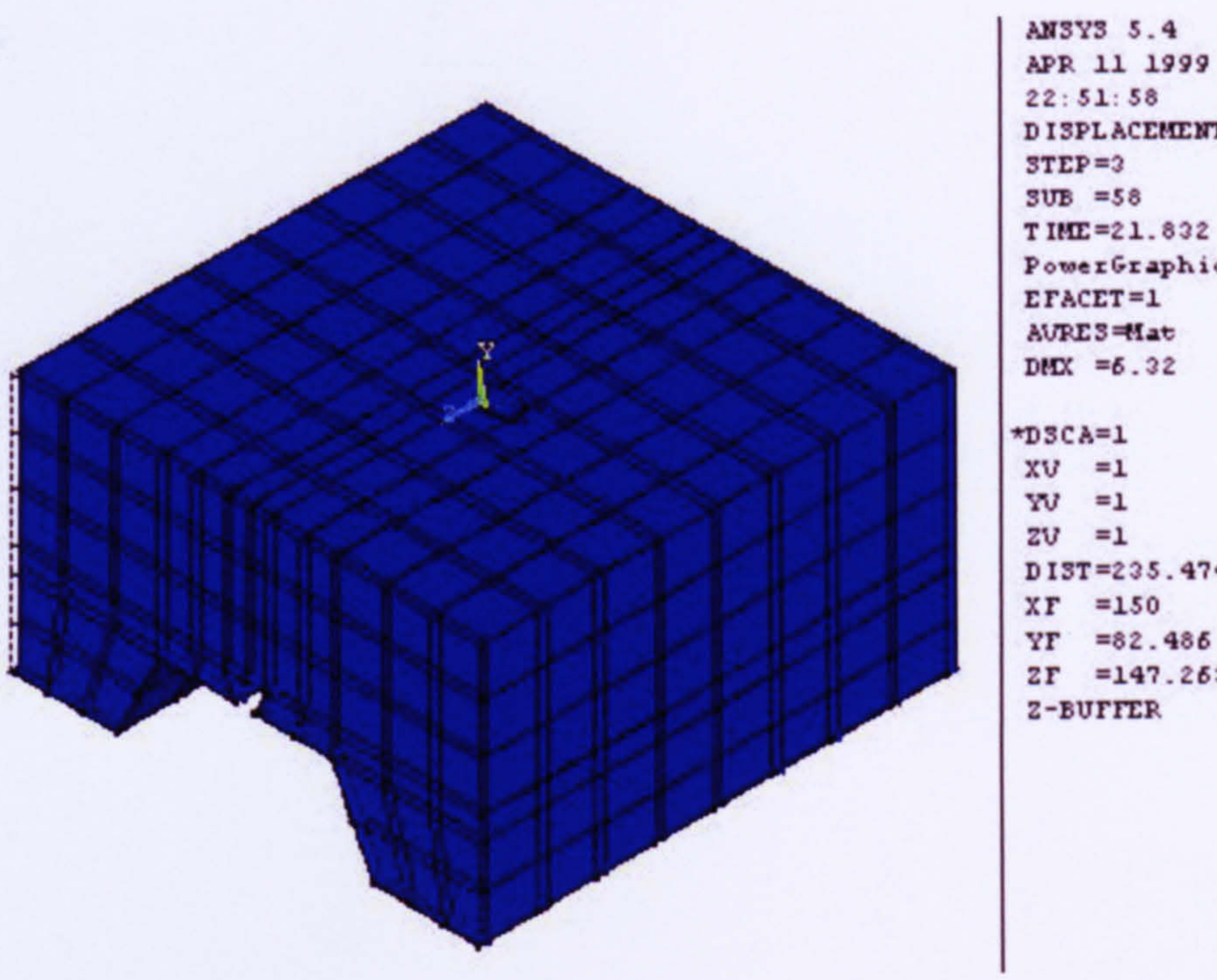

Figure 6.33.d Deformation of the model at load 21.83 kN.

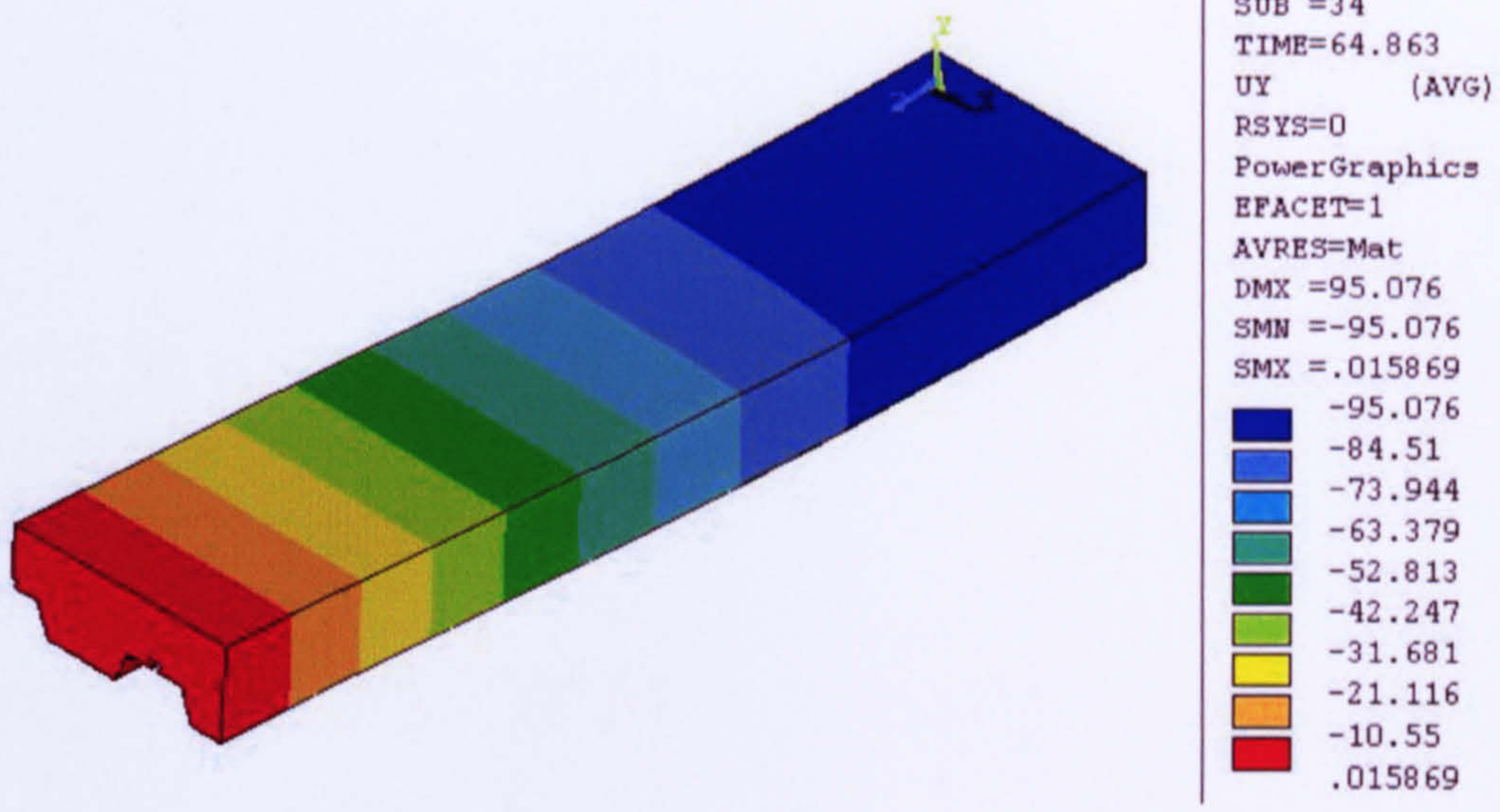

Figure 6.34 a Deflection (95mm) of the composite slab at load of 64.86 kN.

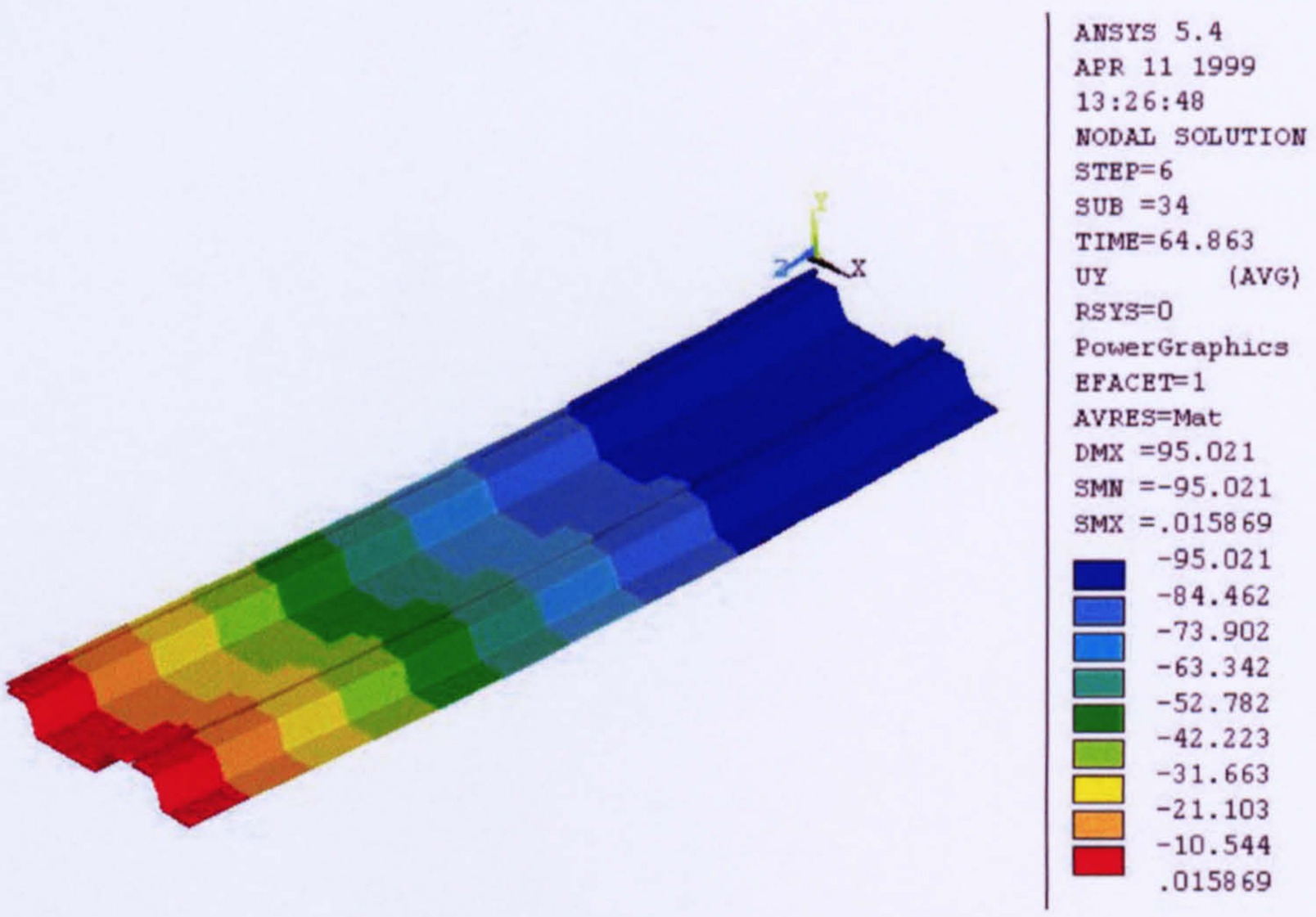

Figure 6.34 b Deflection (95mm) of the profiled steel sheet at load of 64.86 kN.

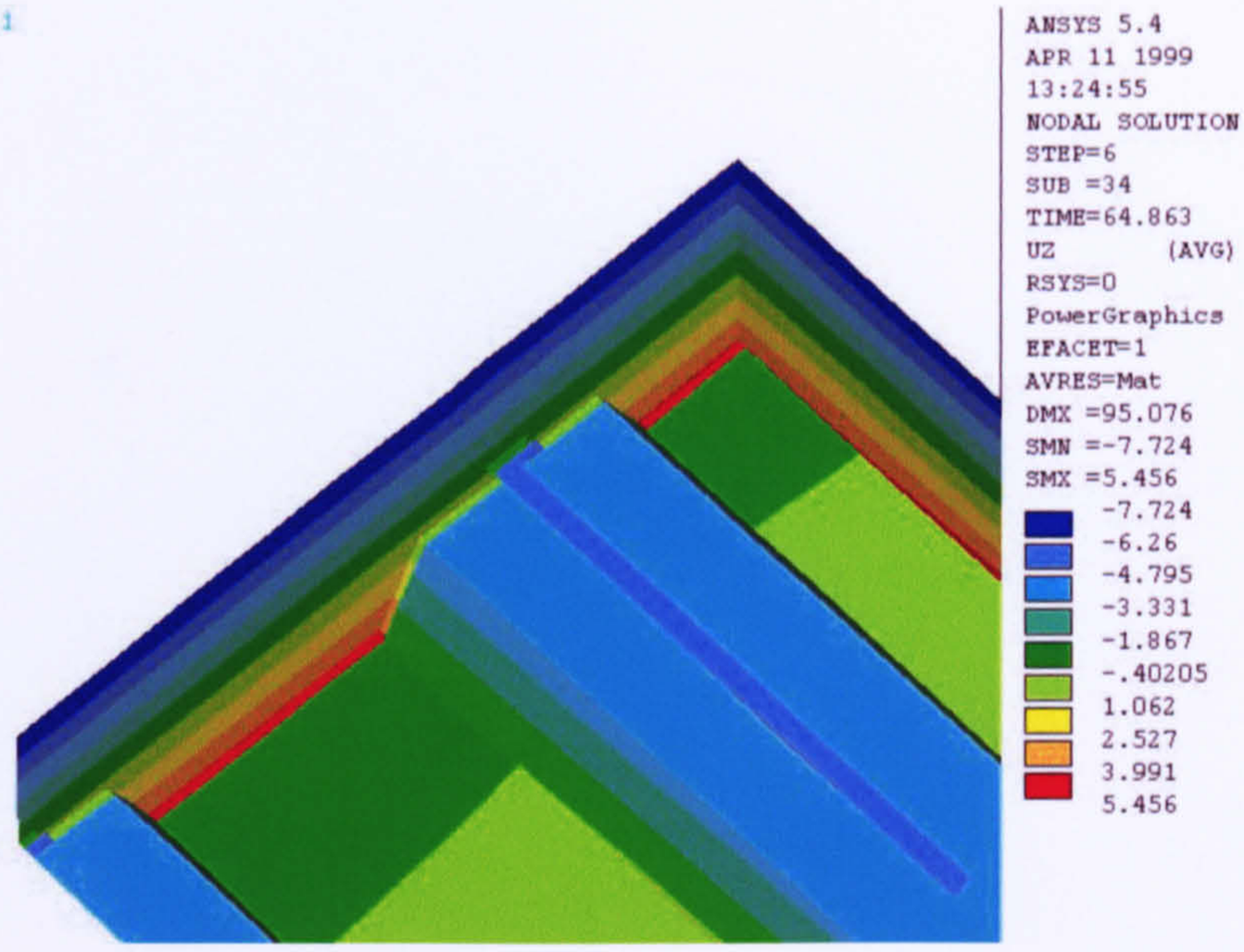

Figure 6.34.c Section of the longitudinal displacement of at load of 64.86 kN.

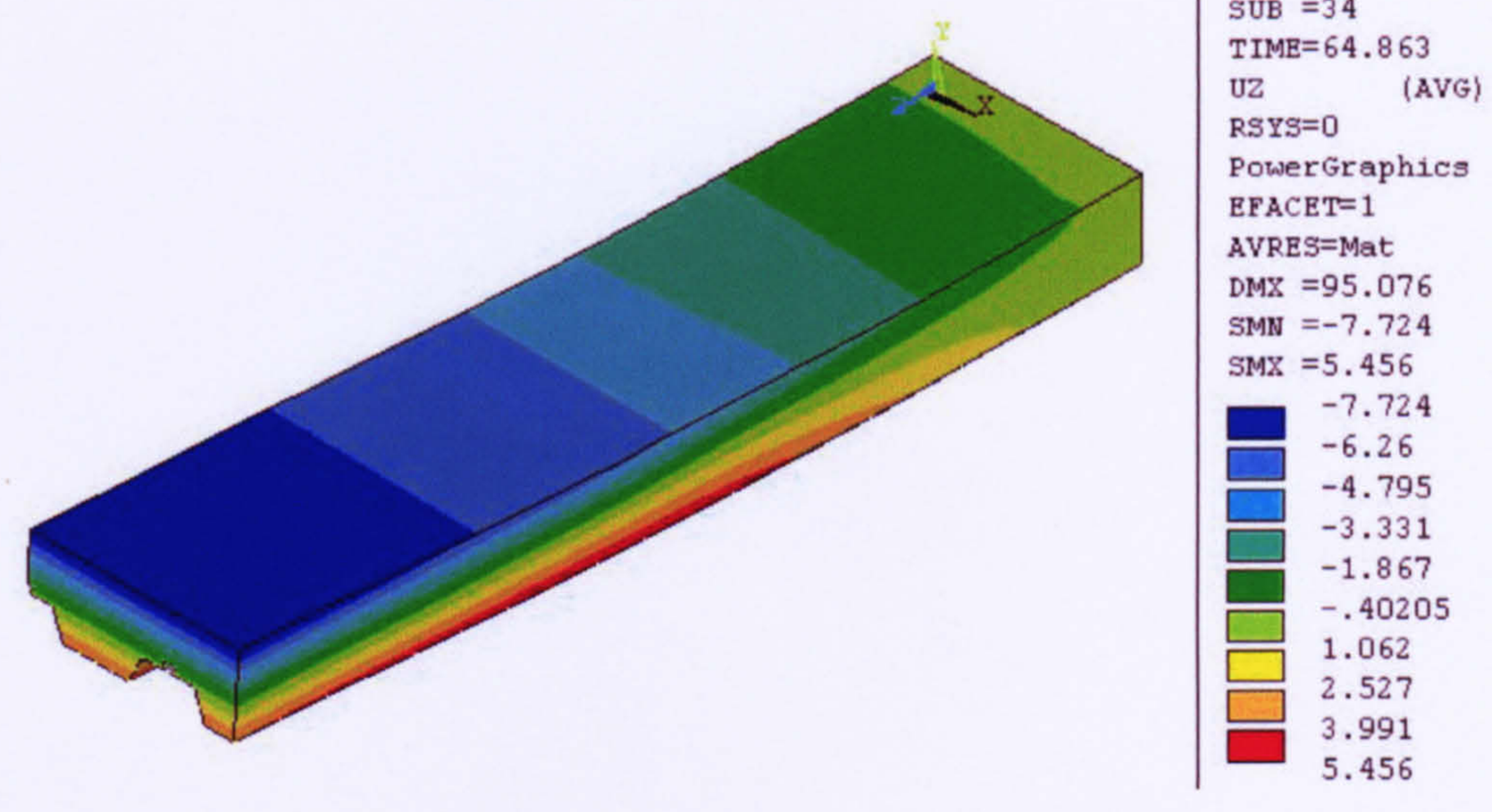

Figure 6.34.d Longitudinal displacement of the composite slab

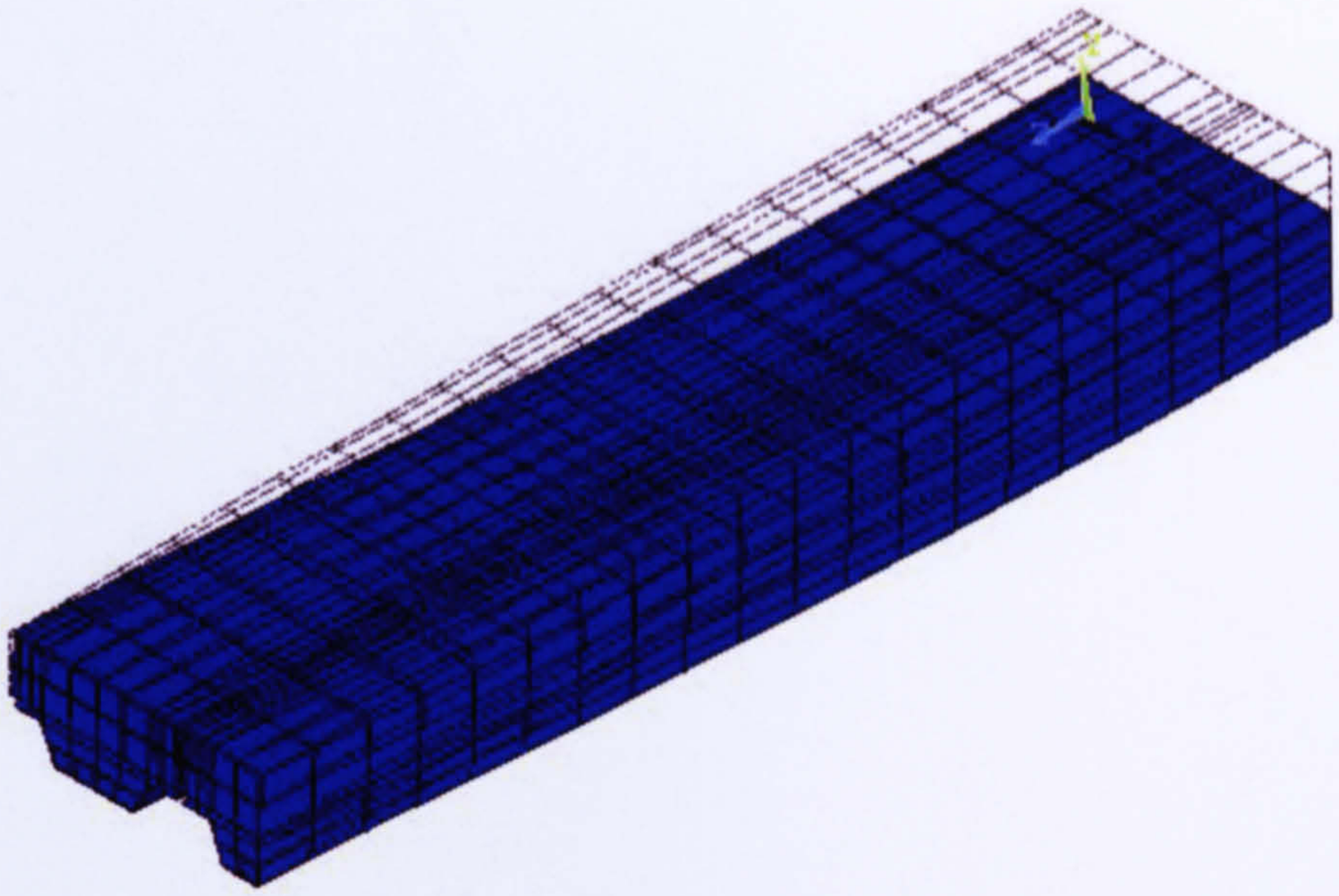

Figure 6.34.e General deformation of composite slab.

Chapter Seven

Finite Element Modelling of Embossment Performance

7.1 Introduction

The behaviour of the profiled steel sheeting/concrete interface is investigated numerically in this chapter. To date, little analytical work has been carried out on shear-bond performance due the complex behaviour at the steel/concrete interface resulting from irregular profile geometry. There is a very wide variation in profiles and embossment types produced by the various manufacturers.

To attempt to increase the capacity and improve the performance of composite slabs, generally the shear-bond resistance needs to be enhanced. Embossments and stiffeners are pressed into most types of profiled steel sheeting for that purpose.

Using the "ANSYS" finite element software programme, a 3-dimensional modelling of embossments is presented in this chapter. The finite element modelling considers the following:

Steel sheet only: studying the effect of varying the aspect ratio, that is the length to width ratio of the plate element, in which the embossment is placed. Studying an incremental number of embossments subjected to horizontal forces applied in the plane of the embossments.

Modelling steel plate element typically a web, or flange with various numbers of embossments.

Concrete and steel sheet: Studying the same aspect ratios and the incremental number of embossments under horizontal forces applied to the concrete face.

7.2 Elements used in modelling

The elements used in the modelling of embossments as shear-connecting devices are ("ANSYS" manual description)[54]:

(a) Finite strain shell element:

The element is suitable for analysing thin to moderately thick shell structures. It is a four-node element with six degrees of freedom at each node; translations in the x, y, and z directions and rotation about the x, y, and z-axes.

It is suited for linear, large rotation, and /or large strain nonlinear applications.

The element is used to represent the profiled steel sheeting and the embossments[57].

(b) 3-D Structural solid element

Used for the three-dimensional modelling of solid structures. The element is defined by eight nodes having three degrees of freedom at each node: translations in the nodal x, y, and z directions.

The element has the capabilities to model plasticity, creep, swelling, stress stiffening, large deflection, and large strains.

The element used to model the concrete material[54].

(c) 3-D Point-to-surface contact element

The element can be used to represent contact and sliding between two surfaces in three dimensions. The element has five nodes with three degrees of freedom at each node: translations in the nodal x, y, and z directions. Contact occurs when the contact node penetrates the target base. Elastic Coulomb friction and rigid Coulomb friction are allowed, where sliding is along the target base.

The element is used to represent the contact and stiffness between the concrete and the profiled steel sheeting[54].

7.3 Material properties

The material properties are required in the modelling of the shear-bond resistance, for profiled steel sheeting, concrete and contact elements. Each material is defined independently, based upon its stress-strain behaviour.

(a) Steel plate element:

Profiled steel sheeting comprises three parts, troughs, webs and flanges. Each part may behave in a different manner due to the pressing of embossments or rolling re-entrant portions or stiffeners. This implies different Young's modules for the different parts. Veljkovic, 1994[41], reported that the pressed embossments reduce the effective yield strength and Young's modulus to about 47% of the original values of the flat sheet. There is however evidence which indicates that work hardening can in fact increase the strength of cold formed sheeting. So, the profiled steel sheeting is modelled with an average value for Young's modulus of different steel sheeting parts obtained from tensile strength tests (Chapter Three).

Young's modulus of the steel = 202777 N/mm^2.

Yield stress of the steel = 354 N/mm^2.

A bilinear Isotropic Hardening (BISO) model was used to model the stress strain curve of the steel material (see section 6.2.3).

Figure 7.1 shows the steel plate geometry.

(b) Concrete:

Figure 7.2 shows the shape and dimensions of the concrete.

The Young's modulus of concrete is calculated as given in BS8110: Part 1, 1985[24], according to the following equation:

$$E_c = 5.5\sqrt{f_{cu}/\gamma_m}$$

Where:

E_c is Young's modulus (kN/mm^2),

f_{cu} is cube strength of concrete (N/mm^2), and

γ_m is partial safety factor.

(γ_m equals 1, in case of comparison with the experimental results).

Young's modulus of concrete = 36482 N/mm^2.

Compressive strength of the concrete = 44 N/mm^2.

Concrete thickness = 15 mm

A Multilinear Isotropic Hardening (MISO) the model was used to model the stress/ strain curve of the concrete material (see section 6.2.3).

7.4 Modelling of steel plate only

7.4.1 General

To study the behaviour of embossments as shear connecting devices, 3-D finite element modelling was used. As a start, 3-D finite element modelling for the sheeting with one embossment only (no concrete) was studied with varying aspect ratios, and secondly a study of the embossments behaviour, when one, two, or three embossments were included in the longitudinal direction.

The aspect ratio is defined as the width of the plate element b divided by the depth of the plate element d. This ratio varied from 2.3 to 6.4 but keeping the embossment depth the same, as shown in Figure 7.3.

After a consideration of various combinations, the boundary conditions were assumed to be fixed along the longitudinal sides of the plate in a steel profile. For example where there may be a line of embossments along the top of a dovetail feature. This would give fixity in the z direction with freedom to rotate in the x-y plane. A more sophisticated study could use a rotational restraint in the x-y plane which would represent the influence of the remainder of the profile adjacent to the top of dovetail. The objective of this study was to investigate the "stiffness" of an embossment(s) in the longitudinal direction, as this property would be important in terms of its ability to transmit longitudinal forces.

7.4.2 Effect of the aspect ratio-single embossment

To model the behaviour of the embossment to resist a longitudinal force, initially one embossment is used. Since the behaviour of the embossment is quite complex and unknown, four different aspect ratios were investigated as shown in Figure 7.3.

Uniform load was applied only on one face of the embossment, and the boundary condition of fixity on the two longitudinal edges was used.

One of the more common cross-sectional shapes of embossments see Figure 7.1, was used. The finite element mesh consists of shell element suitable for analysing thin to moderately thick structures has been used to represent the profiled steel sheet (the embossment) shown in Figure 7.4.a to d.

Figure 7.5.a to d shows the final results of the displacement in z direction (the direction normally associated with slip), and Figure 7.6.a to d represents the final results of the displacement in y direction (vertical deflection). These should be studied along with Figures 7.7 and 7.8, which shows the comparison between load against the deflection, and the horizontal displacement for the four different aspect ratios.

Regarding the horizontal displacement generally, the displacement is a maximum at the loaded edge, which at failure spreads to the free front edge of the plate. As the aspect ratio increases, the maximum displacement spreads from the front to the back edge, which confirms the lower longitudinal stiffness and hence increased flexibility. The shear capacity of the plate also reduced with increased aspect ratios as shown in Figure 7.8.

The pattern for the vertical displacement shows that for the front plates there is an upward displacement, which is maximum at the free front edge, which increases with aspect ratio. The upward displacement probably results from the application of the load at the top of the embossment, which may not represent behaviour in practice, where the load is more evenly applied through the concrete over the entire interface. The load deflection graphs, in Figure 7.7 confirm the behaviour for horizontal displacement, which shows a significant reduction in capacity as the aspect ratio increases. This confirms the intuitive conclusion that embossments are most effective in the stiffer regions of the profile where the plate widths are smallest.

7.4.3 Behaviour of several embossments under horizontal load

To study the effect of horizontal load on several embossments, three models have been studied as shown in Figure 7.9.a to c, the first with one, the second with two,

and the third with three embossments. The finite element mesh for the model was similar to that in the previous model (in section 7.4.1) with the same boundary condition, and same height and elements (geometric properties).

The load was applied to all the embossments on the 'front' face of each of them.

The finite element mesh for the profiled steel sheeting with the same boundary condition as previously used, and the applied load on the one face of embossments are shown in Figure 7.9.a to c.

Figure 7.10.a to c shows the final results of the displacement in y direction (deflection direction), and Figure 7.11.a to c shows the final results of the displacement in z direction (longitudinal direction). Figure 7.12.a to c shows the principal stresses of the steel plate.

The vertical deflection, Figure 7.10 a to d, confirm the upward movement with a maximum at the front edge although the movements are lower for the embossments after the first. This suggests a more uniform behaviour in a continuous line of embossments. The longitudinal displacement, Figure 7.11 a to c, shows an even distribution of maximum movement which does not mirror the vertical displacement effect. The stress patterns indicate yield at the front face of the embossment together yield within the general field but these are at failure. Yield did initiate at the front face of the embossments at lower load levels.

The graphs, Figure 7.13, 7.14, indicate that for the load up to yield the capacities are approximately proportional to the number of embossments. For the loading up to failure, there appears to be a slight increase in capacities/embossment with the number of embossments.

7.5 Modelling concrete with steel sheet and embossments

7.5.1 General

A 3-D finite element model, for a one, two and, three embossments, with four different plate elements was again modelled to study the effect of aspect ratio and number of embossments.

All models have the same boundary conditions, same geometry and material properties.

In all cases concrete was modelled using 3-D structural solid elements, for steel embossment the finite strain shell element used, with point-to-surface element acting between the steel plate and the concrete.

7.5.2 Effect of the aspect ratio of the embossments

Four models with the same sheeting dimensions of section 7.4.2, and same material properties have been used, with a normal weight concrete layer 15 mm thick placed on top of the sheet. Figure 7.15.a to d shows the finite element modelling, with the boundary conditions and the horizontal load applied to one face of the concrete at the top level of the embossment. Figure 7.16.a to d shows the finite element modelling of the steel plate, with two edges fixed, and the other edges free. The results for vertical deflection are shown in Figure 7.17.a to d for each model, and in figure 7.21.a comparison is made between the applied load and the deflection for the four models. In all the models there appeared to be downward deflection at the front edge and upward displacement at the back edge. The graphs display similar movements with only models with the largest aspect ratios, c and d, displaying a well defined transition from linear behaviours.

The results for longitudinal displacement are shown in Figure 7.18.a to d together with the comparison in Figure 7.22. Here the graph indicates clearly that the load capacity decreases with increasing aspect ratio. The individual model results and the graph indicate that the longitudinal displacements increase with increasing aspect ratios.

The stresses (tensile stresses positive, compressive stresses negative) in the concrete at two load levels and in the steel plate are shown in Figures 7.19.a to d and Figures 7.20.a to h. Generally they display compressive stresses along the back edge. The influence of the embossment is to increase the compressive stresses immediately in front of the embossment, the effect being more significant for the lowest aspect ratio. The tensile stresses in the concrete close to the edge of the embossment are

consistent with damage to concrete at these portions where composite slab test samples are examined after failure. The steel plate stresses are generally at a maximum on the front and rear edge of embossment and also at the points of the support for the plate with the highest aspect ratio. Figure 7.17.a to d shows the final results of the displacement in y direction (deflection).

Figure 7.18.a to d shows the final results of the displacements in z direction (longitudinal displacement). Figure 7.19.a to d represents the stresses in the concrete when the model approaching the yield, and Figure 7.20.a to h represents the stresses of the concrete facing the embossment.

Figure 7.21 and Figure 7. 22 show the comparison between the applied load with the deflection and the longitudinal displacement. The longitudinal displacement/load graph indicates that the load capacities decreases as the aspect ratio increases.

7.5.3 Behaviour of several embossments under horizontal load

A 3-D finite element model was created, for three different cases, with one, two, or three embossments combined with concrete on the top. Figure 7.23.a to c shows the finite element meshes for the model with the boundary condition. The uniform horizontal load applied to the concrete at the same level as the embossments is shown in Figure 7.23.a to c. Figure 7.24.a to c shows the finite element mesh for the three models, first with one embossment, second with two, and the third with three embossments for the profiled steel sheeting. Similar material properties and elements have been used.

Figure 7.25.a to c shows the deflection in the y direction, and Figure 7.26.a to c shows the displacements in the z direction.

In Figure 7.27.a to c shows the principal stresses on the steel plate only when the load approaches the yield point, and figure 7.28.a to c shows the principal stresses in the concrete when the load approached yield.

Figure 7.29.a to c, and Figure 7.30.a to c shows the final principal stresses for the steel plate, and the concrete.

Figure 7.31, and Figure 7.32 shows the comparison between the applied load with the deflection, and displacement. Figure 7.31 indicates that the number of

embossments does not significantly affect the vertical stiffness. Figure 7.32 shows a variation in behaviour with the one embossment, which exhibited the lowest capacity.

7.5.4 Effect of uniform load distribution

Two alternative 3-D finite element models were created of one embossment (comprising profiled steel/concrete). For the first, uniform load was applied as a level with the top of the embossment, and for the second, the uniform load was applied to the whole area of the concrete. Figure 7.33.a and b show the finite elements mesh of the model with the uniform distribution force, and the boundary conditions.

Similar elements have been used to model the small composite models, for the concrete, the solid element, for the steel embossment, the finite strain shell element, and 3-D Point-to-Surface contact element for the interface between the materials.

Figure 7.34.a and b shows the displacements in y direction (deflection), and Figure 7.35.a and b shows the displacements in z direction longitudinal displacement.

In Figure 7.36.a to b shows the principal stresses on the profiled steel sheeting only when the load approaching the yield point, and Figure 7.37.a to b shows the total stresses for the concrete only at the same time when the load approached the yield point.

The vertical deflection (Figure 7.34a) shows a variation from the behaviour of the steel sheet alone in that there is a combination of upward and downward movements.

The slip between the concrete and steel is shown in Figures 7.35a and, 7.35b. Larger slip values occur away from the embossment.

The longitudinal stresses in Figures 7.36a to 7.37.b confirm the type of damage to concrete and sheet, which was observed when the failed slabs are inspected. The concrete is generally crushed near the centre of embossment. Likewise the steel stresses at the top of the embossment have also reached their maximum value.

7.6 Conclusions and future work

In the chapter it has been possible to study the behaviour of a typical embossment(s) in various forms. The effect of varying the aspect ratio has been demonstrated, when combined with the slip and stress behaviour of a concrete layer.

Finite element modelling was used to study the behaviour of embossments as shear-connecting devices. Steel plate element only, and steel plate element and concrete were modelled. Since the behaviour of the steel/concrete interface and the profiled steel sheeting itself are quite complex, further boundary conditions should be studied. The steel sheeting thickness should be varied for the profiled steel sheeting and embossments because this can have a significant effect on the embossment as shear-connecting devices.

In the study of steel sheet only, the comparison between one, two, and three embossments indicates no significant difference in overall behaviour with the capacities being a function of the number of embossments. Future studies of embossment shape, spacing and edge boundary conditions should therefore be sufficiently covered with one embossment.

It is interesting; also, to note that similar failure loads were recorded for each of the load cases studied (ie. (i) Load distributed over the entire area and (ii) a concentrated load at the embossment level).

Due to the capacity required for modelling large models and the increased running time only one concrete thickness was considered (15mm) therefore it is suggested a range of thicknesses should be studied in order to determine the significance of the effect of concrete thickness on behaviour.

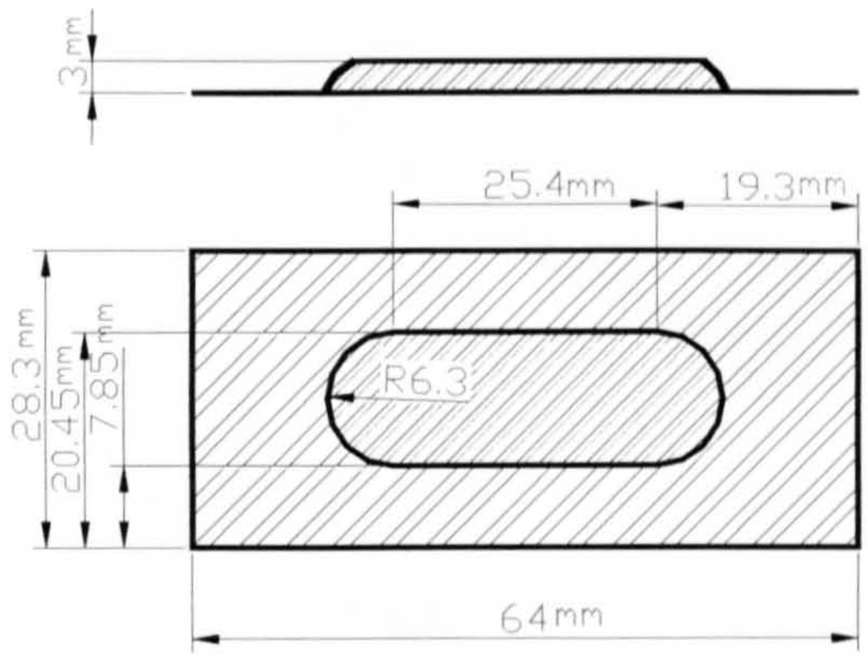

Figure 7.1 Profiled steel sheet dimensions.

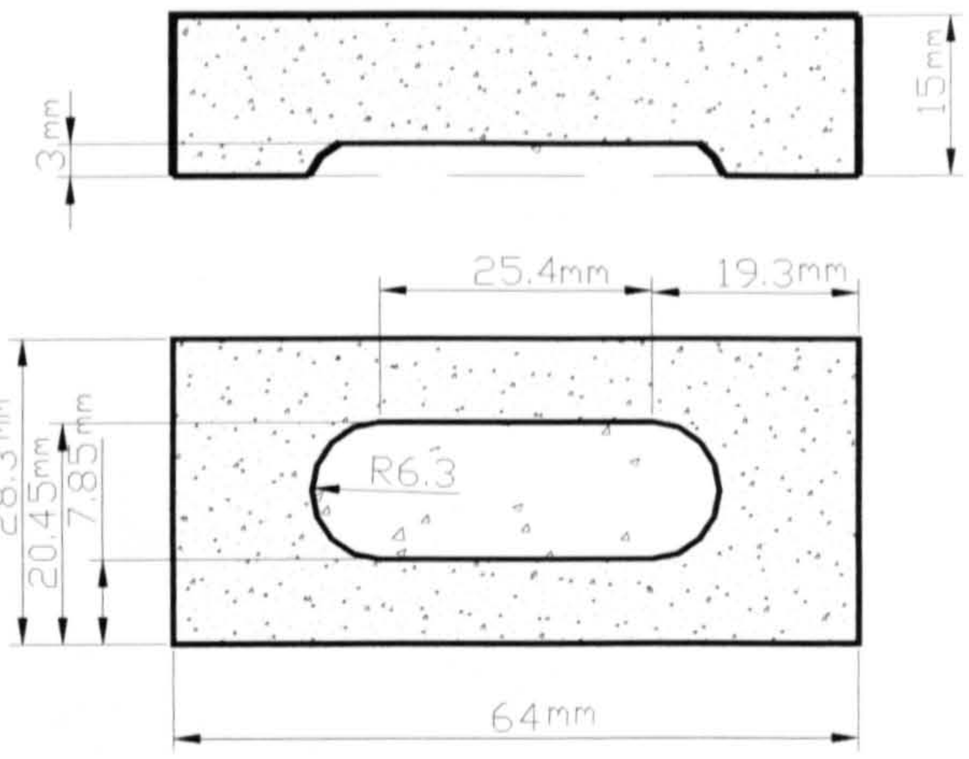

Figure 7.2 Concrete layer dimensions.

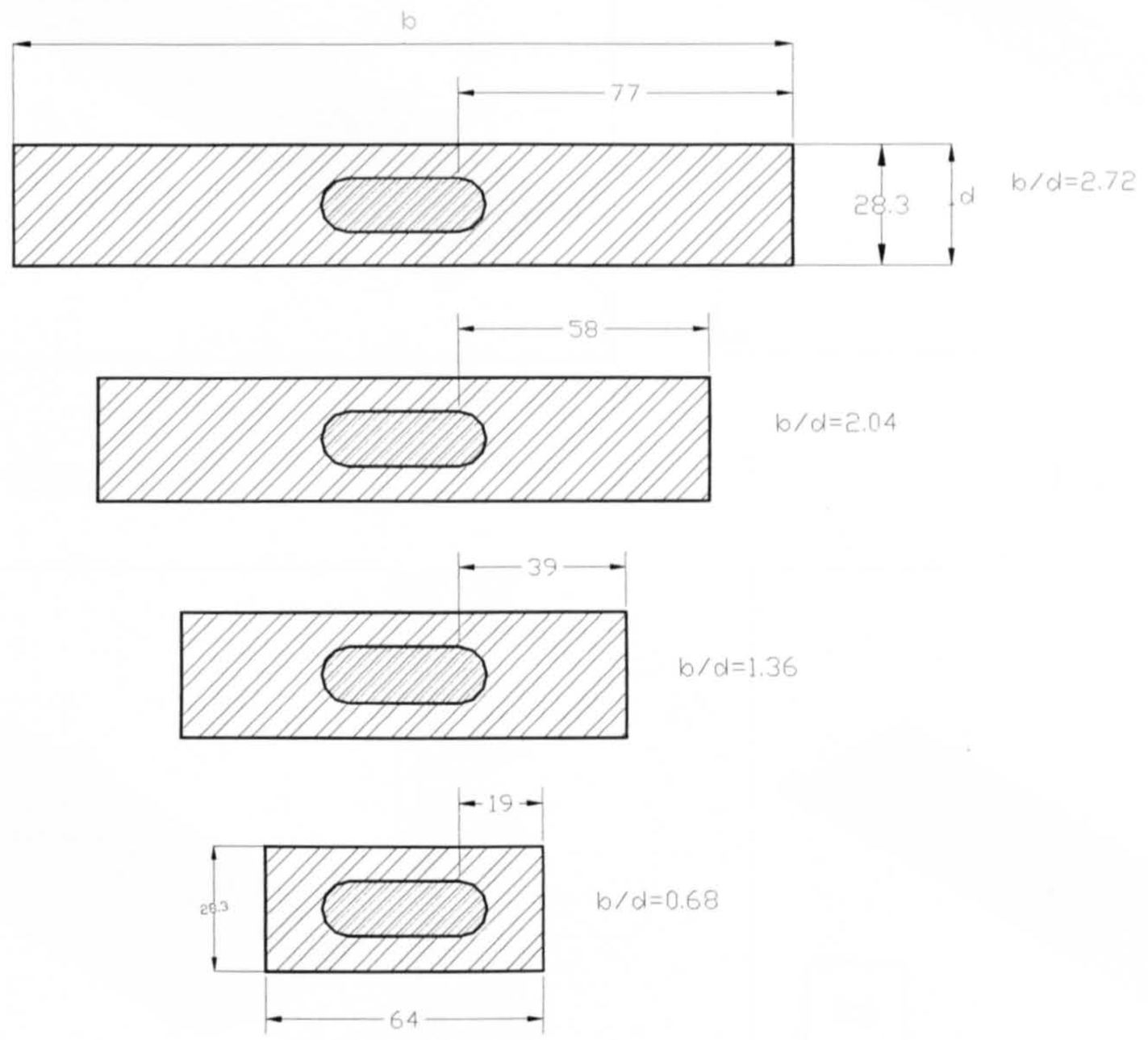

Figure 7.3 Definition of aspect ratio (b/d) for embossment modelling.

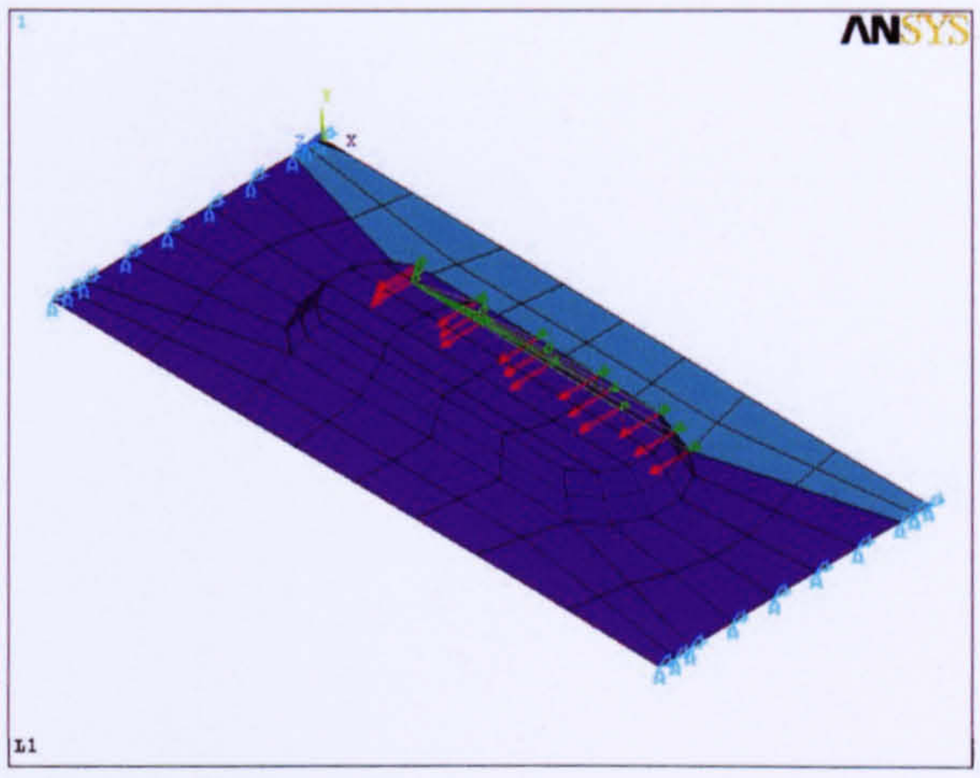

Figure 7.4.a

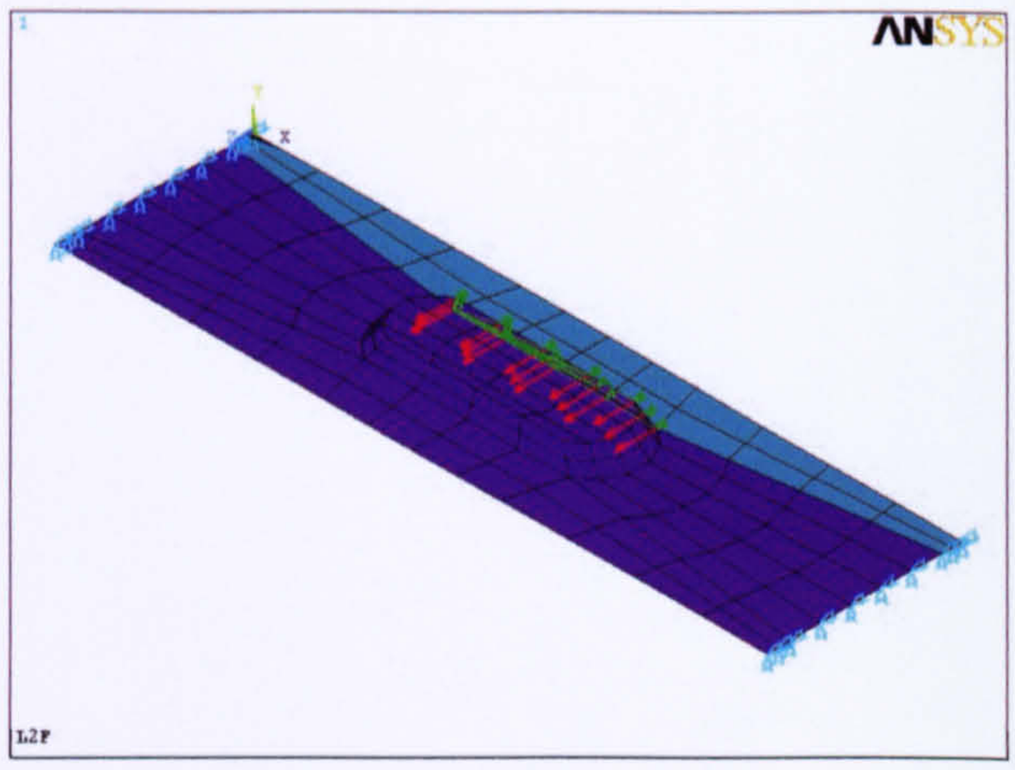

Figure 7.4.b

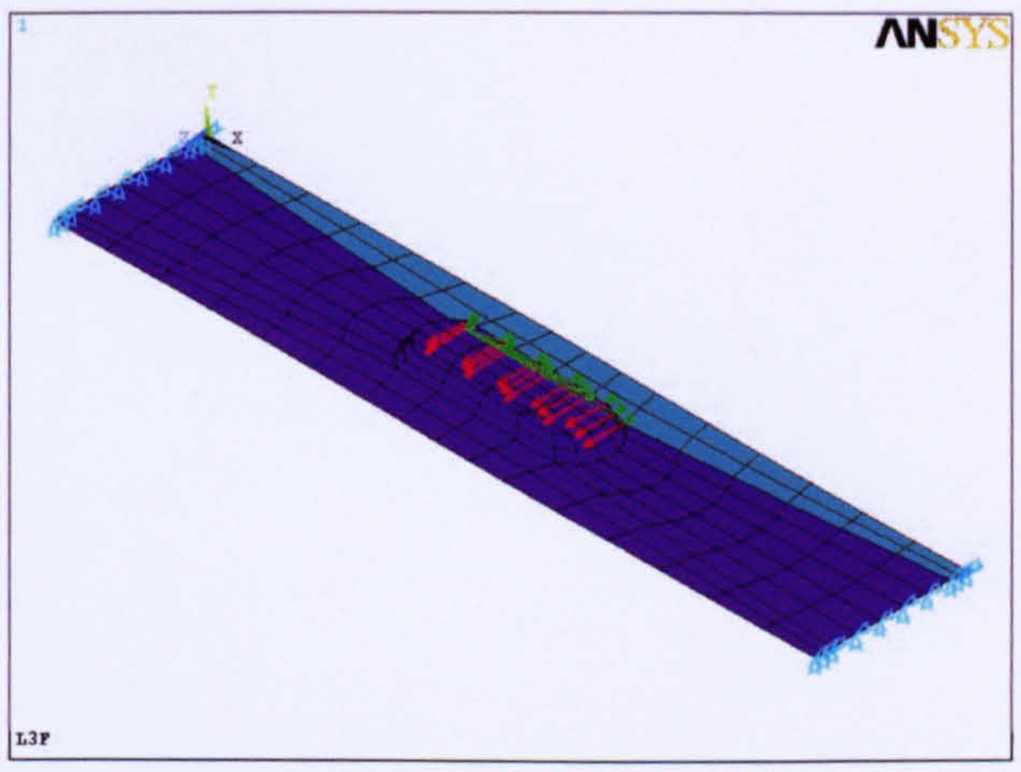

Figure 7.4.c

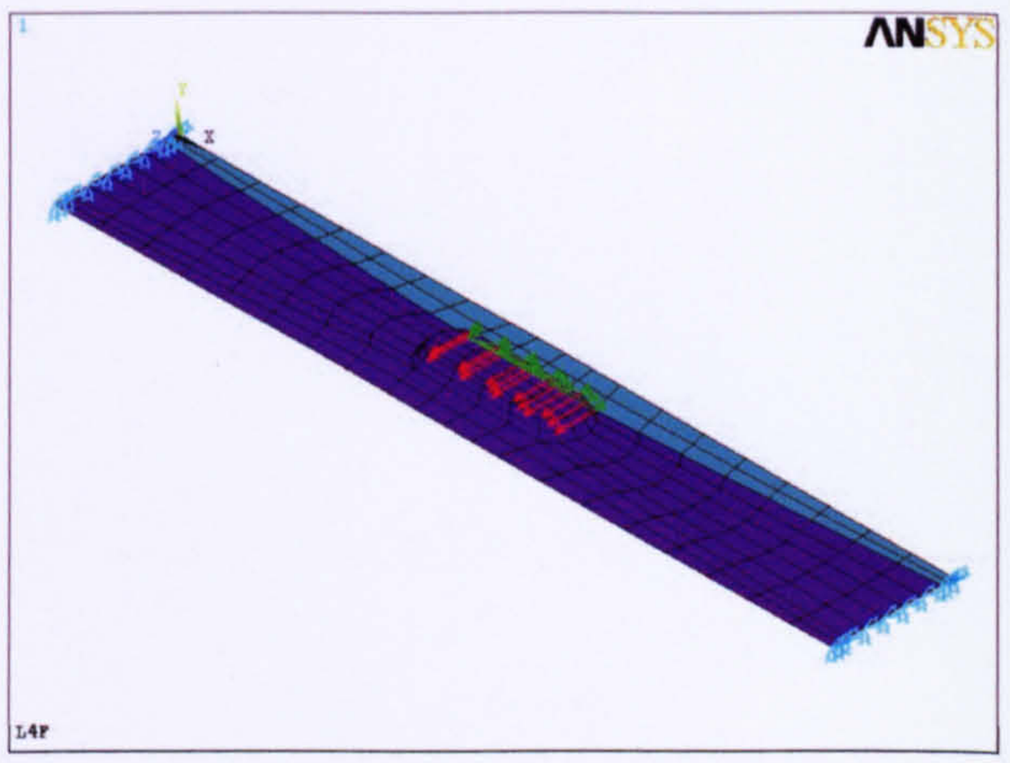

Figure 7.4.d

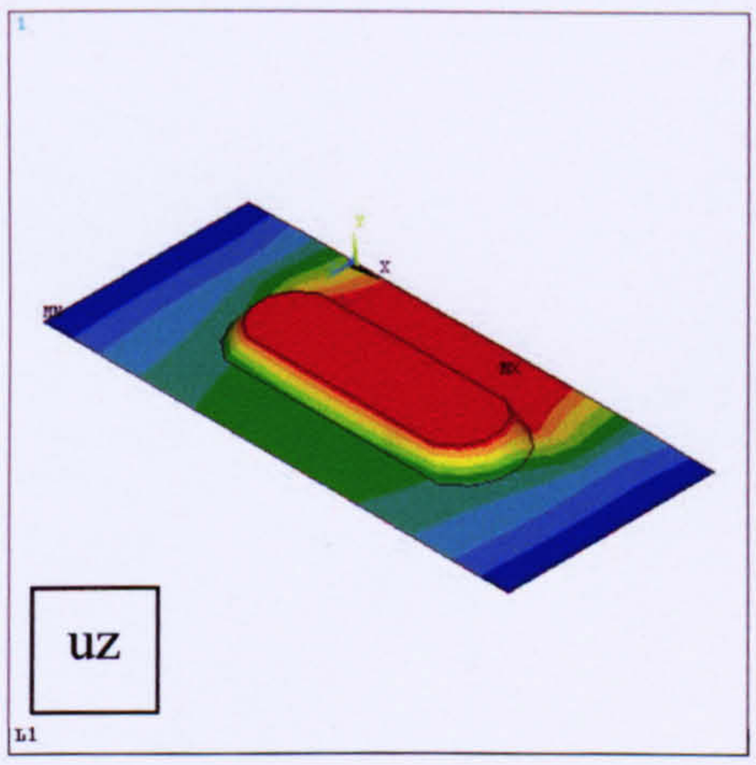

Figure 7.5.a

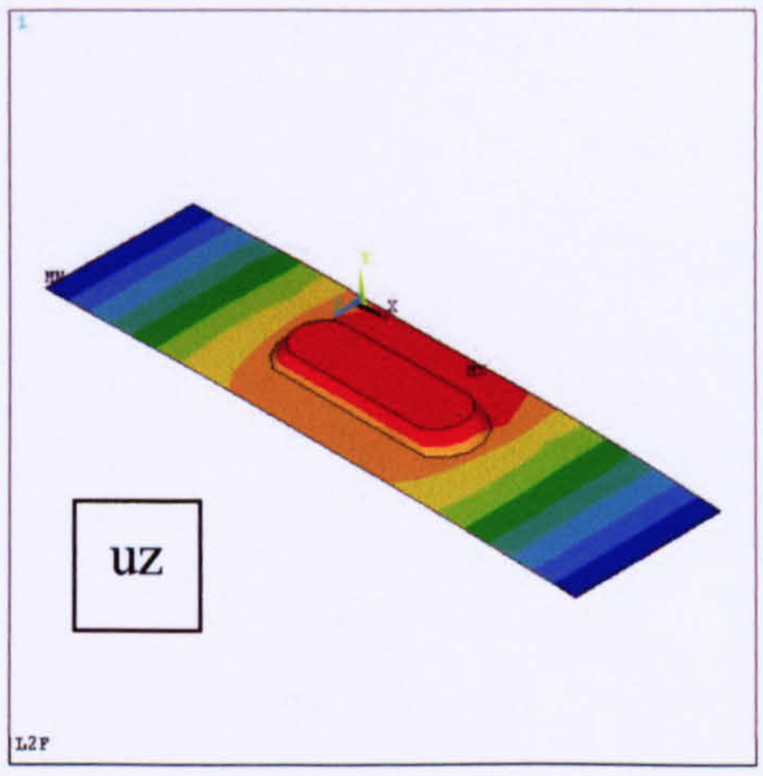

Figure 7.5.b

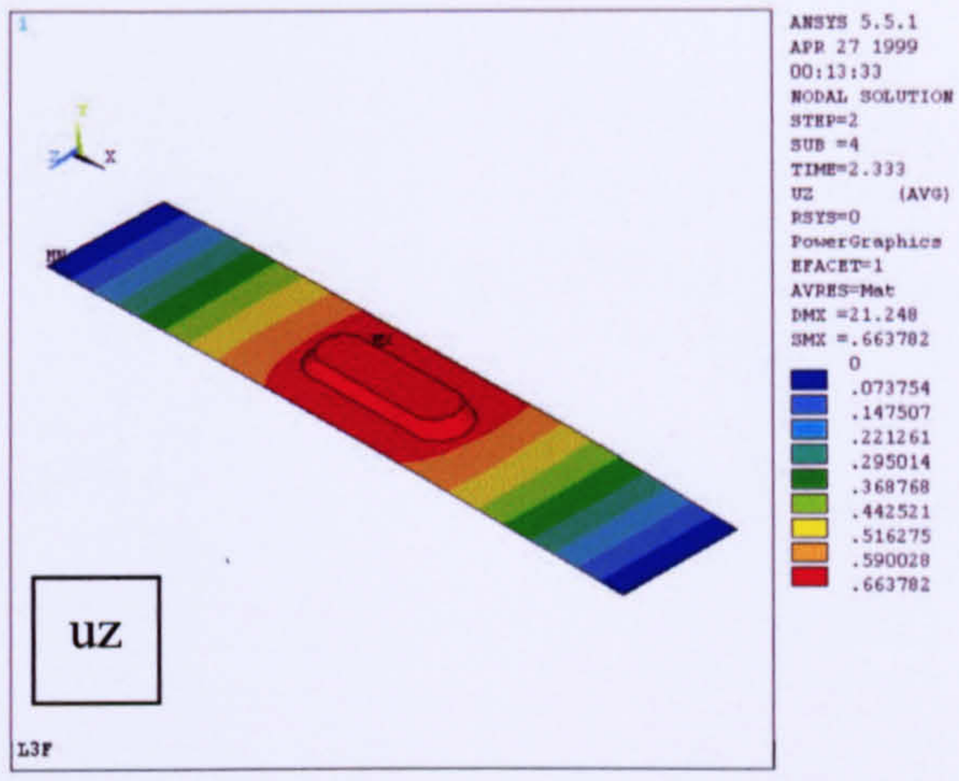

Figure 7.5.c

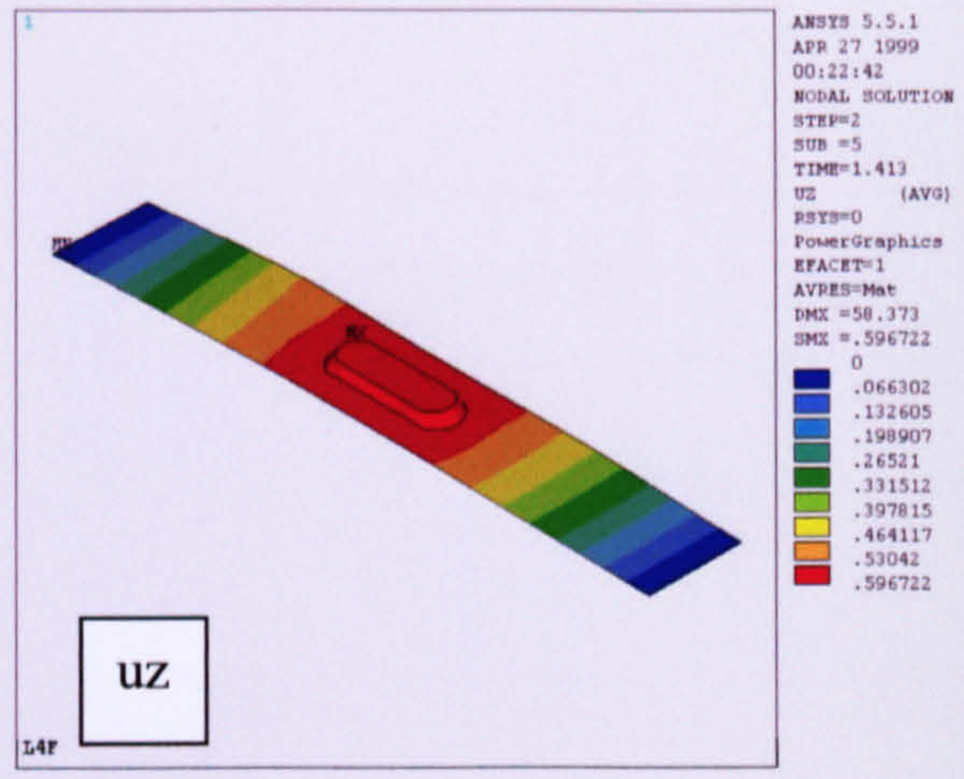

Figure 7.5.d

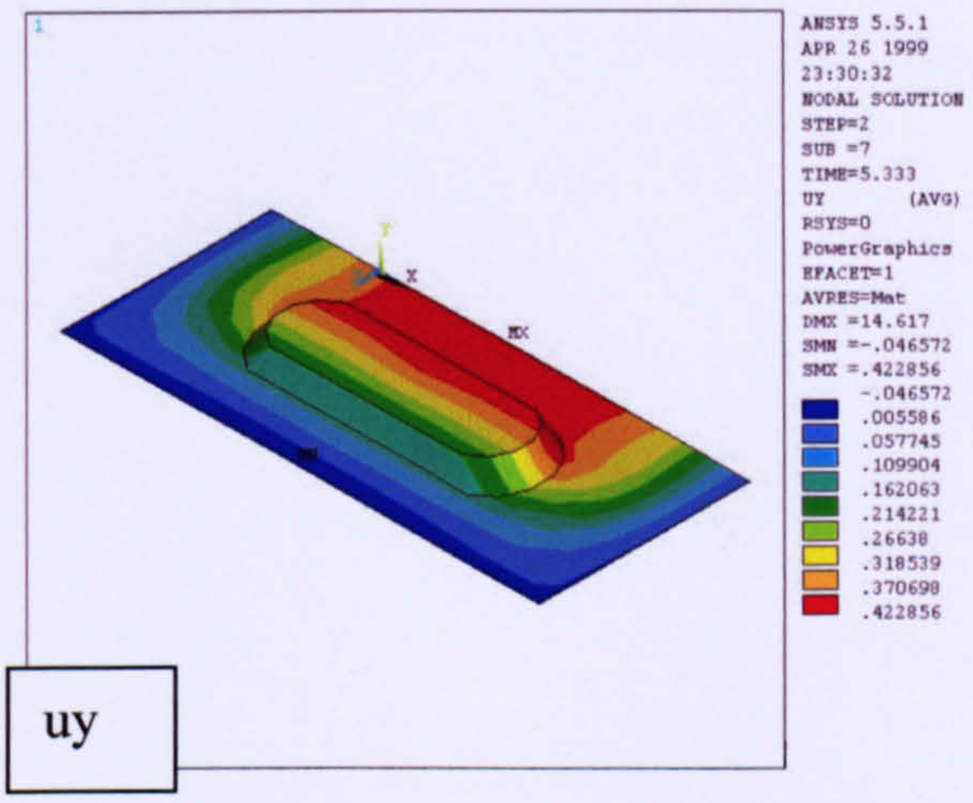

Figure 7.6.a

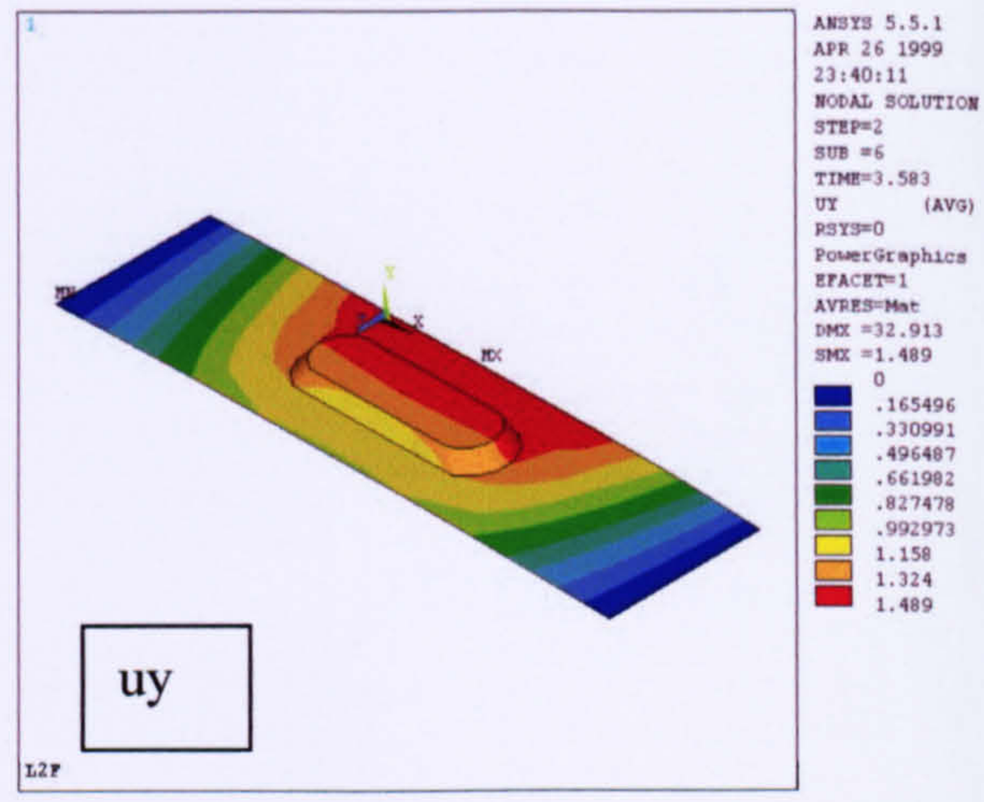

Figure 7.6.b

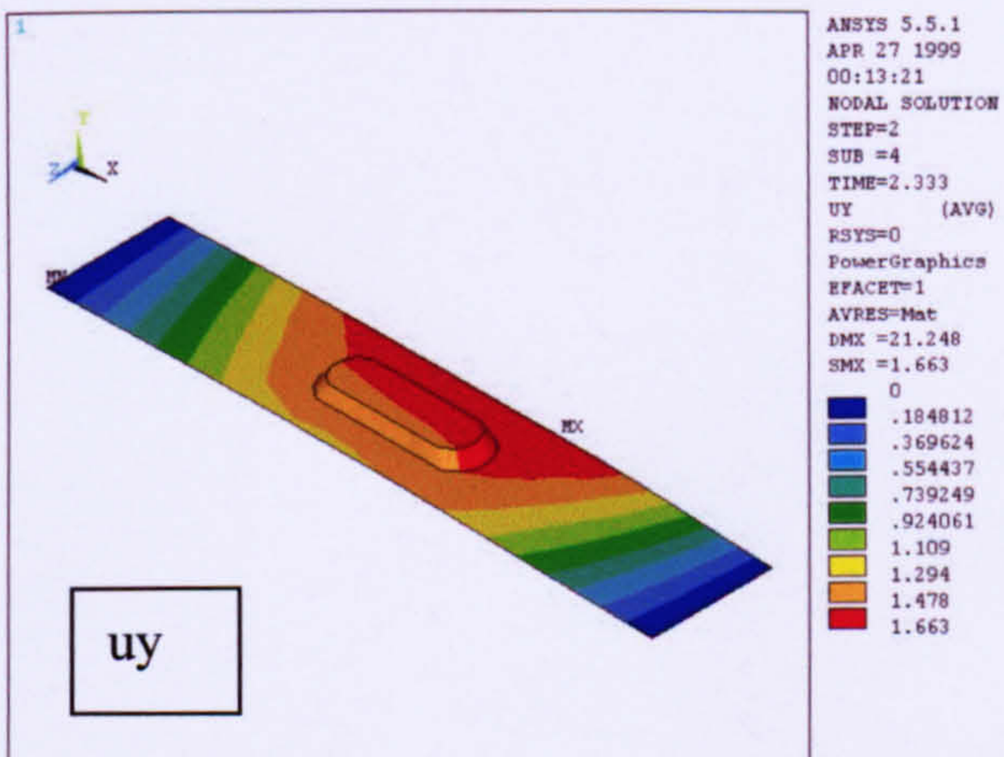

Figure 7.6.c

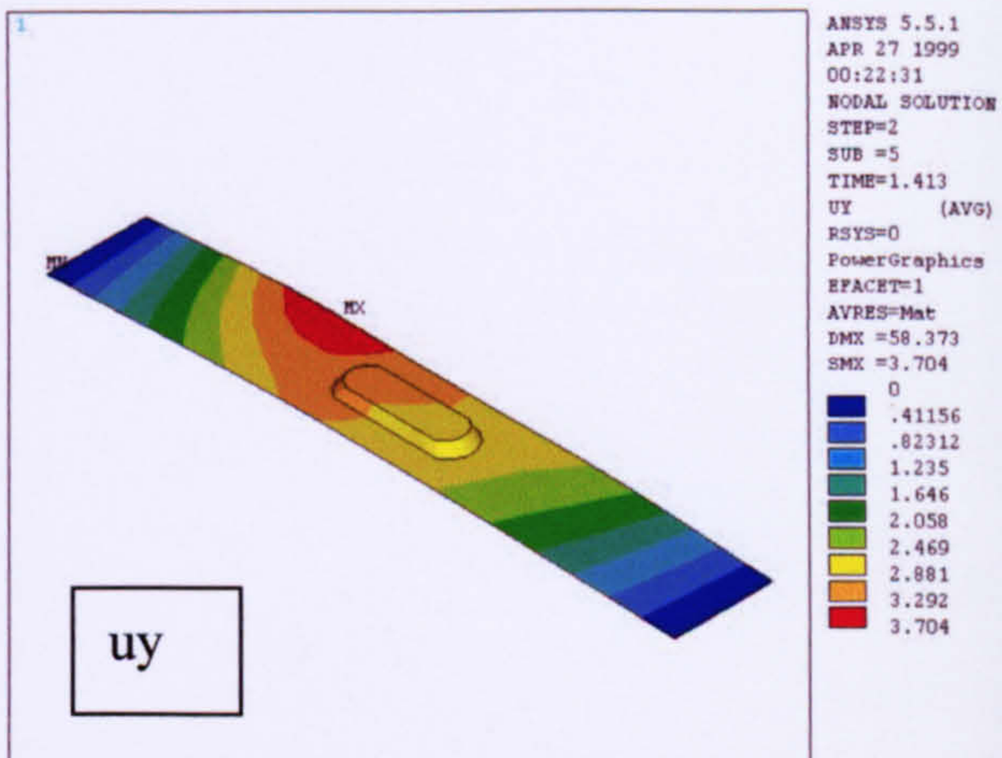

Figure 7.6.d

Figure 7.7 Comparison of applied load versus deflection for various aspect ratios.

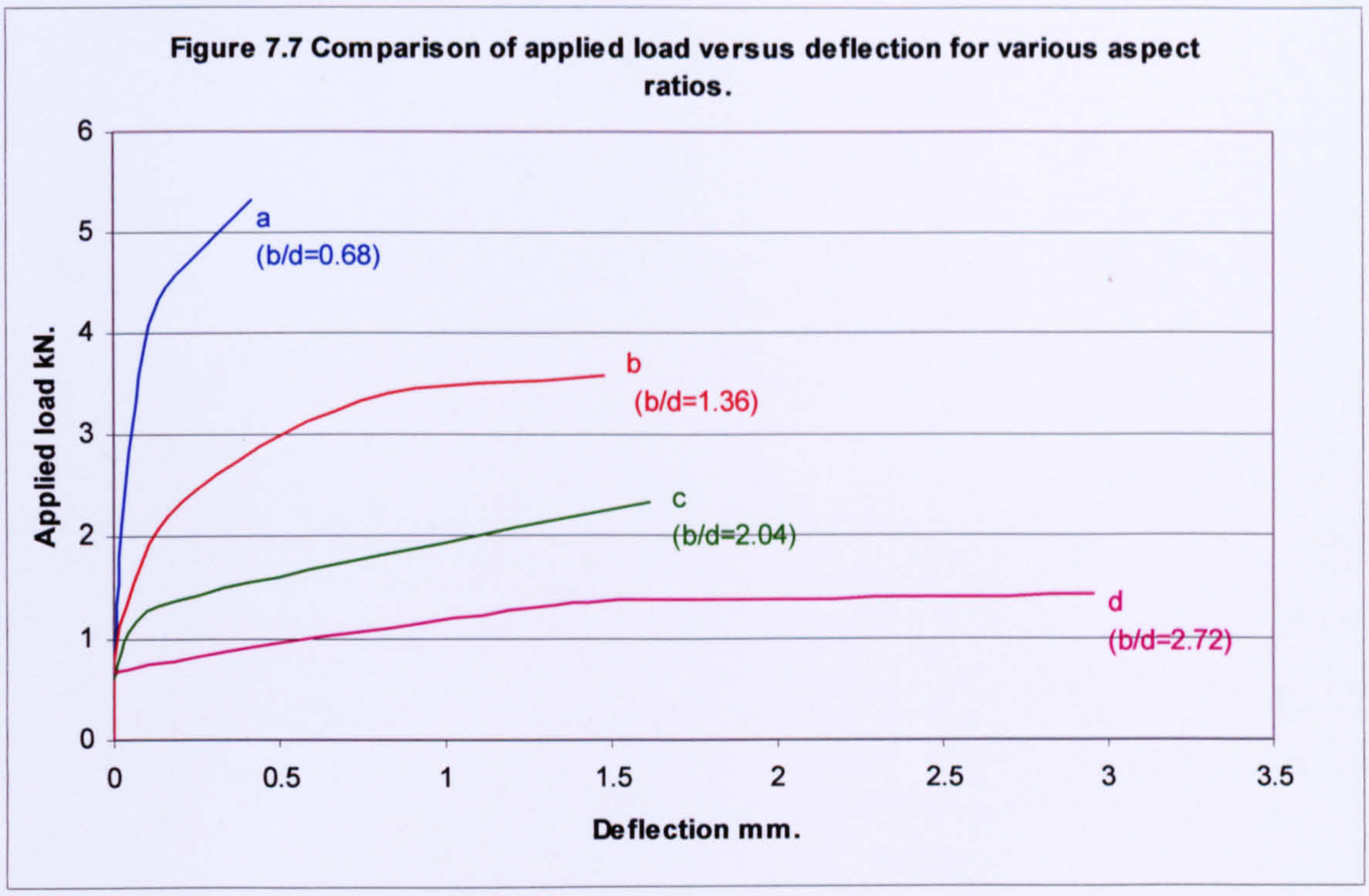

Figure 7.8 Comparison of applied load versus longitudinal displacement various aspect ratios.

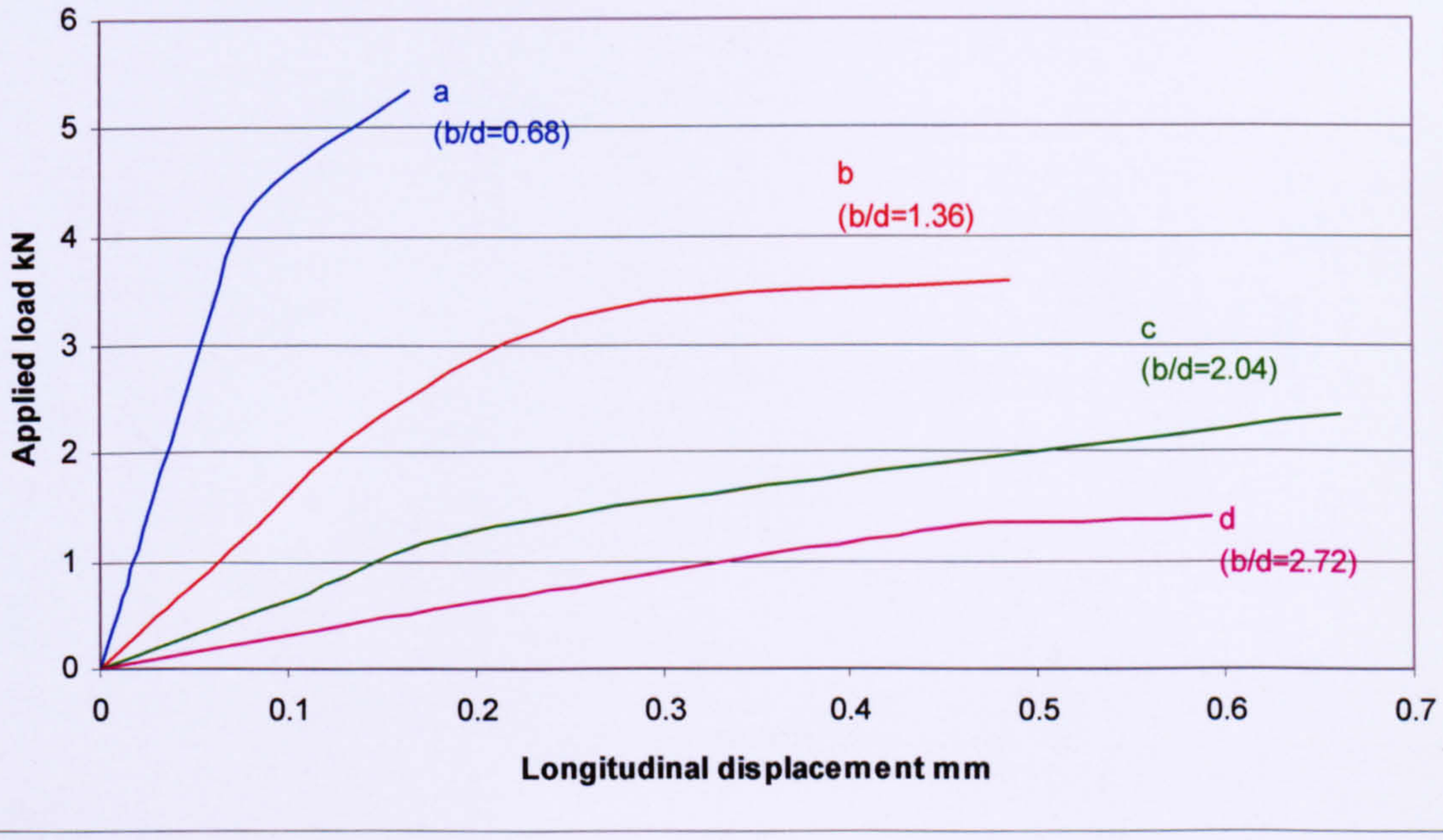

MISSING

PRINT

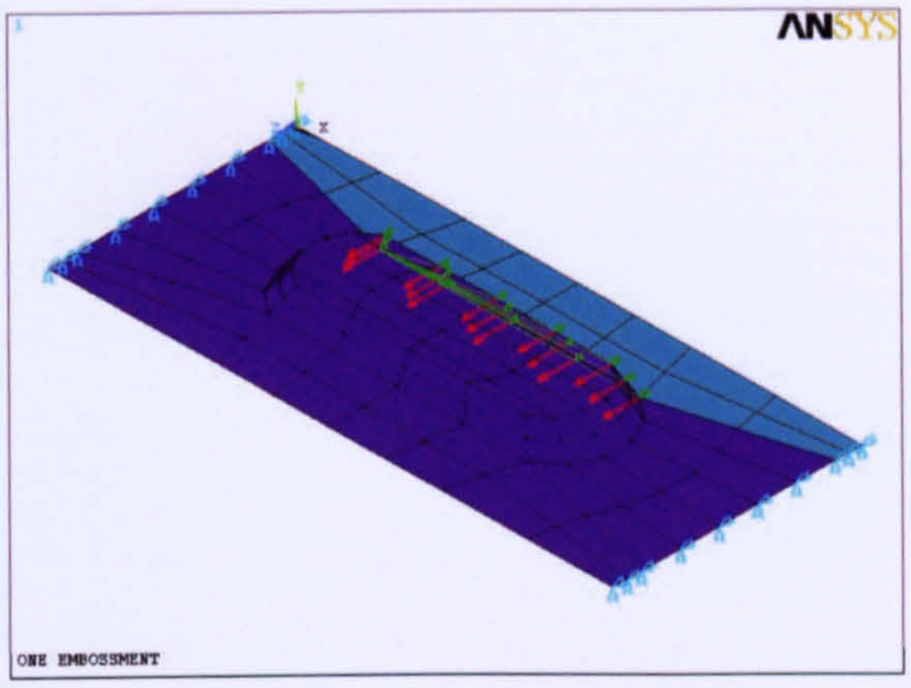

Figure 7.9.a

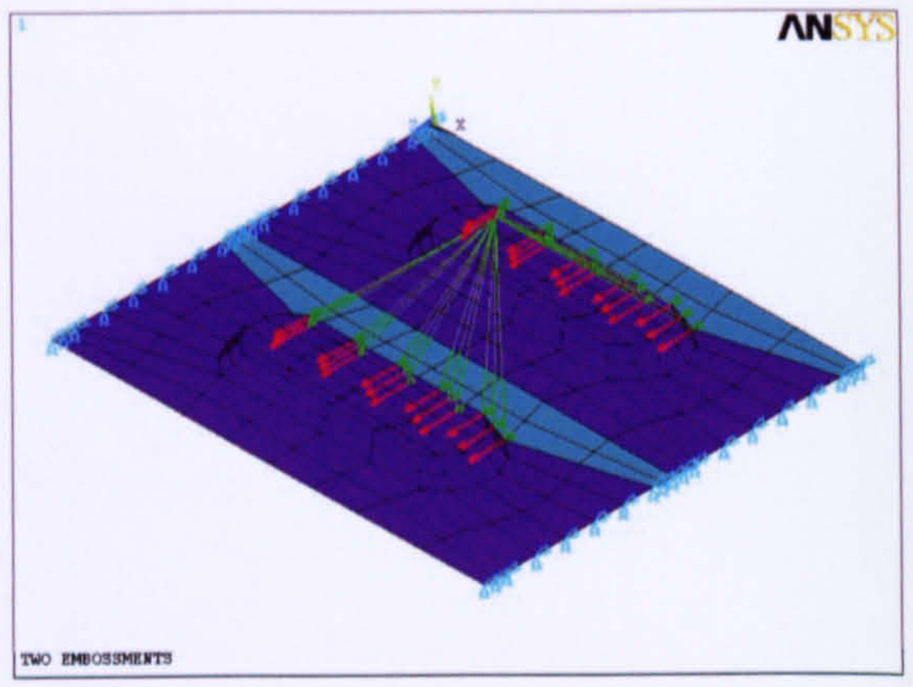

Figure 7.9.b

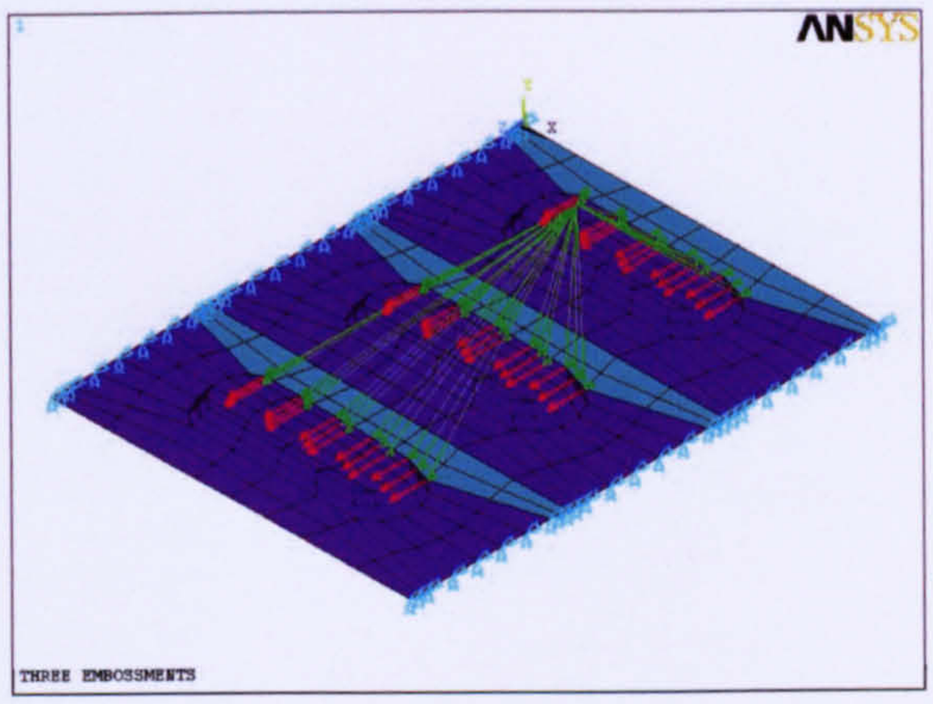

Figure 7.9.d

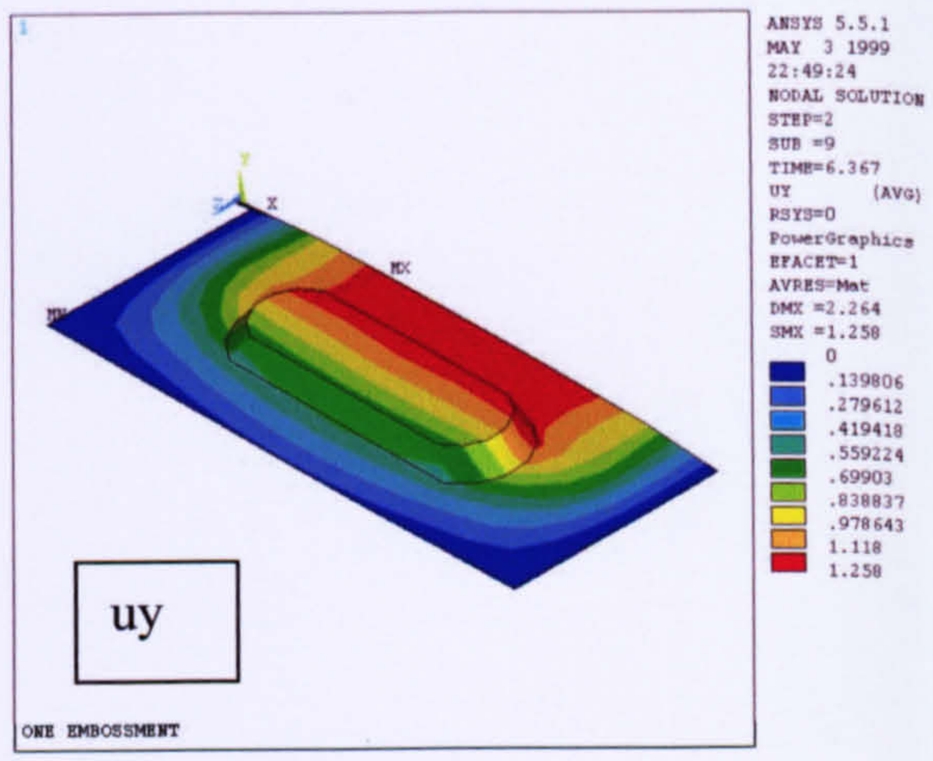

Figure 7.10.a

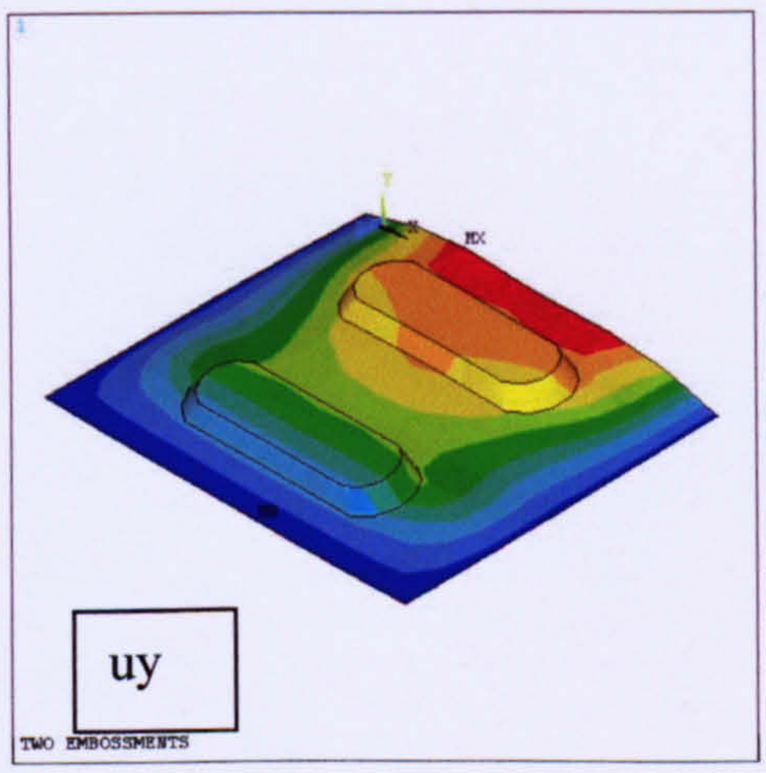

Figure 7.10.b

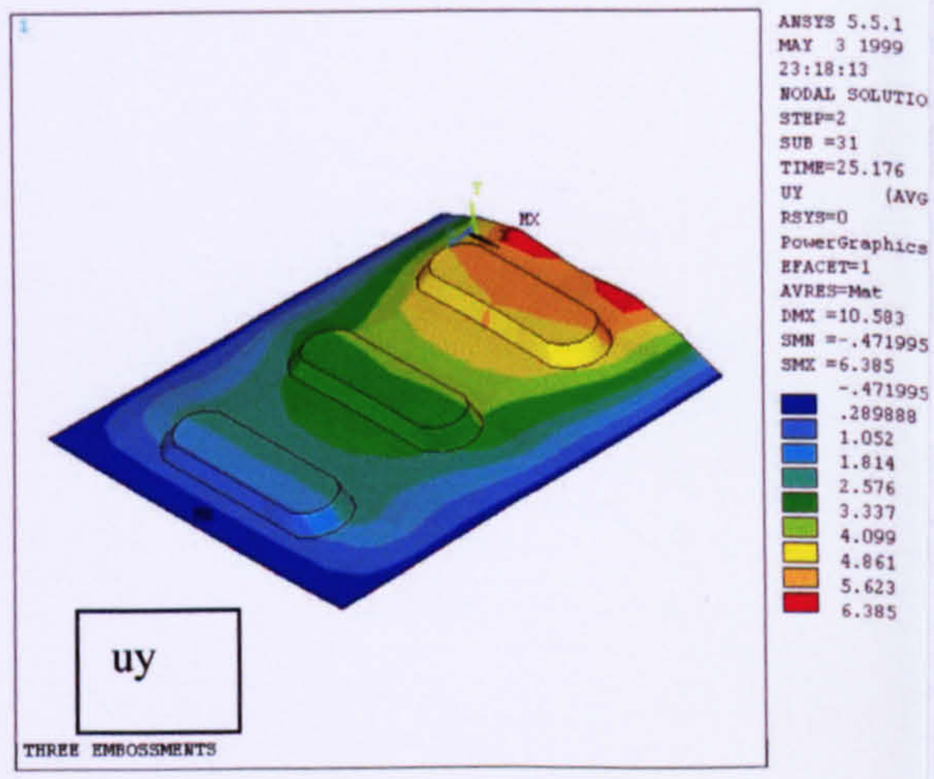

Figure 7.10.d

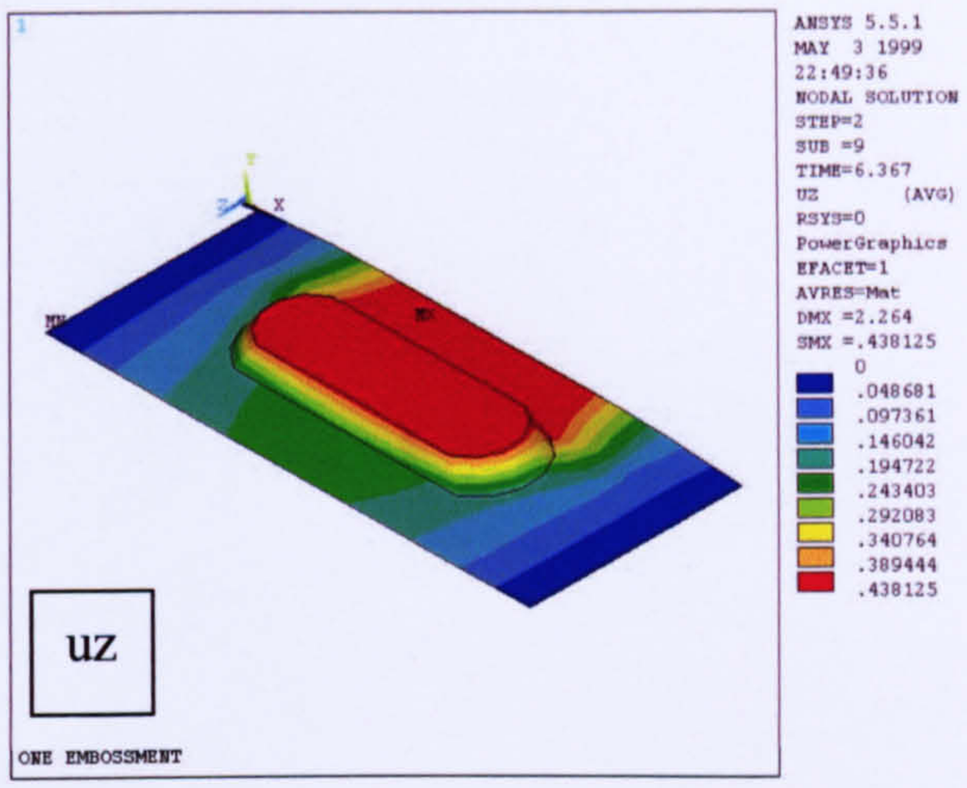

Figure 7.11.a

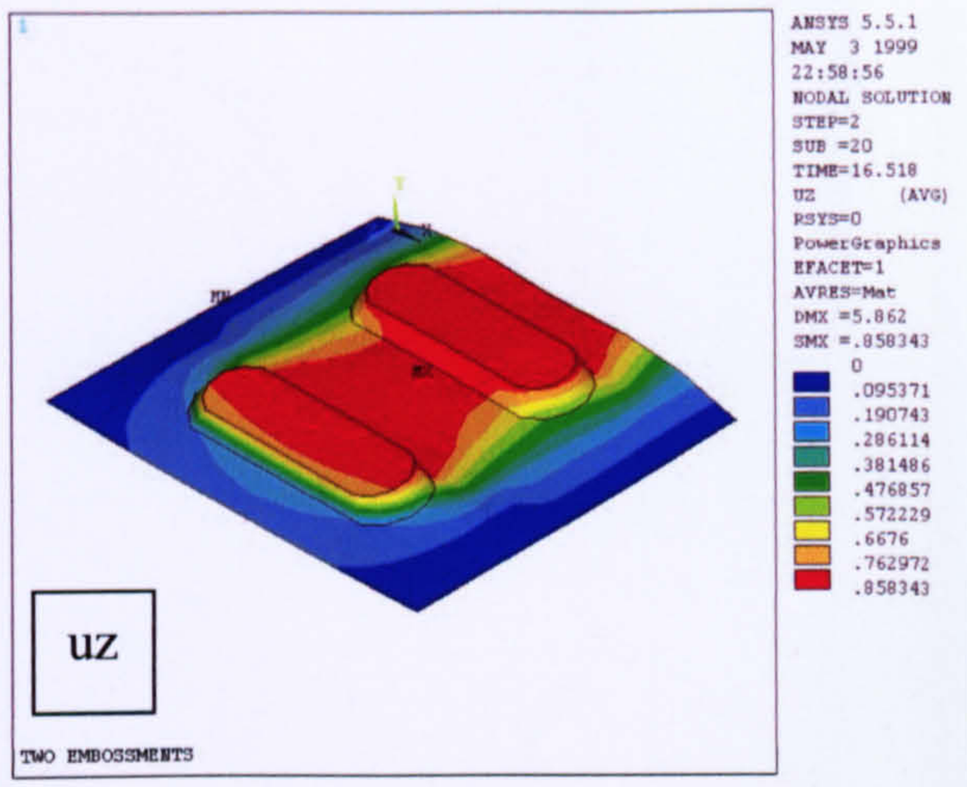

Figure 7.11.b

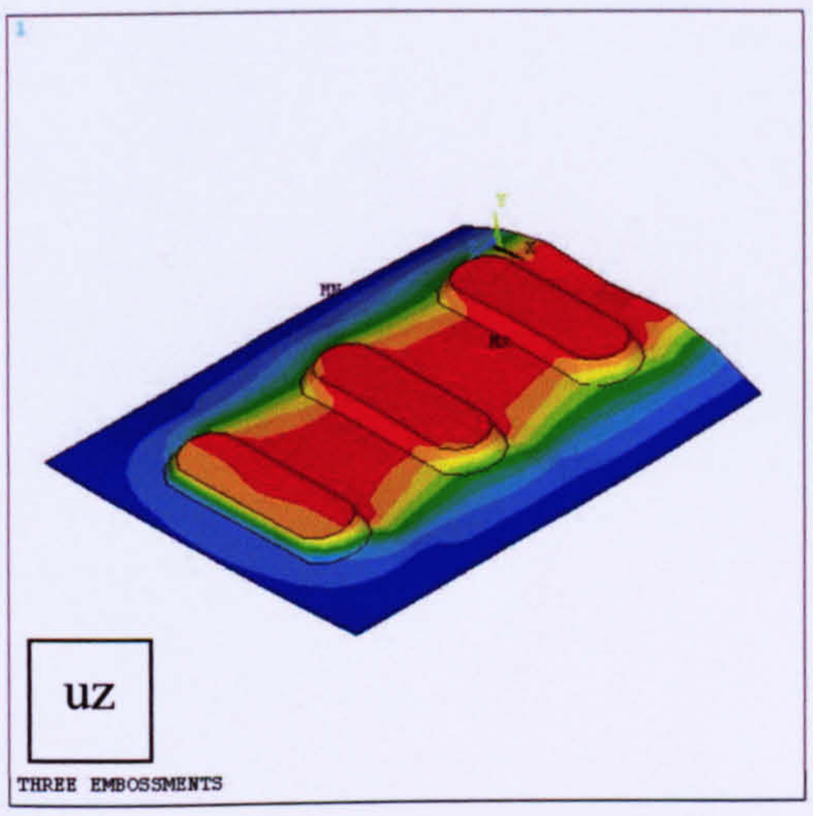

Figure 7.11.c

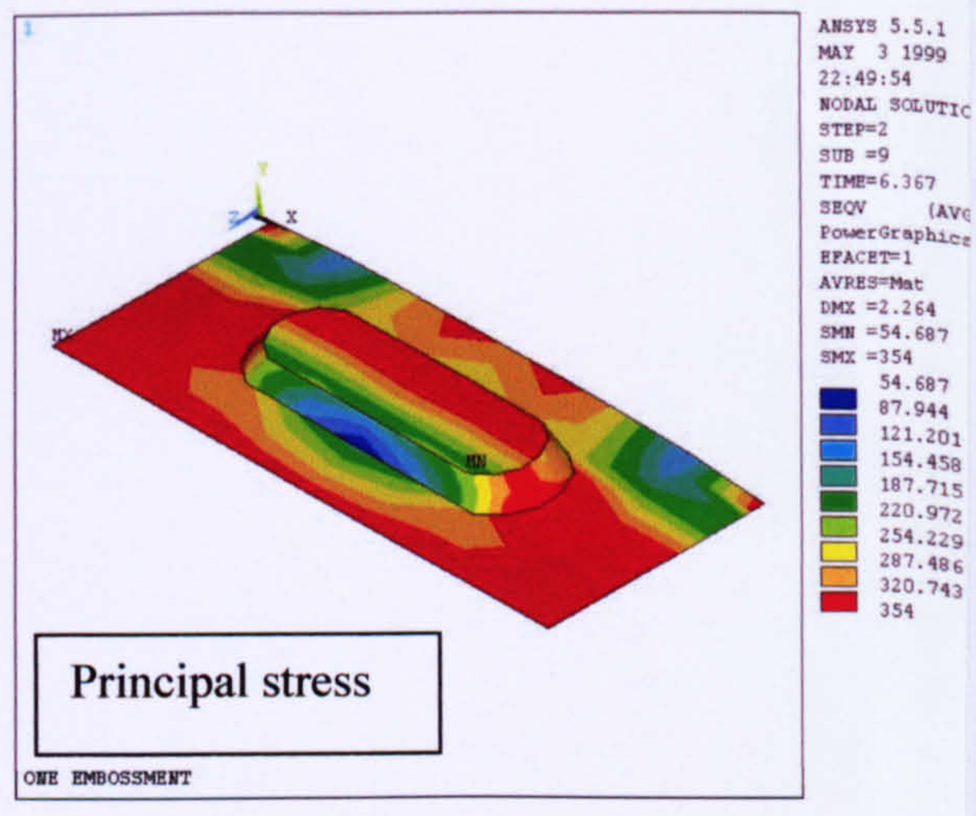

Figure 7.11.d

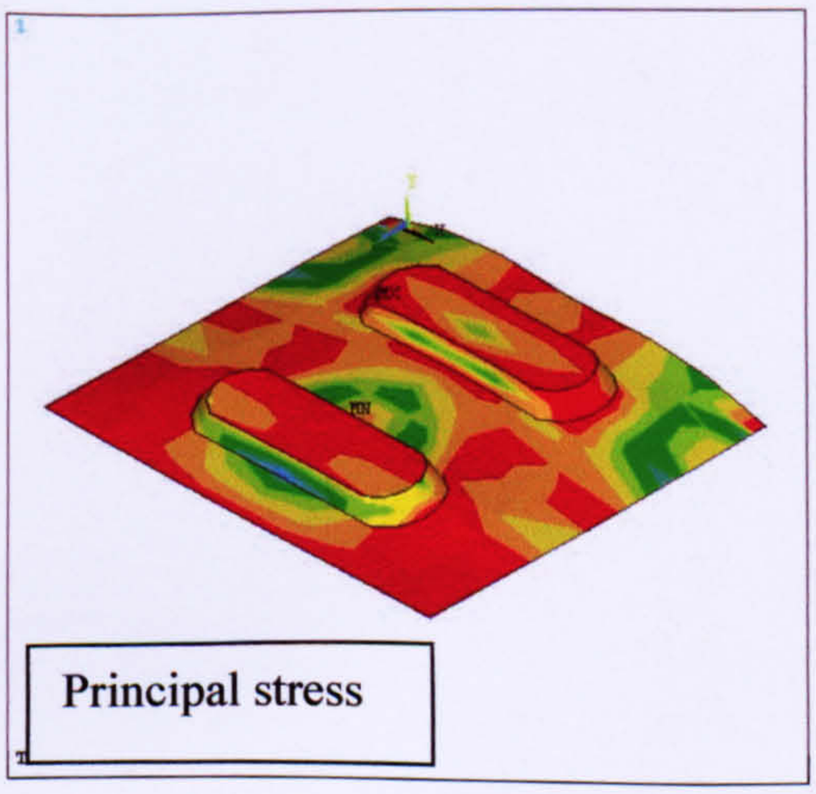

Figure 7.12.a

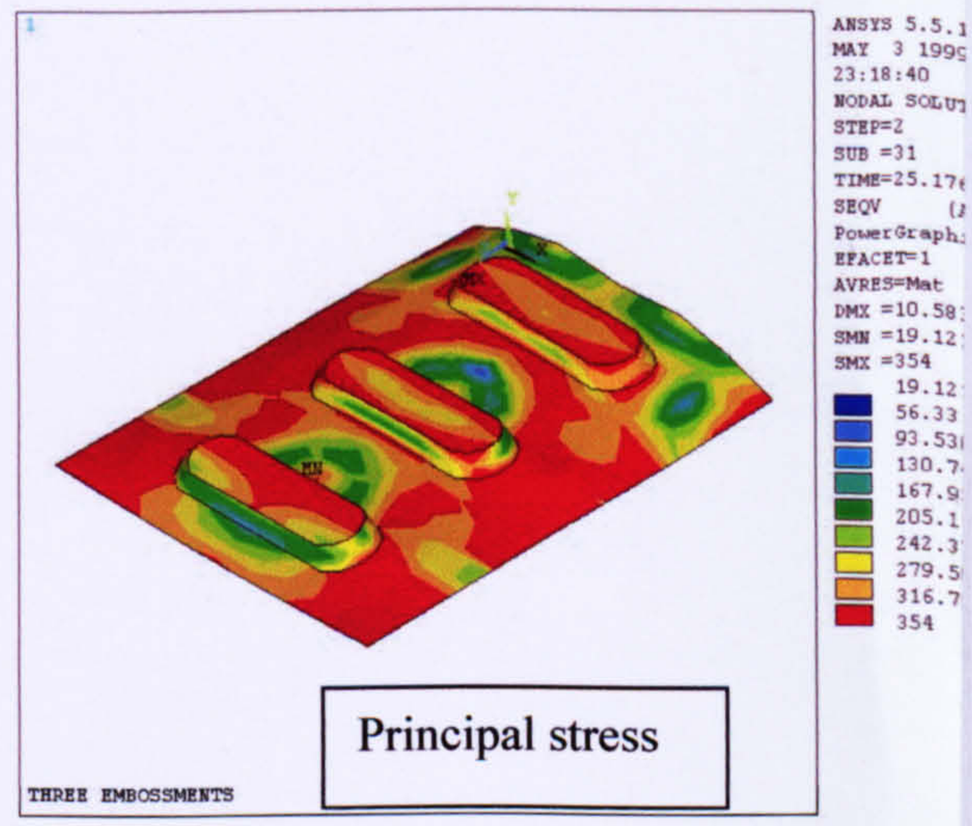

Figure 7.12.b

Figure 7.12.c

Figure 7.13 Comparison of applied load versus longitudenal displacement for numbers of embossments

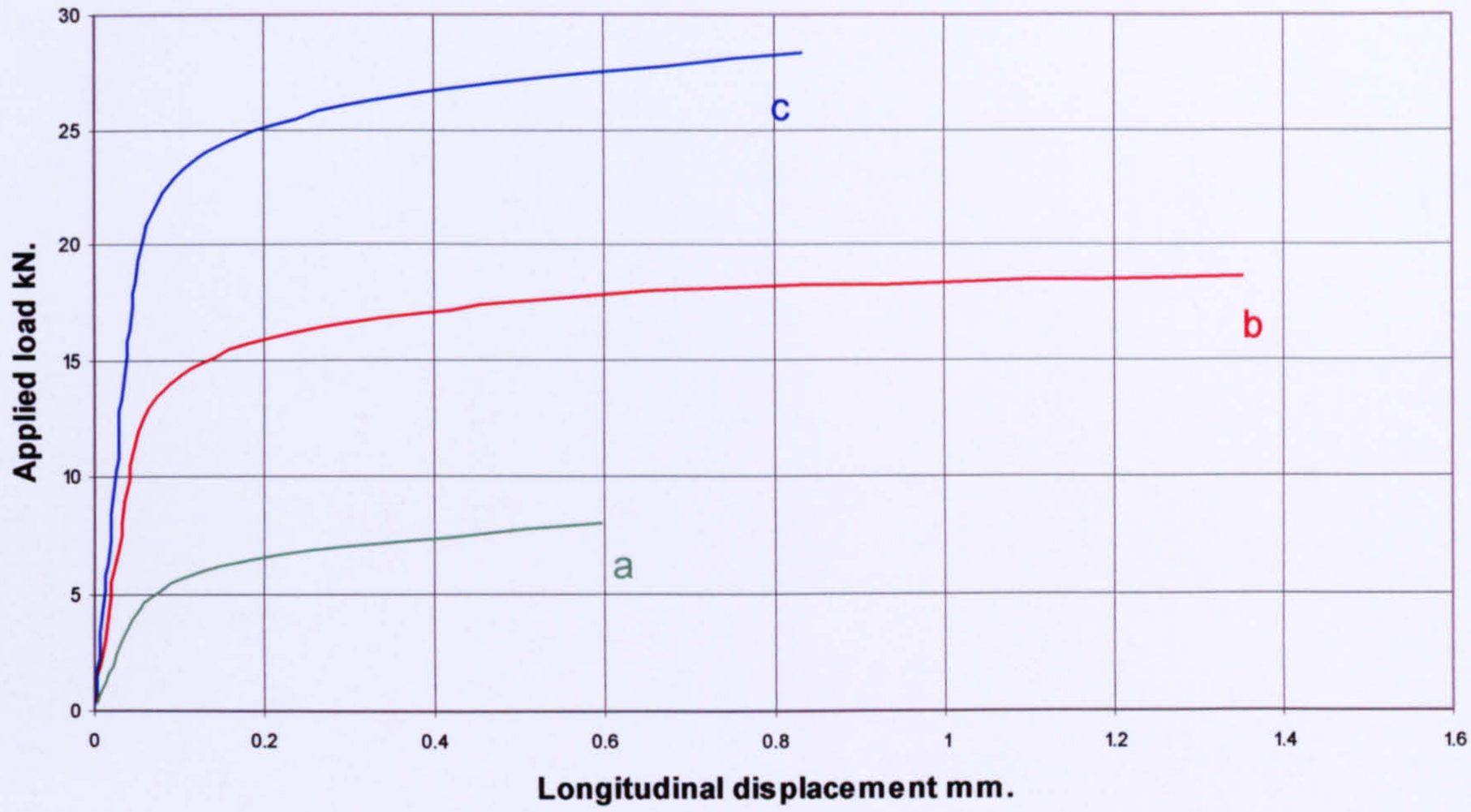

Figure 7.14 Comparison of profiled load versus deflection for numbers of embossments

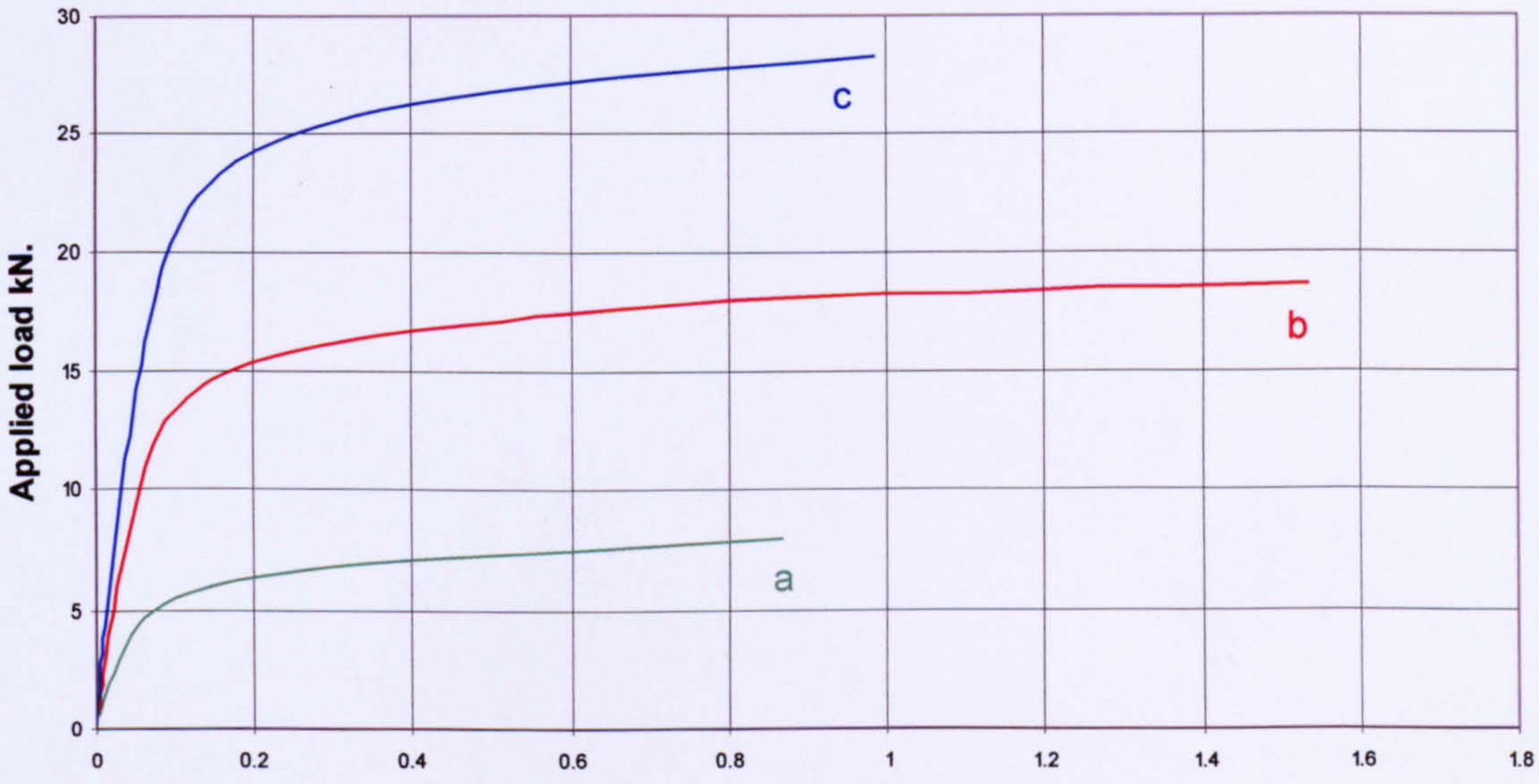

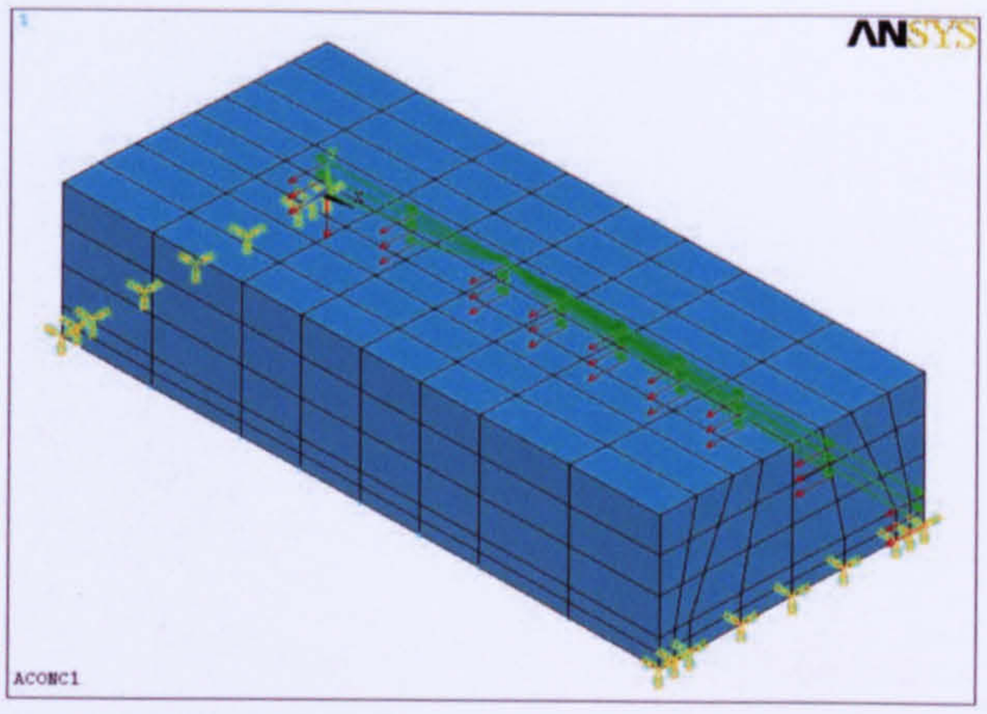

Figure 7.15.a

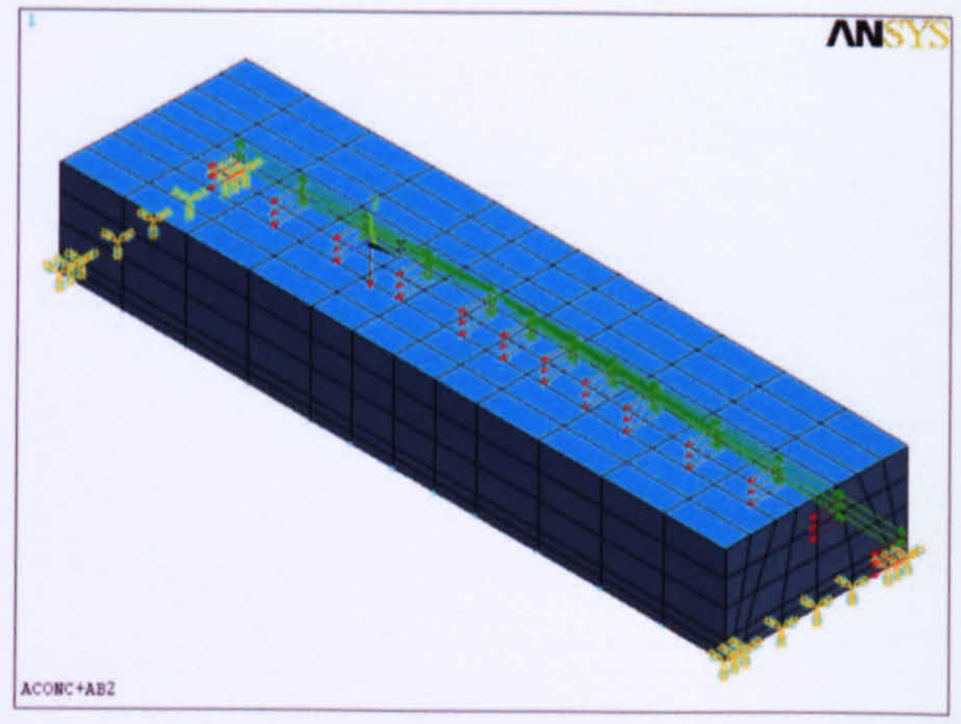

Figure 7.15.b

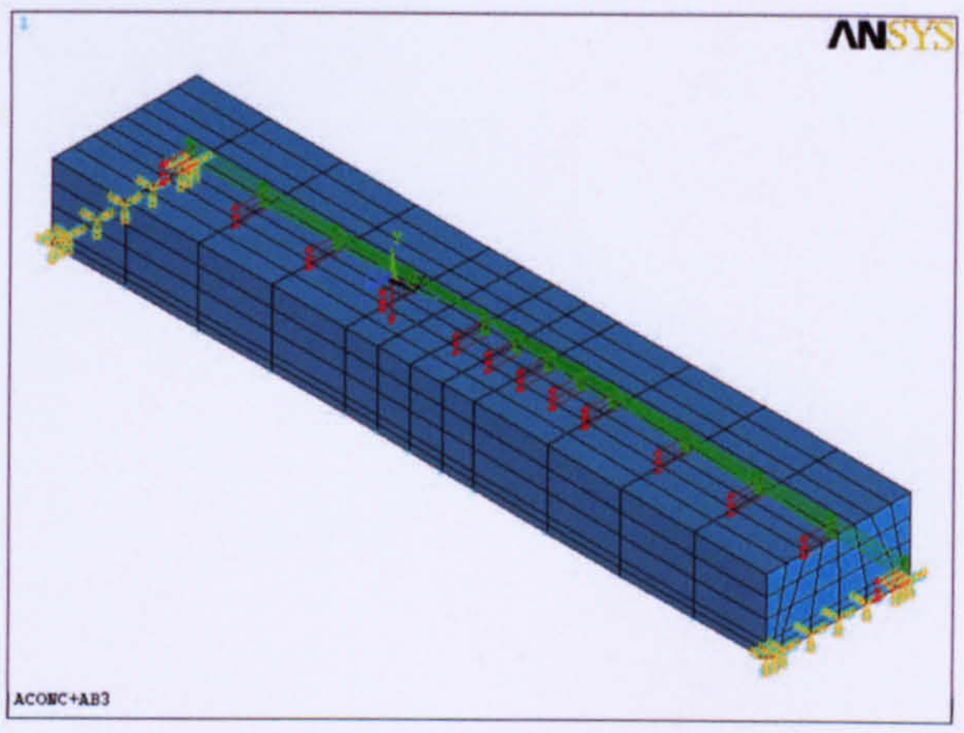

Figure 7.15.c

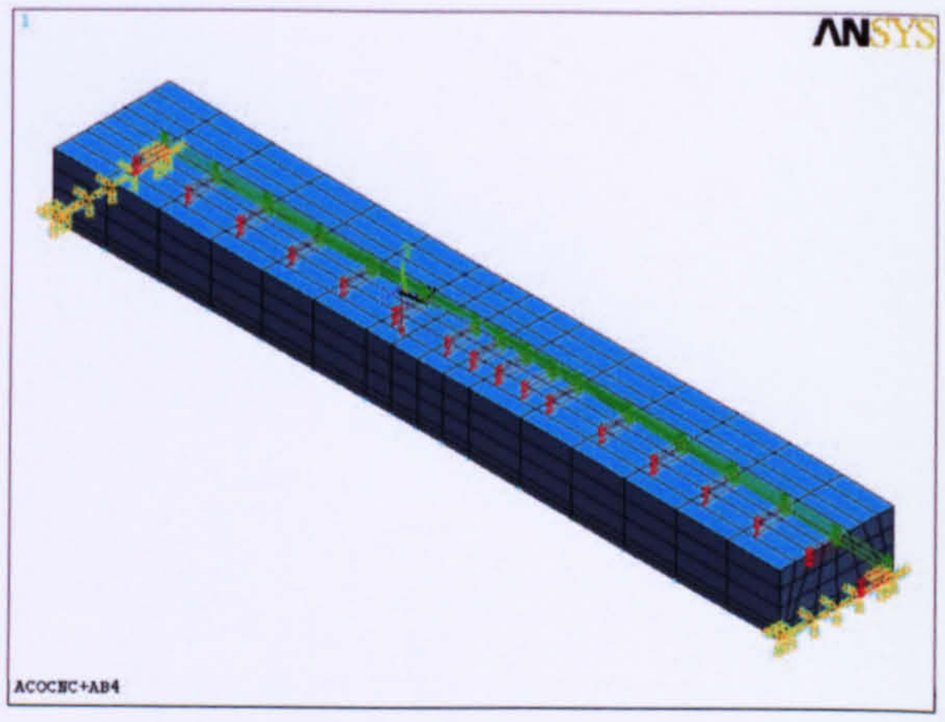

Figure 7.15.d

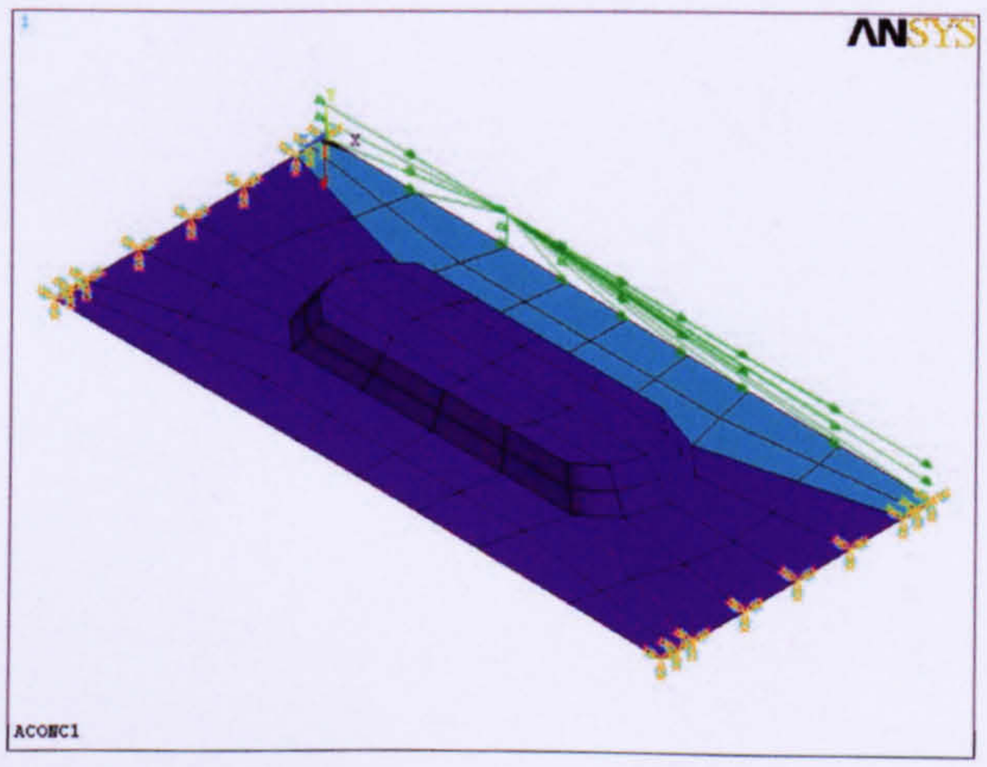

Figure 7.16.a

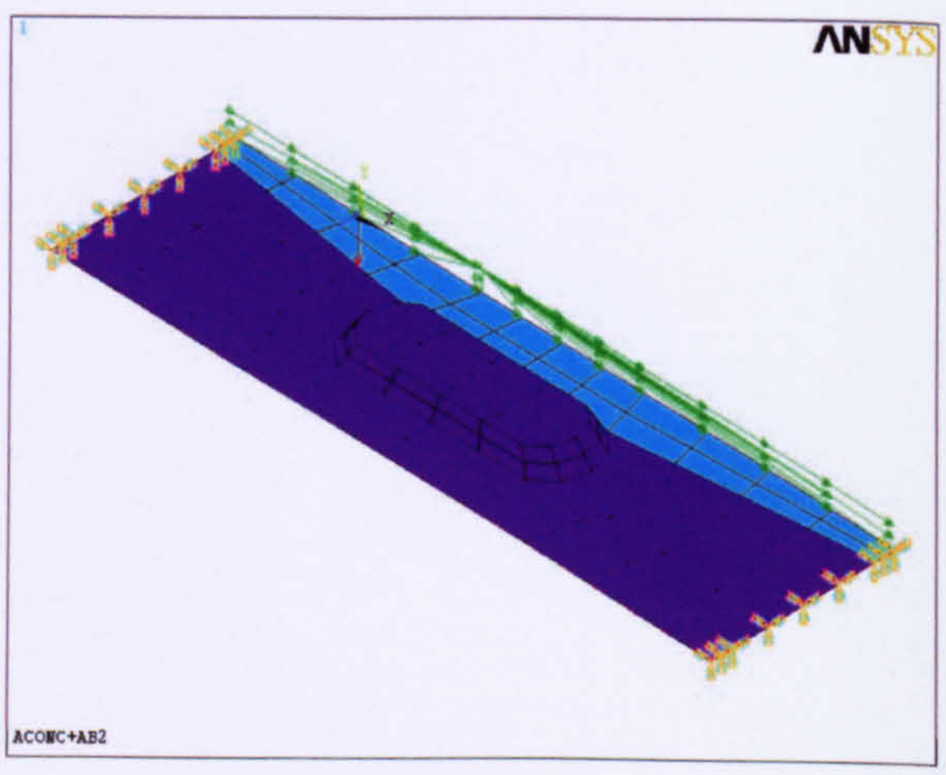

Figure 7.16.b

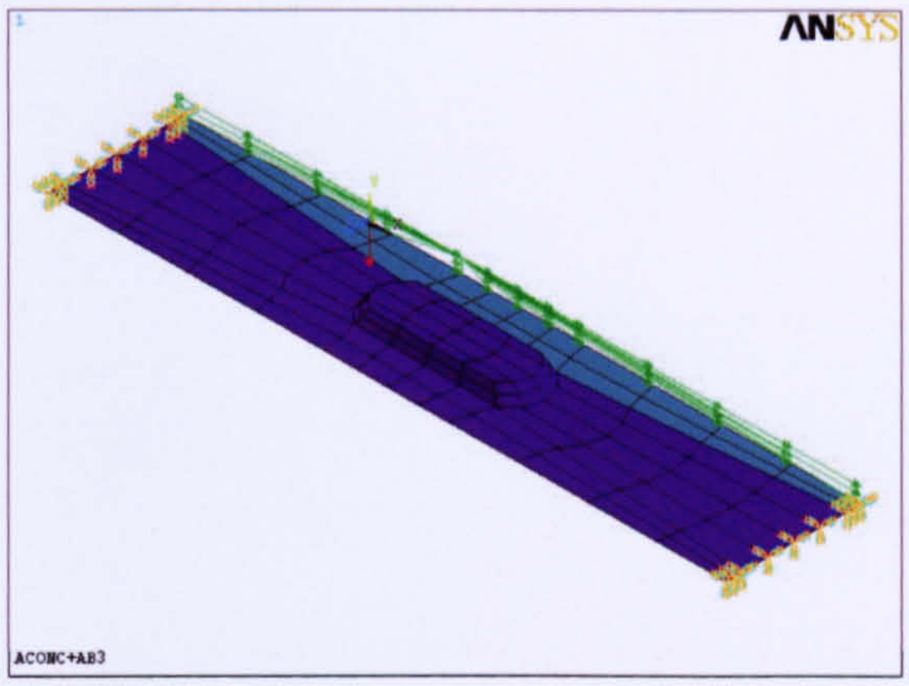

Figure 7.16.c

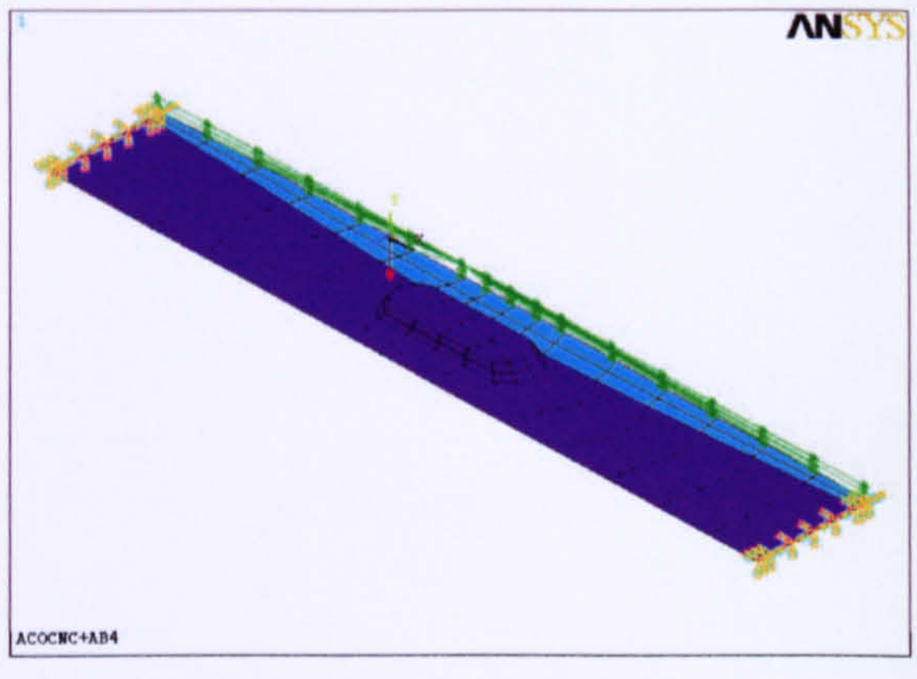

Figure 7.16.d

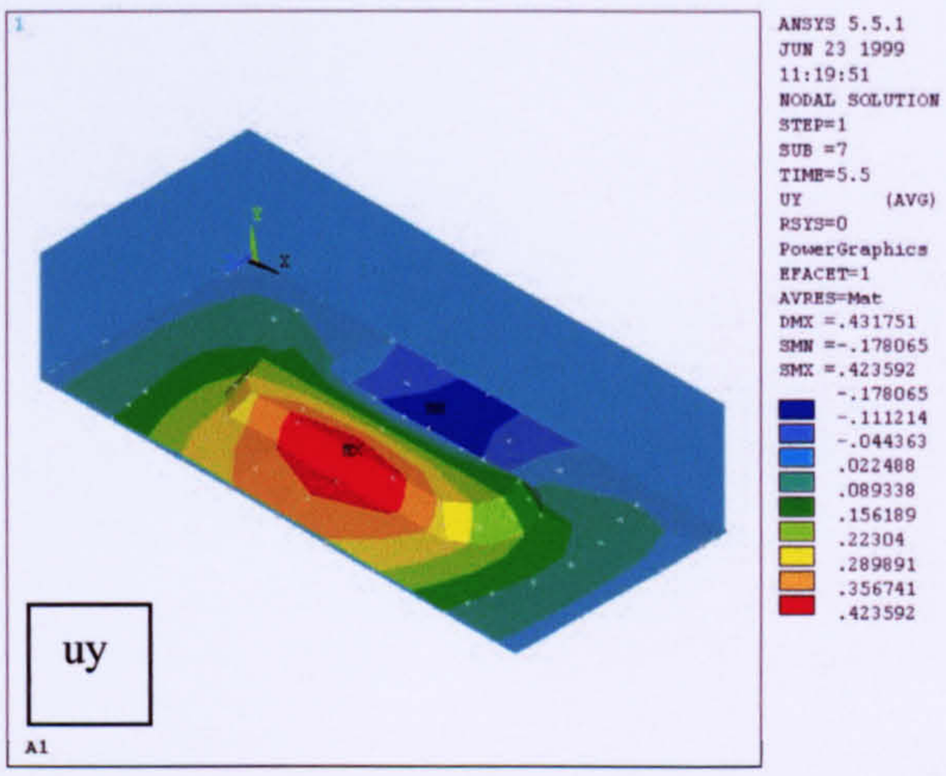

Figure 7.17.a

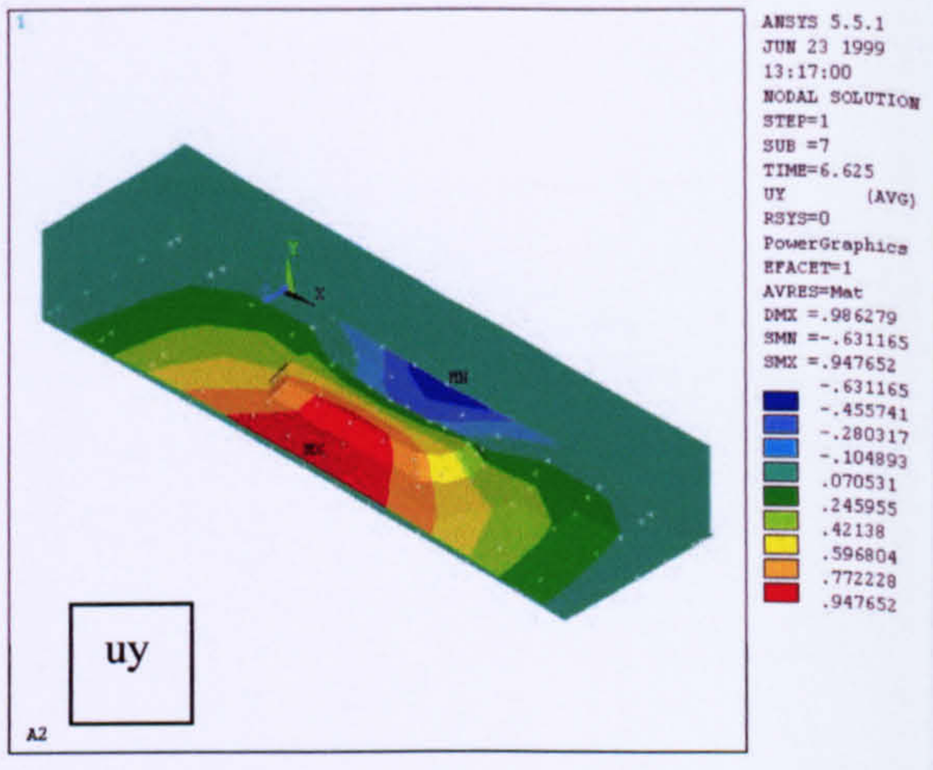

Figure 7.17.b

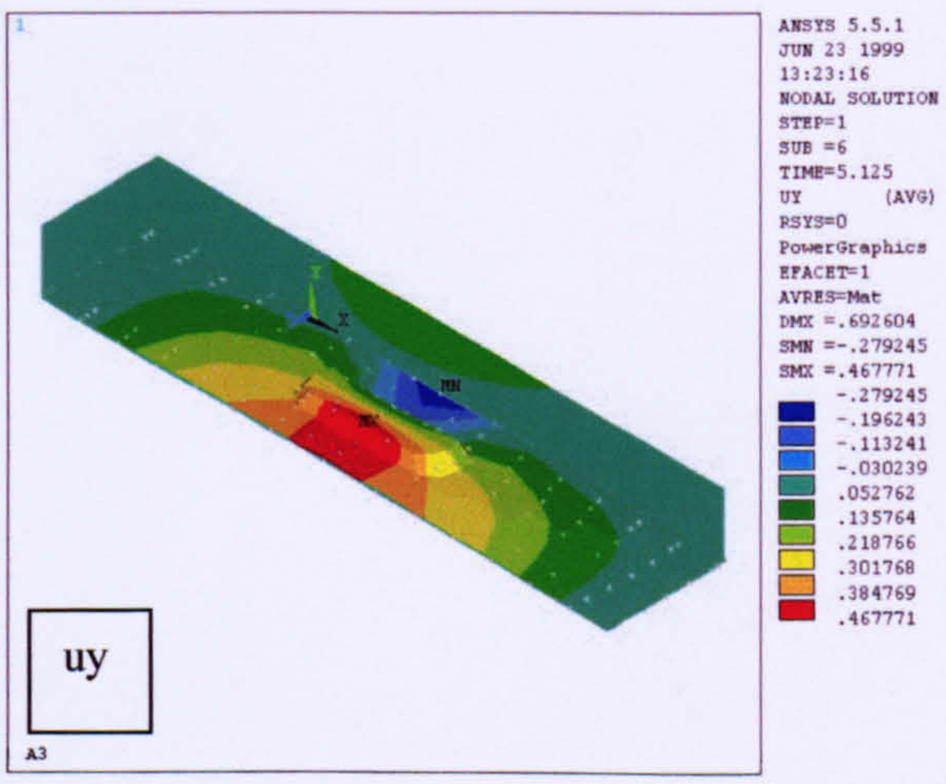

Figure 7.17.c

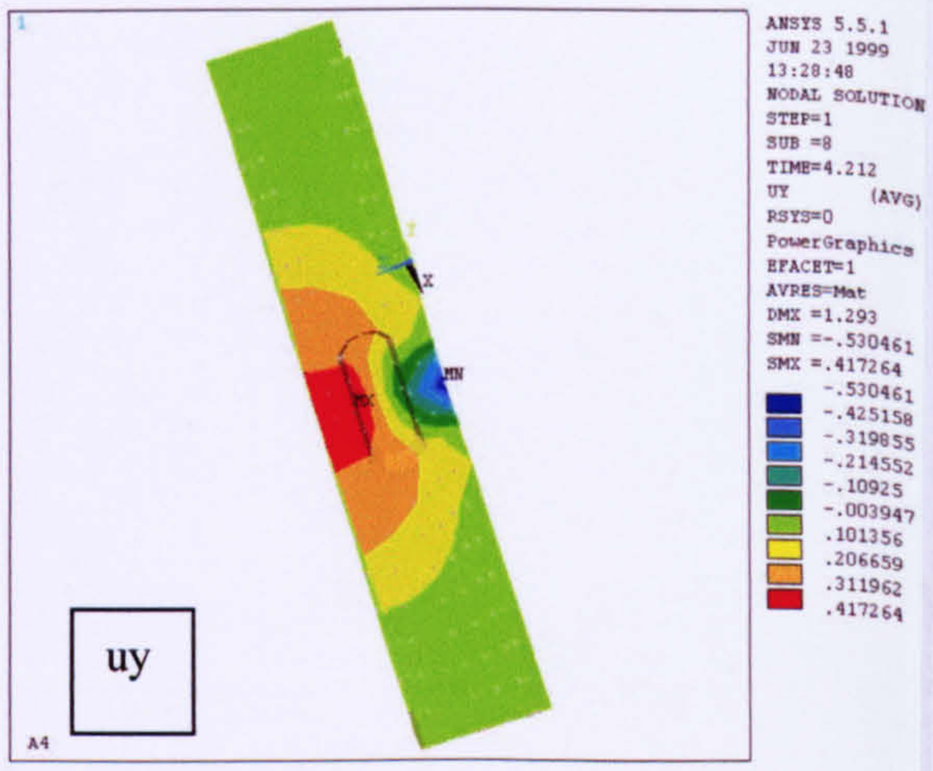

Figure 7.17.d

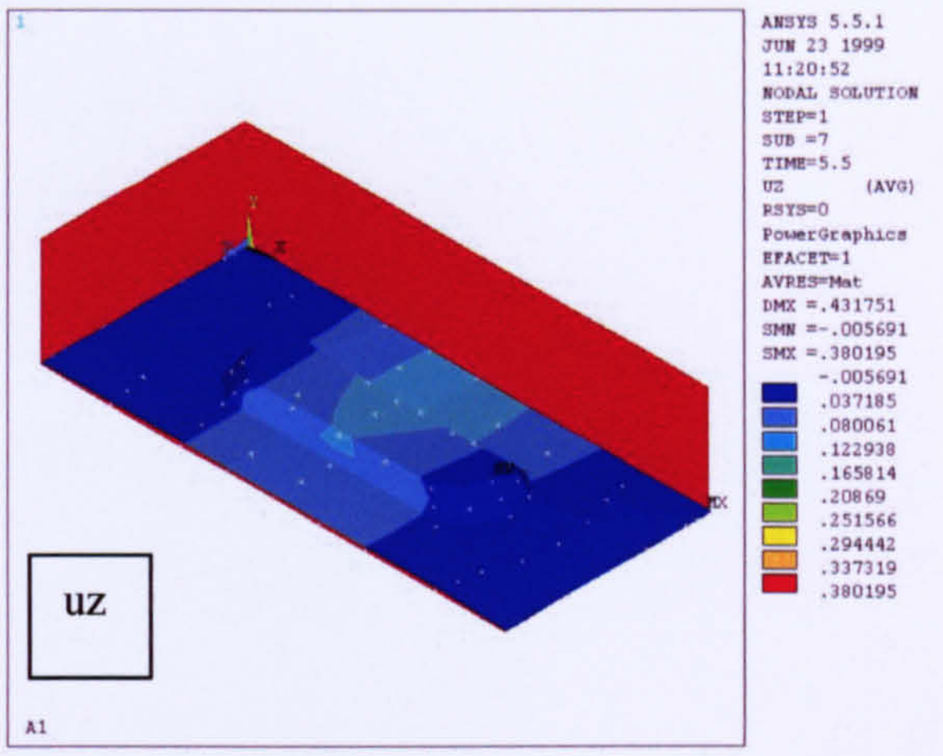

Figure 7.18.a

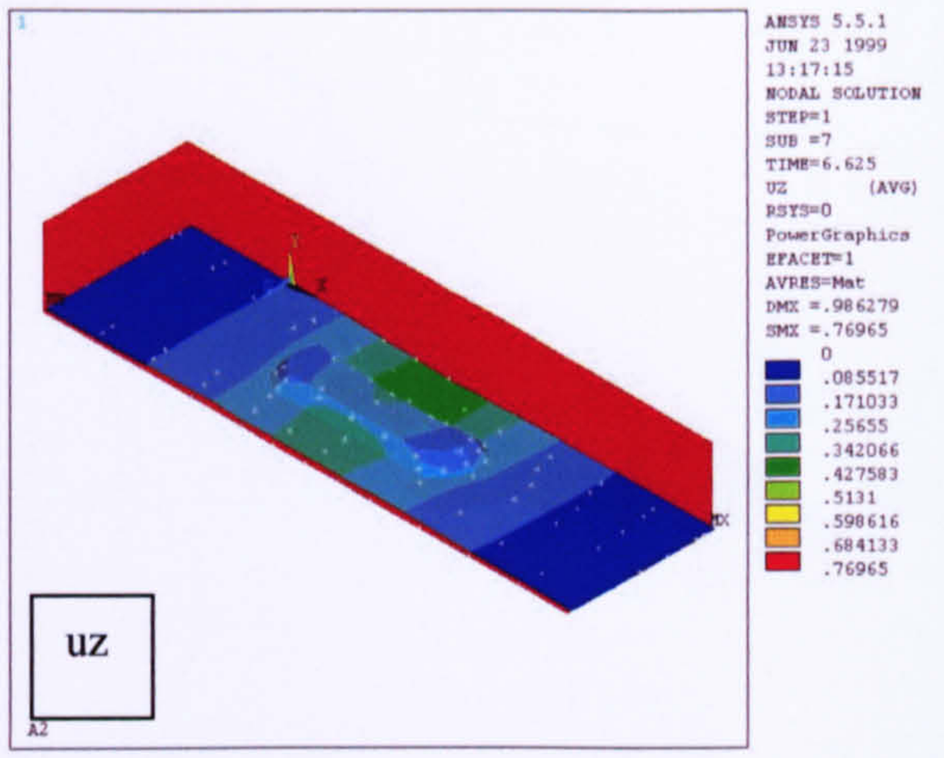

Figure 7.18.b

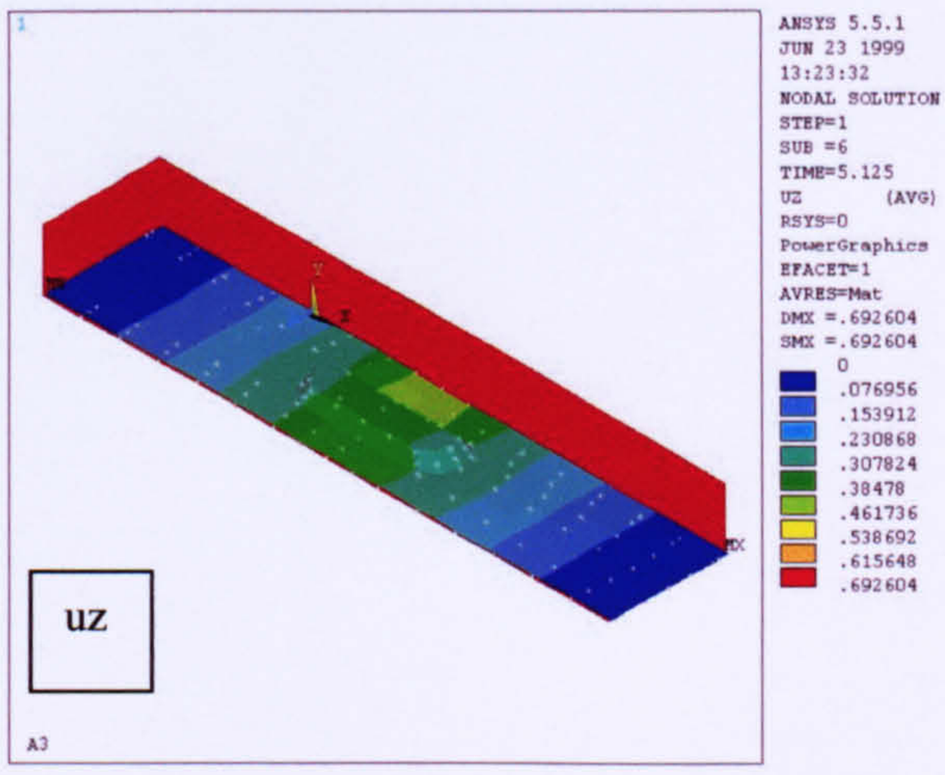

Figure 7.18.c

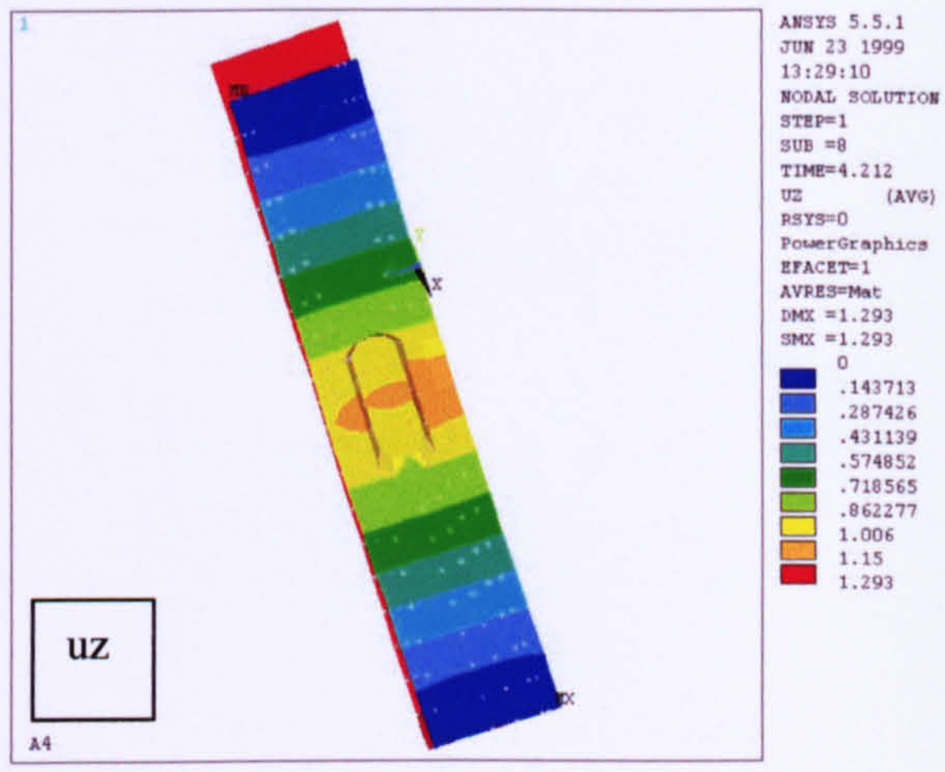

Figure 7.18.d

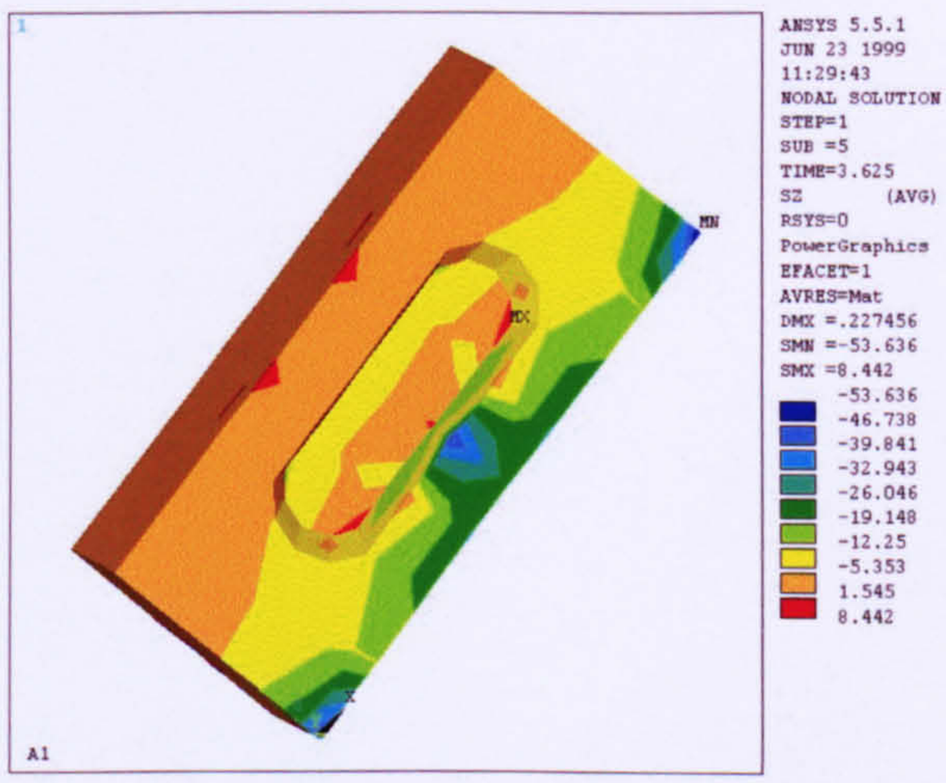

Figure 7.19.a Concrete stresses near yield

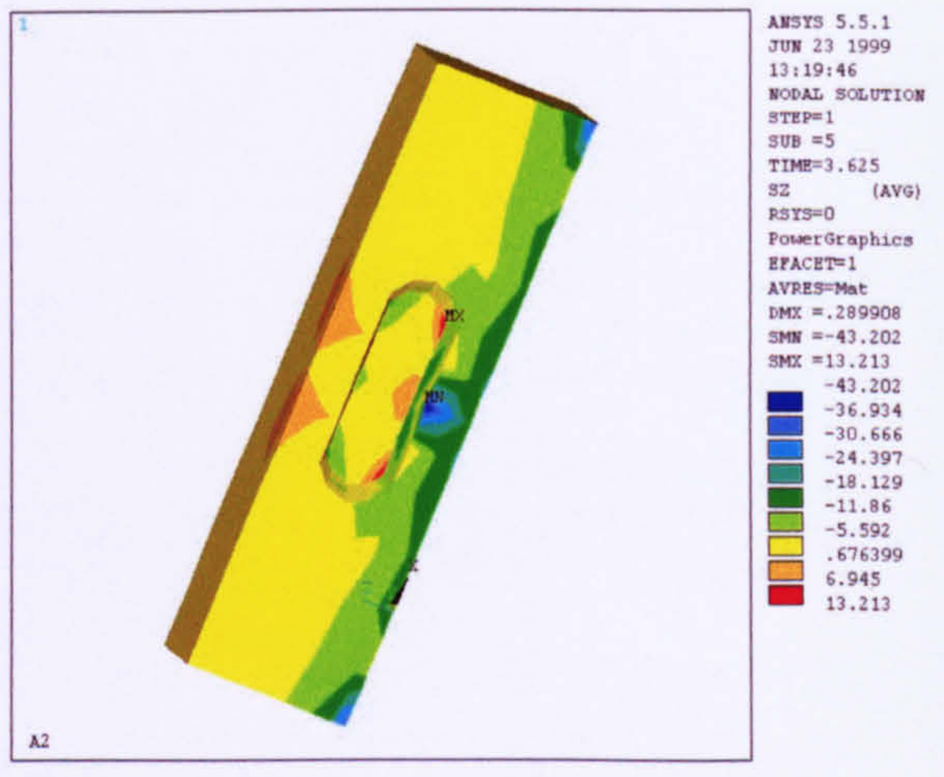

Figure 7.19.b Concrete stress near yield

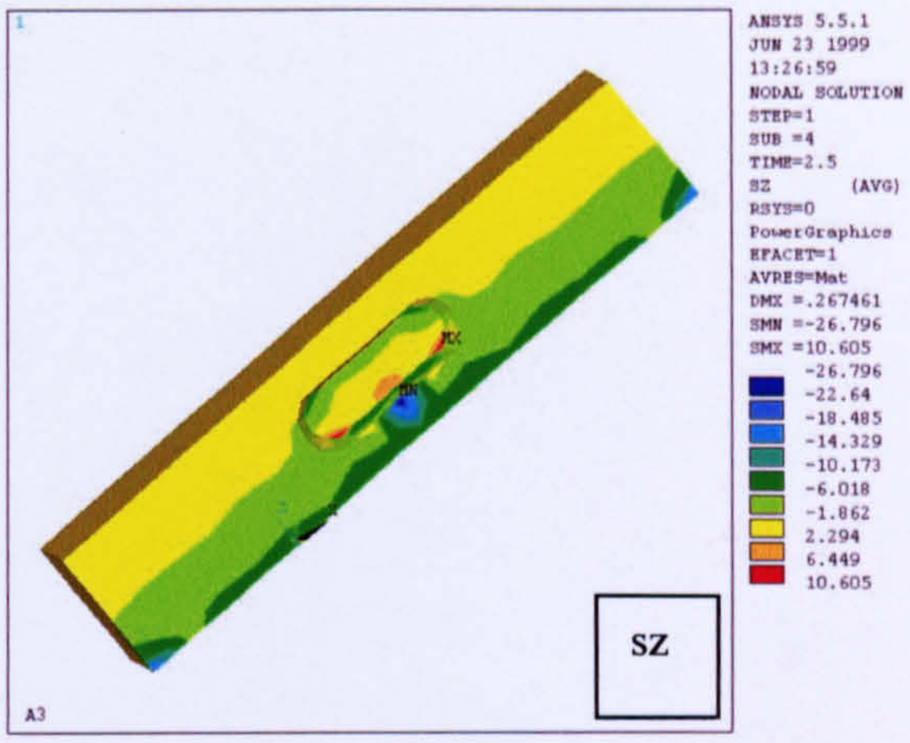

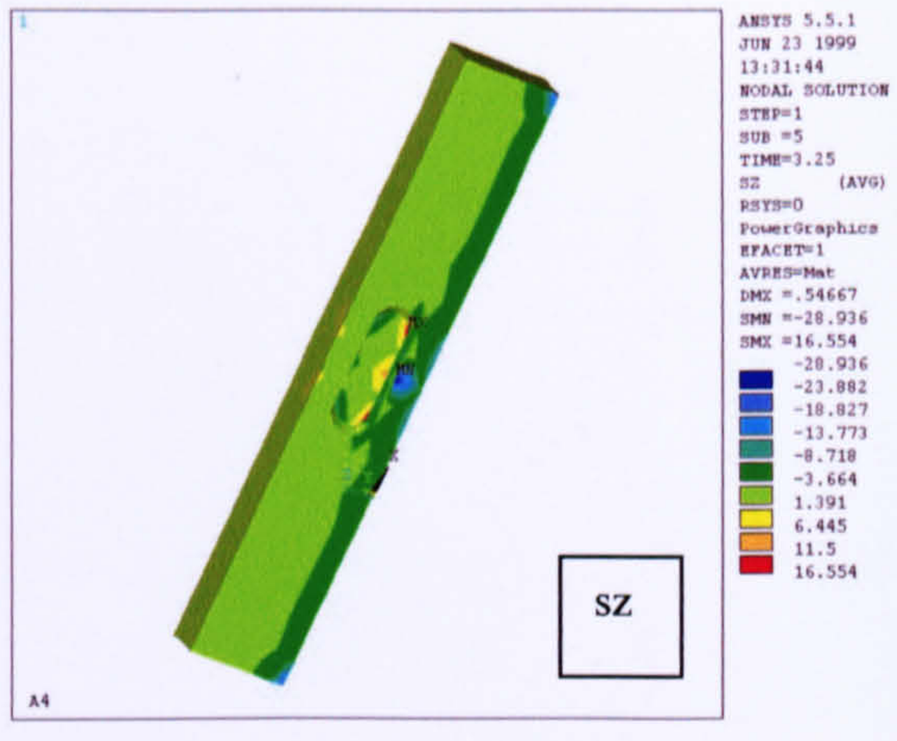

Figure 7.19.c Concrete stresses near yield

Figure 7.19.d Concrete stresses near yield

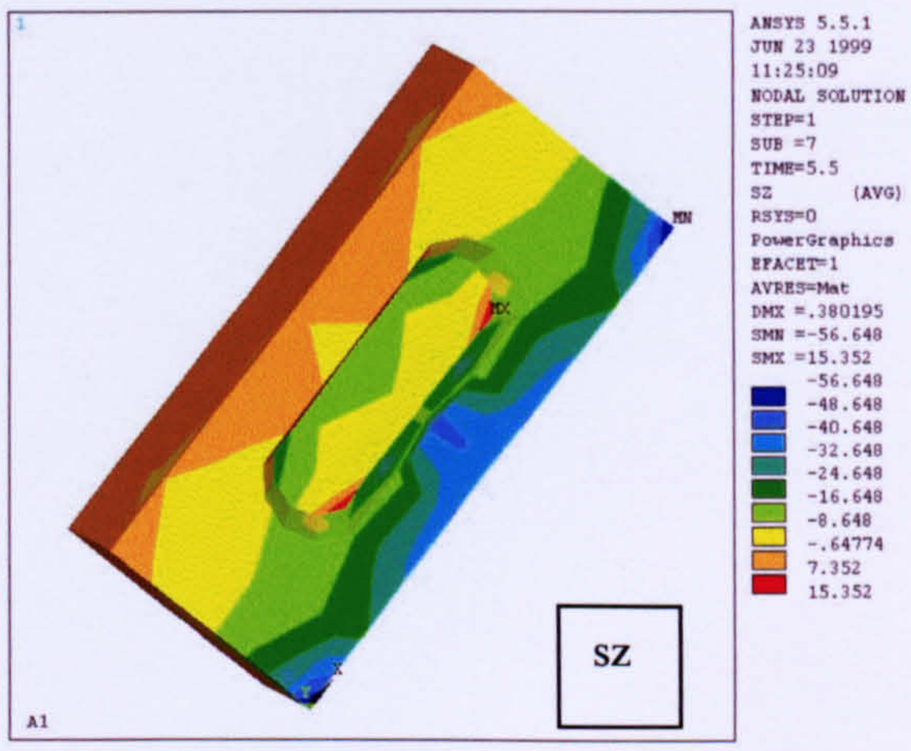

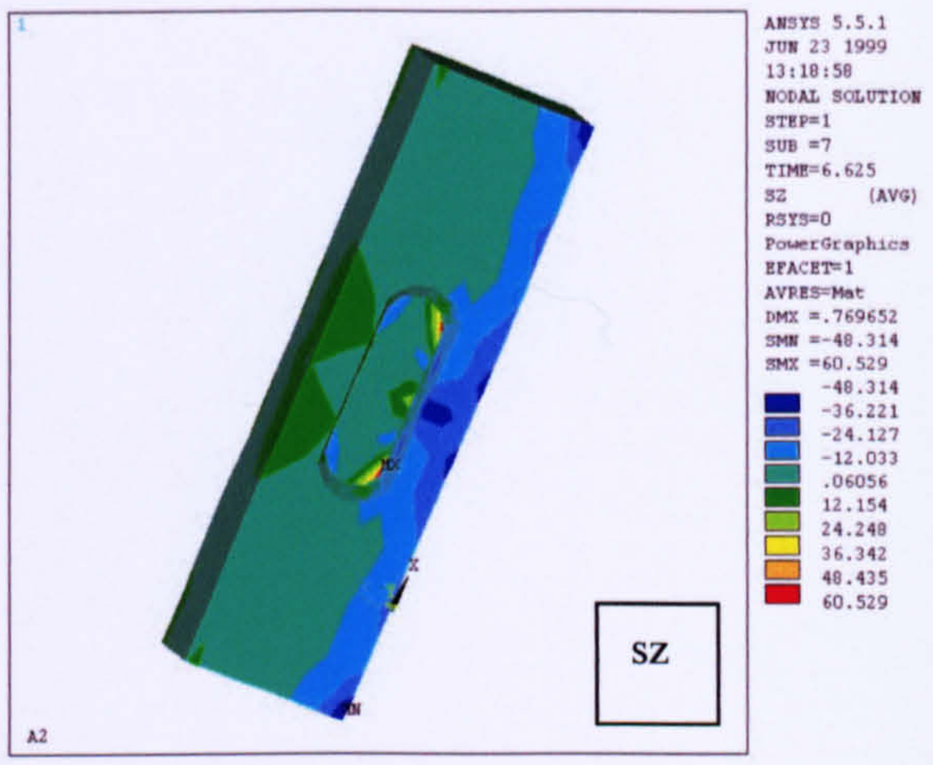

Figure 7.20.a

Figure 7.20.b

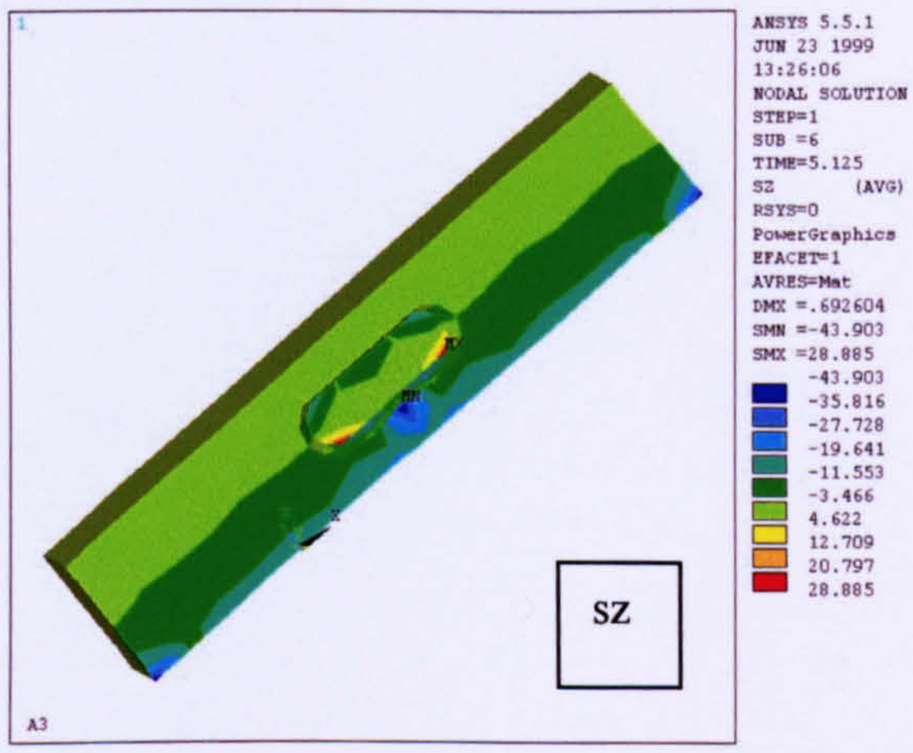

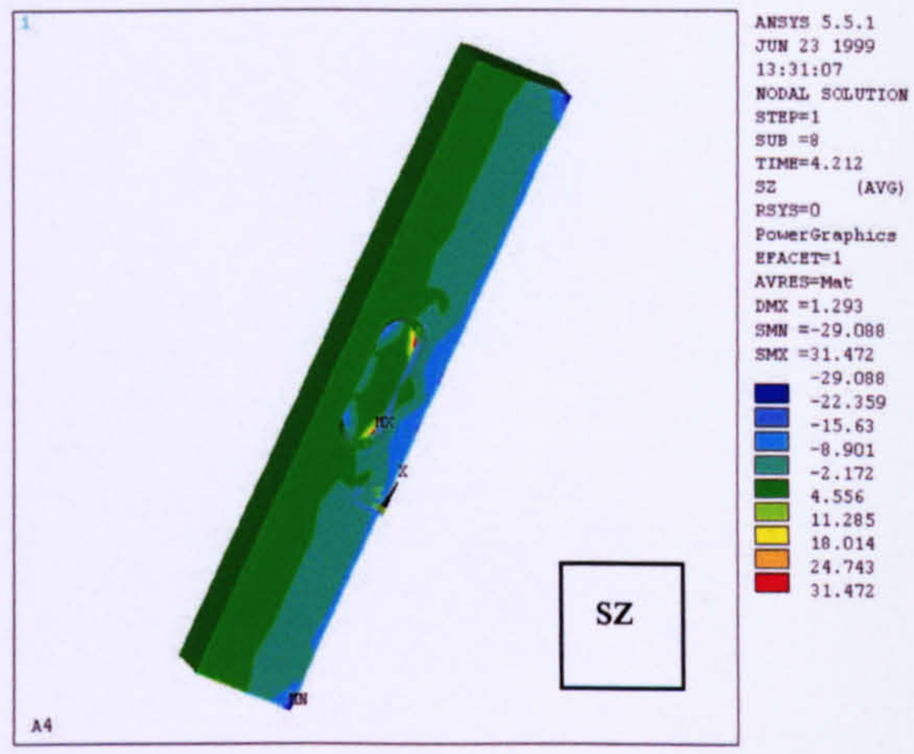

Figure 7.20.c

Figure 7.20.d

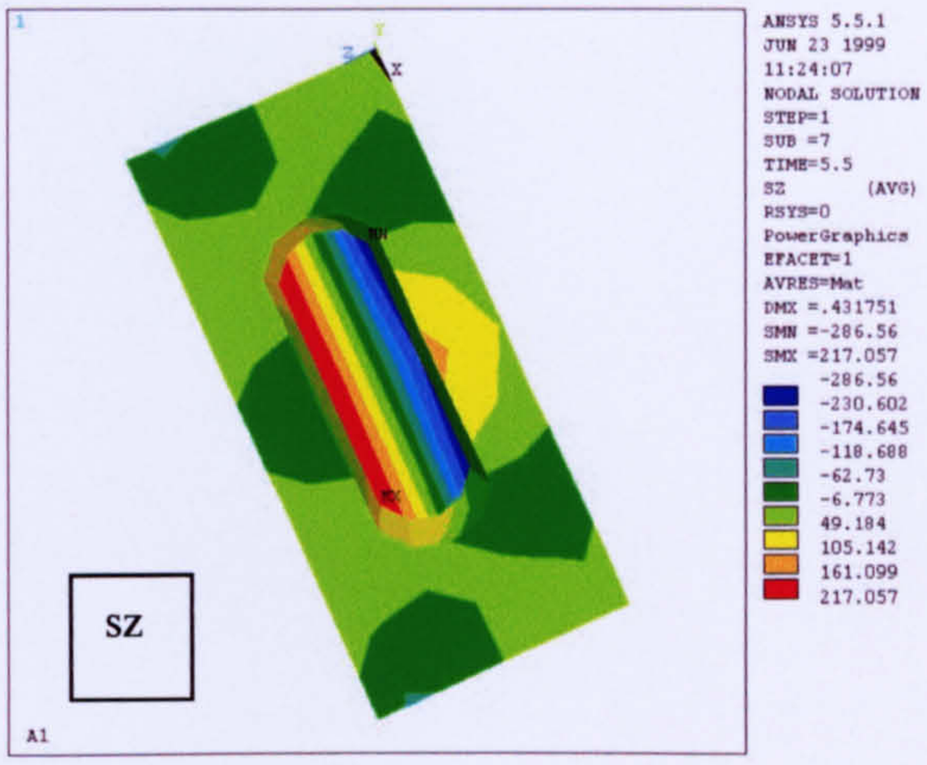

Figure 7.20.e Steel plate stresses

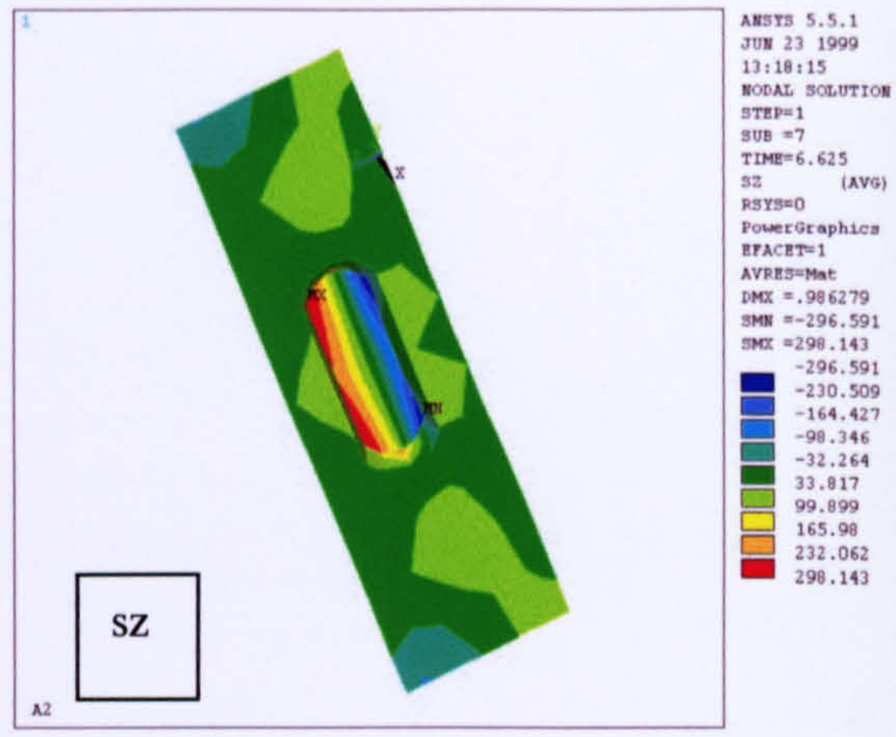

Figure 7.20.f Steel plate stresses

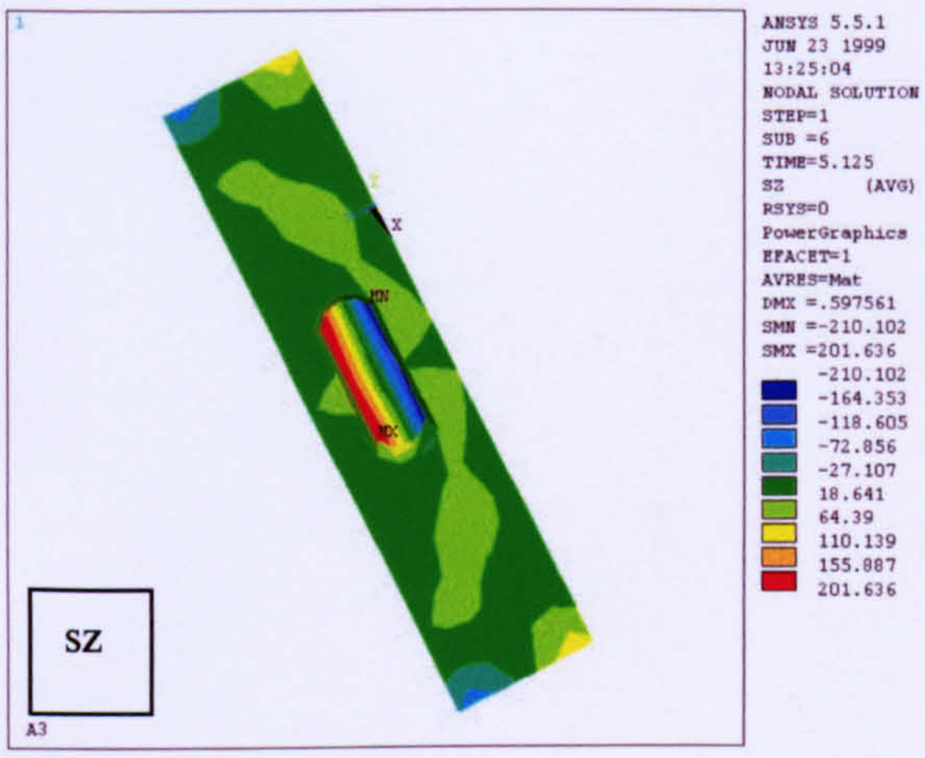

Figure 7.20.g Steel plate stresses

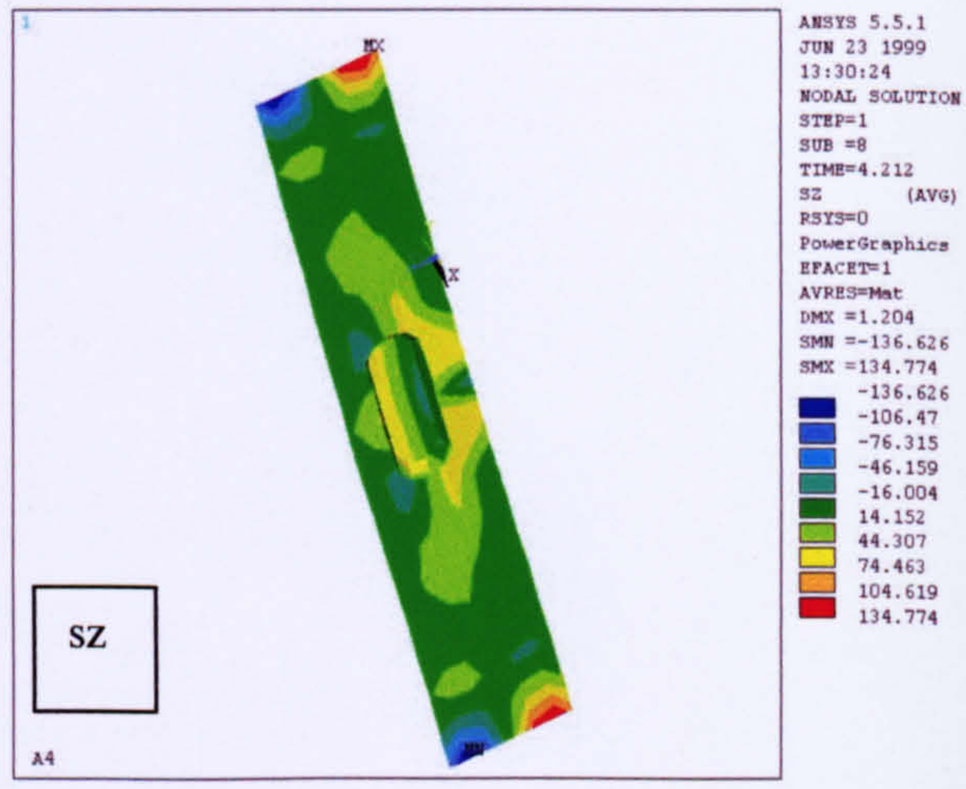

Figure 7.20.h Steel plate stresses

Figure 7.21 Comparison of the applied load versus deflection for various aspect ratio.

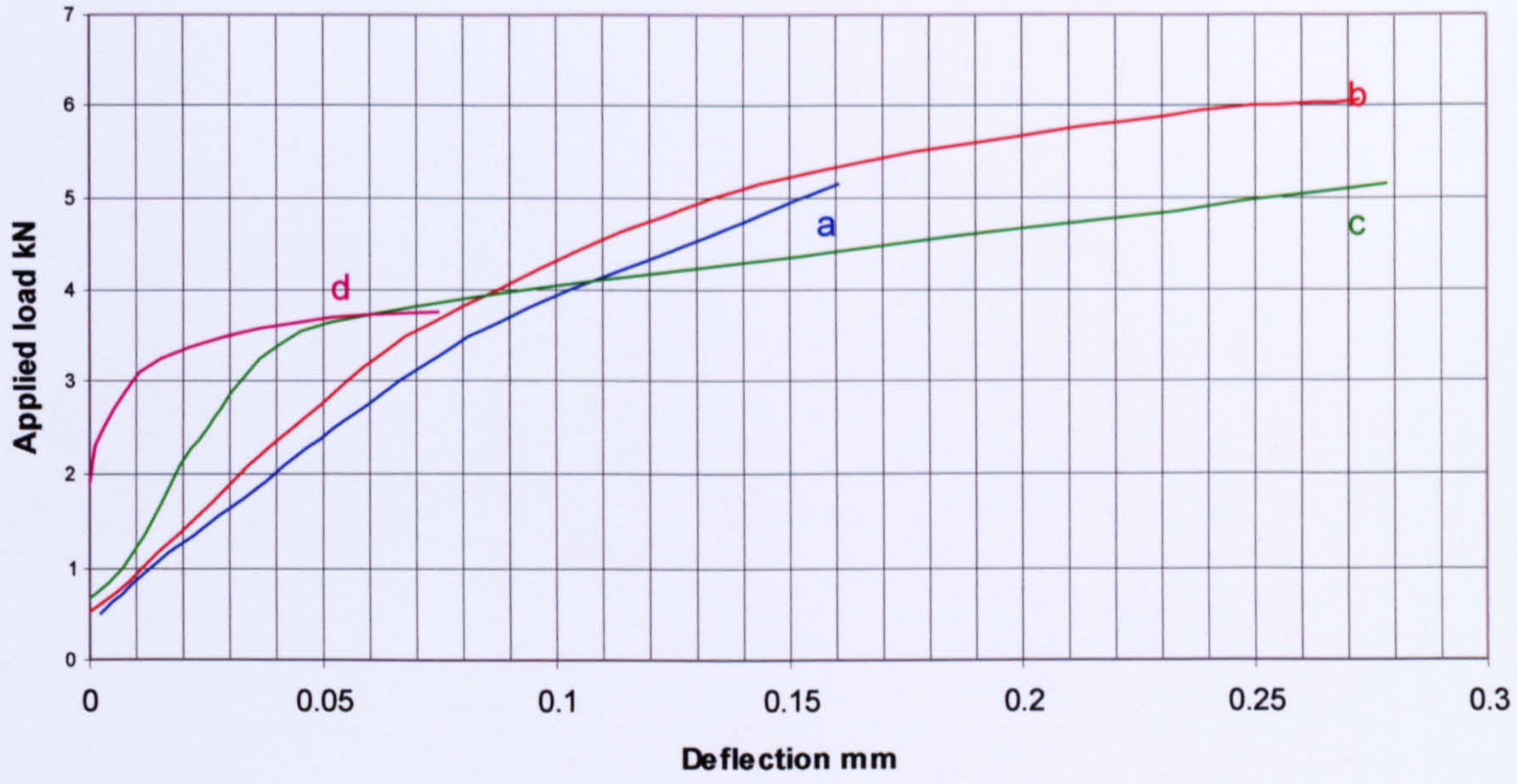

Figure 7.22 Comparison of the applied load versus longitudinal displacement.

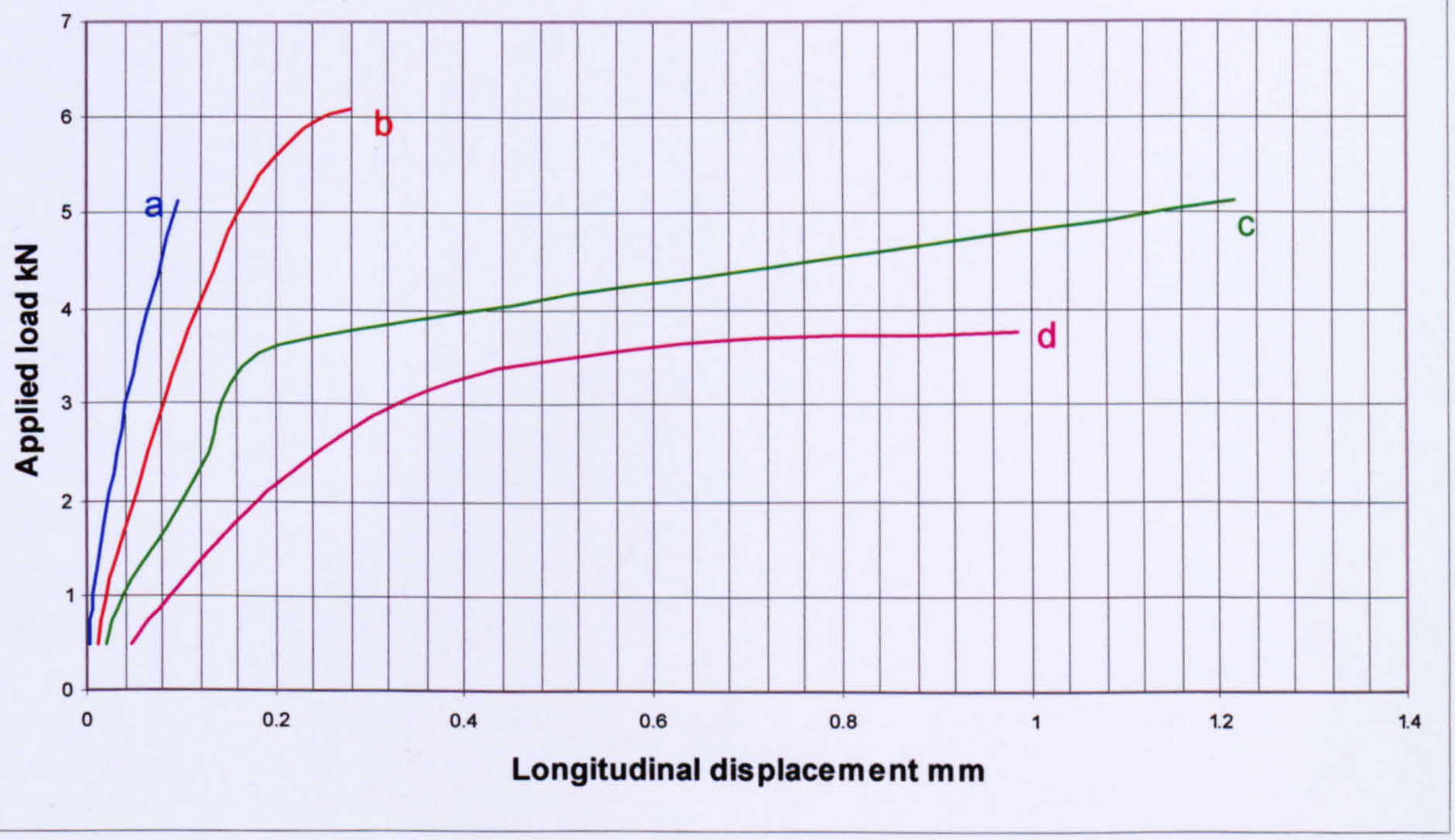

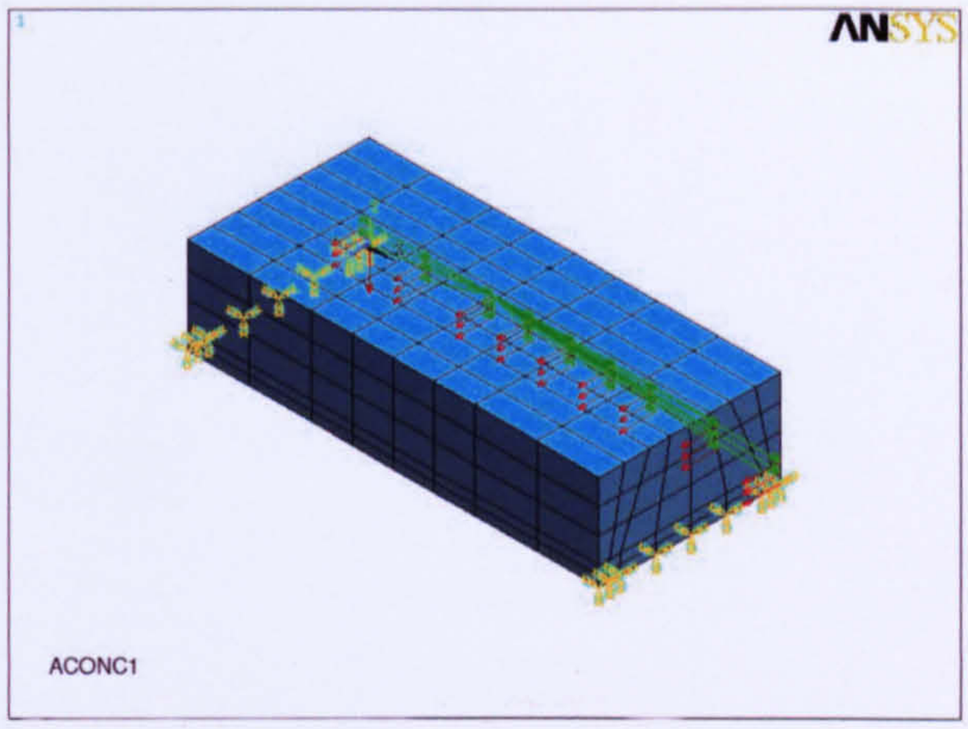

Figure 7.23.a

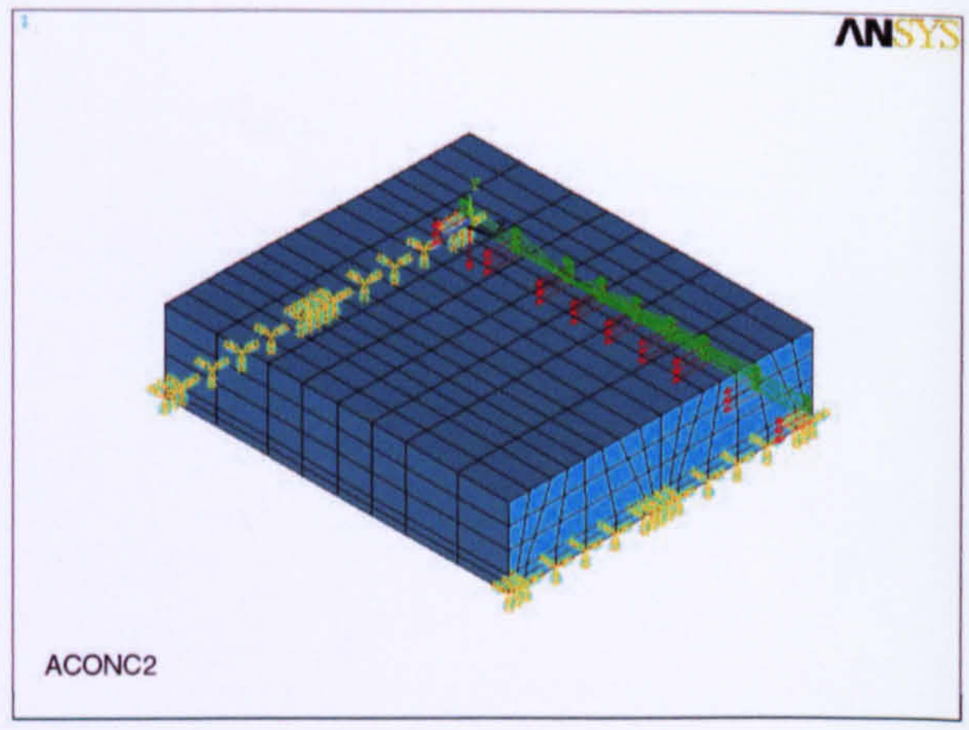

Figure 7.23.b

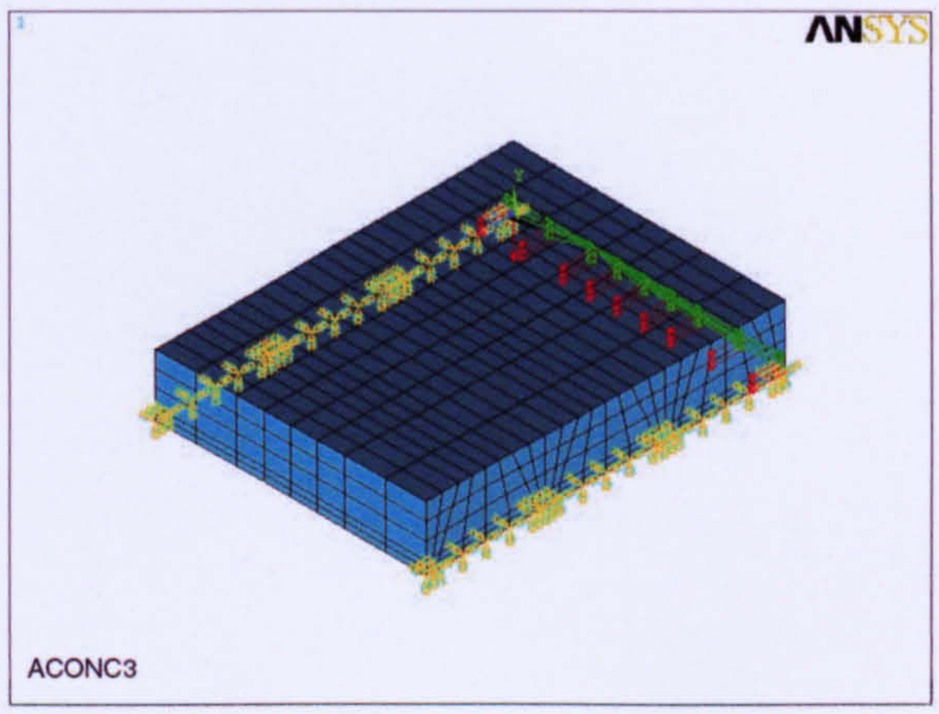

Figure 7.23.c

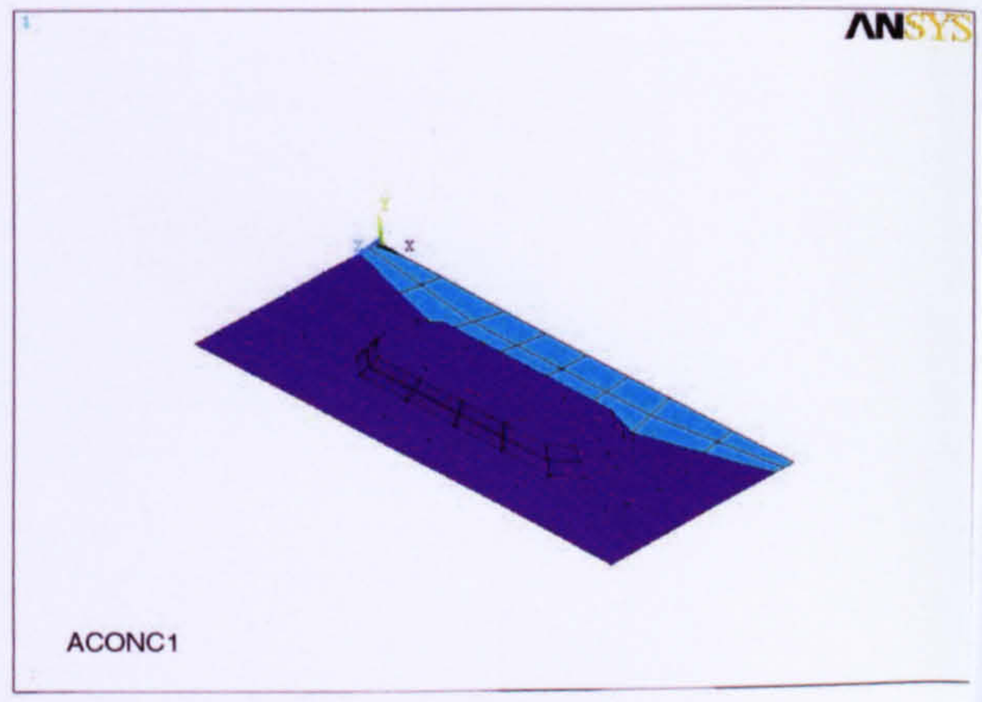

Figure 7.24.a

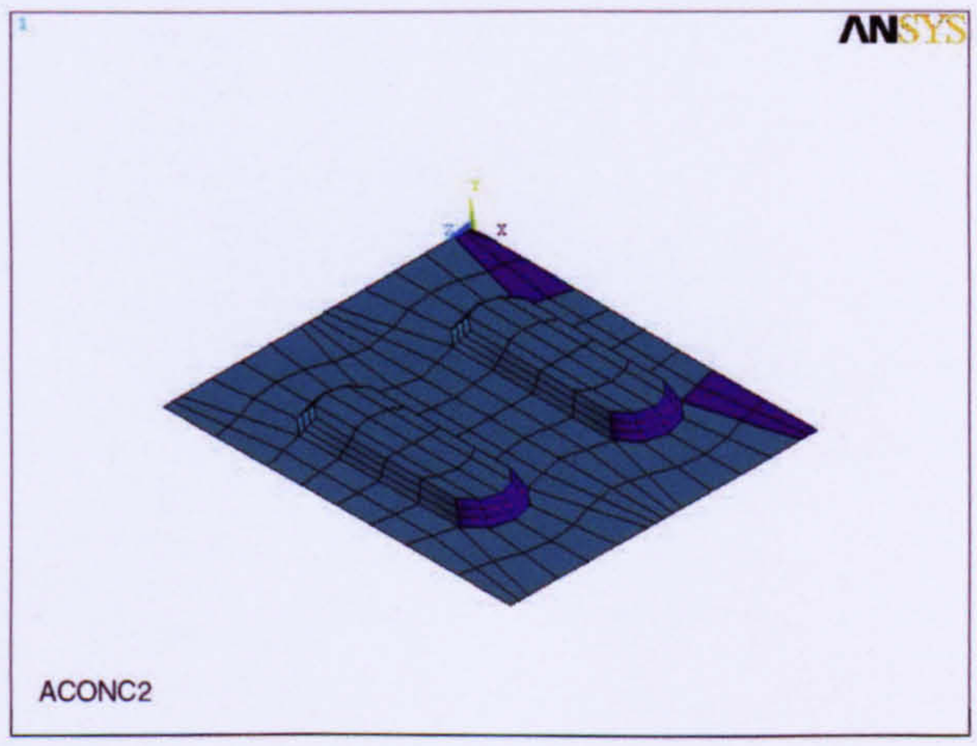

Figure 7.24.b

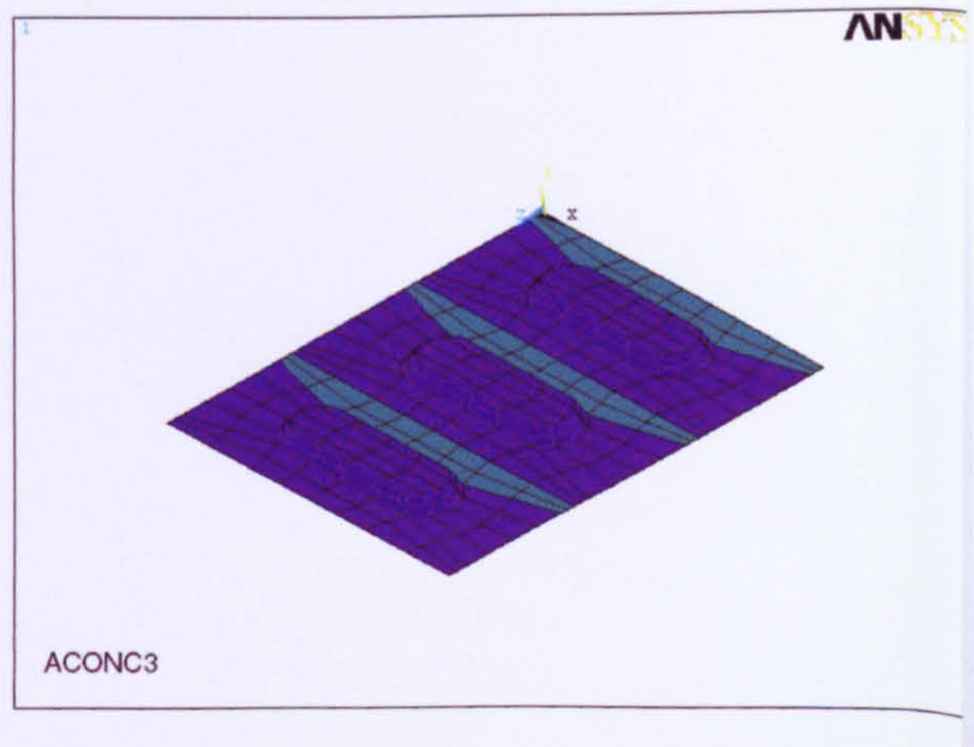

Figure 7.24.c

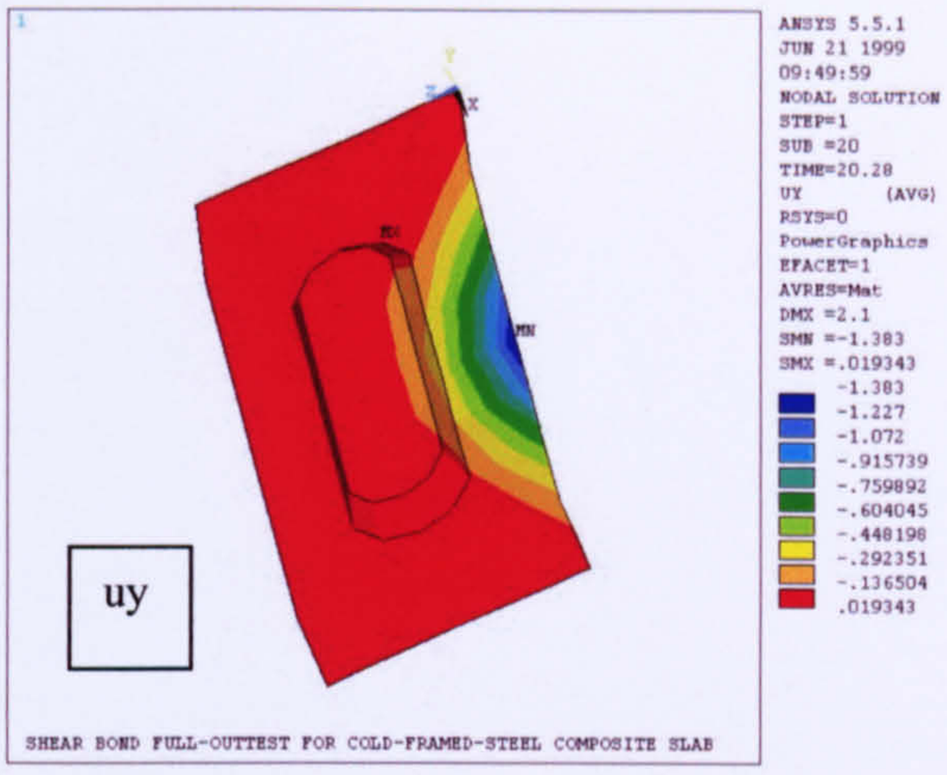

Figure 7.25.a

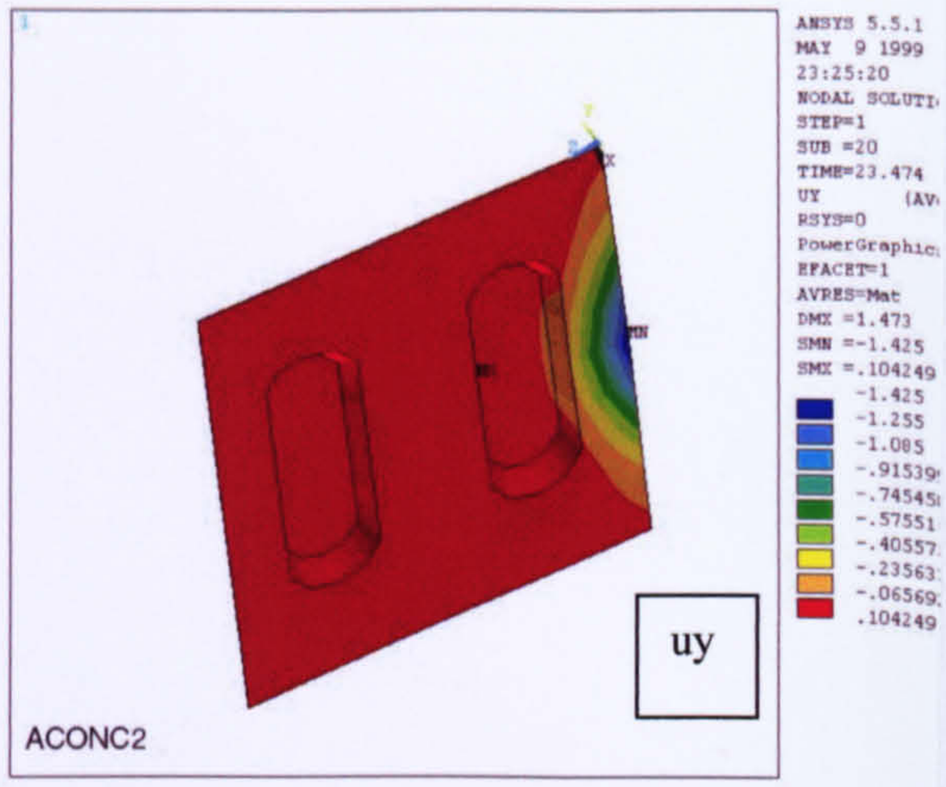

Figure 7.25.b

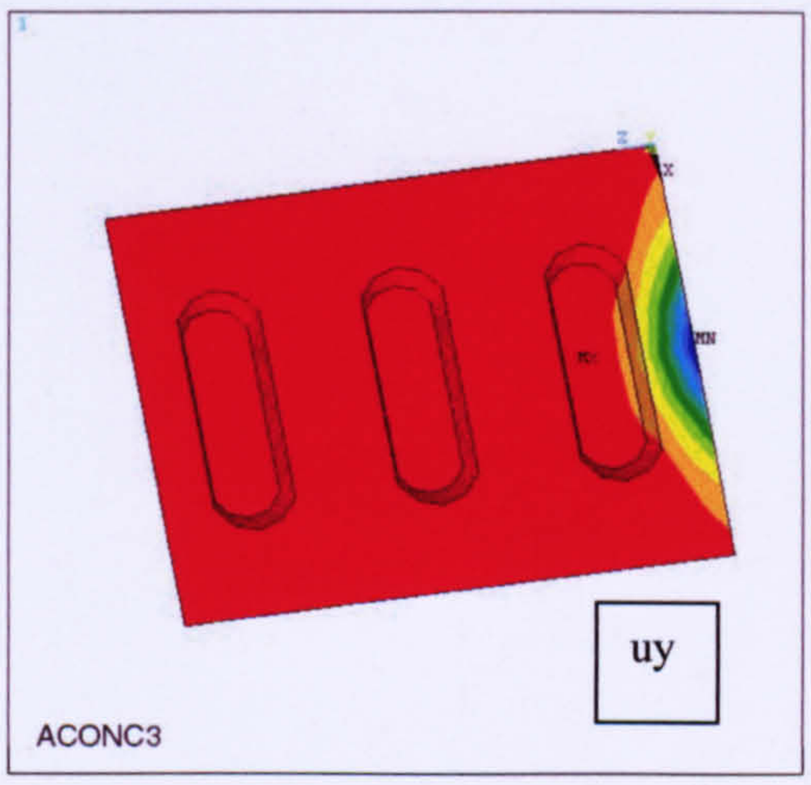

Figure 7.25.c

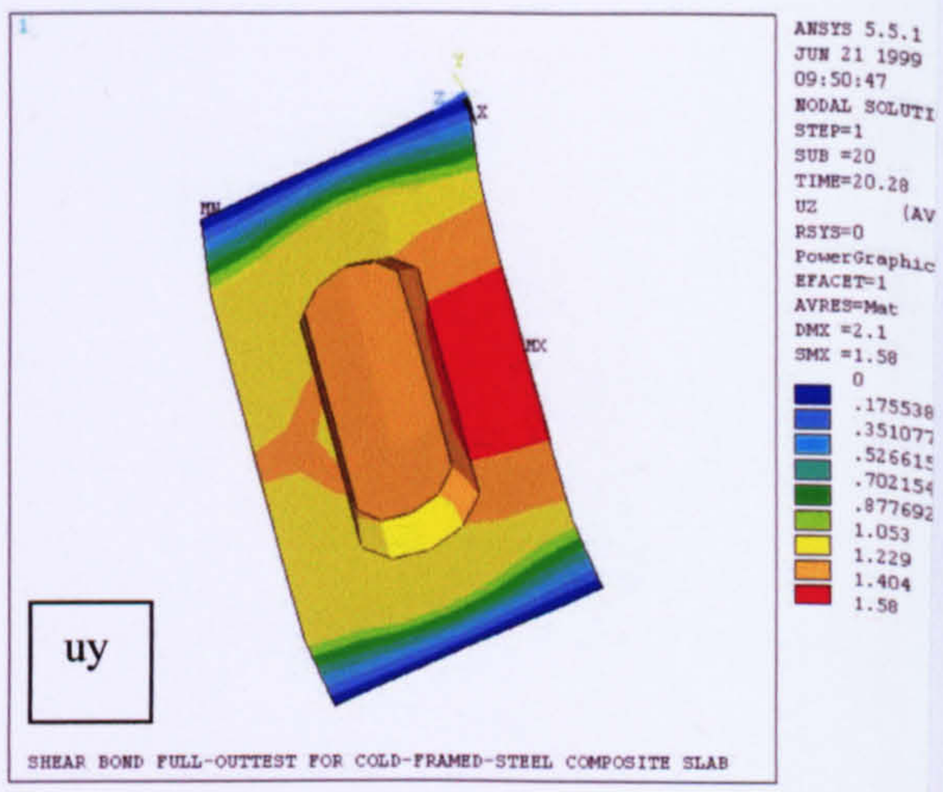

Figure 7.26.a

Figure 7.26.b

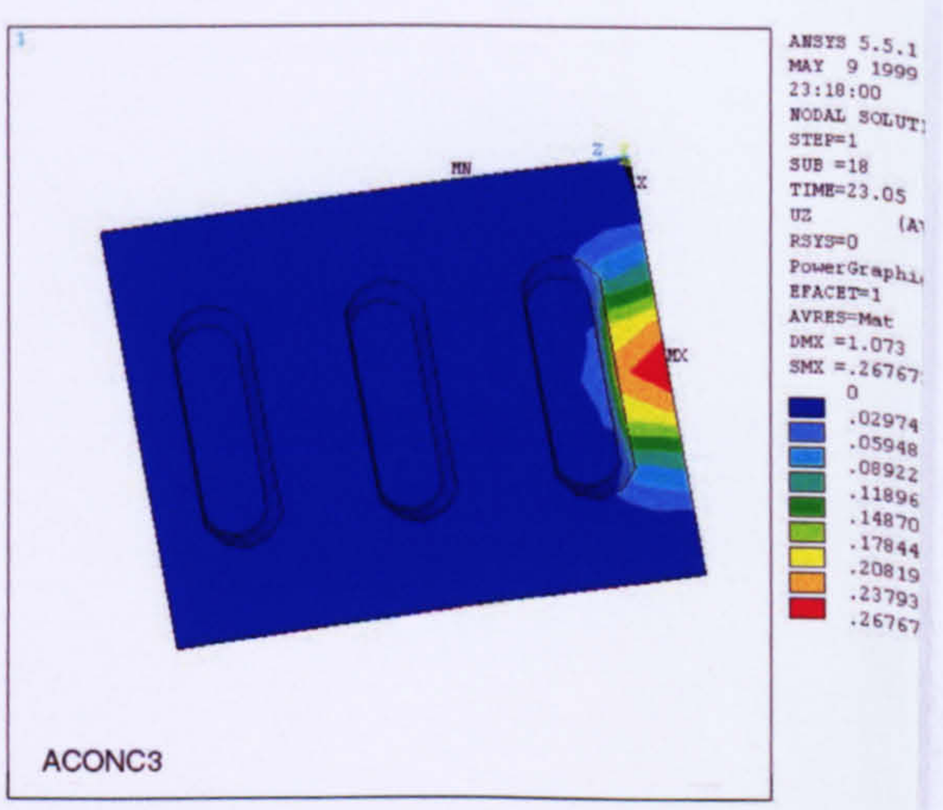

Figure 7.26.c

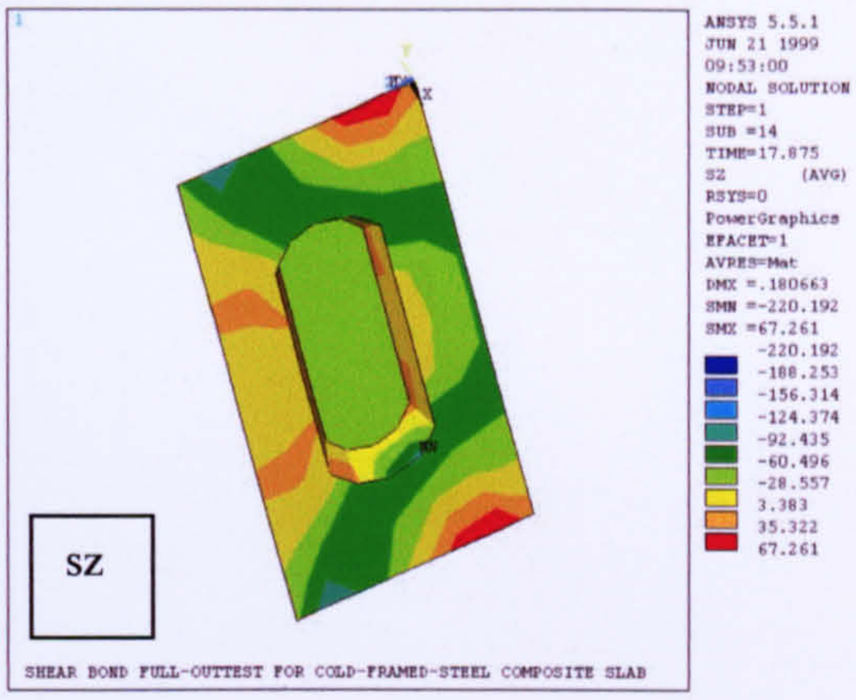

Figure 7.27.a Steel plate stresses

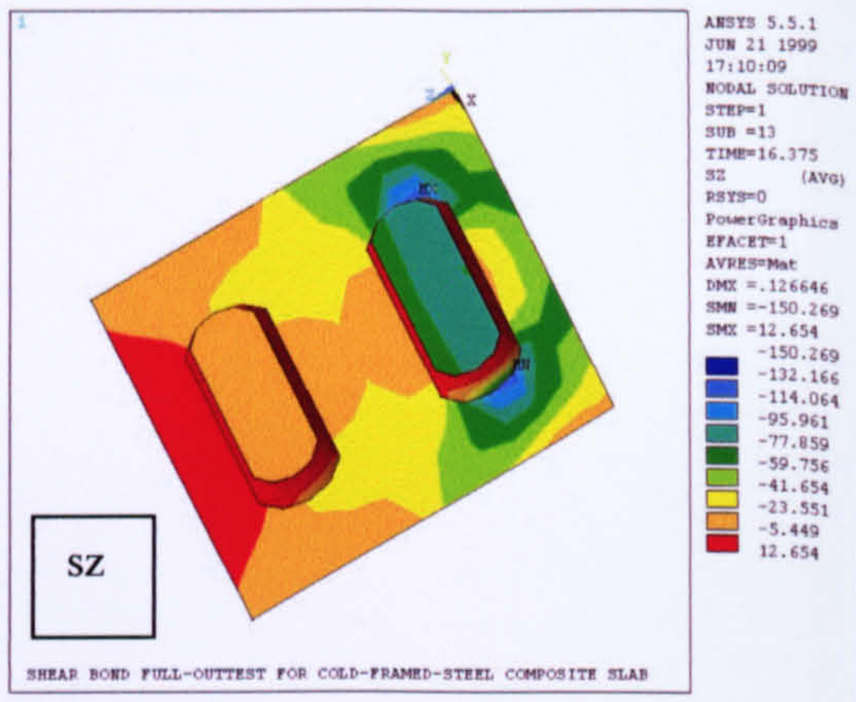

Figure 7.27.b Steel plate stresses

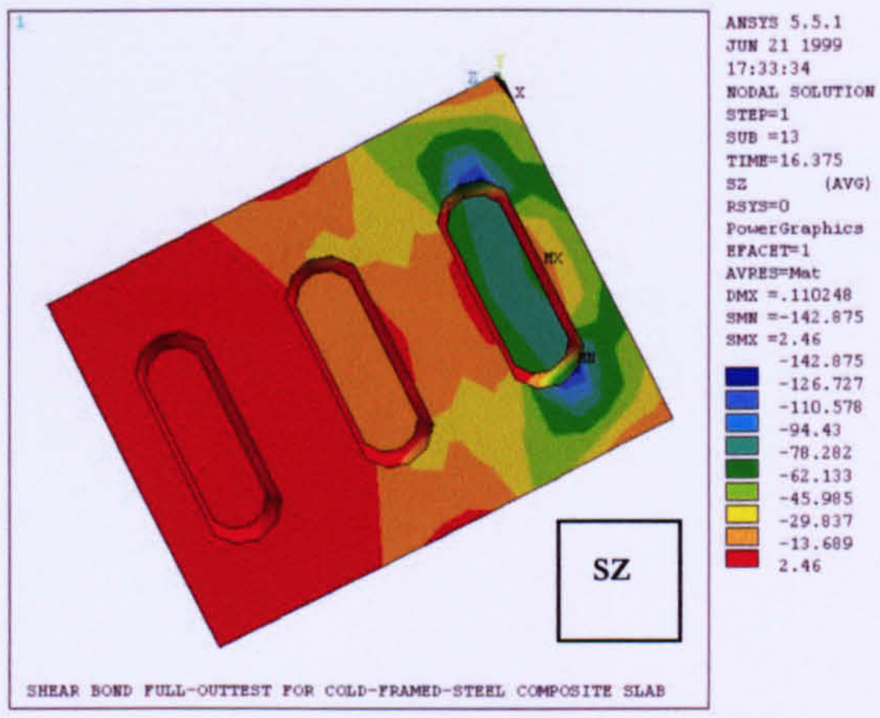

Figure 7.27.c Steel plate stresses

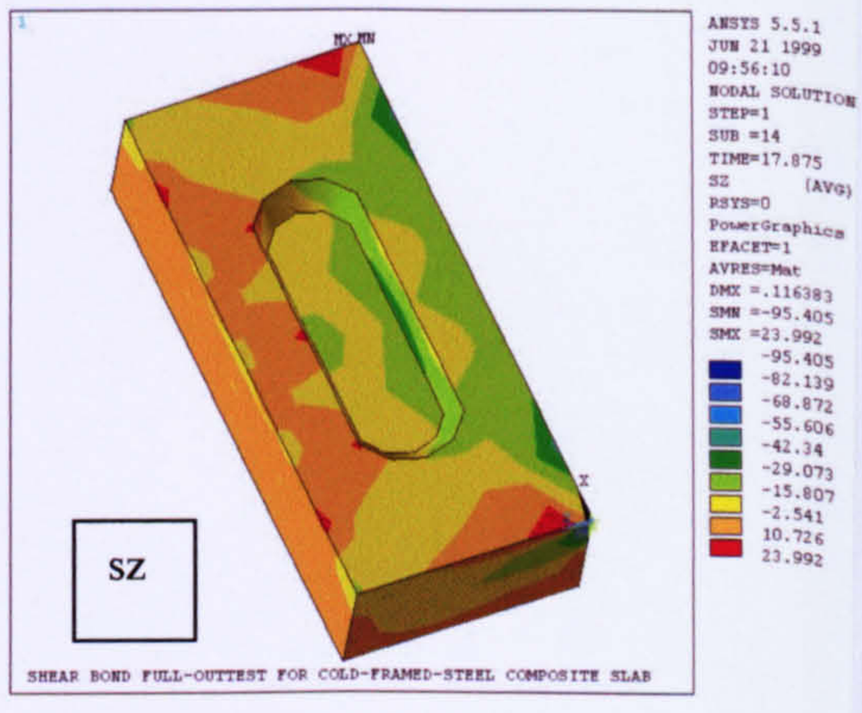

Figure 7.28.a Concrete stresses

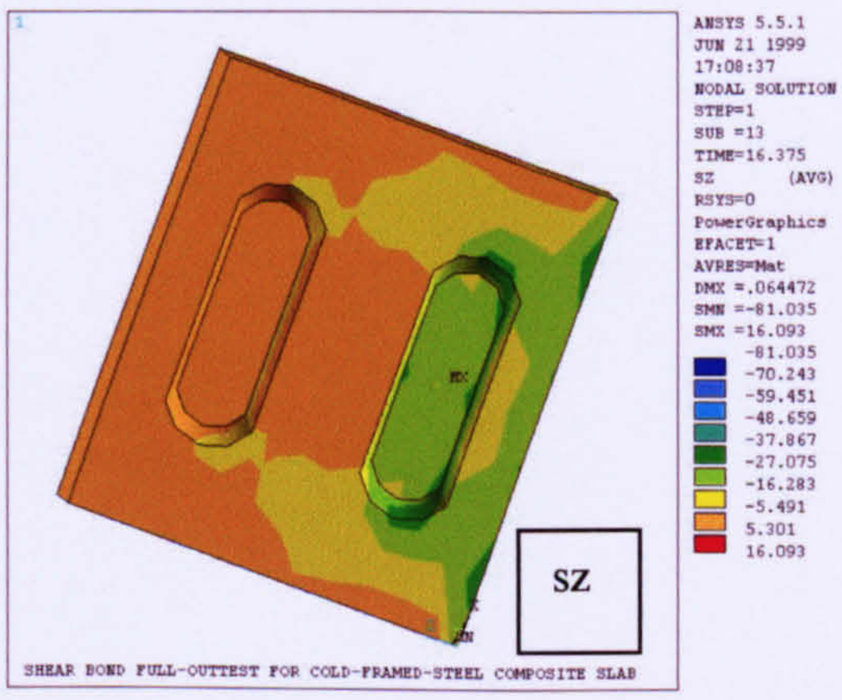

Figure 7.28.b Concrete stresses

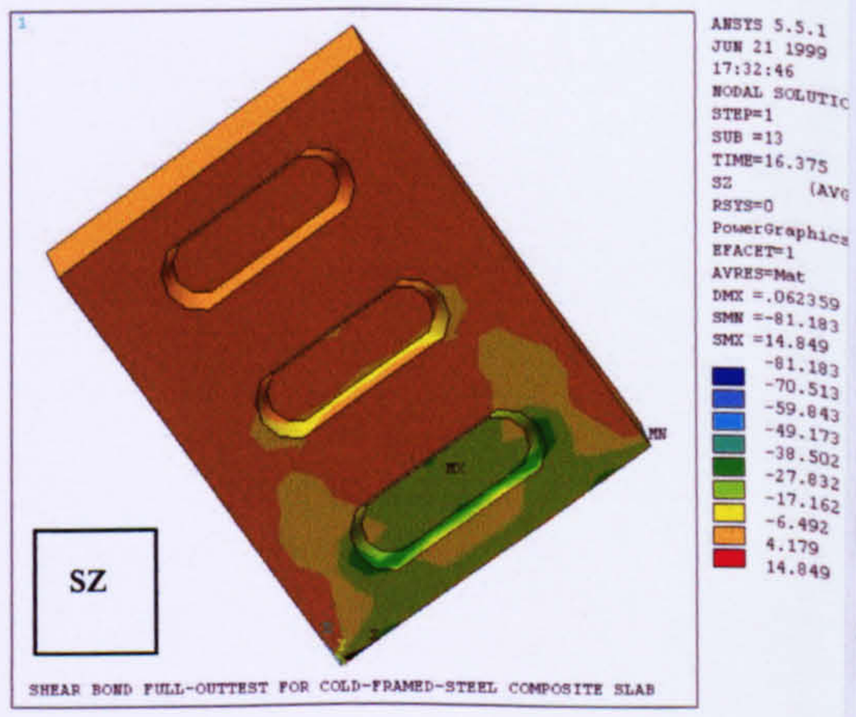

Figure 7.28.c Concrete stresses

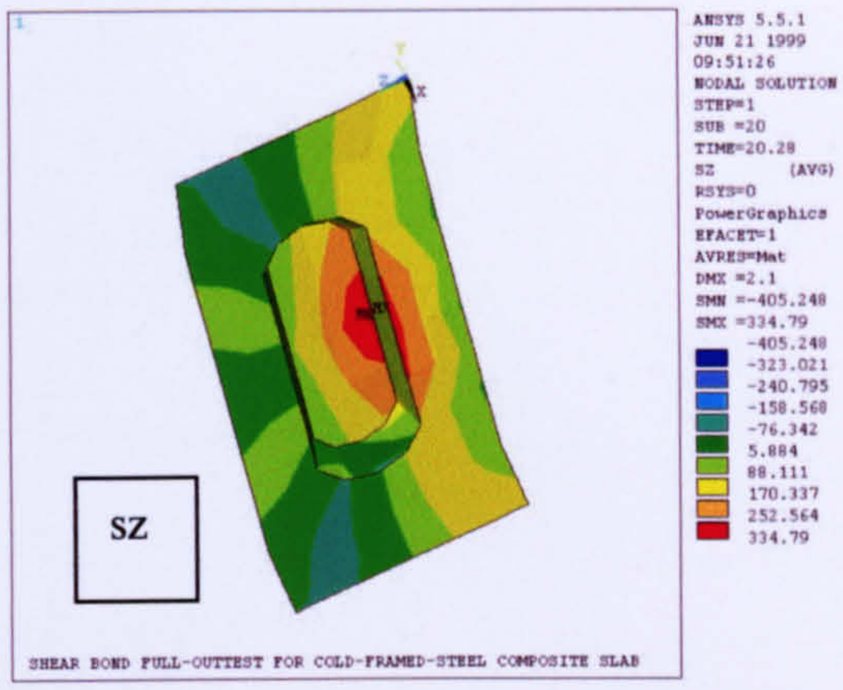

Figure 7.29.a Steel plate stresses

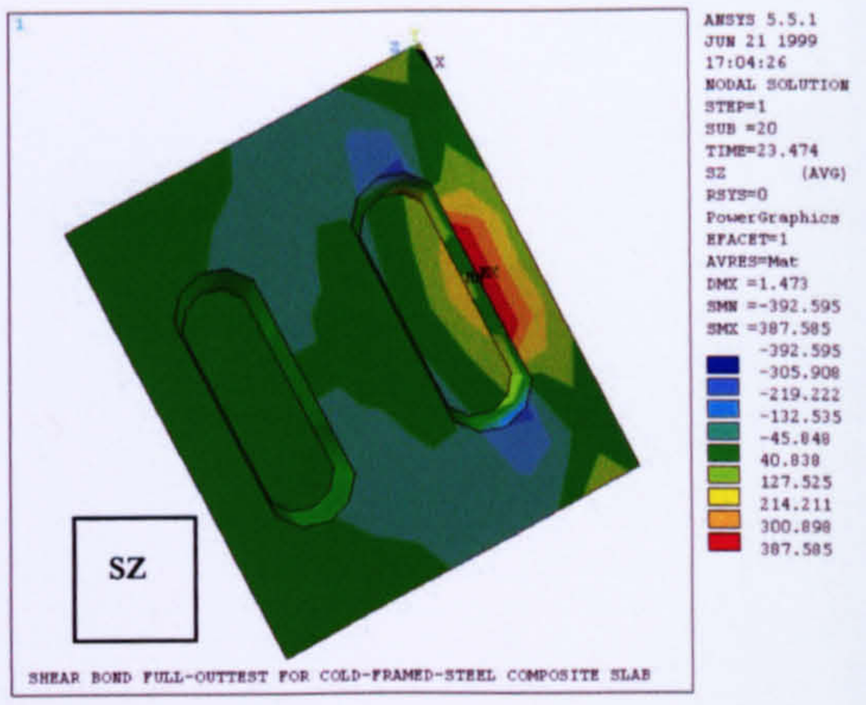

Figure 7.29.b Steel plate stresses

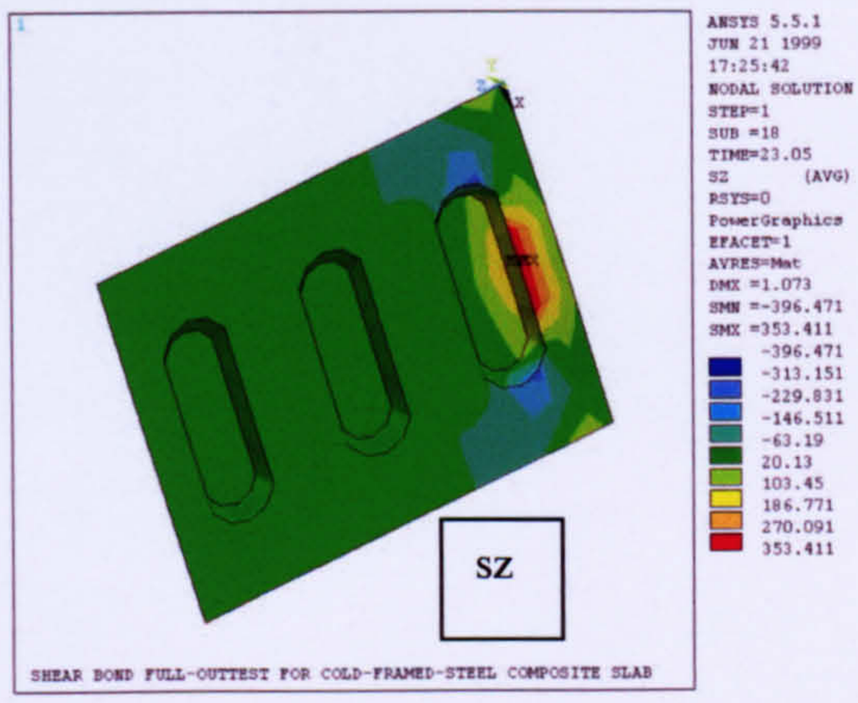

Figure 7.29.c Steel plate stresses

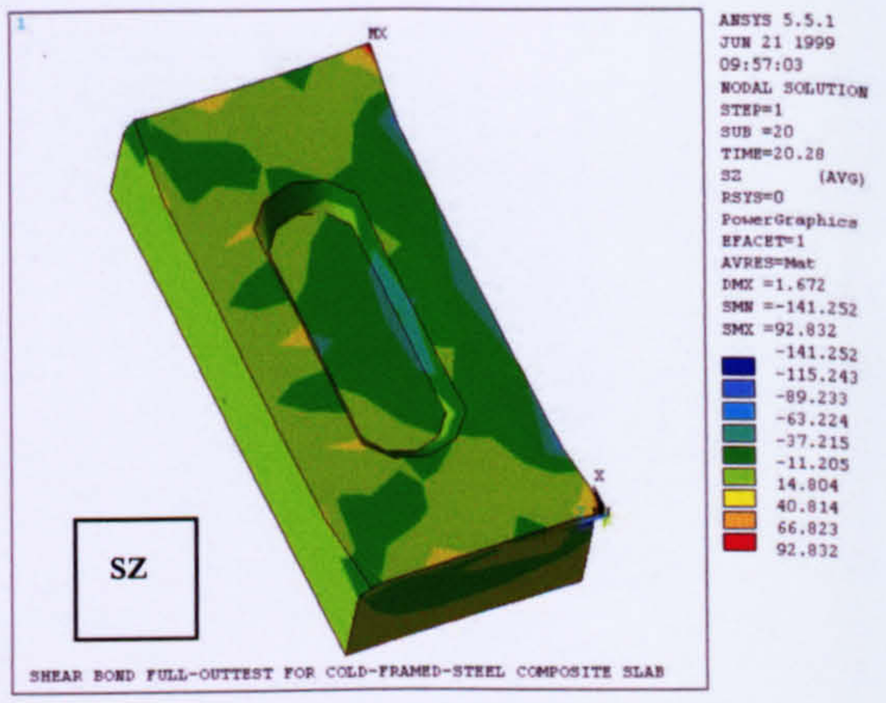

Figure 7.30.a Concrete stresses

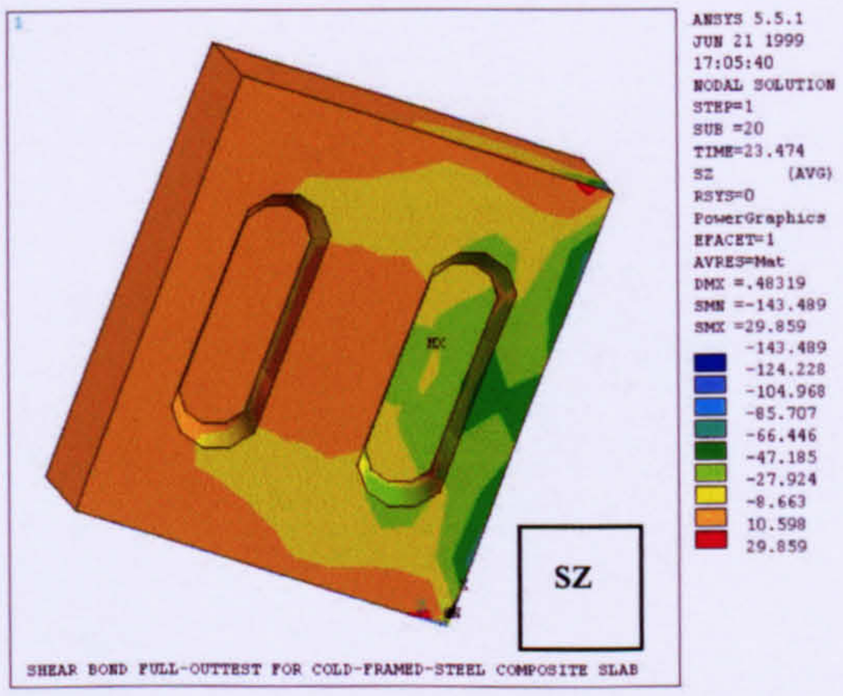

Figure 7.30.b Concrete stresses

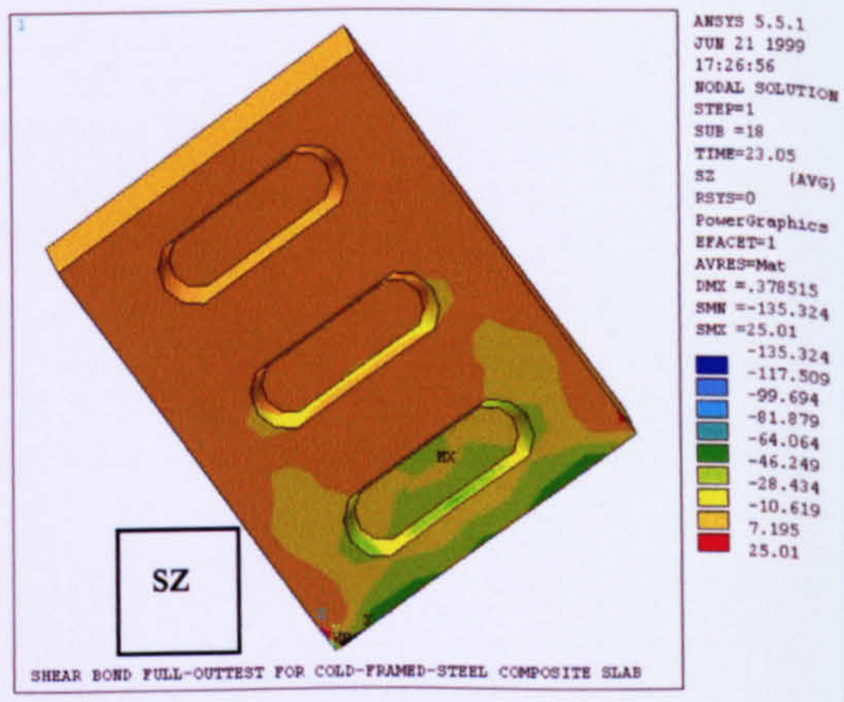

Figure 7.30.c Concrete stresses

Figure 7.31 Comparison of applied load versus deflection for various numbers of embossments.

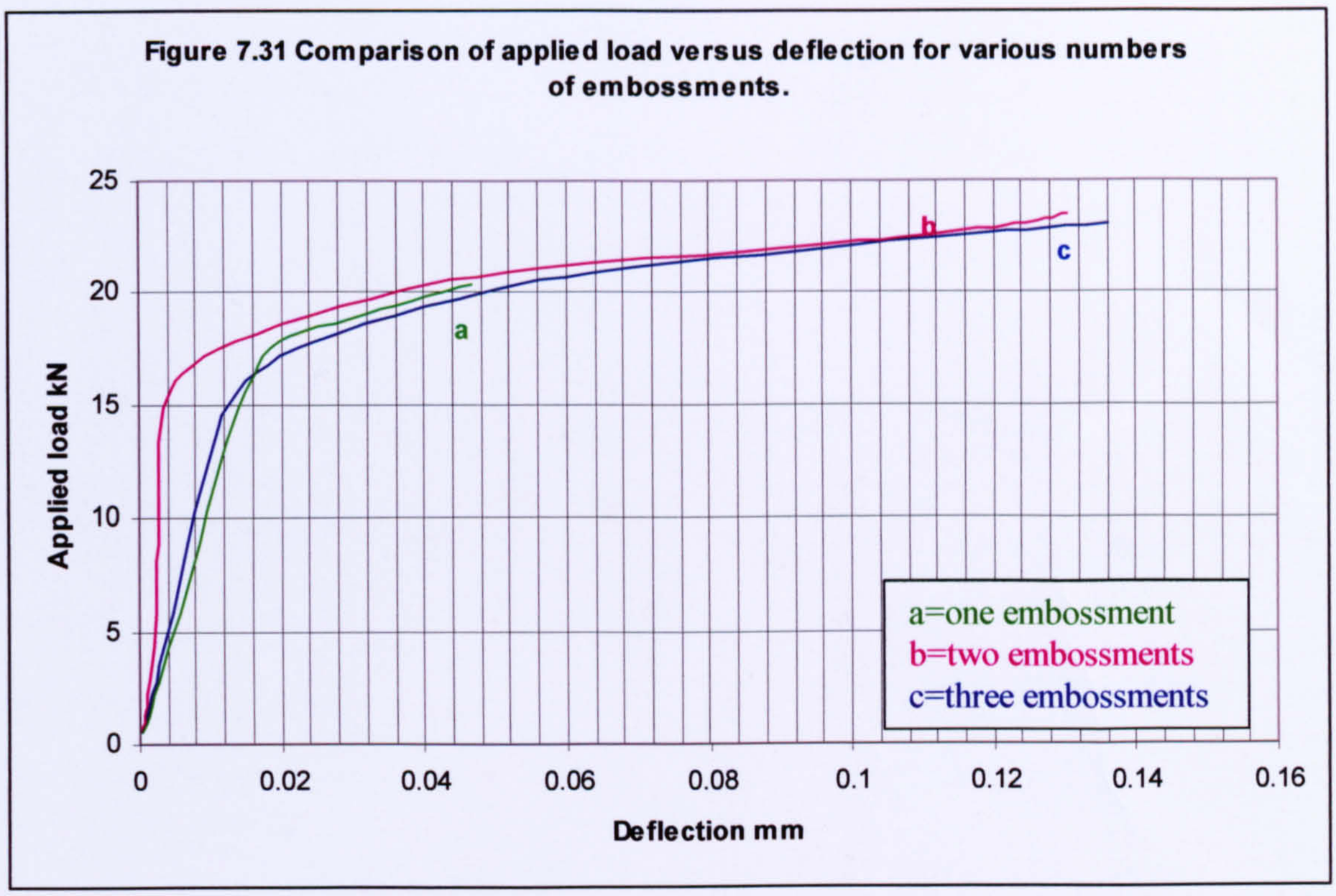

Figure 7.32 Comparison of applied load versus longitudinal slip for various numbers of embossments.

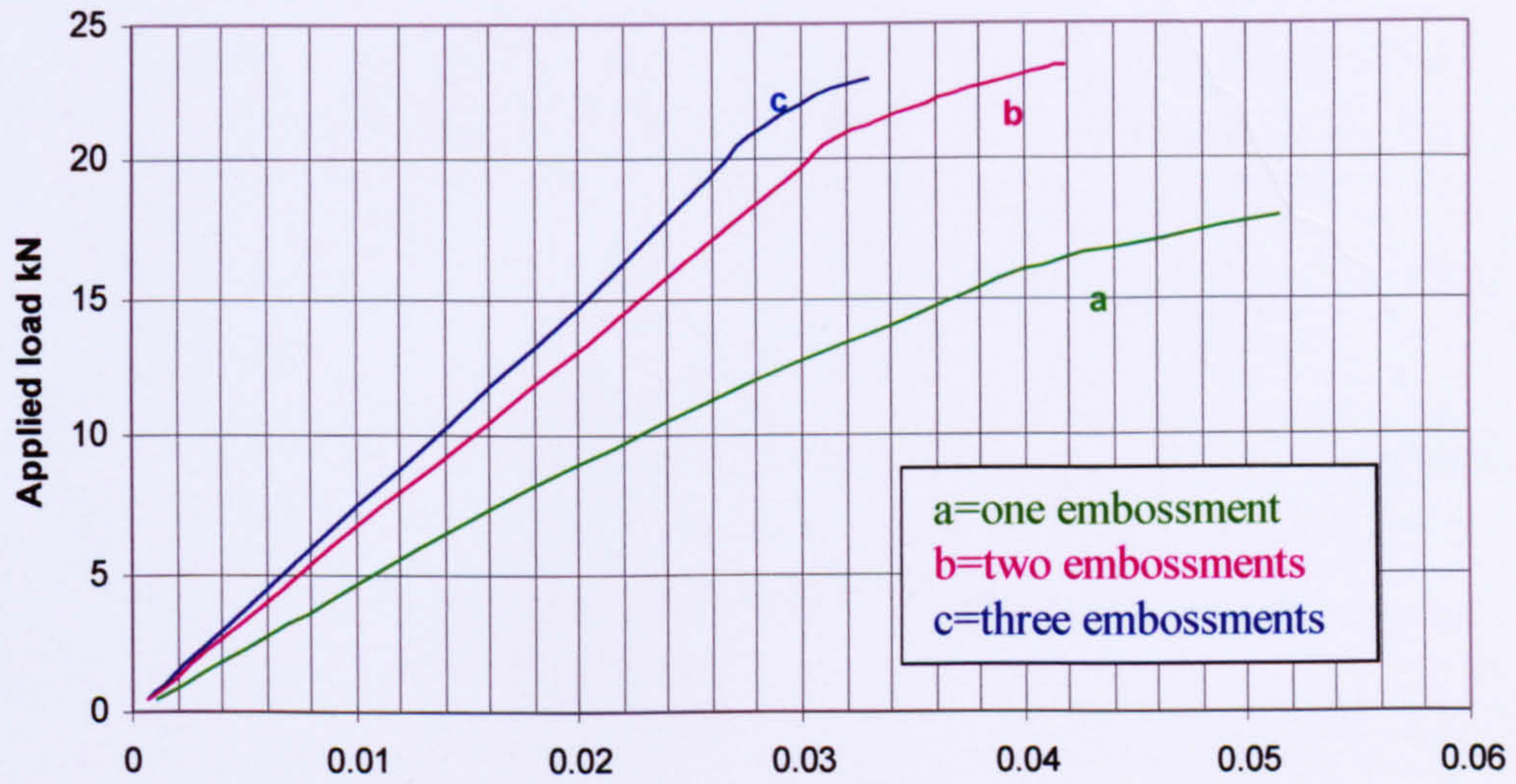

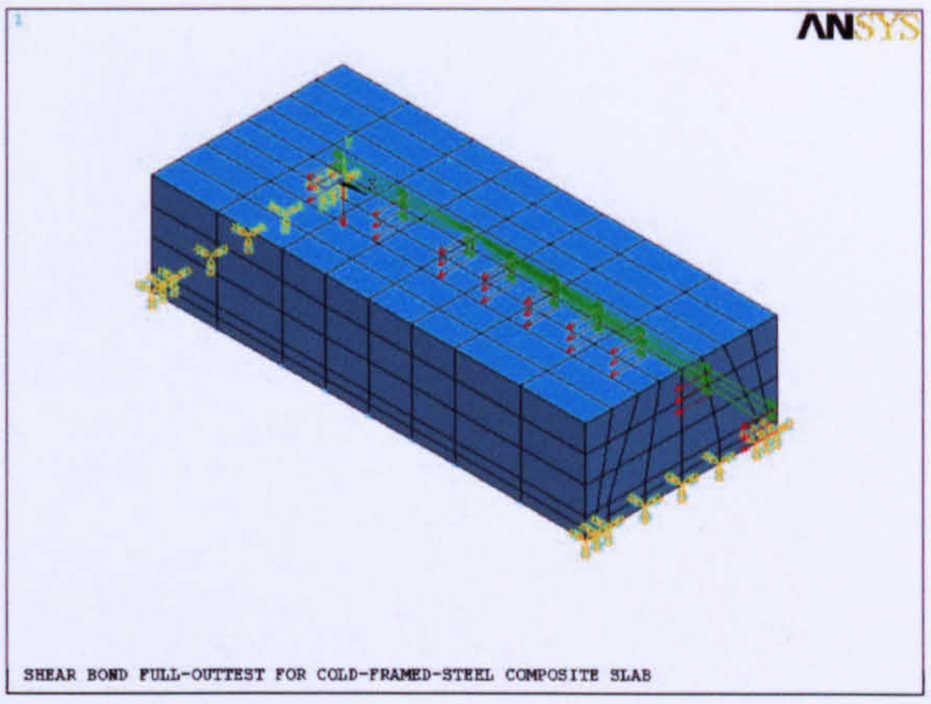

Figure 7.33.a

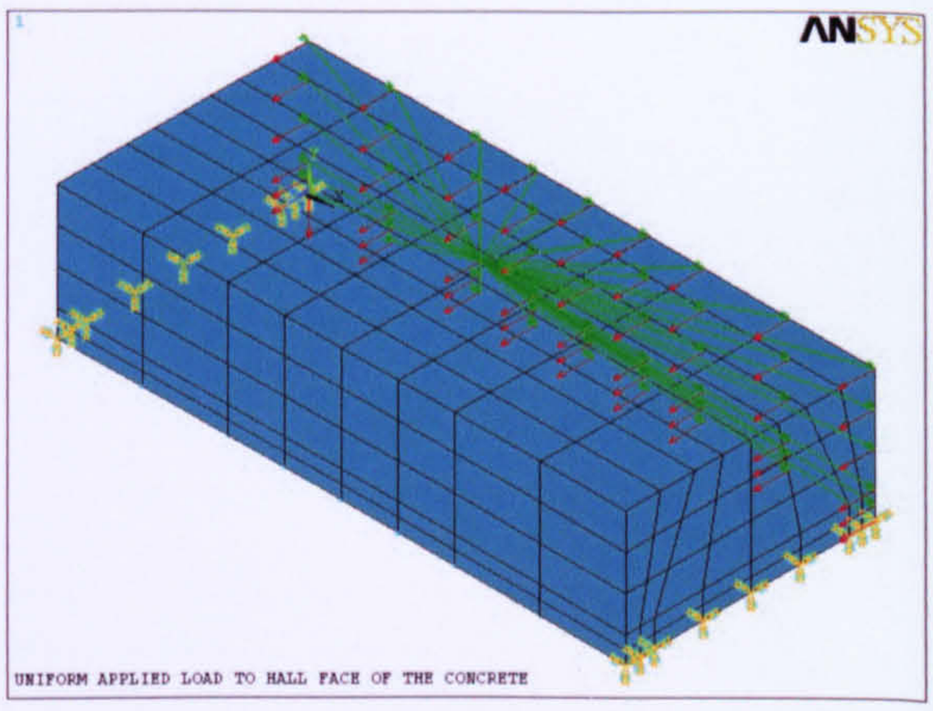

Figure 7.33.b

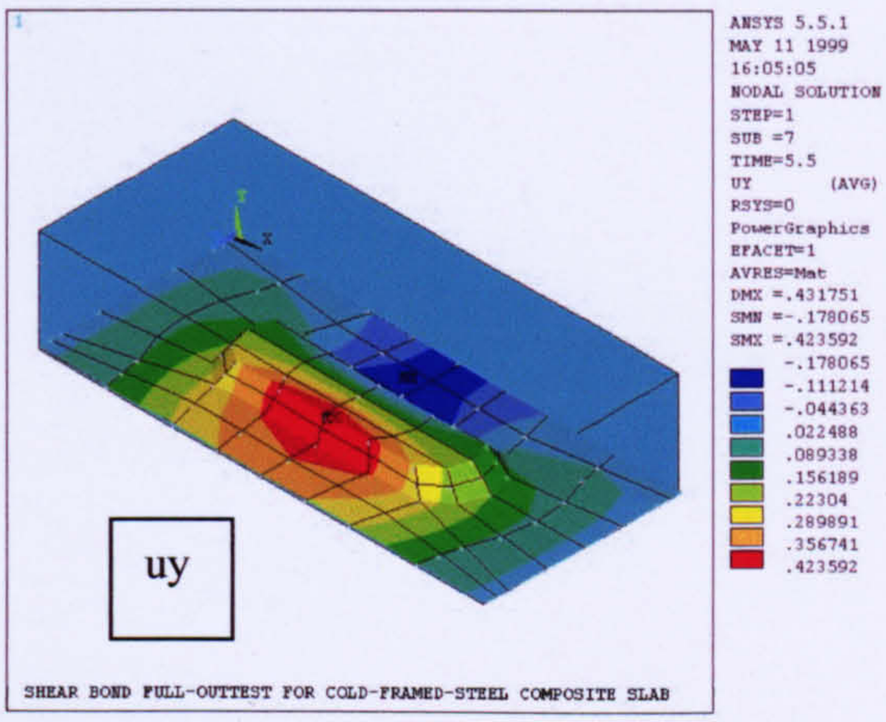

Figure 7.34.a

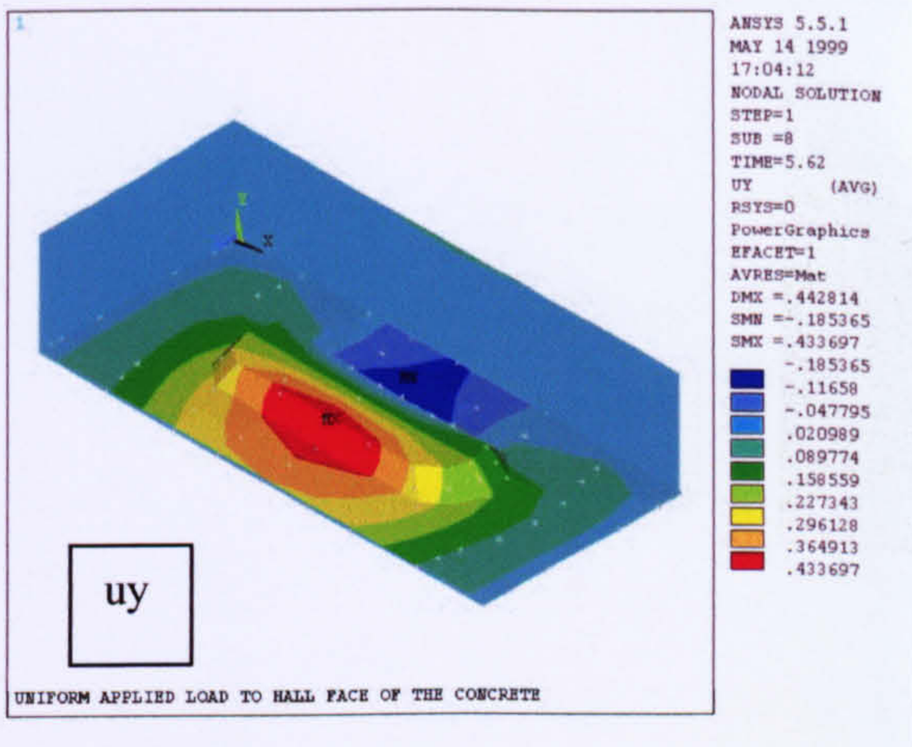

Figure 7.34.b

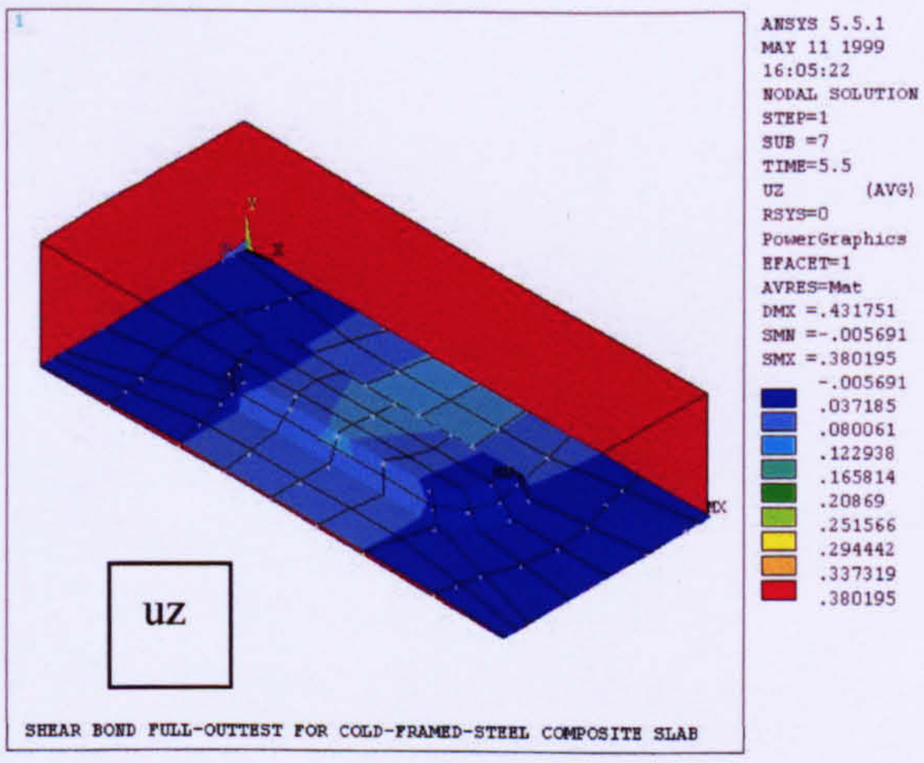

Figure 7.35.a

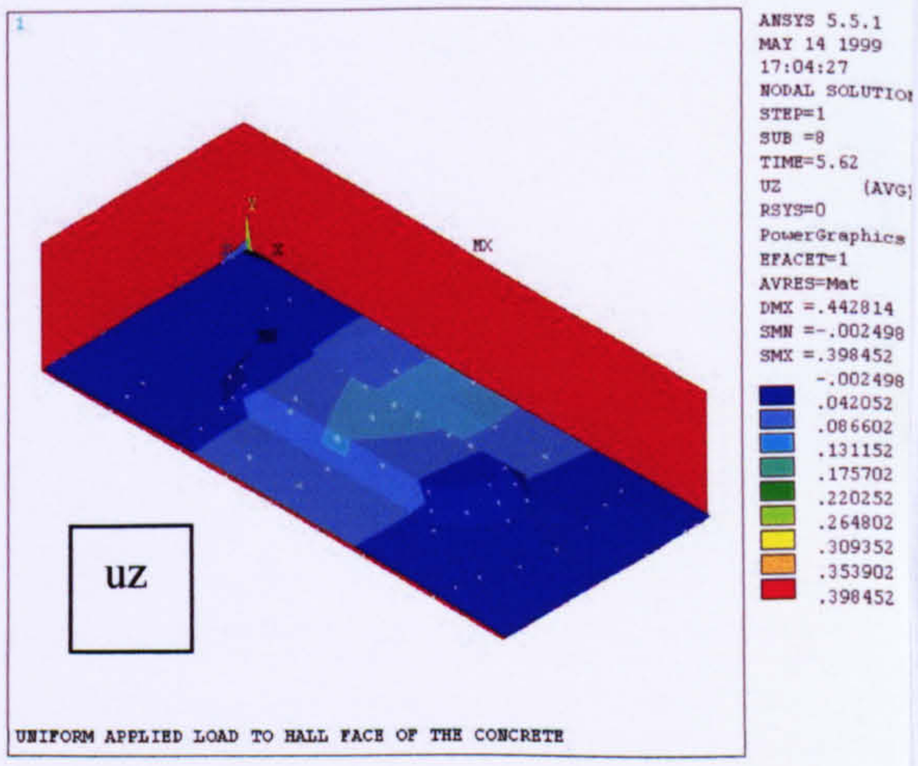

Figure 7.35.b

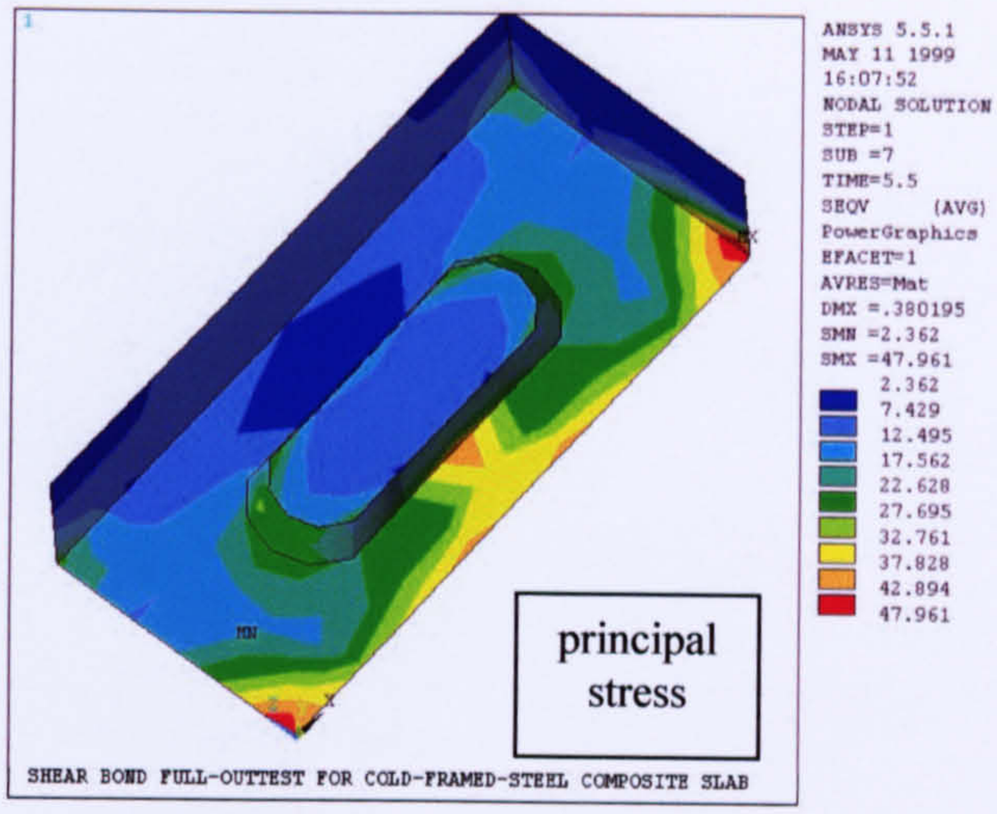

Figure 7.36.a

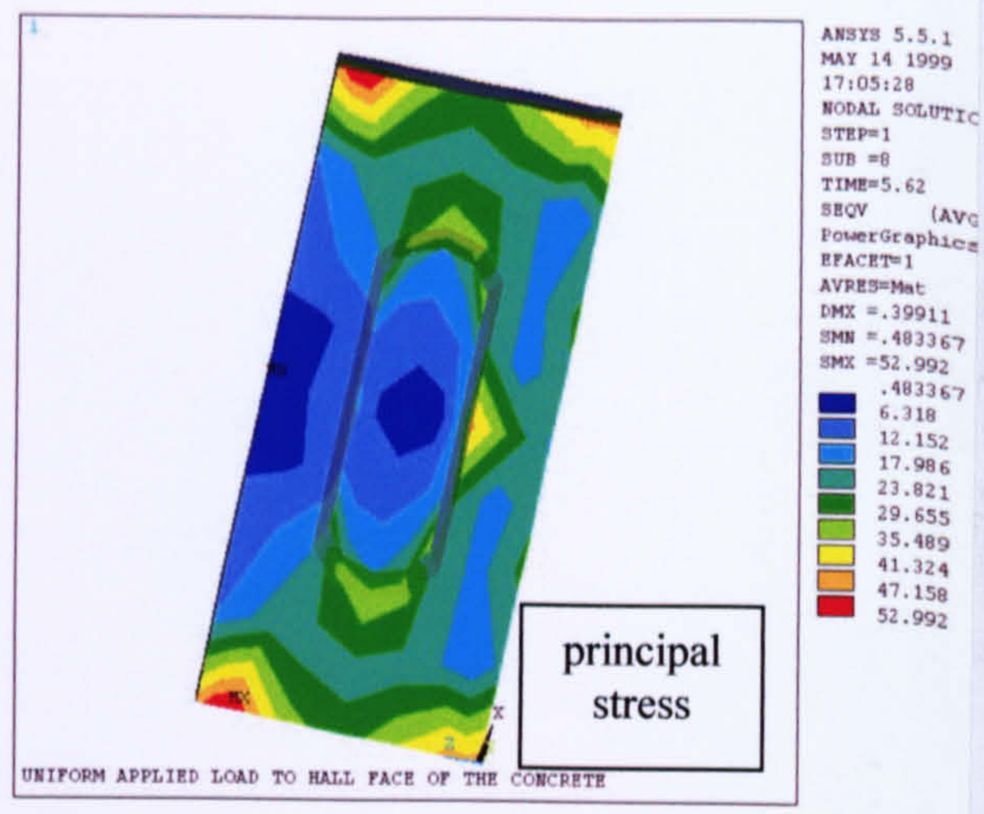

Figure 7.36.b

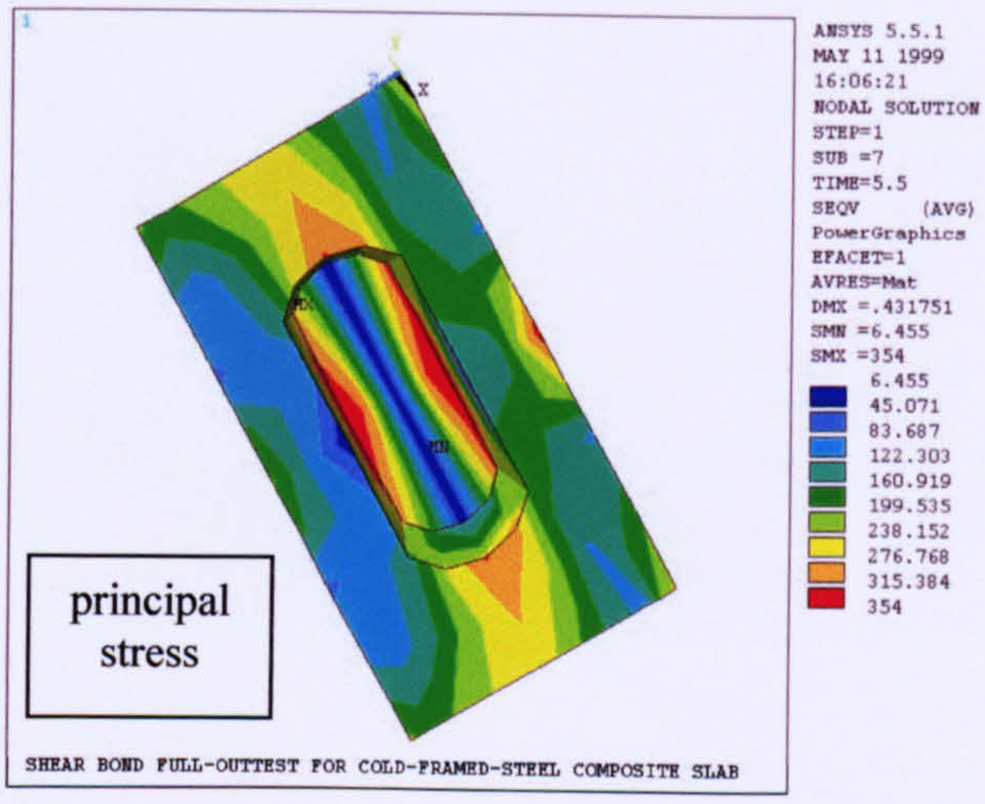

Figure 7.37.a

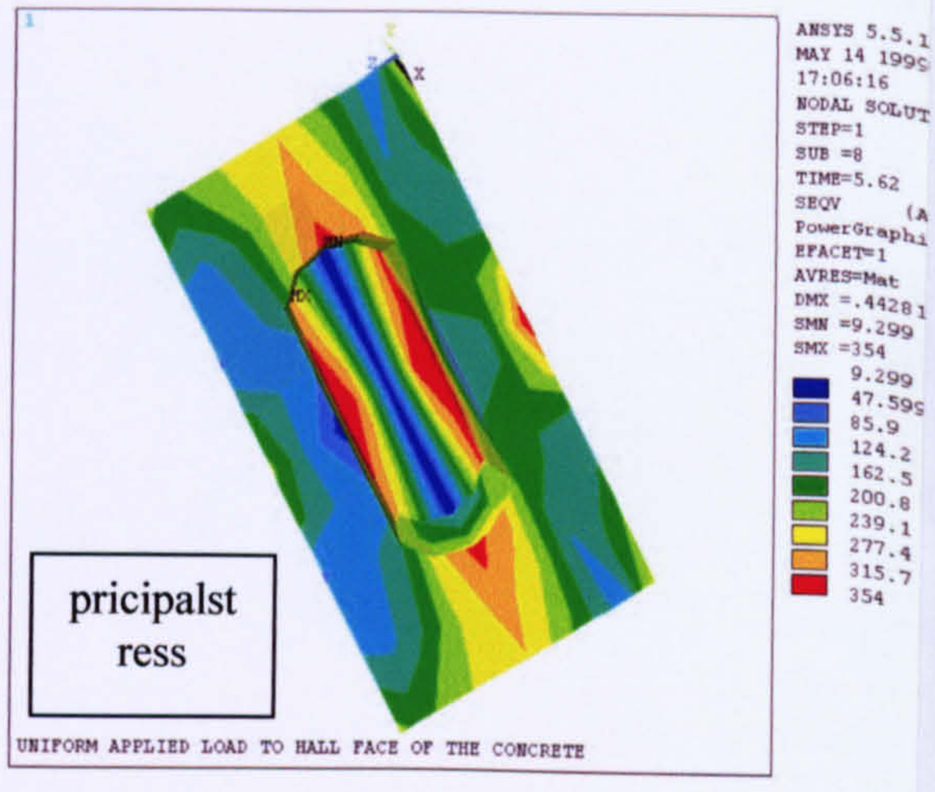

Figure 7.37.b

Chapter Eight

Review, Conclusions and Future Work

8.1 Introduction

Through experimental studies and finite element simulations, the performance of profiled composite slabs has been examined. The major factor affecting the behaviour involve the shear-bond characteristics at the steel/concrete interface.

The experiments included small-scale (push-off, and pull-out tests) for two arrangements of profiled steel sheeting Two tests, for each arrangement were carried out, one push-off, and the other pull-out test. Nine full-scale composite slabs were tested, with various spans and concrete thicknesses.

Push-off and pull-out specimens were simulated using the 'ANSYS' finite element program. Subsequently, the numerical modelling was extended to cover different aspect ratios, and embossment numbers for the profiled steel sheet (three different geometries for the profiled steel sheeting with and without a concrete slab). Different interface elements available in the 'ANSYS' programme were used. The composite slabs were also modelled in three dimensions.

8.2 Summary of research and main conclusions

8.2.1 Introduction

Composite construction with profiled steel sheeting was introduced in Chapter One and the general advantages of composite construction were highlighted including the reduced construction time, the action of the profiled steel sheeting as formwork and main reinforcement, easier services, stability and weight reduction. The different types of thin profiled steel sheeting and their geometric details (embossments, re-entrant portions and stiffness) were also briefly described. The different components of shear-bond; chemical adhesion, friction and mechanical interlock, were defined.

The mechanical interlock component (through the effect of embossments and the re-entrant portions) was defined as being critical to the shear-bond behaviour.

8.2.2 Shear-bond in composite construction

The shear-bond equations used for profiled composite slabs were discussed in Chapter Two. Chapter two contains a general review of shear-bond strength in conventional reinforced concrete and composite beams. Also, it contains a detailed review of shear bond equations for profiled composite slabs for which there are similarities and differences with shear bond behaviour in the common form of composite construction. The two most frequently used design methods for composite slabs; namely the m-k method and the partial interaction method, are reviewed and compared.

None of the previous shear-bond equations has any parameter relating to embossments or the geometry of the profile steel sheeting. More experimental and numerical studies were seen to be required to include the effect of the embossments. By including the effect of steel geometry and the embossments, there will be an improved chance of developing a general numerical formula for shear-bond strength of composite slabs.

8.2.3 Push-off and pull-out tests

The pull-out test used for determining the bond resistance of reinforcing bars in conventional reinforced concrete was reviewed. Also, different push-off tests used for composite beams and composite slabs were briefly presented and discussed. A push-off, and pull-out test presented by the author was used to study the effect of both the embossments and the re-entrant portions in the shear-bond capacities for one type of profiled steel sheeting. The small test presented was used to determine the coefficient of friction between the steel sheeting and the concrete.

The results from the small tests provide a very clear indication of the effectiveness of the re-entrant profile in enhancing the shear bond strength of the profile. The work

also indicates the value of re-entrant shape in providing interlock and the relative properties of the re-entrant should be investigated further.

The results in chapter three (small-scale tests) showed no significant difference between pull-out and push-off tests. A more reproducible value of frictional coefficient (with a closer linear relationship between longitudinal and vertical load) was obtained in the push-off test as opposed to the pull-out test. The push-off test easier to conduct, control and set up. Therefore, the push-off test is recommended with full-encasement of the portion of the profiled steel sheet, which is identified as being the primary factor in shear transfer. For this sheet it was evidently the re-entrant dovetail. For other profiles in which contribution is not clear it is recommended that the full sheet width be included in the test.

Push-off, and pull-out tests are relatively quick, simple and economical to apply, and can yield essential information about the shear connection performance of profiles with very different characteristics. Adhesion bond, mechanical interlock and friction can collectively contribute toward the total longitudinal slip resistance of a profile and can be separately identified using the test. In particular, parametric values determined from the test can be used directly in a physical model using partial shear connection theory, which accurately predicts the strengths of slabs. The test can therefore complement a test program involving full-scale slab tasting. The results of the small-scale tests were used in predicting finite element modelling in chapter six. In addition small-scale tests can be used as an early indication of potentially poor shear bond capacity in a new profile which could give opportunity to either improve the profile or cut the cost of expensive full-scale testing.

Further work to be done in this field of study includes further modelling of embossment shapes, the influence of steel thickness, and the effect of local profile geometry on the stiffness/flexibility of the embossments, which provide the mechanical key.

8.2.4 Full-scale tests

Chapter Four describes the history of composite slab development, with special reference to the research undertaken to predict their behaviour. There is a well-documented database, from which the behaviour and maximum load-carrying capacity may be predicted by calculation based on previous test information of each individual profile type. The deformation of the sheeting, together with the slip between the concrete and the sheet is considered, and the behaviour of the shear connection is also investigated.

Sections 7, 10 and Annex E in Eurocode 4 standards for composite slab construction are considered and a study has been made of the design methods which are available (the m-k and the partial connection method). Current design codes and specifications use the shear-bond model for predicting the strength of simply-supported composite slabs and relies on testing to either determine a regression line which is used in the design method, alternatively or the permissible longitudinal shear strength.

All codes require testing of slabs with a particular profile to cover the full range of the design parameters, e.g. span, shear span, gauge thickness, depth and concrete strength. A series of full-scale composite slabs (nine full-scale composite slabs, with ComFlor 70 profiled steel sheet) were tested in the Structures Laboratory at University of Salford to provide experimental evidence for these studies.

The data and calculations obtained from this chapter were used to model the composite slab behaviour using Finite Element Analysis soft ware (ANSYS), and the results obtained from the experimental work compared with the Finite Element results in chapter six.

The full-scale composite slabs were tested to failure under two concentrated line loads. Early end-slip before reaching the ultimate load occurred in all the slabs but nevertheless, ductile behaviour was observed in the slabs. The tests showed differences between the slabs with and without additional reinforcement, together with the effect of the depth and span of the slabs. The loss of interaction between the steel sheet and the concrete occurred gradually in the tested slabs.

The test results were evaluated by the m-k method and with the partial connection theory in EC4.

Recalculation of the shear strength of the composite slabs was then carried out by both methods. The comparison of the calculated strength with measured maximum load was expressed by a model factor for both methods. This factor indicated the safety margin in the calculations of the strength. It appears that the safety factor by the m-k method was at the same level for this group of slabs, but the results were more scattered for the partial connection theory. A further overall factor was calculated using both methods which gave the ratio of the failure load to the predicted maximum load from the design procedures making all partial factors unity. In both cases the margins were satisfactory.

The main conclusions from testing nine composite slabs with profiled steel sheeting under static and dynamic loading were:

1. Both methods of design (m-k method and Partial Shear Connection method) are satisfactory in predicting the design capacities of the slabs.

2. Testing under static and dynamic loading gave information on the behaviour of composite slabs after breakdown of chemical bond between steel and concrete. This enabled comparison to be made between the behaviour under test and the predicted behaviour given by the finite element modelling.

3. The use of additional reinforcing bars increases the load carrying capacity and ductility of the slabs. Moreover, it decreases the cracks in the tension zone of the composite slab. The "reinforced" and "composite" behaviour was compatible allowing the two capacities to be considered separately.

4. All slabs exhibited signified end slip before reaching the failure load.

5. All slabs reached deflections close to span/50 before failure.

6. The difference between the full-scale and the small-scale values of the shear stress is significant and requires further study. The curvature experienced in the full-scale test may enhance the longitudinal shear resistance and this together to the manner of load application and differences between test format could give rise to these differences.

The form of failure for all the composite slabs (without additional reinforcement) was longitudinal shear. This is confirmed in Table 4.6.a indicating for those slabs that, M_{test} was lower than the ultimate flexural capacity, $M_{p,Rm}$, leading to a range of η_{test} between 0.58 and 0.75.

8.2.5 Modelling of composite slabs

Composite steel-concrete construction allows designers to take advantage of the most favourable mechanical material properties of both steel and concrete, to produce economical structures.

In Chapter Six, a method is described for the calculation of behaviour of composite floor slabs. The method mainly uses the ANSYS finite element to provide the solution to such problems.

Material and interaction properties have been determined from standard and originally designed tests. Plasticity of the concrete, non-linear shear resistance, and friction at interface between concrete and sheeting are included in the numerical model.

The finite element (FE) model developed used a combination of element types from the ANSYS library in order to model the composite slab. Three-dimensional Solid Elements were used to model the concrete, and Strain Shell element was used to model the profile steel sheeting.

The composite action was completed by connecting together each of Solid and Shell Elements with 3-D Point-to-Point Contact Element and Combination Element.

The non-linear analysis of composite slab structures using ANSYS has been investigated in order to examine the capability of ANSYS in dealing with composite slab structures. The procedure was to study a series of problems with different thickness and different dimensions, demanding the accuracy of the behavioural models used in the analysis.

The problems examined demonstrate that the existing program capability is adequate to model behaviour of composite slab structures.

Further information can be obtained from the use of ANSYS. Besides the deflection in each node and stress strain in each element, the shear stress distribution along the slab in the horizontal direction, and further information for instance elastic strains,

equivalent stress, stress, average plastic strains, average equivalent plastic strain can be obtained.

Testing under static and dynamic loading gave information on the behaviour of composite slabs after breakdown of chemical bond between steel and concrete. This enabled comparison to be made between the behaviour under test and the predicted behaviour given by the finite element modelling.

The use of the contact stiffness from the small-scale tests modified by between –5% and 7% provides a reasonable agreement between the experimental and theoretical values. This variation may be partly explained by the failure of the small tests to fully represent the full-scale behaviour. Contributory factors to this may be the lack of curvature in the small-scale test together with effects such as load distribution and the secondary benefit, which may arise from mesh reinforcement in the full scale-test.

8.2.6 Finite element modelling of embossments

Finite element modelling was used to study the behaviour of embossments as shear-connecting devices in three-dimensions. Profiled steel sheeting only, and profiled steel sheeting and concrete were modelled with different interface elements using the 'ANSYS' finite element programme.

One set of boundary conditions were assumed for a mesh with embossment as a simple example in 3-dimensions to predict its real behaviour in the experimental work.

The effects of the aspect ratio and an increasing number of embossments subjected to horizontal forces applied to one face of the embossments have been studied.

The embossments are most effective in the stiffer regions of the profile where the plate widths are smallest.

Two models have been studied for the effect of load position either on the whole face of the concrete or at the level of the embossment.

Further work to be carried out includes:

- Different boundary conditions in the profile local to the embossment.
- Different shapes of embossments including trapezoidal, circular, inclined and chevron types.

- Arrangements of embossments and the effects of different loading profiles.

8.3 Recommendations (for future work)

For the small-scale tests it would be useful to carry out future tests to study the following:

a- Identical profiled steel sheeting with different steel thicknesses.

b- Identical profiled steel sheeting with same embossment geometry but with different heights.

c- Various positions (webs, flanges or troughs) for an identical embossment geometry,

d- Varying embossment shapes.

e- Different geometry of profiled steel sheeting with same embossment.

The results of push-off and pull-out tests may be used to present a numerical equation which include the geometry of both steel sheeting and embossments.

For composite slabs with reinforcement the m-k procedure required extra analysis to allow for the presence of the reinforcing bars. The capacity of the reinforced concrete slab was used to determine the contribution of the composite slab to the ultimate shear obtained in the test. From these tests it would appear that additional reinforcement could be used to increase the capacity of composite slabs without the need to carry out additional tests.

In order to further study the analytical and experimental behaviour it would be interesting to carry out further full-scale tests to determine the strain distribution in concrete and profiled steel sheeting close to steel/concrete interface. These tests could include the size and portion of the re-entrant or other feature in the profile.

The difference between the full-scale and the small-scale values of the shear stress is significant and requires further study. The curvature experienced in the full-scale test may enhance the longitudinal shear resistance and this together to the manner of load application and differences between test format could give rise to these differences.

Further study for the small-scale tests to be carried out including the possibility of applying curvature similar to that of the full-scale tests.

Finite element modelling needs more study and new interface elements should be developed to represent the complex behaviour of the steel/concrete interface in composite slab construction (full-scale, small-scale, and embossment behaviour). Other software as "ANSYS the new version" or "ABAQUS" is being developed, will result in an improved ability to deal with complex problems. This study has demonstrated the power of finite element analysis to represent the composite behaviour of concrete and the complex form of the profile steel sheeting, which is being continually developed into more efficient forms. The ultimate objective with improved finite element packages and faster computers with large memories will be to model the full-scale composite slab, which will enable all the primary parameters to be studied together.

References

1. Lawson, R. M.: 'Design of Composite Slabs and Beams with Steel Decking' The Steel Construction Institute, 1989.
2. Crisinel, M.: 'Composite Slabs' European Steel Design Education Programme, Working Group No.10, Lecture No.9, August 1991, Switzerland.
3. Davies, C.: 'Steel-Concrete Composite Beams for Buildings' George Godwin Limited, Ref No. ISBN 0711449066, 1975.
4. Zubair, A.K.M.: 'Improvement of shear-bond in composite steel and concrete floor slabs'. Ph.D. Thesis, Civil Engineering Dept., University of Southampton, 1987, UK.
5. Evans, H.R. and Wright, H.D. 'Steel-concrete composite flooring deck structures'. In Steel-concrete composite structures: Stability and Strength. Edited by R. Narayanan, Elsevier Applied Science, London and New York, Ch. 2. pp. 21-52,1988.
6. BS5950: Part 4. 'Code of practical for design of composite slabs with profiled steel sheeting'. British Standard Institution, London,1994.
7. DD ENV Eurocode 4 (1994). 'Design of Composite steel and Concrete structures'. Part 1.1. General rules and rules for buildings (with UK. National Application Document). British Standards Institution. London.
8. Mathys, J.H. 'The current scene: multi story steel buildings a new generation'. The Structural Engineer, 1987, Vol. 65A, No. 2, pp. 47-51.
9. Wright, H.D. and Evans, H.R. 'Observations on the design and testing of composite floor slabs'. Steel Construction Today, 1987, No. 1, pp. 91-99.
10. BS 5950; Part 4. Code of Practice for design of composite slabs with profiled steel sheeting. British Standards Institution London, 1982.
11. Eurocode 4 Part 1.1. 'Design of Composite Steel and Concrete Structures' Ref. No. prENV 1994-1-1: 1992, April 1992.
12. Duffy C., O'Leary D. 'Full-Scale load tests on Composite floor slabs using indented steel sheeting'. University of Salford, January 1977.

13. O'Leary D. 'Shear-Bond Capacity tests for QL 59 Composite slabs'. University of Salford, Department of civil Engineering, 1984.
14. Naway, E.G. 'Reinforced Concrete: a fundamental approach'. Prentice Hall, Englewood Cliffs, New Jersey, 1990, Ch. 10, pp. 376-418.
15. Abrishami, H.H. and Mitchell, D. 'Simulation of uniformed bond'. ACI Materials Journal, 1992, Vol. 89, No. 2, pp. 161-168.
16. Cairns, J. and Abdullah, R. 'Performance of epoxy-coated reinforcement at the serviceability limit state'. Proceedings of Institution of Civil Engineers-Structures and Buildings, 1994, Vol. 104, No. 1, pp. 61-73.
17. Carins, J. and Jones, K. ' The splitting forces generated by bond'. Magazine of Concrete Research.1995, Vol. 47, No. 171, pp. 153-165.
18. Hamad, B.S. 'Bond strength improvement of reinforcing bars with especially designed rib geometries'. ACI Structural Journal, 1995, Vol. 92, No. 1, pp. 3-13.
19. Essway M.I. 'Shear-bond in profiled composite construction' PhD thesis, Strathclyde University, 1996, UK.
20. Treece, R.A. and Jirsa, J.O. 'Bond strength of epoxy-coated reinforcing bars'. ACI Materials Journal, 1989, Vol. 86, No. 2, pp. 167-174.
21. Cleary, D.B. and Ramirez, J.A. 'Epoxy-coated reinforcement under repeated loading'. ACI Structural Journal, 1993, Vol. 90, No. 4, pp. 451-458.
22. Yan, C. and Mindess, S. 'Bond between epoxy-coated reinforcing bars and concrete under impact loading'. Canada Journal of Civil Engineering,1994, Vol, 21, No. 1, pp. 89-100.
23. Gambarova, P.G., Rosati, G.P. and Zasso, B. 'Steel-to-concrete bond after concrete splitting: test results'. Materials and Structures, 1989, Vol. 22, pp. 35-47.
24. BS8110: Part 1. 'Structural use of concrete': Code of practice for design and construction. British Standards Institution, London, 1985.
25. BS5950: Part 3: Section 3.1. 'Code of practice for design of simple and continuous composite beams'. British Standards Institution, London, 1990.

26. Loyd, R.M. and Wright, H.D. 'Shear connection between composite slabs and steel beams'. J. Construct. Steel Research, 1990, Vol. 15, pp. 255-285.
27. Johnson, R.P. and Anderson D. Designers 'handbook to Eurocode 4: part 1.1. Design of steel and composite structures'. Published by Thomas Telford, London.1993, Ch. 6, pp. 94-123.
28. Wright H D, Evans RA'A review of Composite Slab Design, Tenth International Specialty Conference. on Cold-formed Steel structures, St. Louis, Missouri, USA, 1990, pp. 27-47.
29. Easterling S.W. Young C.G., 'Strength of Composite Slab'. Journal of Structural Engineering. Vol.118, No 9, 1992, pp. 2370-2389.
30. Patrick M. 'A New Partial Shear Connection Strength Model for Composite Slabs'. Steel Construction, Australian Institute of Steel Construction, V61.24, Num 3, 1990, pp. 2-17.
31. Bode H., and Sauerborn, I. 'Modern Design Concept for Composite Slabs with Ductile Behavior.' Composite Construction in Steel and Concrete II, Proc. of Engineering Foundation Conference, Eds. W. Samuel Easterling and W.M. Klm Roddis, 1992, pp. 125-141
32. Patrick M.and Bridge R.Q. 'Partial Shear Connection design of Composite Slabs'. Engineering Structures. 1994, Vol. 16 Num. 5, pp. 348-362.
33. Bode H., Minas F., Sauerborn I. 'Partial Connection Design of Composite slabs'. Structural Engineering International, Journal of the International Association for Bridge and Structural Engineering (AIBSE), Vol. No. 1, 1996, pp. 53-56.
34. Johnson R.P. and.May I.M. 'Partial-interaction Design of Composite Beam'. The Structural Engineer No 53, August 1975, pp. 305-3 11.
35. Johnson R.P. 'Loss of Interaction in Short-span Composite Beams and Plates'. Journal of Constructional Steel Research, Vol.1, No 2, January 1981, pp. 11-16.
36. Patrick M. 'Shear Connection Performance of Profiled Steel Sheeting in Composite Slabs'. 2 volume, Doctoral thesis presented at School of Civil and Mining Engineering, The University of Sydney, February, 1994.

37. Stark, J.W.B. 'Design of composite floors with profiled steel sheet'. Proceeding of the 4th International Specialty Conference on Cold Formed Steel Structures, University of Missouri, Rolla, MO, USA, 1978.
38. Veljković M.'Development of new sheeting profile for composite floors'. Experimental study and interpretation, Tulea 1993:47, p.92, Luleå University of Technology, Luleå 1993, Sweden
39. Veljkovic M. '3D Nonlinear Analysis of Composite slabs'. p. 395-404 in G.M.A. Kusters and M.A.N Hendriks (eds.) DIANA Computational Mechanics '94, Kluwer Academic Publisher.
40. Jolly CK. and Lawson R.M. 'End anchorage in composite slabs: an increased load carrying capacity'. p. 202-205, The Structural Engineer, Volume 70, No. 1112, June 1992
41. Daniels B. 'Shear Bond Pull-out Tests for Cold-formed-steel Composite slabs'. Publication ICOM 194, June 1988, p.62
42. Veljkovic M. 'Composite slabs, p. 107-128 in Eurocode 4 - Samverkanskonstruktioner (Proc. of Eurocode4 Seminarium 15-16 sept. 1994), Swedish Institute of Steel Construction, Stockholm, Sweden
43. Seliem S S, 'Ultimate Shear-bond Capacity of Composite Deck Concrete Slabs' M Sc. Thesis, University of Waterloo, Ontario Canada, 1979.
44. Daniels J. 'Nonlinear analysis of composite members in bending and shear, ICOM – Construction Metallique, Lausanne, November 1989.
45. Wright H. & Veljkovic M. 'Towards a numerical procedure for composite slab assessment'. Thirteenth International Specialty Conference on Cold-Formed Steel Structures, pp. 415-435, October 17-18, 1996, St. Louis, Missouri, U.S.A.
46. Cescotto S. & Charlier R. 'Frictional contact finite elements based on mixed variational principles'. International Journal for numerical methods in engineering, Vol. 36, 1681-1701, 1993.
47. Wright H., Essawy M.I. 'Bond in thin gauge steel concrete composite structures'. Engineering Foundation Conferences, Composite Construction III, Composite Slab Session.1996, pp. 86-99, 9-14 June, Irsee, Germany.

48. Ping Ren & Crisinel M. 'Non-linear analysis of composite members'. ICOM-Construction Metallique, October 1992.
49. Li An, and Cederwall K. "Slip and Separation at the interface of Composite Slabs". Twelfth International Specialty Conference on Cold Formed Structures, St Louis; Missouri, USA, 1994, pp 385-397.
50. Neulichedl A. 'Behaviour of Composite Slabs with Non-linear Horizontal Shear Slips' Int. Symp on Mixed Structures, Brussels, IABSE, Vol 60 pp 143-148 (in German).
51. Mathey R.C. and Watstein D. (1961). 'Investigation of bond in beam and pull-out specimens with high yield-strength deformed bars'. ACI Journal, Vol. 57, No. 9, pp. 1071-1090.
52. BS 5400: Part 5, (1979). 'Code of practice for design of composite bridges'. British Standard Institution, London.
53. Precision Metal Forming Limited. 'PMF Composite Floor Decking Systems, ComFlor 70'. Swindon Road, Cheltenham, Gloucetershire GL51 9LS.
54. Ansys 'The "Theory", "Procedures", and "Elements" manuals'. Swanson Analysis inc., Houston, U.S.A. V.5.3 58 1997.
55. Frank L. Stasa, 1985. 'Applied finite element Analysis for Engineers'.
56. Daniels & Crisinel; 'Composite slab tests with profiled steel sheeting' Hibond 55, ICOM-Construction Metallique, Publication icom 148, Aug. 1987.
57. Wright H.D. & Evans R; 'Observation on the design and testing of composite floor slabs' Steel Construction Today 1987, 1, 91-99.
58. G. Abdel-Syed; 'Response of Composite Slabs to Dynamic Loads' Department of civil Engineering, University of Windsor, Windsor, Ontario N9B 3P4, October, 1974.
59. Daniels B; 'Shear bond pull-out tests for cold-formed-steel composite slabs' ICOM-Construction Metallique, Publication icom 194, Junin. 1988.
60. Veljkovic M; 'Development of a new sheeting profile for composite floors' research report, division of steel structures, ISSN 0347 – 0881, 1993:47

61. Li An; 'Load bearing capacity and behaviour of composite slabs with profiled steel sheet' Chalmers University of Technology, Gothenburg 1993.

Appendix A

Self weight of concrete slab and spreader beams

Slabs No.	Concrete density kN/m^3	Self-weight +spreader beams kN
1	23.79	10.01
2	23.79	10.01
3	23.18	7.8
4	23.18	6.84
5	23.23	6.9
6	23.23	8.53
7	23.36	12.7
8	23.36	5.68
9	22.79	12.42

Appendix B

Determination of design load using the partial shear connection method

To calculate the ultimate resistance of the composite section, the equal area axis is required.
For steel sheeting of 0.9 mm thick, the cross-section area is:
Area of profile steel $A_p = 1166$ mm^2 per 1000 mm width

$$= 1166 \times \frac{300}{1000}$$

$= 349.8$ mm^2 per 300 mm width
$= 1049.4$ mm^2 per 900 mm width (profiled steel sheet)
Distance from plastic neutral axis of steel sheet to its underside $e_p = 30.34$ mm
The measured ultimate strength of sheeting, $f_{up} = 438.5$ N/mm^2
The measured yield strength of sheeting, $f_{yp} = 349$ N/ mm^2
The design strength of sheeting, $f_{dp} = 330$ N/ mm^2
(Company design strength is recommended 320 N/mm^2).
The distance from plastic neutral axis of steel sheet to its under side (N.A), e_p.
$e_p = 30.34$ mm (given from the company)

Ultimate bending moment of profiled steel, $M_{R.ult}$
$M_{R.ult} = 349 \times 2 \times 0.9 [68 \times 30.34 + 60.83 \times 2.84 + 50 \times (55 - 30.34) + 16.55 (7.5 + 24.66) + 13 \times 39.66]$
$= 2837394.2$ N.mm

$$= \frac{2837394.2}{1000 \times 1000}$$

$= 2.83$ kN.m per 300 mm width
$= 9.433$ kN.m per 1000 mm width
$= 8.49$ kN.m per 900 mm width
Design bending moment of profiled steel sheet, $M_{R.\,design}$
$M_{R.\,design} = M_{pa}$

$$= M_{R.ult} \times \frac{0.87 \times f_{dp}}{f_{yd}}$$

$$= 2.83 \times \frac{0.87 \times 330}{349}$$

$= 2.32$ kN.m per 300 mm width
$= 7.76$ kN.m per 1000 mm width
$= 8.98$ kN.m per 900 mm width
To fined the centroidal axis of the steel, e, the sum of (the area of each element multiplied by vertical distance from the datum line passing through the centreline of the lower flange to the centre of the element) is divided by the sum of the area.

$$e = \frac{\sum A.Y}{\sum A}$$

$$\sum AY = 2\times 60.83\times 0.9\times \frac{55}{2} + 2\times 50\times 0.9\times 55 + 2\times 16.55\times [55+\frac{15}{2}]\times 0.9 + 26\times 0.9\times 70$$

$$= 11460 \text{ mm}^3$$

$$\sum A = 2\times 60.83\times 0.9 + 2\times 50\times 0.9 + 2\times 16.55\times 0.9 + 26\times 0.9 + 68\times 2\times 0.9$$

$$= 375 \text{ mm}^2$$

$$e = \frac{11460}{375}$$

$$e = 30.56 \text{ mm}$$

The distance from plastic neutral axis of steel sheet to its under side (N.A), e_p.

$e_p = 30.34$ mm

Slab No. 1 (2.9 m span, 165 mm total depth)

The ultimate resistance of the composite section $M_{p.Rm}$ using measured strengths.

The ultimate force in sheeting, $N_{st} = A_p \cdot f_{yp}$

$N_{st} = 1166 \times 349 = 406934$ N

The ultimate force in concrete, $N_{cf} = 406934$ N

$$x = \frac{N_{cf}}{f_{cu}.\gamma.b}$$

$$x = \frac{406934}{44\times 0.67\times 1000}$$

$$= 13.8 \text{ mm}$$

From annex E E2(2),

$$M = N_c \cdot Z + M_{pr}$$

or

$$M_{pRm} = N_{cf} \cdot Z + M_{pr}$$

where

$$Z = h_t - \frac{x}{2} - e_p + (e_p - e)\frac{N_{cf}}{A_p.f_{yp}}$$

$$Z = 165 - \frac{13.8}{2} - 30.34 + (30.34 - 30.56)\times \frac{406934}{1166\times 349}$$

$$Z = 127.54 \text{ mm}$$

Bending moment, $M_{pRm} = N_{st} \cdot Z + M_{R.ult}$

$= 406934 \times 127.54 + 9.433 \times 10^6$

$= 61.33$ kNm per 1000 mm width

For test, the maximum bending moment, M_{test} is:

$M_{test} = [(\text{max. load} + \text{self weight}) / 2] \times L/4$

$= [(96.2 + 10.01) / 2] \times (2.9 / 4)$

$= 38.5$ kNm per 900 mm width

$M_{test} = 42.77$ kNm per 1000 mm width

From Figure B.1, the degree of interaction for slab No.1 is seen to be given by $\eta_{test} = 0.62$

Ultimate Shear Strength, $\tau_{u.test}$ is:

$$\tau_{u.test} = \frac{\eta_{test} . N_{ct}}{b(L_s + L_o)}$$

$$\tau_{u.test} = \frac{0.62 \times 406934}{1000 \times (725 + 100)}$$

$$\tau_{u.test} = 0.36 \text{ N/mm}^2$$

Where:

η_{test} = degree of interaction from test results = 0.74

N_{ct} = full interaction force = 406934 N

b = 1000 mm

L_s = shear span L/4 2900/4 = 725 mm

L_o = overhang = 100 mm

Characteristic shear strength $\tau_{u.Rk} = \tau_{u.test} \times 0.9$

$= 0.36 \times 0.9$

$= 0.27$ N/mm^2

Design shear strength $\tau_{u.Rd} = \tau_{u.Rk} / \gamma_v$

Where:

γ_v = partial safety coefficient, normally taken as 1.25

$\tau_{u.Rd} = 0.27 / 1.25$

$= 0.22$ N/mm^2

The length for development of full shear resistance, L_{sf} is:

$$L_{sf} = \frac{N_{ct}}{b.\tau_{u.Rd}}$$

$$= \frac{1166 \times 330 \times 0.87}{1000 \times 0.22}$$

$L_{sf} = 1521.63$ mm

Design resistance for full interaction, $M_{p.Rd}$:

$$x = \frac{N_{cf}}{\gamma . f_{cu} . b}$$

$$x = \frac{1166 \times 330 \times 0.87}{0.4 \times 44 \times 1000}$$

x = 19 mm.

Lever arm Z:

$$Z = h_t - \frac{x}{2} - e_p + (e_p - e)\frac{N_{cf}}{A_p . f_{yp}}$$

= 124 mm

$$= 165 - \frac{19}{2} - 30.34 + (30.34 - 30.56) \times \frac{1166 \times 330}{1166 \times 330}$$

$M_{p.Rd} = N_{cf} . Z + M_{pr}$

$= 1166 \times 330 \times 0.87 \times 124 + 7.76 \times 10^6$

$= 49270066.4 \times 10^{-6}$

= 49.27 kN.m per 1000mm width.

Design resistance for L_x = 900 mm

(assumed for $L_x < L_{sf}$, the shear is partial, so the longitudinal shear resistance is critical.).

Force in concrete in compression, N_c,

$N_c = b . L_x . \tau_{u.Rd}$

$= 300 \times 900 \times 0.22$

= 59400 N

Depth of concrete block:

$$x = \frac{N_c}{\gamma . f_{cu} . b}$$

$$= \frac{59400}{0.4 \times 44 \times 300}$$

= 11.25 mm

Maximum force in steel, N_{st} $= A_p \times f_{dp} \times 0.87$

$= 348.8 \times 330 \times 0.87$

= 100427 N

Force in steel in compression $= (N_{st} - N_c)/2$

$= (100427 - 59400) / 2$

= 20513.5 N

Force in steel in tension $= N_c + (N_{st} - N_c)/2$

$= 59400 + 20513.5$

= 79913.5 N

Force in the upper part of flange $= (26 + 16.55 \times 2) \times 0.9 \times 330 \times 0.87$

= 15270.85 N

The neutral axis is positioned at a distance, **t**, in the lower part of flange.

$$2 \times 50 \times 330 \times t \times 0.87 = 20513.5 - 15270.85$$

$$t = 0.18 \text{ mm}$$

Depth of flange in compression = 15 – 0.45 + 0.18

= 14.73 mm

to fined the centroid of steel in compression, e_{sc}:

$$e_{sc} = \frac{2 \times 16.55 \times 0.9 \times \frac{15}{2} + 2 \times 50 \times 0.18 \times (15 - 0.45 + \frac{0.18}{2})}{26 \times 0.9 + 2 \times 16.55 \times 0.9 + 2 \times 50 \times 0.18}$$

= 6.84 mm

$$Z = h_t - \frac{x}{2} - e_p + (e_p - e) \times \frac{N_c}{A_p . f_{dp}}$$

$$Z = 165 - \frac{11.25}{2} - 30.34 + (30.34 - 30.56) \times \frac{59400}{349.8 \times 330}$$

Z = 128.92 mm.

Taking moment about the centre of the profile,

$M_{p.Rd} = 59400 \times 128.92 + 20513.5 \times (55+15-46.17 - 6.84) \times 2 + 2.32 \times 10^6$

= 10.67 kN.m per 300 mm width

= 35.582 kN.m per 1000 mm width

Design loads using partial connection method:

For two point loads at L/4 = 2900/4 = 725 mm from each support, the maximum bending moment is found from figure B.2.

M_{Rd} = 30.22 kN.m

W = 83.31 kN (total load)

$$= \frac{WL}{8}$$

where L = 2.9 m

Design load = 83.31 / (2.9×1)

= 28.7 kN/m^2

Slab No 2 (2.9 m span, with additional reinforcement):

The composite slab has one reinforcement bar 12 mm diameter in each trough.

$A_s = \pi (12/2)^2$

= 113.1 mm^2

f_{sk} = Yield strength of steel reinforcement.

f_{sk} =460 N/mm^2

γ_s = Partial safety factor for steel reinforcement.

γ_s = 1.15

Design moment of resistance:

a) consider section at distance from end of slab, $L_x = L_{sf}$

$L_x = 1521$ mm.

Using Annex E5(1).

Bending moment, $M_{p.Rd} = N_p \cdot Z_1 + M_{pr} + N_{as} \cdot Z_2$

Force in profile steel sheet, $N_p = b \cdot L_x \cdot \tau_{u.Rd}$

$N_p = 300 \times 1521 \times 0.22$

$= 100386$ N

Force in steel reinforcement, $N_{as} = A_s \cdot f_{sk}/\gamma_s$

$= 113.1 \times 460/1.15$

$= 45240$ N

$$x = \frac{N_p + N_{as}}{b(0.4 \times f_{cu})}$$

$$x = \frac{100386 + 45240}{300 \times 0.4 \times 44}$$

$x = 27.59$ mm

$Z_2 = d_s - 0.5x$

$= (165 - 50 - (12/2)) - 0.5 \times 27.59$

$= 95.205$ mm.

$$Z_1 = h_t - 0.5\chi - e_p + (e_p - e) \times \frac{N_p}{A_p f_{yp}/\gamma_{ap}}$$

$$Z_1 = 165 - 0.5 \times 27.59 - 30.34 + (30.34 - 30.56) \times \frac{100386}{349.8 \times 330/1.1}$$

$=120.64$ mm.

$$M_{pr} = 1.25 \times M_{pa} \times (1 - \frac{N_p}{A_p . f_{yp}/\gamma_{ap}})$$

$$M_{pr} = 1.25 \times 2.54 \times (1 - \frac{100386}{349.8 \times 330/1.1})$$

$= 0.125$ kN.m per 300 mm width, ($<M_{pa}$ O.K)

$M_{p.Rd} = N_p \cdot Z_1 + M_{pr} \times 10^6 + N_{as} \cdot Z_2$

$= (100386 \times 120.6 + 0.125 \times 10^6 + 45240 \times 95.205)\ 10^{-6}$

$= 16.53$ kN.m per 300 mm width.

$= 55.10$ kN.m per 1000 mm width.

From test, the maximum bending moment, M_{test} is:

$M_{test} = \{[\text{maximum load} + \text{self weight}]/2\} \times (L/4)$

$= [(192.7 + 10.01)/2] \times (2.9/4)$

$=73.22$ kN.m per 900 mm width.

$= 81.64$ kN.m per 1000 mm width.

b) Consider a section at distance from end of slab of $L_x = 900$ mm

$N_p = b \cdot L_x \cdot \tau_{u.Rd}$

$= 300 \times 900 \times 0.22$

$= 59400$ N

$$\chi = \frac{N_p + N_{as}}{0.4 \times f_{cu} \times b}$$

$$\chi = \frac{59400 + 45240}{0.4 \times 44 \times 300}$$

$= 19.81$ mm

$Z_2 = d_s - 0.5\,\chi$

$= [165 - 50 - (12/2)] - 0.5 \times 19.81$

$= 99$ mm

$$Z_1 = h_t - 0.5\chi - e_p + (e_p - e) \times \frac{N_p}{A_p f_{yp}/\gamma_{ap}}$$

$$Z_1 = 165 - 0.5 \times 19.81 - 30.34 + (30.34 - 30.65) \times \frac{59400}{349.8 \times 330/1.1}$$

$Z_1 = 124.45$ mm.

$$M_{pr} = 1.25 \times M_{pa} \times (1 - \frac{N_p}{A_p . f_{yp}/\gamma_{ap}})$$

$$M_{pr} = 1.25 \times 2.32 \times (1 - \frac{59400}{349.8 \times 330/1.1})$$

$= 1.25$ kN.m per 300 mm width ($<M_{pa}$ O.K)

$M_{p.Rd} = N_p \,.\, Z_1 + M_{pr} \times 10^6 + N_{as} \,.\, Z_2$

$= (59400 \times 124.45 + 1.25 \times 10^6 + 45240 \times 99)\, 10^{-6}$

$= 13.12$ kN.m per 300 mm width.

$= 43.73$ kN.m per 1000 mm width.

Design load using partial connection method:

For two point loads at L/4 = 2900/4 = 725mm.

From each support, the maximum bending moment is found from figure B.3.

$M_{Rd} = 40$ kN.m

$= WL/8 \quad \Rightarrow L = 2.9$ m

$W = 110.34$ kN (total load)

Design load = 110.34 / (2.9×1)

$= 38$ kN/m^2.

Calculation of flexural capacity of reinforced concrete slab used for back calculation of η_{comp} for composite slabs with reinforcement:

This calculation is made assuming that the flexural capacity of the reinforced concrete slab is attainable in the tests in addition to the longitudinal shear capacity of the composite slab.

According to figure B.4

The ultimate force in concrete $F_c = 0.67\, f_{cu}.b.x$ (with γ_m taken as unity)

The ultimate force for the reinforcement $F_s = A_s f_{ys}$

$F_s = F_c$

$f_{ys}.\, A_s = 0.67\, f_{cu}.\, b.\, x$

$823 \times 2 \times 113.1 = 0.67 \times 44 \times 900 \times x$

$\therefore$ The depth of the rectangular stress block x = 7 mm

$z = 165 - 30 - 6 - x/2$

$\therefore$ The lever arm z = 125.5 mm

The flexural capacity of the reinforced slab

$M_{Rc} = f_{ys.} A_s. z$

$M_{Rc} = (186162.6 \times 125.5)/1000000$

$= 23.4$ kN.m

For test No 2 $M_{test} = 73.48$ kN.m

Assuming full compatibility

$M_{comp} = M_{test} - M_{Rc}$

$M_{comp} = 73.48 - 23.4$

$M_{comp} = 50.1$ kN.m

$\therefore$ The adjusted partial interaction $\eta_{comp} = M_{comp}/M_{p,Rm}$

$\eta_{comp} = 50.1/55.2$

$\eta_{comp} = 0.91$

for test No.5 $M_{Rc} = 23.0$ kN.m

and for test No.7 $M_{Rc} = 22.9$ kN.m

With these values the contribution of the reinforcement in the composite slabs can be deducted in order to calculate the contribution of the composite action to the failure load.

Figure B.1 Determination of the degree of shear connection from M_{test} for slab No. 1

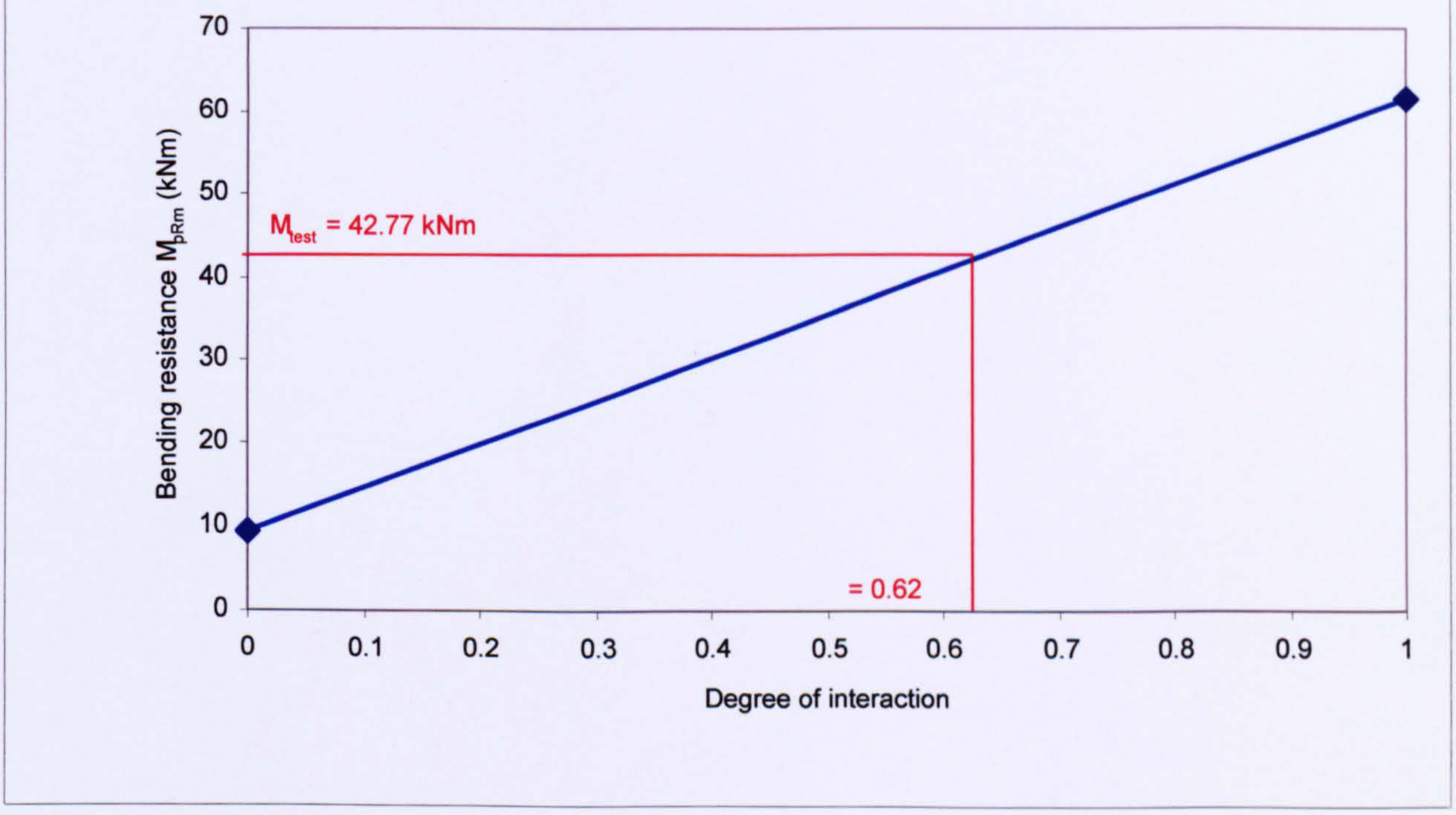

Figur B.2 Design partial interaction diagram for slab No.1

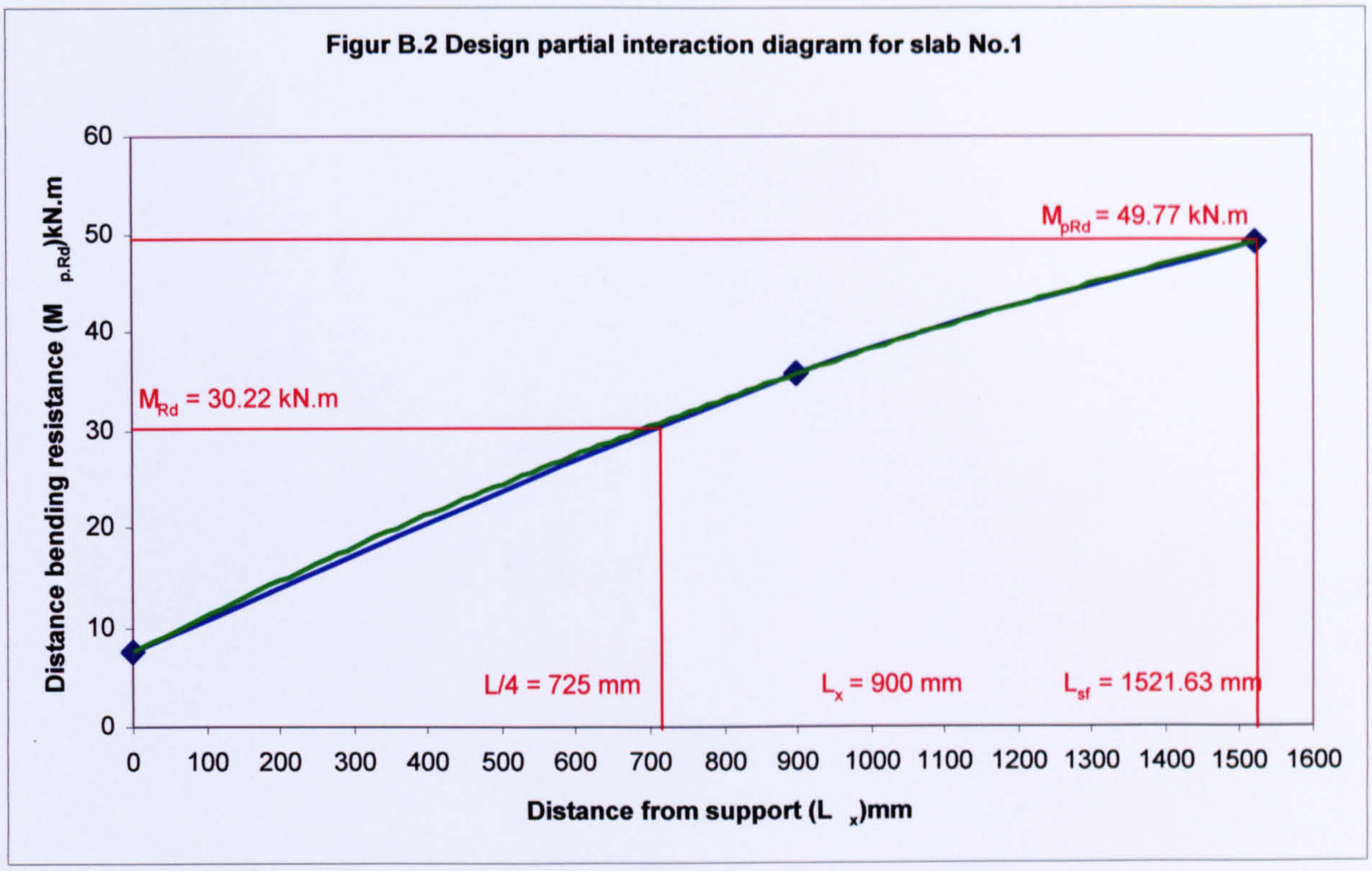

Figure B.3 Design partial interaction diagram for slab No.2

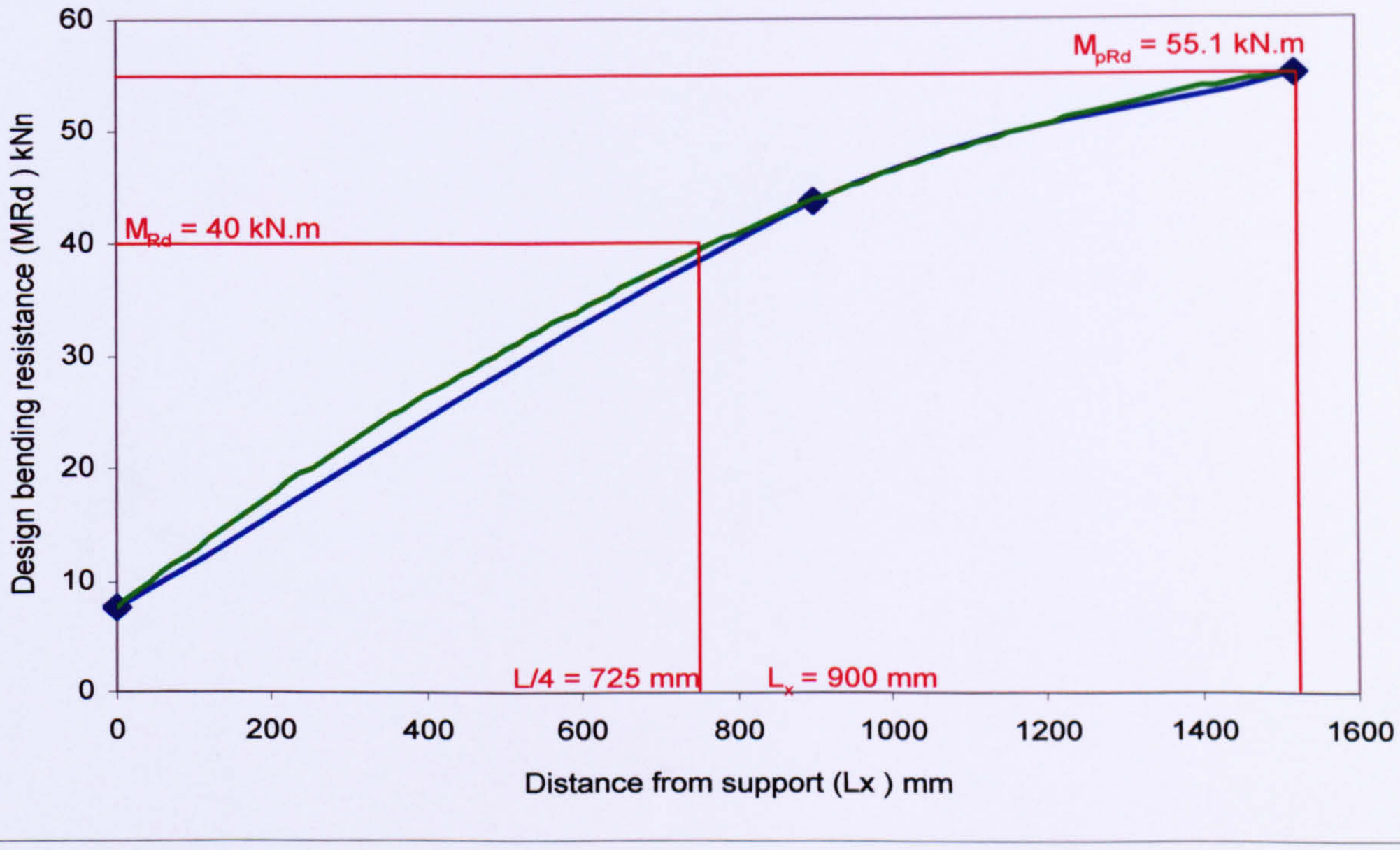

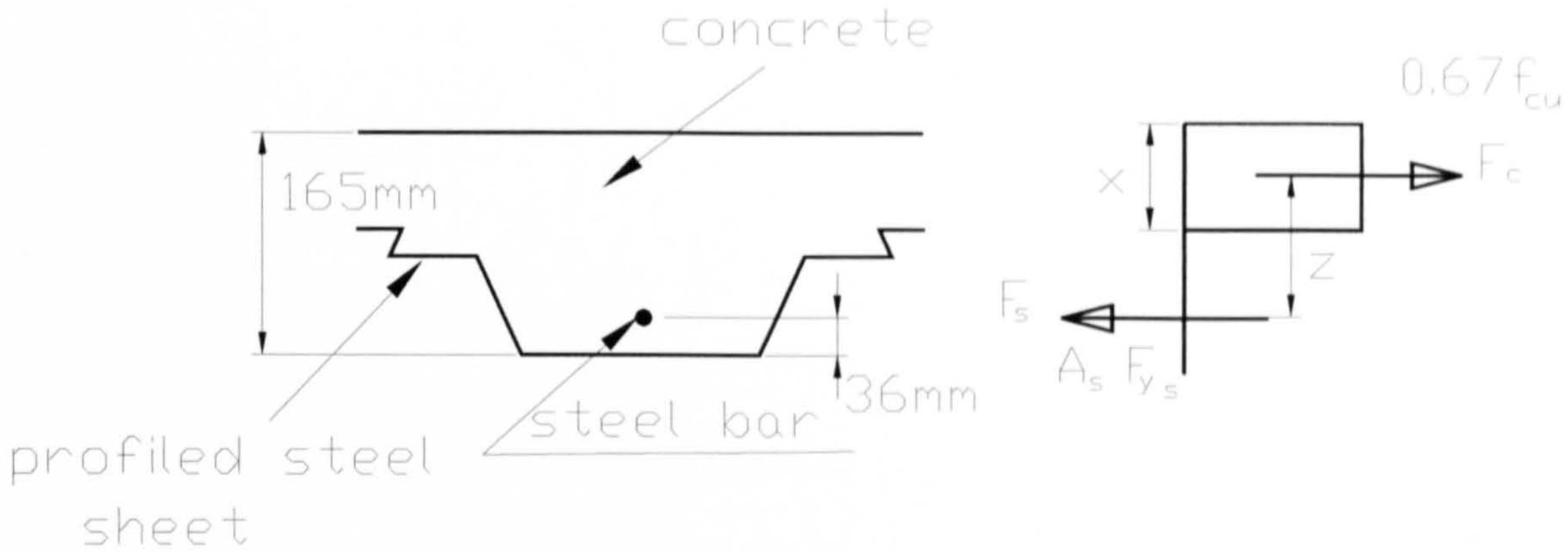

Figure B.4 Cross section of composite slab with reinforcement

APPENDIX C
Determination of design loads using the m-k method

Using the m-k method, the maximum design shear is:

$V_{1.Rd} = V_{1.k} / \gamma_{vs}$

$= b \cdot d_p [(m.A_p / b \cdot L_s) + k] / \gamma_{vs}$

where:

$V_{1.Rd}$ = Maximum design shear resistance

$V_{1.k}$ = Characteristic resistance of end anchorage

γ_{vs} = Partial safety coefficient, normally taken as 1.25

b = Width of cross-section considered

d_p = Distance from top of slab to centred of steel sheet

Note:

The values obtained for m & k are reduced by 10%.

The first series of composite slabs:

From Figure C.1, we calculate the value of m & k.

$m = 169$ N/mm^2 $\Rightarrow m_r = 169 - (169 \times 10/100)$

$= 152$ N/mm^2

$k = 0.12$ N/mm^2 $\Rightarrow k_r = 0.12 - (0.12 \times 10/100)$

$= 0.11$ N/mm^2

Where:

m or m_r = Slope of regression line

k or k_r = Intercept of regression line

Slab No. 1 (span = 2.9 m):

$V_{1.Rd} = 1000 \times 134.66 [(152 \times 1166) / (1000 \times 725) + 0.11] / 1.25$

$= 37960$ N

$= 37.96$ kN

Therefore, the total applied load $w = 37.96 \times 2$

$= 75.93$ kN

The design load $= 75.93 / (2.9 \times 1)$

$= 26.18$ kN/m^2

Slab No. 4 (span = 1.9 m):

$V_{1.Rd} = 1000 \times 134.66 [(152 \times 1166) / (1000 \times 475) + 0.11] / 1.25$

$= 51830.095$ N

$= 51.83$ kN

Therefore, the total applied load, $w = 51.83 \times 2$

$= 103.66$ kN

The design load $= 103.66 / (1.9 \times 1)$

$= 54.55$ kN/m^2

Slab No. 9 (span = 3.9 m):

$V_{1.Rd} = 1000 \times 134.66 [(152 \times 1166) / (1000 \times 975) + 0.11] / 1.25$

$= 31217.03$ N

$= 31.2$ kN

Therefore, the total applied load $w = 31.2 \times 2$

$= 62.43$ kN

The design load = 62.43 / (3.9 × 1)
= 16.0 kN/m^2

Slab No. 3 (span = 2.9 m) (135 depth):

$V_{1.Rd}$ = 1000 × 104.66 [(152× 1166) / (1000 × 725) + 0.11] / 1.25
= 29510.59 N
= 29.51 kN

Therefore, the total applied load w = 29.51 × 2
= 59 kN

The design load = 59 / (2.9 × 1)
= 20.35 kN/m^2

Slab No. 6 (span = 3.9 m) (135 depth):

$V_{1.Rd}$ = 1000 × 104.66 [(152 × 1166) / (1000 × 975) + 0.11 / 1.25
= 24262.39 N
= 24.26 kN

Therefore, the total applied load w = 24.26 × 2
= 48.52 kN

The design load = 48.52 / (3.9 × 1)
= 12.44 kN/m^2

Slab No. 8 (span = 1.9 m) (135 depth):

$V_{1.Rd}$ = 1000 × 104.66 [(152 × 1166) / (1000 × 475) + 0.11] / 1.25
= 40283.2 N
= 40.28 kN

Therefore, the total applied load w = 40.28 × 2
= 80.56 kN

The design load = 80.56 / (1.9 × 1)
= 42 kN/m^2

The second series of composite slabs (with additional reinforcement):

From Figure C.2, we calculate the value of m & k.

m = 257.1 N/mm^2 ⇒ m_r = 257.1 – (257.1 × 10/100)
= 231.39 N/mm^2

k = 0.25 N/mm^2 ⇒ k_r = 0.25 – (0.25 × 10/100)
= 0.225 N/mm^2

Slab No. 2 (span = 2.9 m):

$V_{1.Rd}$ = 1000 × 134.66 [(231.39 × 1166) / (1000 × 725) + 0.225] / 1.25
= 134660 × [(269800 / 725000) + 0.225] / 1.25
= 64328.5 N
= 64.32 kN

Therefore, the total applied load w = 64.32 × 2
= 128.65 kN

The design load = 128.65/(2.9 × 1)
= 44.36 kN/m^2

Slab No. 5 (span = 1.9 m):

$V_{1.Rd}$ = 1000 × 134.66 [(231.39 × 1166) / (1000 × 475) + 0.225] / 1.25

$= 134660 \times [(269800 / 475000) + 0.225] / 1.25$
$= 85428.47$ N
$= 85.42$ kN

Therefore, the total applied load $w = 85.42 \times 2$
$= 170.85$kN

The design load $= 170.85 / (1.9 \times 1)$
$= 89.92$ kN/m^2

Slab No. 7 (span = 3.9 m):

$V_{1.Rd} = 1000 \times 134.66 [(231.39 \times 1166) / (1000 \times 975) + 0.225] / 1.25$
$= 134660 \times [(269800 / 975000) + 0.225] / 1.25$
$= 54049.15$ N
$= 54$ kN

Therefore, the total applied load $w = 54 \times 2$
$= 108$ kN

The design load $= 108 / (3.9 \times 1)$
$= 27.7$ kN/m^2

The second series of composite slabs (with additional reinforcement):

For slab No.2

$V_t = 101$ kN.

$V_{t"Rc"} \times L/4 = M_{Rc}$
$V_{t"Rc"} \times 2.9/4 = 23.4$
$V_{t"Rc"} = 32.27$
$V_{t"Comp"} = V_t - V_{t"Reinf"}$
$V_{t"Comp"} = 101 - 32.27$
$= 68.7$ kN

Similarly for slab No. 5 and 7

$V_{t"Rc"} = 48.42$ and 23.48 kN
$V_{t"Comp"} = 60.97$ and 38.97 kN

For design vales for the "reinforced slab" is obtained by using the appropriate partial safety factor. In this case the factor are 0.87 for the reinforcement and 0.4 for the rectangular concrete stress block.

So for slab No. 2

The ultimate force in concrete $F_c = 0.87 f_{cu}.b.x$ (with γ_m taken as unity)
The ultimate force for the reinforcement $F_s = 0.4 A_s f_{ys}$
$F_s = F_c$
$0.87 f_{ys.} A_s = 0.4 f_{cu}. b. x$
$0.87 \times 823 \times 2 \times 113.1 = 0.4 \times 44 \times 900 \times x$
$x = (0.87 \times 1646 \times 113.1)/(0.4 \times 44 \times 900)$
$x = 10.22$ mm
∴ The depth of the rectangular stress block $x = 10.22$ mm
$z = 165 - 30 - 6 - x/2$
∴ The lever arm $z = 123.9$ mm
The flexural capacity of the reinforced slab
$M_{Rc} = 0.87 f_{ys.} A_s. z$
$M_{Rc} = (0.87 \times 113.1 \times 823 \times 2 \times 123.9)/1000000$
$= 20.06$ kN.m

$V_{Rc} \times L/4 = 20.06$
$V_{Rc} = (4 \times 20.06)/2.9$
$V_{Rc} = 27.66$ kN
$w_r = (27.66 \times 2)/(2.9 \times 0.9) = 21.19$ kN/m^2
$w_r = 21.19$ kN/m^2
$w_o = w_r + w_{comp} = 47.39$
$w_{failure} = 77.66$ kN/m^2
$w_{failure}/w_o = 1.64$

Figure C.1 Evaluation of m & k for the composite slabs

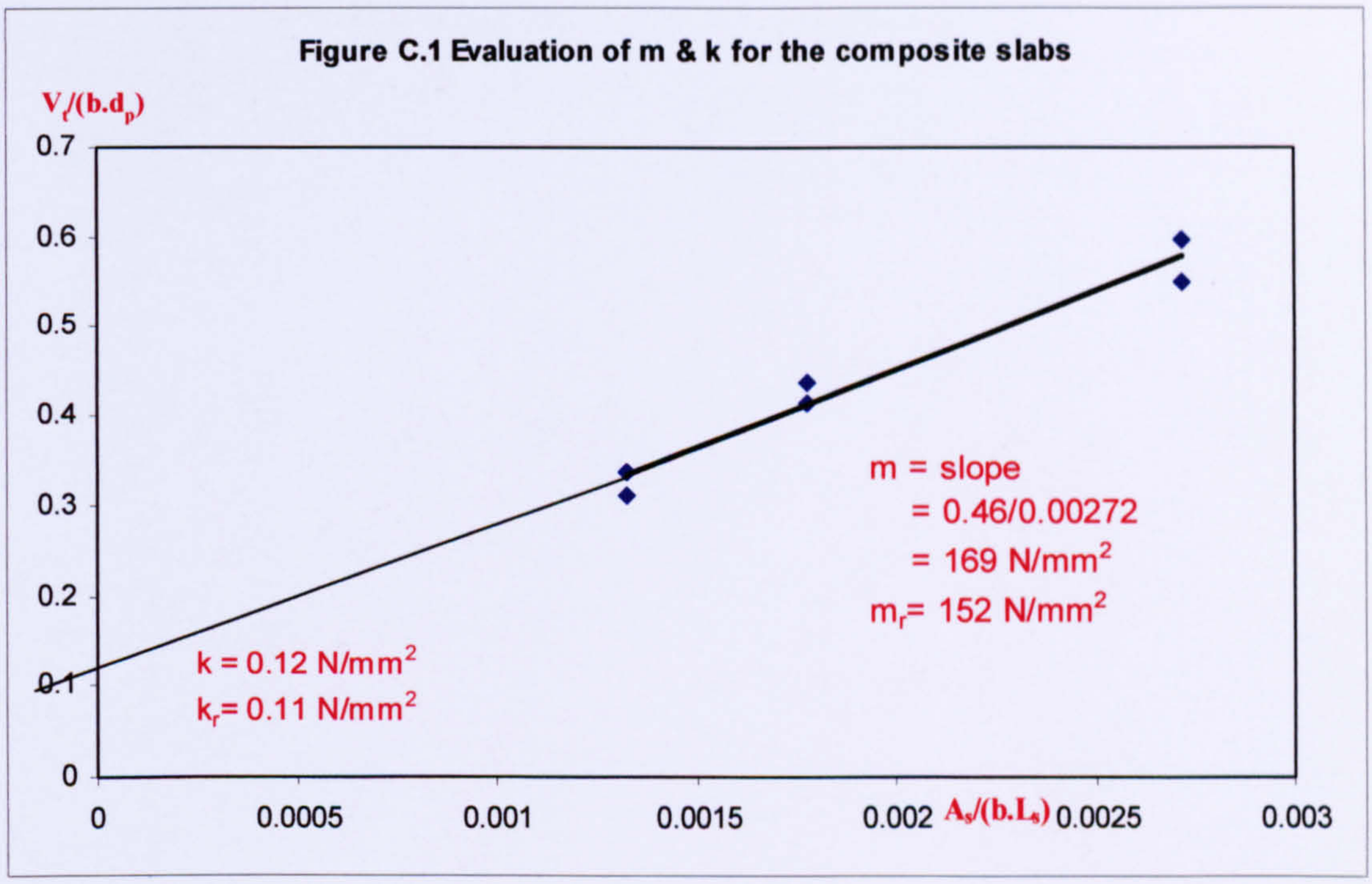

Figure C.2 Evaluation of m&k for second series of composite slabs

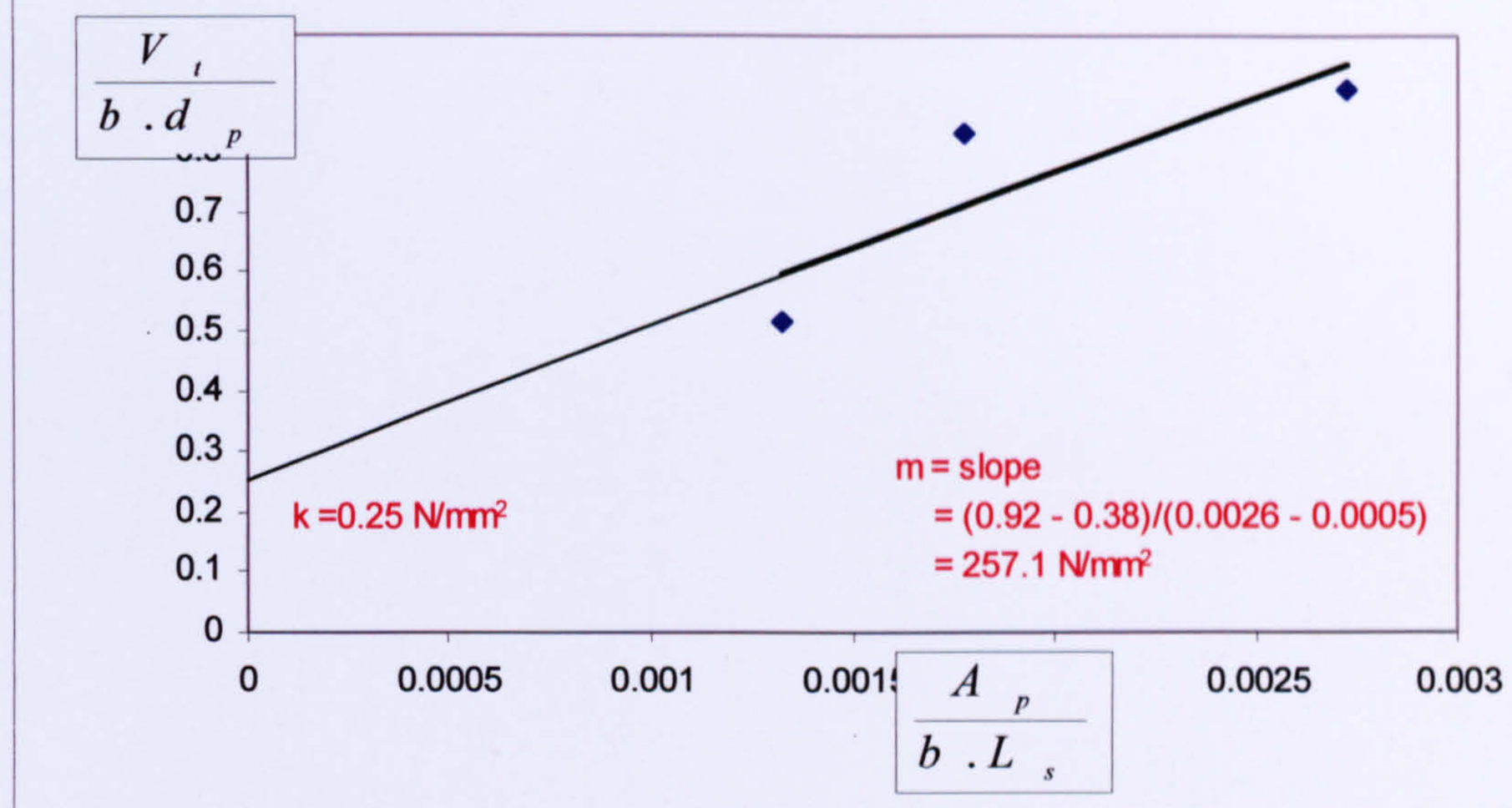

Appendix D

Example of input data

```
/TITLE,slab No 4 (S4) L = 3900 mm H = 165mm
/STITLE,slab 4 H = 165 L = 3900 mm
! MATERIAL PROPERTIES
E1 = 202777             ! YOUNG'S MODULUS FOR STEEL, CONVERTED TO N/MM SQ.
                        ! CONVERTING TO N/MM²
E2 = 26832              ! YOUNG'S MODULUS FOR CONCRETE,
                        ! CONVERTING TO N/MM²
NUIND = 0.3             ! POISSON'S RATIO
ETANI = 0.0
PLS = 975               ! THE LOAD DISTANCE IN MM
P = -(65×1000)/4        ! APPLYING LOAD IN N
H = 165                 ! COMPOSITE SLAB DEPTH IN MM
L = 1950                ! HALF OF THE SPAN LENGTH IN MM
L1 = 20
L2 = 1
L3 = 2
L4 = 4
L5 = 2
L6 = 1
L7 = 2
LS = L
/PREP7
/VIEW,1,1,1,1
/ANG,1
/STITLE,,3-D COMPOSITE SLAB WITH CONTACT ELEMENTS
ET,1,45                 ! 3-D SOLID ELEMENT (FOR CONCRETE)
ET,2,SHELL181           ! 3-D SOLID ELEMENTS  (FOR THE STEEL SHEET)
R,2,.9,.9,.9,.9         ! THICKNESS OF STEEL SHEET
ET,3,COMBIN40,1,,2      ! COMBINATION ELEMENT
R,3,10E5,,,,(18.49×1000)/2 ! FSLIDE = (18.49×1000)/2 N/MM
ET,4,CONTAC52,,,,1      ! KEYOPT(4) = 1 GAP SIZE BY NODE LOCATION
R,4,(18.49×1000)/2,-0.0001
MP,MU,4,0.4             ! COEFFICIENT OF FRICTION

! CONCRETE MATERIAL **********************
MP,EX,1,E2              ! YOUNG'S MODULUS
MP,NUXY,1,0.2           ! POISSON'S RATIO
TB,MISO,2,1             ! ACTIVATE A DATA TABLE FOR MULTIINEAR ISOTROPIC
                        ! HARDENING OPTION-ONLY 1 SET OF TEMP.
TBTEMP,20               ! TEMPERATURE = 20
TBPT,DEFI,0.000302,10   ! STRAIN, STRESS AT TEMP. 20°
TBPT,DEFI,0.00047,15
TBPT,DEFI,0.000654,20

!STEEL MATERIAL   **********************
MP,EX,2,E1              ! YOUNG'S MODULUS
MP,NUXY,2,0.3           ! POISSON'S RATIO
TB,BISO,2,1             ! ACTIVATE A DATA TABLE FOR BILINEAR ISOTROPIC
                        ! HARDENING OPTION-ONLY 1 SET OF TEMP.
TBDATA,1,354,0.0        ! YIELD STRESS N/MM. SQ.;
                        ! TANGENT MODULUS = 1.2E6
TBLIST,BISO,2           ! LIST THE DATA TABLE
/XRANGE,0,0.01          ! X-AXIS
TBPLOT,BISO,2           ! DISPLAY THE DATA TABLE
```

```
K,1,0,70,L
K,2,13,70,L
K,3,6,55,L
K,4,56,55,L
K,5,82,0,L
K,6,224,0,L
K,7,250,55,L
K,8,300,55,L
K,9,293,70,L
K,10,319,70,L
K,11,312,55,L
K,12,362,55,L
K,13,388,0,L
K,14,450,0,L
K,15,450,55,L
K,16,450,70,L
K,17,450,H,L
K,18,362,H,L
K,19,319,H,L
K,20,293,H,L
K,21,250,H,L
K,22,56,H,L
K,23,13,H,L
K,24,0,H,L
K,25,56,70,L
K,26,250,70,L
K,27,362,70,L

K,28,0,70,0
K,29,13,70,0
K,30,6,55,0
K,31,56,55,0
K,32,82,0,0
K,33,224,0,0
K,34,250,55,0
K,35,300,55,0
K,36,293,70,0
K,37,319,70,0
K,38,312,55,0
K,39,362,55,0
K,40,388,0,0
K,41,450,0,0
K,42,450,55,0
K,43,450,70,0
K,44,450,H,0
K,45,362,H,0
K,46,319,H,0
K,47,293,H,0
K,48,250,H,0
K,49,56,H,0
K,50,13,H,0
K,51,0,H,0
K,52,56,70,0
K,53,250,70,0
K,54,362,70,0

K,55,0,70.00001,L
K,56,13,70.00001,L
K,57,6,55.00001,L
K,58,56,55.00001,L
K,59,82,0.00001,L
K,60,224,0.00001,L
K,61,250,55.00001,L
K,62,300,55.00001,L
```

```
K,63,293,70.00001,L
K,64,319,70.00001,L
K,65,312,55.00001,L
K,66,362,55.00001,L
K,67,388,0.00001,L
K,68,450,0.00001,L

K,69,0,70.00001,0
K,70,13,70.00001,0
K,71,6,55.00001,0
K,72,56,55.00001,0
K,73,82,0.00001,0
K,74,224,0.00001,0
K,75,250,55.00001,0
K,76,300,55.00001,0
K,77,293,70.00001,0
K,78,319,70.00001,0
K,79,312,55.00001,0
K,80,362,55.00001,0
K,81,388,0.00001,0
K,82,450,0.00001,0
KPLOT

L,1,28
L,2,29
L,3,30
L,4,31
L,5,32
L,6,33
L,7,34
L,8,35
L,9,36
L,10,37
L,11,38
L,12,39
L,13,40
L,14,41
L,15,42
L,16,43
L,17,44
L,18,45
L,19,46
L,20,47
L,21,48
L,22,49
L,23,50
L,24,51
L,25,52
L,26,53
L,27,54
L,1,2
L,2,3
L,3,4
L,4,5
L,5,6
L,6,7
L,7,8
L,8,9
L,9,10
L,10,11
L,11,12
L,12,13
L,13,14
L,14,15
```

```
L,15,16
L,16,17
L,17,18
L,18,19
L,19,20
L,20,21
L,21,22
L,22,23
L,23,24
L,24,1
L,23,2
L,22,25
L,2,25
L,4,25
L,4,7
L,25,26
L,7,26
L,26,21
L,9,20
L,10,19
L,27,18
L,10,27
L,12,27
L,27,16
L,12,15    !66
L,28,29
L,29,30
L,30,31
L,31,32
L,32,33
L,33,34
L,34,35
L,35,36
L,36,37
L,37,38
L,38,39
L,39,40
L,40,41
L,41,42
L,42,43
L,43,44
L,44,45
L,45,46
L,46,47
L,47,48
L,48,49
L,49,50
L,50,51
L,51,28    !90
L,29,50
L,52,49
L,29,52
L,31,52
L,31,34
L,52,53
L,34,53
L,53,48
L,53,36
L,36,47
L,37,46
L,54,45
L,37,54
L,39,54
L,39,42
```

```
L,54,43
L,26,9! !107

L,55,69
L,56,70
L,57,71 !110
L,58,72
L,59,73
L,60,74
L,61,75
L,62,76
L,63,77
L,64,78
L,65,79
L,66,80
L,67,81 !120
L,68,82
L,55,56
L,56,57
L,57,58
L,58,59
L,59,60
L,60,61
L,61,62
L,62,63
L,63,64 !130
L,64,65
L,65,66
L,66,67
L,67,68
L,69,70
L,70,71
L,71,72
L,72,73
L,73,74
L,74,75
L,75,76
L,76,77
L,77,78
L,78,79
L,79,80
L,80,81
L,81,82
LPLOT!

AL,1,2,28,67
AL,2,3,29,68
AL,3,4,30,69
AL,4,5,31,70
AL,5,6,32,71 !5
AL,6,7,33,72
AL,7,8,34,73
AL,8,9,35,74
AL,9,10,36,75
AL,10,11,37,76 !10
AL,11,12,38,77
AL,12,13,39,78
AL,13,14,40,79
AL,14,15,41,80
AL,15,16,42,81 !15
AL,16,17,43,82
AL,17,18,44,83
AL,18,19,45,84
AL,19,20,46,85
```

```
AL,20,21,47,86 !20
AL,21,22,48,87
AL,22,23,49,88
AL,23,24,50,89
AL,24,1,51,90
AL,23,2,52,91 !25
AL,22,25,53,92
AL,2,25,54,93
AL,25,4,55,94
AL,4,7,56,95
AL,25,26,57,96 !30
AL,26,7,58,97
AL,26,9,107,99
AL,21,26,59,98
AL,20,9,60,100
AL,19,10,61,101 !35
AL,18,27,62,102
AL,10,27,63,103
AL,27,12,64,104
AL,27,16,65,106
AL,12,15,66,105 !40
AL,50,51,28,52
AL,49,52,53,54
AL,29,30,55,54
AL,48,53,57,59
AL,55,56,57,58 !45
AL,31,32,33,56
AL,47,59,107,60
AL,58,34,35,107
AL,46,60,36,61
AL,45,61,62,63 !50
AL,37,38,63,64
AL,44,62,65,43
AL,64,65,66,42
AL,39,40,41,66
AL,89,90,91,67 !55
AL,88,91,92,93
AL,68,69,93,94
AL,87,92,96,98
AL,94,95,96,97
AL,95,70,71,72 !60
AL,86,98,99,100 !61
AL,99,97,73,74
AL,85,100,101,75
AL,101,102,84,103
AL,103,76,77,104
AL,83,82,102,106
AL,106,104,105,81
AL,105,80,79,78        !68

AL,108,109,122,135
AL,109,110,123,136 !70
AL,110,111,124,137
AL,111,112,125,138
AL,112,113,126,139
AL,113,114,127,140
AL,114,115,128,141 !75
AL,115,116,129,142
AL,116,117,130,143
AL,117,118,131,144
AL,118,119,132,145
AL,119,120,133,146 !80
AL,120,121,134,147 !81
APLOT
```

```
VA,1,23,24,25,41,55
VA,22,25,26,27,42,56
VA,2,3,27,28,43,57
VA,21,26,30,33,44,58
VA,30,28,29,31,45,59
VA,29,4,5,6,46,60
VA,20,33,32,34,47,61
VA,7,8,32,31,48,62
VA,19,34,9,35,49,63
VA,18,35,37,36,50,64
VA,37,10,11,38,51,65
VA,17,36,39,16,52,66
VA,39,38,40,15,53,67
VA,40,12,13,14,54,68 !14
VPLOT

LSEL,S,LINE,,1,27
LSEL,A,LINE,,108,121
LESIZE,ALL,,,L1

LSEL,S,LINE,,28
LSEL,A,LINE,,50
LSEL,A,LINE,,67
LSEL,A,LINE,,89

LSEL,A,LINE,,122
LSEL,A,LINE,,135
LESIZE,ALL,,,L2

LSEL,S,LINE,,30
LSEL,A,LINE,,54
LSEL,A,LINE,,49
LSEL,A,LINE,,69
LSEL,A,LINE,,93
LSEL,A,LINE,,88
LSEL,A,LINE,,124
LSEL,A,LINE,,137

LSEL,A,LINE,,34
LSEL,A,LINE,,107
LSEL,A,LINE,,47
LSEL,A,LINE,,73
LSEL,A,LINE,,99
LSEL,A,LINE,,86
LSEL,A,LINE,,128
LSEL,A,LINE,,141

LSEL,A,LINE,,36
LSEL,A,LINE,,46
LSEL,A,LINE,,75
LSEL,A,LINE,,85
LSEL,A,LINE,,130
LSEL,A,LINE,,143

LSEL,A,LINE,,38
LSEL,A,LINE,,63
LSEL,A,LINE,,45
LSEL,A,LINE,,77
LSEL,A,LINE,,103
LSEL,A,LINE,,84
LSEL,A,LINE,,132
LSEL,A,LINE,,145
```

```
LSEL,A,LINE,40
LSEL,A,LINE,,40
LSEL,A,LINE,,66
LSEL,A,LINE,,65
LSEL,A,LINE,,44
LSEL,A,LINE,,79
LSEL,A,LINE,,105
LSEL,A,LINE,,106
LSEL,A,LINE,,83
LESIZE,ALL,,,L3

LSEL,S,LINE,,32
LSEL,A,LINE,,56
LSEL,A,LINE,,57
LSEL,A,LINE,,48
LSEL,A,LINE,,71
LSEL,A,LINE,,95
LSEL,A,LINE,,96
LSEL,A,LINE,,87
LSEL,A,LINE,,126
LSEL,A,LINE,,139
LESIZE,ALL,,,L4

LSEL,S,LINE,,31
LSEL,A,LINE,,33
LSEL,A,LINE,,39
LSEL,A,LINE,,41
LSEL,A,LINE,,70
LSEL,A,LINE,,72
LSEL,A,LINE,,78
LSEL,A,LINE,,80
LSEL,A,LINE,,125
LSEL,A,LINE,,127
LSEL,A,LINE,,133
LSEL,A,LINE,,138
LSEL,A,LINE,,140
LSEL,A,LINE,,146
LESIZE,ALL,,,L5

LSEL,S,LINE,,29
LSEL,A,LINE,,55
LSEL,A,LINE,,58
LSEL,A,LINE,,35
LSEL,A,LINE,,37
LSEL,A,LINE,,42
LSEL,A,LINE,,68
LSEL,A,LINE,,94
LSEL,A,LINE,,97
LSEL,A,LINE,,74
LSEL,A,LINE,,76
LSEL,A,LINE,,104
LSEL,A,LINE,,81
LSEL,A,LINE,,123
LSEL,A,LINE,,129
LSEL,A,LINE,,131
LSEL,A,LINE,,136
LSEL,A,LINE,,142
LSEL,A,LINE,,144
LESIZE,ALL,,,L6

LSEL,S,LINE,,51,53
LSEL,A,LINE,,60,62
LSEL,A,LINE,,90,92
LSEL,A,LINE,,98
```

```
LSEL,A,LINE,,100,102
LESIZE,ALL,,,L7
LSEL,ALL

TYPE,1
MAT,1
REAL,1
ESHAPE,2
VMESH,ALL

TYPE,2
MAT,2
REAL,2
ESHAPE,2
AMESH,69,81

TYPE,3
REAL,3
MAT,3
EINTF,0.0001

TYPE,4
REAL,4
MAT,4
EINTF,0.0001

NSEL,S,LOC,Z,LS   ! SUPPORT FOR THE STEEL
NSEL,R,LOC,Y,0
D,ALL,UY
NSEL,ALL

NSEL,S,LOC,Z,0.0    ! SYMMETRY
D,ALL,UX
D,ALL,UZ
NSEL,ALL

NSEL,S,LOC,X,0.0    ! SYMMETRY
D,ALL,UX
NSEL,ALL

NSEL,S,LOC,Y,H      ! SELECT TOP EDGE OF MODEL
NSEL,R,LOC,Z,PLS
CP,1,UY,ALL         ! COUPLE NODES ON TOP EDGE
NSEL,ALL
SAVE
FINISH

/SOLU                 ! APPLY LOADS AND OBTAIN THE SOLUTION**********
ANTYPE,STATIC         ! STATIC
NLGEOM,ON             ! TURN EFFECT OF LARGE GEOMETRICAL DEFORMATION ON
NROPT,FULL,,ON
PRED,ON               ! TURN PREDITOR ON
CNVTOL,F,,0.05,2,10
TIME,0.0000001        ! TIME AFTER THE LOAD STEP!
AUTOTS,ON             ! AUTOMATIC TIME STEPING
NSEL,S,LOC,Y,H
NSEL,R,LOC,Z,PLS
F,ALL,FY,-0.0000001 ! ULT. LOAD (KN)
NSEL,ALL
SOLVE

TIME,0.000001         ! TIME AFTER THE LOAD STEP!
AUTOTS,ON             ! AUTOMATIC TIME STEPING
NSEL,S,LOC,Y,H
```

```
NSEL,R,LOC,Z,PLS
F,ALL,FY,-0.000001   ! ULT. LOAD (KN)
NSEL,ALL
SOLVE

TIME,0.0001          ! TIME AFTER THE LOAD STEP!
AUTOTS,ON            ! AUTOMATIC TIME STEPING
NSEL,S,LOC,Y,H
NSEL,R,LOC,Z,PLS
F,ALL,FY,-0.0001     ! ULT. LOAD (KN)
NSEL,ALL
SOLVE

TIME,100
NSUBST,50,1000,50
AUTOTS,ON            ! AUTOMATIC TIME STEPING
NSEL,S,LOC,Y,H
NSEL,R,LOC,Z,PLS
F,ALL,FY,P           ! LOAD IN N
NSEL,ALL

OUTPR,ALL,all        ! LIST ALL SOLN. ITEMS TO OUTPUT FILE EVERY SUBSTEP
OUTRES,ALL,all       ! LIST ALL RESULTS TO DATABASE FILE FOR EVERY
                     ! SUBSTEP
LSWRITE
SAVE
SOLVE
SAVE
FINISH
exit
```